Oxydation des polyphénols des vins rouges

Stacy Deshaies

THÈSE POUR OBTENIR LE GRADE DE DOCTEUR DE L'UNIVERSITÉ DE MONTPELLIER

En sciences des aliments et nutrition

École doctorale GAIA – Biodiversité, Agriculture, Alimentation, Environnement, Terre, Eau

Unité de recherche : UMR Sciences Pour l'Œnologie

Etude de l'oxydation des polyphénols du vin rouge

Présentée par Stacy DESHAIES

Le 29 Novembre 2021

Sous la direction de M. Cédric SAUCIER

Devant le jury composé de

Patricia TAILLANDIER, Professeur, Toulouse INP-ENSIACET	Rapporteur
Jorge RICARDO DA SILVA, Professeur, Université de Lisbonne	Rapporteur
Olivier DANGLES, Professeur, Université d'Avignon	Président
François GARCIA, Maître de conférences, Université de Montpellier	Examinateur
Laetitia MOULS, Maître de conférences, Institut Agro – Montpellier SupAgro	Examinateur
Cédric SAUCIER, Professeur, Université de Montpellier	Directeur de thèse

UNIVERSITÉ DE MONTPELLIER

Table des matières

Remerciements

Je tiens en premier lieu à remercier M. Olivier DANGLES, Mme Patricia TAILLANDIER et M Jorge RICARDO DA SILVA pour avoir accepté de juger mon travail.

Je tiens aussi à remercier mon directeur de thèse, Cédric SAUCIER, sans qui ces travaux de recherches n'auraient pas été fructueux. Merci également à mes deux autres encadrants Laetitia MOULS et François GARCIA pour leurs conseils, leur travail et leur investissement à mes côtés durant ces trois années et également pour avoir accepté d'être examinateurs de ce manuscrit de thèse.

Merci aussi aux chercheurs et techniciens qui ont étroitement travaillé avec moi et qui ont permis d'achever ces travaux. Je pense particulièrement à Lucas SUC pour son accompagnement en chimie analytique, ses idées et sa patience au cours de manipulations qui n'ont pas toujours été simples ; Fréderic VERAN pour son soutien en électrochimie et Thibaut CONSTANTIN pour ses connaissances en chimie organique. Merci également à Luca GARCIA qui a bien voulu m'aider dans mes dernières analyses et à l'équipe de la plateforme polyphénols de l'INRAe qui m'a accueilli et m'a donné l'opportunité d'approfondir d'avantage mes travaux de thèse, et plus particulièrement à Christine LE GUERNEVE pour avoir pris le temps de m'expliquer la RMN et de réaliser de nombreuses analyses qui m'ont été plus qu'utiles pour ces recherches.

Un grand merci aux enseignants et chercheurs du DNO qui ont été d'une grande gentillesse et qui m'ont très bien accueilli. Je pense notamment à Mary, Marithé, François mais aussi Vincent et Audrey qui m'ont accompagné durant mes missions d'enseignement. Merci également aux autres collègues de la faculté de pharmacie pour ces excellents moments passés en votre compagnie, en particulier Chantal, Jérôme, Yvan, TibO, Jessica et Cynthia. Merci aussi aux collègues de SPO : Arnaud, Emmanuelle, Aude, Thierry, Aurélie, Pascale, les Stéphanie, Véronique… avec qui j'ai toujours eu d'excellents moments.

Un merci particulier aux filles qui m'ont extrêmement bien accueillies et qui sont devenues de véritables amies Mélodie, Auriane, Sarah, Nawel, Noémie, Anaïs, Marie et Hélène mais aussi à Luca et TibO sans qui la vie à Pharma ne serait pas la même.

Finalement je remercie ma famille, mes frères Mickaël et Nicolas et ma mère Sylvie pour leur soutien et leur présence. Je pense aussi particulièrement à mon père qui a su me donner la force et le courage de mener mes projets et qui aura toujours une place très chère à mon cœur.

Valorisation des travaux de recherches

PUBLICATIONS

1. Deshaies, S.; Cazals, G.; Enjalbal, C.; Constantin, T.; Garcia, F.; Mouls, L.; Saucier, C. **Red Wine Oxidation: Accelerated Ageing Tests, Possible Reaction Mechanisms and Application to Syrah Red Wines.** *Antioxidants* 2020, *9*, 663.

2. Deshaies, S.; Garcia, L.; Veran, F.; Mouls, L.; Saucier, C.; and Garcia, F. **Red wine oxidation characterization by accelerated ageing tests and cyclic voltammetry**. *Antioxidants 2021, 10, 1943.*

3. Deshaies, S.; Le Guernevé, C.; Suc, L.; Mouls, L.; Garcia, F.; and Saucier, C. **Unambiguous NMR structural determination of (+)-Catechin-Laccases dimeric reaction products as potential markers of grape and wine oxidation.** *Molecules, 2021, 26, 6165*

4. Deshaies, S.; Sommerer, N.; Garcia, F,; Mouls, L.; and Saucier, C. **UHPLC-Q-Orbitrap /MS² identification of (+)-Catechin oxidation reaction dimeric products in red wines and grape seed extracts: Effect of grape maturation and wine age**. Soumis (novembre 2021) dans le journal *Food Chemistry.*

5. Deshaies, S.; Garcia, F.; Suc, L.; Saucier, C.; and Mouls, L.; **Study of the oxidative evolution of tannins during Syrah red wines aging by tandem mass spectrometry.** Soumis (octobre 2021) dans le journal *Journal of agricultural and food chemistry.*

COMMUNICATIONS A DES CONGRES INTERNATIONAUX

1. Stacy DESHAIES, Thibaut CONSTANTIN, François GARCIA, Laetitia MOULS, Cédric SAUCIER. « Oxygen consumption kinetics during accelerated oxidation of red wine ». **OenoIVAS, Bordeaux, France, 25-28 juin 2019 – *Poster***

2. Stacy DESHAIES, Christine LE GUERNEVE, François GARCIA, Laetitia MOULS, Cédric SAUCIER. « (+)-catechin oxidation dimers as potential ageing biomarkers ». **Macrowine virtual, Verone, Italie, 23-30 juin 2021 – *Poster***

3. Stacy DESHAIES, Christine LE GUERNEVE, François GARCIA, Laetitia MOULS, Cédric SAUCIER « Structural determination of (+)-catechin-laccases reaction dimeric products ». **XXX International congress on polyphenols, virtual ; Turkü, Finlande, 13-15 juillet 2021 – *Présentation orale***

Abréviations

A	Anthocyane
ARP	Acetaldehyde-reactive polyphenols
C	Catéchine
Cd	Cadmium
CV	Cyclic voltammetry
Cx	Carbone x
DOSY	Diffusion order spectroscopy
DRO	Dérivés réactifs de l'oxygène
DPm	Degré de polymérisation moyen
E_0	Potentiel initial
E_{max}	Potentiel maximum
E_{min}	Potentiel minimum
EC	Epicatéchine
E.C.	Enzyme commission number
ECG	Epicatéchine gallate
EGC	Epigallocatéchine gallate
Glu	Glucose
GCE	Glassy carbon electrode (électrode carbone vitreux)
GRP	Grape reaction product
GSH	Glutathione
HAT	Hydrogen atom transfer
HMBC	Heteronuclear multi-bond connectivity
HPLC	Chromatographie liquide haute performance
HSQC	Heteronuclear single quantum correlation experiment
IFL	Liaison interflavanique
MS	Spectrométrie de masse
OCR	Oxygen consumption rate
o-quinone	*Ortho*-quinone
PA	proanthocyanidines
POD	Peroxydase
PPO	Polyphenol oxydase

RMN	Résonnance magnétique nucléaire
ROESY	Rotating-frame nuclear overhausser effect spectroscopy
SET	Single electron transfer
SO_2	Dioxyde de soufre
SWCNT-SPCE	Single walled carbon nanotubes modified screen printed carbon electrode
T	Tannin
TOCSY	Total correlation spectroscopy
UHPLC	Chromatographie liquide ultra haute performance
UV	Ultraviolet
3SH	3-sulfanylhexan-1-ol
3SHA	3-sulfanylhexal acetate
4MSP	4-methyl-4-sulfanylpentan-2-one

Introduction générale

Les polyphénols sont des composés largement présents dans la nature, ils peuvent notamment être retrouvés dans de nombreux végétaux comme le thé(Khan & Mukhtar, 2007), le cacao(Fayeulle et al., 2018; Rimbach et al., 2009), le raisin(Antoniolli et al., 2015) et dans les produits fermentés correspondant tels que le chocolat(Allgrove & Davison, 2014) ou le vin(Saucier, 2010). Ils possèdent des structures chimiques variées et complexes, les rendant ainsi des cibles privilégiées de nombreuses réactions chimiques(Oliveira et al., 2011; Singleton, 1987a). Parmi ces réactions, les réactions d'oxydation sont d'un intérêt majeur en sciences de aliments puisqu'elles peuvent avoir un impact important sur l'évolution et la conservation des produits, elles sont par exemple responsables des phénomènes de brunissement(Hui et al., 2008; « Roles of o-quinones and their polymers in the enzymic browning of apples », 1990).

En ce qui concerne les réactions d'oxydation du vin impliquant les polyphénols, leur impact, positif ou négatif, dépend fortement des quantités d'oxygène apportées au vin. En effet, un apport modéré et contrôlé permet d'atteindre une qualité optimale(Gambuti et al., 2013; Ugliano, 2013), notamment en réduisant certains aspects négatifs des vins tels que l'amertume ou l'astringence(de Beer et al., 2016; Ugliano, 2013). Cependant, des apports trop faibles ou trop importants en oxygène peuvent également engendrer un développement d'arômes indésirables ou une instabilité de la couleur(V. Cheynier, Dueñas-Paton, et al., 2006).

Les vins rouges diffèrent des autres vins (blancs et rosés) par leur processus de vinification et la composition polyphénolique qui en découle. Etant plus riches en polyphénols(Chevion et al., 2000), les phénomènes d'oxydation pour ces vins vont être nombreux et provoquer de nombreuses réactions chimiques au sein du produit depuis la vinification jusqu'à son évolution en bouteille, impactant ainsi leur qualité(Somers & Wescombe, 1987). La compréhension des mécanismes d'oxydation du vin constitue donc un réel challenge en œnologie. L'étude de l'évolution oxydative des vins a largement été décrit dans la littérature(V. Ferreira et al., 2015; Petrozziello et al., 2018) mais ces études nécessitent souvent des temps de vieillissements relativement longs. Ainsi, afin de disposer de mesures objectives de l'état d'oxydation des vins, de leur capacité antioxydante et de leur potentiel de vieillissement, des travaux visant à élaborer des tests de vieillissements accélérés ont été récemment développés(Castro et al., 2014a; V. Ferreira et al., 2015; Gambuti et al., 2017a; Mercurio & Smith, 2008; Picariello et al., 2017; Sheridan & Elias, 2015; Teng et al., 2019) mais ils restent peu nombreux.

Des techniques électrochimiques ont également récemment été mises au point dans l'analyse de l'oxydation des vins, notamment utilisant la voltammétrie cyclique(Benbouguerra et al.,

2020; Hoyos-Arbeláez et al., 2017). Ces techniques s'avèrent rapides, sensibles et peu coûteuses dans l'analyse des vins et fournissent des informations précieuses quant au potentiel d'oxydation des vins. Les études les plus récentes ont principalement ciblé les vins blancs(Gonzalez et al., 2018)

Parmi les polyphénols, deux principales sous familles sont primordiales dans les vins d'un point de vue organoleptique : les anthocyanes et les tannins condensés, aussi appelés proanthocyanidines, qui sont des polymères de flavan-3-ols. Ces derniers sont majoritaires dans le vin et proviennent principalement de la pellicule et des pépins, extraits au cours des macérations et de la fermentation alcoolique. Les tannins condensés jouent un rôle particulièrement important dans l'évolution sensorielle des vins notamment par leur faculté à réagir avec les anthocyanes ou les protéines salivaires(Atanasova et al., 2002a; V. Cheynier, Dueñas-Paton, et al., 2006). Les tannins, structurellement complexes, ont souvent été étudiés par des méthodes d'analyse globale par précipitation(Mercurio & Smith, 2008) n'incluant pas d'informations sur leurs structures chimiques. Ainsi, de récentes méthodes étudiant les tannins après dépolymérisation chimique ont été développées(Rigaud, Perez-Ilzarbe, et al., 1991a), en faisant notamment intervenir des marqueurs d'oxydation(Mouls et al., 2011a; Mouls & Fulcrand, 2015a).

L'objectif de cette thèse est d'étudier l'oxydation des polyphénols des vins rouges ainsi que leur potentiel d'oxydation.

Il est à noter que ce manuscrit a été réalisé sous forme de thèse sur publications. Il est divisé en cinq chapitres.

Le premier chapitre de ce manuscrit présente une étude bibliographique détaillant la structure des principaux polyphénols présents dans le vin, les réactions d'évolution et d'oxydation les impactant tout au long du vieillissement du vin et les différentes techniques permettant le suivi de ces phénomènes. Les problématiques liées à la thèse seront finalement explicitées à la fin de ce chapitre.

Le second chapitre présente les travaux portant sur la mise au point de tests d'oxydation accélérée et l'acquisition d'empreintes globales en spectrométrie de masse sur trois vins du cépage Syrah et issus de trois millésimes différents.

Le troisième chapitre traite des propriétés redox des vins rouges, étudiées par voltammétrie cyclique et mises en relation avec les vitesses de consommation d'oxygène,

développées au chapitre précèdent. Neuf vins rouges (dont les trois vins de Syrah précédents) de différents cépages et millésimes ont été sélectionnés et oxydés de manière accélérée.

Le quatrième chapitre aborde une approche ciblée et comporte deux parties. La première est centrée sur l'identification et l'obtention de marqueurs d'oxydation dimériques polyphénoliques. La deuxième traite de l'identification de ces marqueurs dans des échantillons de vins rouges et des extraits de pépins, les effets de la maturation des baies et du vieillissement d'un vin rouge y sont abordés.

Le cinquième chapitre présente l'étude de l'évolution oxydative des tannins au cours du vieillissement des vins rouges et s'intéresse à l'évolution structurale des unités constitutives des tannins.

Chapitre I – Bibliographie

1. Composition chimique du vin rouge

1.1. Composition générale

Issu d'un processus de transformation de la baie de raisin, le vin constitue un mélange chimique complexe extrêmement apprécié dans le monde entier et plus particulièrement en France, premier consommateur mondial.

Il existe une grande diversité de vins, se caractérisant principalement par leur cépage, c'est-à-dire la « variété » du raisin dont ils sont issus. Chaque cépage correspond à un climat et confère au produit son goût, sa qualité et des caractéristiques qui lui sont propres. Cette diversité s'accompagne d'un processus de vinification typique à chaque grand type de vin (blanc, rosé et rouge) et entraîne une composition chimique complexe de plus de 600 substances identifiées.

Tableau 1: *composition générale du vin. D'après UC Santa Cruz.*

Composés non-volatiles		**Composés volatiles**	
intitulé	*Teneur dans le vin ($g.L^{-1}$)*	*intitulé*	*Teneur dans le vin ($g.L^{-1}$)*
Glycérol	10	Acides volatiles (acide acétique)	0,45
Acides organiques (acide tartrique, acide lactique, acide succinique,…)	4	Esters (acétate d'éthyle,…)	0,25
Glucides	2	Espèces azotées (acides aminés, protéines)	0,25
Minéraux (calcium, cuivre, zinc, fer, magnésium, potassium)(Drava & Minganti, 2019)	2	Aldéhydes (acétaldéhyde, vanilline,…)	0,04
Tannins et composés phénoliques (dont pigments)	1	Autres alcools (amyl, iso-amyl, butyl, iso-butyl, hexyl, propyl, méthyl)	0,01

Un vin standard est composé à 86 % d'eau et 12 % d'alcools, le principal alcool étant l'éthanol, provenant de la fermentation des sucres du raisin par les levures. Un ordre de grandeur des concentrations des autres composés majoritaires est présenté dans le ***tableau 1***.

1.2. Processus de vinification du vin

Le processus de vinification des vins blanc et rosé suit les mêmes étapes (***figure 1***).

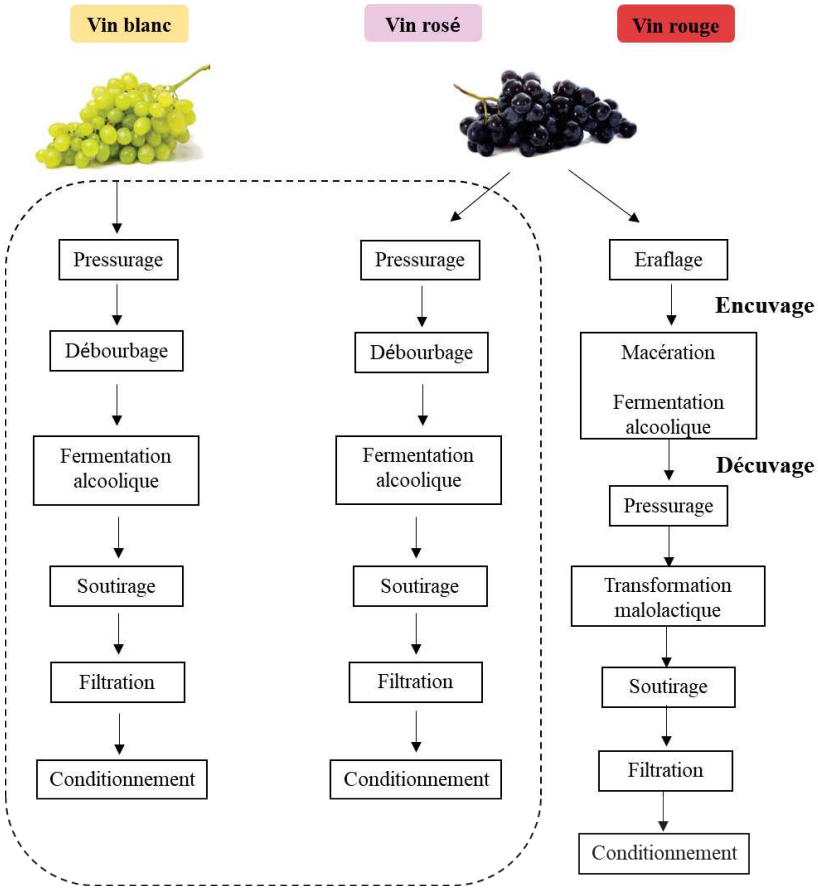

Figure 1: *étapes de vinification du vin blanc, rosé et rouge*

La vinification du vin rouge est différente. Même si le raisin utilisé est le même que pour le vin rosé, le vin rouge n'est pas directement pressuré mais, suite à une éventuelle étape de macération, la fermentation alcoolique se déroule en présence des parties solides du raisin. Il y a donc une extraction des composés présents dans les parties solides tout au long de la fermentation alcoolique ce qui lui confère une grande partie de ses propriétés organoleptiques comme la couleur et l'astringence. Ainsi, plus la macération est longue, plus un vin rouge sera coloré et riche en tannins, composés particulièrement présents dans les pellicules et pépins (Chira et al., 2008). Particulièrement sensibles aux phénomènes

d'oxydation, celui-ci va subir de nombreuses transformations structurelles au cours de l'étape d'élevage qui se fait par échange à travers le fût, perméable à l'oxygène. Les différentes étapes de l'élaboration du vin rouge sont illustrées sur la ***figure 2.***

Figure 2: *Etapes détaillées de l'élaboration du vin rouge*

2. Les polyphénols dans le vin

Les polyphénols sont des composés très réactifs et particulièrement sensibles aux phénomènes d'oxydation qui surviennent tout au long de la vie du vin, du processus de vinification au vieillissement en bouteille. Ces réactions entraînent la formation de composés avec de nouvelles propriétés organoleptiques et structurelles. La connaissance des structures chimiques des produits formés et mécanismes réactionnels impliqués dans ces phénomènes d'oxydation est indispensable pour mieux comprendre la qualité du vin. Dans le cas du vin rouge, cela permet d'améliorer et contrôler la couleur ainsi que l'astringence et d'envisager les différentes altérations possibles du produit(Singleton, 1987a).

Les composés polyphénoliques sont divisés en deux groupes : les flavonoïdes et les non-flavonoïdes.

2.1. Les non- flavonoïdes

Les non-flavonoïdes principalement présents dans les raisins et le vin sont des dérivés d'acides benzoïque et cinnamique (acides hydroxybenzoiques et hydroxycinnamiques). Ils regroupent aussi les stilbènes et les stilbènes glycosides (trans-resveratrol) ainsi que les tannins hydrolysables (***figure 3***).

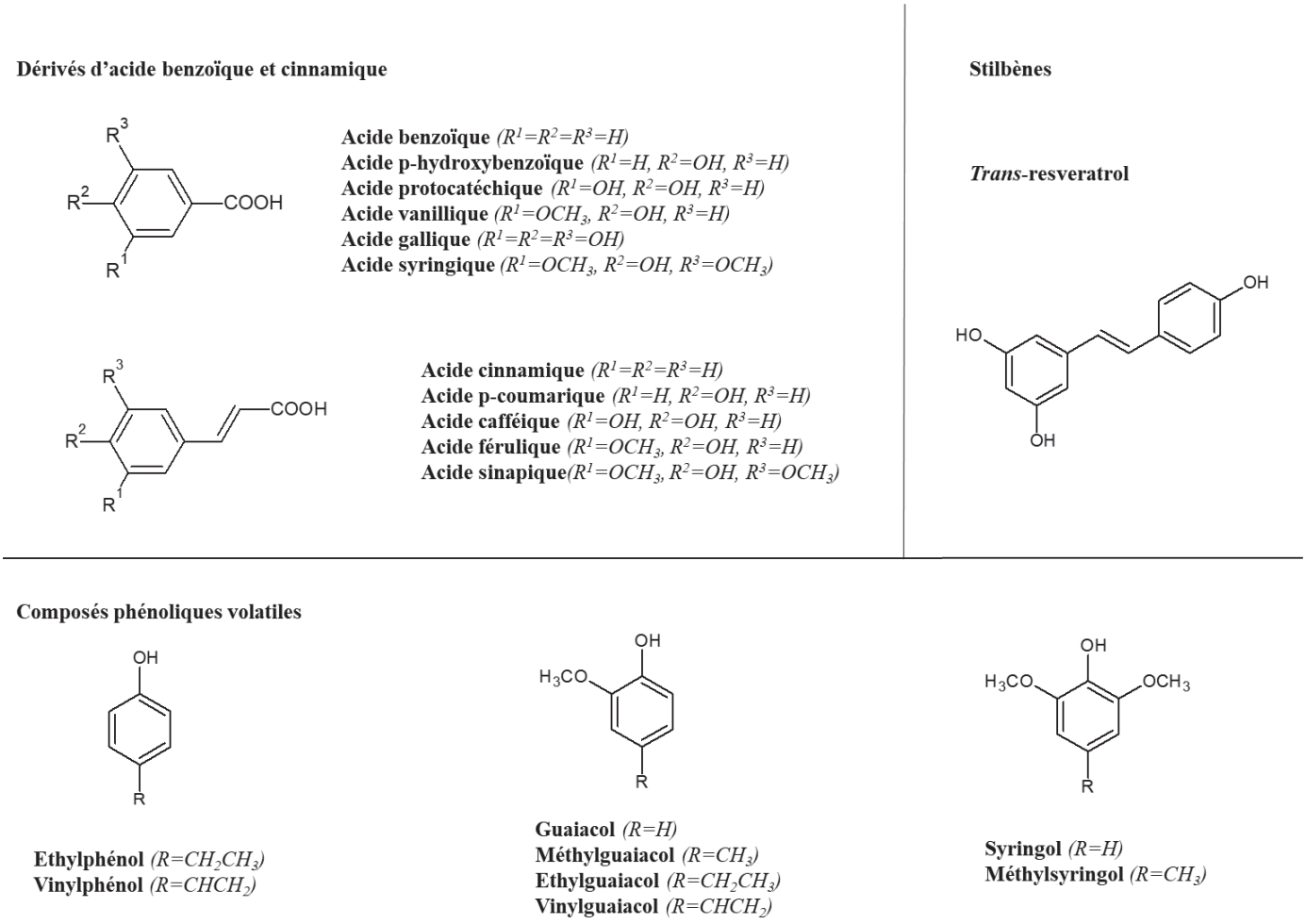

Figure 3: *structures moléculaires des principaux non - flavonoïdes du vin*

2.2. Les flavonoïdes

Les principaux flavonoïdes présents dans le raisin et le vin de *Vitis vinifera* sont les flavonols, les flavan-3-ols et les anthocyanes ainsi que les flavanonols et les flavones présents en plus faible quantité. Les flavonoïdes sont constitués d'un noyau flavane C6-C3-C6 (cycles benzène A et B reliés par un noyau pyrane C contenant un oxygène) et se différencient en plusieurs groupes, caractérisés par le degré d'oxydation de l'hétérocycle C et par l'hydroxylation ou méthoxylation des trois cycles.

On distingue les flavonols, les flavan-3-ols et les anthocyanes. La ***figure 4*** décrit leur structure et présente les plus communs d'entre eux.

Flavonols

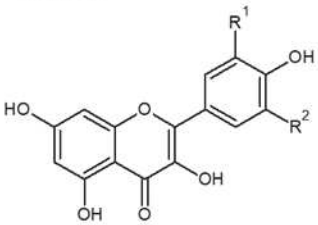

Kaempferol *(R^1=R^2=H)*
Quercetine *(R^1=OH, R^2=H)*
Myricetine *(R^1=R^2=OH)*

Anthocyanes

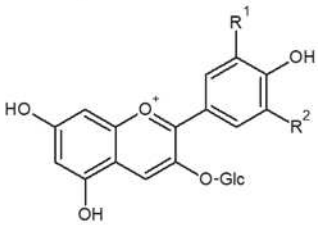

Cyanidine 3-glucoside *(R^1=OH, R^2=H)*
Peonidine 3-glucoside *(R^1=OCH_3, R^2=H)*
Delphinidine 3-glucoside *(R^1=R^2=OH)*
Petunidine 3-glucoside *(R^1=OH, R^2=OCH_3)*
Malvidine 3-glucoside *(R^1=R^2=OCH_3)*

Flavan-3-ols

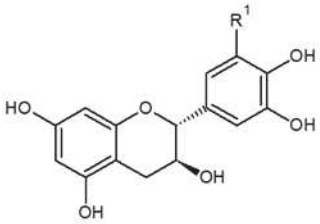

(+)-Catéchine *(R^1=H)*
(+)-Gallocatéchine *(R^1=OH)*

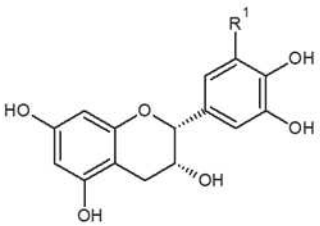

(-)-Epicatéchine *(R^1=H)*
(-)-Epigallocatéchine *(R^1=OH)*

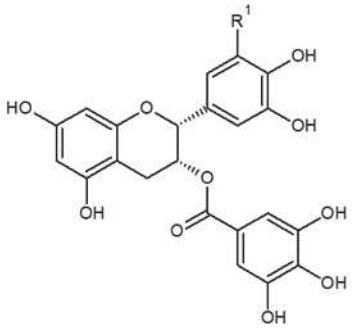

(-)-Epicatéchine gallate *(R^1=H)*
(-)-Epigallocatéchine gallate *(R^1=OH)*

Figure 4: *structures moléculaires des principaux flavonoïdes du vin*

Les flavan-3-ols se retrouvent principalement dans les parties solides de la grappe (pépins, rafle et pellicules) sous forme monomériques, oligomériques et polymériques.

Les tannins des pépins sont des oligomères et polymères constitués d'unités (+)-catéchine , (-)-épicatéchine et (-)-épicatéchine gallate (ECG)(Prieur et al., 1994) tandis que les tannins de la pellicule contiennent également des unités (-)-épigallocatéchine et des traces de (+)-gallocatéchine et (-)-épigallocatéchine gallate(Escribano-Bailón et al., 1995; Souquet et al., 1996). Les tannins des pépins diffèrent surtout de ceux de la pellicule car ils contiennent un plus grand pourcentage d'ECG (20-23 % pépins / 3-5 % pellicule) et possèdent un degré de polymérisation moyen (DPm) plus faible.

Au sein des tannins différentes structures peuvent être observées. Cependant, il est impossible de les séparer en différentes catégories car, au sein d'un tannin avec un DP >3, plusieurs cas de figures peuvent se présenter, on parle alors de polymères.

En revanche, les dimères peuvent être classés en plusieurs catégories en fonction de leurs structures respectives. Les dimères de type A se caractérisent par des liaisons interflavane C4-C8 et des liaisons éther C2-O-C7 ou C2-O-C5. Les polymères de type B possèdent des liaisons C4-C6. Les structures des PA de type A et B sont présentées dans la ***figure 5***.

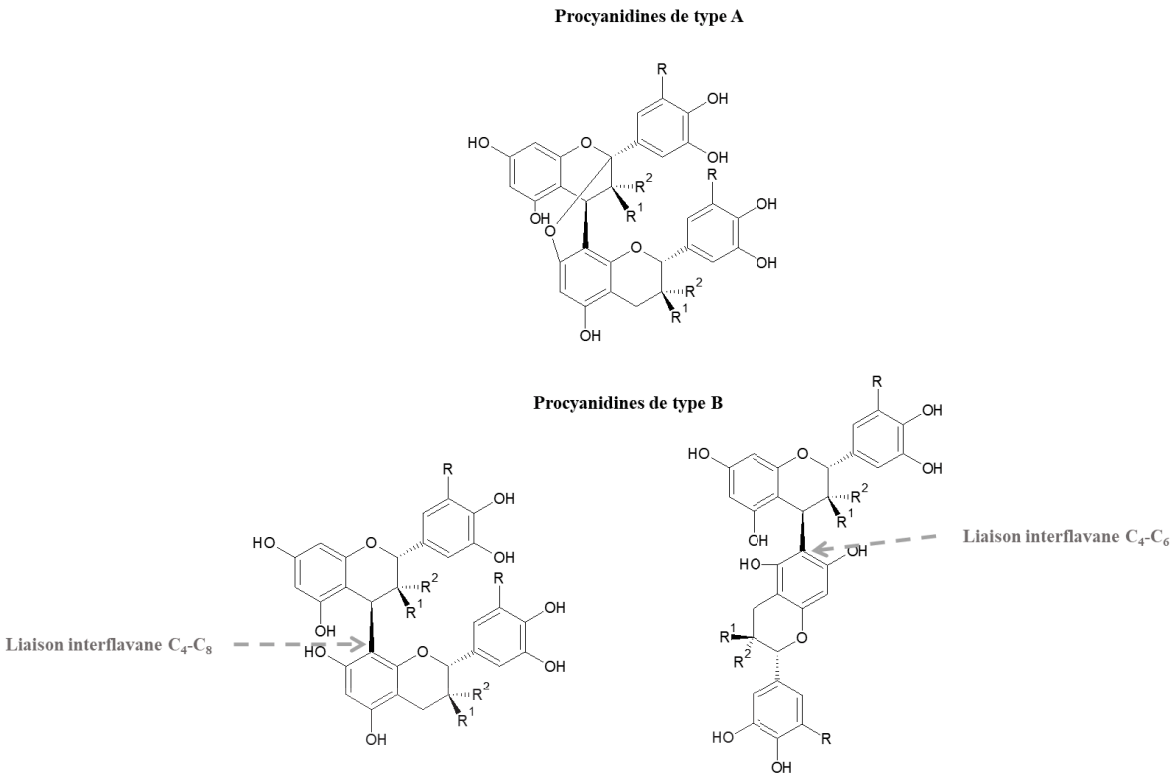

Figure 5: *Structures des dimères de flavan-3-ols de type A et B*

2.3. Impact des tannins condensés sur les propriétés sensorielles des vins

D'un point de vue œnologique, les polyphénols, et plus particulièrement les tannins condensés jouent un rôle essentiel dans l'évolution des propriétés organoleptiques des vins : (i) en réagissant avec les anthocyanes de nombreux pigments dérivés sont générés et permettant une stabilisation de la couleur(Atanasova et al., 2002b; V. Cheynier, Dueñas, et al., 2006); (ii) par des interactions avec les protéines salivaires, les tannins entrainent un dessèchement de la bouche plus ou moins important en fonction de leur composition(McRae & Kennedy, 2011). La force des interactions entre les tannins et les protéines salivaires dépend de la taille moléculaire des tannins (les interactions augmentent avec le degré de polymérisation(V. Cheynier, Prieur, et al., 1997)) et de leur structure chimique: elles augmentent avec le pourcentage de galloylation(V. Cheynier, Prieur, et al., 1997) et/ou en fonction de leur flexibilité conformationnelle(P. McManus et al., 1985). Ainsi l'évolution chimique des tannins au cours du temps module la sensation d'astringence.

Les tannins se retrouvent en faible quantité dans les vins blancs et en quantité importante dans les vins rouges. Chaque type de vin peut ainsi se différencier par sa teneur en tannins, les

rouges étant donc les plus concentrés (1 à 4 g/L)(Ribéreau-Gayon et al., 2006), leur donnant ainsi cette robe foncée et cette sensation astringente caractéristique des vins rouges.

La richesse du vin rouge en tannins condensés et anthocyanes(Brossaud et al., 2008; Kennedy et al., 2006; Ma et al., 2014; Noble, 1994; Robichaud & Noble, 1990; Soares et al., 2017) le distingue des autres vins et en a fait un sujet de recherche privilégié ces dernières années. En effet, ces composés jouent un rôle majeur dans le vieillissement des vins rouges, principalement en raison de leur sensibilité aux phénomènes d'oxydation impactant l'ensemble du processus de fabrication et de stockage du vin. Si tous les paramètres sont bien maitrisés l'évolution chimique des polyphénols dans les vins rouges tend en général à réduire l'astringence ainsi qu'à stabiliser la couleur(Echave et al., 2021).

Nous allons dans la partie suivante décrire les différentes voies d'évolution et d'oxydation des vins rouges.

3. Evolution des polyphénols du vin rouge

3.1. Réactions d'évolution non oxydatives

3.1.a. Sulfonation des anthocyanes

Dans les vins, les anthocyanes, pigments rouges, sont en équilibre physico-chimique entre plusieurs formes : la forme hémiacétal incolore, le cation flavylium qui est la forme rouge de l'anthocyane, la base quinonique de couleur bleue-mauve, et la chalcone C de couleur jaune(Castañeda-Ovando et al., 2009). Au pH du vin (pH 3,2-4), la forme incolore hémiacétal est largement majoritaire (70 à 80 %), au détriment de la forme rouge (cation flavylium) qui est la seule qui participe à la coloration des vins. Dans les vins, les anthocyanes sous la forme flavylium peuvent former des combinaisons instables avec les sulfites pour former des adduits bisulfitiques(Berké et al., 1998; Fulcrand et al., 2006; Wrolstad et al., 2005) (***figure 6***). L'équilibre entre l'adduit bisulfitique incolore et le cation flavylium rouge dépend du pH mais aussi des autres combinaisons des sulfites qui peuvent avoir lieu, par exemple, avec l'acétaldéhyde.

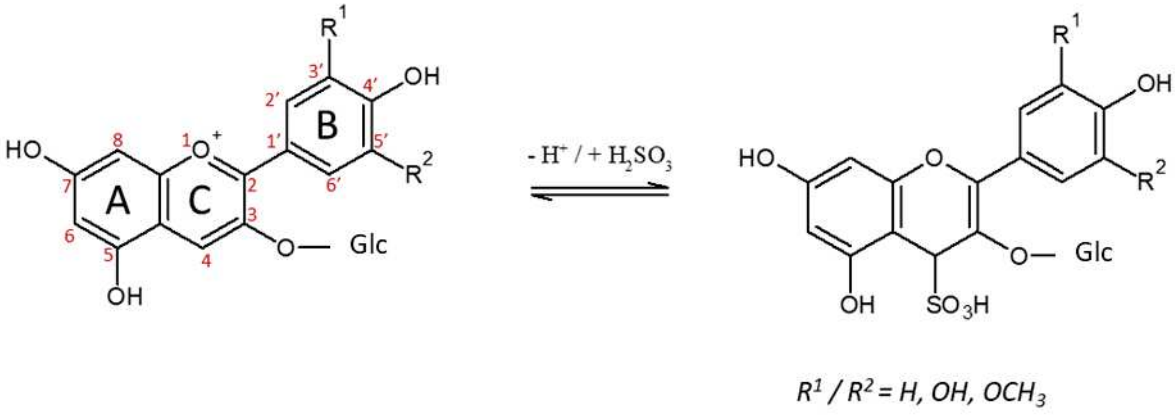

Figure 6 : *Formation d'un adduit bisulfitique par réaction entre les cations flavylium et les sulfites*

3.1.b. Réactions directes et réactions de polycondensation : tannin/tannin, tannin/anthocyane ou anthocyane /anthocyane

Les composés polyphénoliques, en plus de leur rôle de cofacteurs dans la copigmentation des vins rouges(Brouillard & Dangles, 1994; Goto & Kondo, 1991), peuvent directement être impliqués dans la coloration du milieu via la formation de pigments polymériques avec les anthocyanes(*Jackson: Wine science: principles and applications - Google Scholar*, s. d.; Quideau et al., 2005). Certains de ces nouveaux pigments sont plus stables que les anthocyanes monomériques vis à vis des attaques nucléophiles et autres modifications chimiques des anthocyanes (décoloration au SO_2)(*Jackson: Wine science: principles and applications - Google Scholar*, s. d.; Jurd, 1969) et participent fortement à la stabilisation de la couleur.

Au pH du vin rouge, les anthocyanes libres sous la forme flavylium peuvent agir comme électrophiles (positions C2 ou C4 du cycle C – *voir numérotation* ***figure 6***) ou nucléophiles dans leur forme hémicetal (positions C6 ou C8 du cycle A)(*Jackson: Wine science: principles and applications - Google Scholar*, s. d.; Nave et al., 2010; Salas et al., 2004) . De plus, la rupture des liaisons C-C des tannins se produit spontanément dans le vin, catalysée par le milieu acide et libérant ainsi des carbocations T^+ électrophiles. Les anthocyanes libres peuvent ainsi se condenser avec les tannins (flavan-3-ols et proanthocyanidines oligomériques) pour générer des adduits anthocyane-tannin (A-T), tannin-anthocyane (T-A)(He et al., 2008), mais également anthocyane-anthocyane (A-A) et tannin-tannin (T-T). Ces condensations se font à

travers deux mécanismes distincts représentés sur la ***figure 7***. Ces réactions sont appelées les « réactions directes ».

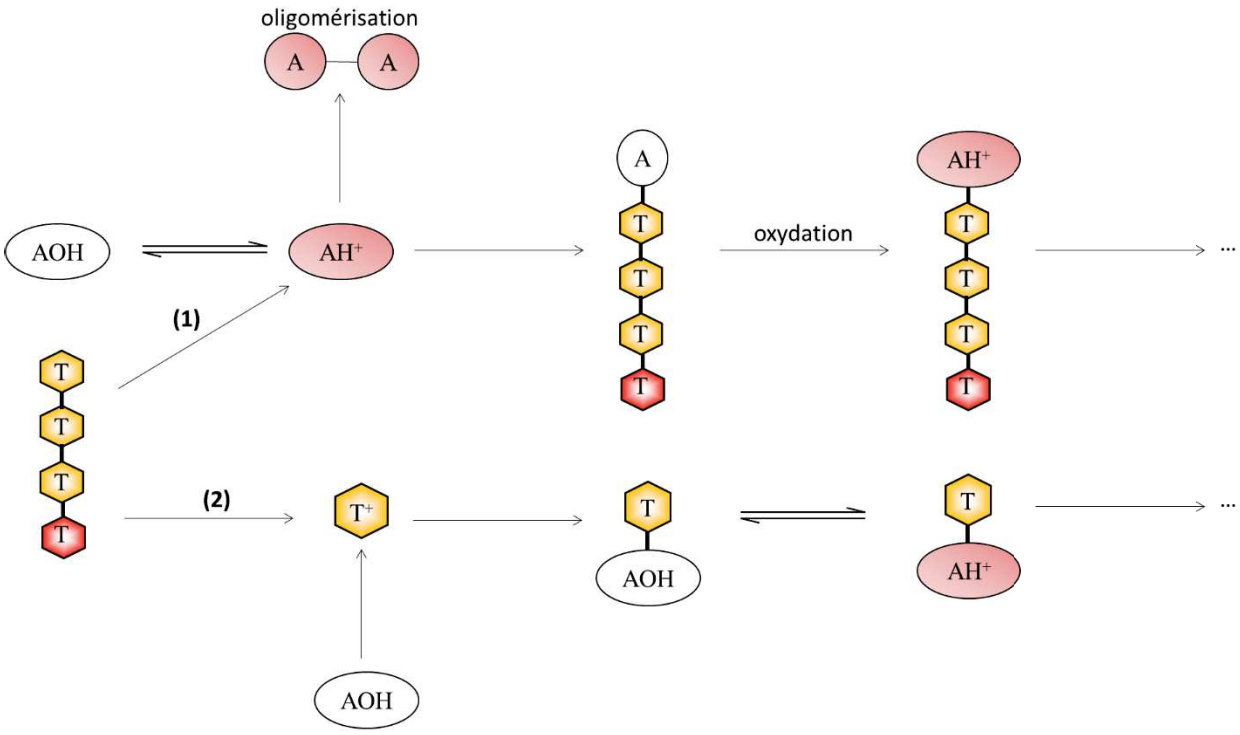

Figure 7 : *Réaction de formation des adduits A-T (1) et T-A (2). (1) : addition d'un tanin sur un carbocation coloré AH^+ aboutissant à la formation d'un adduit A-T incolore ou coloré en fonction de l'évolution de la structure. (2) : rupture des liaisons interflavaniques et addition de l'anthocyane hydratée AOH sur le carbocation T^+ aboutissant à la formation d'un adduit T-AOH incolore et T-AH^+ coloré en équilibre dans le milieu.*

En plus de ces réactions de condensation directe avec les flavonoïdes, les anthocyanes peuvent engendrer la formation de pigments polymériques rougeâtres ou violets via l'intervention de l'acétaldéhyde(Es-Safi et al., 2000; Francia-Aricha et al., s. d.; Sousa et al., 2007), aldéhyde le plus abondant dans le vin rouge(Timberlake & Bridle, 1976). Les réactions faisant intervenir l'acétaldéhyde aboutissent à la formation de dérivés identiques à ceux présentés sur la ***figure 7*** et reliés par des ponts éthyl CH-CH_3 tels que des dérivés de tannins (T-é*thyl*-T), des adduits tannin/anthocyane (A-é*thyl*-T) et des oligomères d'anthocyanes (A-*ethy*l-A)(Dallas et al., 1996; Forino et al., 2020; Timberlake & Bridle, 1976) .

Enfin, ces produits peuvent subir d'autres arrangements structurales et générer des pigments xanthylium jaunes-orangés.

3.1.c. Pyranoanthocyanes

Comme évoqué précédemment, les anthocyanes sont des molécules très réactives et vont évoluer dans les vins selon différentes voies réactionnelles pouvant conduire à leur dégradation, à la formation de pigments dérivés ou à la formation de composés dérivés non colorés. Ces réactions impliquent des métabolites des levures (acétaldéhyde, acide pyruvique, vinylphénols) et/ou d'autres composés phénoliques, en particulier les 6,8-vinylflavanols (monomères ou tannins condensés) ainsi que les acides hydroxycinnamiques. Parmi les composés dérivés formés et colorés une classe importante est représentée par les pyranoanthocyanes(Bakker & Timberlake, 1997; Canals et al., 2005; Freitas & Mateus, 2011; Rentzsch et al., 2007; Schwarz et al., 2003). En effet, les pyranoanthocyanes constituent la classe la plus importante de pigments dérivés des anthocyanes présents naturellement dans le vin rouge(Hayasaka & Asenstorfer, 2002; Mateus et al., 2001a, 2001b; Vivar-Quintana et al., 1999), elles sont issues de la réaction entre une anthocyane native avec n'importe quel composé contenant une double liaison riche en électrons (nucléophile)(von Baer et al., 2008) et possèdent ainsi deux cycles hétéroatomiques (***figure 7***) . Les pyranoanthocyanes se forment principalement à partir des anthocyanes des raisins durant la fermentation du moût ou pendant la maturation et le vieillissement des vins rouges(Freitas & Mateus, 2011; Rentzsch et al., 2007) et ont généralement une couleur plus orangée que les anthocyanes natives et sont plus résistantes aux variations de pH. Elles sont également résistantes à la décoloration par le SO_2.

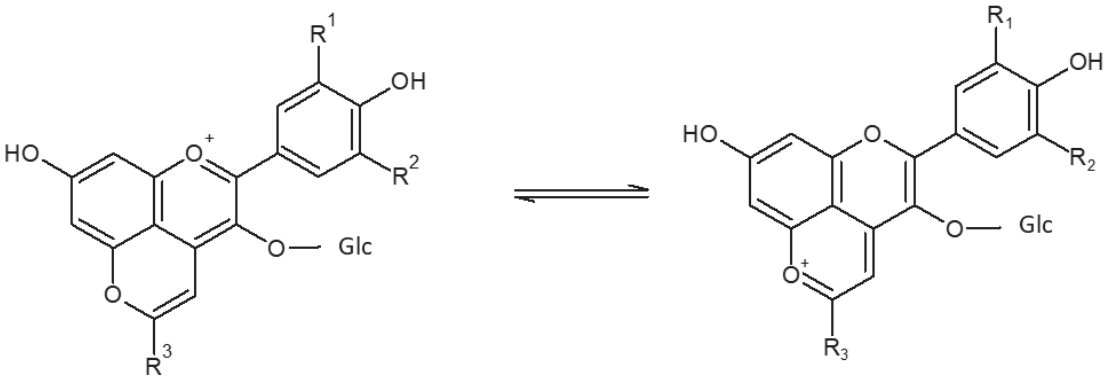

Figure 8 : *Structures des pyranoanthocyanes issues de l'anthocyanidine-3-O-glucoside dans les vins rouges et équilibre dynamique entre les différentes formes du cation flavylium*

3.1.d. Influence du vieillissement du vin rouge sur les anthocyanes

La concentration des anthocyanes libres diminue progressivement durant le vieillissement du vin(Monagas & Bartolomé, 2009; Monagas, Bartolomé, & Gómez-Cordovés, 2005; Alcade-Eon et al., 2006; Monagas, Bartolomé, & Gomez-Cordoves, 2005; Jackson, 2008), avec une tendance pour les anthocyanes acylées à décroître plus rapidement que les non acylées. Cela pourrait provenir de l'hydrolyse de la forme acylée vers la forme non acylée durant le vieillissement du vin(Monagas, Bartolomé, & Gómez-Cordovés, 2005). Cependant, les différentes formes d'anthocyanes libres non acylées montrent les mêmes cinétiques de diminution, tout comme les pyranoanthocyanes issues de ces précurseurs(Monagas, Bartolomé, & Gómez-Cordovés, 2005). Alors que les formes monomériques diminuent, les anthocyanes sous forme d'adduits et les pigments dérivés augmentent, permettant ainsi une stabilisation de la couleur, avec cependant un léger changement de teinte vers une teinte tuilée.

Ces réactions d'évolution s'accompagnent bien souvent de réactions d'oxydations des polyphénols, ces composés étant les cibles prioritaires des phénomènes d'oxydation et ayant un fort impact sur les propriétés organoleptiques du vin rouge. Ces phénomènes sont décrits dans la partie suivante(Waterhouse & Laurie, 2006a).

3.2. Réactions d'oxydation

3.2.a. Définition des dérivés réactifs de l'oxygène (DRO)

Les réactions d'oxydation dans de nombreux systèmes biologiques se produisent via les espèces réactives de l'oxygène (ERO), terme regroupant les radicaux libres de l'oxygène tels que l'anion superoxide $O_2^{\bullet -}$, formé par la capture d'un électron par la molécule d'oxygène, ou les radicaux hydroperoxyle $HOO^{\bullet}$, hydroxyle $HO^{\bullet}$, peroxyles $ROO^{\bullet}$, alkoxyles $RO^{\bullet}$ (R= substrat organique). Il est également possible de trouver des espèces non radicalaires qui sont de potentielles espèces oxydantes ou qui peuvent facilement devenir des radicaux, comme le peroxyde d'hydrogène H_2O_2, l'ozone O_3, l'acide hypochloreux HOCl, le singulet de l'oxygène $^1O_2$ ou les hydroperoxydes lipidiques LOOH(Pourova et al., 2010; Shchepinov, 2007).

La formation des dérivés réactifs de l'oxygènes dans le vin est présentée en ***figure 9***. La réduction du peroxyde d'hydrogène H_2O_2 en radical hydroxyl $HO^{\bullet}$, catalysée par les ions Fe

(II), présents en faible quantité dans les vins,correspond à la réaction de Fenton et libère des radicaux capables d'oxyder de nombreux composés du vin comme l'éthanol en acétaldéhyde mais s'avère également être une étape clé dans l'oxydation non enzymatique des polyphénols(Danilewicz, 2003a; Elias & Waterhouse, 2010; Waterhouse & Laurie, 2006b).

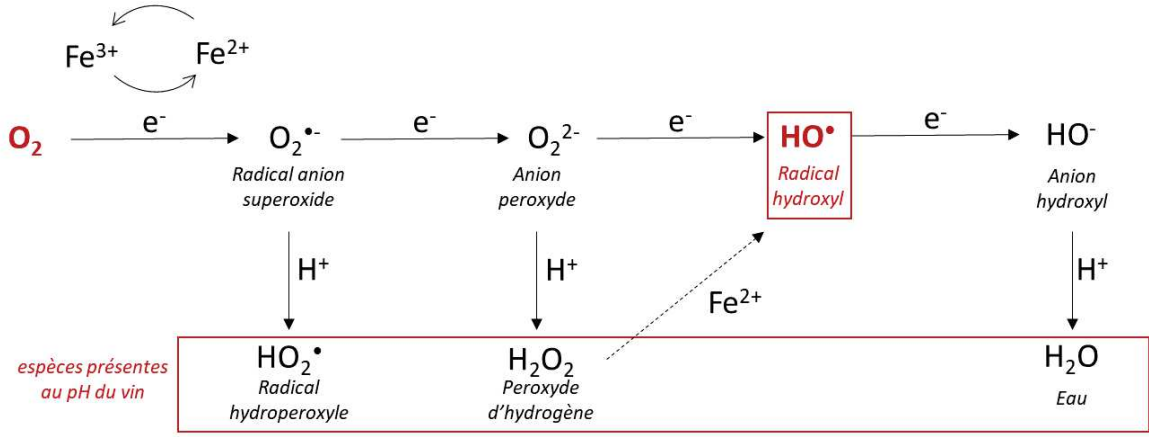

Figure 9: *Réactions de réduction de l'oxygène*

3.2.b. Antioxydants non phénoliques

Sont qualifiés d'antioxydants des composés capables de retarder ou empêcher les phénomènes d'oxydation. Les espèces antioxydantes peuvent agir par différents modes d'action (interruption de la chaîne de propagation radicalaire, chélation des métaux de transitions, inhibition de l'activité des enzymes de peroxydation, désactivation des espèces réactives de l'oxygène , abaissement de la pression partielle en oxygène)(Choe & Min, 2009; Cillard & Cillard, 2006; Sarni-Manchado & Cheynier, s. d.). De par leur structure chimique, les polyphénols sont des antioxydants naturels très efficaces du vin. En effet, par rupture homolytique de la liaison O-H, ils sont capables de céder un atome d'hydrogène aux radicaux peroxyles ROO• (R= substrat organique). Ce mécanisme (HAT : hydrogen atom transfer) est le plus communément décrit dans la littérature(Akoh, 2017; Cillard & Cillard, 2006; Sarni-Manchado & Cheynier, s. d.) avec le mécanisme de transfert d'électron (SET : single electron transfer)(Leopoldini et al., 2011).

Cependant il existe d'autres antioxydants non phénoliques dans les vins, principalement le dioxyde de soufre SO_2 et l'acide ascorbique(Barril et al., 2012).

Bisulfite

L'ion bisulfite HSO_3^- est reconnu pour ses propriétés antimicrobiennes et antioxydantes dans le vin, régulant la croissance des microorganismes et empêchant le brunissement. Il peut également protéger le vin d'une dégradation sensorielle par addition avec des composés carbonylés(Danilewicz et al., 2008) (***figure 10*** *: action de l'anion bisulfite sur l'acétaldéhyde*).

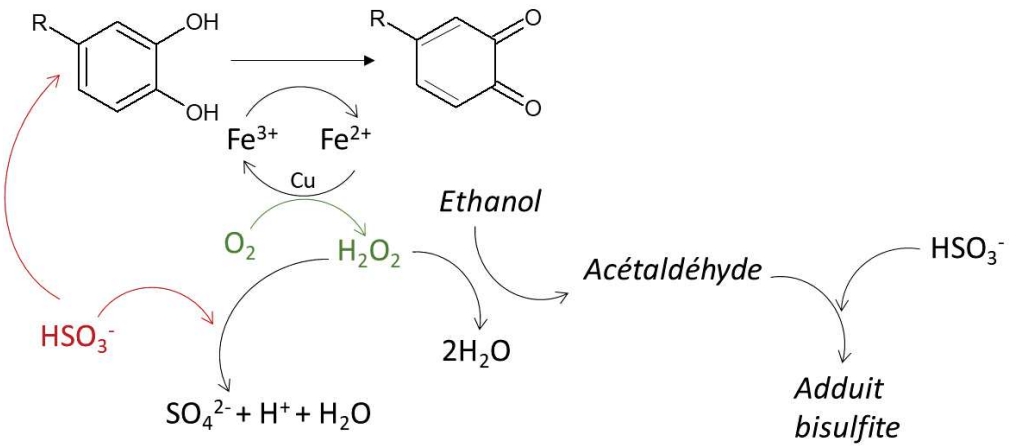

Figure 10 : *Interaction du SO_2 avec les peroxyde d'hydrogène et les quinones après oxydation du groupement catéchol, empêchant l'oxydation de l'éthanol par la réaction de Fenton $Fe^{2+}_{(aq)} + H_2O_2 \rightarrow Fe^{3+} + OH^- + HO^{\bullet}$. La réaction directe entre le SO_2 et l'oxygène moléculaire est lente et requiert la présence d'un catalyseur tel que le fer ou le cuivre. En conditions œnologiques, le SO_2 libre peut réduire les quinones, produits d'oxydation, en phénols ce qui ralentit le processus d'oxydation. Il réagit également avec un oxydant puissant, le peroxyde d'hydrogène, généré par l'oxydation des composés phénoliques et prévient ainsi la formation d'éthanal. Ces deux mécanismes conduisent à une diminution de la concentration en SO_2 libre et total lors du stockage du vin.*

Les taux de SO_2 ajoutés lors de la vinification peuvent varier de 50 à 200 mg/L(Oliveira et al., 2011). Dans le vin, SO_2 est quasi-exclusivement sous forme d'ion bisulfite HSO_3^- correspondant au SO_2 libre. Lorsqu'il est lié à d'autres composés insaturés sous sa forme libre il est qualifié de SO_2 lié. De plus, il ne réagit pas directement avec l'oxygène (***figure 10***) mais avec une forme réduite de l'oxygène : le peroxyde d'hydrogène, limitant ainsi la formation d'aldéhydes(Elias & Waterhouse, 2010). Il joue également un rôle important dans la réduction des quinones dans leur forme phénolique initiale, éliminant ainsi un potentiel électrophile(Danilewicz, 2007; Danilewicz et al., 2008). Cependant, la présence d'ions fer et cuivre et primordiale dans l'oxydation des catéchols en quinones et donc dans l'action du SO_2 sur le peroxyde d'hydrogène(Danilewicz, 2011). En effet, les différents substrats du vin ne sont

pas en mesure de réagir directement avec l'oxygène moléculaire qui existe sous la forme d'un diradical et donc d'un état triplet de charge qui ne peut pas accepter une paire d'électrons (Danilewicz, 2003b; Miller et al., 1990).

Acide ascorbique

L'acide ascorbique est naturellement présent dans les raisins(Bradshaw et al., 2011) mais il est rapidement consommé après l'étape de pressurage (***figure 1***) soit en piégeant l'oxygène induit par cette étape, soit en réduisant les *ortho*-quinones issues de l'oxydation enzymatiques de composés phénoliques. Il est particulièrement ajouté en priorité aux vins blancs, moins riches en acide ascorbique de par leur processus de vinification. Les taux d'acide ascorbique dans les vins varient généralement de 50 à 150 mg/L(Barril et al., 2009) et il est principalement utilisé pour sa capacité à piéger efficacement l'oxygène. Cependant, cette réaction provoque également la formation de peroxyde d'hydrogène et d'acide déhydroascorbique, qui se dégrade rapidement en acides carboxyliques, cétones, aldéhydes, etc... (Kilmartin et al., 2001) Ainsi les taux de SO_2 doivent être adaptés en conséquence afin d'éliminer le peroxyde d'hydrogène formé et de réagir avec les composés résultant de l'oxydation de l'acide ascorbique.

Des études récentes ont mis en avant des alternatives à l'utilisation du SO_2 et de l'acide ascorbique pour protéger les composés volatiles aromatiques du vin durant sa conservation comme par exemple l'utilisation d'acide caféique, d'acide gallique et de glutathion(Lambropoulos & Roussis, 2007; Lavigne et al., 2007; Roussis et al., 2007; Roussis & Sergianitis, 2008). Des mesures de voltammétrie cyclique ont confirmé ces études en montrant le caractère antioxydant du glutathion par addition nucléophile de GSH sur les quinones (Makhotkina & Kilmartin, 2009)

3.2.c. Différents types d'oxydation des polyphénols

Parmi les réactions d'oxydation faisant intervenir les composés phénoliques dans le vin, on distingue les oxydations enzymatiques des réactions chimiques. Elles font toutes les deux intervenir l'oxygène moléculaire comme substrat.

Oxydation enzymatique

En œnologie, l'oxydation enzymatique des composés phénoliques est catalysée par des enzymes appartenant à la catégorie E.C.1 des oxydoreductases (*Nomenclature Committee of the international union of biochemistry and molecular biology*). Les trois principales catégories qui catalysent l'oxydation des polyphénols sont (i) les oxydoreductases qui utilisent l'oxygène comme accepteur d'électron (E.C.1.10.3) (ii) les tyrosinases (E.C.1.14.18.1) et les peroxydases POD (E.C.1.11.1) (***figure 11***)

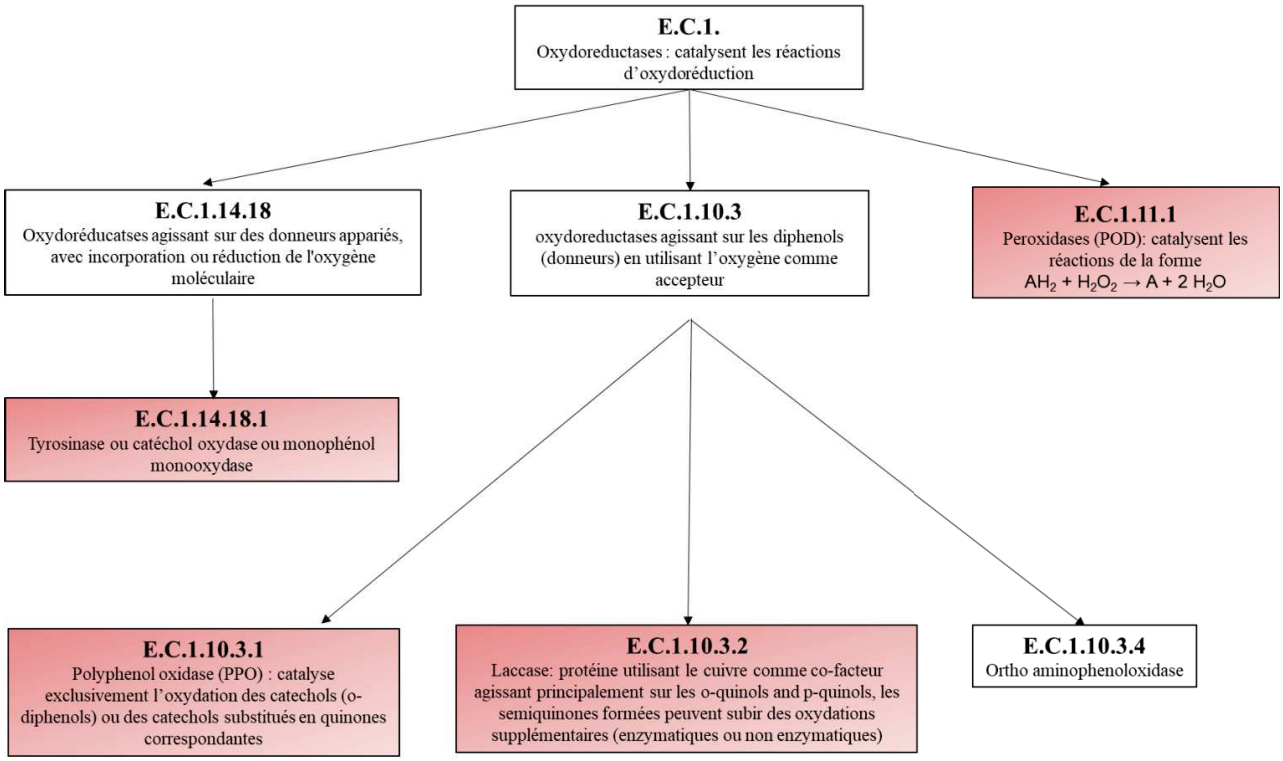

Figure 11: *classification des principales enzymes intervenant dans l'oxydation enzymatique du raisin et du vin*

Les principales enzymes qui agissent au sein des raisins sont :

- Les polyphénoloxidases PPO, utilisant le cuivre comme co-facteur.
- Les tyrosinases(Li et al., 2008; Singleton, 1987b), naturellement produites dans les baies et qui peuvent catalyser l'oxydation des monophénols et des catéchols
- Les laccases, produites par les moisissures des baies infectées par *Botrytis cinerea*(Jackson, 2008; Ployon et al., 2020)et capables d'oxyder de nombreux substrats, notamment les 1,2 et 1,4-dihydroxybenzenes. Leur mécanisme d'action est décrit dans la figure 12.

- Les peroxidases POD(Li et al., 2008; Whitaker & Lee, 1995), utilisant le fer comme co-facteur

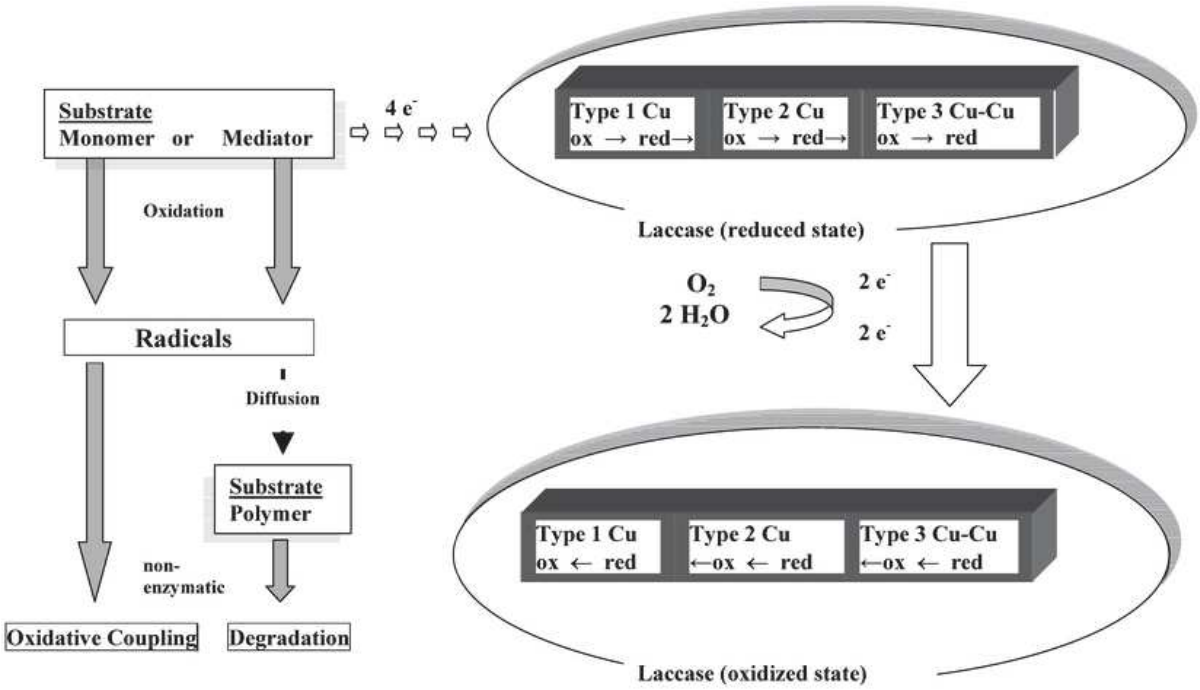

Figure 12 Réactions catalytiques des laccases fongiques : l'enzyme oxyde les molécules de substrat avec le cuivre de type 1 par quatre transferts d'un électron. La réoxydation de la laccase est provoquée par la paire de cuivre diamagnétique de type 3, qui transfère quatre électrons (par étapes de deux électrons) à l'oxygène(Claus, 2003).

Le brunissement causé par les POD est négligeable dans la plupart des fruits sauf si cette enzyme est associée aux PPO(Robards et al., 1999). La majorité des réactions d'oxydation enzymatique ayant lieu avec les PPO dans les baies, la suite de cette étude concernera donc principalement cette enzyme.

Ce type d'oxydation est également appelé brunissement enzymatique et intervient lors des étapes de pressurage des raisins. Bien que particulièrement important dans les vins blancs, il est possible de le retrouver dans les autres types de vins également. En effet, même si les anthocyanes et les tannins condensés (oligomères et polymères) de ne sont pas des substrats privilégiés pour la PPO du fait de l'encombrement stérique(V. Cheynier et al., 1994; V. Cheynier & Ricardo da Silva, 1991), les effets de cette enzyme peuvent être visibles lors de la vinification du vin rouge mais peuvent également avoir un impact sur sa décoloration.

Les premiers substrats de l'oxydation enzymatique dans le moût sont l'acide caftarique (acide cafeoyltartarique) et l'acide coutarique (acide *p*-coumaroyl-tartarique), donnant lieu à

leurs *ortho*-quinones associées (***figure 13***) après action de la PPO(Singleton et al., 1985) sur le groupement catéchol.

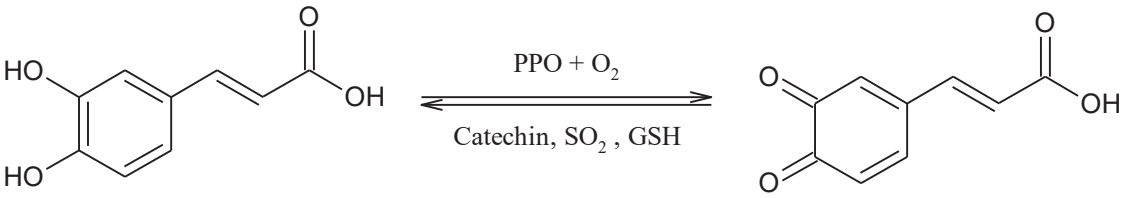

Figure 123 : *Oxydation enzymatique de l'acide caftarique*

La PPO peut également aboutir à la formation de dimères suite à l'oxydation de la catéchine (ou épicatéchine) et addition nucléophile du monomère en excès dans le milieu. Ces dimères diffèrent de leurs isomères de procyanidines de par la nature et la position de leurs liaisons interflavaniques (IFL)(Gaulejac et al., 2001; Guyot et al., 1996; Sanoner et al., 2002) (***figure 14***)

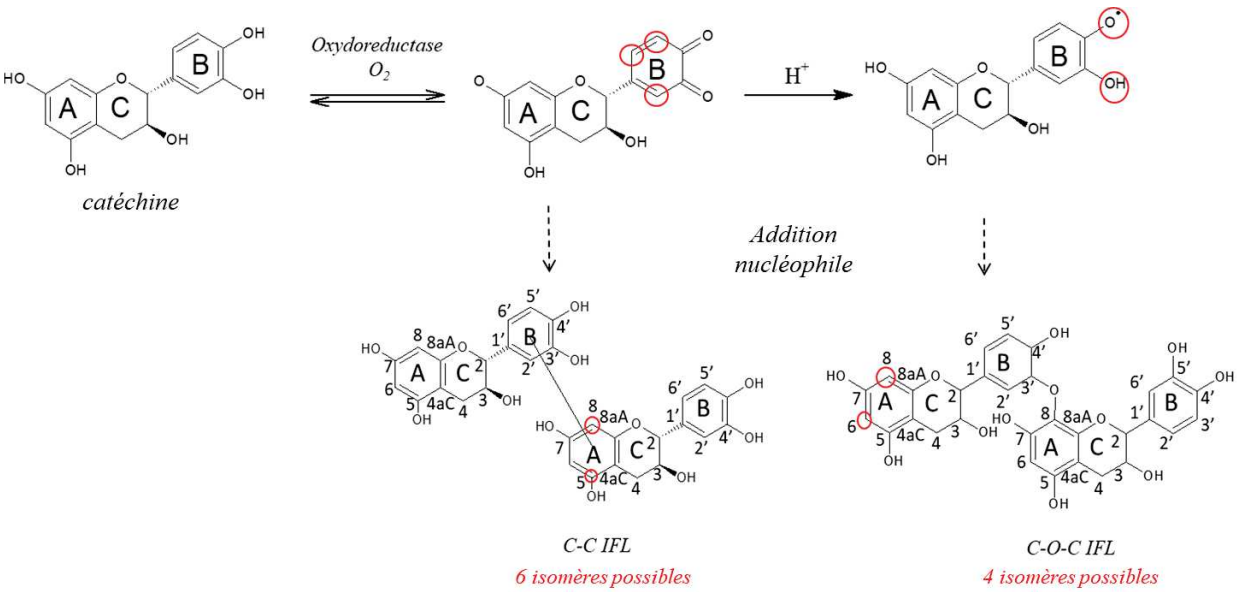

Figure14 : *oxydation enzymatique de la catéchine*

Il est également possible de retrouver, dans des solutions contenant de la PPO, des produits de condensation entre la catéchine (ou EC) et l'acide caftarique(V. Cheynier, Basire, et al., 1989a) ainsi que des dimères d'acide caféique(Veronique. Cheynier & Moutounet, 1992).

Les *o*-quinones issues de l'oxydation enzymatique des acides hydroxycinnamiques (comme les acides caftarique et coutarique) étant très réactives, elles sont en mesure de réagir rapidement

(oxydation couplée) avec d'autres composés présents dans le moût tels que l'acide ascorbique, le SO_2(Rigaud, Cheynier, et al., 1991) ou d'autres *o*-diphénols qui ne sont pas des substrats de la PPO. Ces réactions engendrent la formation d'espèces réductrices(V. Cheynier et al., 1988) qui vont protéger les anthocyanes des altérations liées à l'oxygène. Cependant, le glutathion (GSH) présent peut également s'additionner (addition nucléophile) aux quinones de l'acide caftarique (***figure 13***) et former l'acide (2-S-glutathionyl) caftarique. Ce produit est appelé GRP(V. F. Cheynier et al., 1986; Singleton et al., 1985) (Grape Reaction Product) et cette réaction s'oppose aux réactions de dégradation du moût et aide à maintenir des concentrations importantes en composés phénoliques non altérés dans le vin(Sarni et al., 1995). Ainsi, dans les raisins à forte teneur en acide hydroxycinnamique et faible teneur en GSH, les composés phénoliques sont plus sensibles aux réactions d'oxydation et peuvent réagir notamment avec les quinones de l'acide caftarique par des réactions d'oxydo-réduction ou de condensation(V. Cheynier et al., 1994; V. Cheynier, Hidalgo Arellano, et al., 1997; V. Cheynier, Souquet, et al., 1989; Sarni-Manchado et al., 1997).

Au cours du processus d'élaboration du vin, l'oxydation enzymatique diminue au profit de l'oxydation chimique (manque d'oxygène et/ou inactivation de la PPO).

Oxydation chimique

L'oxydation chimique (ou non enzymatique) est généralement plus lente que l'oxydation enzymatique. Elle est favorisée par la présence de polyphénols contenant un noyau catéchol (groupement *ortho*-dihydroxybenzene) ou un groupement galloyl (groupement 1,2,3-trihydroxybenzene) comme par exemple la (+)-catéchine, la (-)-épicatéchine, la gallocatéchine, l'acide gallique et ses esters associés et l'acide caféique, qui font partie des composés les plus facilement oxydables présents dans le vin (Danilewicz, 2003b; Kilmartin et al., 2001; Li et al., 2008; Singleton, 1987b, 2001). Ces substrats sont d'abord oxydés en radicaux semi-quinones puis benzoquinones sous l'action de l'oxygène réduit en peroxyde d'hydrogène (***figure 15***)(Danilewicz et al., 2008).

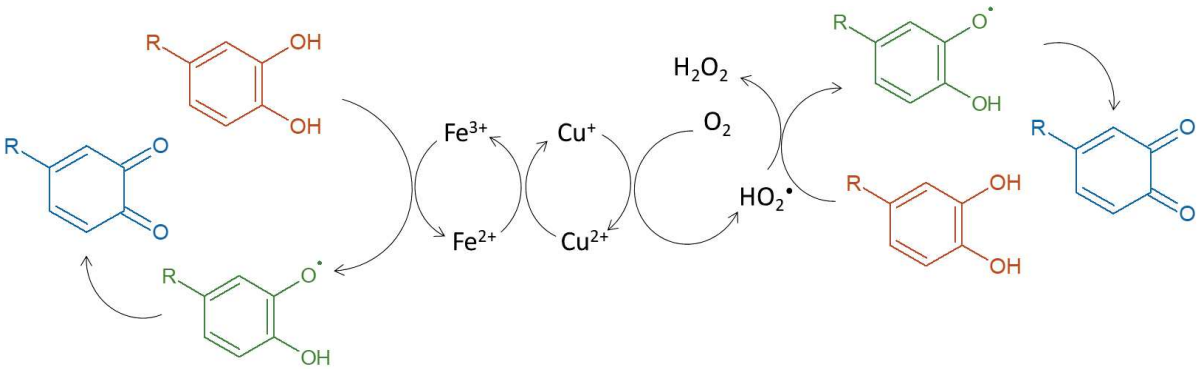

Figure 135 : *mécanisme d'oxydation des groupements catéchols, catalysé par les ions fer et cuivre*

D'autres composés peuvent ensuite s'oxyder à plus haut potentiel comme la malvidine-3-*O*-glucoside, l'acide *para*-coumarique ou le resveratrol(Kilmartin, 2016). Comme évoqué précédemment, les polyphénols ne réagissent pas directement avec l'oxygène mais nécessitent la présence de métaux de transition comme le fer (< 20mg/L) ou le manganèse (<500 mg/L)(Cacho et al., 1995) est nécessaire à leur oxydation chimique.

Par la suite les quinones, composés primaires d'oxydation particulièrement instables, vont subir spontanément d'autres réactions. De par leur caractère électrophiles(Singleton, 1987b), elles sont particulièrement réactives et peuvent former des liaisons covalentes avec les composés nucléophiles du vin(V. F. Cheynier et al., 1986) tels que les flavonoïdes (nucléophiles grâce à leur noyau phloroglucinol), les composés aromatiques possédant une fonction thiol (3SH, 3SHA, 4MSP) ou les peptides contenant une cystéine comme le glutathion. L'oxydation chimique de la catéchine (ou épicatéchine) aboutit aux mêmes composés que l'oxydation enzymatique (***figure 14***) bien que les vitesses de formation soient différentes(Gaulejac et al., 2001; Guyot et al., 1996; Oszmianski et al., 1985). Les réactions entre les quinones et les principaux composés nucléophiles(Oliveira et al., 2016) du vin sont résumés sur la ***figure 16***.

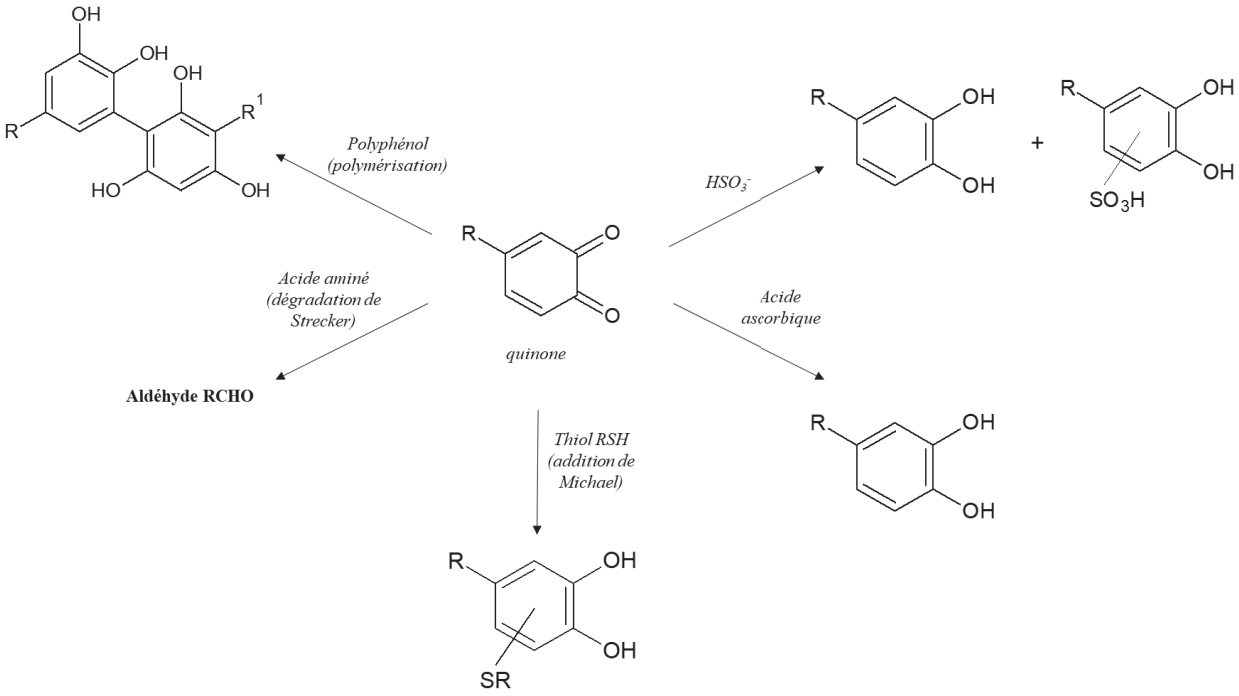

Figure 146 : *principales réactions entre les quinones et les nucléophiles du vin.*

Aussi, les produits issus de l'oxydation chimique des composés non phénoliques du vin (éthanol, acide tartrique) favorisent la formation des produits de polycondensation des tannins(Atanasova et al., 2002a), d'évolution anthocyane/tannin et anthocyanes (*section 3.1.b*) et les réactions de polymérisation des tannins[28].

En conclusion de cette partie, les produits d'évolution et d'oxydation des vins sont nombreux et variés de par la complexité du milieu, la multitude de composés présents et les nombreuses interactions possibles. Tous ces composés nouvellement formés peuvent être qualifiés de marqueurs d'évolution puisqu'ils traduisent de l'état de vieillissement et/ou d'oxydation d'un vin.

Cependant, les vins, et plus particulièrement les vins rouges peuvent prendre des mois voire des années pour s'oxyder naturellement. Récemment, des tests de vieillissements accélérés ont été mis au point afin d'évaluer plus rapidement les capacités d'évolution des vins en fonction de leur composition et la formation de potentiels marqueurs d'oxydations. Le paragraphe suivant présente ces différents tests.

3.2.d. Tests de vieillissements accélérés des vins

Le vieillissement forcé est une simulation des modifications chimiques apportées au vin. Même si ces conditions extrêmes ne sont pas totalement représentatives de la réalité, elles, permettent de reproduire une évolution en laboratoire en un temps raisonnable, en dépit du risque de provoquer/favoriser des réactions indésirables.

Saturations en oxygène

Parmi les tests pour étudier l'évolution oxydative des vins rouges, un des plus utilisés consiste à étudier l'évolution de la consommation d'oxygène après un ou plusieurs cycles successifs de saturations en oxygène, afin d'évaluer le comportement des pigments, des tannins et des composés aromatiques.(V. Ferreira et al., 2015; Gambuti et al., 2018) Des corrélations importantes ont ainsi été établies et confirmées sur vin rouge entre les différents constituants du vin et la vitesse de consommation moyenne de l'oxygène (OCR), les plus importantes étant avec la structure chimique des tannins(V. Ferreira et al., 2015; Vivas & Glories, 1996), la teneur en anthocyanes monomères et totaux (Carrascon et al., 2015; Gambuti et al., 2018) (corrélation négative) et le ratio T/A (corrélation positive), les concentrations en cuivre et fer(Danilewicz, 2007), le pH(Singleton, 1987a) et le SO_2 (Danilewicz et al., 2008; Gambuti et al., s. d.; Singleton, 1987a) . Les mécanismes faisant intervenir le dioxyde de soufre restent cependant complexes et dépendent grandement de la composition du vin étudié. Ferreira *et al.*(V. Ferreira et al., 2015) ont mis en avant la faible consommation de SO_2 suite à une première saturation en oxygène pour certains vins, ce phénomène pouvant notamment s'expliquer par des phénomènes compétitifs avec un autre antioxydant plus réactif que le SO_2 ou avec d'autres composés nucléophiles du milieu qui réagissent davantage avec les quinones générées.

De plus, des résultats contradictoires sur les corrélations avec les taux d'acétaldéhyde (Carrascón et al., 2018; Gambuti et al., 2018) traduisent la complexité du milieu et la difficulté d'analyse des vins rouges, nécessitant parfois la mise en place d'études complémentaires. En effet, la présence d'ARP (acetaldehyde-reactive polyphenols) comme la catéchine qui réagissent très rapidement(Sheridan & Elias, 2015) peut concurrencer la présence d'autres cibles privilégiées de l'acétaldéhyde(Peterson & Waterhouse, 2016), comme le SO_2, rendant parfois difficile la mise en place de corrélations simples avec un groupe de molécules.

Acétaldéhyde

L'ajout de taux variable d'acétaldéhyde peut se révéler être un outil efficace pour accentuer la modification des structures des tannins, notamment grâce à la présence d'ARP(Coppola et al., 2021; Sheridan & Elias, 2015; Teng et al., 2019). Différentes études ont mis en évidence qu'un taux élevé d'acétaldéhyde exogène provoque une augmentation des modifications des structures des tannins, notamment des pigments polymériques mais n'a pas d'influence sur les taux d'acétaldéhyde liés au SO_2. Ces résultats, associés à une diminution des précipitations tannins/protéines suggèrent une utilisation potentielle de cette méthode pour contrôler la couleur et l'astringence des vins rouges.

Peroxyde d'hydrogène

Plus récemment, des oxydations accélérées au peroxyde d'hydrogène(Coppola et al., 2021; Picariello et al., 2017) ont été testées, oxydation forte puisqu'elle accentue la réaction de Fenton (***figure 11***) qui libère le radical hydroxyle $HO^{\bullet}$, particulièrement réactif et capable d'oxyder indifféremment n'importe quel composé organique et entraine notamment la dégradation des anthocyanes(Özkan, 2002; Satake & Yanase, 2018), particulièrement fragiles et responsables de la couleur des vins.

De ce fait, ce test peut facilement et rapidement s'envisager pour prédire l'évolution des polyphénols et de la couleur dans les vins rouges, donnant des résultats similaires à l'oxydation par des saturations successives(Coppola et al., 2021).

Température

Différents tests de vieillissement accélérés ont pu être menés avec des températures pouvant aller de 27 à 60°C(Castro et al., 2014b; Karbowiak et al., 2009; Macías et al., 2001; Oliveira et al., 2015; Tindal et al., 2021; Toit et al., 2006). Ce test accélère globalement toutes les réactions d'évolution des polyphénols, déjà identifiées lors de saturations successives en oxygène. En effet, il a été montré une décroissance de la teneur en anthocyanes (clivage), flavan-3-ols, esters hydroxycinnamiques et acide férulique(Oliveira et al., 2015; Toit et al., 2006). Seules les concentrations en acides hydroxycinnamiques (issus de l'hydrolyse de leurs esters respectifs) et hydroxybenzoiques (issus de la dégradation des anthocyanes) sont susceptibles d'auglenter.

Les composés les plus impactés sont les anthocyanes et les flavan-3-ols (C/EC et tannins condensés) qui se modifient ou se clivent vers des pigments colorés plus stables, réactions caractéristiques des réactions d'évolution naturelle du vin mais largement accélérées par une augmentation de la température(Macías et al., 2001). La température est d'ailleurs un paramètre contrôlé et maitrisé lors de la conservation des bouteilles(Avizcuri et al., 2016; Hopfer et al., 10754; Scrimgeour et al., 2015), il s'agit donc un test prometteur pour l'identification de marqueurs d'oxydations issus du vieillissement des vins(Macías et al., 2001).

3.2.e. Etude de l'évolution oxydative des vins par électrochimie

Voltammétrie cyclique

Récemment, les techniques électrochimiques se sont largement développées grâce à leur sensibilité, leur rapidité, leur facilité d'utilisation notamment avec la mise au point d'électrodes sérigraphiées jetables (Screen Printed electrodes)(Benbouguerra et al., 2020; C. Ferreira et al., 2021) et l'impact réduit de l'environnement chimique sur les mesures(Lorrain et al., 2013). Parmi les méthodes électrochimiques existantes, la voltammétrie cyclique est plus particulièrement utilisée permettant de détecter et caractériser des composés oxydables et réductibles en solution. Un balayage croissant en potentiel est appliqué à l'électrode de travail et, lorsqu'une espèce chimique en solution va être électrolysée (oxydée), cela va se traduire sur le voltammogramme par un pic anodique (transfert de charge et de masse à l'électrode). Lors du balayage dans le sens retour, la réduction de l'espèce chimique qui a été électrolysée va se traduire par un pic cathodique dans le cas d'une réaction réversible. Si plusieurs états d'oxydation avec différents potentiels d'oxydation sont accessibles dans la solution étudiée (un ou plusieurs composés) le voltammogramme montre plusieurs vagues successives.

A partir de la courbe intensité-potentiel obtenue sur le voltammogramme il est possible de caractériser les propriétés réductrices (anti-oxydantes) par :

- Le potentiel du pic qui traduit la facilité du composé à s'oxyder, plus le potentiel est bas, plus le composé sera facilement oxydable ;
- Le courant du pic, proportionnel à la concentration de l'espèce oxydée.

Pour les milieux complexes dès lors que plusieurs espèces sont présentes comme c'est le cas pour le vin, il est préférable d'utiliser la charge (aire sous la courbe anodique sur le voltammogramme) qui est proportionnelle aux nombre d'électrons échangés entre l'électrode

et les espèces présentes plutôt que l'intensité du pic(Chevion et al., 2000; Kilmartin et al., 2002; Makhotkina & Kilmartin, 2010). En effet, il peut se produire en particulier un élargissement du pic dû à l'oxydation des différentes espèces à des potentiels voisins que l'intensité du pic ne prend pas en compte (Kilmartin et al., 2002).

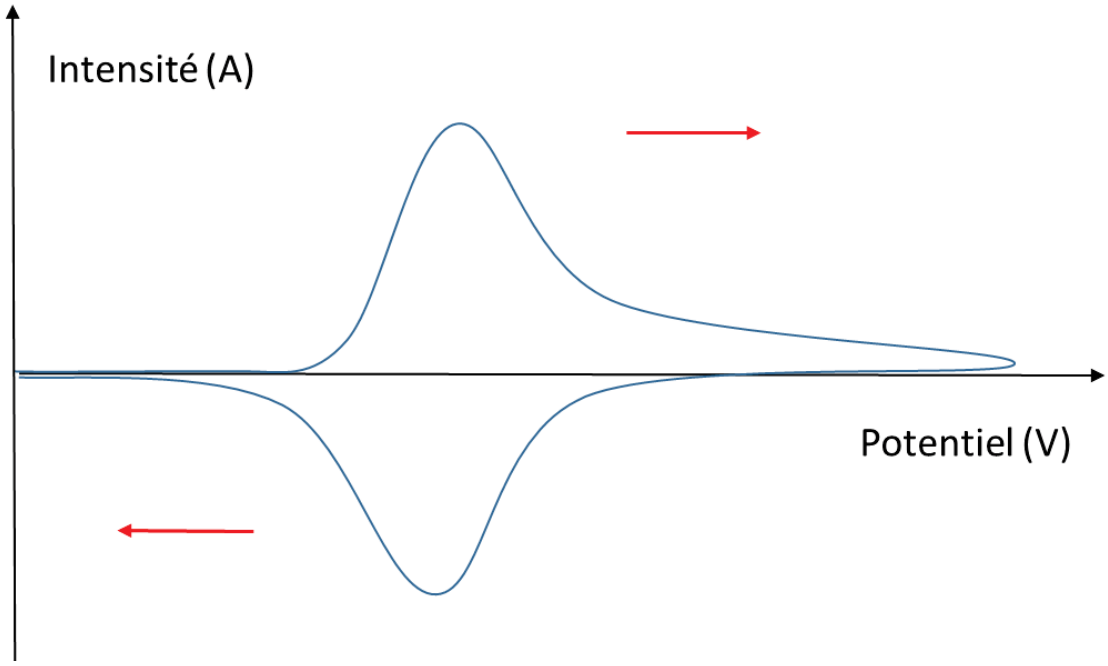

Figure17 : *Exemple de voltammogramme obtenu par voltammétrie cyclique*

Application à l'étude de l'évolution oxydative des vins

La voltammétrie cyclique permet d'obtenir des informations importantes sur le comportement oxydatif des vins en corrélant les paramètres électrochimiques à d'autres paramètres tels que la composition phénolique(C. Ferreira et al., 2021; Kilmartin, 2016; Motta et al., 2020; Ricci et al., 2019; Ugliano, 2016; Ugliano et al., 2015) ou les vitesses de consommation d'oxygène, ces corrélations se sont déjà avérées importantes pour certains vins blancs(Gonzalez et al., 2018). De plus, les voltammogrammes obtenus par soustraction des voltammogrammes de vins oxydés à ceux de leurs références non oxydées donnent la possibilité d'obtenir une image rapide des changements impactant les substrats oxydables du vin. Un ou plusieurs pics cathodiques et/ou anodiques peuvent être visibles sur les voltamogrammes des vins, traduisant la composition de ces derniers en composés oxydables.

A terme, l'application de cette méthode à un grand nombre d'échantillons de vin pourrait constituer un test prédictif de la tendance d'évolution des vins à partir d'une analyse

électrochimique. Une discrimination des vins en fonction de leur composition et de leur comportement électrochimique est alors possible(Geană et al., 2020; Gonzalez et al., 2018).

3.2.f. Etude des marqueurs d'oxydation des vins

Dégradation oxydative des anthocyanes

Les anthocyanes étant des composés réactifs, ils subissent facilement des phénomènes de dégradation(He et al., 2012; Sadilova et al., 2007) et notamment d'oxydation directes(Lopes et al., 2007) suite à l'action du peroxyde d'hydrogène présent en solution. L'ensemble de ces produits d'évolution ou d'oxydation peuvent être des marqueurs de l'état de vieillissement d'un vin.

Durant ces dernières années, plusieurs études ont été menées afin de mettre en évidence ces nouveaux marqueurs d'oxydation. On relève notamment l'utilisation de la fluorescence des produits d'oxydation des anthocyanes comme indice d'oxydation(Bartosz et al., 2020) ou encore l'identification structurale par différentes méthodes analytiques de nouveaux marqueurs de dégradation oxydative de la cyanidine-3-*O*-glucoside et de la malvidine-3-*O*-glucoside (Kamiya et al., 2014; Satake & Yanase, 2018; Zhang et al., 2020), (***figure 18***)

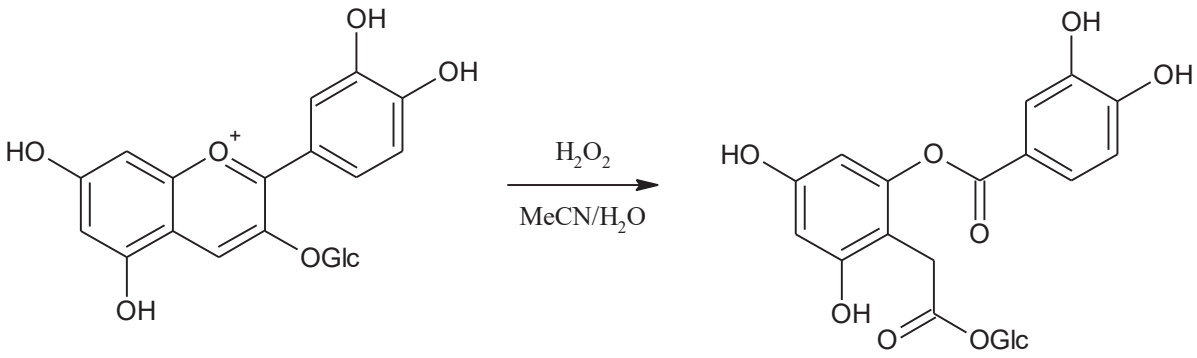

Figure 158: *Exemple de dégradation oxydative d'une anthocyane par action du peroxyde d'hydrogène (Satake & Yanase, 2018)*

Marqueurs d'oxydation issus des unités monomériques de flavanols

Comme évoqué précédemment, les flavanols sont également des cibles privilégiées des phénomènes d'oxydation du vin. De par leur réactivité, leur grande diversité structurale ne va cesser de s'accroitre durant l'élaboration des vins jusqu'à leur consommation. En effet, la présence d'au moins un noyau catéchol au sein de leur structure rend ces molécules vulnérables aux oxydations. Une fois oxydé en quinone ce noyau électrophile(Singleton, 1987a) peut alors induire la formation de liaisons covalentes par addition d'autres composés nucléophiles. Les polyphénols peuvent donc être impliqués dans de nombreuses réactions au cours des procédés de vinification et du vieillissement des vins (***figure 19***).

Les unités monomériques de flavanols (catéchine, épicatéchine, épigallocatéchine) peuvent ainsi subir des réactions d'oxydation(V. Cheynier, Basire, et al., 1989b; Jiang et al., 2011; Jiménez-Atiénzar et al., 2004; Leontieş et al., 2017; Oszmianski et al., 1996; Tanaka & Kouno, 2003) et notamment d'autoxydation (couplage oxydatif) pouvant aboutir aux dimères présentés en ***figure 14*** obtenus par oxydation enzymatique

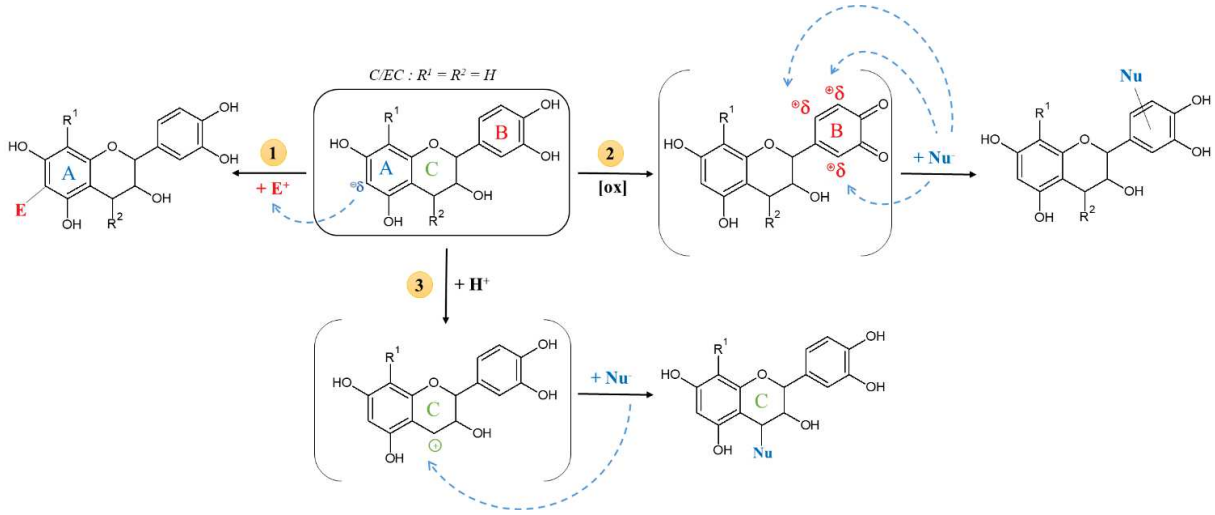

Figure19 : *Réactivité du flavanol (monomère constitutif des tannins – C/EC : R^1=R^2=H) : (1) nucléophile (noyau phloroglucinol, cycle A), (2) oxydable (noyau catéchol, cycle B) →formation de la quinone (électrophile) et (3) électrophile après rupture de la liaison interflavanique (noyau pyrane, cycle C).*

Ces dimères d'oxydation nouvellement formés peuvent ensuite subir des oxydations supplémentaires soit en réagissant avec d'autres composés (formation d'oligomères) soit en créant d'autres liaisons interflavaniques, c'est notamment le cas de la déhydrodicatéchine A et B4(Jiménez-Atiénzar et al., 2004).

Marqueurs d'oxydation issus des chaînes de tannins

Parmi les flavanols plus complexes, l'analyse des tannins condensés ou proanthocyanidines présente un intérêt majeur pour acquérir une meilleure compréhension des relations existant entre ces structures et les propriétés qu'elles confèrent aux vins mais reste encore un défi.

En effet ces flavanols peuvent présenter une forte hétérogénéité(He et al., 2008) en termes de composition et de degrés de polymérisation (DP) qui va s'accroître tout au long des étapes de vinification et de conservation des vins. Ils peuvent subir différentes modifications(Berrueta et al., 2020; Mouls et al., 2011b) par création de liaisons entres les chaînes tanniques ou au sein d'une même chaîne (***figure 20***), ou encore réagir avec d'autres composés du vin comme les arômes(Suc et al., 2021; Vivas, 1997, 2000). Ainsi, le nombre de composés tanniques différents ne cesse d'augmenter mais leur identification présente un véritable enjeu. En effet, il est impossible de caractériser de façon précise la fraction tannique des échantillons et il est donc impossible de comprendre réellement l'impact des modifications structurales des tannins sur les propriétés du vin. La difficulté de caractériser ces molécules est due :

- à leur très grande diversité moléculaire déjà existante dans le raisin et qui va s'accroitre durant la transformation et la conservation du produit. Cette variété structurale provient de (i) leur composition en monomères constitutifs : épicatéchine (C), catéchine (EC), épigallocatéchine (EGC) et épicatéchine gallate (ECG) (ii) du nombre de monomères par molécule (de deux à plus d'une centaine d'unités monomériques) (iii) de la position et le nombre des liaisons qui relient les unités monomères entre elles (structures linéaires et/ou branchées) (iv) leur réactivité : les tannins subissent de nombreuses modifications chimiques durant la vinification et le vieillissement du vin
- à leurs propriétés physico-chimiques (Duval & Avérous, 2016)

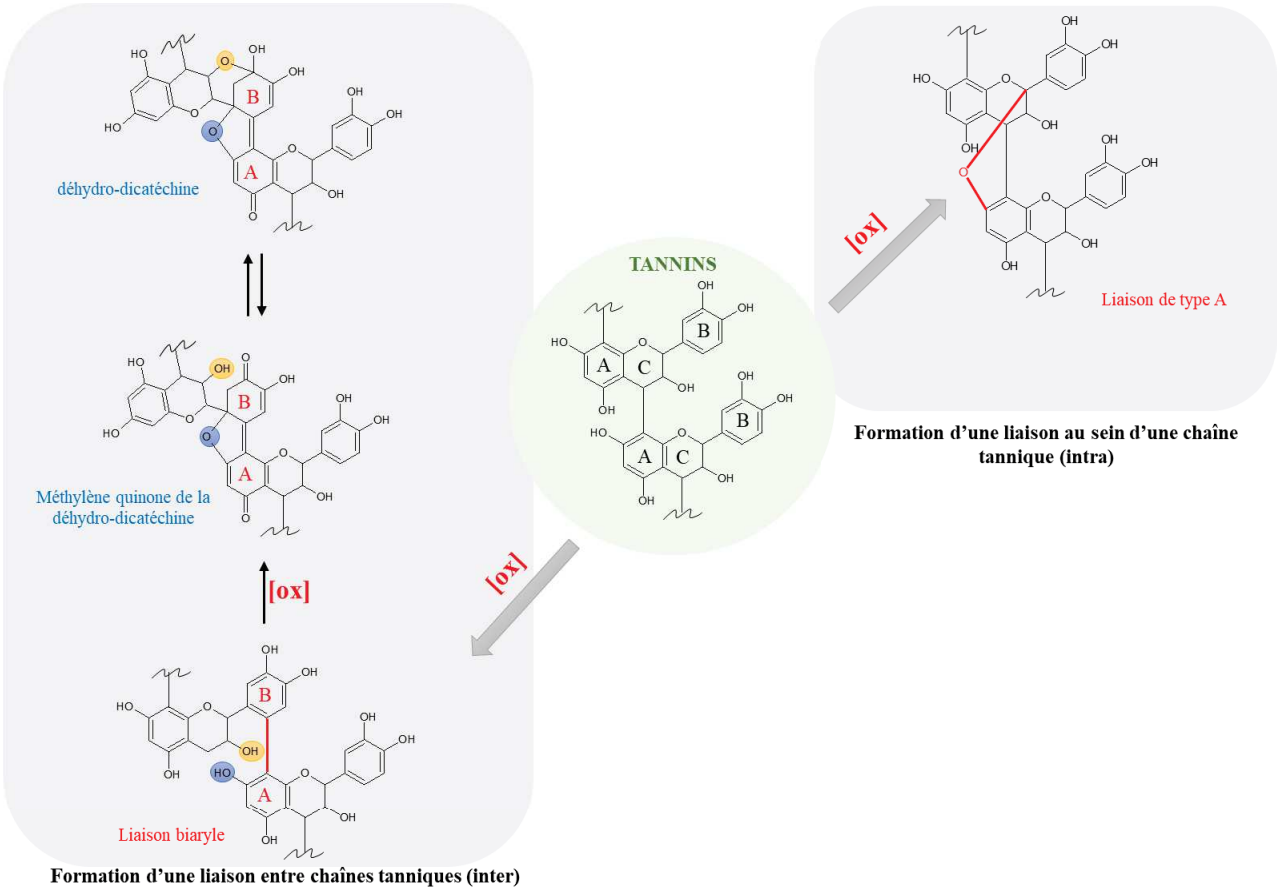

Figure 20 : *exemples de réactions potentielles d'oxydation au sein des structures des tannins dans le vin.*

L'ensemble de ces caractéristiques rendent les tannins difficilement analysables par les techniques actuelles(Mouls et al., 2011b). En effet, les tannins de plus hauts poids moléculaires ne s'ionisent pas par ESI-MS et ne sont également pas séparables par chromatographie liquide. En effet, sur le chromatogramme HPLC en phase inverse à 280 nm obtenu après analyse d'un échantillon de vin rouge, les tannins apparaissent co-élués dans un large pic étendu et plus ou moins abondant en fonction de la concentration tannique, sous les pics des composés de plus faibles poids moléculaires.

Une méthode d'analyse alternative, couramment utilisée, consiste à réaliser une dépolymérisation chimique(Mouls & Fulcrand, 2012, 2015a) en présence d'un réactif nucléophile (phloroglucinol, benzylthiol, acide thioglycolique ou mercaptoéthanol). Les liaisons covalentes formées suite à l'oxydation des tannins vont résister à la réaction de dépolymérisation tandis que les liaisons natives entre les unités constitutives des tannins vont se rompre. Les différentes unités constitutives libérées par dépolymérisation, beaucoup plus petites, vont ensuite pouvoir être analysés par chromatographie liquide. Au final, on retrouve ainsi les unités non-modifiées (terminales et d'extension) et les marqueurs d'oxydation qui

peuvent être classés en trois groupes : marqueurs terminaux, marqueurs d'extension et marqueurs terminaux/extension (***figure 21***)(Mouls & Fulcrand, 2012).

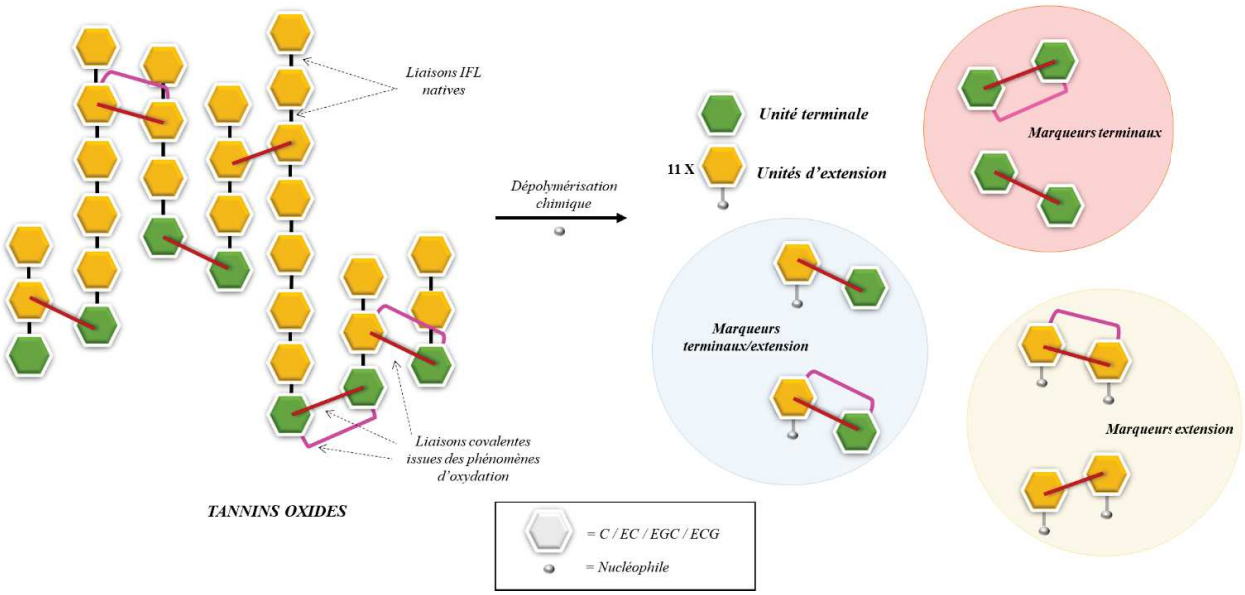

Figure 21 : *exemple réaction de dépolymérisation des tannins condensés et des marqueurs d'oxydation associés.*

4. Problématiques et enjeux globaux de la thèse

Cette étude bibliographique a permis d'effectuer un état des lieux des connaissances sur les polyphénols du vin, et plus précisément, sur les différents phénomènes d'évolution et d'oxydation les caractérisant lors du vieillissement des vins, de nombreuses réactions intervenant simultanément entre les nombreux composés du vin. Nous avons également pu nous apercevoir que l'étude de ces phénomènes et des composés issus de ces réactions est un véritable enjeu pour mieux comprendre l'évolution du vin. Cependant, cela reste difficile dans le vin de par l'environnement chimique complexe, la diversité structurale des composés, leurs propriétés physico-chimiques et le temps nécessaire pour un vin à s'oxyder naturellement, particulièrement pour les vins rouges.

En effet, de nombreuses interrogations, énumérées ci-après, gravitent autour de ces processus d'oxydation des vins rouges. Les objectifs de ce mémoire de thèse visent à répondre aux questions suivantes :

1) Est-il possible de mettre au point des tests rapides et reproductibles de veillissement d'un vin rouge ?

2) Peut-on prédire l'évolution des vins rouges par voltammétrie cyclique ? Y-a-t-il un effet cépage ?

3) Est-il possible d'isoler et de caractériser complètement certains marqueurs d'oxydation des flavan-3-ols ?
   Peut-on retrouver ces marqueurs dans des extraits de pépins (différents stades de maturation) et de vins rouges (différents millésimes) ?

4) Comment évoluent les marqueurs d'oxydation des tannins dans les vins ? Y-a-t-il un effet millésime ? Ces marqueurs se retrouvent-ils dans des vins ayant subi un vieillissement accéléré ?

Chapitre II – Approche polyphénomique globale semi-ciblée

Les objectifs de ce chapitre étaient :

- La mise au point trois tests de vieillissements accélérés répétables de vins rouges :
    - un test chimique utilisant le peroxyde d'hydrogène
    - un test enzymatique utilisant des laccases de *Trametes versicolo*r
    - un test d'oxydation par chauffage à 60°C.
- D'identifier de potentiels marqueurs moléculaires d'oxydation impliqués dans ces tests par LC-MS
- L'application de ces nouveaux tests à des échantillons de vins issus du même cépage (Syrah) et du même producteur mais avec des millésimes différents (2018, 2014 et 2010)

Les méthodes utilisées dans ces travaux ont été :

1. Les méthodes de référence décrites par l'OIV (organisation internationale de la vigne et du vin) pour les analyses globales chimiques des vins
2. Des mesures non-invasives de taux d'oxygène dissous par luminescence et fibre optique
3. Des mesures spectrométriques afin d'acquérir des mesures d'absorbances de 400 à 800nm
4. Des analyses par UHPLC-Q-Tof-MS afin d'acquérir et comparer les empreintes de masse d'échantillons de vins ayant subi un test accéléré (Syrah 2018) aux échantillons correspondant à un vieillissement naturel (Syrah 2018, 2014, 2010)

Les hypothèses étaient les suivantes :

1. Des tests de vieillissements accélérés et reproductibles peuvent être mis au point en entrainant une modification de leur contenu en polyphénols et des cinétiques de consommation d'oxygène différentes selon les vins.
2. Les différents tests de vieillissements accélérés peuvent entraîner une modification semi-ciblée de certains polyphénols du vin.

Conclusions obtenues

1. Trois tests de vieillissements accélérés reproductibles et rapide de vins rouges ont été mis au point. Ils ont permis d'accélérer significativement la consommation d'oxygène dans les échantillons de vins rouges. En effet, un taux d'oxygène inférieur à 1ppm a été atteint en quelques heures pour un vieillissement accéléré et en plusieurs jours pour une consommation naturelle.

2. Les résultats des différents tests se sont révélées significativement différentes pour tous les échantillons, amenant à emmètre l'hypothèse que les trois tests n'oxydent pas les mêmes composants du vin.
3. L'oxydation accélérée de trois millésimes de vins de Syrah a révélé que les cinétiques d'oxydation ne sont pas seulement corrélées à leur millésime mais également à leur cépage et leur composition chimique.
4. L'analyse LC-QTOF-MS a mis en évidence une évolution différente des empreintes différentes en spectrométrie de masse avant et après les tests mais aussi entre les diffèrent tests. D'après les intensités des ions moléculaires observées pour les oxydations naturelles et accélérées, les anthocyanes et les polyphénols avec un groupement galloyl ou catéchol sont les marqueurs moléculaires les plus affectés. Les spectres de masse des échantillons correspondant à l'oxydation naturelle ont montré une diminution des intensités des ions moléculaires caractérisant les anthocyanes libres et une augmentation de celles des flavanols monomériques. Ces résultats ont également été observés pour le vieillissement accéléré au peroxyde d'hydrogène. Ce type d'oxydation accélérée semble être le plus proche du vieillissement naturel, observation également faite sur spectres d'absorption visible.

Cette étude a fait l'objet d'un article scientifique, publié dans le journal *Antioxidants*, sous la référence :

Deshaies, S.; Cazals, G.; Enjalbal, C.; Constantin, T.; Garcia, F.; Mouls, L.; Saucier, C. ***Red Wine Oxidation: Accelerated Ageing Tests, Possible Reaction Mechanisms and Application to Syrah Red Wines***. *Antioxidants* 2020, *9*, 663.

Et ci-après présenté.

antioxidants

MDPI

Article

Red Wine Oxidation: Accelerated Ageing Tests, Possible Reaction Mechanisms and Application to Syrah Red Wines

Stacy Deshaies [1], Guillaume Cazals [2], Christine Enjalbal [2], Thibaut Constantin [3], François Garcia [1], Laetitia Mouls [1] and Cédric Saucier [1,*]

1 SPO, Université de Montpellier, INRAE, Institut Agro, 34000 Montpellier, France; stacy.deshaies@umontpellier.fr (S.D.); francois.garcia@umontpellier.fr (F.G.); laetitia.mouls@supagro.fr (L.M.)
2 IBMM, Université de Montpellier, 34093 Montpellier, France; guillaume.cazals@umontpellier.fr (G.C.); christine.enjalbal@umontpellier.fr (C.E.)
3 Laboratoire d'Œnologie, UFR Pharmacie, Université de Montpellier, 34000 Montpellier, France; thibaut.constantin@umontpellier.fr
* Correspondence: cedric.saucier@umontpellier.fr

Received: 23 June 2020; Accepted: 21 July 2020; Published: 24 July 2020

Abstract: Wine oxidation and ageing involve many complex chemical pathways and reaction mechanisms. The purpose of this study is to set up new and reproducible accelerated red wine ageing tests and identify chemical oxidation or ageing molecular markers. Three accelerated and reproducible ageing tests were developed: a heat test (60 °C); an enzymatic test (laccase test; a chemical test (hydrogen peroxide test). Depending on the test, oxygen consumption was significantly different. For a young wine (2018), the oxygen consumption rate moved from 2.40 ppm·h^{-1} for the heat test to 3.33 ppm·h^{-1} for the enzymatic test and 2.86 ppm·h^{-1} for the chemical test. Once applied to two other vintages (2010 and 2014) from the same winery, the tests revealed different comportments corresponding to wine natural evolution. High resolution UPLC-MS was performed on forced ageing samples and compared to naturally aged red wines. Specific oxidation or ageing ion markers were found with significant differences between tests, revealing the specificity of each test and different possible molecular pathways involved. The hydrogen peroxide test seems to be closer to natural oxidation with an important decrease in absorbance at 520 nm and similar molecular ion variations for $[M+H]^+$ = 291, 331, 347, 493, 535, 581, 639 Da.

Keywords: wine; oxidation; polyphenol; Syrah; mass spectrometry; oxygen; vintage; markers

1. Introduction

Oxygen has an important role in chemical reactions in red wines from the winemaking process to bottle ageing. Oxidation reactions have an impact on the chemical and sensory characteristics, such as wine color [1–3] or organoleptic properties [4,5].

An optimal red wine quality is correlated with a moderate oxygen exposure during the whole wine lifetime [3]. One example is its consumption by yeasts to produce sterols during alcoholic fermentation. This allows them to have better alcohol resistance and nitrogen nutrient absorption. From an organoleptic point of view, an optimal oxygen exposure may reduce some wine negative aspects, such as bitterness or astringency [3,6]. Unwanted aroma or color instability may also occur in the case of too high or too low oxygen exposures [7]. For red wines, a too high oxygen exposure will reduce antioxidant concentrations (sulfur dioxide or ascorbic acid) and desirable volatile compounds, affecting wine quality [8].

Managing oxygen exposure then is a real challenge for winemakers. Each step of the winemaking process involves a specific oxygen level exposure, provided in continuous diffusion manner or at a given moment. This oxygen transfer occurs during different winemaking steps, such as barrel aging (exchange through or with the barrel wood), micro-oxygenation or even bottle storage, which is particularly important for the improvement of red wine quality [9]. As the wine composition is closely related to its ability to react with oxygen, it is often difficult to predict the outcomes for a specific wine and a given oxygen amount, without mentioning accidental and uncontrolled oxygen exposure. Even if some tools were developed to precisely control the dissolved oxygen levels in wines, there is a lack of techniques to predict the wine evolution depending on its oxygen exposure and its aging capacity in bottles.

From a chemical point of view, polyphenols are among the most readily oxidized wine constituents [8,10]. Chemical oxidation reactions occur in red wines, and involve polyphenols, such as anthocyanins, proanthocyanidins and flavan-3-ols [11,12]. Enzymatic oxidation can also occur in botrytized wines containing laccases, which are polyphenol oxidase enzymes [13]. Polyphenols containing a galloyl or catechol group will be oxidized in *ortho*-quinones, which are very reactive and electrophilic oxidation intermediates [14]. Many reactions with wine nucleophile compounds will also occur, like those involving sulfur dioxide, ascorbic acid, amino acids, thiols or the A-ring of other flavonoid compounds [15–17]. Red wine is a very complex medium and many different chemical reactions may occur in a wine-dependent manner. Antioxidant species, such as sulfites, can also form adducts with condensed tannins on C4 position, preventing them from further undesirable reactions, such as nucleophilic addition [18]. Polyphenols can also act as hydroxyl radical scavengers. These radicals are formed through the Fenton reaction [19]. Some of these reactions involving the polyphenols catechol groups are summarized in Scheme 1.

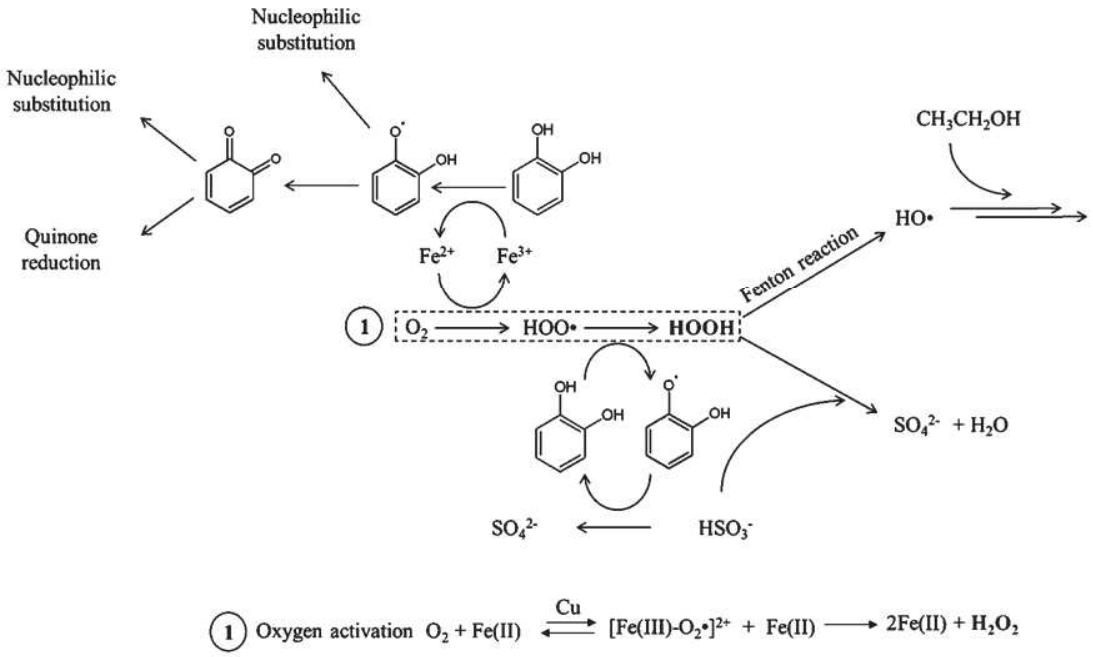

Scheme 1. Partial iron-catalyzed wine oxidation scheme.

Wine evolution (color, chemical composition, impact on polyphenolic composition), regarding different levels of oxygen, has already widely been described, notably by Petrozziello et al. [20]. Ferreira et al. [21] evaluated oxygen consumption for different wines. For both studies, it took several days or months to characterize and follow wine evolution. Accelerated ageing tests are very few and are mainly focused on heat test at 60 °C [22].

There is a need to develop new artificial wine ageing protocols to accelerate these oxidation processes in a shorter period at the laboratory compared to natural oxidations.

The objectives of this article are:

- To set up new and reproducible accelerated ageing tests for red wines.
- Identify oxidation markers involved in these tests by LC-MS.
- Apply the new tests to red wine samples from different vintages.

2. Materials and Methods

2.1. Materials

Hydrogen peroxide solution 30% (ACS reagent) and Laccase from Trametes versicolor (0.94 U/mg) were obtained from Sigma-Aldrich (Saint-Louis, MO, USA).

2.2. Model Wine Solution

The model wine solution was an ethanol water solution (12/88; *v/v*) with 0.033 M tartaric acid, adjusted to pH 3.6 with NaOH 1 M [23].

2.3. Wine Samples

Three red wines samples, 100% Syrah, 13.5% alcoholic strength, were obtained from the same producer (Domaine des Bouzons, Côtes du Rhône, France) and from three different vintages (2018, 2014, 2010). Wine production: 20 days vatting time in stainless steel vats; maturing of Syrah (40%) in oak barrels for 10 months. Two 750 mL bottles of each vintage were opened and slowly homogenized under nitrogen to avoid oxidation reactions. Aliquots of 50 mL tubes were then immediately frozen at −80 °C.

2.4. Wine Global Chemical Characterization

Global chemical analyses of the wine were performed by the Natoli laboratory (St Clément de Rivière, France) according to OIV procedures (www.oiv.int). Analyses included: alcoholic percentage (Fourier transformed infrared spectroscopy—FTIR); glucose and fructose (FTIR–Foss wine scan auto); total acidity (FTIR–Foss wine scan auto); volatile acidity; free, active and total sulfur dioxide (automated colorimetric method); pH; malic and lactic acid (FTIR–Foss wine scan auto); total polyphenols index (FTIR–Foss wine scan auto); CO_2 (FTIR–Foss wine scan auto); Fe (Colorimetric method, reaction with disodium salt of (pyrildil-2)-3bis(phenyl-4-sulfonic 5–6 triazin-1,2,3,4) acid); absorbance read at 570 nm on a sequential analyzer (Olympus AU2700); Cu (colorimetric method 4-(3,5-Dibromo-2-Pyridilazo)-N-Ethyl-N-(3-Sulfopropyl)Aniline reaction; absorbance read at 570 nm on a sequential analyzer (Olympus AU2700). (supplementary data: Tables S1–S3).

2.5. Accelerated Ageing Tests

(a) Oxygen saturation: A previously −80 °C frozen wine sample (50 mL) was thawed and 35 mL was placed in a 500 mL closed flask. This wine sample was then saturated with air by vigorously shaking the flask for 10 s, after which the cap was opened (5 s) to let fresh air get into the flask. This saturation operation was repeated three times. Hermetic Pyrex 11 mL cultures tubes (VWR 734-4224, Radnor, PA, USA) containing Pst3 oxygen sensors (Presens—Precision Sensing GmbH, Regensburg, Germany) were filled with wine (11 mL) with a minimum headspace. It was previously shown that this procedure allows a headspace volume between 0 µL and 120 µL [21]. Further studies confirmed that less than 0.5 mg/L oxygen could pass through this closure, which is negligible for our accelerated test conditions. (b) Accelerated ageing heat test: Tubes containing oxygen saturated wine were heated (60 °C) and stirred (200 rpm) with a thermostatically-controlled stirrer (Hettich Benelux, Bäch, Switzerland). The dissolved oxygen level was monitored with an oxygen analyzer (Presens—Precision Sensing

GmbH, Regensburg, Germany). The acquisition began when the temperature reached 60 °C in the tube. (c) Enzymatic and chemical oxidation: A tube containing wine saturated with oxygen was thermostatically-controlled (22 °C) and stirred (200 rpm). A 10 g/L laccase solution (50 µL) or a 30% vol. H_2O_2 solution (20 µL) was then added to the tube. The acquisition began 30 s after this addition. The oxidation test was stopped once O_2 levels had values lower than 1 mg/L. All tests were performed in triplicate.

2.6. UV–Visible Measurements

The UV–vis spectra were determined with an Agilent Carry 60 spectrometer (Agilent technologies, Santa Clara, CA, USA) equipped with 1 mm cells. Model wine was used for the blank (see model wine section). Spectra were determined in a 400–800 nm UV range.

2.7. UPLC-ESI-Tof Parameters

Analyses were performed using the same UPLC system and method, as described in Gil et al. [24] with slight modifications. The binary mobile phase consisted of Milli-Q water (solvent A) and acetonitrile (solvent B) both acidified with 0.1% formic acid. The separation was performed at a constant flow rate of 0.6 mL/min, using the following short gradient: 1% B for 1 min; 1–100% B in 0.5 min; 100% B for 2 min; 100–1% B in 1.5 min; equilibration at 1% B for 2 min. The injection volume was 10 µL. The mass spectrometer was operated in the positive ESI mode and data were collected for m/z from 100 to 2000 under the following conditions: capillary voltage, 2 kV; cone gas flow, 0 L/h; nitrogen desolvation gas flow, 1000 L/h; desolvation temperature, 350 °C; cone voltage, 60 V. All UPLC-ESI-Tof analyses were performed in triplicate.

2.8. Statistical Analysis

Statistical analyses were done by using XLSTAT 2020.1.1 software. For each oxidation protocol, sample color and intensity measurements were submitted to univariate analysis of variance (ANOVA) followed by a Tukey multiple comparison test (significance for $p < 0.05$).

3. Results and Discussion

3.1. Set Up and Application of Three Different Forced Oxidation Protocols for Syrah Wine Samples (2018, 2014, 2010)

The dissolved oxygen concentration kinetics were monitored in a 2018 Syrah wine sample with three different accelerated oxidation protocols: heat test at 60 °C, laccase oxidation at 22 °C and hydrogen peroxide oxidation at 22 °C. Initial levels of dissolved oxygen were between 5.8 and 7 ppm for each experiment, as shown in Figure 1 and decreased rapidly under 1 ppm in less than 3 h until a final plateau was reached. The concentrations of dissolved oxygen at the plateau were: 0.1 ± *0.02* ppm for 60 °C experiment; 0.2 ± *0.04* ppm for hydrogen peroxide experiment; 0.2 ± *0.02* ppm for laccase experiment. No significant evolution was observed for the control sample over the experiment time; however, after 24 h the oxygen level in the control sample was measured at 4.36 ppm (average, $n = 4$). A complete oxygen consumption ($[O_2] < 1$ ppm) was reached after five days. Even if the total oxygen consumption in a given wine sample is closely related to the wine composition [21], this consumption is significantly faster with an ageing test from five days to a few hours in the present experiment.

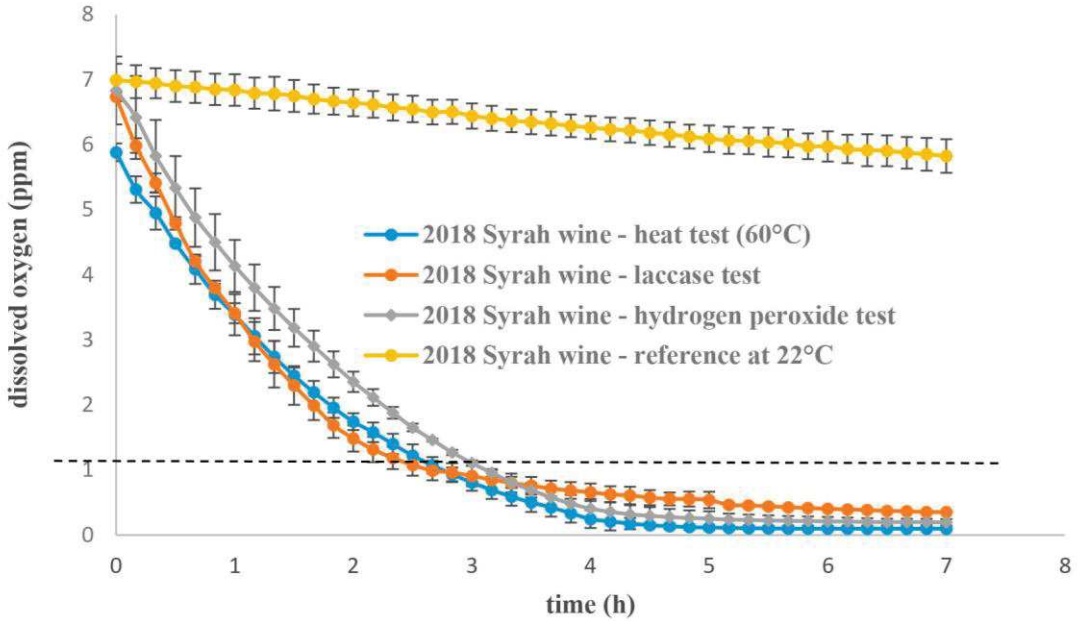

Figure 1. Rate of dissolved oxygen consumption in three different ageing tests used on a 2018 red wine sample (average, $n = 3$ or 4, and standard deviation for each point). Data are available in supplementary data: Tables S4–S7.

The curve profiles and the different threshold values indicated different behaviors depending on the oxidation test, indicating that different oxidation pathways may have occurred for each protocol.

Oxygen consumption rates were also investigated and revealed significant differences between oxidation tests. Oxygen is consumed approximately 1.4-times faster with the laccase test than the heat test at 60 °C and 1.2-times faster than with the hydrogen peroxide test, as shown in Table 1. The three different accelerated oxidation tests may target different wine constituents.

Table 1. Dissolved oxygen consumption rates in three different accelerated ageing tests. Rates are expressed as mean values ± standard error. Different letters indicate a significant difference (Tukey test, $\alpha = 0.05$) between oxidation protocols.

Oxidation Protocol	Oxygen Consumption Rate (ppm·h^{-1})
Heat test −60 °C	2.40 ± 0.06 ^{a}
Laccase test	3.33 ± 0.05 ^{b}
Hydrogen peroxide test	2.86 ± 0.28 ^{c}

Temperature test: It has been established that wine oxidation is accelerated when the temperature increases [25]. This is the case for quinone formation which will lead to important changes in the wine evolution, as shown in Scheme 1. Another main oxidation reaction catalyzed by metals and accelerated with temperature is the anthocyanin degradation [26]. Anthocyanin are red grape pigments which accumulate in the skin during maturation [27,28]. As thermolabile compounds [29], they are the primary targets of chemical changes caused by an increase in temperature. The deglycosylation and cleavage of anthocyanins will lead to the release of the A and B rings of anthocyanins [30]. New compounds resulting from the degradation of anthocyanin are obtained, as benzoic acids. For example, malvidin 3-*O*-glucoside Baeyer–Villiger oxidation produces 2,4,6-trihydroxybenzaldehyde [31], syringic acid or anthocyanone A [32].

The three oxidation protocols were then applied to three different wines from the same winery but from three different vintages—2018, 2014 and 2010—to identify different comportments between vintages regarding oxygen consumption, as shown in Figure 2.

Antioxidants **2020**, *9*, 663

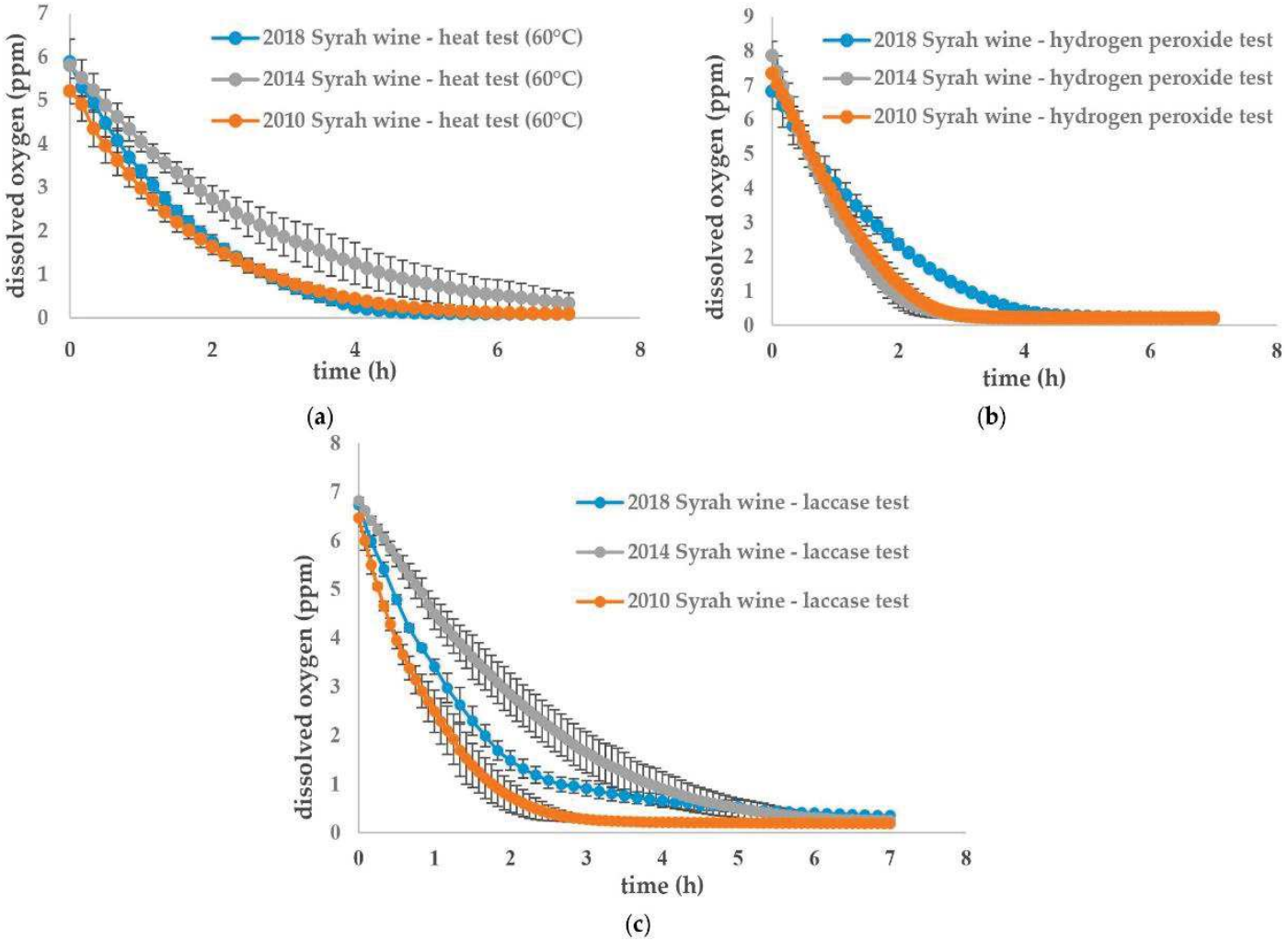

Figure 2. Evolution of dissolved oxygen concentration for three different wines (2018, 2014, 2010) oxidized with (**a**) heat test (60 °C); (**b**) hydrogen peroxide test; (**c**) laccase test. Data are available in supplementary data: Tables S4–S13.

For the 60 °C test, oxygen consumption rates, shown in Table 2a, indicate no significant difference between the three vintages. For the two other treatments, as shown in Table 2b,c, oxygen consumption was significantly different in the three different vintages. For the 2018 and 2010 vintages, the oxygen consumption rate was accelerated in the older wine. It can be hypothesized that oxidizable compound concentration decreases with years due to wine intrinsic oxidation mechanisms and that total oxidation is then faster. The 2014 wine follows this trend with the hydrogen peroxide test but not with the laccase test. The wine oxidation kinetic is not only correlated with age as some differences in vintages and wine composition may have an influence, as shown by Carascon et al. [33].

Table 2. Dissolved oxygen consumption rates for three different oxidized wines: (**a**) at 60 °C; (**b**) with a hydrogen peroxide solution; (**c**) with a laccase solution. Means with different lowercase letters are significantly different (Tukey test, $\alpha = 0.05$).

Wine Sample	Oxygen Consumption Rate ($ppm \cdot h^{-1}$)
(a)	
2018 Syrah wine—heat test (60 °C)	2.40 ± 0.06 [a]
2014 Syrah wine—heat test (60 °C)	1.77 ± 0.45 [a]
2010 Syrah wine—heat test (60 °C)	2.28 ± 0.28 [a]
(b)	
2018 Syrah wine—hydrogen peroxide test	2.86 ± 0.28 [a]
2014 Syrah wine—hydrogen peroxide test	4.41 ± 0.33 [b]
2010 Syrah wine—hydrogen peroxide test	3.65 ± 0.08 [c]
(c)	
2018 Syrah wine—laccase test	3.33 ± 0.06 [a]
2014 Syrah wine—laccase test	2.45 ± 0.34 [b]
2010 Syrah wine—laccase test	4.54 ± 0.66 [c]

3.2. Colorimetric Analysis and Comparison of Three Untreated Wines from Different Vintages (2018, 2014 and 2010) and Three from 2018 Vintage Artificially Oxidized

As red wine oxidation induces color changes, UV measurements were done to compare natural and forced oxidation. Anthocyanins being the main compounds responsible for red color [27,28], their degradation due to oxidation could explain the differences in absorbance measurements, as shown in Table 3. At 520 nm, as shown in Figure 3, corresponding to the flavylium ring of anthocyanin, the 2018 Syrah wine sample had a profile significantly different from the other aged samples (2014 and 2010), which is coherent with a normal wine aging browning process. The 2018 wine at 60 °C followed the 2018 natural wine profile, as did the laccase one, with a maximal absorbance at 520 nm. It is possible that brown oxidized polyphenols were formed and could also increase the absorbance at 520 nm in this case, even if their maximal absorbance is around 420 nm [34]. The sample in the hydrogen peroxide test followed the natural oxidation profile of 2014 and 2010 natural samples, with a maximal absorbance around 420 nm corresponding to yellow and brown pigments. Forced oxidation with hydrogen peroxide seems to be closer to natural oxidation for absorbance measurements.

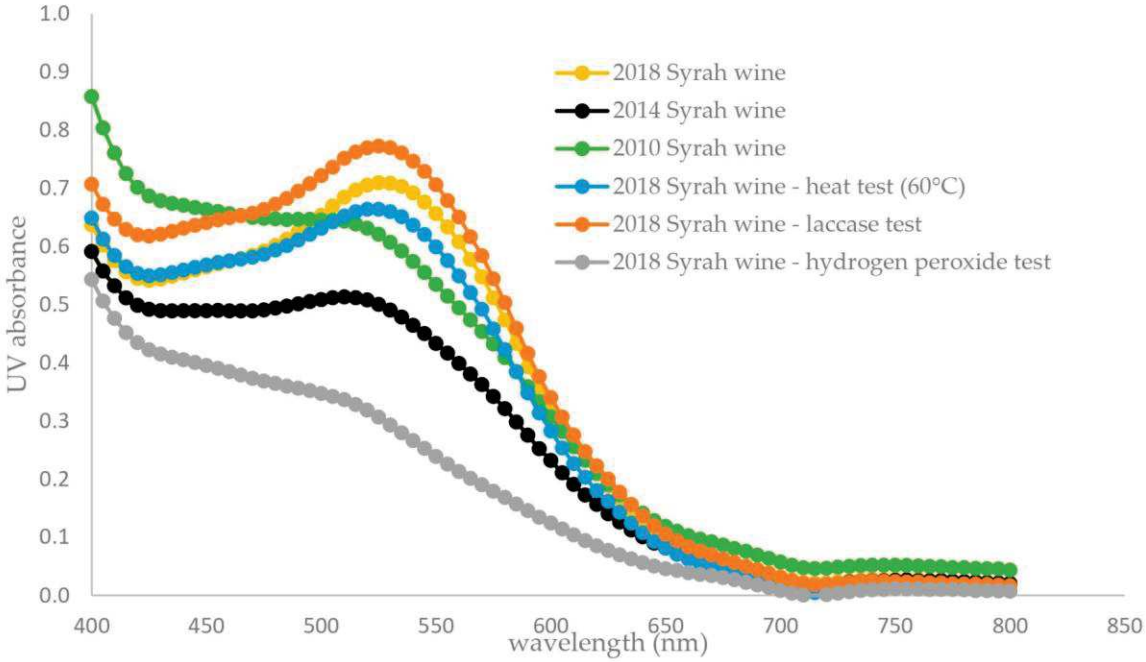

Figure 3. Absorbance measurements (400–800 nm) for six different wine samples: three untreated wines from different vintages (2018, 2014 and 2010) and three from 2018 vintage artificially oxidized. Data are available in supplementary data: Tables S14–S19.

Table 3. Mean of three replicates ± standard error. Means in the same column with different lowercase letters are significantly different (Tukey test, $\alpha = 0.05$).

Wine Sample	Abs 420	Abs 520	420/520
2018	0.545 ± 0.002 ^{a}	0.705 ± 0.003 ^{a}	0.773 ± 0.001 ^{a}
2014	0.499 ± 0.003 ^{b}	0.508 ± 0.004 ^{b}	0.982 ± 0.001 ^{b}
2010	0.702 ± 0.006 ^{c}	0.631 ± 0.006 ^{c}	1.111 ± 0.001 ^{c}
2018—heat test (60 °C)	0.554 ± 0.002 ^{a}	0.664 ± 0.003 ^{d}	0.834 ± 0.002 ^{a}
2018—hydrogen peroxide test	0.435 ± 0.006 ^{e}	0.318 ± 0.007 ^{f}	1.365 ± 0.013 ^{d}
2018—laccase test	0.620 ± 0.02 ^{d}	0.770 ± 0.025 ^{e}	0.806 ± 0.002 ^{a,b}

Other reactions resulting from the temperature increase can occur, such as the production of dioxane, dioxalane isomeres, furfural and 5-hydroxymethylfurfural, derived from carbohydrate dehydration and by cyclisation in Maillard type reactions. These reactions were investigated by Castro in Porto wines [22] under extreme oxidation procedures at 60 °C.

Hydrogen peroxide test: Hydrogen peroxide is notably involved in the Fenton reaction in wine, releasing a hydroxyl radical which is a strong oxidant, as shown in Scheme 1. It will then oxidize ethanol in acetaldehyde or accelerate quinone formation from polyphenols. This last reaction is more important in red wine than in other wine types.

This type of oxidation may be increased by a fast and high oxygen intake, favoring the formation of an intermediate ethoxyl radical, as shown in Scheme 2, instead of an immediate acetaldehyde formation from ethanol [19]. This radical leads to the formation of both acetaldehyde and $HOO^{\bullet}$ oxidizing polyphenols, oxygen consumption is consequently strongly increased by this mechanism.

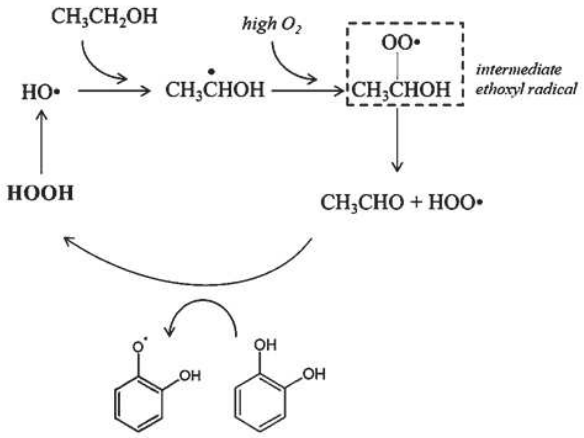

Scheme 2. Proposed scheme depicting the pathway of non-enzymatic wine oxidation under high dissolved oxygen concentration.

Oxidation with hydrogen peroxide induces a radical color change. According to Figure 3, the absorbance spectrum for the sample with hydrogen peroxide is clearly different from the 2018 wine sample with a ratio of absorbance *Abs*(*420 nm*)/*Abs*(*520 nm*) and is significantly higher compared to other wine samples ratios, revealing a predominant yellow color of the oxidized sample and a strong decrease in the red pigments. It can be explained by the oxidation of malvidin 3-*O*-diglucoside in the presence of hydrogen peroxide under acidic conditions, which leads to the formation of ortho-benzoyloxyphenylacetic acid esters through Baeyer–Villiger oxidation type [35–37].

Laccase test: Laccase are polyphenoloxidaze enzyme types (PPO) which come from fungus and which especially oxidize 1,2 and 1,4-dihydroxybenzenes to ortho-benzoquinones, which are easily oxidisable species [8]. This enzymatic oxidation induces wine browning. As presented in Table 2, the absorbance at 420 nm and the ratio *Abs*(*420 nm*)/*Abs*(*520 nm*) for the wine enzymatically treated is significantly higher to the 2018 wine and close to the 2014 wine. The color is consequently browner (yellow pigments increase) and closer to the natural aging color. PPO action in wine is closely correlated to the hydroxycinnamates content and larger non-flavonoid polyphenols group in wine. In the presence of PPO, caffeoyl tartaric acid will be oxidized in benzoquinones [38], which act as electrophiles and as oxidants on substances with lower pH as polyphenols.

Laccases seem to be more selective concerning the oxidation targets as they lead to the formation of electrophile *ortho*-quinones on the flavonoids B-ring containing a catechol group, suffering then from nucleophilic attack by other polyphenols [39,40], particularly from the flavonoids A-ring [41]. The two other oxidation types have a larger range of action, not only attacking a specific site. Moreover, hydrogen peroxide releases a very strong oxidant HO•, which can impact a wide range of polyphenols, even less accessible ones, whereas a high temperature leads to numerous secondary reactions, such as anthocyanin degradation. The three different forced oxidations can generate other unknown reactions with the numerous antioxidant species present in wine (ascorbic acid, sulfites), which can also explain the different trends observed in Figure 3.

3.3. UPLC-ESI-QTof

High resolution UPLC-Q-Tof-MS was performed on three Syrah vintages—2018, 2014 and 2010—to observe natural wine oxidation. It was also performed on three 2018 forced oxidation samples (heat test, laccase test, hydrogen peroxide test) and compared to previous samples issued from natural evolution to detect similarities or differences between forced and natural ageing. Full scan positive mass spectra were acquired by a rapid metabolomics method [31]. A prefiltering of the ions with an intensity equal to or above 20% of the maximal intensity was applied to all samples to focus on the major ions. The intensities of these ions are presented in Figure 4 (natural oxidation samples) and

Figure 5 (comparison between 2018 non oxidized and forced oxidation samples) The ion intensities are standardized compared to the 2018 sample.

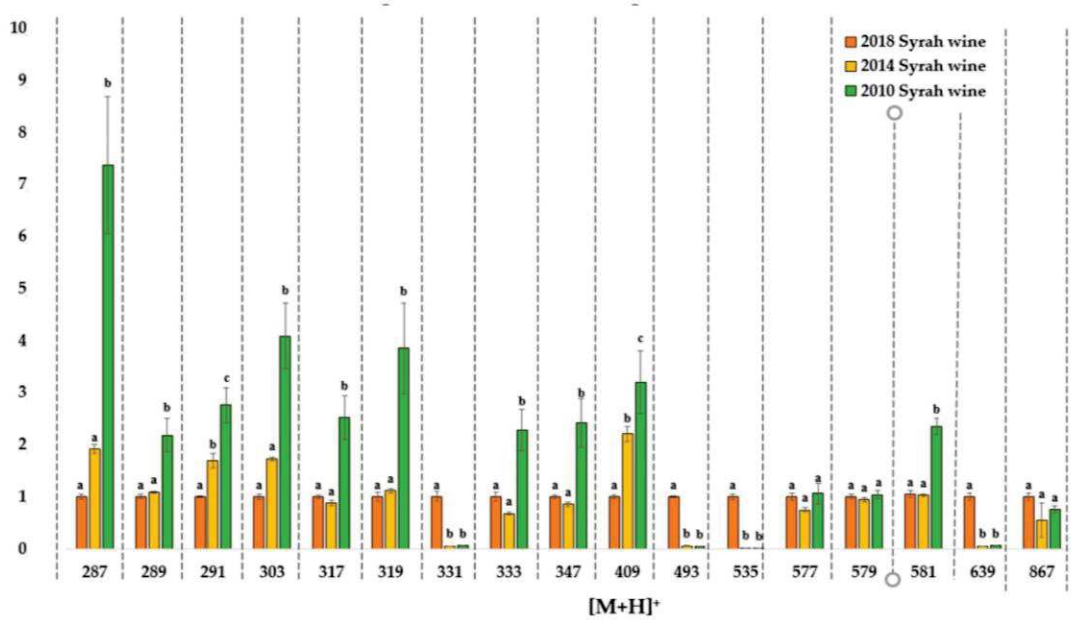

Figure 4. Natural oxidation samples. Ion intensity comparison of high-resolution MS spectra. Intensities for the three wine samples (2018, 2014 and 2010) are given for each $[M+H]^+$ ion and normalized compared to the 2018 sample values. Figures are expressed as mean values (n = 3) with standard deviation. Different letters indicate a significant difference (Tukey test, α = 0.05) between vintages for a same $[M+H]^+$ ion. Data are available in supplementary data: Tables S20–S22.

Possible molecular attributions of the ions are presented in Table 4. The effect on some specific polyphenols (anthocyanin, flavanols and their derivatives) were observed on mass spectra in both naturally or artificially aged wines samples and differed depending on the oxidation protocol, as shown in Figure 5.

Table 4. Ion annotation in high-resolution MS spectra.

$[M+H]^+$	Ion Annotation
287	*Cyanidin, Kaempferol*
289	*Fragment from polymeric proanthocyanidin*
291	*(+)-catechin, (-)-epicatechin, Fragment from polymeric proanthocyanidin*
303	*Quercetin, delphinidin, fragment from quercetin 3-glucoside, fragment from quercetin glucuronide*
317	*Petunidin, isorhamnetin*
319	*Fragment from myricetin 3-glucoside, fragment from myricetin glucuronide*
331	*Malvidin*
333	*unknown*
347	*Syringetin*
409	*Retro Diels Alder fragment*
493	*Malvidin 3-O-glucoside*
535	*Malvidin 3-O-acetyl glucoside*
577	*Oxidized dimeric proanthocyanidin*
579	*Dimeric proanthocyanidin, p-hydroxyphenylpyranopeodin 3-O-glucoside*
581	*Oxidized dimeric proanthocyanidin*
639	*Guaiacylpyranomalvidin 3-O-glucoside*
867	*Trimeric proanthocyanidins*

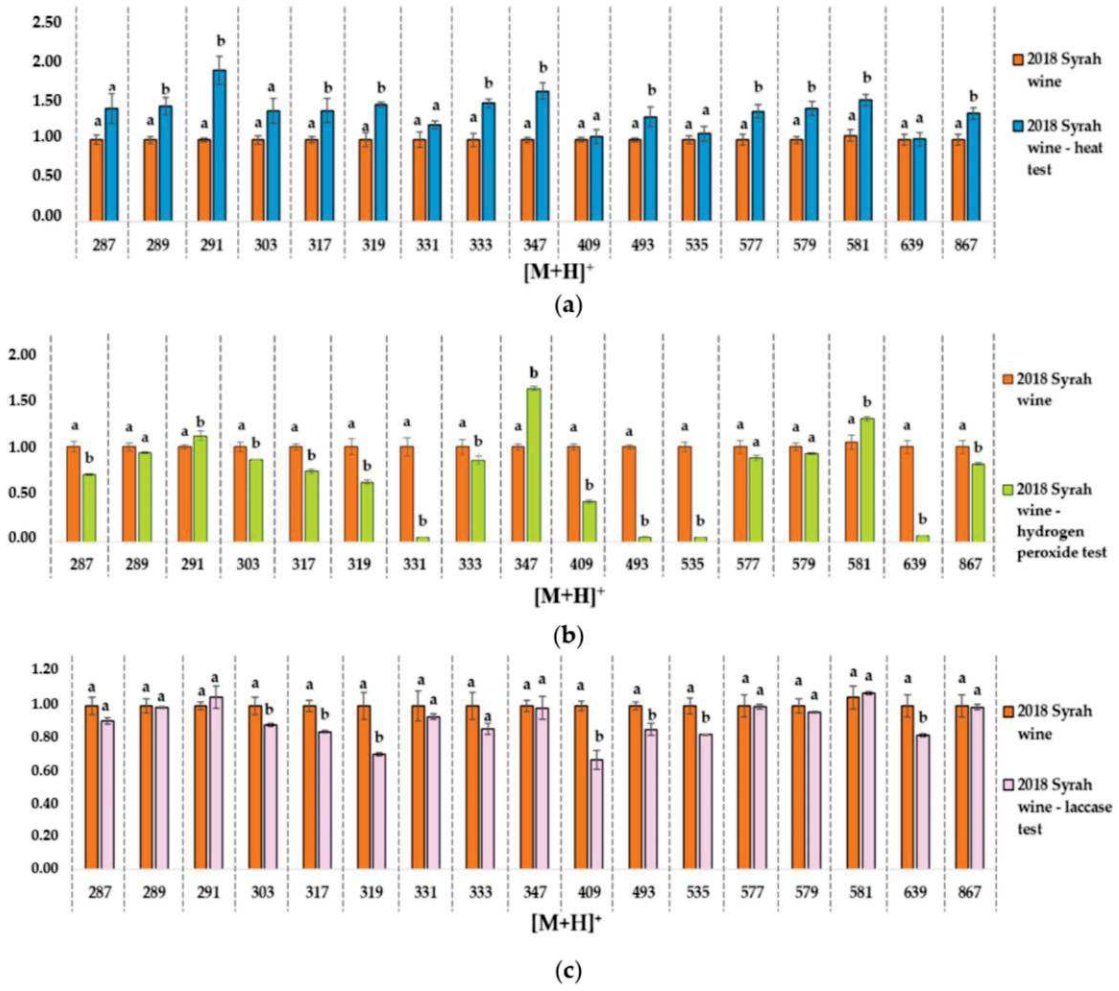

Figure 5. Ion intensity evolution in high resolution MS spectra. Intensity for the control wine aged 2018 and the ageing tests (**a**). Heat test −60 °C (**b**). Hydrogen peroxide test (**c**). Laccase tests. Results are given for each $[M+H]^+$ ion compared to the 2018 sample. Intensities are expressed as mean values with standard deviation. Different letters indicate a significant difference (Tukey test, $\alpha = 0.05$) between samples for the same $[M+H]^+$ ion. Data are available in supplementary data: Tables S20, S23–S25.

This semi-targeted approach allowed us to identify some specific ageing or vintage ion markers in the Syrah wines from different vintages. Ion intensities increased in mass spectra with the wine age for ions with $[M+H]^+$ = 287, 289, 291, 303, 319, 333, 347, 409, 581 Da, which can be attributed to ageing markers, with significant differences between the three vintages for $[M+H]^+$ ions detected at 291 and 409 Da. The 2014 wine can be too close to the 2018 one to observe significant differences for the following ions: 287, 289, 303, 319, 581 Da. However, the 2010 wine is old enough to observe very significant differences compared to the 2018 wine for some ions. For example, a 750% intensity increase was observed for the $[M+H]^+$ ion at 287 Da and 250% for 581 Da between the 2018 and 2010 wines, which corresponds to an increase in the monomeric flavanol ions on the mass spectra.

Some ion intensities decreased with the age of the wines, such as 331, 493, 535, 639 $[M+H]^+$. This was observed both for the 2014 and 2010 wine samples. It can be hypothesized that these ions correspond to malvidin derivatives, as shown in Table 4. Malvidin 3-*O*-glucoside is one of the main red pigments in wine and it is particularly sensitive to oxidation, as with most of the anthocyanins [2,5]. This intensity decrease was not observed for the 60 °C aging test, as shown in Figure 5a, and the laccase test, suggesting that other more sensitive molecules are impacted in these tests, as shown in Figure 5c.

Similarities can be observed between natural aging and the different artificial ageing tests.

Heat test: The same tendency for the ions at $[M+H]^+$ = 289, 291, 303, 317, 319, 333, 347, 581 Da is observed between natural aging and oxidation protocol at 60 °C, as shown in Figure 5a. Ions intensities increased both with wine ageing and after the heat test.

Hydrogen peroxide test: An intensity increase for $[M+H]^+$ = 581 Da is reported for this test, as shown in Figure 5b, as for the natural aging between 2018 and 2010 wines. An opposite tendency, correlated to natural aging, is noted for ions with $[M+H]^+$ = 493, 535, 639 Da. This oxidation test had a stronger impact on anthocyanin ($[M+H]^+$ = 331, 493, 535 and 639 Da) and a more moderate impact on low molecular weight flavonoids ($[M+H]^+$ = 291, 347 and 581 Da). Forced oxidation with hydrogen peroxide seems to be closer to natural oxidation than the two other tests for the chosen markers.

Laccase test: The same decreasing tendency as for hydrogen peroxide test is reported for ions with $[M+H]^+$ = 493, 535, 639 Da. It is the only test with no similarities with natural ageing for increasing intensities.

4. Conclusions

Three reproducible accelerated ageing tests based on three oxidation protocols were developed in this study and tested on three Syrah red wine samples. Each test revealed specific oxidation or ageing ion markers with significant differences between tests.

Intensities of their corresponding molecular ions were measured on MS spectra and revealed differences between wines with different vintages and between wines with different ageing tests, potentially revealing the presence of fragments from molecule degradation. Anthocyanins and polyphenols containing a galloyl or catechol group were among these potential oxidation markers both for natural ageing and accelerated ageing tests. MS spectra measured for natural ageing showed that the intensity for molecular ions corresponding to free anthocyanins decreased and the intensities increased for those corresponding to monomeric flavanols. The same result was observed for the hydrogen peroxide test on 2018 wine, which seems to be closer to natural oxidation than other tests for these oxidation markers.

Further research is needed to compare the slow and "natural" ageing kinetics of different red wines and the results of these ageing tests. The ultimate objective will be to determine which test is the most accurate to predict red wine ageing capacity.

Supplementary Materials: The following are available online at http://www.mdpi.com/2076-3921/9/8/663/s1, Table S1: analytical characterization of 2018 wine; Table S2: analytical characterization of 2014 wine; Table S3: analytical characterization of 2010 wine; Table S4: evolution of dissolved oxygen in 2018 red wine at 22 °C; Table S5: evolution of dissolved oxygen in 2018 red wine at 60 °C; Table S6: evolution of dissolved oxygen in 2018 red wine—laccase oxidation test; Table S7: evolution of dissolved oxygen in 2018 red wine—hydrogen peroxide oxidation test; Table S8: evolution of dissolved oxygen in 2014 red wine at 60 °C; Table S9: evolution of dissolved oxygen in 2014 red wine—laccase test; Table S10: evolution of dissolved oxygen in 2014 red wine—hydrogen peroxide oxidation test; Table S11: evolution of dissolved oxygen in 2010 red wine at 60 °C; Table S12: evolution of dissolved oxygen in 2010 red wine—laccase oxidation test; Table S13: evolution of dissolved oxygen in 2010 red wine—hydrogen peroxide oxidation test; Table S14: Absorbance measurements in UVvis (400–800 nm) for 2018 red wine; Table S15: Absorbance measurements in UVvis (400–800 nm) for 2014 red wine; Table S16: Absorbance measurements in UVvis (400–800 nm) for 2010 red wine; Table S17: Absorbance measurements in UVvis (400–800 nm) for 2018 red wine at 60 °C; Table S18: Absorbance measurements in UVvis (400–800 nm) for 2018 red wine—laccase oxidation test; Table S19: Absorbance measurements in UVvis (400–800 nm) for 2018 red wine—hydrogen peroxide oxidation test; Table S20: High resolution UPLC-MS for 2018 red wine; Table S21: High resolution UPLC-MS for 2014 red wine; Table S22: High resolution UPLC-MS for 2010 red wine; Table S23: High resolution UPLC-MS for 2018 wine at 60 °C; Table S24: High resolution UPLC-MS for 2018 red wine—laccase oxidation test; Table S25: High resolution UPLC-MS for 2018 wine—hydrogen peroxide oxidation test.

Author Contributions: Conceptualization: C.S.; Data curation: S.D.; Formal analysis: S.D.; Funding acquisition: C.S.; Investigation: S.D. and G.C.; Methodology: S.D., T.C., G.C. and C.S.; Project administration and validation: C.S; Supervision: L.M., F.G. and C.S.; Visualization: S.D.; Writing—original draft: S.D.; Writing—review and editing: S.D., C.S., L.M., F.G., G.C., T.C. and C.E. All authors have read and agreed to the published version of the manuscript.

Funding: This work was supported in part by a PhD grant (S.D.) from the University of Montpellier (Bourse école doctorale GAIA).

Conflicts of Interest: The authors declare no conflict of interest.

References

1. Ferreira, V.; Bueno, M.; Franco-Luesma, E.; Culleré, L.; Fernández-Zurbano, P. Key Changes in wine aroma active compounds during bottle storage of spanish red wines under different oxygen levels. *J. Agric. Food Chem.* **2014**, *62*, 10015–10027. [CrossRef] [PubMed]
2. Gambuti, A.; Siani, T.; Picariello, L.; Rinaldi, A.; Lisanti, M.T.; Ugliano, M.; Dieval, J.B.; Moio, L. Oxygen exposure of tannins-rich red wines during bottle aging. influence on phenolics and color, astringency markers and sensory attributes. *Eur. Food Res. Technol.* **2017**, *243*, 669–680. [CrossRef]
3. Ugliano, M. Oxygen contribution to wine aroma evolution during bottle aging. *J. Agric. Food Chem.* **2013**, *61*, 6125–6136. [CrossRef] [PubMed]
4. Caillé, S.; Samson, A.; Wirth, J.; Diéval, J.-B.; Vidal, S.; Cheynier, V. Sensory characteristics changes of red grenache wines submitted to different oxygen exposures pre and post bottling. *Anal. Chim. Acta* **2010**, *660*, 35–42. [CrossRef]
5. Gambuti, A.; Rinaldi, A.; Ugliano, M.; Moio, L. Evolution of phenolic compounds and astringency during aging of red wine: Effect of oxygen exposure before and after bottling. *J. Agric. Food Chem.* **2013**, *61*, 1618–1627. [CrossRef]
6. De Beer, D.; Joubert, E.; Marais, J.; du Toit, W.; Fouché, B.; Manley, M. Characterisation of pinotage wine during maturation on different oak products. *South Afr. J. Enol. Vitic.* **2016**, *29*. [CrossRef]
7. Cheynier, V.; Dueñas-Paton, M.; Salas, E.; Maury, C.; Souquet, J.-M.; Sarni-Manchado, P.; Fulcrand, H. Structure and properties of wine pigments and tannins. *Am. J. Enol. Vitic.* **2006**, *57*, 298–305.
8. Oliveira, C.M.; Ferreira, A.C.S.; De Freitas, V.; Silva, A.M.S. Oxidation mechanisms occurring in wines. *Food Res. Int.* **2011**, *44*, 1115–1126. [CrossRef]
9. Somers, T.C.; Wescombe, L.G. Evolution of red wines II. an assessment of the role of acetaldehyde. *VITIS J. Grapevine Res.* **1987**, *26*, 27.
10. Singleton, V.L. Oxygen with phenols and related reactions in musts, wines, and model systems: Observations and practical implications. *Am. J. Enol. Vitic.* **1987**, *38*, 9.
11. Kilmartin, P.A. The oxidation of red and white wines and its impact on wine aroma. *Res. Gate* **2009**, *73*.
12. Waterhouse, A.L.; Laurie, V.F. Oxidation of wine phenolics: A critical evaluation and hypotheses. *Am. J. Enol. Vitic.* **2006**, *57*, 306–313.
13. Ployon, S.; Attina, A.; Vialaret, J.; Walker, A.S.; Hirtz, C.; Saucier, C. Laccases 2 & 3 as biomarkers of botrytis cinerea infection in sweet white wines. *Food Chem.* **2020**, *315*, 126233. [CrossRef] [PubMed]
14. Nikolantonaki, M.; Waterhouse, A.L. A method to quantify quinone reaction rates with wine relevant nucleophiles: A key to the understanding of oxidative loss of varietal thiols. *J. Agric. Food Chem.* **2012**. [CrossRef] [PubMed]
15. Nikolantonaki, M.; Magiatis, P.; Waterhouse, A.L. Measuring protection of aromatic wine thiols from oxidation by competitive reactions vs wine preservatives with ortho-quinones. *Food Chem.* **2014**, *163*, 61–67. [CrossRef] [PubMed]
16. Fulcrand, H.; Dueñas, M.; Salas, E.; Cheynier, V. Phenolic reactions during winemaking and aging. *Am. J. Enol. Vitic.* **2006**, *57*, 289–297.
17. Danilewicz, J.C.; Seccombe, J.T.; Whelan, J. Mechanism of interaction of polyphenols, oxygen, and sulfur dioxide in model wine and wine. *Am. J. Enol. Vitic.* **2008**, *59*, 128–136.
18. Ma, L.; Watrelot, A.A.; Addison, B.; Waterhouse, A.L. Condensed tannin reacts with SO_2 during wine aging, yielding flavan-3-ol sulfonates. *J. Agric. Food Chem.* **2018**, *66*, 9259–9268. [CrossRef]
19. Elias, R.J.; Waterhouse, A.L. Controlling the fenton reaction in wine. *J. Agric. Food Chem.* **2010**, *58*, 1699–1707. [CrossRef]
20. Petrozziello, M.; Torchio, F.; Piano, F.; Giacosa, S.; Ugliano, M.; Bosso, A.; Rolle, L. Impact of increasing levels of oxygen consumption on the evolution of color, phenolic, and volatile compounds of nebbiolo wines. *Front. Chem.* **2018**, *6*. [CrossRef]
21. Ferreira, V.; Carrascon, V.; Bueno, M.; Ugliano, M.; Fernandez-Zurbano, P. Oxygen consumption by red wines. part I: Consumption rates, relationship with chemical composition, and role of SO_2. *J. Agric. Food Chem.* **2015**, *63*, 10928–10937. [CrossRef] [PubMed]

22. Castro, C.C.; Martins, R.C.; Teixeira, J.A.; Silva Ferreira, A.C. Application of a high-throughput process analytical technology metabolomics pipeline to port wine forced ageing process. *Food Chem.* **2014**, *143*, 384–391. [CrossRef] [PubMed]
23. Zou, H.; Kilmartin, P.A.; Inglis, M.J.; Frost, A. Extraction of phenolic compounds during vinification of pinot noir wine examined by hplc and cyclic voltammetry. *Aust. J. Grape Wine Res.* **2002**, *8*, 163–174. [CrossRef]
24. Gil, M.; Reynes, C.; Cazals, G.; Enjalbal, C.; Sabatier, R.; Saucier, C. Discrimination of rosé wines using shotgun metabolomics with a genetic algorithm and ms ion intensity ratios. *Sci. Rep.* **2020**, *10*. [CrossRef] [PubMed]
25. Macías, V.M.P.; Pina, I.C.; Rodríguez, L.P. Factors influencing the oxidation phenomena of sherry wine. *Am. J. Enol. Vitic.* **2001**, *52*, 151–155.
26. Kumar, K.; Ajar, N.Y.; Pritesh, V.; Singh, K. Chemical changes in food during processing and storage. *Res. Gate* **2016**. [CrossRef]
27. Carbonneau, A.; Deloire, A.; Torregrosa, L.; Jaillard, B.; Pellegrino, A.; Metay, A.; Ojeda, H.; Lebon, E.; Abbal, P. *Traité de La Vigne: Physiologie, Terroir, Culture*; Dunod: Malakoff, France, 2015.
28. Tanaka, Y.; Sasaki, N.; Ohmiya, A. Biosynthesis of plant pigments: Anthocyanins, betalains and carotenoids. *Plant J.* **2008**, *54*, 733–749. [CrossRef]
29. Aurelio, D.-L.; Edgardo, R.G.; Navarro-Galindo, S. Thermal kinetic degradation of anthocyanins in a roselle (hibiscus sabdariffa l. cv. 'criollo') infusion. *Int. J. Food Sci. Technol.* **2008**, *43*, 322–325. [CrossRef]
30. Redus, M.; Baker, D.C.; Dougall, D.K. Rate and equilibrium constants for the dehydration and deprotonation reactions of some monoacylated and glycosylated cyanidin derivatives. *J. Agric. Food Chem.* **1999**, *47*, 3449–3454. [CrossRef]
31. Piffaut, B.; Kader, F.; Girardin, M.; Metche, M. Comparative degradation pathways of malvidin 3,5-diglucoside after enzymatic and thermal treatments. *Food Chem.* **1994**, *50*, 115–120. [CrossRef]
32. Lopes, P.; Richard, T.; Saucier, C.; Teissedre, P.-L.; Monti, J.-P.; Glories, Y. Anthocyanone a: A quinone methide derivative resulting from malvidin 3- *o* -glucoside degradation. *J. Agric. Food Chem.* **2007**, *55*, 2698–2704. [CrossRef] [PubMed]
33. Carrascón, V.; Vallverdú-Queralt, A.; Meudec, E.; Sommerer, N.; Fernandez-Zurbano, P.; Ferreira, V. The kinetics of oxygen and so2 consumption by red wines. what do they tell about oxidation mechanisms and about changes in wine composition? *Food Chem.* **2018**, *241*, 206–214. [CrossRef] [PubMed]
34. Singleton, V.L.; Kramlinga, T.E. Browning of white wines and an accelerated test for browning capacity. *Am. J. Enol. Vitic.* **1976**, *27*, 157–160.
35. Jurd, L. Anthocyanidins and related compounds—XIII. *Tetrahedron* **1968**, *24*, 4449–4457. [CrossRef]
36. Hrazdina, G. Oxidation of the anthocyanidin-3,5-diglucosides with H_2O_2: The structure of malvone. *Phytochemistry* **1970**, *9*, 1647–1652. [CrossRef]
37. Hrazdina, G.; Franzese, A.J. Oxidation products of acylated anthocyanins under acidic and neutral conditions. *Phytochemistry* **1974**, *13*, 231–234. [CrossRef]
38. Cheynier, V.; Ricardo da Silva, J.M. Oxidation of grape procyanidins in model solutions containing trans-caffeoyltartaric acid and polyphenol oxidase. *J. Agric. Food Chem.* **1991**, *39*, 1047–1049. [CrossRef]
39. McDonald, P.D.; Hamilton, G.A. Mechanisms of Phenolic Oxidative Coupling Reactions. In *Organic Chemistry*; Elsevier: Amsterdam, The Netherlands, 1973; Volume 5, pp. 97–134. [CrossRef]
40. Fulcrand, H.; Cheminat, A.; Brouillard, R.; Cheynier, V. Characterization of compounds obtained by chemical oxidation of caffeic acid in acidic conditions. *Phytochemistry* **1994**, *35*, 499–505. [CrossRef]
41. Guyot, S.; Vercauteren, J.; Cheynier, V. Structural determination of colourless and yellow dimers resulting from (+)-catechin coupling catalysed by grape polyphenoloxidase. *Phytochemistry* **1996**, *42*, 1279–1288. [CrossRef]

Chapitre III – Propriétés redox des vins rouges

Après la mise au point des tests de vieillissements accélérés répétables, ces derniers ont été appliqués à un nombre plus important de vins (9 vins rouges de différents cépages et millésimes) en parallèle d'une étude électrochimique. Pour cette dernière, la voltammétrie cyclique utilisant des électrodes jetables a été choisie, technique rapide, sensible, peu coûteuse et nécessitant une petite quantité d'échantillon. Les objectifs de ce chapitre étaient :

- De mesurer les cinétiques de consommation d'oxygène de ces neuf vins soumis au trois protocoles de vieillissements accélérés décris dans le chapitre précèdent
- De caractériser leur comportement électrochimique par voltammétrie cyclique. Pour cela, les vins avant et après oxydation ont été analysés. Les soustractions des valeurs des charges obtenues (avant - après oxydation) ont permis ainsi d'obtenir des valeurs représentatives des phénomènes d'oxydation uniquement.
- D'évaluer de potentielles corrélations entre les paramètres électrochimiques (charges), la composition phénolique des vins et leurs cinétiques de consommation d'oxygène lors des tests de vieillissement accéléré afin de conclure quant à l'utilisation de la voltammétrie cyclique pour prédire l'évolution oxydative des vins rouges

Les méthodes utilisées pour mener cette étude ont été les suivantes :

1. Des mesures non-invasives de la concentration en oxygène dissous par luminescence et fibre optique
2. Une méthode électrochimique (voltammétrie cyclique) utilisant des électrodes jetables (nanotubes de carbone simple-feuillet) afin de déterminer la capacité réductrice (antioxydante) des vins et caractériser les composés les plus facilement oxydables.
3. Une méthode de mesure quantitative des taux de SO_2 présents dans les vins par GC-MS

Les hypothèses étaient les suivantes :

1. Des vins avec des compositions polyphénoliques différentes peuvent avoir des vitesses de consommation d'oxygène différentes et des comportements différents d'un point de vue électrochimique.
2. Les résultats des mesures électrochimiques utilisant des électrodes jetables peuvent être corrélés aux vitesses de consommation d'oxygène et/ou à la composition phénolique des vins
3. La sensibilité d'un vin face à certains phénomènes d'oxydation peut être prédit grâce à la voltammétrie cyclique.

Conclusions :

1. Le comportement oxydatif des vins dépend à la fois du vin considéré et du type de vieillissement accéléré utilisé.
2. Les valeurs issues de la soustraction des voltammogrammes des vins non oxydés des voltammogrammes des vins oxydés correspondants permettent une vue d'ensemble de l'impact des différents tests sur les vins.
3. Des corrélations significatives négatives ont été observées entre les paramètres électrochimiques (charges) des vins non oxydés (référence) et les vitesses de consommation d'oxygène lors de tests de vieillissement accélérés avec la température et les laccases. Ainsi, la voltammétrie cyclique semble être une technique prometteuse pour prédire ces deux tests de vieillissements accélérées et reflète la sensibilité des vins face aux phénomènes d'oxydation. En revanche, il n'est pas possible d'utiliser la voltammétrie cyclique pour prédire l'oxydation chimique des vins par le peroxyde d'hydrogène à partir des vins de référence.

Cette étude a fait l'objet d'un article scientifique, publié dans le journal *Antioxidants* (octobre 2021), sous la référence :

Deshaies, S.; Garcia, L.; Veran, F.; Mouls, L.; Saucier, C. ; Garcia, F. ***Red wine oxidation characterization by accelerated ageing tests and cyclic voltammetry***

Et présenté ci-après.

antioxidants

MDPI

Article

Red Wine Oxidation Characterization by Accelerated Ageing Tests and Cyclic Voltammetry

Stacy Deshaies, Luca Garcia, Frédéric Veran, Laetitia Mouls, Cédric Saucier and François Garcia *

SPO, Université de Montpellier, INRAE, Institut Agro, 34000 Montpellier, France; stacy.deshaies@umontpellier.fr (S.D.); luca.garcia@umontpellier.fr (L.G.); Frederic.veran@inrae.fr (F.V.); laetitia.mouls@supagro.fr (L.M.); cedric.saucier@umontpellier.fr (C.S.)
* Correspondence: francois.garcia@umontpellier.fr

Abstract: In order to obtain information on the oxidative behavior of red wines, oxygen consumption rates and electrochemical changes (cyclic voltammetry) were measured for nine red wines subject to three different accelerated ageing tests: chemical (with hydrogen peroxide), enzymatic (with laccase from *Trametes versicolor*), and temperature (at 60 °C). Oxidative behavior depended both on the wine sample and accelerated ageing test type. A good correlation was observed between electrochemical parameters of charges for reference/non-oxidized wines, in accordance with their antioxidant capacity, and the variation of charges after enzymatic and temperature tests, meaning that cyclic voltammetry could be used in order to predict these two oxidation tests and reflect the wine sensitivity towards respective oxidation targets. However, it was not possible to predict wine chemical oxidation test based on hydrogen peroxide from the electrochemical measurements.

Keywords: cyclic voltammetry; phenolic compounds; red wine; oxygen consumption rate; oxidation

Citation: Deshaies, S.; Garcia, L.; Veran, F.; Mouls, L.; Saucier, C.; Garcia, F. Red Wine Oxidation Characterization by Accelerated Ageing Tests and Cyclic Voltammetry. *Antioxidants* **2021**, *10*, 1943. https://doi.org/10.3390/antiox10121943

Academic Editor: Ehab A. Abourashed

Received: 29 October 2021
Accepted: 24 November 2021
Published: 3 December 2021

Publisher's Note: MDPI stays neutral with regard to jurisdictional claims in published maps and institutional affiliations.

1. Introduction

During the winemaking process and storage, red wines can undergo many undesirable changes, particularly oxidative degradation due to numerous atmospheric oxygen intakes. This spoilage can deeply impact organoleptic properties [1–5] and color stabilization [6] but its impact is strongly wine dependent [7–9].

Phenolic compounds constitute primary targets to oxidation reactions [10–12], particularly those possessing an *ortho*-diphenol functional group which are going to be quickly converting into quinones; unstable and highly reactive compounds. Indeed, quinones are able to undergo nucleophilic addition, which is one of the main mechanisms responsible for oxidative degradation [5]. Numerous nucleophiles are available in wines, including SO_2, phenolic compounds, amino acids, ascorbic acid, and volatile and non-volatile thiols [7,13–17].

Consequently, due to the manifold possible reactions and the complexity of the media, oxidation reactions effects are still difficult to predict. Thus, for example, Ferreira et al. [8] recently highlighted the unusual behavior of certain red wines towards antioxidants as SO_2 and so the presence and competition of more reactive antioxidants.

Electrochemical methods, in particular linear sweep voltammetry and cyclic voltammetry (CV), using either carbon paste or glassy carbon electrodes, were developed and applied to the analysis of wine phenolic compounds [18–21]. Recently, electrochemical techniques became widely used to determine antioxidant capacities of food or beverages as well as to analyze polyphenols [22,23] as they appear as sensitive, fast, and easy to use techniques [24].

Cyclic voltammetry is among the most commonly used method to characterize total polyphenols content, antioxidant capacity, as well as to discriminate wine samples [25,26]. Voltammograms represent both anodic and cathodic curves. Concerning the anodic one, corresponding to the oxidation phenomenon, information can be drawn from the following

parameters: (i) the peak current, proportional to the concentration of oxidizable compounds in solution; (ii) the peak potential, corresponding to the ease of oxidation of involved compounds (the more the potential is low and the more the compounds are easy to oxidize); (iii) the charge (corresponding to the area under the curve) which allows for the characterization of antioxidant capacity [22].

Glassy carbon is used as a material for classical electrochemical electrodes but presently, carbon based disposable screen-printed electrodes appear as a promising tool and are become more widely used [27]. Indeed, they offer numerous advantages, including disposability [28], reproducibility, practicality, high sensitivity, their ability to limit samples consumption thanks to miniaturization, and low detection limits [29,30]. Among these, carbon nanotubes are used, allowing for the increase in, among others, sensitivity. Two categories of carbon nanotubes electrodes exist: multi-walled carbon nanotubes (MWCNTs) and single-walled carbon nanotubes (SWCNTs) [27,31,32]. SWCNTs were privileged in this work for their good results concerning wine polyphenols characterization and antioxidant capacity as shown by Newair et al. [33]. The objectives of this article were first to determine the phenolic composition of nine different red wines (different varieties and vintage). Then, for each wine, their oxygen consumption rates (initial and average) and their voltammetry behavior with different accelerated ageing tests (H_2O_2, laccase and temperature) were analyzed. Finally, the possible correlations of electrochemical parameters with ageing tests results, and phenolic compounds were evaluated in order to use them as a quick method of characterization of red wine oxidation.

2. Materials and Methods

2.1. Chemicals and Reagents

Ethanol (absolute), tartaric acid (≥99.5%), laccase from *Trametes versicolor* (0.94 U·mg^{-1}), Folin–Ciocalteu reagent, sodium hydroxide, chloride acid (1 M), (+)-catechin, (−)-epicatechin, quercetin and caffeic acid were purchased from Sigma-Aldrich (Saint-Quentin Fallavier, France). Oenin chloride was obtained from Extrasynthese (Genay, France).

2.2. Model Wine Solution

The model wine solution used as blank for electrochemical measurements was composed as follows: 12% vol. ethanol in water, 0.033 M tartaric acid and pH adjusted to 3.6 (sodium hydroxide 1 N).

2.3. Red Wines

Wines with different characteristics were selected for experiments. Commercial red wines were selected from various grape varieties from four vintages, 2019, 2018, 2014 and 2010, and origins: Côtes du Rhône (Syrah 2018, 2014 and 2010 from the same winery) corresponding to R1 to R3, Chinon (Cabernet Franc, 2018) corresponding to R4, Morgon (Gamay, 2018) corresponding to R5, Alsace rouge (Pinot noir, 2018) for R6, Ardèche (Syrah, 2019) for R7, Côteaux de Béziers (Syrah 2019) for R8 and Grès-de-Montpellier (Syrah, 2019) for R9.

A bottle of each wine was opened and slowly homogenized under nitrogen to avoid oxidation reactions. Aliquots of 50 mL tubes were then immediately frozen at −80 °C.

2.4. Wine Global Chemical Characterization

2.4.1. Wine Global Chemical Characterization

Studied wines were characterized with enological usual chemical analyses (Natoli laboratory, St Clément de Rivière, France) according to OIV procedures (www.oiv.int, accessed on 23 November 2021). Analyses included: alcoholic percentage (Fourier transformed infrared spectroscopy: FTIR); total acidity (FTIR); volatile acidity; total sulfur dioxide (automated colorimetric method); pH (FTIR); Fe (colorimetric method, reaction with disodium salt of (pyrildil-2)-3bis(phenyl-4-sulfonic 5–6 triazin-1,2,3,4) acid), absorbance read at 570 nm on a sequential analyzer (Olympus AU2700); Cu (colorimetric method 4-(3,5-

Dibromo-2-Pyridilazo)-*N*-Ethyl-*N*-(3-Sulfopropyl) aniline reaction, absorbance read at 570 nm on a sequential analyzer (Olympus AU2700) (Supplementary Data Table S1).

2.4.2. Quantitative Analysis of Free SO_2 Levels (GC-MS)

Free SO_2 level (samples after oxygen saturation) was determinate by head-space gas chromatography coupled to a quadrupole mass spectrometer detector (HS-GC-MS) following the method described in Carrascon et al. [34] with slight modifications. GC-MS analysis was carried out on a GC Trace Ultra gas chromatograph (Thermo Fisher, Waltham, MA, USA) and coupled to an ISQ Series mass spectrometer (Thermo Fisher, Waltham, MA, USA). A DB-WAX (30 m × 0.25 mm i.d. × 0.25 µm) capillary column (Agilent Technologies, Santa Clara, CA, USA) was used for the chromatographic separation. For the analysis, 4.5 mL of sample was placed into a 10 mL headspace vial and 500 µL of *ortho*-phosphoric acid (85%) was added before closing and vials were incubated at 40 °C for 15 min. After this, 400 µL of the headspace was injected into a PTV injector, working in split mode (1:7 split ratio) and kept at 200 °C. An AOC-5000 autosampler (Shimadzu, Kyoto, Japan) with a static headspace unit was used and the 1mL gas-tight syringe was heated at 50 °C. After the injection, the hot syringe was cleaned by purging for 5 min with nitrogen. The temperature method started at 50 °C for 4 min then raised to 220 °C at 50 °C/min and was kept at this temperature for 5 min. The carrier gas employed was helium at 1.5 mL/min. The mass spectrometer was used with an electron impact (EI) ion source and acquisition was performed in single ion monitoring (SIM) mode. The m/z used for quantification were 48 and 64.

External calibration curves in model wine containing known amounts of SO_2 (as potassium metabisulfite) were prepared.

2.5. Accelerated Ageing Tests

Three accelerated oxidation tests were applied to the nine wines after oxygen saturation. Each wine sample was saturated with air by vigorously shaking a 500 mL flask containing 35 mL of wine for 10 s, after which the cap was opened (5 s) to let fresh air enter the flask. This saturation operation was repeated three times. The procedure and the test optimization have been previously described by Deshaies et al. [35]:

Briefly, enzymatic test was performed by the addition of 50 µL of a 10 $mg{\cdot}L^{-1}$ laccase from *Trametes versicolor* solution in 11 mL of red wine.

For chemical test, 20 µL of hydrogen peroxide solution (30% in water) was added to 11 mL of red wine.

Finally, the heat treatment was performed by heating 11 mL of wine at 60 °C.

For each test, red wine was put in Hermetic Pyrex 11 mL culture tubes (VWR 734–4224, Radnor, PA, USA) containing Pst3 oxygen sensors (Presens—Precision Sensing GmbH, Regensburg, Germany) with a minimum headspace.

2.6. Determination of Phenolic Composition

2.6.1. Determination of Total Phenolic Content (TPC)

The Folin–Ciocalteu method, revised by Magalhaes et al. [36], was used to determine total phenolic content. Absorbances were measured on a multiplate reader (Spectrostar Nano—BMG Labtech) equipped with spectrophotometric detection and 96-well plates. Each well contained: 50 µL diluted wine (1/100) + 50 µL Folin Ciocalteu reagent (1:5 *v*/*v* in water) + 100 µL sodium hydroxide solution (0.35 M). Absorbance at 750 nm of formed blue complex was read after 3 min.

The absorbance values for the wine samples were related to the calibration curve (gallic acid solution: 10 $mg{\cdot}L^{-1}$ to 200 $mg{\cdot}L^{-1}$). They reflected the total phenolic content in the considered wine. TPC was expressed in gallic acid equivalent (mg/L) and the result was multiplied by the associated dilution factor.

2.6.2. Total Tannins Content (TC)

The Bate-Smith method was used to determine total tannins content (TC) [37]. To 4 mL 1/50 diluted wine (in water) in a tube was added 2 mL water and 6 mL HCl (12 N). The tube was then heated in a water bath at 100 °C for 30 min. The reference tube was identically treated without the heating step. A total of 1 mL ethanol (95%) was added to both tubes and absorbances at 550 nm were measured on spectrophotometer UV-1900 (Shimadzu, Marne-La-Vallée, France) against water under one cm of optical path. A_{550} values were plotted on a standard curve drawn from reference oligomers.

2.6.3. Total Pigments Index (TP)

Wine samples were diluted in HCL 1 M (1/100) in a hermetic flask. After 30 min out of light, absorbance at 520 nm was read on spectrophotometer UV-1900 (Shimadzu, Marne-La-Vallée, France) against water under 1 mm of optical path. The result was multiplied by the associated dilution factor [1,38].

2.6.4. SO_2 Bleaching Resistant Pigments Index (RP)

To 10 mL wine in a hermetic flask, 150 µL of SO_2 solution was added ($Na_2S_2O_5$ in water at 200 g/L). After 30 min out of light, absorbance at 520 nm was read on spectrophotometer UV-1900 (Shimadzu, France) against water under 1 mm of optical path. The result was multiplied by the associated dilution factor [39].

2.7. Electrochemical Apparatus and Measurements

Electrochemical measurements were performed with potentiostat/galvanostat (Autolab PGSTAT 302N) using software Nova 2.1.5 (Metrohm, Herisau, Switzerland). Model wine solution was used to dilute wine samples (1/75). Measurements were performed in the range of −0.2 V to 0.8 V (vs. $Ag_{(s)}$) with a scan rate of 100 mV/s using single-walled carbon nanotubes-modified screen-printed carbon electrode SWCNTs-SPCE (4 mm diameter, Dropsens, Oviedo, Spain) in a three-electrode configuration (silver solid reference electrode and carbon counter electrode). A total of 200 µL of sample were dropped at the electrode surface and measurements were immediately carried out. The experimental set-up is presented in Figure 1.

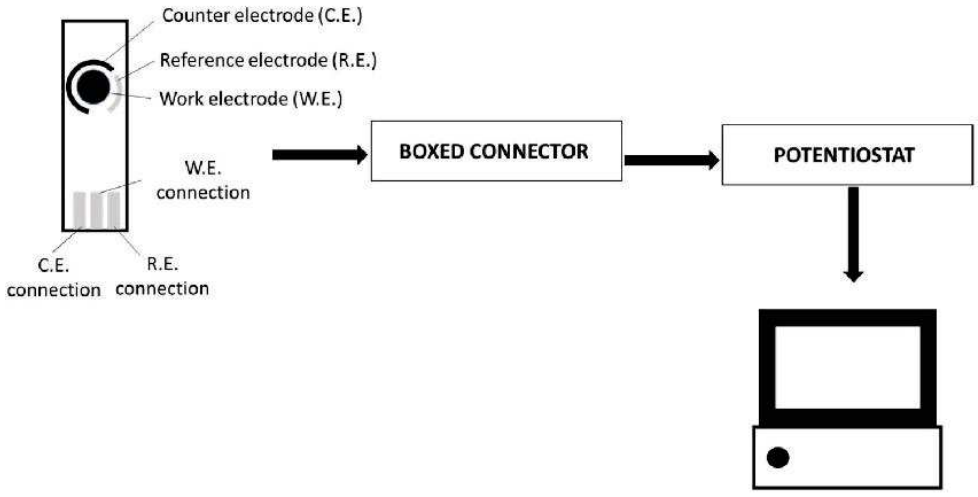

Figure 1. Cyclic voltammetry experimental set-up.

2.8. Statistical Analysis

The ANOVA, correlation and PCA (principal component analysis) tests were performed using XLSTAT software (Addinsoft version 19.02, Paris, France). A Tukey test was carried out and where p-values were <0.05 was considered as significant. Pearson's correlation coefficient was carried out for the determination of correlations between electrochemical parameters, oxygen consumption rates and phenolic composition. All analyses, experiments and tests were performed in triplicate.

3. Results and Discussion

3.1. Wines Phenolic Characterization

According to Table 1, phenolic and tannin contents were mostly in accordance, with significant highest contents for R8 wine concerning phenolic content (3.1 g GAE·L^{-1}), and R8 (4.6 g·L^{-1}), R3 (4.4 g·L^{-1}) and R4 (4.2 g·L^{-1}) concerning total tannins content, whereas lowest contents were observed for R7 (1.4 g·L^{-1} and 2.1 g·L^{-1} respectively). These values were also in accordance with pigment index ones, with total pigment index values ranging from 4.8 for R6 to 21.2 for R9 and also the SO_2 bleaching resistant pigments index from 1.7 to 7.2 for the same wines. Finally, it can be concluded that, although some wines were from the same cultivar, the nine wines presented very different initial phenolic composition.

Table 1. Phenolic characterization of the different red wines. Values represent means of triplicate determination ± SD. GAE: gallic acid equivalent. Different letters indicate the significant differences between samples in one column according to Tukey's test, $p < 0.05$.

Wine Sample	Total Phenolic Content (g GAE/L)	Total Tannins Content (g/L)	Total Pigments Index	SO_2 Bleaching Resistant Pigments Index
R1	1.9 ± 0.1^{d}	2.8 ± 0.2^{d}	19.2 ± 0.9^{a}	5.4 ± 0.4^{b}
R2	1.9 ± 0.1^{d}	$3.2 \pm 0.1^{c,d}$	4.9 ± 0.1^{d}	$4.3 \pm 0.1^{c,d}$
R3	2.5 ± 0.1^{b}	$4.4 \pm 0.1^{a,b}$	6.0 ± 0.5^{d}	$4.8 \pm 0.1^{b,c}$
R4	2.4 ± 0.1^{b}	$4.2 \pm 0.1^{a,b}$	8.35 ± 1.1^{c}	$4.6 \pm 0.3^{b,c}$
R5	$2.6 \pm 0.1^{b,c}$	3.4 ± 0.1^{c}	9.1 ± 0.1^{c}	3.5 ± 0.2^{d}
R6	2.7 ± 0.2^{b}	2.8 ± 0.1^{d}	4.8 ± 0.3^{d}	1.7 ± 0.1^{e}
R7	1.4 ± 0.1^{e}	2.1 ± 0.1^{e}	14.7 ± 0.5^{b}	3.5 ± 0.4^{d}
R8	3.1 ± 0.05^{a}	4.6 ± 0.1^{a}	16.2 ± 1.3^{b}	6.8 ± 0.2^{a}
R9	2.5 ± 0.1^{b}	4.1 ± 0.2^{b}	21.2 ± 1.9^{a}	7.2 ± 0.1^{a}

3.2. Accelerated Ageing Tests: Oxygen Consumption Parameters

The red wines were submitted to three accelerated ageing tests experiments [36]: chemical (H_2O_2 added), enzymatic (by laccase from *Trametes versicolor*) and heat treatment (at 60 °C). The oxygen consumption was monitored non-destructively by means of fluorescence oxygen sensors. The wine samples submitted to ageing test oxidations consumed an oxygen concentration of approximately 6.5 mg·L^{-1} whereas, in the case of non-oxidized controls, average total consumed oxygen was only 0.20 ± 0.15 mg·L^{-1}.

Table 2 data confirm that wines can differ for their kinetics to consume oxygen, in agreement with recent studies [7,8].

Table 2. Oxygen consumption rates (ppm·h^{-1}) of wines for the accelerated ageing tests. Values represent means of triplicate determination ± SD. Initial O_2 rate (iOCR) is calculated as tangent to the linear regression O_2 = f (time) in the first 30 min. Average O_2 rate (aOCR) is calculated between the first O_2 value before the aging test and the first O_2 value of the final threshold. Different letters indicate the significant differences between samples in one column according to Tukey's test, $p < 0.05$.

	Initial O_2 Rate iOCR	Average O_2 Rate aOCR		Initial O_2 Rate iOCR	Average O_2 Rate aOCR		Initial O_2 Rate iOCR	Average O_2 Rate aOCR
R1 60 °C	2.40 ± 0.06 ^{a,b}	1.27 ± 0.05 ^{a}	R1 lac	3.33 ± 0.05 ^{b,c}	1.35 ± 0.21 ^{a,b}	R1 H_2O_2	2.86 ± 0.28 ^{c,d}	1.44 ± 0.21 ^{c}
R2 60 °C	1.83 ± 0.52 ^{a,b,c}	0.71 ± 0.30 ^{b,c,d}	R2 lac	2.58 ± 0.40 ^{c,d}	1.19 ± 0.13 ^{b,c}	R2 H_2O_2	5.1 ± 0.19 ^{b}	2.65 ± 0.74 ^{b}
R3 60 °C	2.59 ± 0.32 ^{a}	1.02 ± 0.10 ^{a,b}	R3 lac	5.47 ± 0.82 ^{a}	1.9 ± 0.50 ^{a}	R3 H_2O_2	3.74 ± 0.05 ^{b,c}	2.35 ± 0.17 ^{b,c}
R4 60 °C	1.07 ± 0.09 ^{c,d}	0.54 ± 0.11 ^{c,d}	R4 lac	1.2 ± 0.04 ^{e,f}	0.77 ± 0.09 ^{b,c,d}	R4 H_2O_2	5.33 ± 0.77 ^{b}	2.9 ± 0.12 ^{b}
R5 60 °C	2.14 ± 0.10 ^{a,b}	0.93 ± 0.11 ^{a,b,c}	R5 lac	1.4 ± 0.05 ^{e,f}	0.8 ± 0.05 ^{b,c,d}	R5 H_2O_2	4.89 ± 0.89 ^{b}	2.4 ± 0.14 ^{b,c}
R6 60 °C	0.87 ± 0.21 ^{c,d}	0.33 ± 0.12 ^{d}	R6 lac	1.85 ± 0.11 ^{d,e}	0.57 ± 0.13 ^{c,d}	R6 H_2O_2	1.69 ± 0.58 ^{d}	0.25 ± 0.08 ^{d}
R7 60 °C	2.4 ± 0.24 ^{a,b}	0.86 ± 0.02 ^{a,b,c}	R7 lac	4.2 ± 0.09 ^{b}	2 ± 0.08 ^{a}	R7 H_2O_2	8.55 ± 0.19 ^{a}	2.72 ± 0.09 ^{b}
R8 60 °C	0.7 ± 0.11 ^{d}	0.37 ± 0.06 ^{d}	R8 lac	0.38 ± 0.10 ^{f}	0.17 ± 0.03 ^{d}	R8 H_2O_2	9.32 ± 0.25 ^{a}	4 ± 0.15 ^{a}
R9 60 °C	1.61 ± 0.43 ^{b,c,d}	0.89 ± 0.01 ^{a,b,c}	R9 lac	1 ± 0.05 ^{e,f}	0.54 ± 0.01 ^{c,d}	R9 H_2O_2	1.69 ± 0.05 ^{d}	0.22 ± 0.06 ^{d}

Oxidation mechanisms in wine start with oxygen activation by metal catalysis (Fe or Cu), inducing radicals named reactive oxygen species (ROS). Quinones are then formed as well as hydrogen peroxide, both capable of reacting with several other wine compounds [5,11,17]. Consequently, a decrease in the dissolved oxygen concentration is systematically observed and the measure of this reflects the evolution of wine oxidative kinetics [8,11].

Experiments were carried out in hermetic culture tubes with minimum headspace. It was previously shown that this procedure allowed a headspace volume between 0 µL and 120 µL [8], and so oxygen ingress through the cap was negligible and only evolution of dissolved oxygen in wine was considered during the time of the experiment. Oxygen consumption parameters are summarized in Table 2. Important differences were observed between wines both for initial and average O_2 rates. Values ranged from 0.17 ppm·h^{-1} (R8 lac) to 4 ppm·h^{-1} (R8 H_2O_2) for average O_2 rates and from 0.38 ppm·h^{-1} (R8 lac) to 9.32 ppm·h^{-1} (R8 H_2O_2) for initial O_2 rates. The wines can have completely opposite behaviors towards the oxidation process. R9 and R7 wines showed similar rates around 1 ppm·h^{-1} whatever the oxidation protocol, whereas R8 and R4 wines also had low consumption rates less or around 1 ppm·h^{-1} for temperature and enzymatic tests but were among the highest rates for chemical oxidation (9.32 and 5.33 ppm·h^{-1} respectively). Globally, chemical oxidation using H_2O_2 showed the equal highest oxygen consumption rates for all considered samples except for R1 and R3, for which enzymatic oxidation (using laccase) showed the highest consumption rates.

Several factors can influence the oxygen consumption rates of wine as pH, ascorbic acid concentration or metals concentration [8,13] pH, and also copper and iron concentrations, are shown in the supplementary data, all play a part in oxygen consumption during experiments. For example, R8, which had the highest metals concentrations, very quickly consumed oxygen when it was oxidized adding H_2O_2 compared to other samples (Table 2). On the contrary, R6 had the lowest metal concentrations and was globally oxidized slower than other samples whatever the considered oxidation protocol. However, it is difficult to conclude on a clear relation between OCRs and the above variables, metals concentrations not completely reflecting the fraction involved in oxidation reactions [13,26,40,41].

As an antioxidant, SO_2 can affect oxygen consumption kinetics during accelerated ageing tests. Free SO_2 values are available in the supplementary data (Tables S1 and S2) and were measured after oxygen saturation (before oxidation) and after the different controlled oxidations. Chemical and temperature tests completely consumed available free SO_2 (if available after saturation) whatever the initial concentration, this latter having consequently a limited impact on OCRs. This decay in SO_2 was primarily due to its reaction with the quinones and H_2O_2 deriving from oxidation of phenolics [42]. Concerning enzymatic oxidation, all the available SO_2 was not systematically consumed. However, R3 and R7

samples were statistically the ones with highest OCR_{lac} (initial and average) but these two samples presented no available free SO_2 before enzymatic oxidation. Consequently, it can be hypothesized that free SO_2 content had no impact on enzymatic oxidation.

Several factors can be responsible for SO_2 consumption as ascorbic acid concentration [43] or sulfonation reactions [44]. Even if a theoretical molar reaction ratio of 2:1 (SO_2/O_2) should be expected [7], it is generally not observed. Recent studies showed that such a molar ratio can hardly be applied to a complex media such as wine [9,45]. Indeed, SO_2 does not directly react with oxygen and other chemical species are involved and other strong reductants can compete with it, as recently observed by Ferreira et al. [8]. For certain wines, oxygen consumption might be really fast but not result in immediate SO_2 loss, other highly reactive reductants can consume O_2 with no involvement of SO_2.

3.3. Electrochemical Behavior of Standard Polyphenols and Wine Samples Oxidized with the Three Different Protocols

3.3.1. Electrochemical Behavior of Standard Polyphenols

Figure 2 represents the cyclic voltammograms of representative wine polyphenols (flavanol, hydroxycinnamic acid, benzoic acid, anthocyanin and flavonol) in model wine solutions using single-walled carbon nanotube (SWCNT) electrodes. The corresponding anodic (oxidation) peak potentials are given in Table 3. Only one anodic peak was present for caffeic acid at a potential of 166 mV, whereas for catechin and gallic acid two peaks were present with a potential of 151 mV for the first one (Ep,a_1). This is attributed to the oxidation of hydroxyl groups (on B-ring for catechin) into corresponding *ortho*-quinones [19,46,47]. The formed *ortho*-quinones can be reduced on the reverse scan generating a well-defined cathodic peak as, for example, for caffeic acid (Figure 2b). The second anodic peak observed only for catechin and gallic acid (Ep,a_2 = 476 mV) corresponded to the oxidation of catechin A-ring hydroxyl group [48] and to the oxidation of the third phenol group adjacent to the *ortho*-diphenol group in gallic acid [49]. For quercetin, only one peak at low potential (166 mV) was present and the second peak was not clearly observable. At last, concerning anthocyanins, electrochemical behavior of oenin chloride in model wine was also investigated showing only one peak at 398 mV. Oenin chloride revealed that anthocyanins tend to be less easily oxidizable compounds than other phenolic compounds.

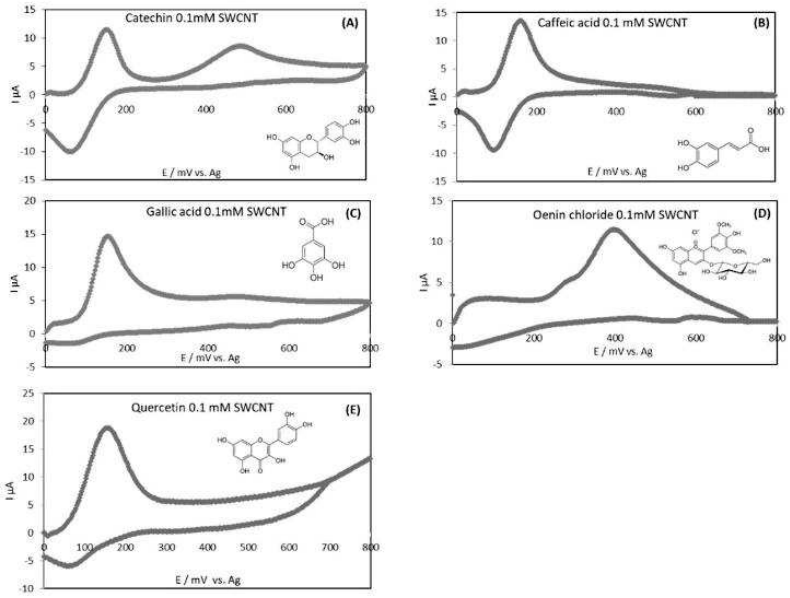

Figure 2. Cyclic voltammograms of different standard polyphenols at SWCNT-SCPE: catechin (**A**); caffeic acid (**B**); gallic acid (**C**); oenin chloride (**D**) and quercetin (**E**) at a concentration of 0.1 mM (blank subtracted); SWCNT-SPCE: single walled carbon nanotubes modified screen printed carbon electrodes.

Table 3. Voltammetric peak potentials of the standard polyphenols (concentration of 0.1 mM) in model wine solution (pH 3.6) using SWCNT-SPCE. Ep,a_1 represents the potential of the first anodic peak and Ep,a_2 represents the potential of the second anodic peak.

Standards	Potential (mV) SWCNT-SPCE (vs. $Ag_{(s)}$)	
	Ep,a_1	Ep,a_2
Catechin	151	476
Caffeic acid	166	/
Gallic acid	154	476
Oenin chloride	398	/
Quercetin	151	/

The classification obtained considering only the first peak potential for the studied standards at equal concentration (0.1 mM) by increasing potential was as follows: quercetin 151 mV/catechin 151 mV < gallic acid 154 mV < caffeic acid 166 mV < oenin chloride 398 mV and revealed the ability of the compounds to oxidize at different potentials. These potentials depend on a molecule structure's chemical reactivity. This ranking appears to be logical when considering substituents to catechol groups. An electro donating group reduces potential values while electro accepting groups (as carboxyl) tend to increase potential values. Moreover, it is noteworthy that the galloyl substitution of gallic acid is more oxidizable than the catechol group of caffeic acid [33].

3.3.2. Electrochemical Behavior of Wines Non-Oxidized and Oxidized with Different Oxidation Protocols

Electrochemical methods, and in particular cyclic voltammetry (CV), involve mechanisms similar to those occurring in wines [20]. CV is consequently of major interest in order to study wine oxidation. It has already been applied to the study of white wine oxidation [26,50,51] and recently, carbon-based screen printed sensors turned out to be a rapid and reproducible device for the analysis of polyphenols [52] and wine components. They give access to voltammograms resulting from the current responses from a large number of polyphenols.

Values in Table 4 showed the high variability in anodic current measurements through the resulting calculated charges, depending on each wine. Wine samples were increasingly diluted (in model wine solution) from 1/100 to 1/10 and acquisitions were performed on 1/75 diluted samples. This dilution allowed for the linear part of the total charge response as a function of wine concentration. Moreover, experiments were performed on wines diluted 75 times in order to discard free SO_2 influence in anodic reactions (oxidation) [53]. Indeed, with higher SO_2 contents, semi quinone radicals formed during electrochemical oxidation can react, leading to quinone reduction back to the original polyphenol [54]. Further reactions could also take place as the formation of sulfonic acid derivatives, disrupting CV results by increasing anodic peak intensity and also decreasing the cathodic peak intensity [54].

Voltammetric experiments were carried out for all reference wines as well as all oxidation protocols. Cyclic voltammograms showed for each sample three peaks at approximately the same potentials: around 220, 480 and 700 mV. Reverse cathodic peak was also observed. An example of obtained cyclic voltammograms for the reference R2 wine and the three accelerated protocols (blank subtracted) is presented in Figure 3.

Table 4. Charges (Q) for reference (non-oxidized) wines (blanck substracted) and difference of charges (ΔQ) between reference wines and oxidized wines with three different accelerated protocols (60 °C, laccase and H_2O_2). Q and ΔQ are expressed in μC. Different letters indicate the significant differences between samples in one column according to Tukey's test, $p < 0.05$.

A		Q_{240mV}	Q_{520mV}	$Q_{520mV}-Q_{240mV}$	Q_{240mV}/Q_{800mV}	Q_{800mV}
R1		7.64 ± 0.76^{d}	20.49 ± 1.74^{d}	12.83 ± 1.12^{e}	$0.21 \pm 0.03^{b,c}$	37.30 ± 1.98^{e}
R2		7.42 ± 1.26^{d}	26.11 ± 2.23^{d}	$18.54 \pm 1.01^{d,e}$	$0.15 \pm 0.02^{c,d}$	$50.25 \pm 3.21^{c,d,e}$
R3		$9.67 \pm 1.55^{c,d}$	27.62 ± 3.32^{d}	$17.94 \pm 1.67^{d,e}$	$0.23 \pm 0.06^{b,c}$	42.57 ± 3.87^{e}
R4		19.00 ± 5.41^{b}	$46.00 \pm 3.02^{b,c}$	$27.96 \pm 2.21^{b,c}$	$0.29 \pm 0.03^{a,b}$	$65.11 \pm 12.92^{b,c,d}$
R5		$16.21 \pm 1.93^{b,c}$	38.25 ± 0.29^{c}	$22.04 \pm 1.42^{c,d}$	0.38 ± 0.01^{a}	$43.29 \pm 6.78^{d,e}$
R6		20.73 ± 0.46^{b}	51.30 ± 4.36^{b}	30.55 ± 3.62^{b}	$0.31 \pm 0.01^{a,b}$	$67.75 \pm 0.96^{b,c}$
R7		3.60 ± 0.74^{d}	17.93 ± 1.82^{d}	14.33 ± 1.07^{e}	0.09 ± 0.01^{d}	37.75 ± 6.28^{e}
R8		29.28 ± 2.77^{a}	96.52 ± 1.12^{a}	69.71 ± 0.87^{a}	$0.30 \pm 0.03^{a,b}$	99.00 ± 1.88^{a}
R9		$10.67 \pm 2.13^{c,d}$	38.98 ± 4.40^{c}	$28.31 \pm 2.25^{b,c}$	$0.14 \pm 0.04^{c,d}$	$75.98 \pm 8.51^{a,b}$
B		ΔQ_{240mV}	ΔQ_{520mV}	$\Delta(Q_{520mV}-Q_{240mV})$	$\Delta(Q_{240mV}/Q_{800mV})$	ΔQ_{800mV}
R1	60 °C	0^{f}	0^{d}	0^{f}	0^{a}	0^{d}
R2	60 °C	$8.20 \pm 0.86^{b,c}$	17.30 ± 0.87^{c}	9.11 ± 0.01^{d}	0.34 ± 0.03^{a}	24.11 ± 0.10^{b}
R3	60 °C	$0.56 \pm 0.53^{e,f}$	3.88 ± 0.46^{d}	3.35 ± 0.07^{e}	0.05 ± 0.05^{a}	$10.62 \pm 0.8^{c,d}$
R4	60 °C	10.70 ± 0.37^{b}	70.20 ± 0.56^{a}	59.53 ± 0.19^{a}	0.24 ± 0.01^{a}	44.32 ± 0.50^{a}
R5	60 °C	$3.36 \pm 2.05^{d,e}$	5.50 ± 4.91^{d}	$2.13 \pm 2.87^{e,f}$	0.52 ± 0.60^{a}	11.70 ± 7.22^{c}
R6	60 °C	10.56 ± 1.06^{b}	23.80 ± 1.64^{b}	13.24 ± 0.58^{c}	0.40 ± 0.03^{a}	26.42 ± 4.41^{b}
R7	60 °C	0^{f}	2.35 ± 1.09^{d}	$2.34 \pm 1.02^{e,f}$	0^{a}	$4.61 \pm 1.12^{c,d}$
R8	60 °C	23.22 ± 1.66^{a}	49.04 ± 6.16^{a}	50.23 ± 0.82^{b}	0.48 ± 0.03^{a}	73.45 ± 2.48^{a}
R9	60 °C	$5.64 \pm 1.06^{c,d}$	16.27 ± 2.15^{c}	$10.64 \pm 1.09^{c,d}$	0.17 ± 0.02^{a}	31.98 ± 5.26^{b}
C		ΔQ_{240mV}	ΔQ_{520mV}	$\Delta(Q_{520mV}-Q_{240mV})$	$\Delta(Q_{240mV}/Q_{800mV})$	ΔQ_{800mV}
R1	Lac.	$3.37 \pm 0.60^{c,d,e}$	$5.74 \pm 1.59^{d,e}$	$2.36 \pm 1.00^{d,e}$	$0.30 \pm 0.09^{a,b}$	11.37 ± 1.48^{c}
R2	Lac.	0.22 ± 0.17^{e}	$0.61 \pm 0.24^{e,f}$	0.40 ± 0.08^{e}	0.02 ± 0.01^{c}	9.49 ± 2.47^{c}
R3	Lac.	0^{e}	0^{f}	0^{e}	0^{c}	1.61 ± 0.53^{c}
R4	Lac.	$2.05 \pm 0.13^{d,e}$	$1.48 \pm 0.52^{e,f}$	0^{e}	0.47 ± 0.19^{a}	4.93 ± 2.11^{c}
R5	Lac.	5.88 ± 1.69^{c}	8.92 ± 2.63^{d}	$3.04 \pm 0.94^{d,e}$	0.41 ± 0.03^{a}	14.15 ± 3.04^{c}
R6	Lac.	11.80 ± 1.29^{b}	32.31 ± 1.48^{b}	20.50 ± 0.22^{b}	0.40 ± 0.02^{a}	29.13 ± 1.43^{b}
R7	Lac.	0.63 ± 0.51^{e}	$4.68 \pm 1.63^{d,e,f}$	4.03 ± 1.12^{d}	0.05 ± 0.03^{c}	12.18 ± 4.83^{c}
R8	Lac.	22.80 ± 2.31^{a}	46.31 ± 8.55^{a}	48.78 ± 1.59^{a}	0.50 ± 0.04^{a}	71.58 ± 0.72^{a}
R9	Lac.	$5.70 \pm 2.09^{c,d}$	16.43 ± 4.40^{c}	10.73 ± 2.31^{c}	$0.18 \pm 0.02^{b,c}$	31.49 ± 8.20^{b}
D		ΔQ_{240mV}	ΔQ_{520mV}	$\Delta(Q_{520mV}-Q_{240mV})$	$\Delta(Q_{240mV}/Q_{800mV})$	ΔQ_{800mV}
R1	H_2O_2	$3.29 \pm 0.13^{c,d}$	$5.73 \pm 0.08^{c,d,e}$	$2.45 \pm 0.05^{b,c}$	0.07 ± 0.01^{a}	45.39 ± 2.64^{a}
R2	H_2O_2	$1.45 \pm 0.04^{d,e}$	$4.05 \pm 1.08^{d,e,f}$	2.7 ± 0.88^{b}	0.55 ± 0.58^{a}	$5.28 \pm 4.12^{c,d}$
R3	H_2O_2	$3.66 \pm 0.88^{b,c}$	$9.56 \pm 1.13^{b,c}$	5.87 ± 0.25^{a}	0.18 ± 0.03^{a}	19.77 ± 1.81^{b}
R4	H_2O_2	$2.22 \pm 0.32^{c,d}$	$8.13 \pm 0.56^{b,c,d}$	5.91 ± 0.23^{a}	0.16 ± 0.08^{a}	$17.22 \pm 9.48^{b,c}$
R5	H_2O_2	$2.68 \pm 0.89^{c,d}$	$5.36 \pm 2.49^{c,d,e}$	2.68 ± 1.57^{b}	0.11 ± 0.03^{a}	23.75 ± 0.53^{b}
R6	H_2O_2	13.11 ± 1.46^{a}	15.50 ± 3.31^{a}	$2.39 \pm 1.85^{b,c}$	0.30 ± 0.01^{a}	43.27 ± 6.75^{a}
R7	H_2O_2	0^{e}	$1.35 \pm 0.19^{e,f}$	$1.35 \pm 0.19^{b,c}$	0^{a}	$3.77 \pm 1.45^{c,d}$
R8	H_2O_2	0^{e}	0^{f}	0^{c}	0^{a}	0^{d}
R9	H_2O_2	5.72 ± 1.03^{b}	$11.92 \pm 1.90^{a,b}$	6.20 ± 0.87^{a}	0.39 ± 0.09^{a}	$15.59 \pm 5.98^{b,c}$

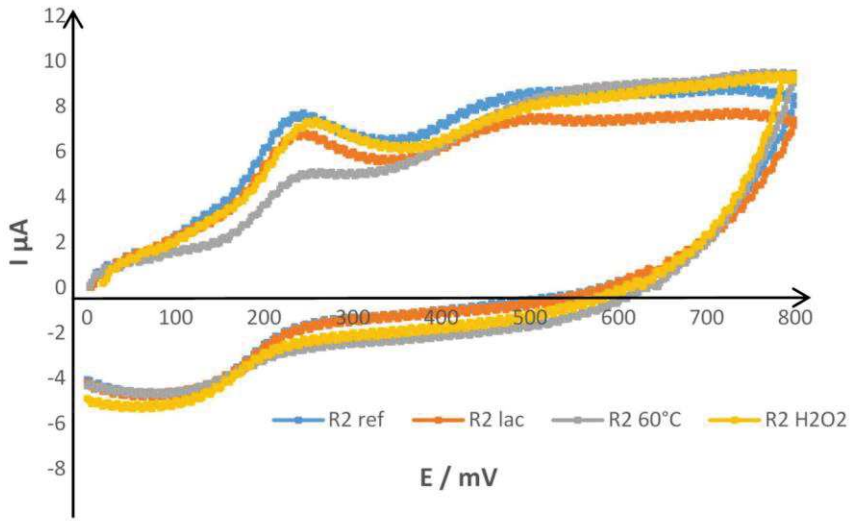

Figure 3. Cyclic voltammograms of R2 wine non-oxidized (ref) and oxidized with three different protocols: temperature (60 °C), chemical (H_2O_2) and enzymatic (laccase) with SWCNT.

The first oxidation peak can be assigned to the most oxidizable compounds as catechin-type flavonoids [52], including oligomers and polymers, caffeic acid and derivatives, flavonols containing a catechol or a galloyl group (Table 3). As described by Newair et al. [33], red wines contain high concentrations of flavan-3-ols, caffeic acid and gallic acid, all responsible for the first anodic peak intensity.

The second peak on the voltammograms at around 520 mV could correspond to overlaps [53] mainly resulting from the malvidin anthocyanins oxidation as well as to the second oxidation of catechin type flavanols and galloyl containing compounds (Table 3). Ferulic acid and trans resveratrol or similar polyphenols could also interact [18].

Concerning the third peak, its presence was less marked on the voltammograms and can corresponds to the oxidation of phenolic compounds with high oxidation potentials, such as para-coumaric or vanillic acids [19,55,56]. The presence of a cathodic peak on the reverse scan on the voltammograms is noteworthy.

As mentioned previously, differences between wines were mainly notables on intensities on cyclic voltammograms. In addition to that, oxidized wine intensities on voltammograms were almost equal or inferior to the reference ones corresponding, reflecting the oxidation protocol impact on the oxidizable compound content in the sample. For example, concerning the R2 wine in Figure 3 representing cyclic voltammograms for reference wine and three accelerated protocols, enzymatic and chemical oxidation protocols appeared to have a moderate impact on the wine compared to temperature oxidation, with the latter having the most important one.

3.3.3. Charges of Non-Oxidized Red Wines and Charge Variation after Accelerated Ageing Tests

The different charges extracted from voltammograms and corresponding to the area under the anodic curve until the given potential value shown in Table 4 allow us to illustrate the polyphenol's capacity to be oxidized at the working electrode [52]. The total charge Q_{800mV} corresponds to all oxidizable phenolic compounds that will contribute to the total antioxidant capacity of the wine sample. Q_{240mV} represents the electrochemical charge of the most easily oxidizable polyphenols (generally hydroxyl group oxidation into quinones for flavan-3-ols, phenol acids and flavonols) that have consequently the highest antioxidant capacity. Q_{520mV} estimates the charge of the compounds which oxidize until 520 mV (the major part). In addition to that, the difference (Q_{520mV}–Q_{240mV}) gives the charge of the compounds that correspond to the second oxidation peak on the voltammograms, whereas

the ratio Q_{240mV}/Q_{800mV} illustrates the contribution of the most antioxidant compounds to the total antioxidant capacity of the wine.

For the reference wines (Table 4A), the charges (Q) values were extracted from voltammograms with blank subtracted (model wine solution), whereas for the oxidized wine samples (Table 4B–D), the difference of charges (ΔQ) values were extracted from voltammograms corresponding to oxidized wines with reference wine subtracted in order to obtain values representing only oxidized compounds.

For non-oxidized wines the obtained charges values (Q_{240mV}, Q_{520mV} and Q_{800mV}) were very different (Table 4A). The lowest values for the charges were observed for R7 wine and these weak values were in accordance with its phenolic and total tannins contents which were also the lowest ones (Table 1). On the opposite end, the highest values were observed for R8 wine which presents a significantly high content of polyphenols and tannins, compared to other wines.

Values in Table 4B–D were those of reference wines minus oxidized wines (ΔQ) in order to take into consideration only oxidation effect. As described by previous researchers [18–20], the majority of compounds involved in wine oxidation reactions (phenolic compounds, ascorbic acid) are able to oxidize at the surface of an electrode and therefore can be analyzed using voltammetric methods. A comparison of oxidized wines with their corresponding non-oxidized ones (subtractive approach) can provide additional information on global wine oxidation. Indeed, due to the numerous simultaneous voltammetric signals occurring during wine analysis, this method is unable to provide specific information on individual wine components.

Interestingly, charge differences (ΔQ) of subtractive voltammograms were also strongly wine-dependent, which provides interesting information on chemical reactions involving the major wine oxidizable compounds during oxygen consumption. Some wines showed important current decrease at 240 mV and consequently high values of difference of charge. It was the case for R8 wine oxidized with laccases or at 60 °C or R6 wine for all oxidation types. It revealed that they contained oxidizable species which were easily degraded upon oxygen consumption. On the other hand, other wines showed opposite behavior, as for R7 wine oxidized with H_2O_2 or at 60 °C. Moreover, the different values of $\Delta(Q_{520mV}-Q_{240mV})$ indicated that oxidation also induced changes in less easily oxidizable compounds.

All these measurements were also very different depending on the considered oxidation protocol, as for R2 wine values, which were among the highest ones with temperature oxidation and among the lowest ones with laccase or H_2O_2 oxidation protocols, whereas R1 wine showed opposite trends for the same protocols. These results are in accordance with the influence of wine composition on its oxidation ability.

It is noteworthy that even older wines (R2 and R3 were respectively from 2014 and 2010) contain oxidizable compounds and can undergo further oxidations. Hydrogen peroxide had an impact on them whereas R7 and R8 wines were very little impacted. On the contrary, enzymatic oxidation had a negligible impact on them. Temperature oxidation impacts R2 and R3 wines whereas it was not true for R1 wine (2018 Syrah wine). Even if oxidation phenomena are strongly wine dependent, these results can suggest that oxidation reactions lead to the formation of different products which are able to further oxidize themselves.

3.4. Correlation between Phenolic Composition, Oxygen Consumption Rates and Electrochemical Parameters

Table 5 represents the Pearson correlation matrix between electrochemical parameters for non-oxidized wines and for all accelerated ageing tests (H_2O_2, laccase and at 60 °C), OCRs (initial and average oxygen consumption rate) and wine composition (tannins, polyphenols, total pigments, and SO_2 bleaching resistant pigments).

Table 5. Pearson's correlation coefficients between electrochemical parameters, phenolic composition, and oxygen consumption rates. * (in green) represents significance at $p \leq 0.05$ and ** (in red) represent significance at $p \leq 0.01$.

	Folin TPC	TC	TP	RP	$Q_{240mV\ ref}$	$Q_{520mV\ ref}$	$Q_{520mV-240mV\ ref}$	$Q_{240/800mV\ ref}$	$Q_{800mV\ ref}$	$\Delta Q_{240mV\ H2O2}$	$\Delta Q_{520mV\ H2O2}$	$\Delta(Q_{520mV-240mV})_{H2O2}$	$Q_{240/800mV\ H2O2}$	$\Delta Q_{800mV\ H2O2}$
Folin TPC	**1.00**	**0.91 ****	−0.08	0.26	**0.86 ****	**0.80 ****	0.74 *	0.53	0.74 *	0.31	0.29	0.09	0.00	0.06
TC		**1.00**	−0.15	0.36	0.72 *	0.69 *	0.65	0.33	0.73 *	0.25	0.36	0.37	0.14	−0.07
TP			**1.00**	0.72 *	−0.10	0.09	0.18	−0.49	0.21	−0.26	−0.25	−0.09	−0.35	−0.06
RP				**1.00**	0.10	0.32	0.41	−0.40	0.45	−0.45	−0.29	0.18	−0.06	−0.38
$Q_{240mV\ ref}$					**1.00**	**0.94 ****	**0.87 ****	0.66	**0.80 ****	0.18	0.03	−0.25	−0.23	−0.03
$Q_{520mV\ ref}$						**1.00**	**0.99 ****	0.43	**0.90 ****	0.00	−0.16	−0.35	−0.23	−0.27
$Q_{520mV-240mV\ ref}$							**1.00**	0.31	**0.90 ****	−0.08	−0.24	−0.39	−0.23	−0.37
$Q_{240/800mV\ ref}$								**1.00**	0.09	0.14	0.00	−0.25	−0.35	0.31
$Q_{800mV\ ref}$									**1.00**	0.14	0.07	−0.09	0.07	−0.30
$\Delta Q_{240mV\ H2O2}$										**1.00**	**0.90 ****	0.21	0.37	0.70 *
$\Delta Q_{520mV\ H2O2}$											**1.00**	0.62	0.47	0.63
$\Delta(Q_{520mV-240mV})_{H2O2}$												**1.00**	0.39	0.14
$\Delta Q_{240/800mV\ H2O2}$													**1.00**	0.00
$\Delta Q_{800mV\ H2O2}$														**1.00**

	$\Delta Q_{240mV\ lac}$	$\Delta Q_{520mV\ lac}$	$\Delta(Q_{520mV-240mV})_{lac}$	$\Delta Q_{240/800mV\ lac}$	$\Delta Q_{800mV\ lac}$	$\Delta Q_{240mV\ 60°C}$	$\Delta Q_{520mV\ 60°C}$	$\Delta(Q_{520mV-240mV})_{60°C}$	$\Delta Q_{240/800mV\ 60°C}$	$\Delta Q_{800mV\ 60°C}$	aOCR H_2O_2	aOCR lac	aOCR 60 °C	iOCR H_2O_2	iOCR lac	iOCR 60 °C
Folin TPC	0.71 *	0.65	0.53	0.62	0.58	0.67 *	0.55	0.49	0.66	0.65	0.02	−0.77 *	−0.49	−0.12	−0.58	−0.63
TC	0.49	0.48	0.33	0.40	0.39	0.63	0.63	0.60	0.43	0.74 *	0.06	−0.61	−0.48	−0.15	−0.43	−0.60
TP	0.23	0.26	−0.49	0.10	0.43	−0.03	−0.03	−0.02	−0.35	−0.03	−0.10	−0.15	0.36	0.08	−0.22	0.07
RP	0.24	0.29	−0.40	0.02	0.36	0.26	0.29	0.28	−0.15	0.35	0.23	−0.27	0.21	0.14	−0.27	−0.06
$Q_{240mV\ ref}$	**0.86 ****	**0.81 ****	0.66	**0.83 ****	0.65	**0.87 ****	**0.80 ****	0.73 *	0.74 *	0.76 *	0.25	**−0.82 ****	−0.75 *	0.21	−0.71 *	**−0.84 ****
$Q_{520mV\ ref}$	**0,93 ****	**0.92 ****	0.43	0.69 *	0.79 *	**0.94 ****	**0.81 ****	0.72 *	0.66	**0.80 ****	0.36	−0.79 *	−0.72 *	0.38	−0.69 *	**−0.82 ****
$Q_{520mV-240mV\ ref}$	**0.93 ****	**0.94 ****	0.31	0.59	**0.83 ****	**0.93 ****	0.78 *	0.68 *	0.60	0.78 *	0.40	−0.74 *	−0.68 *	0.44	−0.65	−0.77 *
$Q_{240/800mV\ ref}$	0.39	0.28	**1.00 ****	0.68 *	0.02	0.34	0.34	0.32	0.62	0.16	0.28	−0.33	−0.33	0.11	−0.25	−0.31
$Q_{800mV\ ref}$	**0.81 ****	**0.82 ****	0.09	0.54	**0.83 ****	**0.90 ****	0.79 *	0.71 *	0.53	**0.91 ****	0.10	**−0.84 ****	−0.74 *	0.16	−0.76 *	**−0.88 ****
$\Delta Q_{240mV\ H2O2}$	0.13	0.08	0.14	0.17	0.20	−0.02	−0.16	−0.20	0.15	0.02	**−0.84 ****	−0.28	−0.27	−0.77 *	−0.10	−0.31
$\Delta Q_{520mV\ H2O2}$	−0.14	−0.19	0.00	0.04	−0.04	−0.18	−0.16	−0.15	−0.03	0.05	**−0.84 ****	−0.17	−0.10	**−0.88 ****	−0.02	−0.17
$\Delta(Q_{520mV-240mV})_{H2O2}$	−0.55	−0.57	−0.25	−0.23	−0.45	−0.35	−0.08	0.02	−0.34	0.07	−0.36	0.12	0.27	−0.59	0.14	0.17
$\Delta Q_{240/800mV\ H2O2}$	−0.28	−0.28	−0.35	−0.38	−0.08	−0.01	−0.14	−0.18	0.16	0.17	−0.44	−0.14	−0.12	−0.55	−0.10	−0.11
$\Delta Q_{800mV\ H2O2}$	−0.09	−0.19	0.31	0.26	−0.15	−0.35	−0.36	−0.34	−0.13	−0.40	−0.70 *	−0.02	0.26	−0.75 *	0.11	0.10

Table 5. *Cont.*

	$\Delta Q_{240mV\ lac}$	$\Delta Q_{520mV\ lac}$	$\Delta(Q_{520mV}-Q_{240mV})_{lac}$	$\Delta Q_{240/800mV\ lac}$	$\Delta Q_{800mV\ lac}$	$\Delta Q_{240mV\ 60°C}$	$\Delta Q_{520mV\ 60°C}$	$\Delta(Q_{520mV}-Q_{240mV})_{60°C}$	$\Delta Q_{240/800mV\ 60°C}$	$\Delta Q_{800mV\ 60°C}$	aOCR H_2O_2	aOCR lac	aOCR 60 °C	iOCR H_2O_2	iOCR lac	iOCR 60 °C
$\Delta Q_{240mV\ lac}$	**1.00**	**0.99** **	0.39	0.68 *	**0.91** **	**0.83** **	0.59	0.48	0.63	0.59	0.17	−0.77 *	−0.62	0.29	−0.66	−0.74 *
$\Delta Q_{520mV\ lac}$		**1.00**	0.28	0.58	**0.92** **	**0.84** **	0.59	0.47	0.55	0.60	0.21	−0.70 *	−0.63	0.36	−0.59	−0.72 *
$\Delta Q_{(520mV-Q_{240mV})lac}$			**1.00**	0.68 *	0.02	0.34	0.34	0.32	0.62	0.16	0.28	−0.33	−0.33	0.11	−0.25	−0.31
$\Delta Q_{240/800mV\ lac}$				**1.00**	0.48	0.61	0.65	0.63	0.60	0.53	0.10	−0.77 *	−0.48	0.08	−0.76 *	−0.70 *
$\Delta Q_{800mV\ lac}$					**1.00**	0.72 *	0.43	0.31	0.50	0.55	−0.06	−0.75 *	−0.54	0.16	−0.67 *	−0.68 *
$\Delta Q_{240mV\ 60°C}$						**1.00**	**0.88** **	0.79 *	0.68 *	**0.89** **	0.39	−0.79 *	**−0.83** **	0.39	−0.72 *	**−0.90** **
$\Delta Q_{520mV\ 60°C}$							**1.00**	**0.99** **	0.46	**0.92** **	0.48	−0.66	−0.75 *	0.41	−0.66	**−0.84** **
$\Delta(Q_{520mV}-Q_{240mV})_{60°C}$								**1.00**	0.36	**0.88** **	0.49	−0.58	−0.68 *	0.40	−0.60	−0.78 *
$\Delta Q_{240/800mV\ 60°C}$									**1.00**	0.55	0.19	−0.76 *	−0.65	0.14	−0.73 *	−0.64
$\Delta Q_{800mV\ 60°C}$										**1.00**	0.26	−0.78 *	−0.79 *	0.21	−0.75 *	**−0.89** **
aOCR H_2O_2											**1.00**	0.07	−0.17	**0.89** **	−0.03	−0.05
aOCR lac												**1.00**	0.62	0.08	**0.95** **	**0.85** **
aOCR 60 °C													**1.00**	−0.27	0.57	**0.90** **
iOCR H_2O_2														**1.00**	−0.06	−0.10
iOCR lac															**1.00**	**0.80** **
iOCR 60 °C																**1.00**

Concerning the phenolic composition, the charges $Q_{240mV\ ref}$ and $Q_{520mV\ ref}$ were well correlated with TPC (itself well correlated with TC (R = 0.91)) with R = 0.86 and 0.80 respectively. A better correlation between TPC and the total charge $Q_{800mV\ ref}$ could have been expected since the Folin–Ciocalteu test (TPC) is a global method for which all hydroxyl groups that are able to react with the F-C reagent are implied [34]. These three charges were also well correlated with the values of their corresponding difference of charge at the same potential for enzymatic and temperature oxidation tests, while no correlation was observed with chemical oxidation using hydrogen peroxide. The fact that the calculated charges of non-oxidized (reference) wines, in accordance with its oxidability, presented high correlations with the difference of the charges for enzymatic as well as temperature oxidized wines (reference subtracted) emphasizes that cyclic voltammetry can partly predict these two oxidation tests and reflects the wine sensitivity towards respective oxidation targets. However, it is not possible to predict the wine chemical oxidation test using hydrogen peroxide. These last results are in accordance with the good negative correlations between the oxygen consumption rates and the charges of the reference wines: between $aOCR_{lac}$ and $Q_{240mV\ ref}$ (R = −0.82) or $Q_{800mV\ ref}$ (R = −0.84), and between $iOCR_{60°C}$ and $Q_{240mV\ ref}$, $Q_{520mV\ ref}$ and $Q_{800mV\ ref}$ (R = −0.84; −0.82 and −0.88 respectively).

Considering the parameters related to oxygen consumption kinetics, for a same oxidation test, iOCR was highly correlated with aOCR: $R(iOCR_{60°C}/aOCR_{60°C})$ = 0.89; $R(iOCR_{lac}/aOCR_{lac})$ = 0.95 and $R(iOCR_{H2O2}/aOCR_{H2O2})$ = 0.90. These results are in accordance with previous studies studying OCR of oxygen saturated white wines [26]. It is worth mentioning that OCRs for enzymatic by laccase and temperature at 60 °C oxidations were partly correlated to each other ($iOCR_{60°C}$ correlated with $aOCR_{lac}$ and $iOCR_{lac}$ with respectively R = 0.85 and 0.80).

Concerning the relation between OCRs and the differences of charges (ΔQ) for oxidized wines, strong negative correlations were observed for the temperature oxidation between the oxygen consumption rates and the charge at low potential $\Delta Q_{240mV\ 60°C}$ as well as the total charge $\Delta Q_{800mV\ 60°C}$ and more particularly for $iOCR_{60°C}$. For the laccase oxidation test, less robust correlations were obtained.

Kinetic parameters for the H_2O_2 ageing test ($iOCR_{H2O2}$ or $aOCR_{H2O2}$) were not correlated with the electrochemical parameters of reference wines but showed a high negative correlation with $\Delta Q_{520mV\ H2O2}$ with R = −0.88 and −0.84, respectively (R = −0.84 between $aOCR_{H2O2}$ and $\Delta Q_{520mV\ H2O2}$).

3.5. Principal Component Analysis

Principal component analysis (PCA) was used in this work in order to classify wines. Factor analysis was calculated with the same parameters as the ones used for Pearson's correlation in Table 5. Figure 4 shows the plots of loadings and scores in the space described by the 1st and 2nd factors.

The first factor explains 51.19% of the total data variability and it is mainly related to the richness in polyphenols and tannins (TPC and TC) and to the electrochemical parameters for non-oxidized wines, enzymatic and temperature oxidations, and their respective OCRs. It allows us to distinguish red wine samples depending on their oxidation rates with laccases or at 60 °C. Indeed, the first factor is positively correlated with electrochemical parameters, TPC and TC, while it is negatively correlated with OCRs. R1, R3, as well as R7, are red wines being the fastest oxidized by laccases and by temperature. R1 and R7 wines are among the lowest in TPC and TC values.

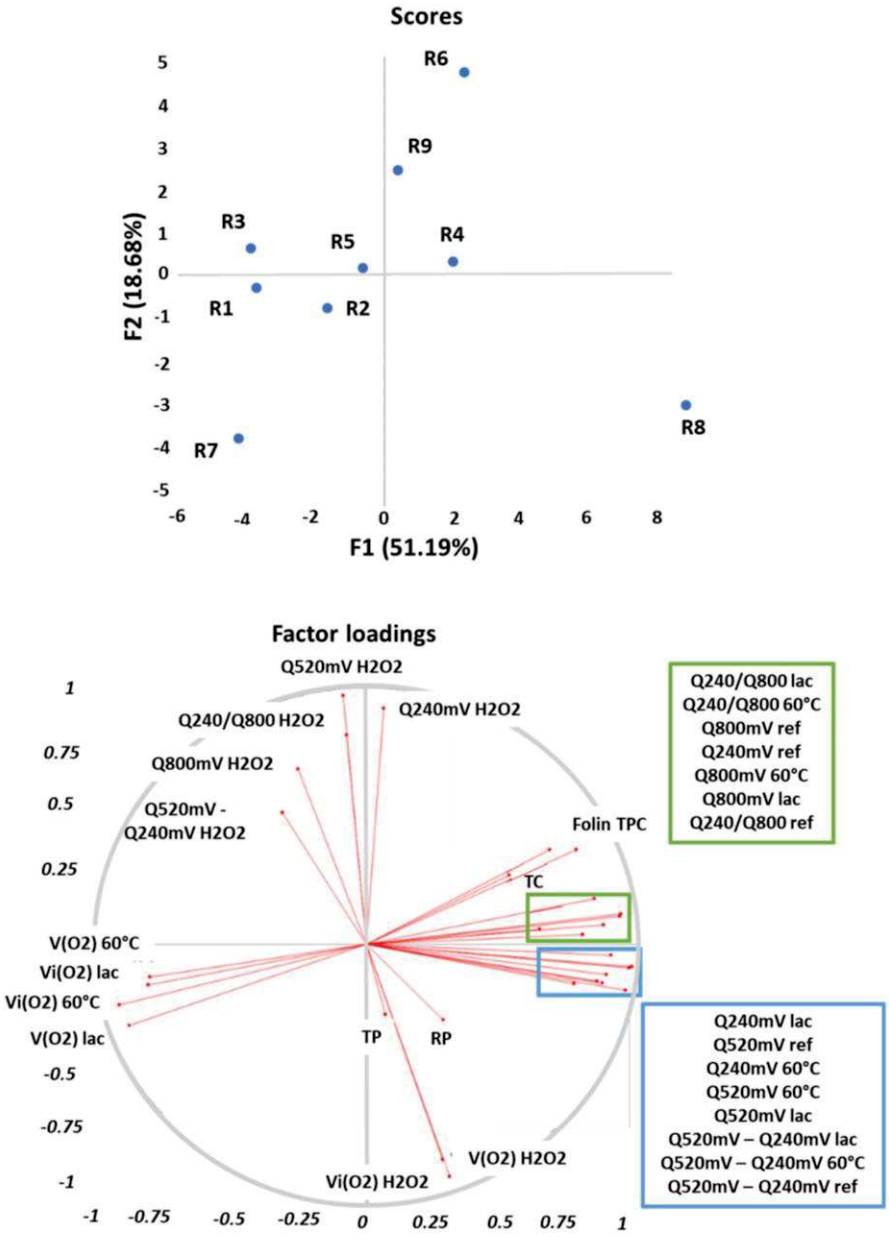

Figure 4. Representation of the loadings (variables) and the scores (wines) in the plane defined by respectively the first (F1) and second (F2) factor (explained variance: 69.87%).

The second factor explains 18.68% of the total data variability. It is positively correlated with electrochemical parameters concerning chemical oxidation with H_2O_2 and negatively correlated with corresponding OCRs and with anthocyanins content (TP and RP). R8 is the red wine with the highest TPC and TC and the fastest oxidized by hydrogen peroxide, and the slowest oxidized by the two other tests.

Wines can consequently be discriminated in Figure 4 into three groups depending on their variable responses. The three Syrah wines (R1, R2 and R3) from the same winery but with different vintages are gathered together on the left of the PCA while both 2019 aged Syrah wines (R7 and R8) are at the bottom of Figure 4. All other wines from different grape cultivars are gathered in a third group, also containing the last 2019 aged Syrah wine (R9), a hypothesis being that it is the only Syrah wine in the study which was aged in barrels.

Figure 5 is a PCA of the reference wines according to their electrochemical parameters (except Q_{240mV}/Q_{800mV} ratio). It shows the plots of loadings and scores in the space described by the 1st and 2nd factors. The first factor explains 92.47% of the total data variability while the second one explains 5.23%. Three groups can be seen on Figure 5 depending on wine OCRs (initial or average). Indeed, the first group contains R1, R3 and R7 wines, and corresponds to the wines which consume oxygen the most quickly when oxidized with temperature or laccases, while R8 wine shows really low OCRs with these two oxidation processes. All other wines (R2, R4, R5, R6 and R9) have intermediate values compared the two previous groups. Consequently, electrochemical measurements on non-oxidized (reference) wines allow us to classify wines depending on their OCRs (for laccase and temperature). It is then possible to predict a wine's sensibility towards oxidation (laccase and temperature) thanks to electrochemical measurements of the reference wines. This method is very promising as it is quick and necessitates a sample diluted drop.

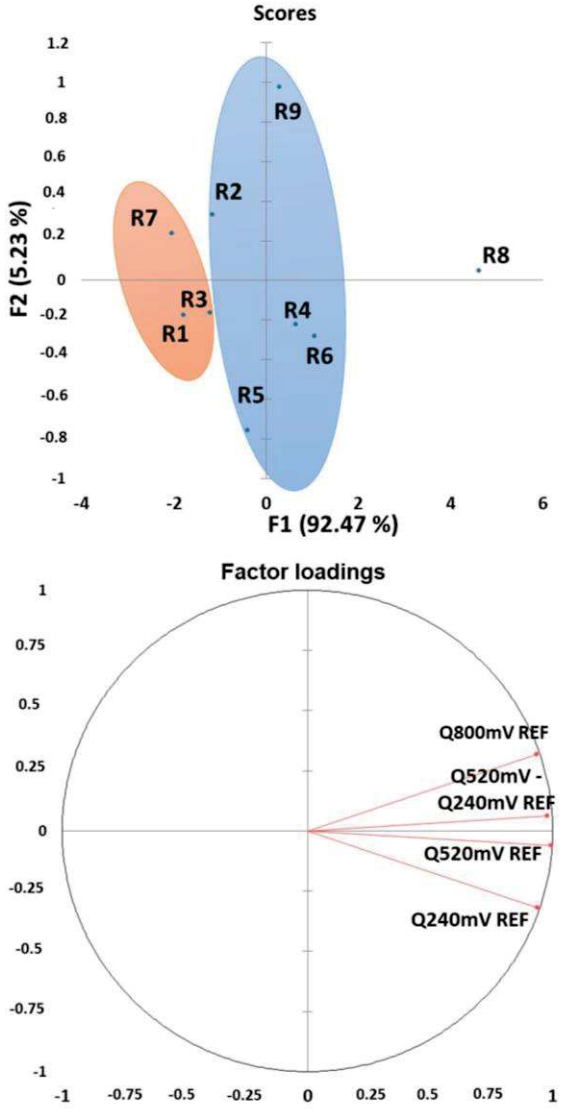

Figure 5. Representation of the loadings (variables—electrochemical parameters (except Q_{240mV}/Q_{800mV} ratio) for the reference wines) and the scores (wines) in the plane defined by respectively the first (F1) and second (F2) factor (explained variance: 97.74%).

Another PCA representation gathering all the electrochemical parameters (before and after oxidation) also reveals a discrimination into three main groups (Supplementary data Figure S1) and confirms previous results.

4. Conclusions

Overall, the results of this work confirm that different wine ageing tests produce distinct results for different red wines, depending on the chemical molecules targeted [8,34,57]. These wines also showed different electrochemical behavior (cyclic voltammetry) before and after oxidation protocols. Wines were discriminated into three main groups depending on their electrochemical behavior, chemical composition, and OCRs: the first group gathered three Syrah wines from the same winery with different ages, the second one gathered two 2019 Syrah wines, while the other samples were gathered in the last group.

Electrochemical parameters before oxidation (temperature and laccases) revealed a discrimination into three groups between red wine samples according to their oxygen consumption rates. Electrochemistry and more specifically cyclic voltammetry appears then as a promising method to predict red wine oxidation and seems to be effective even on older vintages. Moreover, this method appears to be fast and allows us to obtain results with really few samples.

Further research is needed in order to confirm the obtained results by the oxidative and electrochemical characterization in a larger series of red wines.

Supplementary Materials: The following are available online at https://www.mdpi.com/article/10.3390/antiox10121943/s1. Table S1: enological analytic characterization of the red wines, Table S2: free SO_2 levels in the red wines after the different oxidation tests, Figure S1: representation of the scores (wines) (variables—electrochemical parameters for the reference wines (Q) and oxidized wines by the three protocols minus reference wines (ΔQ)) in the plane defined by respectively the first (F1) and second (F2) factor (explained variance: 79.55%).

Author Contributions: Conceptualization: F.G.; data curation: S.D.; formal analysis: S.D., L.G. and F.V.; funding acquisition: C.S.; investigation: S.D. and F.G.; methodology: S.D., L.G. and F.G.; project administration and validation: C.S; supervision: L.M., F.G. and C.S.; visualization: S.D.; writing—original draft: S.D.; writing—review and editing: S.D., C.S., L.M., F.G., F.V. and L.G. All authors have read and agreed to the published version of the manuscript.

Funding: This work was supported in part by a PhD grant (S.D.) from the University of Montpellier (Bourse école doctorale GAIA).

Institutional Review Board Statement: Not applicable.

Informed Consent Statement: Not applicable.

Data Availability Statement: Data is contained within the article and Supplementary Material.

Conflicts of Interest: The authors declare no conflict of interest.

References

1. Atanasova, V.; Fulcrand, H.; Cheynier, V.; Moutounet, M. Effect of oxygenation on polyphenol changes occurring in the course of wine-making. *Anal. Chim. Acta* **2002**, *458*, 15–27. [CrossRef]
2. Kilmartin, P. The Oxidation of Red and White Wines and Its Impact on Wine Aroma. *Chem. N. Z.* **2009**, *73*, 18–22.
3. Ferreira, V.; Bueno, M.; Franco-Luesma, E.; Culleré, L.; Zurbano, P.F. Key Changes in Wine Aroma Active Compounds during Bottle Storage of Spanish Red Wines under Different Oxygen Levels. *J. Agric. Food Chem.* **2014**, *62*, 10015–10027. [CrossRef]
4. Gambuti, A.; Siani, T.; Picariello, L.; Rinaldi, A.; Lisanti, M.T.; Ugliano, M.; Dieval, J.B.; Moio, L. Oxygen exposure of tannins-rich red wines during bottle aging. Influence on phenolics and color, astringency markers and sensory attributes. *Eur. Food Res. Technol.* **2017**, *243*, 669–680. [CrossRef]
5. Ugliano, M. Oxygen Contribution to Wine Aroma Evolution during Bottle Aging. *J. Agric. Food Chem.* **2013**, *61*, 6125–6136. [CrossRef] [PubMed]
6. Echave, J.; Barral, M.; Fraga-Corral, M.; Prieto, M.; Simal-Gandara, J. Bottle Aging and Storage of Wines: A Review. *Molecules* **2021**, *26*, 713. [CrossRef] [PubMed]
7. Danilewicz, J.C. Reaction of Oxygen and Sulfite in Wine. *Am. J. Enol. Vitic.* **2016**, *67*, 13–17. [CrossRef]

8. Ferreira, V.; Carrascón, V.; Bueno, M.; Ugliano, M.; Fernandez-Zurbano, P. Oxygen Consumption by Red Wines. Part I: Consumption Rates, Relationship with Chemical Composition, and Role of SO_2. *J. Agric. Food Chem.* **2015**, *63*, 10928–10937. [CrossRef]
9. Waterhouse, A.L.; Frost, S.; Ugliano, M.; Cantu, A.R.; Currie, B.L.; Anderson, M.; Chassy, A.W.; Vidal, S.; Diéval, J.-B.; Aagaard, O.; et al. Sulfur Dioxide-Oxygen Consumption Ratio Reveals Differences in Bottled Wine Oxidation. *Am. J. Enol. Vitic.* **2016**, *67*, 449–459. [CrossRef]
10. Oliveira, C.; Ferreira, A.C.S.; Freitas, V.; Silva, A. Oxidation mechanisms occurring in wines. *Food Res. Int.* **2011**, *44*, 1115–1126. [CrossRef]
11. Singleton, V.L. Oxygen with Phenols and Related Reactions in Musts, Wines, and Model Systems: Observations and Practical Implications. *Am. J. Enol. Vitic.* **1987**, *38*, 9.
12. Waterhouse, A.L.; Laurie, V.F. Oxidation of Wine Phenolics: A Critical Evaluation and Hypotheses. *Am. J. Enol. Vitic.* **2006**, *57*, 306–313.
13. Danilewicz, J.C. Review of Reaction Mechanisms of Oxygen and Proposed Intermediate Reduction Products in Wine: Central Role of Iron and Copper. *Am. J. Enol. Vitic.* **2003**, *54*, 73–85.
14. Nikolantonaki, M.; Chichuc, I.; Teissedre, P.-L.; Darriet, P. Reactivity of volatile thiols with polyphenols in a wine-model medium: Impact of oxygen, iron, and sulfur dioxide. *Anal. Chim. Acta* **2010**, *660*, 102–109. [CrossRef]
15. Nikolantonaki, M.; Waterhouse, A.L. A Method to Quantify Quinone Reaction Rates with Wine Relevant Nucleophiles: A Key to the Understanding of Oxidative Loss of Varietal Thiols. *J. Agric. Food Chem.* **2012**, *60*, 8484–8491. [CrossRef]
16. Nikolantonaki, M.; Magiatis, P.; Waterhouse, A.L. Measuring protection of aromatic wine thiols from oxidation by competitive reactions vs. wine preservatives with ortho-quinones. *Food Chem.* **2014**, *163*, 61–67. [CrossRef] [PubMed]
17. Oliveira, C.M.; Santos, S.A.; Silvestre, A.J.; Barros, A.S.; Ferreira, A.C.S.; Silva, A.M. Quinones as Strecker degradation reagents in wine oxidation processes. *Food Chem.* **2017**, *228*, 618–624. [CrossRef]
18. Kilmartin, P.A.; Zou, H.; Waterhouse, A.L. A Cyclic Voltammetry Method Suitable for Characterizing Antioxidant Properties of Wine and Wine Phenolics. *J. Agric. Food Chem.* **2001**, *49*, 1957–1965. [CrossRef]
19. Kilmartin, P.A.; Zou, H.; Waterhouse, A.L. Correlation of Wine Phenolic Composition versus Cyclic Voltammetry Response. *Am. J. Enol. Vitic.* **2002**, *53*, 294–302.
20. Makhotkina, O.; Kilmartin, P.A. Uncovering the influence of antioxidants on polyphenol oxidation in wines using an electrochemical method: Cyclic voltammetry. *J. Electroanal. Chem.* **2009**, *633*, 165–174. [CrossRef]
21. Ugliano, M. Rapid fingerprinting of white wine oxidizable fraction and classification of white wines using disposable screen printed sensors and derivative voltammetry. *Food Chem.* **2016**, *212*, 837–843. [CrossRef] [PubMed]
22. Hoyos-Arbeláez, J.; Vázquez, M.; Contreras-Calderón, J. Electrochemical methods as a tool for determining the antioxidant capacity of food and beverages: A review. *Food Chem.* **2017**, *221*, 1371–1381. [CrossRef] [PubMed]
23. Piljac-Žegarac, J.; Valek, L.; Stipčević, T.; Martinez, S. Electrochemical determination of antioxidant capacity of fruit tea infusions. *Food Chem.* **2010**, *121*, 820–825. [CrossRef]
24. Lorrain, B.; Ky, I.; Pechamat, L.; Teissedre, P.-L. Evolution of Analysis of Polyhenols from Grapes, Wines, and Extracts. *Molecules* **2013**, *18*, 1076–1100. [CrossRef]
25. Geană, E.-I.; Ciucure, C.T.; Artem, V.; Apetrei, C. Wine varietal discrimination and classification using a voltammetric sensor array based on modified screen-printed electrodes in conjunction with chemometric analysis. *Microchem. J.* **2020**, *159*, 105451. [CrossRef]
26. Gonzalez, A.; Vidal, S.; Ugliano, M. Untargeted voltammetric approaches for characterization of oxidation patterns in white wines. *Food Chem.* **2018**, *269*, 1–8. [CrossRef]
27. Dai, Y.-Q.; Shiu, K.-K. Glucose Biosensor Based on Multi-Walled Carbon Nanotube Modified Glassy Carbon Electrode. *Electroanalysis* **2004**, *16*, 1697–1703. [CrossRef]
28. Liu, M.; Xiang, J.; Zhou, J.; Ding, H. A disposable amperometric sensor for rapid detection of serotonin in the blood and brain of the depressed mice based on Nafion membrane-coated colloidal gold screen-printed electrode. *J. Electroanal. Chem.* **2010**, *640*, 1–7. [CrossRef]
29. Bordonaba, J.G.; Terry, L. Electrochemical behaviour of polyphenol rich fruit juices using disposable screen-printed carbon electrodes: Towards a rapid sensor for antioxidant capacity and individual antioxidants. *Talanta* **2012**, *90*, 38–45. [CrossRef]
30. Pasakon, P.; Mensing, J.P.; Phokaratkul, D.; Karuwan, C.; Lomas, T.; Wisitsoraat, A.; Tuantranont, A. A high-performance, disposable screen-printed carbon electrode modified with multi-walled carbon nanotubes/graphene for ultratrace level electrochemical sensors. *J. Appl. Electrochem.* **2019**, *49*, 217–227. [CrossRef]
31. Chowdhry, A.; Kaur, J.; Khatri, M.; Puri, V.; Tuli, R.; Puri, S. Characterization of functionalized multiwalled carbon nanotubes and comparison of their cellular toxicity between HEK 293 cells and zebra fish in vivo. *Heliyon* **2019**, *5*, e02605. [CrossRef] [PubMed]
32. Gokceli, G.; Eksik, O.; Zayim, E.O.; Karatepe, N. A Comparative Study of Single- and Multi-Walled Carbon Nanotube Incorporation to Indium Tin Oxide Electrodes for Solar Cells. *Int. J. Mater. Metall. Eng.* **2019**, *13*, 24–27.
33. Newair, E.F.; Kilmartin, P.A.; Garcia, F. Square wave voltammetric analysis of polyphenol content and antioxidant capacity of red wines using glassy carbon and disposable carbon nanotubes modified screen-printed electrodes. *Eur. Food Res. Technol.* **2018**, *244*, 1225–1237. [CrossRef]

34. Carrascón, V.; Vallverdu-Queralt, A.; Meudec, E.; Sommerer, N.; Fernandez-Zurbano, P.; Ferreira, V. The kinetics of oxygen and SO_2 consumption by red wines. What do they tell about oxidation mechanisms and about changes in wine composition? *Food Chem.* **2018**, *241*, 206–214. [CrossRef] [PubMed]
35. Deshaies, S.; Cazals, G.; Enjalbal, C.; Constantin, T.; Garcia, F.; Mouls, L.; Saucier, C. Red Wine Oxidation: Accelerated Ageing Tests, Possible Reaction Mechanisms and Application to Syrah Red Wines. *Antioxidants* **2020**, *9*, 663. [CrossRef]
36. Magalhães, L.M.; Santos, F.; Segundo, M.A.; Reis, S.; Lima, J.L. Rapid microplate high-throughput methodology for assessment of Folin-Ciocalteu reducing capacity. *Talanta* **2010**, *83*, 441–447. [CrossRef]
37. Ribéreau-Gayon, P.; Stonestreet, E. Le Dosage Des Tannins Du Vin Rouge et La Détermination de Leur Structure. *Chim. Anal.* **1966**, *48*, 188–196.
38. Labarbe, B. Le Potentiel Polyphenolique de La Grappe de *Vitis vinifera* var. Gamay Noir et Son Devenir En Vinification Beaujolaise. Ph.D. Thesis, Ecole Nationale Supérieure Agronomique, Montpellier, France, 2000.
39. Ducasse, M.-A.; Canal-Llauberes, R.-M.; de Lumley, M.; Williams, P.; Souquet, J.-M.; Fulcrand, H.; Doco, T.; Cheynier, V. Effect of macerating enzyme treatment on the polyphenol and polysaccharide composition of red wines. *Food Chem.* **2010**, *118*, 369–376. [CrossRef]
40. Clark, A.C.; Kontoudakis, N.; Barril, C.; Schmidtke, L.; Scollary, G.R. Measurement of labile copper in wine by medium exchange stripping potentiometry utilising screen printed carbon electrodes. *Talanta* **2016**, *154*, 431–437. [CrossRef] [PubMed]
41. Kontoudakis, N.; Smith, M.; Guo, A.; Smith, P.A.; Scollary, G.R.; Wilkes, E.N.; Clark, A.C. The impact of wine components on fractionation of Cu and Fe in model wine systems: Macromolecules, phenolic and sulfur compounds. *Food Res. Int.* **2017**, *98*, 95–102. [CrossRef]
42. Danilewicz, J.C.; Seccombe, J.T.; Whelan, J. Mechanism of Interaction of Polyphenols, Oxygen, and Sulfur Dioxide in Model Wine and Wine. *Am. J. Enol. Vitic.* **2008**, *59*, 128–136.
43. Bradshaw, M.P.; Barril, C.; Clark, A.C.; Prenzler, P.; Scollary, G.R. Ascorbic Acid: A Review of its Chemistry and Reactivity in Relation to a Wine Environment. *Crit. Rev. Food Sci. Nutr.* **2011**, *51*, 479–498. [CrossRef]
44. Arapitsas, P.; Ugliano, M.; Perenzoni, D.; Angeli, A.; Pangrazzi, P.; Mattivi, F. Wine metabolomics reveals new sulfonated products in bottled white wines, promoted by small amounts of oxygen. *J. Chromatogr. A* **2016**, *1429*, 155–165. [CrossRef] [PubMed]
45. Carrascón, V.; Bueno, M.; Fernandez-Zurbano, P.; Ferreira, V. Oxygen and SO_2 Consumption Rates in White and Rosé Wines: Relationship with and Effects on Wine Chemical Composition. *J. Agric. Food Chem.* **2017**, *65*, 9488–9495. [CrossRef]
46. Souza, L.P.; Calegari, F.; Zarbin, A.J.G.; Marcolino-Júnior, L.H.; Bergamini, M.F. Voltammetric Determination of the Antioxidant Capacity in Wine Samples Using a Carbon Nanotube Modified Electrode. *J. Agric. Food Chem.* **2011**, *59*, 7620–7625. [CrossRef]
47. Petrovic, S.C. Correlation of Perceived Wine Astringency to Cyclic Voltammetric Response. *Am. J. Enol. Vitic.* **2009**, *60*, 373–378.
48. Rebelo, M.; Rego, R.; Ferreira, M.; Oliveira, M. Comparative study of the antioxidant capacity and polyphenol content of Douro wines by chemical and electrochemical methods. *Food Chem.* **2013**, *141*, 566–573. [CrossRef]
49. Novak, I.; Šeruga, M.; Komorsky-Lovrić, Š. Square-wave and cyclic voltammetry of epicatechin gallate on glassy carbon electrode. *J. Electroanal. Chem.* **2009**, *631*, 71–75. [CrossRef]
50. Martins, R.C.; Oliveira, R.; Bento, F.; Geraldo, D.; Lopes, V.; de Pinho, P.G.; Oliveira, C.; Ferreira, A.C.S. Oxidation Management of White Wines Using Cyclic Voltammetry and Multivariate Process Monitoring. *J. Agric. Food Chem.* **2008**, *56*, 12092–12098. [CrossRef]
51. Rodrigues, A.; Ferreira, A.C.S.; de Pinho, P.G.; Bento, F.; Geraldo, D. Resistance to Oxidation of White Wines Assessed by Voltammetric Means. *J. Agric. Food Chem.* **2007**, *55*, 10557–10562. [CrossRef] [PubMed]
52. Benbouguerra, N.; Richard, T.; Saucier, C.; Garcia, F. Voltammetric Behavior, Flavanol and Anthocyanin Contents, and Antioxidant Capacity of Grape Skins and Seeds during Ripening (*Vitis vinifera var. Merlot*, *Tannat*, and *Syrah*). *Antioxidants* **2020**, *9*, 800. [CrossRef] [PubMed]
53. Vilas-Boas, Â.; Valderrama, P.; Fontes, N.; Geraldo, D.; Bento, F. Evaluation of total polyphenol content of wines by means of voltammetric techniques: Cyclic voltammetry vs. differential pulse voltammetry. *Food Chem.* **2019**, *276*, 719–725. [CrossRef]
54. Makhotkina, O.; Kilmartin, P.A. The phenolic composition of Sauvignon blanc juice profiled by cyclic voltammetry. *Electrochim. Acta* **2012**, *83*, 188–195. [CrossRef]
55. Singleton, V.L.; Salgues, M.; Zaya, J.; Trousdale, E. Caftaric Acid Disappearance and Conversion to Products of En-zymic Oxidation in Grape Must and Wine. *Am. J. Enol. Vitic.* **1985**, *36*, 50–56.
56. Lopes, P.; Richard, T.; Saucier, C.; Teissedre, P.-L.; Monti, J.-P.; Glories, Y. Anthocyanone A: A Quinone Methide Derivative Resulting from Malvidin 3-*O*-Glucoside Degradation. *J. Agric. Food Chem.* **2007**, *55*, 2698–2704. [CrossRef] [PubMed]
57. Coppola, F.; Picariello, L.; Forino, M.; Moio, L.; Gambuti, A. Comparison of Three Accelerated Oxidation Tests Applied to Red Wines with Different Chemical Composition. *Molecules* **2021**, *26*, 815. [CrossRef] [PubMed]

Chapitre IV – Approche ciblée : identification et obtention de marqueurs d'oxydation

Le prochain chapitre aborde une approche ciblée des marqueurs d'oxydation. Il se divise en deux parties

Partie I – Analyse structurale par RMN de marqueurs d'oxydation dimériques obtenus par oxydation enzymatique de la (+)-catéchine.

Partie II – identification de ces marqueurs par UHPLC-Q-Orbitrap/MS^2 dans des extraits de pépins et de vin rouge. Impact de la maturation des baies et du vieillissement du vin.

Partie I

Les objectifs de la première partie étaient

- D'effectuer une étude comparative du profil produits d'oxydation de type dimère de la (+)-catéchine par trois types d'oxydoreductases :
    - laccases de *Trametes versicolor* (commerciales)
    - laccases de *Botrytis cinere*a (extraites)
    - polyphenoloxidases (PPO) extraites de pépins
- D'isoler certains produits d'oxydation de la catéchine par les laccases de *Trametes versicolor* et de déterminer leurs structures moléculaires

Les méthodes utilisées étaient les suivantes :

1. UHPLC-MS afin d'acquérir les chromatogrammes UV (280nm) des produits de réaction de la catéchine par les différentes enzymes et de suivre les avancements de réaction
2. Des méthodes de purification telles que la chromatographie flash pour séparer les différents oligomères entre eux, et la chromatographie semi-préparative pour séparer les dimères les uns des autres et obtenir des produits purs.
3. Acquisitions RMN :
    - 1D ^{1}H et ^{13}C
    - 2D homonucléaire ^{1}H TOCSY et ROSEY and heteronucléaire $^{1}H/^{13}C$ HSQC et HMBC

Les hypothèses étaient les suivantes

1. Les produits de réaction de différentes oxydoreductasess peuvent entrainer des différences de produits formés et de niveau d'oxydation.
2. L'utilisation du nitrate de cadmium pour les analyses RMN pourrait permettre d'obtenir des signaux OH phénoliques résolus et ainsi d'aboutir à des structures complètes de composés phénoliques.

Conclusions

1. Les trois différentes oxydoréductases utilisées dans cette étude ont produit globalement des profils UV similaires contenant 8 pics. Parmis ces 8 produits, différents états d'oxydation sont relevés (m/z=579 ou 577 en fonction du nombre de liaisons créées entres les unités de catéchine)
2. Un produit supplémentaire est visible pour les laccases de *Botrytis cinerea* et la polyphenoloxidases extraite du raisin. Les ions moléculaires des produits obtenus ont également des masses similaires dans les trois cas. Ainsi les laccases commerciales de *Trametes versicolor* peuvent être utilisées comme moyen biologique d'obtention par hémisynthèse de potentiels marqueurs d'oxydation du raisin et du vin.
3. Six produits d'oxydation dimériques ont été structurellement identifiés par RMN : N2, N3, N4, N6 et N8. N2 et N4 présentent des liaisons interflavaniques de type C-C, avec N4 contenant deux isomères. N3 et N6 présentent des liaisons interflavanes de type C-O-C. N8 présente un état d'oxydation supérieur et plusieurs liaisons interflavanes, il est connu sous le nom de déhydrodicatéchine A.
4. L'utilisation du nitrate de cadmium pour les analyses RMN permets l'identification de N6 et N8 directement. Il permet de réduire les échanges intermoléculaires entre les protons des OH et ceux du solvant, et ainsi d'accroitre la résolution des OH phénoliques
5. Des signaux OH phénoliques résolus ont été obtenus pour N2, N3 et N4 avec également utilisation du nitrate de cadmium mais aussi grâce à une étape supplémentaire d'évaporation et de resolubilisation.
6. L'ajout de cadmium n'a pas d'effet sur les OH aliphatiques. Des ajouts croissants de cadmium n'ont pas d'effet croissants sur la résolution des OH phénoliques. Une température d'acquisition à 15°C permets de séparer certains signaux superposés entre les OH aliphatiques et phénoliques.

Les principaux spectres utilisés pour la détermination structurale des composés sont présentés en **annexes (p 97 à 124)**. Cette étude a également fait l'objet d'un article scientifique, publié dans le journal *Molecules* en septembre 2021 sous la référence :

Stacy Deshaies, Christine Le Guernevé, Lucas Suc, Laetitia Mouls, François Garcia and Cédric Saucier. ***Unambiguous NMR structural determination of (+)-Catechin-Laccases dimeric reaction products as potential markers of grape and wine oxidation.***

Et présenté ci-après

molecules

MDPI

Article

Unambiguous NMR Structural Determination of (+)-Catechin—Laccase Dimeric Reaction Products as Potential Markers of Grape and Wine Oxidation

Stacy Deshaies, Christine le Guernevé, Lucas Suc, Laetitia Mouls, François Garcia and Cédric Saucier *

SPO, Université de Montpellier, INRAE, Institut Agro, 34000 Montpellier, France; stacy.deshaies@umontpellier.fr (S.D.); christine.le-guerneve@inrae.fr (C.l.G.); lucas.suc@inrae.fr (L.S.); laetitia.mouls@supagro.fr (L.M.); francois.garcia@umontpellier.fr (F.G.)
* Correspondence: cedric.saucier@umontpellier.fr

Abstract: (+)-Catechin—laccase oxidation dimeric standards were hemi-synthesized using laccase from *Trametes versicolor* in a water-ethanol solution at pH 3.6. Eight fractions corresponding to eight potential oxidation dimeric products were detected. The fractions profiles were compared with profiles obtained with two other oxidoreductases: polyphenoloxidase extracted from grapes and laccase from *Botrytis cinerea*. The profiles were very similar, although some minor differences suggested possible dissimilarities in the reactivity of these enzymes. Five fractions were then isolated and analyzed by 1D and 2D NMR spectroscopy. The addition of traces of cadmium nitrate in the samples solubilized in acetone-d_6 led to fully resolved NMR signals of phenolic protons, allowing the unambiguous structural determination of six reaction products, one of the fractions containing two enantiomers. These products can further be used as oxidation markers to investigate their presence and evolution in wine during winemaking and wine ageing.

Keywords: oxidation marker; (+)-catechin; phenolic NMR signals; laccase; cadmium nitrate; polyphenol oxidase

Citation: Deshaies, S.; le Guernevé, C.; Suc, L.; Mouls, L.; Garcia, F.; Saucier, C. Unambiguous NMR Structural Determination of (+)-Catechin—Laccase Dimeric Reaction Products as Potential Markers of Grape and Wine Oxidation. *Molecules* **2021**, *26*, 6165. https://doi.org/10.3390/molecules26206165

Academic Editors: Dalene De Beer, Lizette Joubert, Elisabetta Damiani and Tiziana Bacchetti

Received: 15 September 2021
Accepted: 7 October 2021
Published: 13 October 2021

1. Introduction

Polyphenols are a family of chemical compounds widely present in nature. They are found in significant amount in tea [1], cacao [2,3], blueberries [4], grapes [5], and fermented products like wine [6]. Being primary oxidation targets [7,8], polyphenols chemical structures continually evolve. These changes impact the organoleptic properties of many types of food; they are responsible for phenomena such as food browning [9] and modifications of wine's sensory characteristics [10,11]. In enology, this oxidation phenomenon takes place in grapes or wines. Concerning enzymatic oxidation, the main enzymes responsible for browning are oxidoreductases, more precisely, polyphenol oxidase present in grapes and laccase produced by *Botrytis cinerea* [12].

Enzymatic oxidation mainly occurs in grape must, but further wine browning may be due to chemical oxidation reactions [7,13] or to *Botrytis cinerea* laccase that can be very stable during wine ageing [14]. Two oxidation enzymatic activities may occur on phenolic substrates: monophenol oxidase activity characterized by the hydroxylation of an existing hydroxyl group adjacent position and diphenol oxidase activity corresponding to the oxidation of *ortho*-dihydroxybenzenes to *ortho*-benzoquinones.

According to the *Nomenclature Committee of the International Union of Biochemistry and Molecular Biology* (NC-IUBMB), these enzymatic activities are catalyzed by E.C.1-class enzymes corresponding to oxidoreductases. Among them, the three main classes of oxidoreductases catalyzing polyphenol oxidation are E.C.1.14.18.1 (monophenol monooxygenase), E.C.1.11.1 (peroxidase/POD), and E.C.1.10.3 (oxidoreductases acting on diphenols).

This last class is divided in different subclasses, and two of them appeared particularly interesting for this study: E.C.1.10.3.1 (polyphenol oxidase/PPO) and E.C.1.10.3.2 (laccase) (See Supplementary Materials Figure S1).

PPO, laccase, and peroxidase are the oxidoreductases mainly responsible for browning during grape processing [13]. Browning caused by POD is negligible in fruits but can increase phenols degradation when combined with PPO [15]. PPO are naturally present in grapes and are able to catalyze the oxidation of monophenols to catechols and of catechols to brown pigments [8,13,16]. Laccases, occurring in *Botrytis*-infected grapes, have a wider action spectrum [17] as they can catalyze the oxidation of many different substrates. The main laccases' oxidation targets remain 1-2 and 1-4 dihydroxybenzene.

In wine, benzoquinone produced by oxidation (PPO or laccases) can easily undergo further reactions depending on their redox properties and electronic affinities [15]. They can either act as electrophiles and react with amino derivatives [18] or act as oxidants and react, among others, with phenolic substrates. Depending on their chemical conformation (quinone or semi-quinone), benzoquinone can lead to different oxidation reaction products. At a neutral pH, (+)-catechin will be oxidized to quinone on the A-ring position C5 or C7 and lead to the formation of six possible dimeric isomers implying a linkage between the B-ring position C2′, C5′, or C6′ of the upper catechin unit and the A-ring position C6 or C8 of the lower unit [19,20]. Dehydrodicatechin is a well-known product of this coupling [21]. The labeling positions of the structures are displayed in Figure 1. Under acidic conditions, semi-quinone forms can also be present on the B-ring (position OH3′ or OH4′) and lead to four possible dimeric isomers [20,22] with the upper catechin unit and the A-ring of the lower unit (position C6 or C8). Catechin enzymatic oxidation was investigated in previous studies [22,23], and the associated oxidation products were characterized by HPLC [24], though more rarely isolated and never completely characterized by NMR.

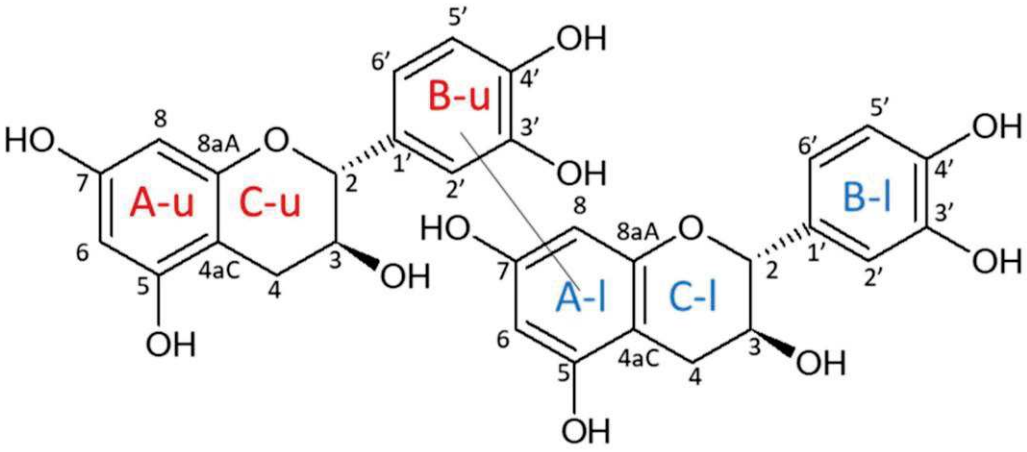

Figure 1. Example of a dimeric oxidation product. A, B, C rings are labelled with u for upper units and with l for lower units.

The aim of this work was first to compare by UHPLC-MS the dimeric (+)-catechin oxidation products profiles in the presence of three oxidoreductase extracts, i.e., PPO extracted from grapes, laccase from the fungus *Botrytis cinerea* present in botrytized sweet wines [14], and laccase from *Trametes versicolor.*

The second objective was to hemisynthesize and characterize the structures of some dimeric oxidation products by NMR spectroscopy obtained with laccase from *Trametes versicolor*.

2. Results and Discussion

2.1. Comparison of Dimeric Reaction Products Profiles with Three Different Oxydoreductases and (+)-Catechin

(+)-Catechin was first oxidized in the presence of laccase from *Trametes versicolor* at pH 3.6 in the model wine solution. After separation of the dimeric fraction from residual (+)-catechin and other polymeric fractions, eight major fractions were collected and analyzed by UHPLC-UV-MS, noted from N1 to N8 in increasing retention time order (Table 1). The electrospray mass spectra in positive mode showed the ion peaks $[M + H]^+$ at *m/z* 579 for N1 to N6, hypothetically corresponding to a dimer formed by a single bond between two catechin units, and $[M + H]^+$ at *m/z* 577 for N7 and N8, hypothetically suggesting the formation of an additional linkage.

Table 1. Analytical reversed-phase UHPLC retention times, absorbance maxima, corresponding *m/z* (Th), and yields (%) for the eight major oxidation products collected.

Compound	R_t (min)	λ_{max} (nm)	*m/z* (Th)	Molar Yield (%)
N1	6.14 ± 0.02	280	579	0.4
N2	6.91 ± 0.02	280	579	0.1
N3	10.34 ± 0.03	280	579	0.7
N4	14.11 ± 0.07	280	579	0.3
N5	17.13 ± 0.02	280	579	0.2
N6	19.03 ± 0.01	280	579	0.7
N7	20.63 ± 0.03	263, 318	577	0.1
N8	25.23 ± 0.01	256, 280, 286	577	0.2

These eight oxidation fractions were potentially observed after the chemical depolymerization of a tannin fraction in previous works [25,26] and could possibly be the same as those already described by Guyot et al. [20], even if the experimental conditions were slightly different. Indeed, in this previous study, a crude PPO extract was used at pH 3 and 6 to obtain eight fractions. In the present study, three different enzymes were compared at pH 3.6 in the model wine solution. The LC-MS comparative analysis of the major oxidation fractions obtained with the three different enzymes (laccase from *Trametes versicolor*, laccase from *Botrytis cinerea*, and polyphenoloxidase extracted from grapes) are presented in Table 2. For each of the eight fractions, the retention times were almost identical with the different enzymes, and similar *m/z* were determined with the MS analysis. These results support the hypothesis that the same fractions were obtained for each enzyme, containing products with structures similar to those hypothesized by Guyot et al. [20]. López-Serrano and Ros Barceló [27] also performed a comparative study of the (+)-catechin oxidation products with two different enzymes: peroxidase and polyphenoloxidase, both extracted from strawberries. They concluded that the products obtained with the two enzymes were qualitatively the same. An additional compound named N4′ with m/z = 578 Th and R_t = 15.66 min was observed in experiments with laccase from *Botrytis cinerea* and extracted PPO but not with laccase from *Trametes versicolor*, which suggests possible differences in reactivity for these enzymes.

2.2. Study and Optimization of Physicochemical Parameters on ^{1}H-NMR Phenolic and Aliphatic OH Signals

The structural characterization of procyanidins dimers can be obtained by NMR analysis. In particular, the precise linkage position between units may be determined using HMBC and/or ROESY correlation spectra [28,29] (Figures S2 and S3). In the case of an ether-type (C–O–C) bond, the attribution of the hydroxyl signal protons is necessary. It may also be crucial in the case of C–C linkages if some aliphatic or aromatic protons overlap or if some key correlations are missing. However, even in an aprotic solvent, the hydroxyl protons of polyphenols often appear as broad signals from which no structural information can be obtained [30]. This issue was tentatively addressed by the addition of traces of

$Cd(NO_3)_2$ in the sample solutions. Indeed, ^1H broad signals of OH groups are due to the intermolecular exchange between these OH protons and other protons in the solvent or solute. By reducing intermolecular bonds, the presence of cadmium nitrate in the samples may decrease these exchanges, thus improving the sharpness of OH proton signals.

2.2.1. Effect of Cadmium Addition

After freeze-drying, the five fractions N2, N3, N4, N6, and N8 were solubilized in acetone-d_6. Then, 1D proton NMR spectra were acquired at 25 °C before (Figure 2A) and after addition of small amounts of cadmium (Figure 2B). In pure acetone-d_6, the phenolic OH protons of all fractions appeared as broad peaks. After the addition of cadmium, these protons showed highly resolved signals in the case of fractions N6 and N8, whereas for fractions N2, N3, and N4 the signals were only a little sharper. It should also be mentioned that increasing the Cd content had no effect upon OH signal resolution, as no sharpness or broadness of peak linewidth was observed when successive small amounts of Cd were added to the samples (data not shown).

Table 2. Qualitative comparison of analytical reversed-phase UHPLC retention times for the eight major oxidation products with the three different oxidative enzymes: laccase from *Trametes versicolor*, laccase from *Botrytis cinerea*, and polyphenoloxidase extracted from grapes. The results are expressed as mean values (n = 3) with standard deviation.

	R_t (min)		
Compound	**Laccase from *Trametes versicolor***	**Laccase from *Botrytis cinerea***	**Polyphenoloxidase Extracted from Grapes**
N1	6.14 ± 0.02	6.14 ± 0.02	6.12 ± 0.01
N2	6.91 ± 0.02	6.86 ± 0.01	6.80 ± 0.01
N3	10.34 ± 0.03	10.29 ± 0.02	10.29 ± 0.01
N4	14.11 ± 0.07	14.10 ± 0.01	14.04 ± 0.05
N4′	/	15.67 ± 0.01	15.66 ± 0.05
N5	17.13 ± 0.02	17.12 ± 0.04	17.11 ± 0.06
N6	19.03 ± 0.01	19.00 ± 0.003	19.00 ± 0.03
N7	20.63 ± 0.03	20.59 ± 0.01	20.60 ± 0.03
N8	25.23 ± 0.01	25.21 ± 0.02	25.22 ± 0.03

Highly resolved phenolic OH signals from products N2, N3, and N4 were achieved thanks to additional drying and resolubilization (Figure 2C,D).

The difference of behavior upon Cd addition between the fractions may be explained by the strength of molecular interactions: stronger in the case of N2, N3, and N4 compared to N6 and N8, a further step being necessary to break these bonds.

This additional step may be the key step when using Cd to obtain highly resolved phenolic OH signals in any situation, whatever the origin of the samples, the synthesis reaction, or the natural polyphenolic products.

A previous work dealing with the unambiguous structural characterization of polyphenol dimers using highly resolved OH phenolic NMR signals thanks to cadmium nitrate addition was published in 1996 [30]. To our knowledge, no other research paper using this methodology has been published since then. Other investigations were subsequently undertaken to reach this goal, either by picric acid dosed additions [31] or by using a low acquisition temperature [32]. This may be explained by the further step necessary to get a decisive effect upon OH peak sharpness with Cd addition, as described above. However, cadmium seems to be of great value, since highly resolved signals can be obtained without the need to add precise amounts, in contrast with picric acid or NMR spectra acquisition at low temperatures.

Molecules **2021**, *26*, 6165

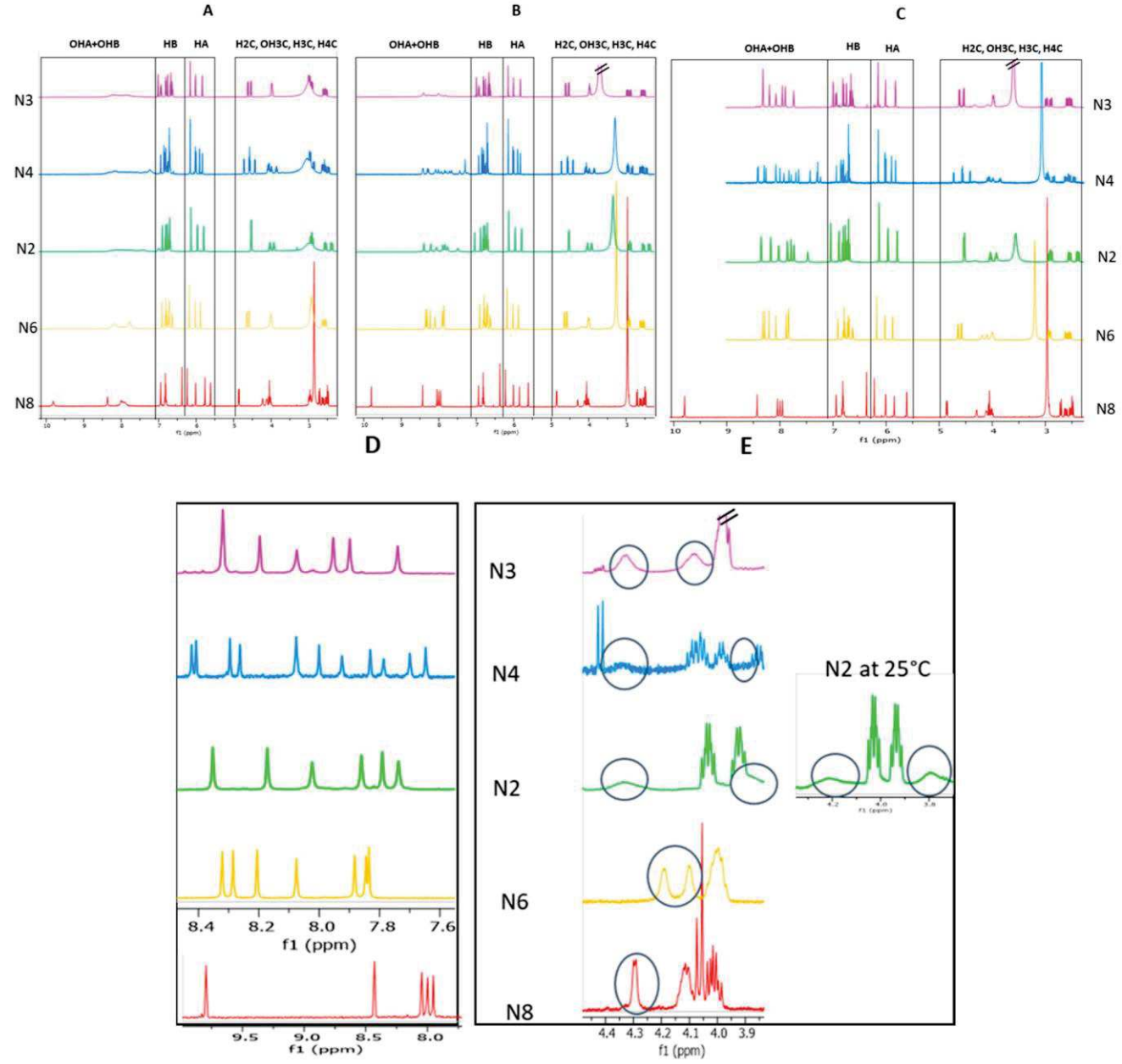

Figure 2. Image of 1D ^{1}H spectra of the fractions N2, N3, N4, N6, and N8 at 25 °C, solubilized in acetone-d_6 (**A**), at 25 °C in acetone-d_6 in the presence of cadmium (**B**), at 15 °C in acetone-d_6 in the presence of Cd (with an additional step consisting in dryness evaporation of the fractions N2, N3, and N4) (**C**), expansion of the phenolic (**D**) and the aliphatic (**E**) OH regions in the same physicochemical conditions as in (**C**).

2.2.2. Effect of the Temperature

A decrease of the temperature from 25 °C to 15 °C had no impact on the sharpness of phenolic OH or aliphatic OH signals. Nevertheless, downfield shifts of exchangeable proton peaks allowed us to separate some overlapping phenolic and aliphatic OH signals, making their identification more obvious (Figure 3). By decreasing the temperature, the proton exchange rate was reduced, and one might expect sharper aliphatic OH peaks [31]. The temperature of 15 °C is obviously not low enough to obtain well-resolved aliphatic OH signals. However, it allowed us to clearly identify the resonance of two aliphatic OH protons in samples N3 and N6 and of one in sample N8. The spectrum of sample N2 also

exhibited two OH aliphatic protons signals, which were more distinguishable at 25 °C than at 15 °C (Figure 2E). In the case of the sample N4, the signals arising from aliphatic OH were only partly visible in the spectra, whether the temperature was set at 25 °C or to 15 °C, due to persistent overlapping (Figure 2E).

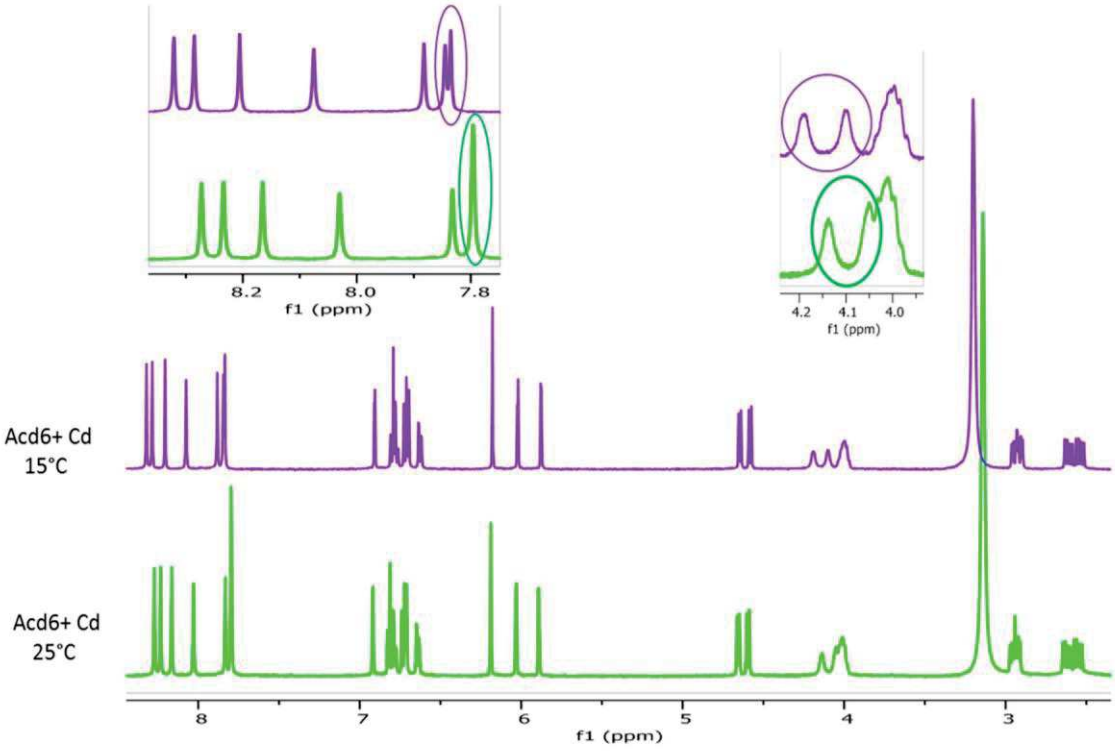

Figure 3. Image of 1D ^{1}H spectra of fraction N6 in acetone-d_6 in the presence of Cd at 25 °C and 15 °C. The expansions show the effect of temperature upon the aromatic and aliphatic OH signal chemical shifts.

2.3. *Structural Characterization of the Dimeric Standards—NMR Spectrum Analysis*

The NMR spectra of fractions N2, N3, N4, N6, and N8 showed that the oxidation products were of high purity, since the signal intensities of other detected compounds were less than 10% compared to those of these products.

In all spectra, four ^{1}H chemical shift regions typical of catechin units may be distinguish (Figure 2C): signals of the aliphatic protons of pyran rings (C rings) are found in the region from 2.3 to 5.0 ppm, and those of the aromatic signal protons of resorcinol rings (A rings) and of catechol rings (B rings) from 5.5 to 6.3 ppm and 6.3 to 7.1 ppm, respectively. The OH phenol signals of both A and B rings appeared from 7.1 to 10 ppm. The NMR spectra of both fractions showed the presence of distinct signal sets of catechin units in a constant intensity ratio: two sets of signals were observed in the spectra of fractions N2, N3, N6, and N8 in accordance with the presence of dimers, and four sets in the N4 spectra, which can correspond to one tetramer, two dimers, or a mixture of different oligomers, that is, one trimer plus one monomer. In order to determine the degree of oligomerization of the products present in fraction N4, an ^{1}H DOSY experiment was performed using a mixture containing aliquots of both fractions N4 and N2. The diffusion coefficients of all signals displayed similar values (Figure 4), indicating the presence of two dimers of catechin in fraction N4.

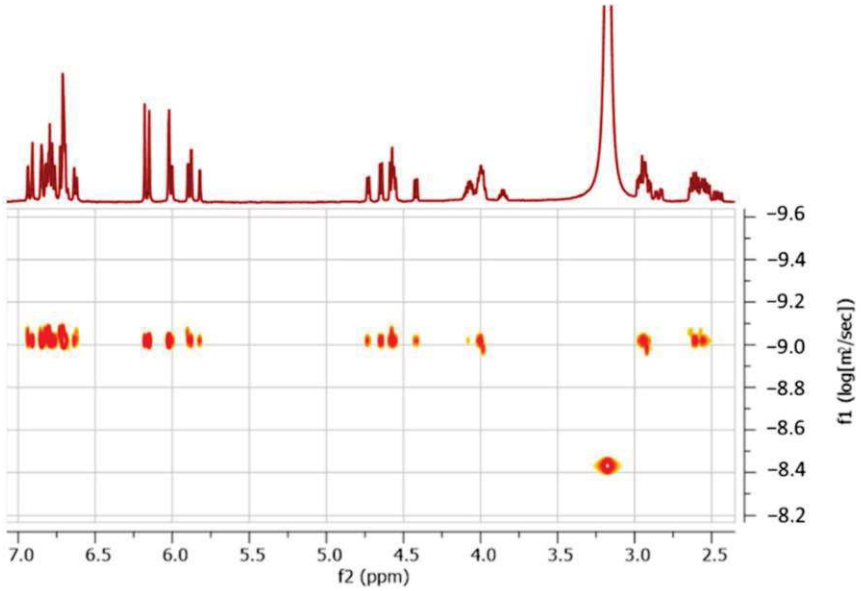

Figure 4. Image of 2D ^{1}H DOSY spectra of a sample containing both fractions N4 and N2.

Thanks to the fully resolved OH phenol signals which provide reliable quantitative results, the type of linkage between the catechin units may be directly deduced from peak surface area integration. Thus, for both fractions N3 and N6, the lack of one OH phenol (belonging either to a resorcinol or to a catechol ring) and the lack of one resorcinol aromatic proton indicated an interflavanic linkage (IFL) of ether type implying an O position in an A or B ring and a C6 or C8 position in an A ring. In the case of sample N2, two aromatic protons were lacking, one of a B ring and one of an A ring, implying a CA-CB IFL. The 1D ^{1}H spectrum of fraction N4 showed that two protons of the B ring were lacking, as well as two protons of the A ring. The bonds between the dimer units of fraction N4 are thus both of the C–C type. The spectra of fraction N8 were quite different from the four others. Some signals were typical of catechin units, in which three OH phenols, one aromatic A ring, and one B ring protons were lacking, as well as one aliphatic OH. On the other hand, some other NMR signals are atypical of a catechin unit: a methylene with deblinded ^{13}C chemical shifts (~40 ppm) and a ketone group (~192 ppm).

The proton spin systems of C, A, and B rings were determined using both ^{1}H 1D and ^{1}H 2D TOCSY spectra (not shown). Two ABMX C-ring spin systems (typical of catechin) were observed in the spectra of fractions N2, N3, N6, and N8, and four for fraction N4. In the spectra of fractions N2, N3, N6, and N8, two meta-coupled doublets (J~2Hz) and a singlet in the aromatic A ring region were assigned, respectively, to the A ring protons of the non-linked catechin unit and to the A ring residual proton of the of C6- or C8-linked catechin unit. In the spectra of N4, due to the presence of two dimers, four meta-coupled doublets and two singlets were detected and assigned as described above. The B ring proton systems were also easily determined from these spectra and allowed us to identify two ABM proton spin systems for the dimers of fractions N3 and N6, whereas one ABM and one AB proton spin systems were detected for dimer N2, and one ABM and one AM proton spin systems for dimer N4. The dimer N8 exhibited only one ABM B-ring spin system typical of a catechin monomer.

2.3.1. Determination of the A Ring Position of the IFL of the Dimers of Fractions N2, N3, N4, and N6

The establishment of the bridge location on the A ring of dimers (i.e., C6A- or C8A-position) requires the attribution of the residual HA proton of the CA-linked catechin unit. Thanks to the highly resolved phenolic OH signals, an easy starting point was the identification of the two OH phenol protons of the A ring-linked units, i.e., the A ring that

had one isolated ^{1}H spin. This may be achieved using ^{1}H-^{13}C long-range correlations, as illustrated in Figure 5. The OH5A was readily identified thanks to a correlation with the C4aC. This quaternary carbon is indeed characterized by both its chemical shift at ~100 ppm and a long-range correlation observed with the H4C protons. OH5A also correlated with two other carbons: the most deshielded (δ > 145 ppm) was obviously C5A, while the other (δ > 125 ppm) was C6A, which also showed a correlation with the other OHA phenol proton, i.e., OH7A. This latter correlated with two other carbons: a deshielded quaternary carbon (δ > 145ppm) and a more shielded carbon (δ > 125 ppm) which were easily attributed to C7A and C8A, respectively. Once C6A and C8A are assigned, the residual HA proton may be directly attributed from the HSQC spectra. It thus was found that this residual HA proton was H6A for all fractions N2, N3, N4, N6. The IFL between catechin units thus implied a C8A position for all dimers.

2.3.2. Determination of the B Ring Position of the IFL

Dimers of fractions N2 and N4. The spectra of fraction N2 showed two different types of B ring proton spin systems: one AMX corresponding to the B ring of the non-linked unit, and one AM with a coupling constant of about 8 Hz, characteristic of H6′B and H5′B of a C2′B-linked unit. The linkage between the units of the N2 dimer is thus C2′B–C8A. The NMR spectra of fraction N4 also showed different B spin systems: two AMX, corresponding to the non-linked B-ring, and two AX spin systems, both displaying coupling constants of about 2 Hz, which are characteristic of H2′B and H6′B protons of C5′B-linked units. The presence of long-range ^{1}H/^{13}C correlations between H6′B and C8A, which were observed in the HMBC spectra of the two dimers, are in accordance with a C5′B–C8A linkage (Figure 5).

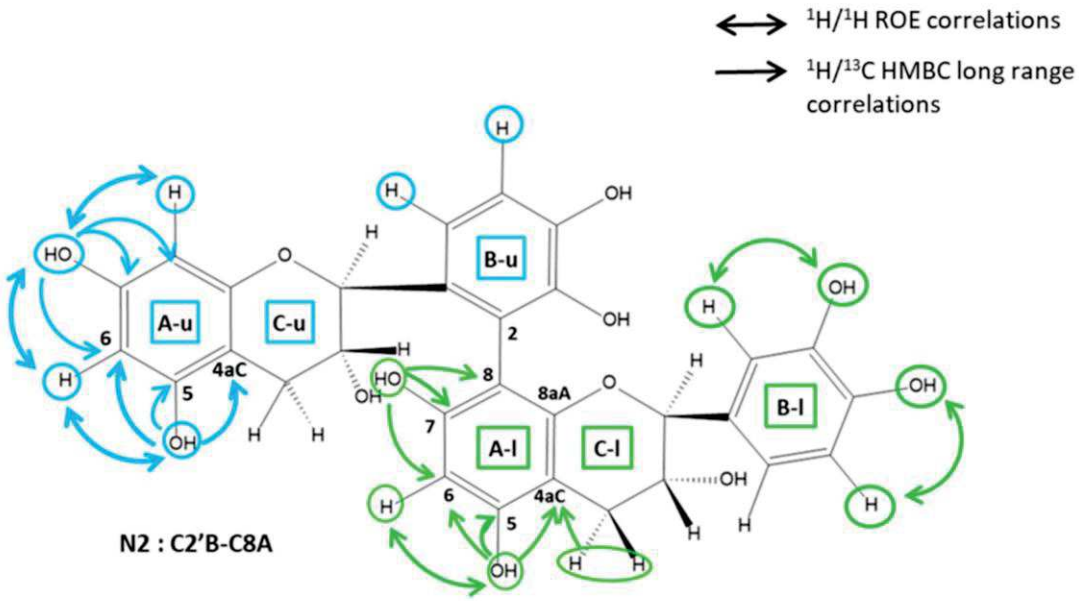

Figure 5. *Cont.*

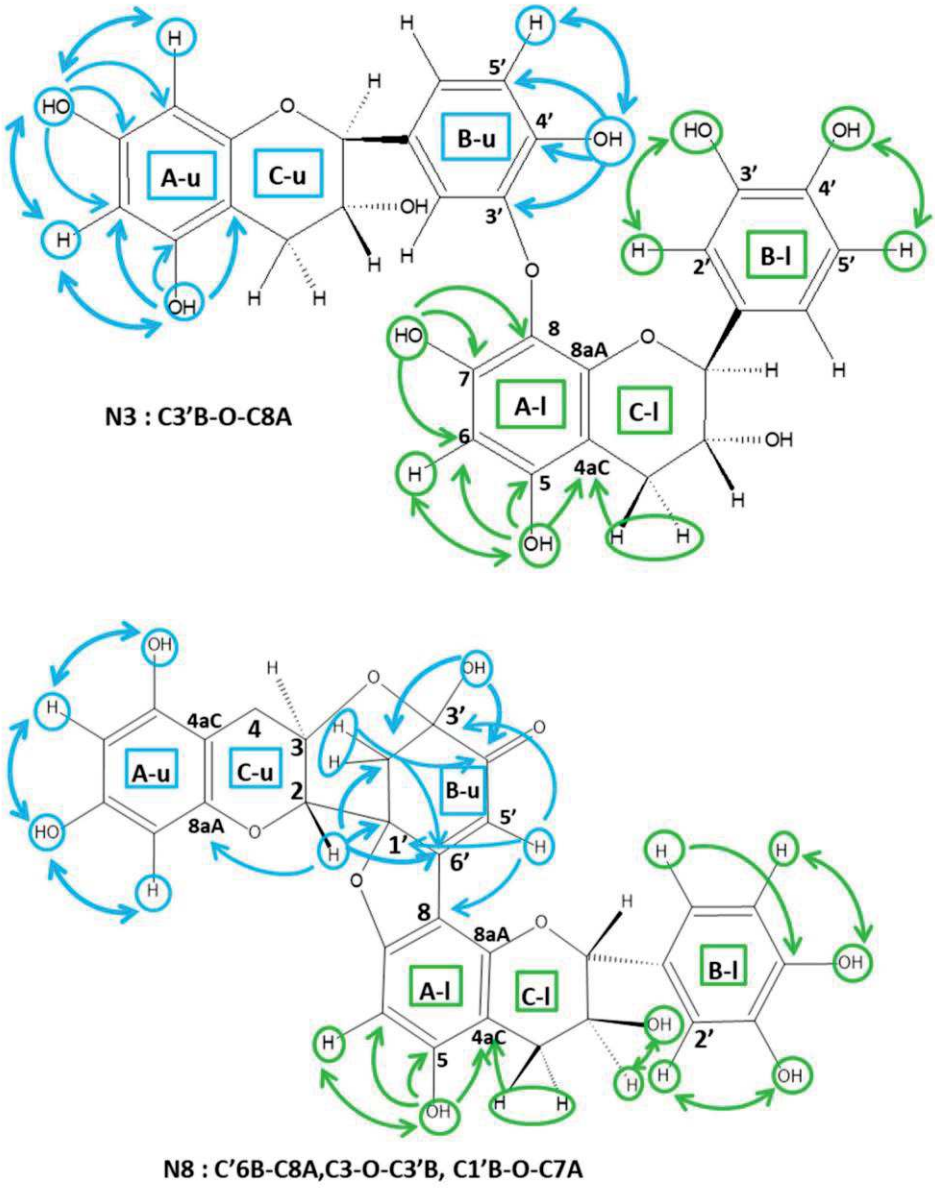

Figure 5. Scheme of catechin dimers (N2, N3, and N8) showing main $^{1}H/^{13}C$ long-range and $^{1}H/^{1}H$ ROE correlations, allowing linkage position determination. Blue arrows: upper unit. Green arrows: Lower units. Single arrows: HMBC correlations. Double arrows: ROEs correlations. A, B, C rings are labelled with u for upper units and with l for lower units.

Dimers of fractions N3 and N6. The spectra of fractions N3 and N6 showed the presence of two AMX B-ring proton systems and the lack of one OH phenol signal. Since all the OHA phenolic protons of the dimer units were identified (as described above), the missing OH phenolic signal can be either that of OH3′B or that of OH4′B.

The OH position (3′B or 4′B) may be easily determined through ROE correlations with H2′B or H5′B, respectively, or using long-range HMBC correlations as illustrated in Figure 5.

The attribution of the residual OH of the B rings was readily performed using either long-range HMBC or ROESY correlations, as illustrated in Figure 5. In the case of dimer N3, a ROE correlation was observed between the H5′B and the residual OH′B of the catechin unit linked through its B ring. This OH was thus identified as OH4′B. In the case of fraction N6, the residual OH′B was assigned to OH3′B, since an ROE correlation was observed between this OH and H2′B. The long-range HMBC correlations are in accordance with these attributions. The linkage positions of these two dimers were then determined as follows: CO3′B–C8A and CO4′B–C8A for N3 and N6. respectively.

Fraction N8. Spectrum analysis of the dimer N8 showed that one unit of this dimer is a catechin with two linkage positions one the A ring, one at the C8A, and the other at the C-O7A position, since the protons H8A and OH7A are missing. The other unit of this dimer exhibited singular spectral features, indicating the loss of the B ring aromaticity and the presence of several linkage positions on both B and C rings.

The ^{1}H NMR signals arising from the B ring were two doublets at 2.49 and 2.71 ppm, exhibiting a geminal coupling of ~15 Hz (12.03 ppm) typical of a methylene group and a singlet at 6.38 ppm arising from an ethylenic proton. Since these methylene and ethylene protons were not coupled, they are likely to be in positions 2′B and 5′B. The HMBC spectrum showed all correlations, allowing accurate attributions of these B ring carbons, as illustrated in Figure 5. The H2C of this unit gave three correlations with B ring carbons: one is the methylene carbon at ~45 ppm, which was thus attributed to C2′B, and the remaining two, with carbons resonating at ~90 ppm and ~162 ppm, which can be assigned to C1′B and C6′B. H5′B gave only strong ^{3}J correlations with two quaternary carbons of this B ring: one is the carbon previously assigned to C3′B (~95 ppm), and the other one, which resonated at ~90 ppm, could thus be attributed to C1′B. The carbon at ~162 ppm was then deduced to be C6′B.

The presence of an aliphatic OH (~5.8 ppm) at the C3′B position (~95 ppm) was determined through its ROE correlation with both H2′B protons. Furthermore, OH3′B gave HMBC correlation with a quaternary carbon at ~192.5 ppm, characteristic of a ketone group at the C4′B position.

The shielding of this C1′B of about 40 ppm is in accordance with a loss of the B ring aromaticity. Furthermore, the lack of OH at the C7A position of the other unit is in agreement with an ether linkage C1′B–O–C7A.

The NMR data showed that the C ring of this unit does not have any OH3C. The presence of a C3C–O–C3′B linkage is in accordance with the shielding of C3C of about 1.5 ppm as well as the chemical shift of C3′B which is typical of a hemiketal carbon (95 ppm).

Altogether, the NMR spectral data allow us to conclude that this dimer corresponds to the dehydrocatechin A described earlier by Weinges et al. [33] and then by Guyot et al. [20].

The structures of the six dimeric compounds determined by these NMR analyses are shown in Figure 6, N2, N3, N6, and N8 being pure products, and N4 being a mixture of two isomers.

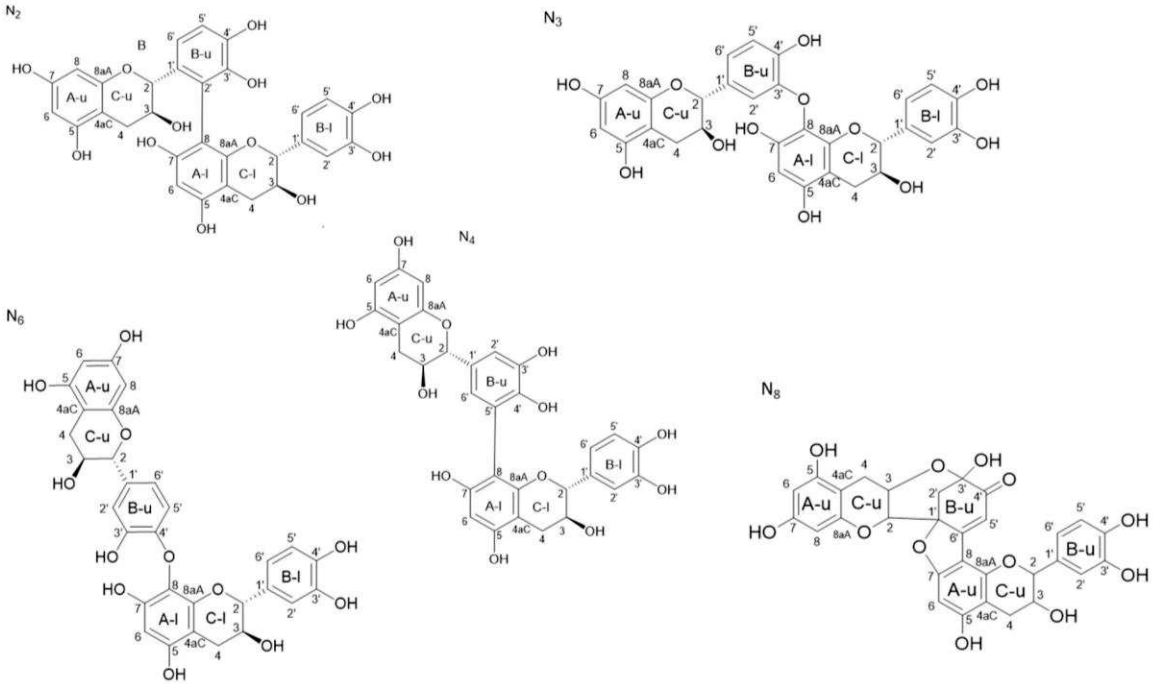

Figure 6. Structures of the six dimeric oxidation products formally identified by NMR analysis, N4 corresponding to a mixture of two isomers. Upper units rings are labelled with u and lower units rings are labelled with l.

3. Materials and Methods

3.1. Chemicals

(+)-Catechin hydrate ≥ 98%; laccase from *Trametes versicolor* (0.94 U·mg^{-1}); sodium phosphate dibasic dihydrate ≥ 98%; citric acid (ACS reagent, cadmium nitrate tetrahydrate 99.997%; formic acid and Amberlite XAD7HP were obtained from Sigma-Aldrich) (Saint-Louis, MO, USA). Acetone-d_6 was purchased from Euriso-top (Saarbrücken, Germany), and trifluoroacetic acid (TFA) from Roth Labo (Karlsruhe, Germany). Water LC-MS, acetonitrile LC-MS (ACN), and methanol LC-MS (MeOH) were all from VWR (Radnor, PA, USA).

3.2. Preparation of the Model Wine Solution

The model wine solution was an ethanol/water solution (12/88; *v*/*v*) with 0.033 M tartaric acid, adjusted to pH 3.6 with NaOH 1 M [34].

3.3. Crude Grape PPO Extracts

The PPO extract was prepared as described previously by Singleton et al. [35]. Frozen grapes were first mixed in an acetate buffer (1.5 M, pH 5; 10 g·L^{-1} ascorbic acid). The mixture was then filtered and centrifuged (3000 g; 10 min). The residue was finally washed with acetone (80%) and air-dried.

3.4. Laccase from Botrytis Cinerea

Laccase from *Botrytis cinerea* was obtained as described by Quijada-Morin et al. [36]. It was produced from the VA612 strain (collected in 2005 in a vineyard in Hautvillers, Champagne, France, from the Pinot Noir cultivar). Briefly, cultures on solid malt yeast medium were left for one week at 24 °C under blue light. The spores were then scraped and inoculated into a 500 mL Erlenmeyer flask containing 125 mL of culture medium (40 g·L^{-1} glucose, 7 g·L^{-1} glycerol, 0.5 g·L^{-1} L-histidine, 0.1 g·L^{-1} $CuSO_4$, 1.8 g·L^{-1} $NaNO_3$, 0.5 g·L^{-1} KCl, 0.5 g·L^{-1} $CaCl_2 \cdot H_2O$, 0.05 g·L^{-1} $FeSO_4 \cdot 7H_2O$, 1.0 g·L^{-1} KH_2PO_4, and 0.7 g·L^{-1} $MgSO_4 \cdot 7H_2O$). After 3 days of incubation and 2 days of growth in the same previous medium, gallic acid (2 g·L^{-1}) was added to the pre-cultures. After 5 days, the

liquid medium was filtered, and the supernatant was submitted to tangential filtration in a Quixstand filtration system (GE Healthcare UK, Little Chalfont, England) equipped with a 30 kDa-molecular weight cut off membrane. The concentrate was finally subjected to a diafiltration against distilled water, and only the fractions that presented oxidant activity against ABTS were kept (−80 °C).

3.5. Oxidation Procedure

A laccase solution (1 $g \cdot L^{-1}$) in phosphate-citrate buffer was previously prepared and added to a 6 $g \cdot L^{-1}$ (+)-catechin solution (model wine) to obtain a laccase final concentration of 0.3 $g \cdot L^{-1}$. The obtained solution was then slowly stirred (180 rpm) at room temperature for 2 h. The concentrations were previously optimized, and the experimentation was performed in triplicate.

3.6. Reaction Stopping on Resin Amberlite XAD7HP

An amberlite column was conditioned with ethanol (absolute) and rinsed with two column volumes of milli-Q water. The previous laccase/(+)-catechin reaction medium was dropped on the column and first eluted with two column volumes of milli-Q water [37]. The column was then eluted with ethanol until the collected fraction was uncolored. Only ethanol fractions were kept, evaporated, and lyophilized. The powder was stored at −80 °C until used.

3.7. Purification Procedure of the Dimeric Fraction Using Flash Chromatography

The lyophilized powder was first purified using a flash chromatography system puriflash430 equipped with a UV detector set at 280 nm and a Puriflash diol 50 µm f0025 column. The binary mobile phase consisted of acetonitrile (solvent A) and methanol (solvent B), both acidified with 0.1% TFA. A series of injection were performed at a constant flow rate of 20 $mL \cdot min^{-1}$, using the following gradient: 100% A for 4.4 min; 0–10% B in 10 min; 10% B for 5 min; 10–90% B in 5 min; 90% B for 3 min; 90–10% B in 2 min; 10% B for 10 min. The injection volume was 1 mL (300 mg lyophilized powder dissolved in 1 mL of solvent A). Three distinct fractions were collected each time. The first one corresponded to residual (+)-catechin, and the third one was a mixture of high-molecular-weight polyphenols. The second eluted fraction, containing a mixture of dimeric oxidation products, was evaporated and lyophilized before the second purification step.

3.8. Purification Procedure of Oxidation Products from the Dimeric Fraction Using a Semi-Preparative Chromatographic System

The fraction containing dimeric oxidation products was purified using a semi-preparative Bio-Rad NGC 10 medium-pressure chromatography system equipped with a reversed-phase Varian Dynamax C18 Microsorb column (250 × 21.2 mm; 3 µm). The binary mobile phase consisted of milli-Q water (solvent A) and 80% acetonitrile, 20% Milli-Q water (solvent B), both acidified with 0.05% TFA. A series of injections (300 µL) of the lyophilized powder (20 mg dissolved in 200 µL of solvent A and 100 µL of ACN) were performed under the following elution conditions: 100% A for 4 min; 0–35% B in 46 min; 35–100% B in 2 min; 100% B for 5 min. Eight distinct fractions were collected each time, corresponding to pure UPLC signals at 280 nm. Each fraction was evaporated and lyophilized before NMR analysis.

3.9. Sample Preparation for NMR Analysis

About 1 mg of each lyophilized powder weighted in Eppendorf tubes was solved into 500 µL of acetone-d_6. Then, ~10 µL of a concentrated solution of cadmium nitrate in acetone-d_6 was added to the samples, and the resulting solutions were transferred to 5 mm NMR tubes for NMR analysis. An additional step was performed for some samples: after solubilization of the lyophilized powders in acetone-d_6 in the presence of traces of

cadmium, the samples were evaporated to dryness and then re-solubilized in acetone-d_6 without further addition of Cd.

3.10. Instrument Specifications

UPLC-MS analysis. The reactions were monitored using two UPLC-MS systems. The first one was used to precisely identify products' retention times using a long gradient method. i.e., Waters reversed-phase Ultra-High-Performance Liquid Chromatography coupled to Mass Spectrometry (UHPLC-MS). The liquid chromatography system was an Acquity UPLC (Waters, Milford, MA, USA) equipped with a photodiode array detector. We used an Acquity UPLC HSS T3 column (1.8 µm, 2.1 × 150 mm). The column temperature was 25 °C. The binary mobile phase consisted of 0.1% formic acid in water (solvent A) and acetonitrile (solvent B). The separation was performed at a constant flow rate of 0.25 mL·min^{-1}, using the following gradient: 8–11% B in 2 min; 11% B for 8 min; 11–25% B in 15 min; 25–55% B in 5 min; 55–99% B in 1 min; 99% B for 4 min; 99–8% B in 1 min; 8% B for 4 min. The injection volume was 5 µL. The mass spectrometer was a Waters Acquity QDa electrospray ionization (ESI) simple quadrupole (Waters, Milford, MA, USA). The capillary voltage was set at 0.8 kV. The mass spectra were acquired over a mass range of 200−900 Th in the positive ion mode.

The second UHPLC-MS system, used for a rapid verification during the purification steps, was the same as described previously, with an Acquity UHPLC HSS T3 column (1.8 µm, 2.1 × 100 mm) heated at 38 °C. The separation was performed at a constant flow rate of 0.55 mL·min^{-1}, using the following fast gradient: 0.1–40% B in 5 min; 40–99% B in 2 min; 99% B for 1 min; 99–0.1% B in 1 min. The injection volume was 2 µL. The mass spectrometer was a Bruker amaZon X electrospray ionization (ESI) ion trap (Bruker Daltonics, Bremen, Germany). The capillary voltage was set at −5.5 kV. The mass spectra were acquired over a mass range of 50−2000 Th in the positive ion mode.

All UPLC-MS analyses were performed in triplicate.

NMR Instrumentation. All the NMR spectra were recorded on an Agilent DD2 500 MHz spectrometer (Agilent Technologies, Santa Clara, CA, USA), operating at 500.05 and 125.74 MHz for proton and carbon-13 nuclei, respectively, using a 5 mm indirect detection probe equipped with a z gradient coil. 1D ^{1}H and ^{13}C, 2D homonuclear ^{1}H TOCSY and ROESY, and heteronuclear ^{1}H/^{13}C HSQC and HMBC experiments were performed using classical pulse sequences and analyzed using both VNMRJ4.2 and MestReNova 14.2.1 (Mestrelab Research, Spain) software. DOSY measurements were acquired and processed as previously described [38]. The acquisition parameters of the DgcsteSL pulse sequence were as follows: the diffusion delay time and the gradient pulse width were set at 50 ms and 2 ms, respectively, the gradient strength (g) was incremented in 16 steps with equal g2 spacing from 0.3 to 32 G·cm^{-1}. After phase correction, 2D DOSY spectra were constructed from the peak height measurement using VNMRJ4.2 software.

All spectra were referenced to the solvent acetone-d_6 signals (^{1}H residual signal at 2.05 ppm and ^{13}C signal at 29.92 ppm).

4. Conclusions

The action of three different oxidoreductases (polyphenoloxidase extracted from grapes, laccase from *Botrytis cinerea*, and laccase from *Trametes versicolor*) on (+)-catechin were investigated, and the LC-UV-MS resulting profiles were very similar, although some minor differences suggested possible dissimilarities in the reactivity of these enzymes.

The structures of six catechin-laccase oxidation products (using laccase from *Trametes versicolor*) were obtained on the basis of specific NMR signatures (four pure products, i.e., N2, N3, N6, and N8, and N4, corresponding to a mixture of two isomers). The complete attribution of phenolic OH signals was possible thanks to the addition of cadmium nitrate with a simple preparation procedure that allowed the unambiguous attribution of the linkages between the catechin units for some of the compounds of interest. This procedure

will greatly simplify NMR analysis of polyphenols mixtures, either synthetized or extracted from natural products.

The standards obtained in this work may be used in the future as oxidation markers to investigate their presence and evolution during grape ripening and wine ageing. Besides catechin, other polyphenol compounds, including flavonoids and non-flavonoids, may also be used as substrates of laccase to obtain additional new standards.

Supplementary Materials: The following are available online, Figure S1: Classification of enzymes responsible for enzymatic browning; Table S1: ^{1}H and ^{13}C NMR assignments for compounds N2, N3, N4, N6, and N8; Figure S2: 2D $^{1}H/^{13}C$ HMBC, top 1D ^{1}H, side 1D ^{13}C spectrum (a) N2; (b) N3; (c) N4; (d) N6, and (e) N8; Figure S3: ^{1}H 2D ROESY spectrum showing correlations (in blue) between phenolic and aromatic protons, ROE correlations between phenolic protons due to chemical exchange appear in red (a) N2, (b) N3, (c) N4, (d) N6, and (e) N8.

Author Contributions: Conceptualization: C.S.; Data curation: S.D.; Formal analysis: S.D.; Funding acquisition: C.S.; Investigation: S.D. and C.l.G.; Methodology: S.D., L.S., C.l.G. and C.S.; Project administration and validation: C.S.; Supervision: L.M., F.G. and C.S.; Visualization: S.D.; Writing—original draft: S.D.; Writing—review and editing: S.D., C.S., L.M., F.G., L.S. and C.l.G. All authors have read and agreed to the published version of the manuscript.

Funding: This work was supported in part by a PhD grant (S.D.) from the University of Montpellier (Bourse école doctorale GAIA).

Institutional Review Board Statement: Not applicable.

Informed Consent Statement: Not applicable.

Data Availability Statement: The data presented in this study are available in the present article and Supplementary Information Section.

Conflicts of Interest: The authors declare no conflict of interest.

Sample Availability: Samples of the compounds are not available from the authors.

Abbreviations

NMR: nuclear magnetic resonance, Cd: cadmium, TOCSY: total correlation spectroscopy, ROESY: Rotating-frame nuclear Overhauser effect spectroscopy, HSQC: heteronuclear single-quantum correlation experiment, HMBC: heteronuclear multi-bond connectivity, DOSY: diffusion ordered spectroscopy.

References

1. Khan, N.; Mukhtar, H. Tea Polyphenols for Health Promotion. *Life Sci.* **2007**, *81*, 519–533. [CrossRef]
2. Fayeulle, N.; Vallverdu-Queralt, A.; Meudec, E.; Hue, C.; Boulanger, R.; Cheynier, V.; Sommerer, N. Characterization of New Flavan-3-Ol Derivatives in Fermented Cocoa Beans. *Food Chem.* **2018**, *259*, 207–212. [CrossRef] [PubMed]
3. Rimbach, G.; Melchin, M.; Moehring, J.; Wagner, A.E. Polyphenols from Cocoa and Vascular Health—A Critical Review. *Int. J. Mol. Sci.* **2009**, *10*, 4290–4309. [CrossRef]
4. Avram, A.M.; Morin, P.; Brownmiller, C.; Howard, L.R.; Sengupta, A.; Wickramasinghe, S.R. Concentrations of Polyphenols from Blueberry Pomace Extract Using Nanofiltration. *Food Bioprod. Process.* **2017**, *106*, 91–101. [CrossRef]
5. Antoniolli, A.; Fontana, A.R.; Piccoli, P.; Bottini, R. Characterization of Polyphenols and Evaluation of Antioxidant Capacity in Grape Pomace of the Cv. Malbec. *Food Chem.* **2015**, *178*, 172–178. [CrossRef]
6. Saucier, C. How Do Wine Polyphenols Evolve during Wine Ageing? *Cerevisia* **2010**, *35*, 11–15. [CrossRef]
7. Oliveira, C.M.; Ferreira, A.C.S.; De Freitas, V.; Silva, A.M.S. Oxidation Mechanisms Occurring in Wines. *Food Res. Int.* **2011**, *44*, 1115–1126. [CrossRef]
8. Singleton, V.L. Oxygen with Phenols and Related Reactions in Musts, Wines, and Model Systems: Observations and Practical Implications. *Am. J. Enol. Vitic.* **1987**, *38*, 69–77.
9. Mathew, A.G.; Parpia, H.A.B. Food Browning as a Polyphenol Reaction. In *Advances in Food Research*; Chichester, C.O., Mrak, E.M., Stewart, G.F., Eds.; Academic Press: Cambridge, MA, USA, 1971; Volume 19, pp. 75–145. [CrossRef]
10. Gambuti, A.; Rinaldi, A.; Ugliano, M.; Moio, L. Evolution of Phenolic Compounds and Astringency during Aging of Red Wine: Effect of Oxygen Exposure before and after Bottling. *J. Agric. Food Chem.* **2013**, *61*, 1618–1627. [CrossRef] [PubMed]

11. Caillé, S.; Samson, A.; Wirth, J.; Diéval, J.-B.; Vidal, S.; Cheynier, V. Sensory Characteristics Changes of Red Grenache Wines Submitted to Different Oxygen Exposures Pre and Post Bottling. *Anal. Chim. Acta* **2010**, *660*, 35–42. [CrossRef]
12. Dubernet, M.; Ribereau-Gayon, P.; Lerner, H.R.; Harel, E.; Mayer, A.M. Purification and Properties of Laccase from Botrytis Cinerea. *Phytochemistry* **1977**, *16*, 191–193. [CrossRef]
13. Li, H.; Guo, A.; Wang, H. Mechanisms of Oxidative Browning of Wine. *Food Chem.* **2008**, *108*, 1–13. [CrossRef]
14. Ployon, S.; Attina, A.; Vialaret, J.; Walker, A.S.; Hirtz, C.; Saucier, C. Laccases 2 & 3 as Biomarkers of Botrytis Cinerea Infection in Sweet White Wines. *Food Chem.* **2020**, *315*, 126233. [CrossRef]
15. Robards, K.; Prenzler, P.D.; Tucker, G.; Swatsitang, P.; Glover, W. Phenolic Compounds and Their Role in Oxidative Processes in Fruits. *Food Chem.* **1999**, *66*, 401–436. [CrossRef]
16. Sánchez-Ferrer, Á.; Neptuno Rodríguez-López, J.; García-Cánovas, F.; García-Carmona, F. Tyrosinase: A Comprehensive Review of Its Mechanism. *Biochim. Biophys. Acta BBA—Protein Struct. Mol. Enzymol.* **1995**, *1247*, 1–11. [CrossRef]
17. Du Toit, W.J.; Marais, J.; Pretorius, I.S.; du Toit, M. Oxygen in Must and Wine: A Review. *S. Afr. J. Enol. Vitic.* **2006**, *27*, 76–94. [CrossRef]
18. Kutyrev, A.A.; Moskva, V.V. Nucleophilic Reactions of Quinones. *Russ. Chem. Rev.* **1991**, *60*, 72. [CrossRef]
19. Guyot, S.; Cheynier, V.; Souquet, J.M.; Moutounet, M. Influence of PH on the Enzymic Oxidation of (+)-Catechin in Model Systems. *J. Agric. Food Chem.* **1995**, *43*, 2458–2462. [CrossRef]
20. Guyot, S.; Vercauteren, J.; Cheynier, V. Structural Determination of Colourless and Yellow Dimers Resulting from (+)-Catechin Coupling Catalysed by Grape Polyphenoloxidase. *Phytochemistry* **1996**, *42*, 1279–1288. [CrossRef]
21. Sun, W.; Miller, J.M. Tandem Mass Spectrometry of the B-Type Procyanidins in Wine and B-Type Dehydrodicatechins in an Autoxidation Mixture of (+)-Catechin and (−)-Epicatechin. *J. Mass Spectrom.* **2003**, *38*, 438–446. [CrossRef]
22. Jiménez-Atiénzar, M.; Cabanes, J.; Gandía-Herrero, F.; García-Carmona, F. Kinetic Analysis of Catechin Oxidation by Polyphenol Oxidase at Neutral PH. *Biochem. Biophys. Res. Commun.* **2004**, *319*, 902–910. [CrossRef]
23. Cheynier, V.; Basire, N.; Rigaud, J. Mechanism of Trans-Caffeoyltartaric Acid and Catechin Oxidation in Model Solutions Containing Grape Polyphenoloxidase. *J. Agric. Food Chem.* **1989**, *37*, 1069–1071. [CrossRef]
24. López-Serrano, M.; Ros Barceló, A. Reversed-Phase and Size-Exclusion Chromatography as Useful Tools in the Resolution of Peroxidase-Mediated (+)-Catechin Oxidation Products. *J. Chromatogr. A* **2001**, *919*, 267–273. [CrossRef]
25. Mouls, L.; Fulcrand, H. UPLC-ESI-MS Study of the Oxidation Markers Released from Tannin Depolymerization: Toward a Better Characterization of the Tannin Evolution over Food and Beverage Processing: Oxidation Markers Released from Tannin Depolymerization. *J. Mass Spectrom.* **2012**, *47*, 1450–1457. [CrossRef] [PubMed]
26. Mouls, L.; Fulcrand, H. Identification of New Oxidation Markers of Grape-Condensed Tannins by UPLC-MS Analysis after Chemical Depolymerization. *Tetrahedron* **2015**, *71*, 3012–3019. [CrossRef]
27. López-Serrano, M.; Ros Barceló, A. Comparative Study of the Products of the Peroxidase-Catalyzed and the Polyphenoloxidase-Catalyzed (+)-Catechin Oxidation. Their Possible Implications in Strawberry (*Fragaria* × *Ananassa*) Browning Reactions. *J. Agric. Food Chem.* **2002**, *50*, 1218–1224. [CrossRef]
28. Appeldoorn, M.M.; Sanders, M.; Vincken, J.P.; Cheynier, V.; Le Guernevé, C.; Hollman, P.C.H.; Gruppen, H. Efficient Isolation of Major Procyanidin A-Type Dimers from Peanut Skins and B-Type Dimers from Grape Seeds. *Food Chem.* **2009**, *117*, 713–720. [CrossRef]
29. Es-Safi, N.E.; Guernevé, C.L.; Ducrot, P.H. Application of NMR Spectroscopy and Mass Spectrometry to the Structural Elucidation of Modified Flavan-3-ols and Their Coupling Reaction Products*. *Spectrosc. Lett.* **2008**, *41*, 41–56. [CrossRef]
30. De Bruyne, T.; Pieters, L.A.C.; Dommisse, R.A.; Kolodziej, H.; Wray, V.; Domke, T.; Vlietinck, A.J. Unambiguous Assignments for Free Dimeric Proanthocyanidin Phenols from 2D NMR. *Phytochemistry* **1996**, *43*, 265–272. [CrossRef]
31. Charisiadis, P.; Primikyri, A.; Exarchou, V.; Tzakos, A.; Gerothanassis, I.P. Unprecedented Ultra-High-Resolution Hydroxy Group 1H NMR Spectroscopic Analysis of Plant Extracts. *J. Nat. Prod.* **2011**, *74*, 2462–2466. [CrossRef]
32. Esatbeyoglu, T.; Jaschok-Kentner, B.; Wray, V.; Winterhalter, P. Structure Elucidation of Procyanidin Oligomers by Low-Temperature 1H NMR Spectroscopy. *J. Agric. Food Chem.* **2011**, *59*, 62–69. [CrossRef] [PubMed]
33. Weinges, K.; Ebert, W.; Huthwelker, D.; Mattauch, H.; Perner, J. Oxydative Kupplung von Phenolen, II1) Konstitution und Bildungsmechanismus des Dehydro-dicatechins A. *Justus Liebigs Ann. Chem.* **1969**, *726*, 114–124. [CrossRef]
34. Zou, H.; Kilmartin, P.A.; Inglis, M.J.; Frost, A. Extraction of Phenolic Compounds during Vinification of Pinot Noir Wine Examined by HPLC and Cyclic Voltammetry. *Aust. J. Grape Wine Res.* **2002**, *8*, 163–174. [CrossRef]
35. Singleton, V.L.; Salgues, M.; Zaya, J.; Trousdale, E. Caftaric Acid Disappearance and Conversion to Products of Enzymic Oxidation in Grape Must and Wine. *Am. J. Enol. Vitic.* **1985**, *36*, 50–56.
36. Quijada-Morin, N.; Garcia, F.; Lambert, K.; Walker, A.S.; Tiers, L.; Viaud, M.; Sauvage, F.X.; Hirtz, C.; Saucier, C. Strain Effect on Extracellular Laccase Activities from Botrytis Cinerea. *Aust. J. Grape Wine Res.* **2018**, *24*, 241–251. [CrossRef]
37. Spinelli, D.; Fatarella, E.; Di Michele, A.; Pogni, R. Immobilization of Fungal (Trametes Versicolor) Laccase onto Amberlite IR-120 H Beads: Optimization and Characterization. *Process Biochem.* **2013**, *48*, 218–223. [CrossRef]
38. Watrelot, A.A.; Le Guernevé, C.; Hallé, H.; Meudec, E.; Véran, F.; Williams, P.; Robillard, B.; Garcia, F.; Poncet-Legrand, C.; Cheynier, V. Multimethod Approach for Extensive Characterization of Gallnut Tannin Extracts. *J. Agric. Food Chem.* **2020**, *68*, 13426–13438. [CrossRef]

Partie II

Les marqueurs d'oxydation précédemment obtenus dans la partie I de ce chapitre et identifiés peuvent ensuite servir de standards analytiques pour leur identification dans des milieux complexes (raisin, vin)

Les objectifs de cette partie étaient de mettre au point une méthode analytique afin d'identifier les marqueurs d'oxydation précédemment décrits dans la partie I dans des extraits de raisin ou de vin. Les échantillons utilisés étaient

- des extraits de pépins de différents cépages : Tannat, Merlot et Syrah à différents stades de maturation : stade vert, véraison et maturité
- des échantillons de vins rouges de Syrah issus du même processus de vinification mais à différents millésimes : 2018, 2014 et 2010.
- **la méthode principale** utilisée dans cette étude était une séparation chromatographique par UHPLC (280nm) suivi d'une séparation/analyse par spectrométrie de masse à trappe orbitale.

Les hypothèses étaient les suivantes :

1. Les marqueurs d'oxydation dimériques identifiés dans la partie I sont identifiables dans des extraits complexes de pépins et de vins.
2. La maturation de la baie et le millésime du vin ont un effet sur la teneur de ces marqueurs

Conclusions

1. Chacun des 8 marqueurs d'oxydation dimériques possède un spectre de fragmentations spécifique qui permets leur identification dans des milieu complexes.
   Ces spectres ont pu être acquis grâce aux standards obtenus par hémisynthèse.
2. Tous les marqueurs d'oxydation (liaisons interflavanes C-C ou C-O-C) présentent un fragment spécifique *m/z* = 393, absent des spectres fragmentation des dimères natifs de type B. La fragmentation des dimères d'oxydation possédant une liaison biaryl éther (C-O-C) présentent un fragment spécifique *m/z* = 291 absent des spectres fragmentation des dimères d'oxydation possédant une liaison biaryl C-C et des spectres de fragmentation des dimères natifs de type B.
3. L'analyse des extraits de pépins de trois variétés différentes (Merlot, Tannat, Syrah) a révélé la présence de trois marqueurs N6, N7 et N8. Leur concentration varie selon l'ordre décroissant suivant Merlot > Tannat > Syrah. Cette différence peut être dû à un

effet variétal ou à une composition en flavanols initiale variable. La concentration de ces marqueurs tend à augmenter avec la maturation de la baie (intensité de l'ion moléculaire multiplié par au moins un facteur 10 entre le stade vert et maturité).

4. L'analyse de trois vins 100% Syrah à trois millésimes différents : 2018, 2014 et 2010 a révélé la présence d'un marqueur d'oxydation N6 et la présence possible de deux autres N2 et N5. Une concentration décroissante de ces marqueurs a été observé avec le vieillissement du vin ce qui peut être révélateur de réactions supplémentaires survenant avec l'évolution du vin.

Cette étude a fait l'objet d'un article scientifique (à soumettre dans le journal *Food chemistry*) sous la référence :

Stacy Deshaies, Nicolas Sommerer, François Garcia, Laetitia Mouls and Cédric Saucier.
« ***UHPLC-Q-Orbitrap /MS² identification of (+)-Catechin oxidation reaction dimeric products in red wines and grape seed extracts: Effect of grape maturation and wine age*** »

Et présenté ci-après

Article 4

UHPLC-Q-Orbitrap /MS² identification of (+)-Catechin oxidation reaction dimeric products in red wines and grape seed extracts: Effect of grape maturation and wine age

Stacy Deshaies [1], Nicolas Sommerer [1], François Garcia [1], Laetitia Mouls [1] and Cédric Saucier [1,*]

[1] SPO, Université de Montpellier, INRAE, Institut Agro, 34000 Montpellier, France;
stacy.deshaies@umontpellier.fr (S.D.); nicolas.sommerer@inrae.fr (N.S.) ;
francois.garcia@umontpellier.fr (F.G.); laetitia.mouls@supagro.fr (L.M.);
cedric.saucier@umontpellier.fr (C.S)

* cedric.saucier@umontpellier.fr (corresponding author)

ABSTRACT

B-type procyanidin dimers (B1, B2, B3 and B4) and (+)-catechin dimeric oxidation products were analyzed in grapes and wine by UHPLC-Q-Orbitrap MS. The different dimers gave different fragmentation patterns according to their interflavan linkage (IFL) position. Oxidation dimeric compounds (C-C or C-O-C type) gave a specific fragment ion at *m/z* 393, missing for B-Type dimers fragmentations. A fragment ion at m/z 291 was also observed as specific for oxidation dimeric compounds with a bi-aryl ether linkage. Higher level oxidation products were relatively resistant to fragmentation with abundant specific fragments at *m/z* 425 (Retro Diels Alder), 397 and 245. These specific fragmentations were very useful to identify them in complex samples such as grape seed extracts and wines. Three grape varieties (Merlot, Tannat, Syrah) and three ripening stages (green stage, veraison and maturity) were used and the corresponding seed extracts were obtained. The UHPLC-Q-Orbitrap MS analyses revealed a global increasing trend for the dimeric-catechin oxidation markers during grape ripening. The analysis of monovarietal Syrah wines (three vintages: 2018, 2014 and 2010) revealed a global decreasing trend of these molecules during wine aging which might be due to further oxidation or other chemical reactions.

Key words: oxidation, red wine, flavanol, markers, grape seed, UHPLC/MS, orbitrap

1. Introduction

Condensed tannins are important for red wines as they are associated with organoleptic properties (astringency, color) and product stability. They undergo many modifications through wine making process and wine evolution due to their structures. Their structures consist in a succession of one or several flavan-3-ols units, each of them containing a catechol ring that can be oxidized to form a quinone which is a highly reactive electrophilic compound [1]. Addition reactions with nucleophilic compounds can then occur [2]. One of them is with other flavonoids which may act as nucleophilic compounds due to their phloroglucinol nucleus.

Browning in most fruit [3,4] and, in the early stages of juice or must preparation for wine is mainly the result of enzymatic oxidation of phenolic substances naturally present in grapes [5] or wines [6]. The phenolic compounds in grapes berries are the primary targets to enzymatic oxidation as they are located in the skins [7,8] and seeds in the grapes [9] and are substrates for polyphenol oxidases [10]. They can then be released in wine, depending on wine-making process, possibly affecting the quality of the product through oxidation reactions.

Numerous oxidation molecular markers with very different molecular weight will develop during wine making process and aging. Many studies on flavanols oxidation focused on the dimeric oxidized forms (molecular positive ions at *m/z* 579 or 577 depending on the oxidation level). They differ from the initial proanthocyanidin dimers by the nature and position of the interflavan linkage (IFL). The latter contains either a C-C IFL or a C-O-C IFL between upper unit B-ring and lower unit A-ring while proanthocyanidin dimers have a C-C IFL at C-4/C-8 between C-ring and A-ring with ion at *m/z* 579. Four major proanthocyanidin dimer isomers are usually found in wines: B1, B2, B3 and B4 [11].

Considering the complexity of oxidation dimer structures and the large number of possible isomers, it remains difficult to obtain information on these molecules and to distinguish them from initial proanthocyanidin dimers rapidly and robustly [12] in a complex environment such as wine. Many studies based on high performance liquid chromatography (HPLC) were designed to analyze natural procyanidin dimers but remain weak to identify and characterize isomers [13]. Methods based on molecular mass information (electrospray ionization mass spectrometry coupled to HPLC) [14-16] are a second step to identify complex composition but

does not allow the identification of two dimers with similar retention time. UHPLC coupled MS/MS is then the best option to obtain specific fragmentations and distinguish dimers from each other and identify them in complex mixtures. (Sun *et al*. [17] and Mouls & Fulcrand [18]).

Recently, UHPLC-LTQ-Orbitrap-high resolution mass spectrometry allowed the investigation of complex polymeric polyphenols in model solution and the determination of numerous adducts after depolymerization [19]. Oxidation marker identification in wine after depolymerization was also done, by UHPLC/MS/MS [20].

In this study, we targeted specifically the dimeric oxidized forms of (+)-catechin resulting from the addition of two monomeric (+)-catechin units that could be present in grape seed or wines. Eight standards of these dimeric oxidation markers were previously detected and five of them fully characterized by NMR *. Their structures are reported in ***figure 1***.

The goal of this paper is to investigate the presence of these 5 compounds together with procyanidin B1, B2, B3, B4 in grapes seeds extracts and Syrah red wines and to follow their evolution during grape ripening and wine ageing. For the grapes, three varieties (Merlot, Tannat and Syrah) and three stages of ripening were considered: green stage, veraison, and maturity. For the wines, three vintages of Syrah wines (2018, 2014 and 2010) were used.

* *reference article 3 "Unambiguous NMR structural determination of (+)-Catechin-Laccases dimeric reaction products as potential markers of grape and wine oxidation*.**"**

77

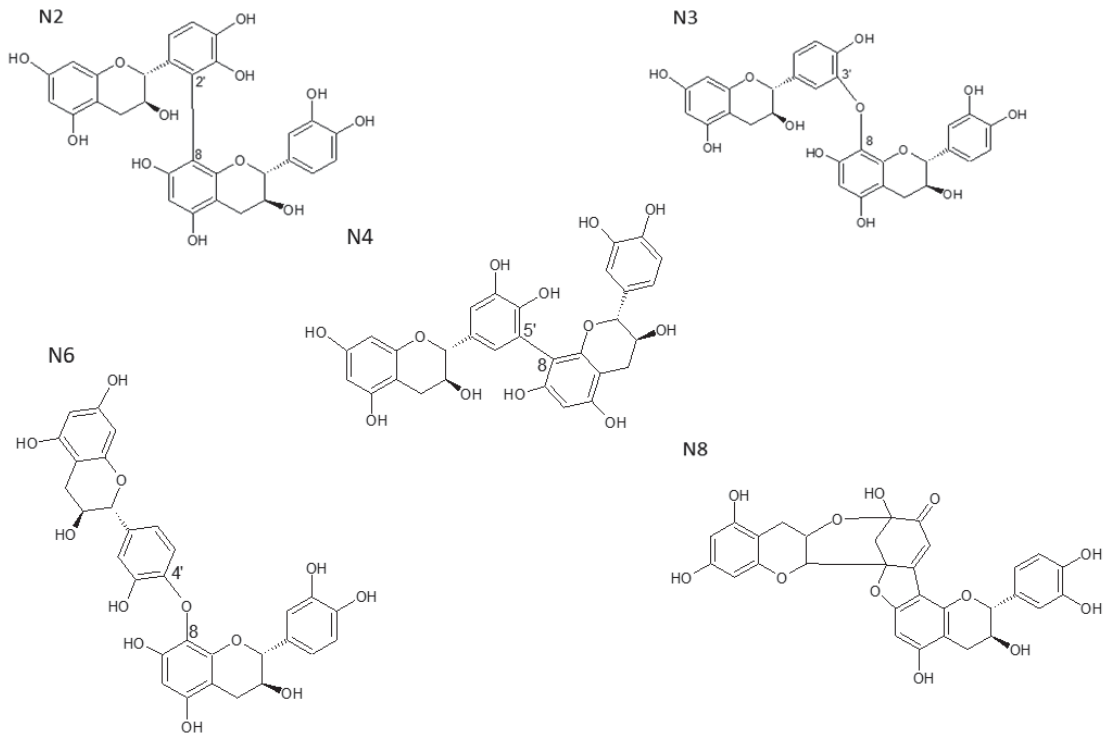

78

79 ***Figure 16 :*** *five identified oxidation markers with different oxidation states: N2, N3, N4 and N6 ions at*
80 *m/z 579 Da and N8 (dehydrodicatechin A) corresponding to a superior oxidation state at m/z 577 Da*
81 *(adapted from *)*

82

83 **3. Material and methods**

84 *2.1. Reagents and Materials*

85 Procyanidin B1 (≥90%), procyanidin B2 (≥90%), procyanidin B3 (≥90%) and procyanidin B4
86 (≥90%) were purchased from Extrasynthese (Genay, France). Formic acid and acetonitrile were
87 obtained from Prolabo (Fontenay S/Bois, France). Deionized water was purified with a Milli-Q
88 water system (Millipore, Bedford, MA) prior to use.

89 *2.2. Wine samples*

90 Three red wines samples, 100% Syrah, 13.5% alcoholic strength, were obtained from the same
91 producer (Domaine des Bouzons, Côtes du Rhône, France) and from three different vintages

* *reference article 3 "Unambiguous NMR structural determination of (+)-Catechin-Laccases dimeric reaction products as potential markers of grape and wine oxidation*."

(2018, 2014, 2010). Wine production: 20 days vatting time in stainless steel vats; maturing of Syrah (40%) in oak barrels for 10 months. Two 750 mL bottles of each vintage were opened and slowly homogenized under nitrogen to avoid oxidation reactions. Aliquots of 50 mL tubes were then immediately frozen at −80 °C.

2.3. Grapes seeds samples

Three *V. vinifera* varieties (Merlot, Tannat, and Syrah) were harvested in 2018 at different stages of ripening: green stage 16/07/2018; veraison 19/07/2018 and maturity 03/09/2018 from INRAE experimental vineyard (Montpellier, France) (coordinates: 43°37′02.7″ N 3°51′22.3″ E, average annual temperature: 15.85 °C, average annual precipitation: 629 mm (the weather was quite dry), and soil: Gravels and river sand). The whole grapes were stored at −80 °C in plastic bags until polyphenols extraction.

2.4. Grapes seeds samples preparation

Polyphenols were extracted from seeds as described previously by Benbouguerra *et al* [21]. Seeds were first manually removed from the pulp. The polyphenols were then extracted with 100 mL of acetone/water (70/30 v/v) deoxygenated with nitrogen for 5 min.

2.5. Instrumentation

The liquid chromatography separation was done on a Vanquish UHPLC (Thermo Fischer Scientific, San José, CA, USA) with an Acquity HSS T3 column (150 mm length, 2.1 mm internal diameter, 1.8 µm particle size; Waters) at 26°C. The mobile phase consisted of H2O/HCO2H (99/1, V/V) (solvent A) and CH3CN/HCO2H (99/1, V/V) (solvent B). The flow rate was 0.25 mL/min and the injection volume 2µL. The elution program was as follows: 8–11% B (0–2 min), isocratic with 11% B (2–10 min), 11–25% B (10–25 min), 25–55% B (25–30 min), 55-99% B (30-31min), isocratic with 99% B (31–35 min), 99-8% B (35-36min) and isocratic with 8% B (36-40min).

The Mass Spectrometer was an Orbitrap Exploris 480 from Thermo Fisher Scientific (San José, CA, USA) equipped with an electrospray ionization (ESI) source and an internal post-source fluoranthen mass calibrant. In the positive and negative ion modes, the voltages were to 3500

and 2500V respectively. Sheath, auxiliary and sweep gases were set to 40, 10 and 2 (arbitrary units) respectively. Ion transfer tube and vaporizer temperatures were set to 280°C and 300°C respectively. The mass range was set to 190-1300 m/z, RF lens was set at 50%, and 1 microscan was used to set the Automatic Gain Control (AGC). The resolution was set to 120k to have an acquisition frequency of ca. 4Hz.

For ion intensity comparison purpose, all MS acquisitions were performed the same day, with blank control between injections. For MS/MS experiments, resolution for the parent ion scan and the MS/MS scan were set to 60k and 15k respectively. The isolation window of the quadrupole was set to 2m/z. The targeted ions were fragmented in the HCD collision cell against Nitrogen with the Stepped Normalized Collision Energy (SNCE) parameter set to 15-30- 45 % or 20-40-60%.

3. Results and discussion

3.1. Standards separation and MS identification

In the whole study, standards untitled N1 to N8 corresponded to oxidation dimers previously hemi-synthesized in a previous work* with unambiguous structures for N2, N3, N4, N6 and N8. The B1, B2, B3, B4 dimers correspond to B-type procyanidins (structures available in supplementary data ***figure S1***). Their retention times and their experimental masses (below 1ppm mass error, exact protonated masses being 577.13405 and 579.14970) are reported in ***figure 2***.

142

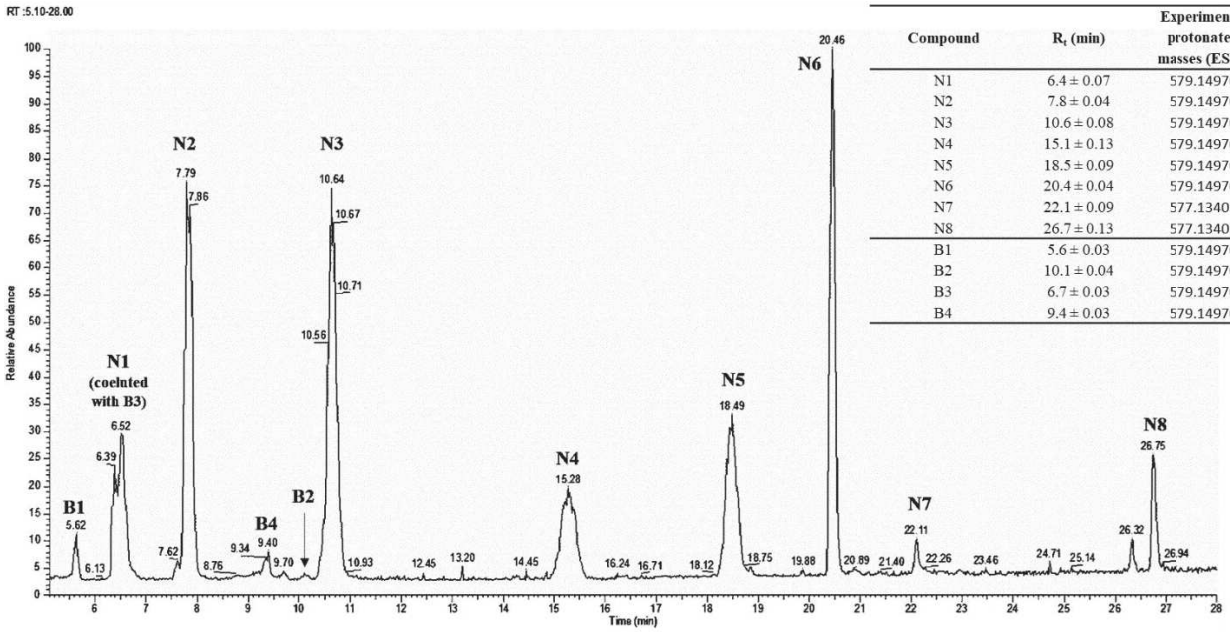

Compound	R_t (min)	Experimental protonated masses (ESI+)
N1	6.4 ± 0.07	579.14970
N2	7.8 ± 0.04	579.14970
N3	10.6 ± 0.08	579.14970
N4	15.1 ± 0.13	579.14970
N5	18.5 ± 0.09	579.14970
N6	20.4 ± 0.04	579.14970
N7	22.1 ± 0.09	577.13405
N8	26.7 ± 0.13	577.13405
B1	5.6 ± 0.03	579.14970
B2	10.1 ± 0.04	579.14970
B3	6.7 ± 0.03	579.14970
B4	9.4 ± 0.03	579.14970

143

144 ***Figure 17 :*** *TIC MS (total ion chomatogram) of dimeric mixture containing four B-type dimeric*
145 *procyanidins (B1 to B4) and eight oxidation dimeric markers (N1 to N8).*

146 The developed method allowed an optimized separation within a short analysis period. A partial
147 coelution was however observed between B1 and N1 around 6.4 min, N1 showing two close
148 peaks at 6.4 and 6.5min (N1a and N1b). B2 retention time (10.1 min) was also close to N3 one
149 (10.6 min). Some of these oxidation dimers were detected and structurally hypothesized in a
150 previous study [17] but it is the first time that fully NMR characterized standards were used
151 with a high resolution UHPLC/MS/MS analysis. Further fragmentations were performed to
152 differentiate isomers. Positive ion mass spectra for N2, N7 and procyanidin B1 are presented in
153 ***figure 3*** (positive ion mass spectrum for N1a, N1b, N3, N4, N6, N8, B2, B3, B4 are available
154 in supplementary data ***figures S2 and S3***).

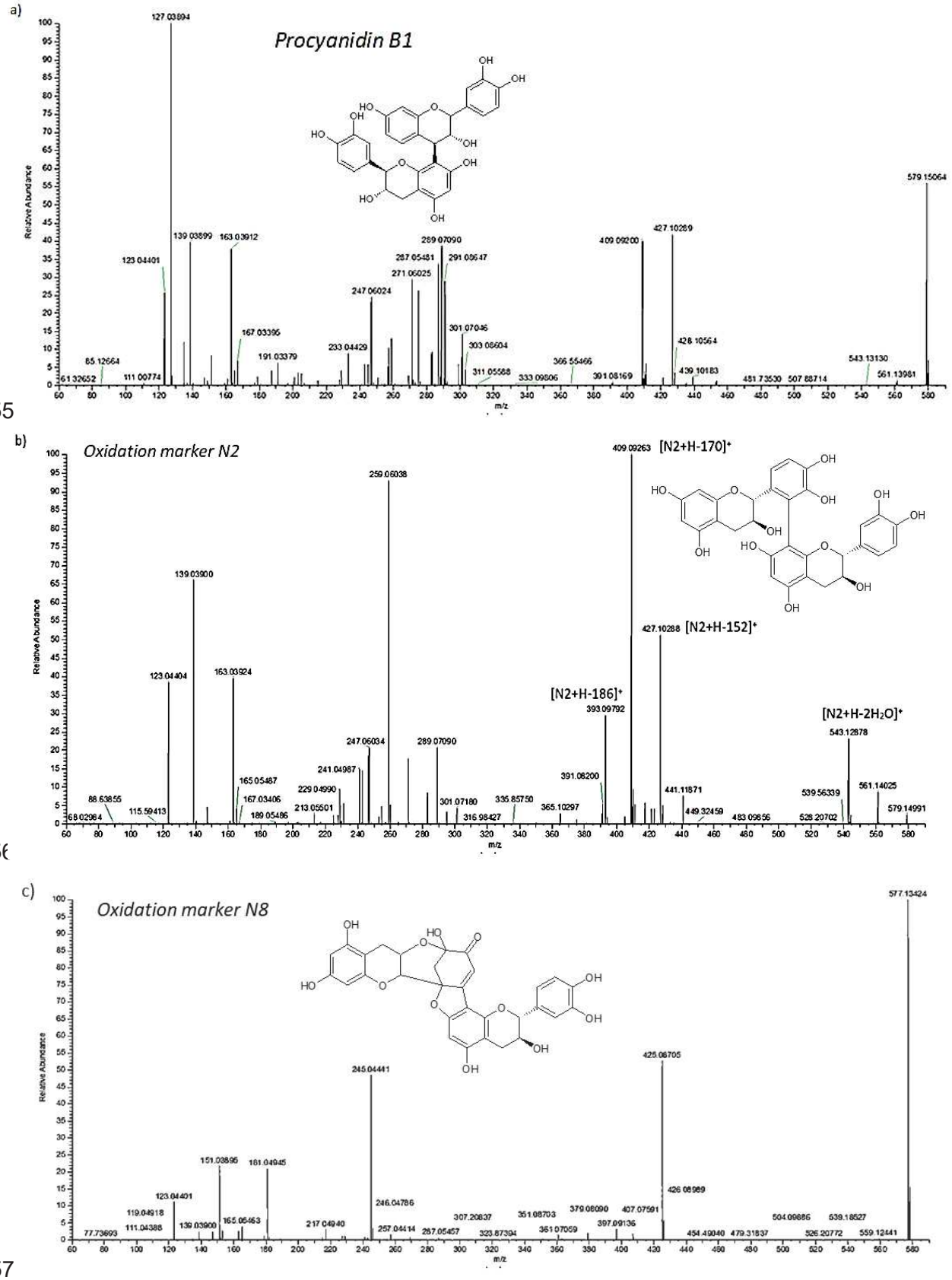

Figure 18 : *Positive ion tandem mass spectra of the procyanidin B1 (a) , the oxidation dimer N2 (b) and oxidation dimer N8 (c) with Stepped Normalized Collision Energy (SNCE), 30% midpoint, 15% range and three steps*

The positive ion tandem mass spectra of B1 (***figure 3.a***) gave characteristic fragment ions at *m/z* 427 (Retro Diels alder), 409 and 289 with residual abundant ions, resulting from fragmentations, at 127, 139 and 163 [22]. These ions were similar for other B-type mass spectra (ion mass spectrum of B2, B3 and B4 available in ***figure S2***). Fragment ion at *m/z* 453 identified as abundant in previous study [17] is really low or missing in our study, probably related with its ability to easily dissociate into *m/z* 289 ion.

Figure 3(b) and (c) represents the tandem mass spectra of the two types of protonated oxidation dimers. Ion at *m/z* 289 was identified in every fragmentation spectrum [17] but does not result from the same fragmentation pathway. This ion is easily formed for natural dimers and consequently shows a high relative abundance (RA) (***figure S2***). For elucidated oxidation dimers containing a C-C IFL this RA is also high, ion at *m/z* 289 may result from successive breaks of upper unit A and C rings followed by a RDA mechanism on the lower unit (***figure S5***).

However, RA for *m/z* 289 is noticeably reduced for elucidated dimers with a C-O-C IFL. In this case, it results from *m/z* 291 deprotonation. It is noteworthy that *m/z* 291 is really specific of C-O-C IFL fragmentation. Indeed, it can be hypothesized that the presence of an oxygen atom on the IFL favors the fragmentation, on the contrary to C-C IFL.

This ion *m/z* 289 is missing for dimers with a second oxidation state as N7 or N8 (dehydrodicatechin A).

Dimers N1 to N6 ($[M+H]^+$ = 579 / ***Figure 3.b***) with a C-C or a C-O-C IFL form a specific fragment ion at *m/z* 393, missing for B type dimers, their C-C bond between C-ring of the upper unit and A-ring of the lower unit being very weak. Structure elucidation hypothesis for fragment ions for N2 and N4 are represented in supplementary data (***figures S5 and S6***). For dimers with a bi-aryl linkage (***figure S5***), this specific fragment may result from the rearrangement of the dimeric structure after successive water losses. For dimers with a bi-aryl linkage (***figure S6***), it can be hypothesized that this fragment ion results from a rearrangement after a HRF mechanism.

For dimers N7 and N8 ($[M+H]^+$ = 577 / ***Figure 3.c***), dissociation in MS/MS experiments was inhibited by a stable hyperconjuguated π- π system within the molecules, whereas in native dimers and N1 to N6, the product ions were stabilized by creating a similar π- π system. At a Stepped Normalized Collision Energy of 30% with 3 steps and a 15% window, abundant

fragment ions for N7 are *m/z* 397 Da and *m/z* 245 Da, and *m/z* 425 Da (RDA $[M+H-152]^+$) and *m/z* 245 Da for N8 (dehydrodicatechin A). A SNCE of 40% with three steps and a 20% window has been investigated and it resulted in better fragmentation efficiency for the compounds (***figure S4***) even if the parent ion at m/z 577 Da remains largely present. Structure elucidation hypothesis for the fragment ions of dehydrodicatechin N8 is represented in supplementary data (***figure S7***).

In summary, our hemisynthetized standard oxidation dimeric molecules gave significative difference in mass fragmentations compared to procyanidin dimers.

3.2. Identification in grape seeds extracts

Grapes seeds extracts were investigated in the study due to their higher polyphenolic content and lower molecular weight flavanols compared to skins [21]. Previous studies report the identification of natural dimers B1 to B4 in wines and grape seeds extracts [9,11].

Nicoletti & al. [23] also identified and quantified a wide selection of phenolic compounds in different grape varieties and noted large differences between samples. Oxidation markers resulting from the reaction between flavanols and volatile thiols were also investigated [24,25]. Numerous B-type oligomeric procyanidins, mostly C4-C6-linked oligomers, with (+)-catechin, (-)-epicatechin and (-)-epicatechin-3-O-gallate units were detected in *Vitis vinifera* grape seeds [9], skins [26] and pulp [27].

However, few references can be found on the topic of polyphenol oxidation marker evolution in grape seeds and in red wines. For the three considered varieties in the study (Syrah, Tannat and Merlot), three of the eight oxidation dimers previously presented in ***figure 2*** were identified. EIC chromatograms for N6 and for the three ripening stages of Merlot, Syrah and Tannat are presented in supplementary data (respectively ***figures S8, S9 and S10***). N6 (Tr 20.3min) intensity tends to increase during berries maturation from 6.8^E5 at green stage to 2.0^E6 at maturation (***table 1***) for Merlot variety. Same observations were made for N7 (Tr 22.03min) and N8 (26.7min) (***figure 4 a.b.c***) with really low signals for N7, especially at green stage.

Tandem mass spectra allowed us to confirm the presence of oxidation dimers N6, N7 and N8 by using specific MS/MS fragmentations that were seen for the standards in part 3.1. Specific fragments for N6 were identified in each variety (***figures S8d. S9d. and S10d***.) at *m/z* 427, 409, 393 and 289 Th. It can be reported that fragmentation is more efficient for the standards than in Merlot wine which was probably due to a matrix effect. Moreover, for low abundance parent

ions, contaminants may be present in the MS/MS spectra as the isolation window for the parent ion mass selection was set to 2 u.m.a. thus leading to a composite (*i.e.* non pure) MS/MS spectrum. Possible fragmentations pathways for N2 and N3 are available in supplementary data.

Similar observations were seen for N7 and N8 (dehydrodicatechin A) both present in Merlot variety based on retention time (figure 4.a.b.c) and specific fragmentations (***figure 4.d.e***.) for ions of interest at 425, 397 and 245. Specific fragmentations for these two compounds N7 and N8 are available in supplementary data (***figure S11***) for Syrah variety at maturity. For Tannat variety, specific fragmentation was only available for N8 (***figure S12***). Indeed, N7 fragmentation spectrum shows, in addition to specific N7 fragmentations, other non-specific fragmentations due to a low parent ion intensity and to the noise surrounding this ion. N7 specific fragments then have low relative abundance, other ions being in the same signal-to-noise ratio (detection limit). However, compared to other varieties and considering that N6 and N8 are observed in Tannat variety, signal at Rt=22.3min can be attributed to N7.

Ion at *m/z* 425 Th was more abundant in Merlot variety than in standard analysis which can be due to matrix effect. A lower relative abundance for *m/z* 245 Th in Merlot variety, which is a supplementary fragmentation of the ion at *m/z* 425 Th was also observed. These differences in relative abundance were not visible for N8 as both the molecular ion and fragments presented a strong signal, less perturbed by the chemical environment: A higher SNCE showed similar results (data not shown).

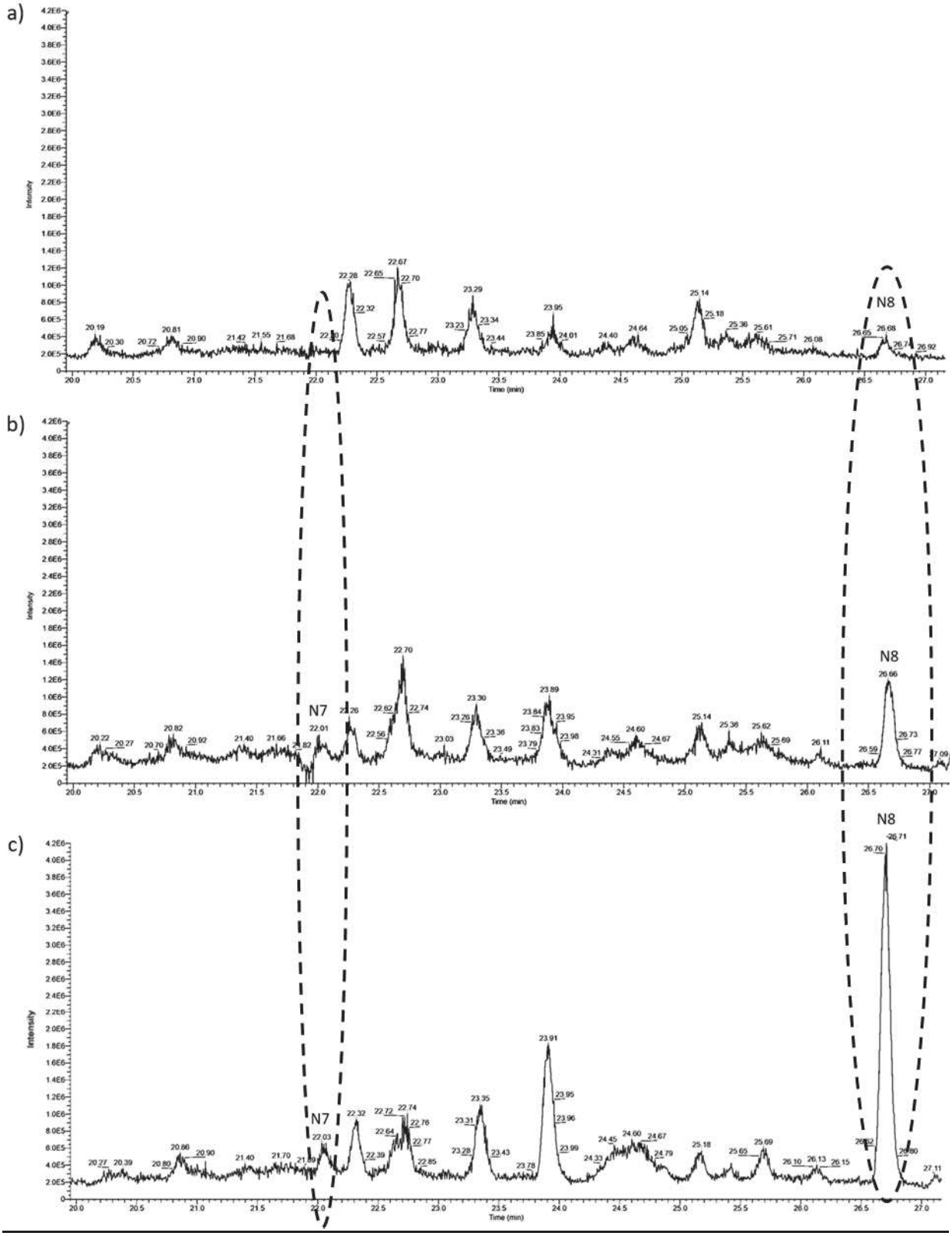

247

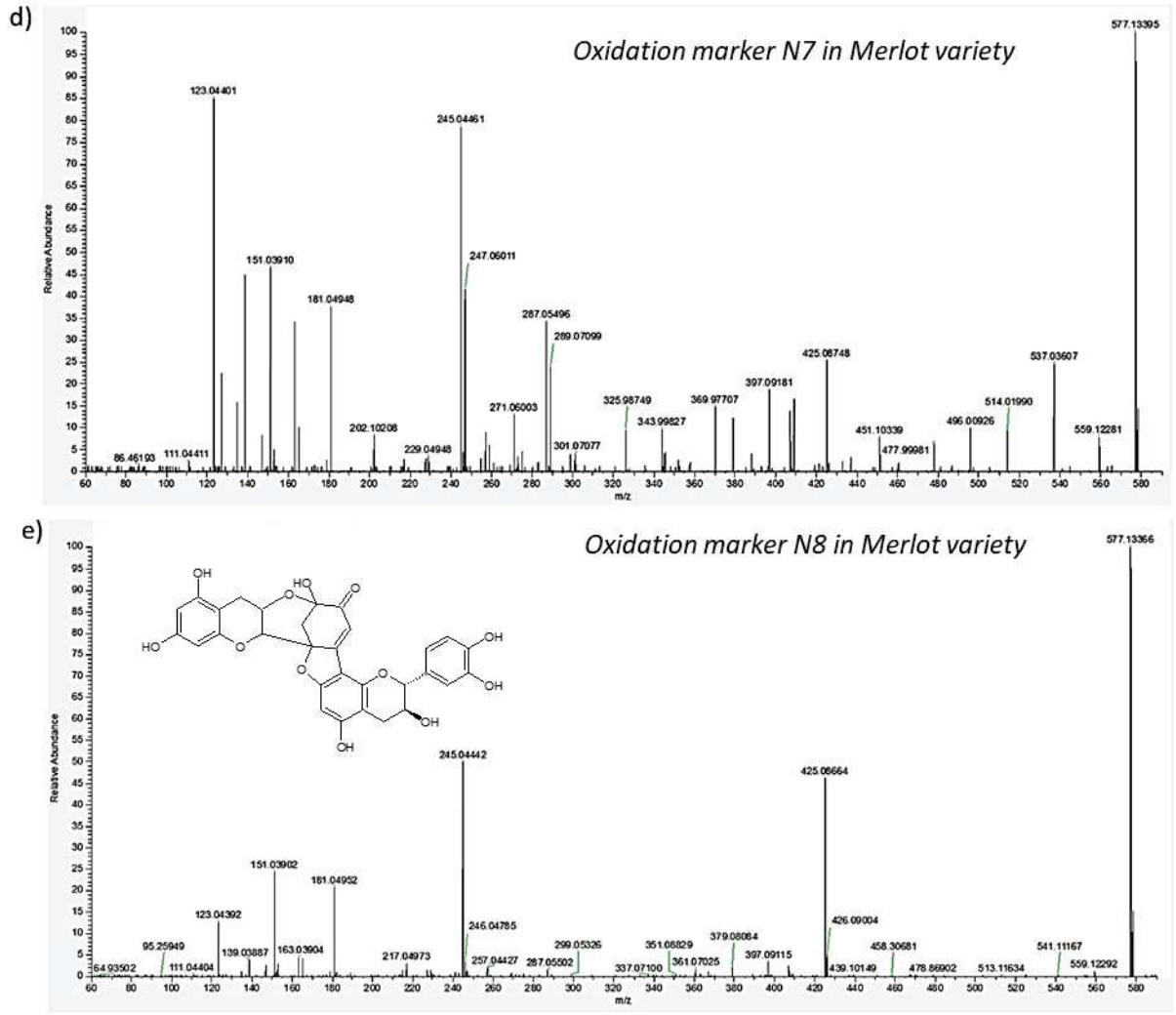

Figure 4: *EIC chromatogram of ion at m/z 577.13405 (+/-1ppm) (Tr 20 – 27min) of three 10g/L grape extracts of Merlot variety at different stage of ripening : green stage (a) ; veraison (b) ; maturity (c) and tandem mass spectra of compound at 22.03min (d) (for maturity) corresponding to N7 and at 26.7 min (e) (for 03/09/2018) corresponding to N8 – SNCE 30% midpoint, 15% range and three steps. Part of the fragment ions of a protonated oxidation dimer N8 is available in supplementary data.*

Table 1 shows the EIC signal intensity evolutions for the three identified markers in three different grape varieties at different date/stages of ripening: 18/06/2018 corresponded to the green stage, 19/07/2018 to veraison and 03/09/2018 to maturity. For all the grape varieties the ion intensities increased with grape evolution for the three markers N6, N7 and N8, with very high signals for N8 at maturity ($5.7^{E}6$ for Merlot at maturity). At green stage, some signals were really low or were missing (less than three times background signal). However, dehydrodicatechin A (N8) was present at each stage which can be representative of its ability to be formed as a result of the grape polyphenoloxidase-catalysed [1,28,29] and/or peroxidase-

catalyzed [5,30] oxidation of (+)-catechin [31] and (-)-epicatechin, largely present in grapes seeds [32].

In our study, the Merlot variety had the highest ion intensities for each marker for the three ripening stages, compared to Tannat and Syrah which was probably related to its higher initial flavanols content. According to *Benbouguerra et al.* [21], the flavanols content in the samples in decreasing order was Merlot > Syrah > Tannat for green stage; Tannat > Syrah > Merlot for veraison and Tannat > Merlot > Syrah for maturity, with an highest flavanols content just before veraison for each variety. It can be explained by a partial oxidation of flavanols starting after veraison [33]. Even if oxidation markers are present before veraison in the extracts, it cannot be confirmed that they are unambiguously present in grape seeds, as extraction process may have caused partial and non-specific flavanol oxidation. However, the very significant ion signal increase for some specific molecular oxidation markers during ripening stages supports the hypothesis of a specific enzymatic oxidation

Table 1: *EIC (extracted ion chromatogram) evolution trend of oxidation markers in three different grape varieties (Merlot, Tannat, Syrah) at different stages of ripening: green stage, veraison and maturity. ND: Not Detected.*

		Ion intensity		
Variety	**Compound identified**	**18/06/2018**	**19/07/2018**	**03/09/2018**
Merlot	N6	$6.8^{E}5 \pm 6\%$	$1.5^{E}6 \pm 2\%$	$2.0^{E}6 \pm 33\%$
	N7	ND	$7.5^{E}5 \pm 17\%$	$9.23^{E}5 \pm 28\%$
	N8	$5.7^{E}5 \pm 26\%$	$8.9^{E}5 \pm 30\%$	$5.7^{E}6 \pm 33\%$
Tannat	N6	ND	$2.0^{E}6 \pm 3\%$	$4.6^{E}6 \pm 1\%$
	N7	ND	$9.7^{E}5 \pm 1\%$	$1.5^{E}6 \pm 1\%$
	N8	ND	$2.1^{E}5 \pm 3\%$	$4.0^{E}6 \pm 3\%$
Syrah	N6	$5.8^{E}5 \pm 10\%$	$1.1^{E}6 \pm 1\%$	$2.4^{E}6 \pm 7\%$
	N7	ND	ND	$8.8^{E}5 \pm 2\%$
	N8	$5.4^{E}5 \pm 0.5$	$1.3^{E}6 \pm 4\%$	$6.6^{E}6 \pm 0.5\%$

3.3. Identification in red wine

In recent years, main research focus on the reactivity and identification of oxidation markers resulting from condensed tannins oxidation [20,25,34]. The latter were analyzed by UHPLC-MS after chemical depolymerization. In the present study, we focused on the specific and direct targeted analysis of (+)-catechin dimeric oxidation products in red wines. Most of the studies

reported in the literature were carried out with monomers in various oxidation conditions (pH, oxidizing reagents) [35,36], and their identification in model wine solutions [10,36] Vivas de Gaulejac *et al.* reported [37,38] the identification of procyanidin A2 (resulting from B2 radical oxidation) and the evolution of stabilized quinones concentration in wine but research work concerning oxidation markers identification in wine, especially using standards, remain few.

For the study, we considered three monovarietal Syrah wines (Domaine des Bouzons, Côtes du Rhône, France) from three different vintages: 2018, 2014 and 2010. The LC-MS analysis revealed the possible presence of five of the eight oxidation markers previously identified (***Table 2***). Fragmentations were not possible on these markers due to the very low signals and the strong background signal resulting matrix effect of wine. However, identifications based on retention times and Extracted Ion Chromatogram at high mass accuracy, below 1ppm, remain precise enough to emit the hypothesis of the presence of these compounds in wine.

N6 was identified in both grape seeds extracts and wines whereas N8 (dehydrodicatechin A) was only present in grape seeds extracts, which may be explained by its ability to undergo further chemical reactions in wine which does not seem to be the case for N6. Two other oxidation markers were only identified in wine (N2 and N5) and for each of the markers we noted a global decreasing trend through the different vintages (except for N5). Wine being a really complex media where numerous chemical reactions occur, oxidation markers between two monomeric units can rapidly occur in a 1-year aged wine (2018) and undergo further chemical modifications during wine aging. Further oxidation steps, involving quinone formation on catechol rings and reaction with other nucleophilic compounds [1].

Table 2 : *identification of oxidation markers in three Syrah wines at different vintages (2018, 2014 and 2010)*

		Ion intensity		
Variety	**Compound identified**	**2018**	**2014**	**2010**
Syrah	N2	$1.7^{E}6 \pm 6\%$	$9.8^{E}5 \pm 3\%$	$8.1^{E}5 \pm 14\%$
	N5	$5.4^{E}5 \pm 3\%$	$6.5^{E}5 \pm 1\%$	$3.0^{E}5 \pm 2\%$
	N6	$4.6^{E}5 \pm 1\%$	$2.6^{E}5 \pm 7\%$	$1.7^{E}5 \pm 4\%$

4. Conclusion

The use of NMR characterized standards for dimeric flavanol oxidation markers and high resolution mass spectrometry allowed the first time detection of some of these new compounds in grape seed extracts and wines. Specific fragmentations were obtained for each oxidation marker and dimeric procyanidins (B1 to B4). One specific fragment at *m/*z 393 Th, corresponding to different structures, was detected for C-C and C-O-C type oxidation markers and was missing for B-type dimeric procyanidins. A specific ion *m/z* = 291 Th was also detected for C-O-C type oxidation markers. These specific ions can be used in further studies to distinguish them from B-type procyanidins, especially when both compounds are coeluted.

Analyses of three grape varieties (Merlot, Tannat, Syrah) revealed the presence of three flavanol oxidation markers (N6, N7 and N8) in theirs seeds during ripening. For all the studied varieties, N6, N7 and N8 were identified and their concentrations increased during ripening as their ion intensities were multiplied by at least a factor 10 from the green to the maturity stage.

The analyses of monovarietal Syrah wines from different vintages (2018, 2014 and 2010) revealed the presence of one oxidation marker (N6) and possibly two other (N2, N5) even if complete fragmentations were not feasible in their cases. A decrease in ion intensity of these markers was observed with wine age, which might indicate further oxidation or chemical reaction during ageing. Relationship between these markers during oxidation steps of winemaking, ageing of red wines should be investigated in futures studies together with sensory properties.

Abbreviations: EIC: extracted ion chromatogram, ESI: electrospray ionization, IFL: Interflavan linkage, NMR: nuclear magnetic resonance, SNCE: stepped normalized collision energy, TIC: total ion chromatogram, UHPLC: ultra-high performance liquid chromatography

Funding: This work was supported in part by a PhD grant (S.D.) from the University of Montpellier (Bourse école doctorale GAIA).

Conflicts of Interest: The authors declare no conflict of interest

References

Akoh, C. C. (2017). *Food Lipids—Chemistry, Nutrition and Biotechnology*. https://www.taylorfrancis.com/books/mono/10.1201/9781315151854/food-lipids-casimir-akoh

Alcade-Eon, C., Escribano-Bailón, M. T., Santos-Buelga, C., & Rivas-Gonzalo, J. C. (2006). Changes in the detailed pigment composition of red wine during maturity and ageing : A comprehensive study. *Analytica Chimica Acta*, *563*(1-2), 238-254.

Allgrove, J., & Davison, G. (2014). Chapter 19—Dark Chocolate/Cocoa Polyphenols and Oxidative Stress. In R. R. Watson, V. R. Preedy, & S. Zibadi (Éds.), *Polyphenols in Human Health and Disease* (p. 241-251). Academic Press. https://doi.org/10.1016/B978-0-12-398456-2.00019-0

Antoniolli, A., Fontana, A. R., Piccoli, P., & Bottini, R. (2015). Characterization of polyphenols and evaluation of antioxidant capacity in grape pomace of the cv. Malbec. *Food Chemistry*, *178*, 172-178. https://doi.org/10.1016/j.foodchem.2015.01.082

Arapitsas, P., Speri, G., Angeli, A., Perenzoni, D., & Mattivi, F. (2014). The influence of storage on the "chemical age" of red wines. *Metabolomics*, *10*, 816-832.

Atanasova, V., Fulcrand, H., Cheynier, V., & Moutounet, M. (2002a). Effect of oxygenation on polyphenol changes occurring in the course of wine-making. *Analytica Chimica Acta*, *458*(1), 15-27. https://doi.org/10.1016/S0003-2670(01)01617-8

Atanasova, V., Fulcrand, H., Cheynier, V., & Moutounet, M. (2002b). Effect of oxygenation on polyphenol changes occurring in the course of wine-making. *Analytica Chimica Acta*, *458*(1), 15-27. https://doi.org/10.1016/S0003-2670(01)01617-8

Avizcuri, J.-M., Sáenz-Navajas, M.-P., Echávarri, J.-F., Ferreira, V., & Fernández-Zurbano, P. (2016). Evaluation of the impact of initial red wine composition on changes in color and anthocyanin content during bottle storage. *Food Chemistry*, *213*, 123-134. https://doi.org/10.1016/j.foodchem.2016.06.050

Bakker, J., & Timberlake, C. F. (1997). Isolation, identification, and characterization of new color-stable anthocyanins occuring in some red wines. *Journal of Agricultural and Food Chemistry*, *45*(1), 35-43.

Barril, C., Clark, A. C., Prenzler, P. D., Karuso, P., & Scollary, G. R. (2009). Formation of Pigment Precursor (+)-1″-Methylene-6″-hydroxy-2H-furan-5″-one-catechin Isomers from (+)-Catechin and a Degradation Product of Ascorbic Acid in a Model Wine System. *Journal of Agricultural and Food Chemistry*, *57*(20), 9539-9546.

Barril, C., Clark, A. C., & Scollary, G. R. (2012). Chemistry of ascorbic acid and sulfur dioxide as an antioxidant system relevant to white wine. *Analytica Chimica Acta*, *732*, 186-193. https://doi.org/10.1016/j.aca.2011.11.011

Bartosz, G., Grzesik-Pietrasiewicz, M., & Sadowska-Bartosz, I. (2020). Fluorescent Products of Anthocyanidin and Anthocyanin Oxidation. *Journal of Agricultural and Food Chemistry*, *68*(43), 12019-12027. https://doi.org/10.1021/acs.jafc.0c04755

Benbouguerra, N., Richard, T., Saucier, C., & Garcia, F. (2020). Voltammetric Behavior, Flavanol and Anthocyanin Contents, and Antioxidant Capacity of Grape Skins and Seeds during Ripening (Vitis vinifera var. Merlot, Tannat, and Syrah). *Antioxidants*, *9*(9), 800. https://doi.org/10.3390/antiox9090800

Berké, B., Chèze, C., Vercauteren, J., & Deffieux, G. (1998). Bisulfite addition to anthocyanins : Revisited structures of colourless adducts. *Tetrahedron Letters*, *39*(32), 5771-5774. https://doi.org/10.1016/S0040-4039(98)01205-2

Berrueta, L. A., Rasines-Perea, Z., Prieto, N., Asensio-Regalado, C., Alonso-Salces, R. M., Sanchez-Ilarduya, M. B., & Gallo, B. (2020). Formation and evolution profiles of anthocyanin derivatives and tannins during fermentations and aging of red wines. *European Food Research and Technology*, *246*, 149-165.

Bradshaw, M. P., Barril, C., Clark, A. C., Prenzler, P. D., & Scollary, G. R. (2011). Ascorbic Acid : A Review of its Chemistry and Reactivity in Relation to a Wine Environment. *Critical Reviews in Food Science and Nutrition*, *51*(6), 479-498. https://doi.org/10.1080/10408391003690559

390 Brossaud, F., Cheynier, V., & Noble, A. C. (2008, mars 12). Bitterness and astringency of
391 grape and wine polyphenols. *Australian Journal of Grape and Wine Research*.
392 Brouillard, R., & Dangles, O. (1994). Anthocyanin molecular interactions : The first step in the
393 formation of new pigments during wine aging? *Food Chemistry*, *51*(4), 365-371.
394 https://doi.org/10.1016/0308-8146(94)90187-2
395 Cacho, J., Castells, J., Esteban, A., Laguna, B., & Sagrista, N. (1995). Iron, Copper, and
396 Manganese Influence on Wine Oxidation. *American Journal of Enology and*
397 *Viticulture*, *46*(3), 380-384.
398 Canals, R., Llaudy, M. C., Valls, J., & Canals, J. M. (2005). Influence of Ethanol
399 Concentration on the Extraction of Color and Phenolic Compounds from the Skin and
400 Seeds of Tempranillo Grapes at Different Stages of Ripening | Journal of Agricultural
401 and Food Chemistry. *Journal of Agricultural and Food Chemistry*, *53*(10), 4019-4025.
402 Carrascon, V., Fernandez-Zurbano, P., Bueno, M., & Ferreira, V. (2015). Oxygen
403 Consumption by Red Wines. Part II: Differential Effects on Color and Chemical
404 Composition Caused by Oxygen Taken in Different Sulfur Dioxide-Related Oxidation
405 Contexts. *Journal of Agricultural and Food Chemistry*, *63*(51), 10938-10947.
406 Carrascón, V., Vallverdú-Queralt, A., Meudec, E., Sommerer, N., Fernandez-Zurbano, P., &
407 Ferreira, V. (2018). The kinetics of oxygen and SO2 consumption by red wines. What
408 do they tell about oxidation mechanisms and about changes in wine composition?
409 *Food Chemistry*, *241*, 206-214. https://doi.org/10.1016/j.foodchem.2017.08.090
410 Castañeda-Ovando, A., Pacheco-Hernández, Ma. de L., Páez-Hernández, Ma. E.,
411 Rodríguez, J. A., & Galán-Vidal, C. A. (2009). Chemical studies of anthocyanins : A
412 review. *Food Chemistry*, *113*(4), 859-871.
413 https://doi.org/10.1016/j.foodchem.2008.09.001
414 Castro, C. C., Martins, R. C., Teixeira, J. A., & Silva Ferreira, A. C. (2014a). Application of a
415 high-throughput process analytical technology metabolomics pipeline to Port wine
416 forced ageing process. *Food Chemistry*, *143*, 384-391.
417 https://doi.org/10.1016/j.foodchem.2013.07.138

418 Castro, C. C., Martins, R. C., Teixeira, J. A., & Silva Ferreira, A. C. (2014b). Application of a
419 high-throughput process analytical technology metabolomics pipeline to Port wine
420 forced ageing process. *Food Chemistry*, *143*, 384-391.
421 https://doi.org/10.1016/j.foodchem.2013.07.138
422 Chevion, S., Roberts, M. A., & Chevion, M. (2000). The use of cyclic voltammetry for the
423 evaluation of antioxidant capacity. *Free Radical Biology and Medicine*, *28*(6),
424 860-870. https://doi.org/10.1016/S0891-5849(00)00178-7
425 Cheynier, V., Basire, N., & Rigaud, J. (1989a). Mechanism of trans-caffeoyltartaric acid and
426 catechin oxidation in model solutions containing grape polyphenoloxidase. *Journal of*
427 *Agricultural and Food Chemistry*, *37*(4), 1069-1071.
428 https://doi.org/10.1021/jf00088a055
429 Cheynier, V., Basire, N., & Rigaud, J. (1989b). Mechanism of trans-caffeoyltartaric acid and
430 catechin oxidation in model solutions containing grape polyphenoloxidase. *Journal of*
431 *Agricultural and Food Chemistry*, *37*(4), 1069-1071.
432 https://doi.org/10.1021/jf00088a055
433 Cheynier, V., Dueñas, M., Salas, E., Maury, C., Souquet, J. M., Sarni-Manchado, & Fulcrand,
434 H. (2006). Structure and Properties of Wine Pigments and Tannins. *American Journal*
435 *of Enology and Viticulture*, *57*, 298-305.
436 Cheynier, V., Dueñas-Paton, M., Salas, E., Maury, C., Souquet, J.-M., Sarni-Manchado, P., &
437 Fulcrand, H. (2006). Structure and Properties of Wine Pigments and Tannins.
438 *American Journal of Enology and Viticulture*, *57*(3), 298-305.
439 Cheynier, V. F., Trousdale, E. K., Singleton, V. L., Salgues, M. J., & Wylde, R. (1986).
440 Characterization of 2-S-glutathionyl caftaric acid and its hydrolysis in relation to grape
441 wines. *Journal of Agricultural and Food Chemistry*, *34*(2), 217-221.
442 https://doi.org/10.1021/jf00068a016
443 Cheynier, V., Hidalgo Arellano, Souquet, J. M., & Moutounet, M. (1997). Estimation of the
444 Oxidative Changes in Phenolic Compounds of Carignane During Winemaking.
445 *American Journal of Enology and Viticulture*, *48*, 225-228.

446 Cheynier, V., Owe, C., & Rigaud, J. (1988). Oxidation of Grape Juice Phenolic Compounds
447 in Model Solutions. *Journal of Food Science*, *53*(6), 1729-1732.
448 Cheynier, V., Prieur, C., Guyot, S., Rigaud, J., & Moutounet, M. (1997). The Structures of
449 Tannins in Grapes and Wines and Their Interactions with Proteins. In *Wine* (Vol. 661,
450 p. 81-93). American Chemical Society. https://doi.org/10.1021/bk-1997-0661.ch008
451 Cheynier, V., & Ricardo da Silva, J. M. (1991). Oxidation of grape procyanidins in model
452 solutions containing trans-caffeoyltartaric acid and polyphenol oxidase. *Journal of*
453 *Agricultural and Food Chemistry*, *39*(6), 1047-1049.
454 https://doi.org/10.1021/jf00006a008
455 Cheynier, V., Souquet, J. M., Kontek, A., & Moutounet, M. (1994). Anthocyanin degradation
456 in oxidising grape musts. *Journal of the Science of Food and Agriculture*, *66*(3),
457 283-288.
458 Cheynier, V., Souquet, J. M., & Moutounet, M. (1989). Glutathione Content and Glutathione
459 to Hydroxycinnamic Acid Ratio in Vitis vinifera Grapes and Musts. *American Journal*
460 *of Enology and Viticulture*, *40*(4), 320-324.
461 Cheynier, Veronique., & Moutounet, Michel. (1992). Oxidative reactions of caffeic acid in
462 model systems containing polyphenol oxidase. *Journal of Agricultural and Food*
463 *Chemistry*, *40*(11), 2038-2044. https://doi.org/10.1021/jf00023a002
464 Chira, K., Suh, J.-H., Saucier, C., & Teissèdre, P.-L. (2008). Les polyphénols du raisin.
465 *Phytothérapie*, *6*(2), 75-82. https://doi.org/10.1007/s10298-008-0293-3
466 Choe, E., & Min, D. B. (2009). Mechanisms of Antioxidants in the Oxidation of Foods.
467 *Comprehensive Reviews in Food Science and Food Safety*, *8*(4), 345-358.
468 https://doi.org/10.1111/j.1541-4337.2009.00085.x
469 Cillard, J., & Cillard, P. (2006). Mécanismes de la peroxydation lipidique et des anti-
470 oxydations. *Oilseeds & fats Crops and Lipids*, *13*(1), 24-29.
471 Claus, H. (2003). Laccases and their occurrence in prokaryotes. *Archives of Microbiology*,
472 *179*(3), 145-150. https://doi.org/10.1007/s00203-002-0510-7

Coppola, F., Picariello, L., Forino, M., Moio, L., & Gambuti, A. (2021). Comparison of Three Accelerated Oxidation Tests Applied to Red Wines with Different Chemical Composition. *Molecules*, *26*(4), 815. https://doi.org/10.3390/molecules26040815

Dallas, C., Ricardo da Silva, J. M., & Laureano, O. (1996). Products Formed in Model Wine Solutions Involving Anthocyanins, Procyanidin B2, and Acetaldehyde | Journal of Agricultural and Food Chemistry. *Journal of Agricultural and Food Chemistry*, *44*(8), 2402-2407.

Danilewicz, J. C. (2003a). *Review of Reaction Mechanisms of Oxygen and Proposed Intermediate Reduction Products in Wine : Central Role of Iron and Copper*. 13.

Danilewicz, J. C. (2003b). Review of Reaction Mechanisms of Oxygen and Proposed Intermediate Reduction Products in Wine : Central Role of Iron and Copper. *American Journal of Enology and Viticulture*, *54*(2), 73-85.

Danilewicz, J. C. (2007). Interaction of Sulfur Dioxide, Polyphenols, and Oxygen in a Wine-Model System : Central Role of Iron and Copper. *American Journal of Enology and Viticulture*, *58*(1), 53-60.

Danilewicz, J. C. (2011). Mechanism of Autoxidation of Polyphenols and Participation of Sulfite in Wine : Key Role of Iron. *American Journal of Enology and Viticulture*, *62*(3), 319-328. https://doi.org/10.5344/ajev.2011.10105

Danilewicz, J. C., Seccombe, J. T., & Whelan, J. (2008). Mechanism of Interaction of Polyphenols, Oxygen, and Sulfur Dioxide in Model Wine and Wine. *American Journal of Enology and Viticulture*, *59*(2), 128-136.

de Beer, D., Joubert, E., Marais, J., du Toit, W., Fouché, B., & Manley, M. (2016). Characterisation of Pinotage Wine During Maturation on Different Oak Products. *South African Journal of Enology and Viticulture*, *29*(1). https://doi.org/10.21548/29-1-1450

Deshaies, S., Cazals, G., Enjalbal, C., Constantin, T., Garcia, F., Mouls, L., & Saucier, C. (2020). Red Wine Oxidation : Accelerated Ageing Tests, Possible Reaction

Mechanisms and Application to Syrah Red Wines. *Antioxidants*, *9*(8), 663. https://doi.org/10.3390/antiox9080663

Drava, G., & Minganti, V. (2019). Mineral composition of organic and conventional white wines from Italy. *Heliyon*, *5*(9), e02464. https://doi.org/10.1016/j.heliyon.2019.e02464

Duval, A., & Avérous, L. (2016). Characterization and Physicochemical Properties of Condensed Tannins from Acacia catechu. *Journal of Agricultural and Food Chemistry*, *64*(8), 1751-1760.

Echave, J., Barral, M., Fraga-Corral, M., Prieto, M. A., & Simal-Gandara, J. (2021). Bottle Aging and Storage of Wines : A Review. *Molecules*, *26*(3), 713. https://doi.org/10.3390/molecules26030713

Elias, R. J., & Waterhouse, A. L. (2010). Controlling the Fenton Reaction in Wine. *Journal of Agricultural and Food Chemistry*, *58*(3), 1699-1707. https://doi.org/10.1021/jf903127r

Escribano-Bailón, M. T., Guerra, M. T., Rivas-Gonzalo, J. C., & Santos-Buelga, C. (1995). Proanthocyanidins in skins from different grape varieties. *Zeitschrift Für Lebensmittel-Untersuchung Und Forschung*, *200*(3), 221-224. https://doi.org/10.1007/BF01190499

Es-Safi, N.-E., Le Guernevé, C., Cheynier, V., & Moutounet, M. (2000). New Phenolic Compounds Formed by Evolution of (+)-Catechin and Glyoxylic Acid in Hydroalcoholic Solution and Their Implication in Color Changes of Grape-Derived Foods | Journal of Agricultural and Food Chemistry. *Journal of Agricultural and Food Chemistry*, *48*(9), 4233-4240.

Fayeulle, N., Vallverdu-Queralt, A., Meudec, E., Hue, C., Boulanger, R., Cheynier, V., & Sommerer, N. (2018). Characterization of new flavan-3-ol derivatives in fermented cocoa beans. *Food Chemistry*, *259*, 207-212. https://doi.org/10.1016/j.foodchem.2018.03.133

Ferreira, C., Sáenz-Navajas, M.-P., Carrascón, V., Næs, T., Fernández-Zurbano, P., & Ferreira, V. (2021). An assessment of voltammetry on disposable screen printed electrodes to predict wine chemical composition and oxygen consumption rates. *Food Chemistry*, *365*, 130405. https://doi.org/10.1016/j.foodchem.2021.130405

528 Ferreira, V., Carrascon, V., Bueno, M., Ugliano, M., & Fernandez-Zurbano, P. (2015).
529 Oxygen Consumption by Red Wines. Part I : Consumption Rates, Relationship with
530 Chemical Composition, and Role of SO_2. *Journal of Agricultural and Food Chemistry*,
531 *63*(51), 10928-10937. https://doi.org/10.1021/acs.jafc.5b02988
532 Forino, M., Picariello, L., Lopatriello, A., Moio, L., & Gambuti, A. (2020). New insights into the
533 chemical bases of wine color evolution and stability : The key role of acetaldehyde.
534 *European Food Research and Technology*, *246*, 733-743.
535 Francia-Aricha, E., Guerra, M. T., Rivas-Gonzalo, J. C., & Santos-Buelga, C. (s. d.). New
536 Anthocyanin Pigments Formed after Condensation with Flavanols | Journal of
537 Agricultural and Food Chemistry. *Journal of Agricultural and Food Chemistry*, *45*(6),
538 2262-2266.
539 Freitas, V. D., & Mateus, N. (2011). Formation of pyranoanthocyanins in red wines : A new
540 and diverse class of anthocyanin derivatives. *Analytical and Bioanalytical Chemistry*,
541 *401*, 1463-1473.
542 Fulcrand, H., Dueñas, M., Salas, E., & Cheynier, V. (2006). Phenolic Reactions during
543 Winemaking and Aging. *American Journal of Enology and Viticulture*, *57*(3), 289-297.
544 Gambuti, A., Han, G., Peterson, A. L., & Waterhouse, A. L. (s. d.). Sulfur Dioxide and
545 Glutathione Alter the Outcome of Microoxygenation. *American Journal of Enology and*
546 *Viticulture*, *66*(4), 411-423.
547 Gambuti, A., Picariello, L., Rinaldi, A., & Moio, L. (2018). Evolution of Sangiovese Wines With
548 Varied Tannin and Anthocyanin Ratios During Oxidative Aging. *Frontiers in*
549 *Chemistry*, *0*. https://doi.org/10.3389/fchem.2018.00063
550 Gambuti, A., Rinaldi, A., Ugliano, M., & Moio, L. (2013). Evolution of phenolic compounds
551 and astringency during aging of red wine : Effect of oxygen exposure before and after
552 bottling. *Journal of Agricultural and Food Chemistry*, *61*(8), 1618-1627.
553 https://doi.org/10.1021/jf302822b
554 Gambuti, A., Siani, T., Picariello, L., Rinaldi, A., Lisanti, M. T., Ugliano, M., Dieval, J. B., &
555 Moio, L. (2017a). Oxygen exposure of tannins-rich red wines during bottle aging.

Influence on phenolics and color, astringency markers and sensory attributes. *European Food Research and Technology*, *243*(4), 669-680. https://doi.org/10.1007/s00217-016-2780-3

Gambuti, A., Siani, T., Picariello, L., Rinaldi, A., Lisanti, M. T., Ugliano, M., Dieval, J. B., & Moio, L. (2017b). Oxygen exposure of tannins-rich red wines during bottle aging. Influence on phenolics and color, astringency markers and sensory attributes. *European Food Research and Technology*, *243*(4), 669-680. https://doi.org/10.1007/s00217-016-2780-3

Gaulejac, N. V. de, Vivas, N., Nonier, M.-F., Absalon, C., & Bourgeois, G. (2001). Study and quantification of monomeric flavan-3-ol and dimeric procyanidin quinonic forms by HPLC/ESI-MS. Application to red wine oxidation. *Journal of the Science of Food and Agriculture*, *81*(12), 1172-1179. https://doi.org/10.1002/jsfa.926

Geană, E.-I., Ciucure, C. T., Artem, V., & Apetrei, C. (2020). Wine varietal discrimination and classification using a voltammetric sensor array based on modified screen-printed electrodes in conjunction with chemometric analysis. *Microchemical Journal*, *159*, 105451. https://doi.org/10.1016/j.microc.2020.105451

Giribaldi, J., Besson, M., Suc, L., Fulcrand, H., & Mouls, L. (2020). The use of extracted-ion chromatograms to quantify the composition of condensed tannin subunits. *Rapid Communications in Mass Spectrometry*, *34*(7), e8619. https://doi.org/10.1002/rcm.8619

Gonzalez, A., Vidal, S., & Ugliano, M. (2018). Untargeted voltammetric approaches for characterization of oxidation patterns in white wines. *Food Chemistry*, *269*, 1-8. https://doi.org/10.1016/j.foodchem.2018.06.104

Goto, T., & Kondo, T. (1991). Structure and Molecular Stacking of Anthocyanins. *Angewandte Chemie International Edition*, 17-33.

Guyot, S., Vercauteren, J., & Cheynier, V. (1996). Structural determination of colourless and yellow dimers resulting from (+)-catechin coupling catalysed by grape

583 polyphenoloxidase. *Phytochemistry*, *42*(5), 1279-1288. https://doi.org/10.1016/0031-
584 9422(96)00127-6
585 Hagerman, A. E., & Butler, L. G. (1978). Protein precipitation method for the quantitative
586 determination of tannins. *Journal of Agricultural and Food Chemistry*, *26*(4), 809-812.
587 https://doi.org/10.1021/jf60218a027
588 Hayasaka, Y., & Asenstorfer, R. E. (2002). Screening for Potential Pigments Derived from
589 Anthocyanins in Red Wine Using Nanoelectrospray Tandem Mass Spectrometry.
590 *Journal of Agricultural and Food Chemistry*, *50*(4), 756-761.
591 https://doi.org/10.1021/jf010943v
592 He, F., Liang, N.-N., Mu, L., Pan, Q.-H., Wang, J., Reeves, M. J., & Duan, C.-Q. (2012).
593 Anthocyanins and Their Variation in Red Wines I. Monomeric Anthocyanins and Their
594 Color Expression. *Molecules*, *17*(2), 1571-1601.
595 https://doi.org/10.3390/molecules17021571
596 He, F., Pan, Q.-H., Shi, Y., & Duan, C.-Q. (2008). Chemical Synthesis of Proanthocyanidins
597 in Vitro and Their Reactions in Aging Wines. *Molecules*, *13*(12), 3007-3032.
598 https://doi.org/10.3390/molecules13123007
599 Hopfer, H., Ebeler, S. B., & Heymann, H. (10754). The Combined Effects of Storage
600 Temperature and Packaging Type on the Sensory and Chemical Properties of
601 Chardonnay. *Journal of Agricultural and Food Chemistry*, *60*(43), 10743.
602 Hoyos-Arbeláez, J., Vázquez, M., & Contreras-Calderón, J. (2017). Electrochemical methods
603 as a tool for determining the antioxidant capacity of food and beverages : A review.
604 *Food Chemistry*, *221*, 1371-1381. https://doi.org/10.1016/j.foodchem.2016.11.017
605 Hui, Y. H., Nip, W.-K., Nollet, L. M. L., Paliyath, G., & Simpson, B. K. (2008). *Food*
606 *Biochemistry and Food Processing*. John Wiley & Sons.
607 Jackson, R. S. (2008, avril 30). Wine Science : Principles and Applications. *Wine Science,*
608 *Third Edition*.
609 *Jackson : Wine science : Principles and applications—Google Scholar*. (s. d.).

610 Jiang, H., Shii, T., Matsuo, Y., Tanaka, T., Jiang, Z.-H., & Kouno, I. (2011). A new catechin
611 oxidation product and polymeric polyphenols of post-fermented tea. *Food Chemistry*,
612 *129*(3), 830-836. https://doi.org/10.1016/j.foodchem.2011.05.031
613 Jiménez-Atiénzar, M., Cabanes, J., Gandía-Herrero, F., & García-Carmona, F. (2004).
614 Kinetic analysis of catechin oxidation by polyphenol oxidase at neutral pH.
615 *Biochemical and Biophysical Research Communications*, *319*(3), 902-910.
616 https://doi.org/10.1016/j.bbrc.2004.05.077
617 Jurd, L. (1969). Review of Polyphenol Condensation Reactions and their Possible
618 Occurrence in the Aging of Wines | American Journal of Enology and Viticulture.
619 *American Journal of Enology and Viticulture*, 191-195.
620 Kamiya, H., Yanase, E., & Nakatsuka, S. (2014). Novel oxidation products of cyanidin 3-O-
621 glucoside with 2,2′-azobis-(2,4-dimethyl)valeronitrile and evaluation of anthocyanin
622 content and its oxidation in black rice. *Food Chemistry*, *155*, 221-226.
623 https://doi.org/10.1016/j.foodchem.2014.01.077
624 Karbowiak, T., Gougeon, R. D., Alinc, J.-B., Brachais, L., Debeaufort, F., Voilley, A., &
625 Chassagne, D. (2009). Wine Oxidation and the Role of Cork. *Food science and*
626 *Nutrition*, *50*(1), 20-52.
627 Kennedy, J. A., Ferrier, J., Harbertson, J. F., & Gachons, C. P. des. (2006). Analysis of
628 Tannins in Red Wine Using Multiple Methods : Correlation with Perceived
629 Astringency. *American Journal of Enology and Viticulture*, *57*(4), 481-485.
630 Kennedy, J. A., & Jones, G. P. (2001). Analysis of Proanthocyanidin Cleavage Products
631 Following Acid-Catalysis in the Presence of Excess Phloroglucinol. *Journal of*
632 *Agricultural and Food Chemistry*, *49*(4), 1740-1746.
633 Khan, N., & Mukhtar, H. (2007). Tea polyphenols for health promotion. *Life Sciences*, *81*(7),
634 519-533. https://doi.org/10.1016/j.lfs.2007.06.011
635 Kilmartin, P. A. (2016). Electrochemistry applied to the analysis of wine : A mini-review.
636 *Electrochemistry Communications*, *67*, 39-42.
637 https://doi.org/10.1016/j.elecom.2016.03.011

638 Kilmartin, P. A., Zou, H., & Waterhouse, A. L. (2001). A Cyclic Voltammetry Method Suitable
639 for Characterizing Antioxidant Properties of Wine and Wine Phenolics. *Journal of*
640 *Agricultural and Food Chemistry*, *49*(4), 1957-1965.
641 Kilmartin, P. A., Zou, H., & Waterhouse, A. L. (2002). Correlation of Wine Phenolic
642 Composition versus Cyclic Voltammetry Response. *American Journal of Enology and*
643 *Viticulture*, *53*(4), 294-302.
644 Lambropoulos, I., & Roussis, I. G. (2007). Inhibition of the decrease of volatile esters and
645 terpenes during storage of a white wine and a model wine medium by caffeic acid and
646 gallic acid. *Food Research International*, *40*(1), 176-181.
647 https://doi.org/10.1016/j.foodres.2006.09.003
648 Lavigne, V., Pons, A., & Dubourdieu, D. (2007). Assay of glutathione in must and wines
649 using capillary electrophoresis and laser-induced fluorescence detection : Changes in
650 concentration in dry white wines during alcoholic fermentation and aging. *Journal of*
651 *Chromatography A*, *1139*(1), 130-135. https://doi.org/10.1016/j.chroma.2006.10.083
652 Leontieş, A.-R., Răducan, A., Gîfu, I. C., & Anghel, D. F. (2017). Catechin oxidation
653 products : Mechanistic aspects and kinetics. *Studia Universitatis Babeș-Bolyai*
654 *Chemia*, *62*(4), 11-19. https://doi.org/10.24193/subbchem.2017.4.01
655 Leopoldini, M., Russo, N., & Toscano, M. (2011). The molecular basis of working mechanism
656 of natural polyphenolic antioxidants. *Food Chemistry*, *125*(2), 288-306.
657 https://doi.org/10.1016/j.foodchem.2010.08.012
658 Li, H., Guo, A., & Wang, H. (2008). Mechanisms of oxidative browning of wine. *Food*
659 *Chemistry*, *108*(1), 1-13. https://doi.org/10.1016/j.foodchem.2007.10.065
660 Lopes, P., Richard, T., Saucier, C., Teissedre, P.-L., Monti, J.-P., & Glories, Y. (2007).
661 Anthocyanone A : A Quinone Methide Derivative Resulting from Malvidin 3-O-
662 Glucoside Degradation. *Journal of Agricultural and Food Chemistry*, *55*(7),
663 2698-2704. https://doi.org/10.1021/jf062875o

664 Lorrain, B., Ky, I., Pechamat, L., & Teissedre, P.-L. (2013). Molecules | Free Full-Text |
665 Evolution of Analysis of Polyhenols from Grapes, Wines, and Extracts. *Molecules*,
666 *18*(1), 1076-1100.
667 Ma, W., Guo, A., Zhang, Y., Wang, H., Liu, Y., & Li, H. (2014). A review on astringency and
668 bitterness perception of tannins in wine. *Trends in Food Science & Technology*, *40*(1),
669 6-19. https://doi.org/10.1016/j.tifs.2014.08.001
670 Macías, V. M. P., Pina, I. C., & Rodríguez, L. P. (2001). *Factors Influencing the Oxidation*
671 *Phenomena of Sherry Wine*. 5.
672 Makhotkina, O., & Kilmartin, P. A. (2009). Uncovering the influence of antioxidants on
673 polyphenol oxidation in wines using an electrochemical method : Cyclic voltammetry.
674 *Journal of Electroanalytical Chemistry*, *633*(1), 165-174.
675 https://doi.org/10.1016/j.jelechem.2009.05.007
676 Makhotkina, O., & Kilmartin, P. A. (2010). The use of cyclic voltammetry for wine analysis :
677 Determination of polyphenols and free sulfur dioxide. *Analytica Chimica Acta*, *668*(2),
678 155-165.
679 Makkar, H. P. S., Blümmel, M., Borowy, N. K., & Becker, K. (1993). Gravimetric
680 determination of tannins and their correlations with chemical and protein precipitation
681 methods. *Journal of the Science of Food and Agriculture*, *61*(2), 161-165.
682 Mateus, N., Silva, A. M. S., Vercauteren, J., & de Freitas, V. (2001a). Occurrence of
683 Anthocyanin-Derived Pigments in Red Wines. *Journal of Agricultural and Food*
684 *Chemistry*, *49*(10), 4836-4840. https://doi.org/10.1021/jf001505b
685 Mateus, N., Silva, A. M. S., Vercauteren, J., & de Freitas, V. (2001b). Occurrence of
686 Anthocyanin-Derived Pigments in Red Wines. *Journal of Agricultural and Food*
687 *Chemistry*, *49*(10), 4836-4840. https://doi.org/10.1021/jf001505b
688 McRae, J. M., & Kennedy, J. A. (2011). Wine and Grape Tannin Interactions with Salivary
689 Proteins and Their Impact on Astringency : A Review of Current Research. *Molecules*,
690 *16*(3), 2348-2364. https://doi.org/10.3390/molecules16032348

691 Mercurio, M., & Smith, P. A. (2008). *Tannin Quantification in Red Grapes and Wine :*
692 *Comparison of Polysaccharide- and Protein-Based Tannin Precipitation Techniques*
693 *and Their Ability to Model Wine Astringency | Journal of Agricultural and Food*
694 *Chemistry*. *56*(14), 5528-5537.
695 Merrell, C., & Hansen, M. (2018). Improving Red Wine Color and Mouthfeel Over Time.
696 *Wines Vines Analytics*, *Wines&Vines*.
697 https://winesvinesanalytics.com/features/203972
698 Miller, D. M., Buettner, G. R., & Aust, S. D. (1990). Transition metals as catalysts of
699 "autoxidation" reactions. *Free Radical Biology and Medicine*, *8*(1), 95-108.
700 https://doi.org/10.1016/0891-5849(90)90148-C
701 Millet, M., Poupard, P., Guilois-Dubois, S., Zanchi, D., & Guyot, S. (2019). Self-aggregation
702 of oxidized procyanidins contributes to the formation of heat-reversible haze in apple-
703 based liqueur wine. *Food Chemistry*, *276*, 797-805.
704 https://doi.org/10.1016/j.foodchem.2018.09.171
705 Monagas, M., & Bartolomé, B. (2009). Anthocyanins and Anthocyanin-Derived Compounds.
706 In M. V. Moreno-Arribas & M. C. Polo (Éds.), *Wine Chemistry and Biochemistry* (p.
707 439-462). Springer New York. https://doi.org/10.1007/978-0-387-74118-5_21
708 Monagas, M., Bartolomé, B., & Gomez-Cordoves, C. (2005). Evolution of polyphenols in red
709 wines from Vitis vinifera L. during aging in the bottle. *European Food Research and*
710 *Technology*, *220*, 331-340.
711 Monagas, M., Bartolomé, B., & Gómez-Cordovés, C. (2005). Evolution of polyphenols in red
712 wines from Vitis vinifera L. during aging in the bottle. *European Food Research and*
713 *Technology*, *220*(3), 331-340. https://doi.org/10.1007/s00217-004-1109-9
714 Motta, S., Guaita, M., Cassino, C., & Bosso, A. (2020). Relationship between polyphenolic
715 content, antioxidant properties and oxygen consumption rate of different tannins in a
716 model wine solution ScienceDirect. *Food Chemistry*, *313*.
717 https://www.sciencedirect.com/science/article/pii/S0308814619321910?casa_token=

F5Za7fqUobkAAAAA:hwgLXeXveMPoNL9XDEjcAvkCPWJ0kBx_10jXTzvEW-2LNhfSXibf9VJfJpPLV8S88MxeXgIthwrWcA

Mouls, L., & Fulcrand, H. (2012). UPLC-ESI-MS study of the oxidation markers released from tannin depolymerization : Toward a better characterization of the tannin evolution over food and beverage processing. *Journal of Mass Spectrometry*, *47*(11), 1450-1457. https://doi.org/10.1002/jms.3098

Mouls, L., & Fulcrand, H. (2015a). Identification of new oxidation markers of grape-condensed tannins by UPLC–MS analysis after chemical depolymerization. *Tetrahedron*, *71*(20), 3012-3019. https://doi.org/10.1016/j.tet.2015.01.038

Mouls, L., & Fulcrand, H. (2015b). Identification of new oxidation markers of grape-condensed tannins by UPLC–MS analysis after chemical depolymerization. *Tetrahedron*, *71*(20), 3012-3019. https://doi.org/10.1016/j.tet.2015.01.038

Mouls, L., Mazauric, J.-P., Sommerer, N., Fulcrand, H., & Mazerolles, G. (2011a). Comprehensive study of condensed tannins by ESI mass spectrometry : Average degree of polymerisation and polymer distribution determination from mass spectra. *Analytical and Bioanalytical Chemistry*, *400*(2), 613-623. https://doi.org/10.1007/s00216-011-4751-7

Mouls, L., Mazauric, J.-P., Sommerer, N., Fulcrand, H., & Mazerolles, G. (2011b). Comprehensive study of condensed tannins by ESI mass spectrometry : Average degree of polymerisation and polymer distribution determination from mass spectra. *Analytical and Bioanalytical Chemistry*, *400*(2), 613-623. https://doi.org/10.1007/s00216-011-4751-7

Nave, F., Teixeira, N., Mateus, N., & de Freitas, V. (2010). The fate of flavanol–anthocyanin adducts in wines : Study of their putative reaction patterns in the presence of acetaldehyde. *Food Chemistry*, *121*(4), 1129-1138. https://doi.org/10.1016/j.foodchem.2010.01.060

Noble, A. C. (1994). Bitterness in wine. *Physiology & Behavior*, *56*(6), 1251-1255. https://doi.org/10.1016/0031-9384(94)90373-5

Oliveira, C. M., Barros, A. S., Ferreira, A. C. S., & Silva, A. M. S. (2016). Study of quinones reactions with wine nucleophiles by cyclic voltammetry. *Food Chemistry*, *211*, 1-7. https://doi.org/10.1016/j.foodchem.2016.05.020

Oliveira, C. M., Barros, A. S., Silva Ferreira, A. C., & Silva, A. M. S. (2015). Influence of the temperature and oxygen exposure in red Port wine : A kinetic approach. *Food Research International*, *75*, 337-347. https://doi.org/10.1016/j.foodres.2015.06.024

Oliveira, C. M., Ferreira, A. C. S., De Freitas, V., & Silva, A. M. S. (2011). Oxidation mechanisms occurring in wines. *Food Research International*, *44*(5), 1115-1126. https://doi.org/10.1016/j.foodres.2011.03.050

Oszmianski, J., Cheynier, V., & Moutounet, M. (1996). Iron-Catalyzed Oxidation of (+)-Catechin in Model Systems. *Journal of Agricultural and Food Chemistry*, *44*(7), 1712-1715. https://doi.org/10.1021/jf9507710

Oszmianski, J., Sapis, J.-C., & Macheix, J.-J. (1985). Changes in Grape Seed Phenols as Affected By Enzymic and Chemical Oxidation in vitro. *Journal of Food Science*, *50*(5), 1505-1506. https://doi.org/10.1111/j.1365-2621.1985.tb10515.x

Özkan, M. (2002). Degradation of anthocyanins in sour cherry and pomegranate juices by hydrogen peroxide in the presence of added ascorbic acid. *Food Chemistry*, *78*(4), 499-504. https://doi.org/10.1016/S0308-8146(02)00165-6

Peterson, A. L., & Waterhouse, A. L. (2016). 1H NMR: A Novel Approach To Determining the Thermodynamic Properties of Acetaldehyde Condensation Reactions with Glycerol, (+)-Catechin, and Glutathione in Model Wine. *Journal of Agricultural and Food Chemistry*, *64*(36), 6869-6878.

Petrozziello, M., Torchio, F., Piano, F., Giacosa, S., Ugliano, M., Bosso, A., & Rolle, L. (2018). Impact of Increasing Levels of Oxygen Consumption on the Evolution of Color, Phenolic, and Volatile Compounds of Nebbiolo Wines. *Frontiers in Chemistry*, *6*. https://doi.org/10.3389/fchem.2018.00137

Picariello, L., Gambuti, A., Picariello, B., & Moio, L. (2017). Evolution of pigments, tannins and acetaldehyde during forced oxidation of red wine : Effect of tannins addition. *LWT*, *77*, 370-375. https://doi.org/10.1016/j.lwt.2016.11.064

Ployon, S., Attina, A., Vialaret, J., Walker, A. S., Hirtz, C., & Saucier, C. (2020). Laccases 2 & 3 as biomarkers of Botrytis cinerea infection in sweet white wines. *Food Chemistry*, *315*, 126233. https://doi.org/10.1016/j.foodchem.2020.126233

P. McManus, J., G. Davis, K., E. Beart, J., H. Gaffney, S., H. Lilley, T., & Haslam, E. (1985). Polyphenol interactions. Part 1. Introduction; some observations on the reversible complexation of polyphenols with proteins and polysaccharides. *Journal of the Chemical Society, Perkin Transactions 2*, *0*(9), 1429-1438. https://doi.org/10.1039/P29850001429

Poncet-Legrand, C., Cabane, B., Bautista-Ortín, A.-B., Carrillo, S., Fulcrand, H., Pérez, J., & Vernhet, A. (2010). Tannin Oxidation : Intra- versus Intermolecular Reactions. *Biomacromolecules*, *11*(9), 2376-2386. https://doi.org/10.1021/bm100515e

Pourova, J., Kottova, M., Voprsalova, M., & Pour, M. (2010). Reactive oxygen and nitrogen species in normal physiological processes. *Acta Physiologica*, *198*(1), 15-35.

Prieur, C., Rigaud, J., Cheynier, V., & Moutounet, M. (1994). Oligomeric and polymeric procyanidins from grape seeds. *Phytochemistry*, *36*(3), 781-784. https://doi.org/10.1016/S0031-9422(00)89817-9

Quideau, S., Jourdes, M., Lefeuvre, D., Montaudon, D., Saucier, C., Glories, Y., Pardon, P., & Pourquier, P. (2005). The Chemistry of Wine Polyphenolic C-Glycosidic Ellagitannins Targeting Human Topoisomerase II. *Chemistry – A European Journal*, *11*(22), 6503-6513. https://doi.org/10.1002/chem.200500428

Rentzsch, M., Schwarz, M., & Winterhalter, P. (2007). Pyranoanthocyanins–an overview on structures, occurrence, and pathways of formation. *Trends in Food Science & Technology*, *18*(10), 526-534.

798 Ribéreau-Gayon, P., Glories, Y., Maujean, A., & Dubourdieu, D. (2006). *Handbook of*
799 *Enology, Volume 2 : The Chemistry of Wine - Stabilization and Treatments*. John
800 Wiley & Sons.
801 Ricci, A., Teslic, N., Petropolus, V.-I., Parpinello, G. P., & Versari, A. (2019). Fast Analysis of
802 Total Polyphenol Content and Antioxidant Activity in Wines and Oenological Tannins
803 Using a Flow Injection System with Tandem Diode Array and Electrochemical
804 Detections. *Food Analytical Methods*, *12*(2), 347-354. https://doi.org/10.1007/s12161-
805 018-1366-z
806 Rigaud, J., Cheynier, V., Souquet, J.-M., & Moutounet, M. (1991). Influence of must
807 composition on phenolic oxidation kinetics. *Journal of the Science of Food and*
808 *Agriculture*, *57*(1), 55-63. https://doi.org/10.1002/jsfa.2740570107
809 Rigaud, J., Perez-Ilzarbe, J., Da Silva, J. M. R., & Cheynier, V. (1991a). Micro method for the
810 identification of proanthocyanidin using thiolysis monitored by high-performance liquid
811 chromatography. *Journal of Chromatography A*, *540*, 401-405.
812 https://doi.org/10.1016/S0021-9673(01)88830-0
813 Rigaud, J., Perez-Ilzarbe, J., Da Silva, J. M. R., & Cheynier, V. (1991b). Micro method for the
814 identification of proanthocyanidin using thiolysis monitored by high-performance liquid
815 chromatography. *Journal of Chromatography A*, *540*, 401-405.
816 https://doi.org/10.1016/S0021-9673(01)88830-0
817 Rimbach, G., Melchin, M., Moehring, J., & Wagner, A. E. (2009). Polyphenols from Cocoa
818 and Vascular Health—A Critical Review. *International Journal of Molecular Sciences*,
819 *10*(10), 4290-4309. https://doi.org/10.3390/ijms10104290
820 Robards, K., Prenzler, P. D., Tucker, G., Swatsitang, P., & Glover, W. (1999). Phenolic
821 compounds and their role in oxidative processes in fruits. *Food Chemistry*, *66*(4),
822 401-436. https://doi.org/10.1016/S0308-8146(99)00093-X
823 Robichaud, J. L., & Noble, A. C. (1990). Astringency and bitterness of selected phenolics in
824 wine. *Journal of the Science of Food and Agriculture*, *53*(3), 343-353.
825 https://doi.org/10.1002/jsfa.2740530307

826 Roles of o-quinones and their polymers in the enzymic browning of apples. (1990).
827 *Phytochemistry*, *29*(2), 435-440.
828 Roussis, I. G., Lambropoulos, I., & Tzimas, P. (2007). Protection of Volatiles in a Wine with
829 Low Sulfur Dioxide by Caffeic Acid or Glutathione. *American Journal of Enology and*
830 *Viticulture*, *58*(2), 274-278.
831 Roussis, I. G., & Sergianitis, S. (2008). Protection of some aroma volatiles in a model wine
832 medium by sulphur dioxide and mixtures of glutathione with caffeic acid or gallic
833 acid—Roussis. *Flavour and Fragrance Journal*, *23*(1), 35-39.
834 Sadilova, E., Carle, R., & Stintzing, F. C. (2007). Thermal degradation of anthocyanins and
835 its impact on color and in vitro antioxidant capacity. *Molecular Nurition Food*
836 *Research*, *51*(12), 1461-1471.
837 Salas, E., Atanasova, V., Poncet-Legrand, C., Meudec, E., Mazauric, J. P., & Cheynier, V.
838 (2004). Demonstration of the occurrence of flavanol–anthocyanin adducts in wine and
839 in model solutions. *Analytica Chimica Acta*, *513*(1), 325-332.
840 https://doi.org/10.1016/j.aca.2003.11.084
841 Sanoner, P., Guyot, S., Bernillon, S., Fulcrand, H., Drilleau, J.-F., & Renard, C. (2002,
842 septembre 9). *Procyanidin B2 oxidation products, multi linked dimers ?* 21.
843 International Conference on Polyphenols. https://hal.inrae.fr/hal-02763559
844 Sarneckis, C. J., Dambergs, R. G., Jones, P., Mercurio, M., Herderich, M. J., & Smith, P. A.
845 (2006). Quantification of condensed tannins by precipitation with methyl cellulose :
846 Development and validation of an optimised tool for grape and wine analysis.
847 *Australian Journal of Grape and Wine Research*, *12*(1), 39-49.
848 https://doi.org/10.1111/j.1755-0238.2006.tb00042.x
849 Sarni, P., Fulcrand, H., Souillol, V., Souquet, J. M., & Cheynier, V. (1995). Mechanisms of
850 anthocyanin degradation in grape must-like model solutions. *Journal of the Science of*
851 *Food and Agriculture*, *69*(3), 385-391.
852 Sarni-Manchado, P., & Cheynier, V. (s. d.). *Les polyphénols en agroalimentaire*.

Sarni-Manchado, P., Cheynier, V., & Moutounet, M. (1997). Reactions of polyphenoloxidase generated caftaric acid o-quinone with malvidin 3-O-glucoside. *Phytochemistry*, *45*(7), 1365-1369. https://doi.org/10.1016/S0031-9422(97)00190-8

Satake, R., & Yanase, E. (2018). Mechanistic studies of hydrogen-peroxide-mediated anthocyanin oxidation. *Tetrahedron*, *74*(42), 6187-6191. https://doi.org/10.1016/j.tet.2018.09.012

Saucier, C. (2010). How do wine polyphenols evolve during wine ageing? *Cerevisia*, *35*(1), 11-15. https://doi.org/10.1016/j.cervis.2010.05.002

Schwarz, M., Wabnitz, T. C., & Winterhalter, P. (2003). Pathway Leading to the Formation of Anthocyanin−Vinylphenol Adducts and Related Pigments in Red Wines. *Journal of Agricultural and Food Chemistry*, 3682-3687.

Scrimgeour, N., Nordestgaard, S., Lloyd, N. D. R., & Wikes, E. N. (2015). Exploring the effect of elevated storage temperature on wine composition. *Australian Journal of Grape and Wine Research*, *21*(S1), 713-722.

Shchepinov, M. S. (2007). Reactive Oxygen Species, Isotope Effect, Essential Nutrients, and Enhanced Longevity. *Rejuvenation Research*, *10*(1), 47-60.

Sheridan, M. K., & Elias, R. J. (2015). Exogenous acetaldehyde as a tool for modulating wine color and astringency during fermentation. *Food Chemistry*, *177*, 17-22. https://doi.org/10.1016/j.foodchem.2014.12.077

Singleton, V. L. (1987a). *Oxygen with Phenols and Related Reactions in Musts, Wines, and Model Systems : Observations and Practical Implications*. *38*(1), 9.

Singleton, V. L. (1987b). *Oxygen with Phenols and Related Reactions in Musts, Wines, and Model Systems : Observations and Practical Implications*. *38*(1), 9.

Singleton, V. L. (2001). A survey of wine aging reactions, especially with oxygen. *Proceedings of the ASEV 50th Anniversary Annual Meeting, Seattle, Washington, June 19-23, 2000, 2001, ISBN 0-9630711-4-9, Págs. 323-336*, 323-336. https://dialnet.unirioja.es/servlet/articulo?codigo=590527

Singleton, V. L., Salgues, M., Zaya, J., & Trousdale, E. (1985). Caftaric Acid Disappearance and Conversion to Products of Enzymic Oxidation in Grape Must and Wine. *American Journal of Enology and Viticulture*, *36*(1), 50-56.

Soares, S., Brandão, E., Mateus, N., & De Freitas, V. (2017). Sensorial properties of red wine polyphenols : Astringency and bitterness. *Food science and Nutrition*, *57*(5), 937-948.

Somers, T. C., & Wescombe, L. G. (1987). Evolution of red wines part II. An assessment of the role of acetaldehyde. *VITIS - Journal of Grapevine Research*, *26*(1), 27-27.

Souquet, J.-M., Cheynier, V., Brossaud, F., & Moutounet, M. (1996). Polymeric proanthocyanidins from grape skins. *Phytochemistry*, *43*(2), 509-512. https://doi.org/10.1016/0031-9422(96)00301-9

Sousa, C., Mateus, N., Silva, A. M. S., González-Paramás, A. M., Santos-Buelga, C., & Freitas, V. de. (2007). Structural and chromatic characterization of a new Malvidin 3-glucoside–vanillyl–catechin pigment. *Food Chemistry*, *102*(4), 1344-1351. https://doi.org/10.1016/j.foodchem.2006.04.050

Suc, L., Rigou, P., & Mouls, L. (2021). Detection and Identification of Oxidation Markers of the Reaction of Grape Tannins with Volatile Thiols Commonly Found in Wine. *Journal of Agricultural and Food Chemistry*, *69*(10), 3199-3208.

Tanaka, T., & Kouno, I. (2003). Oxidation of Tea Catechins : Chemical Structures and Reaction Mechanism. *food science and technology research*, *9*(2), 128-133.

Teng, B., Hayasaka, Y., Smith, P. A., & Bindon, K. A. (2019). *Effect of Grape Seed and Skin Tannin Molecular Mass and Composition on the Rate of Reaction with Anthocyanin and Subsequent Formation of Polymeric Pigments in the Presence of Acetaldehyde* | *Journal of Agricultural and Food Chemistry*. *67*(32), 8938-8949.

Timberlake, C. F., & Bridle, P. (1976). Interactions Between Anthocyanins, Phenolic Compounds, and Acetaldehyde and Their Significance in Red Wines. *American Journal of Enology and Viticulture*, *27*(3), 97-105.

907 Tindal, R. A., Jeffery, D. W., & Muhlack, R. A. (2021). Mathematical modelling to enhance
908 winemaking efficiency : A review of red wine colour and polyphenol extraction and
909 evolution. *Australian Journal of Grape and Wine Research*, *27*(2), 219-233.
910 Toit, W. J. du, Marais, J., Pretorius, I. S., & Toit, M. du. (2006). Oxygen in Must and Wine : A
911 review. *South African Journal of Enology and Viticulture*, *27*(1), 76-94.
912 https://doi.org/10.21548/27-1-1610
913 Ugliano, M. (2013). Oxygen Contribution to Wine Aroma Evolution during Bottle Aging.
914 *Journal of Agricultural and Food Chemistry*, *61*(26), 6125-6136.
915 https://doi.org/10.1021/jf400810v
916 Ugliano, M. (2016). Rapid fingerprinting of white wine oxidizable fraction and classification of
917 white wines using disposable screen printed sensors and derivative voltammetry.
918 *Food Chemistry*, *212*, 837-843. https://doi.org/10.1016/j.foodchem.2016.05.156
919 Ugliano, M., Wirth, J., Bégrand, S., Dieval, J.-B., & Vidal, S. (2015). Oxidation Signature of
920 Grape Must and Wine by Linear Sweep Voltammetry Using Disposable Carbon
921 Electrodes. In S. B. Ebeler, G. Sacks, S. Vidal, & P. Winterhalter (Éds.), *Advances in*
922 *Wine Research* (Vol. 1203, p. 325-334). American Chemical Society.
923 https://doi.org/10.1021/bk-2015-1203.ch020
924 Vernhet, A., carillo, S., & Poncet-Legrand, C. (2014). Condensed Tannin Changes Induced
925 by Autoxidation : Effect of the Initial Degree of Polymerization and Concentration.
926 *Journal of Agricultural and Food Chemistry*, *62*(31), 7833-7842.
927 Vivar-Quintana, A. M., Santos-Buelga, C., Francia-Aricha, E., & Rivas-Gonzalo, J. C. (1999).
928 Formation of anthocyanin-derived pigments in experimental red wines / Formación de
929 pigmentos derivados de antocianos en vinos tintos experimentales. *Food Science*
930 *and Technology International*, *5*(4), 347-352.
931 https://doi.org/10.1177/108201329900500407
932 Vivas, N. (1997). Composition et propriétés des préparations commerciales de tanins à
933 usage oenologique. *Revue des oenologues et des techniques vitivinicoles et*
934 *oenologiques: magazine trimestriel d'information professionnelle*, *24*(84), 15-21.

Vivas, N. (2000). Propriétés et intérêts des tanins œnologiques extraits du raisin. *Revue française d'oenologie*, *183*, 15-18.

Vivas, N., & Glories, Y. (1996). Role of Oak Wood Ellagitannins in the Oxidation Process of Red Wines During Aging. *American Journal of Enology and Viticulture*, *47*(1), 103-107.

von Baer, D., Rentzsch, M., Hitschfeld, M. A., Mardones, C., Vergara, C., & Winterhalter, P. (2008). Relevance of chromatographic efficiency in varietal authenticity verification of red wines based on their anthocyanin profiles : Interference of pyranoanthocyanins formed during wine ageing. *Analytica Chimica Acta*, *621*(1), 52-56.

Waterhouse, A. L., & Laurie, V. F. (2006a). Oxidation of Wine Phenolics : A Critical Evaluation and Hypotheses. *American Journal of Enology and Viticulture*, *57*(3), 306-313.

Waterhouse, A. L., & Laurie, V. F. (2006b). Oxidation of Wine Phenolics : A Critical Evaluation and Hypotheses. *American Journal of Enology and Viticulture*, *57*(3), 306-313.

Whitaker, J. R., & Lee, C. Y. (1995). Recent Advances in Chemistry of Enzymatic Browning. In *Enzymatic Browning and Its Prevention* (Vol. 600, p. 2-7). American Chemical Society. https://doi.org/10.1021/bk-1995-0600.ch001

Wrolstad, R. E., Durst, R. W., & Lee, J. (2005). Tracking color and pigment changes in anthocyanin products. *Trends in Food Science & Technology*, *16*(9), 423-428. https://doi.org/10.1016/j.tifs.2005.03.019

Zanchi, D., Poulain, C., Konarev, P., Tribet, C., & Svergun, D. (2008). Colloidal stability of tannins : Astringency, wine tasting and beyond. *journal of physics: condensed matter*.

Zhang, Z., Li, J., Fan, L., & Duan, Z. (2020). Effect of organic acid on cyanidin-3-O-glucoside oxidation mediated by iron in model Chinese bayberry wine. *Food Chemistry*, *310*, 125980. https://doi.org/10.1016/j.foodchem.2019.125980

Chapitre V – Recherche de marqueurs d'oxydation issus des tannins

Dans ce chapitre, six types de marqueurs d'oxydation des tannins condensés à deux niveaux d'oxydation ont été étudiés. Ces derniers ont été recherchés dans des échantillons de vins rouges (Syrah 2018, Syrah 2014, Syrah 2010 et Syrah 2018 oxydé au peroxyde d'hydrogène) après dépolymérisation afin de comparer l'état d'oxydation de la fraction tannique des différents échantillons. Ces marqueurs ont été sélectionnées car ils peuvent être discriminés selon deux approches donnant des informations sur (i) l'orientation de l'évolution structurale des tannins en fonction des proportions relatives entre les marqueurs d'oxydation des unités terminales (*m/z* 579 et 577), terminales et d'extension (*m/z* 683 et 681) et d'extension (*m/z* 787 et 785) (ii) le niveau d'oxydation des tannins en fonction des proportions relatives entre les marqueurs d'oxydation du « premier niveau » d'oxydation (*m/z* 579, 683 et 787) et du « deuxième niveau » d'oxydation (*m/z* 577, 681 et 785).

L'objectif final de ce travail est de mesurer l'impact du vieillissement accéléré sur la fraction tannique et de le comparer au vieillissement naturel.

Les méthodes utilisées étaient les suivantes

- Une chromatographie liquide semi-préparative basse pression par chromatographie flash afin de fractionner les échantillons de vins et d'isoler la fraction tannique ;
- Une dépolymérisation chimique des différentes fractions par thioglycolyse acide, afin de rompre les liaisons natives des tannins et d'obtenir des unités constitutives des tannins non-modifiées et les marqueurs d'oxydation plus facilement analysables ;
- Des analyses par UHPLC-MS^2 ont permis de détecter et d'identifier les marqueurs d'oxydation obtenus après dépolymérisation.

Les hypothèses étaient les suivantes

1. Une méthode d'oxydation accélérée du vin rouge permettrait de prédire l'évolution de la fraction tannique durant le vieillissement du vin. Est-elle similaire à celle de l'oxydation naturelle ?
2. Le suivi de six types de marqueurs d'oxydation par spectrométrie de masse permet de témoigner de l'état d'oxydation de la fraction tannique. Ces marqueurs pertinemment sélectionnés sont susceptibles de se retrouver dans tous les échantillons et l'analyse de leurs aires EIC permettraient d'étudier l'évolution oxydative de la fraction tannique entre les échantillons.
3. En fonction de l'état d'oxydation, les marqueurs d'oxydation des tannins peuvent avoir différents niveaux d'oxydation (premier niveau, deuxième niveau…), l'analyse des EIC

des marqueurs à deux niveaux d'oxydation nous donnera des informations sur l'état d'oxydation de la fraction tannique.

Conclusions

1. Le pourcentage d'unités modifiées au sein des tannins augmente avec le vieillissement naturel et accéléré des vins, ce qui correspond à une évolution logique de ces composés en milieu œnologique. Le pourcentage de modifications des tannins pour les millésimes 2014, 2010 et 2018 oxydé au peroxyde d'hydrogène est équivalent et il est plus élevé que pour le millésime 2018. Cette méthode d'oxydation accélérée semble suivre l'oxydation naturelle en ce qui concerne le pourcentage global d'unités modifiées.
2. La quantité totale de tannins présents dans chaque vin elle diminue au cours au cours du vieillissement du vin. Cette perte peut être due à une précipitation d'une partie de tannins au cours du vieillissement.
3. Après dépolymérisation des tannins, le suivi de 18 marqueurs d'oxydation (6 types de marqueurs à deux niveaux d'oxydation – 3 isomères pour chaque type) a mis en évidence une évolution de l'état d'oxydation des tannins au cours du vieillissement du vin. En effet, on note augmentation des marqueurs du deuxième niveau d'oxydation au fur et à mesure des années ce qui témoigne d'un état d'oxydation plus avancé de la fraction tannique.
4. Dans le vin de 2018 oxydé artificiellement, d'après les aires EIC obtenues, la quantité de marqueurs au premier niveau d'oxydation (*m/z* 579, 683 et 787) est similaire à celle du vin de 2014. Ainsi, le suivi des marqueurs d'oxydation du premier niveau permet (pour les vins étudiés) de prédire l'évolution naturelle du vin. Tandis que le suivi des marqueurs d'oxydation du deuxième niveau donne un reflet plus réaliste de l'état d'oxydation global de la fraction tannique des vins

Cette étude a fait l'objet d'un article scientifique, soumis dans le journal JAFC (*journal of agricultural and food chemistry*) en octobre 2021 sous la référence :

Deshaies, S.; Garcia, F.; Suc, L.; Saucier, C.; and Mouls, L.; **Study of the oxidative evolution of tannins during red wines aging by tandem mass spectrometry.**

Et présenté ci-après

Article 5:

STUDY OF THE OXIDATIVE EVOLUTION OF TANNINS DURING SYRAH RED WINES AGING BY TANDEM MASS SPECTROMETRY

Stacy Deshaies, François Garcia, Lucas Suc, Cédric Saucier, and Laetitia Mouls*

SPO, Univ Montpellier, INRAE, Institut Agro, Montpellier, France

GRAPHICAL ABSTRACT

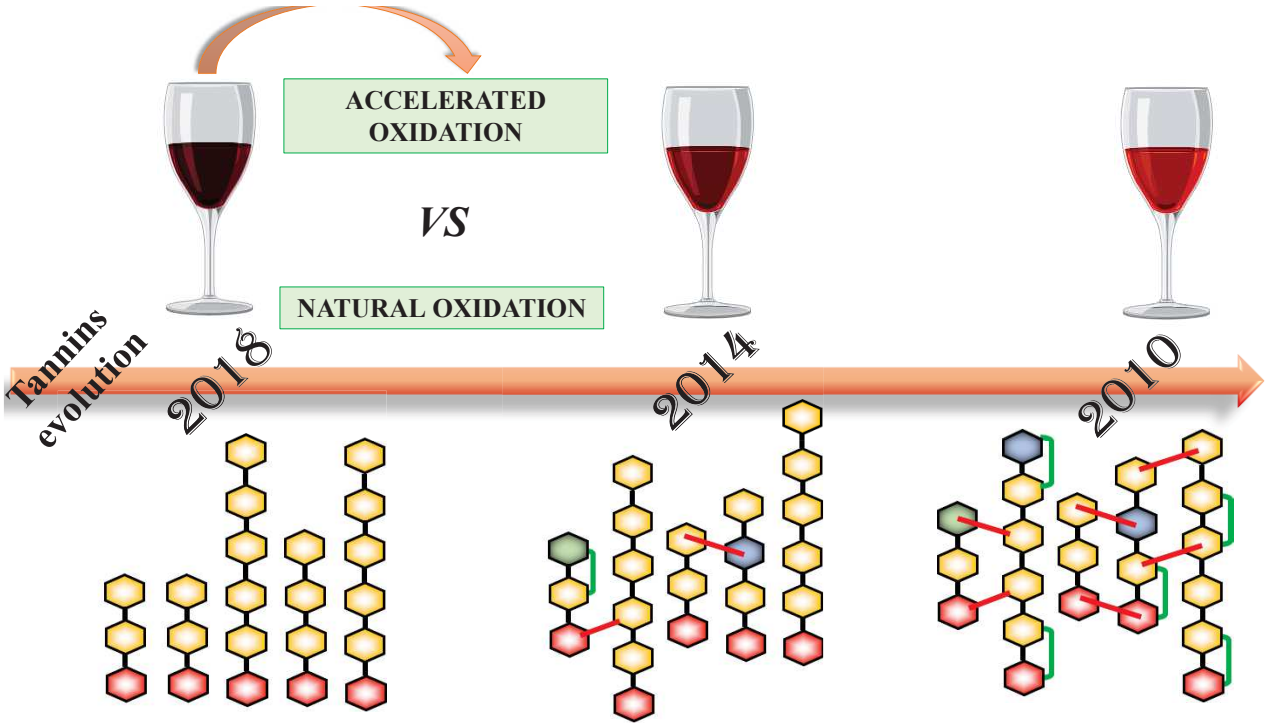

ABSTRACT

Red wine is a very complex medium in which condensed tannins undergo many modifications during winemaking and bottle aging. These reactions have an impact on the organoleptic properties. This work aimed to highlight tannins evolution related to wine evolution by studying three vintages of Syrah wines. An accelerated oxidation is also correlated to the natural

* Corresponding author. Tel.: +3-349-961-3111; fax: +3-349-961-2857; e-mail: laetitia.mouls@supagro.fr

evolution in order to evaluate the ability of this oxidation to imitate natural evolution. After chemical depolymerization of the tannins, the monitoring of 6 types of markers at two oxidation levels was investigated. An evolution of the tannin oxidation state during ageing by the increase of the markers of the second oxidation level over the vintages was observed. In the 2018 oxidized wine sample, the first oxidation level markers are similar to the 2014 vintage but the second oxidation level markers are higher than other vintages, indicating a more advanced state of tannin oxidation.

KEYWORDS

Proanthocyanidin

Flavan-3-ol

Oxidation marker

Polyphenol

Accelerated ageing

Depolymerization.

1. Introduction

During wine aging, a moderate and regular oxygen intake at the cork allows the wine to evolve through time. But this evolution depends on conservation parameters (temperature, humidity and time) (Arapitsas et al., 2014) and on wine chemical composition. A wine intended for long ageing must have a sufficient important tannin level (Merrell & Hansen, 2018). Red wines phenolic composition is particularly rich compared to white wines one, mainly due to the presence of condensed tannins and anthocyanins which play a major role in red wine organoleptic properties (Brossaud et al., 2008; Kennedy et al., 2006; Ma et al., 2014; Noble, 1994; Robichaud & Noble, 1990; Soares et al., 2017). If all parameters are correctly controlled during wine storage, polyphenols chemical evolution in red wines tends generally to reduce astringency and contributes to color stabilization (Echave et al., 2021). Polyphenols, in particular condensed tannins, are of primary importance in these sensorial evolutions (i) by reacting with anthocyanins and giving numerous by-products pigments, thus allowing a color stabilization (Atanasova et al., 2002b; V. Cheynier, Dueñas, et al., 2006); (ii) by interacting with salivary proteins, leading to varying degrees of mouth dryness, depending on their composition (McRae & Kennedy, 2011). The interaction strength between tannins and salivary proteins depends on tannins molecular structures: the interactions increase with polymerization degree (V. Cheynier, Prieur, et al., 1997), galloylation percentage (V. Cheynier, Prieur, et al., 1997) and/or their conformational flexibility (P. McManus et al., 1985). Tannins chemical evolution through time thus modulates astringency perception.

Depending on its phenolic composition and on its oxidation state, a wine has a more or less important ageing potential. In order to better predict the optimal time from a qualitative point of view for its consumption, it is necessary to have objective measurements of the wine oxidation state as well as its antioxidant capacity and ageing potential. In this context, studies have been recently carried out (Castro et al., 2014a; V. Ferreira et al., 2015; Gambuti et al., 2017b; Mercurio & Smith, 2008; Picariello et al., 2017; Sheridan & Elias, 2015; Teng et al., 2019) aiming to develop accelerated ageing tests to predict the oxidative evolution of wines.

Until now, tannins evolution in a sample has often been studied using global precipitation analysis methods (Hagerman & Butler, 1978; Makkar et al., 1993; Mercurio & Smith, 2008; Sarneckis et al., 2006). These methods estimate an order of magnitude of the tannin fraction amount but do not give information on the tannin chemical structures.

In view of the structural complexity of the tannin fraction in the samples and in order to have more information on its composition, methods studying tannins after chemical depolymerization have been developed (Kennedy & Jones, 2001; Rigaud, Perez-Ilzarbe, et al., 1991b). However, in these research works, the interpretation of the results was generally carried out on the basis of the unmodified units present in the tannin chains (catechin, epicatechin, epigallocatechin, epicatechin-3-*O*-gallate…), which constitutes a variable part of the tannins, depending on their oxidation level. Indeed, in wines, tannins are more or less oxidized through time. Tannins chemical structures are consequently modified as new intramolecular and intermolecular linkages are generated (Mouls & Fulcrand, 2012, 2015b; Poncet-Legrand et al., 2010).

These structural modifications can potentially change the tannins conformational flexibility and then have an impact on their organoleptic properties (Millet et al., 2019; Mouls & Fulcrand, 2015a; Vernhet et al., 2014; Zanchi et al., 2008). The new covalent bonds resulting from tannins oxidation resist to the depolymerization conditions (Mouls & Fulcrand, 2012, 2015a). Dimeric and trimeric oxidation markers are consequently observed after tannins chemical depolymerization. The mean degree of polymerization (mDP) estimated on the basis of non-modified units is an « apparent » mDP which can be, in some cases, very far from the real mDP, depending on the tannins oxidation state and transformation degree (Giribaldi et al., 2020). The consideration of tannins oxidation markers obtained after depolymerization is essential to better characterise them. In order to understand more precisely the oxidations impact on tannins evolution, the study of oxidation markers resulting from chemical depolymerization have been investigated (**Scheme S1**) (Mouls & Fulcrand, 2012).

After identifying the oxidation markers in model solutions in previous studies, this work proposes to follow, for the first time, oxidative evolution of tannins during aging of wine through oxidation markers observed after chemical depolymerization.

This UHPLC-MS/MS analysis of the tannins was carried out on the three wine samples of the study (3 vintages: 2018, 2014 and 2010) and on the wine of the 2018 vintage that had undergone accelerated ageing according to the chemical method (oxidation in the presence of H_2O_2) which, according to the first results obtained by polyphenomics, proved to be the method that might be closely related to the "natural" momoners flavanols evolution during wine ageing (Deshaies et al., 2020).

As a follow-up to this study and go further in the characterization of polyphenols, the present work has a double objective: (i) to follow the oxidation state of tannins according to the age of the wine, (ii) to compare the impact of an accelerated oxidation on the tannin fraction with the natural evolution.

2. Materials and Methods

2.1.Reagents, Chemicals, and Materials

(+)-catechin hydrate (≥ 98%), (-)-epicatechin (≥ 90%), laccase from *Trametes versicolor* (≥ 0.5 unit/mg); specific activity: 0.94 U/mg); thioglycolic acid (≥ 98%); hydrogen peroxide solution (30% in water); methanol (absolute), ethanol (absolute) and hydrochloric acid were purchased from Merck/Sigma-Aldrich (Saint-Quentin Fallavier, France). Procyanidin B2 (≥ 90%) was purchased from Extrasynthese (Genay, France). Tartaric acid (≥ 99.5%) was purchased from Prolabo (Paris, France).

2.2. Wine samples

Three red wines samples have been elaborated according to an identical traditional winemaking method in mono-varietal (100% Syrah), 13.5% alcoholic strength, were obtained from the same producer (Domaine des Bouzons, Côtes du Rhône, France) and from three different vintages (2018, 2014, 2010). Wine production: 20 days vatting time in stainless steel vats, maturing of Syrah in oak barrels during 10 months. Two 750 mL bottles of each vintage were opened, slowly homogenized under nitrogen to avoid oxidation reactions. Aliquots of 50 mL tubes were then immediately frozen at -80°C.

2.3. Dimeric standards preparation (oxidation markers)

In a wine model solution (12% EtOH, 0.033 M tartaric acid, pH 3.6) catechin (or epicatechin) was dissolved at a final concentration of 6 $g.L^{-1}$ and laccase from *Trametes versicolor* at a final concentration 10 $g.L^{-1}$. The reaction media was then stirred 2 hours at 180 rpm at 22°C. Reaction was stopped on an Amberlite XAD7HP column according to the following protocol: resin was first conditioned in ethanol and rinsed with water (two column volumes). The reaction media was then dropped on the column and washed with water (two column volumes) and eluted with ethanol until the collected fractions were not colored anymore. In this step, the enzyme was retained while compounds of interest were eluted with ethanol. Ethanol fractions were then collected, evaporated and lyophilized before UHPLC-MS/MS analysis.

2.4. Accelerated ageing test with H_2O_2

The accelerated ageing test was performed on Syrah 2018 sample as previously described (Deshaies et al., 2020). *Oxygen saturation:* First, 50 mL of wine was thawed and 35 mL was placed in a 500 mL hermetic bottle. The wine was then vigorously shaken 10 seconds to saturate it in oxygen. The cap was then opened 5 seconds to allow oxygen intake. This operation was repeated 3 times. The wine was finally put in 11 mL hermetic Pyrex tubes (VWR 734-4224, Radnor, PA, USA) equipped with a Presens spot (Presens-Precision Sensing GmbH, Regensburg, Germany) with minimum headspace. *Chemical oxidation:* Secondly, the tubes were maintained at 22°C and stirred at 200 rpm. A hydrogen peroxide solution (30% in water) was added (20 µL). Dissolved oxygen rate acquisition began 30 seconds after H_2O_2 addition. The oxidation test was considered finished when oxygen rates were under 1 $mg.L^{-1}$. All tests were performed in triplicate.

2.5. Fraction isolation before depolymerization by low pressure liquid gel chromatography

After thawing, 30 mL of wine were centrifuged and concentrated (evaporation of 20 to 30% of the initial volume). The wine was then deposited on fractogel HW50F (approximately 200 mL column volume). Each wine was treated in duplicate.

Solvents used were: EtOH acidified with 0.05% TFA (A); water acidified with 0.05% TFA (B); acetone acidified with 0.05% TFA (C). The separation was performed at a constant flow rate of 20 $mL.min^{-1}$, using the following gradient: 0-5 min à 100% B; 5-10 min 100-95% B 5% C; 10-38 min 95-69% B / 5-31% C; 38-90 min 69-20% B / 31-80% C; 90-110 min 20% B / 80% C; 110-120 min 0-45% A / 20-25% B / 80-30% C; 120-135 min 45% A / 25% B / 30% C; 135-140 min 45-100% A; 140-160 min 100% A.

After separation, fractions were collected and grouped according to their retention time, before evaporation and lyophilization. Separation was as follow:

- F1: polyphenolic fraction (anthocyanins, flavonoïds including tannins at low molecular weight) – tubes 1 to 49 (38 to 110 min);
- F2: fraction containing exclusively tannins - tubes 50 to 61 (110 to 140 min).

2.6. Depolymerization

Each fraction (F1 and F2) of each duplicate was depolymerized 3 times. In a 10 mL graduated flask was added 166 µL of hydrochloric acid (0.2 M) and 80 µL of thioglycolic acid. Volume was then completed with methanol. Lyophilized fractions F1 and F2 were dissolved in 100 µL of methanol (2 $mg.mL^{-1}$), plus 100 µL of the previous thioglycolysis solution. The reaction media was then placed in a microvial with a crimp cap. The latest were finally incubated 6 minutes at 90°C and cooled down in an ice-water bath.

2.7. UPLC−MS/MS analyses

The samples were analyzed using a Waters reversed-phase ultra-performance liquid chromatography system coupled to a Bruker AmaZon X mass spectrometer. The liquid chromatography system was an Acquity UPLC (Waters, Milford, MA, U.S.A.) equipped with a photodiode array detector. The column was an Acquity UPLC HSS T3 (1.8 µm, 2.1 × 100 mm) preceded by a Waters column in-line filter (0.2 µm, 2.1 mm). The binary mobile phase consisted in Milli-Q water (solvent A) and acetonitrile/water 80:20 (solvent B) both acidified with 0.1% formic acid. The separation was performed at a constant flow rate of 0.55 $mL.min^{-1}$, using the following short gradient: 0.1-25 % B in 2 min; 25-35 % B in 2 min; 35 % B for 1 min; 35-45 % B in 1 min; 40-99.9% B in 2 min; 99.9% B for 2 min; 99.9-0.1% B in 1 min and equilibration at 0.1 % B for 2 min.

The « apparent » mDP of each sample was estimated these terminal and extension units obtained after depolymerization from UV chromatogram at 280 nm using the following formula $mDP = \frac{\sum extension\ units}{\sum terminal\ units}$.

The percentage of modifications within the tannin structures was estimated from the UV chromatogram after depolymerisation (**Scheme S1**) according to the following formula:

$$\% \text{ modified tannins} = \frac{\Omega}{\Delta + \Omega} \text{ X } 100$$

with

□ : area of the peaks corresponding to the unmodified terminal and extension tannins constitutive units

□□□□ area of the hump under the peaks of the unmodified units, i.e. area of the tannins modified constitutive units.

The mass spectrometer was a Bruker amaZon X electrospray ionization (ESI) ion trap (Bruker Daltonics, Bremen, Germany). The nebulizer pressure was 3.03 bar; the temperature of the drying gas was set at 200 °C with a 12 L min^{-1} flow; and the capillary voltage was set at −5.5 kV. The mass spectra were acquired over a mass range of 50−2000 Th in the positive ion mode. The mass spectrum acquisition speed was set at *m/z* 8100 s^{-1}. The target mass was tailored to each reaction between *m/z* 500 and 900. Complementary analyses were performed with inclusion of *m/z* 577, 579, 683, 681, 787, 785 and exclusion of *m/z* 291. All UHPLC-MS/MS analyses were performed in triplicate.

2.8. Selection of oxidation markers of tannins

In this work, after chemical depolymerization of tannins, six types of oxidation markers have been selected among those previously identified so as to be researched in samples. These markers present in all samples have been chosen because they reflect the oxidation level and the location of the modification within the tannin chains. Indeed, these markers can be classified according to two approaches giving information based on:

- The tannin structural oxidation evolution in relation to the relative proportions between the oxidation markers of the terminal (*m/z* 579 and 577), terminal and extension (*m/z* 683 and 681) and extension (*m/z* 787 and 785) units.

- The level of tannin oxidation depending on the relative proportions between the oxidation markers of the "first level" of oxidation (*m/z* 579, 683 and 787) and the "second level" of oxidation (*m/z* 577, 681 and 785). The oxidation markers of the second oxidation level underwent further oxidation (more advanced oxidation) resulting in the formation of a new covalent bond (loss of 2 umas corresponding to two hydrogen atoms).

The relative proportions of the different oxidation markers in the tannin fraction of the samples were estimated from the EIC obtained by UHPLC-MS/MS of the tannin fractions after chemical depolymerisation by thioglycolysis (Giribaldi et al., 2020).

3. Results and discussion

3.1. Global tannin study in wines

3.1.1. Tannin study before depolymerization

Throughout its multi-step production process (fermentation, maturation...), wine develops an increasingly complex chemical matrix containing numerous families of molecules with varying molecular weights. Thus, the study of tannins in this environment becomes difficult or even impossible and a prior chemical treatment of the sample is necessary to isolate tannins from this matrix.

To carry out this study, wine samples were fractionated using flash chromatography. Two distinct fractions were obtained based on their elution times: F1 and F2.

The first eluted fraction was a polyphenolic fraction containing mainly low molecular weight tannins and anthocyanins, remarkable for their distinct UV peaks (**Figure S1A**). The second fraction, eluted at the end of the sequence, contained mainly polymeric tannins, clearly noticeable by the "polymeric hump" visible in UV at 280 nm which resulted from the co-elution of a large number of bio-polymers (**Figure S1B**). It can also be noticed that the absorbance intensity of F1 observed on the UV chromatograms at 280 nm is clearly higher than that of fraction 2. Indeed, contrary to fraction 2 which contains only tannins, fraction 1 contains many other phenolic compounds and in particular anthocyanins which have a higher response coefficient than flavanols at 280 nm (in our experimental conditions, the response coefficient of malvidin is 3.6 times higher than that of catechin).

Similar profiles were observed for the other wines fractions (2018, 2010 and 2018 oxidized, **Figure S1**).

From the MS/MS fragment analyses, we note that the F1 fractions contained mostly anthocyanins (*m/z* 493, 611, 625, 639, 641...), low molecular weight tannins (dimers and trimers, *m/z* 595, 579, 867, 881...) and reaction products between flavanols and anthocyanins (*m/z* 781, ...). Under the distinct peaks on the UV chromatogram at 280 nm was a large 'hump' indicating a complex mixture of co-eluted molecules which most probably corresponds to a mixture of tannins, more or less modified.

A polymeric hump (**Figure S1B**) was also clearly visible and predominant for F2 fraction. In this hump, polymers up to an mDP of 8 (monocharged ions: dimers, trimers and tetramers and bicharged ions) could be detected and identified by mass spectrometry.

The molecular diversity of tannins in wines, due to their degree of polymerisation and their chemical structures, creates a polymeric hump and does not allow their separation by liquid chromatography. Their analysis by mass spectrometry is also limited because the tannin

ionisation decreases with molecular weight, and it becomes very difficult to detect tannins of with mDP above DP>8 by mass spectrometry (Mouls et al., 2011a).

An alternative method to overcome these analytical limits is to study them after chemical depolymerization which released monomers (C, EC, EGC and ECG: unmodified units) and dimers/trimers (oxidation markers). Analysis of the samples after depolymerization by UHPLC-MS gives access to a lot of information: apparent mDP, proportion of unmodified units. In order to confirm the previous hypotheses regarding the presence and distribution of tannins in fractions F1 and F2, the apparent mDP of each fraction was estimated after depolymerization.

3.1.2. « apparent » mDP

In this study, thioglycolic acid ($C_2H_4O_2S$) was used as nucleophilic reagent in chemical tannins depolymerization under acidic conditions. After reaction, a mixture of extension and terminal constitutive units of the tannins were obtained. Extension units can be easily discriminated from the terminal units by mass spectrometry as they are linked to the nucleophilic reagent in C4 position (**Scheme S1**).

This apparent mDP, depending on the modification state of the tannins may be more or less different from the real mDP, which is currently impossible to determine. However, the calculation of the apparent mDP allows a comparative study between the different fractions. Calculated apparent mDP of the different fractions of the samples are presented in **table 1**.

	2010		**2014**		**2018**		**2018 oxidized**	
	F1	**F2**	**F1**	**F2**	**F1**	**F2**	**F1**	**F2**
Dry extract ($g.L^{-1}$)	3.8 ± 0.1	0.5 ± 0.1	2.6 ± 0.4	0.8 ± 0.2	3.0 ± 0.7	1.1 ± 0.2	2.8 ± 0.1	0.8 ± 0.1
% unmodified units	-	34	-	36	-	62	-	36
% modified units	-	65	-	64	-	38	-	64
Apparent mDP (UV)	2.2 ± 0.1	8.4 ± 0.1	2.0 ± 0.1	6.2 ± 0.5	1.7 ± 0.1	8.7 ± 0.2	1.7 ± 0.1	6.8 ± 0.4
Apparent mDP (EIC)	2.6 ± 0.2	8.0 ± 0.9	2.2 ± 0.1	5.8 ± 0.2	2.6 ± 0.2	8.7 ± 0.6	2.2 ± 0.1	6.5 ± 0.1

Table 1: Dry weight, percentage of unmodified and modified units, apparent mDP (estimated by UV and EIC) of both F1 and F2 fractions for 4 different Syrah wine samples

Typically, the apparent mDP is calculated from the UV chromatograms areas at 280 nm, which can be biased in the case of samples with a complex matrix. Indeed, many co-elutions can lead

to an error in the mDP estimation. A recent study showed that the determination of the apparent mDP by mass spectrometer from the EIC area of each constitutive tannins unit generated after chemical depolymerization could be used to eliminate this co-elution phenomenon and to be more precise. Indeed, the use of EIC allows it to be specific and more sensitive than UV (Giribaldi et al., 2020). The different constitutive units (extension and terminal) do not have the same mass spectrometry response coefficient, so the apparent mDP estimation from EIC requires the use of a corrective factor. Extension units (EC-Nu) have a higher response coefficient than terminal units (EC). This corrective factor was estimated for this study to 2.9 ± 0.1 from the method describe previously (Suc et al., 2021; Giribaldi et al., 2020). The values obtained from the UV and EIC chromatograms are close, indicating that potential co-elutions in liquid chromatography lead to a small error in the estimation of apparent mDP for the study samples (**Table 1**).

For the time being, only the apparent mDP is available, but in the future the mDP calculation should also take into account the modified units in order to get as close as possible to the real mDP of the wine tannin fraction. This cannot be done from UV chromatograms but could be possible from EICs. For this purpose, the study of tannin oxidation markers was conducted on the basis of the EIC.

According to **table 1**, for the samples studied the apparent mDP calculated from UV chromatogram is close to that estimated by EIC. They are of the same order of magnitude for the vast majority of the fractions: between 1.7 and 2.6 for F1 fraction and between 5.8 and 8.7 for F2 fraction. However, we note a more significant difference for the F1 fraction obtained from the 2018 wine (apparent mDP 1.7 and 2.6, estimated from UV and EIC respectively). This can be explained by a higher amount of monomeric polyphenols (Figure S1, 2018 A) which complicates the estimation of the mDP from the UV chromatogram and in this case underestimates it. In order to estimate the total amount of tannins in the wine and their evolution between the different samples, the proportion of tannins in the F1 fraction was then determined.

3.1.3. *Total tannin proportion evolution*

Modified tannin constitutive units were present in very low concentrations compared to the unmodified units. They have a high structural diversity and were therefore not detectable as a distinct peak on the UV chromatograms but it cannot be excluded that their total amount was greater than the unmodified units. The modified units are also co-eluted with the unmodified units as a large bump (formation of a « polymeric hump ») (**Figure S1**). As mentioned above,

297 the F2 fraction is exclusively composed of tannins with a certain oxidation level. Due to their
298 reactivity, these tannins have undergone different modifications during the wine elaboration
299 and evolution. The quantity of dry extract weighed for F2 at the end of the separation
300 corresponded to a wine tannic fraction with more or less modification due to some oxidation or
301 rearrangements.

302 The total amount of tannins corresponds to the sum of the unmodified and modified units (total
303 chromatogram area). **Table 1** shows the dry extracts quantities weighed for each fraction and
304 the percentages of modified and unmodified units of the tannin fraction F2.

305 The F1 fraction corresponded to a mixture of various polyphenols (anthocyanins, monomers,
306 dimers...). It is then impossible to directly determine the real weight of tannins in this fraction.
307 To estimate the amount of tannins in F1 it is necessary to determine the amount of tannin
308 constitutive units in the F1 fraction. The unmodified extension and terminal units are not
309 directly visible on the UV chromatogram, due to the complexity of the medium. They were then
310 estimated from the EIC areas.

311 According to the oxidation marker study below, the oxidation state of the F1 fraction is 10 times
312 lower than the F2 one. Thus, a weight of tannins in the F1 fraction was estimated from the EICs
313 obtained for F2 and by introducing a corrective factor due to the difference in ESI-MS
314 ionization of extension and terminal units. Thus after determining the ratio between the
315 modified and unmodified part in the F2 fraction, the unmodified units were determined by the
316 EICs in F1 and the modified part was estimated at a ratio ten times lower than that observed for
317 the F2 fraction. The evolution of the total tannin concentration in each sample is shown in
318 **figure 1.**

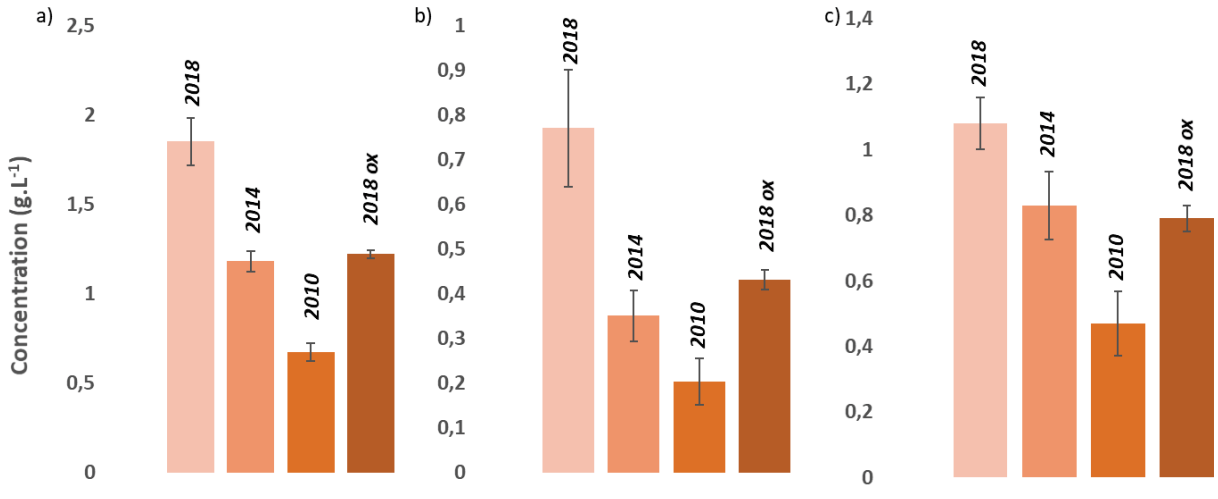

319

Figure 1: Tannins concentration evolution ($g.L^{-1}$) in 4 red wine samples: 2018, 2014, 2010 and 2018 oxidized with hydrogen peroxide: (a) total tannin fraction, (b) F1 and (c) F2.

The percentage of modified tannin units increases significantly in the first four years with wine natural which corresponds to an excepted evolution of these compounds in the oenological environment (**Table 1**). A similar evolution has been estimated for 2018 vintages oxidized with hydrogen peroxide is equivalent (64%) reflecting the impact of the use of hydrogen peroxide on tannin evolution and is higher than for the 2018 vintage for which only 38% of the tannin constituent units are modified. The proportion of modified units appears to be equivalent for the 2014 2010 and 2018 vintages oxidized higher than the 2018 vintage. This accelerated oxidation method seems to follow the natural oxidation according to the percentage of modified units. As for the total amount of tannins (**Figure 1.a.**) present in each wine, it seems to decrease during the aging of the wine (about 1.9 $g.L^{-1}$ in 2018, 1.2 $g.L^{-1}$ in 2014 and 0.6 $g.L^{-1}$ in 2010). This loss can be due to a precipitation of some tannins during aging. However, this result must be moderated because these are three different vintages and the initial tannin composition of each of the vintages is not known and could differ even if the vinifications were carried out in an identical manner (20-day vatting, 40% Syrah aged in oak barrels for 10 months).

Nevertheless, if we compare the 2018 vintage before and after accelerated aging we also notice a loss of part of the tannin fraction for the oxidized 2018 sample (1.2 $g.L^{-1}$). Thus the accelerated aging conditions also seem to follow the natural evolution of the tannin fraction in terms of total amount. If we observe the amount of tannins in the F1 and F2 fractions for each of the wines we observe a higher mass concentration in F2 for all wines (0.8 $g.L^{-1}$ and 1.1 $g.L^{-1}$ for F1 and F2 respectively i.e. F1/F2 = 0. 7 for the 2018 vintage; 0.35 $g.L^{-1}$ and 0.8 $g.L^{-1}$ for F1 and F2 respectively i.e. F1/F2 = 0.4 for the 2014 vintage; 0.2 $g.L^{-1}$ and 0.5 $g.L^{-1}$ for F1 and F2 respectively i.e. F1/F2 = 0.4 for the 2010 vintage). This decrease in the tannin fraction with time and the increase in the proportion of tannins in the F2 fraction compared to the F1 fraction reflects the evolution of tannin structures. These hypotheses are supported by the results obtained for the oxidized 2018 wine which has a concentration of tannins twice as high in the F2 fraction as in the F1 fraction (0.4 $g.L^{-1}$ and 0.8 $g.L^{-1}$ for F1 and F2 respectively F1/F2= 0.5) and a total amount of tannins approximately 2 times lower than that of the 2018 wine before accelerated oxidation.

3.2. Study of tannins oxidation markers in wines

Tannins will undergo many chemical changes during wine aging. Among the reactions, the oxidation of the catechol nucleus present on each tannins constitutive unit into a quinone (electrophile) can lead to the formation of new covalent bonds within the same tannin chain (intra-molecular bonding) or between tannins (inter-molecular bonding) (**Schemes S1 and S3**).

In contrast to the C4-C6 and C4-C8 inter-flavanic bonds, the new intra- and intermolecular bonds created between the tannin chains as a result of wine aging will resist under chemical depolymerization conditions (**Figure S1**). Due to their high diversity and low concentration these oxidation markers were not distinctly observable on UV chromatogram but can be studied by mass spectrometry from their EIC. The oxidative evolution of epicatechin is a good element to monitor the oxidation state of tannins because it is the preponderant tannins constitutive unit in wine. In the studied wines the total sum of epicatechin units was more than 3 to 4 times higher than the catechin units (**Table S1**).

In this study, six types of markers (M1, M2, M3, M4, M5 and M6 with *m/z* 579, 577, 683, 681, 787 and 785 respectively)[34,37] were chosen because they can reflect the tannin oxidation level (*m/z* 579, 683 and 787: markers for the first oxidation level and *m/z* 577, 681 and 785 for second oxidation level) and the structural evolution of the tannins (*m/z* 579 and 577: terminal markers, *m/z* 683 and 681: extension/terminal markers and *m/z* 787 and 785: extension markers). For each type of marker, several isomers were detected in the samples. The three major isomers (a, b and c) were detected for the four wines and eluted by liquid chromatography at different retention times were selected for this study (**Table 2**). The evolution of the EIC intensities of these 18 oxidation markers was then monitored in order to compare the 4 wine samples (2018; 2014; 2010 and 2018 oxidized with hydrogen peroxide). As the mass spectrometry response coefficients of the markers were not known, the EIC evolution was compared as a function of marker type between samples.

Oxidation markers		Oxidation level	*m/z*	Name	Tr (min)	Fragments ions MS^2
terminal		1	579	M1a	2,6	561, 543, **441**, **427**, 425, 409, 393, 331, 301, 289, 271, 259
				M1b	2,9	561, 543, **559**, 427, **425**, 415, 409, 393, 289,271, 259
				M1c	3,1	559, 425, 251, 165
	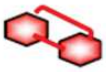	2	577	M2a	3,2	559, 541, 439, 437, 425, **409**, 391, 299, 287, 271
				M2b	3,9	559, 557, 541, **451**, 437, 425, **407**, 299, 287, 271
				M2c	4,3	559, 557, 541, **451**, 449, 437, 425, **407**, 331, 299, 287
terminal/ extension	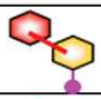	1	683	M3a	3,8	**577**, 559, 557, **531**, 451, 425, **409**, **395**, 289, 247
				M3b	4,3	577, **575**, 557, **529**, 449, 425, **407**, 299, 247
				M3c	5,1	**577**, 559, **531**, 449, 425, **407**, 299, 247
	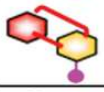	2	681	M4a	4,1	663, 575, 557, 529, 513, 465, **449**, **425**, **407**, 395
				M4b	4,4	663, 575, 559, 557, 529, 469, 425, 407, 331, 299, 247
				M4c	5,1	663, 575, 557, **455**, 437, **413**, 287, 227
extension	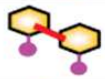	1	787	M5a	4,1	681, 575, 557, 529, 511, 449, 431, 407, 395
				M5b	4,5	681, 625, 622, 575, 479, 447, 405, 301
				M5c	4,9	681, 663, 635, 575, 557, 529, 511, 449, 287, 227
	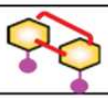	2	785	M6a	4	765, 677, 631, 621, 573, 557, 529, 469
				M6b	4,5	681, 679, **625**, 592, **575**
				M6c	5	679, 625, 622, 479, 301

Table 2: Studied oxidation markers: retention time (UHPLC) and principal fragments ions observed on the MS/MS spectrum.

First, the wines were compared through the global evolution of the 6 marker types, then through the evolution of each of the 3 isomers for the same marker type. This comparison was carried out on the whole tannin fraction of each wine as well as on the F1 and F2 fractions obtained for each wine.

Results are correlated to the total tannins concentration in the samples and to the proportion of unmodified units within the tannins.

3.2.1. *Analysis of MS/MS spectra.*

During tannins oxidation, the new covalent bonds generated between a terminal unit and an extension unit or between two extension units the markers will give, after chemical depolymerization, tannin oxidation markers with one or two nucleophilic adducts respectively. The standards for these markers are not available and the exact structure of each of these markers cannot be determined but some structural hypotheses can be made based on the MS/MS spectra for each of the markers (**Table 2** and **Scheme 1**).

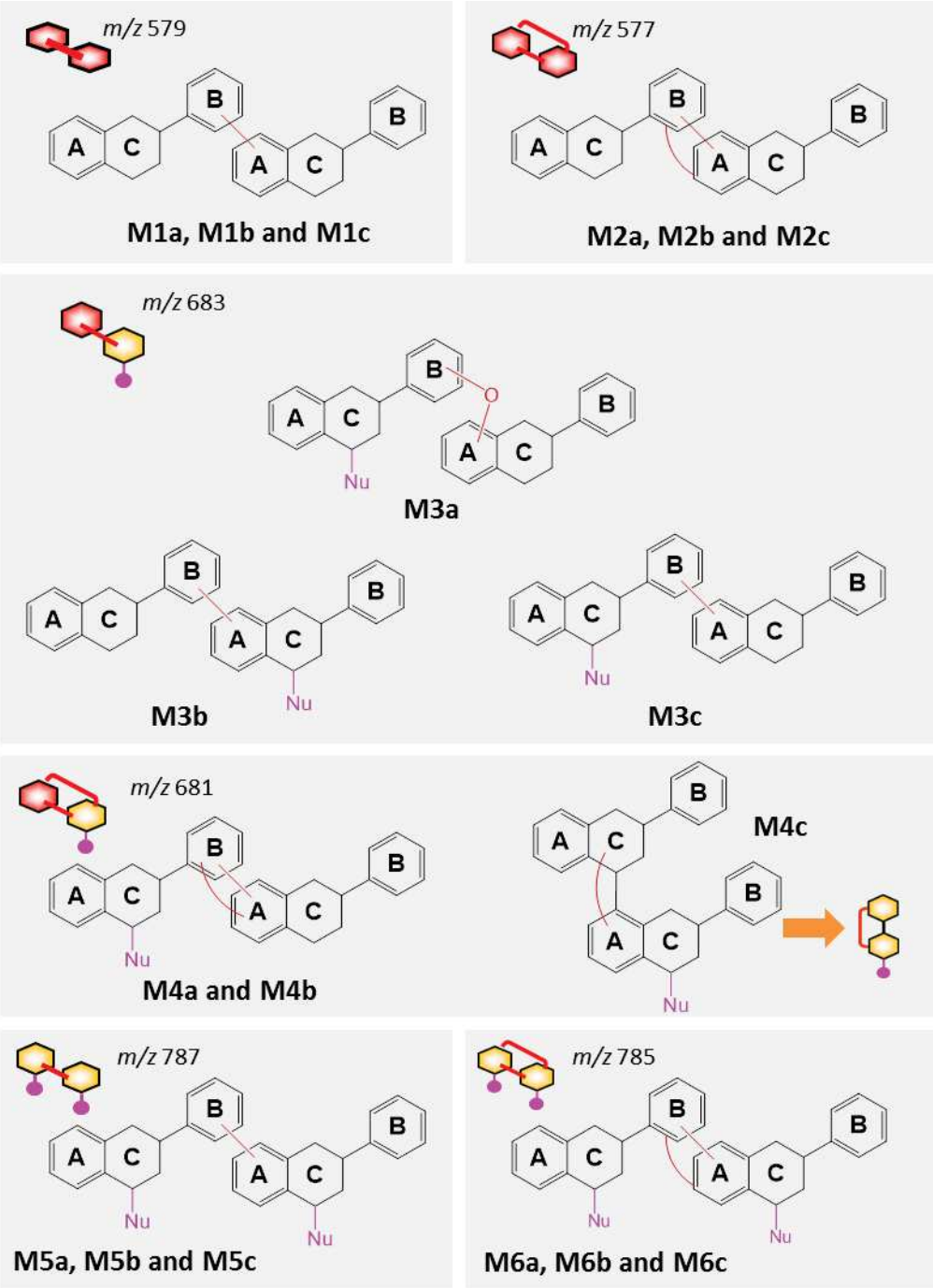

Scheme 1: Structure hypotheses for some oxidation markers, resulting from their MS/MS spectra.

On the markers MS/MS spectra, a loss of a neutral molecule of 152 Da can correspond to a loss of the B-ring by RDA (Retro-Diels-Alder). If on the same MS/MS spectrum we also observe a loss of 126 Da, which can correspond to the loss of an A-ring, this indicates that the covalent bond which was created by oxidation is very probably between the A-ring of a unit and the B-

ring of the other unit (usual dissociation mass spectrometry of epicatechin monomer are available in **scheme S4**). These neutral losses were obtained for most of the considered markers:

- fragment ions 427 Th (for M1), 425 Th (for M2), 529 Th (or 531 Th) (for M3), 635 Th (for M5) reflect the loss of a B-ring from the parent ion;
- fragment ions 451 Th (for M2) and 557 Th (or/and 559 Th) (for M3 and M4), reflect the loss of an A-ring from the parent ion. This loss of A-ring can also be observed from a fragment ion and in particular after the loss of B-ring (-152 Da): 301 Th (for M1), 299 Th (for M2) and 407 Th (for M4).

On the M1 type markers MS/MS spectra, the presence of fragment ions at 561, 543, 441, 427, 409, 393 and/or 289 Th indicate a B-dehydrodicatechin[29] type structure. These ions are observed on the MS/MS spectrum of M1a and M1b with different relative abundances. The M1a and M1b markers are, at first sight, B-dehydrodicatechin[29] type isomers. For M1c, the lack of quality of the MS/MS spectrum obtained does not allow us to make structural hypothesis.

Similarly, on the M2 type markers MS/MS spectra the presence of fragment ions at 559, 541, 439, 425, 407, 391 and/or 287 Th indicate an A-dehydrodicatechin[29] type structure. For M2a, M2b and M2c these fragment ions are present on their MS/MS spectrum (except for 439 Th for M2b and M2c). Thus these marker ions are, at first sight, A-dehydrodicatechin[29] type isomers.

For markers with one or two nucleophiles (M3, M4, M5 and M6): a loss of one (or two) nucleophile(s) is usually first observed and the losses of 152 Da and 126 Da are obtained from this fragment ion (-Nu) (supplementary material).

Thus the isomers M3a, M3b and M3c are oxidation markers of extension/terminal tannins and the covalent bond created by oxidation connects the A-ring of one unit to the B-ring of the other unit. This bond is probably a bi-aryl bond. For M3a the abundant presence of the fragment ion *m/z* 395 could indicate that, for this oxidation marker, a bi-aryl ether bond is implicated. Indeed, a break in the bi-aryl ether bond would lead to the formation of an EC-Nu fragment ion at *m/z* 395.

For M3a, contrary to the other isomers, we observe a loss of the B-ring directly from the parent ion (*m/z* 683 → *m/z* 531). The presence of this fragment ion could indicate a difference in the positioning of the nucleophile on the marker. Indeed, two main types of structure can be obtained for M3 markers: (i) the extension unit carrying the nucleophile can be linked to the B-ring terminal unit by its a-ring or (ii) the extension unit carrying the nucleophile can be linked

to the A-ring terminal unit by its B-ring. The loss of B-ring directly from the parent ion (*m/z* 683 → *m/z* 531) might indicate that in the case of M3a it is the second case (ii) which would be more favorable to this loss of neutral.

For M4a and M4b, the fragment ions present on the MS/MS spectra indicate that the bond created by oxidation is between an A-ring and a B-ring. The presence of the fragment ion *m/z* 395 for M4a could indicate as previously for M3a that it is a bi-aryl ether bond. The presence of the fragment ion *m/z* 529 could indicate, as seen before for M3a, that the extension unit is linked to the A-ring of the terminal unit by its B-ring.

The fragment ions observed on the MS/MS spectrum of M4c (*m/z* 455 [-Nu + BFF] (*benzofuran forming*) and 413 [-Nu + HRF - H_2O] (*heterocyclic ring fission*)) show that it is an extension unit marker[29].

As described by Mouls & Fulcrand in 2012 (Mouls & Fulcrand, 2012) the MS/MS spectrum of M5a and M5c correspond to the extension marker whose units are linked by a bi-aryl bond between the A and B rings (possibly bi-aryl ether for M5a *m/z* 395 but to be confirmed).

For M5b as for M5a and M5c the fragment ions *m/z* 681 and 575 show the loss of one and two nucleophiles. However, the MS/MS spectrum of M5b differs by the presence of *m/z* 625, 479 and 301 ions. These fragment ions are also observed on the MS/MS spectrum of M6c.

For M5 and M6 markers it is difficult to make structural assumptions from the MS/MS spectra obtained. However, considering that the nucleophile can only be located on C-ring, structure hypotheses can be made and are presented in **scheme 1.**

3.2.2. *Oxidation markers evolution in four wines*

Epicatechin and catechin are among the four main flavanol monomers identified in grapes. A part of these monomers will be found "intact" in wines and a more or less important part of these monomers can also oxidize and react to give oxidized dimers at *m/z* 579 and 577. These oxidized dimers have similar structures to the terminal tannin oxidation markers (M1 and M2 type) obtained after chemical depolymerization. In our study, in order to take into account only the oxidation markers from tannins and not to count the epicatechin oxidation markers that have identical structures, a UHPLC-MS analysis of the samples before depolymerization was performed. This allowed subtracting the epicatechin oxidation markers from the EIC obtained after depolymerization. This operation was not necessary for the other markers selected in this study that have one or two nucleophiles (terminal/extension markers and extension markers,

464 *m/z* 683 or 681 and 787 or 785 respectively) because they were not present in the medium before
465 depolymerization and are therefore tannin specific.

466 According to the evolution (EIC areas) of each marker types in the whole tannin fraction
467 (**Figure 2.a**.), a clear decrease is observed with the wine aging for the markers at the first level
468 of oxidation (M1, M3 and M5; *m/z* 579, 683 and 787 respectively). This trend is also observed
469 for the oxidized 2018 sample (chemical oxidation with hydrogen peroxide). This decrease
470 reflects an evolution of these markers towards different structures, related to more advanced
471 oxidation states, these states may correspond to the creation of new bonds between different
472 tannic chains (intermolecular bonding) or within the same chain (intramolecular bonding) or to
473 the association with other wine compounds, thus reducing the number of *m/z* 579 available
474 terminal units.

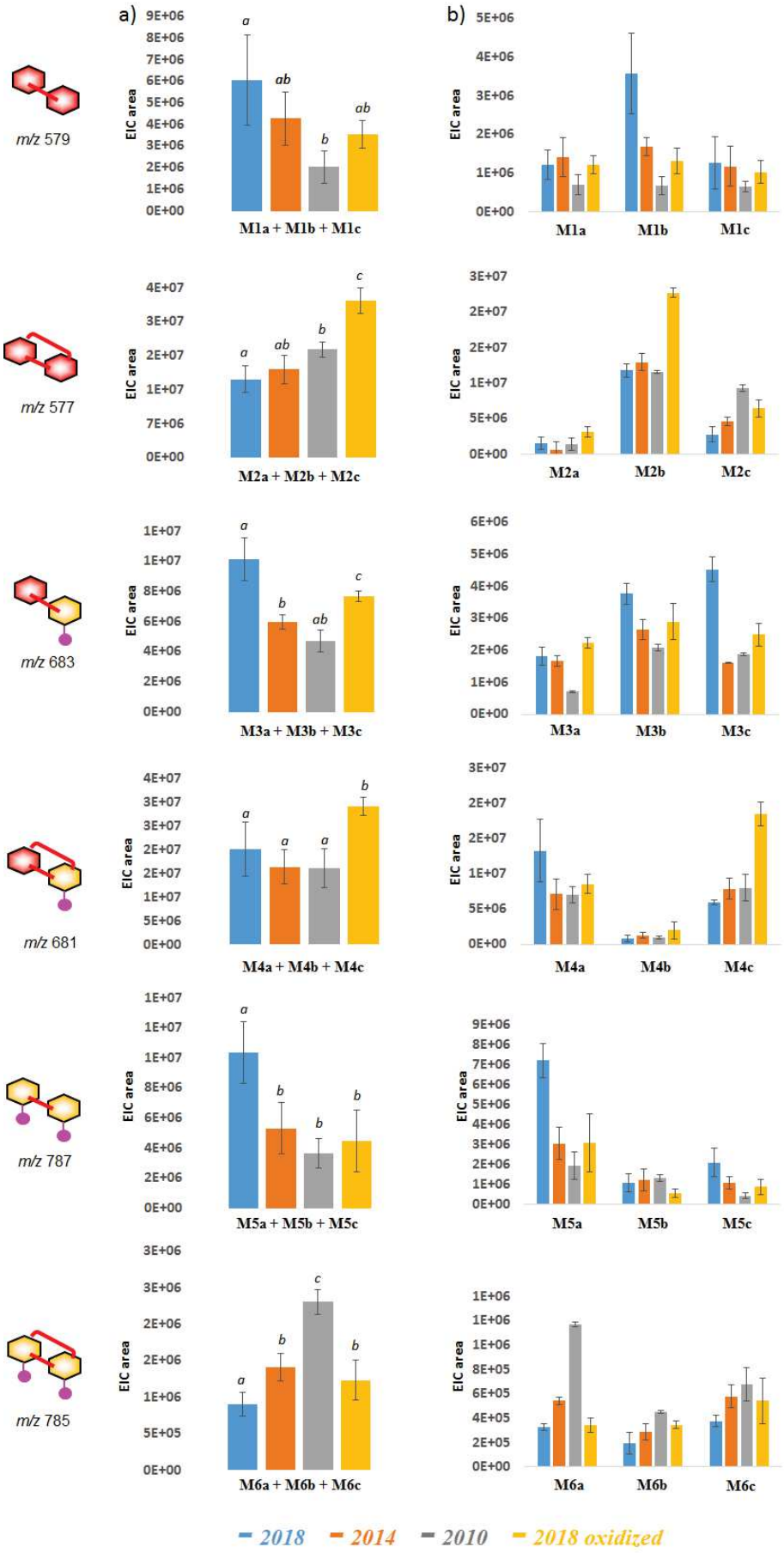
a)
b)
m/z 579
m/z 577
m/z 683
m/z 681
m/z 787
m/z 785
EIC area
M1a + M1b + M1c
M1a
M1b
M1c
M2a + M2b + M2c
M2a
M2b
M2c
M3a + M3b + M3c
M3a
M3b
M3c
M4a + M4b + M4c
M4a
M4b
M4c
M5a + M5b + M5c
M5a
M5b
M5c
M6a + M6b + M6c
M6a
M6b
M6c
2018
2014
2010
2018 oxidized

Figure 2: Comparative evolution of each oxidation markers (a) in different Syrah wines: 2018, 2014, 2010 and 2018 oxidized (b) and global evolution marker. Different letters indicate the significant differences between samples according to Tukey's test, $p<0.05$.

On the contrary, the total proportion of second oxidation state markers (M2, M4 and M6; *m/z* 575, 683 and 785 respectively) increases with wine aging, except for *m/z* 681 (M4) where the increase does not appear to be significant for wines of all three vintages. This difference is due to the M4a marker whose trend is reversed compared to the other markers of the second level of oxidation (more abundant content in the 2018 wine) (**Figure 2.b**.). An evolution of this marker towards a higher oxidation level (level 3) seems to be favored.

For the 2018 oxidized wine, however, there is a significant total increase for this M4 marker type. This is mainly due to the M4c marker whose abundance for the 2018 oxidized wine is more than twice as high as for the other wines. The 2014 and 2010 wines have a similar and slightly higher content than the 2018 wine. Unlike the M4a and M4b markers which are, at first sight, oxidation markers of intermolecular reactions, the M4c marker is derived from intramolecular reactions. Thus, accelerated oxidation seems to favor intramolecular reactions for this type of marker (M4, *m/z* 681).

Thus, through the study of these 6 types of markers, we observe a decrease of the markers of the first oxidation level which evolve towards more advanced oxidation forms (markers of the second oxidation level or even third level).

Accelerated oxidation of wine impacts the evolution of tannins in a similar or more important way than the natural aging of wines. Indeed, for markers *m/z* 579, 683, 787 (first oxidation level; M1, M3, M5) and 785/787 (second oxidation level; M6) the evolution is comparable to the 2014 vintage. Regarding the markers *m/z* 577 and 681 (second level of oxidation; terminal M2 and terminal/extension M4 respectively and extension for M4c) their concentration is higher than that obtained for the three vintages reflecting a probably slightly more advanced oxidation state.

3.2.3. Oxidation markers evolution in F1 and F2 fractions of each wine

In a second step, the sum of the global EIC areas by marker type (M1, M2, M3, M4, M5 and M6) and then by marker was represented for the two fractions F1 and F2 (**Figure 3**). Regardless of the type of marker we observe a decrease in markers over time in the F1 and F2 fractions.

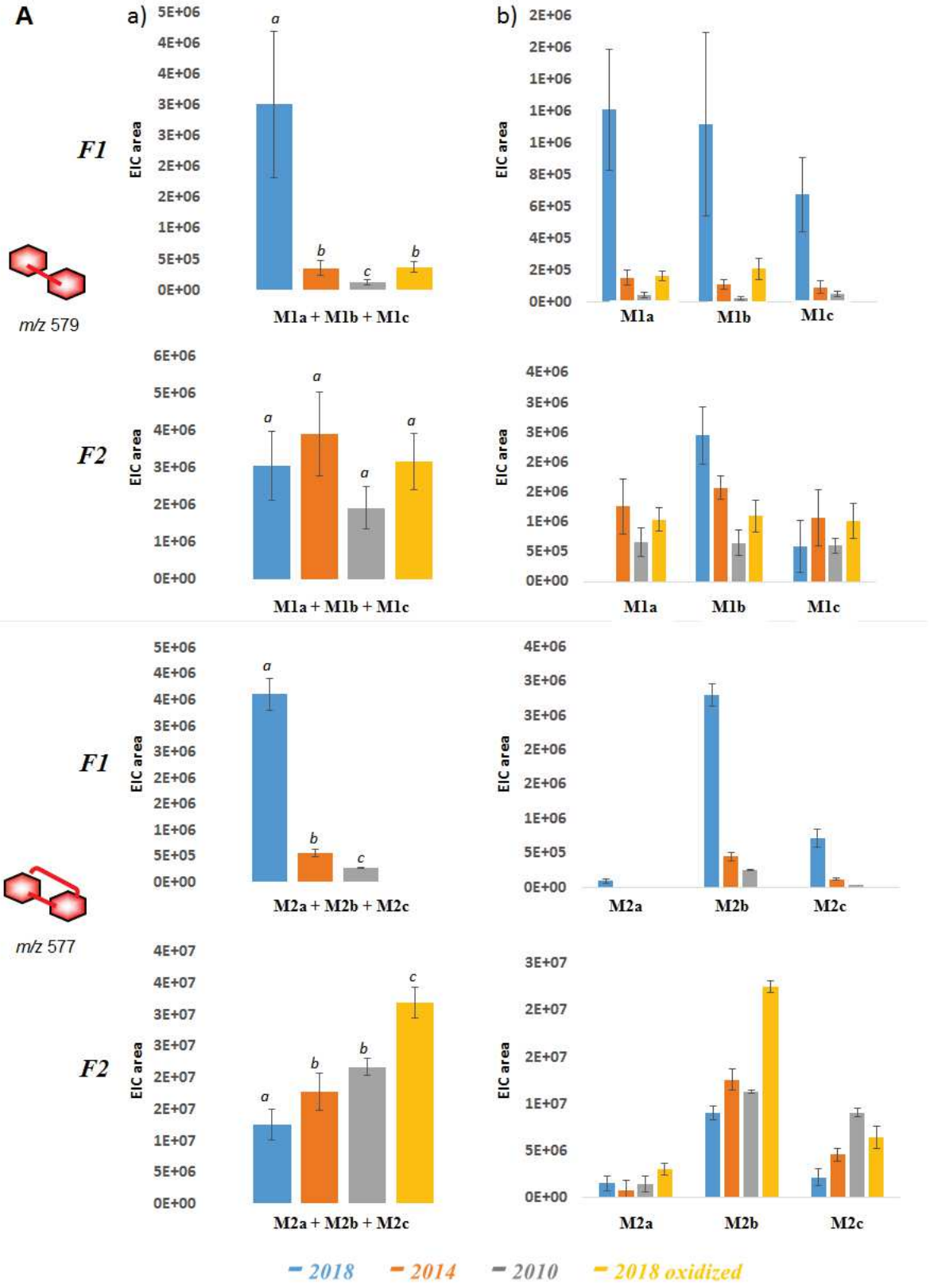
A
a)
b)
F1
F2
m/z 579
m/z 577
EIC area
M1a + M1b + M1c
M2a + M2b + M2c
M1a
M1b
M1c
M2a
M2b
M2c
2018
2014
2010
2018 oxidized

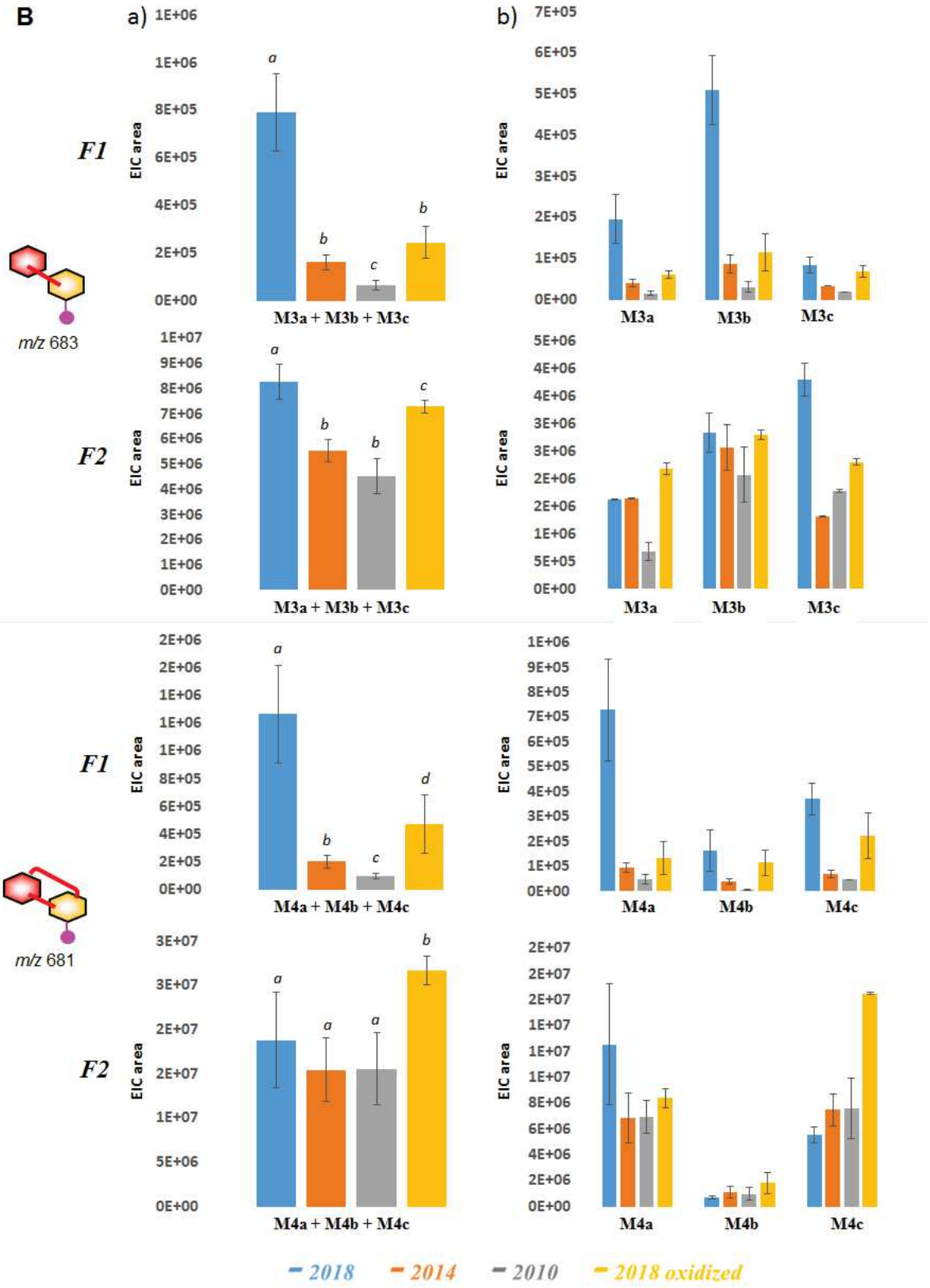
B
a)
b)
F1
F2
m/z 683
m/z 681
EIC area
M3a + M3b + M3c
M4a + M4b + M4c
M3a
M3b
M3c
M4a
M4b
M4c
2018
2014
2010
2018 oxidized

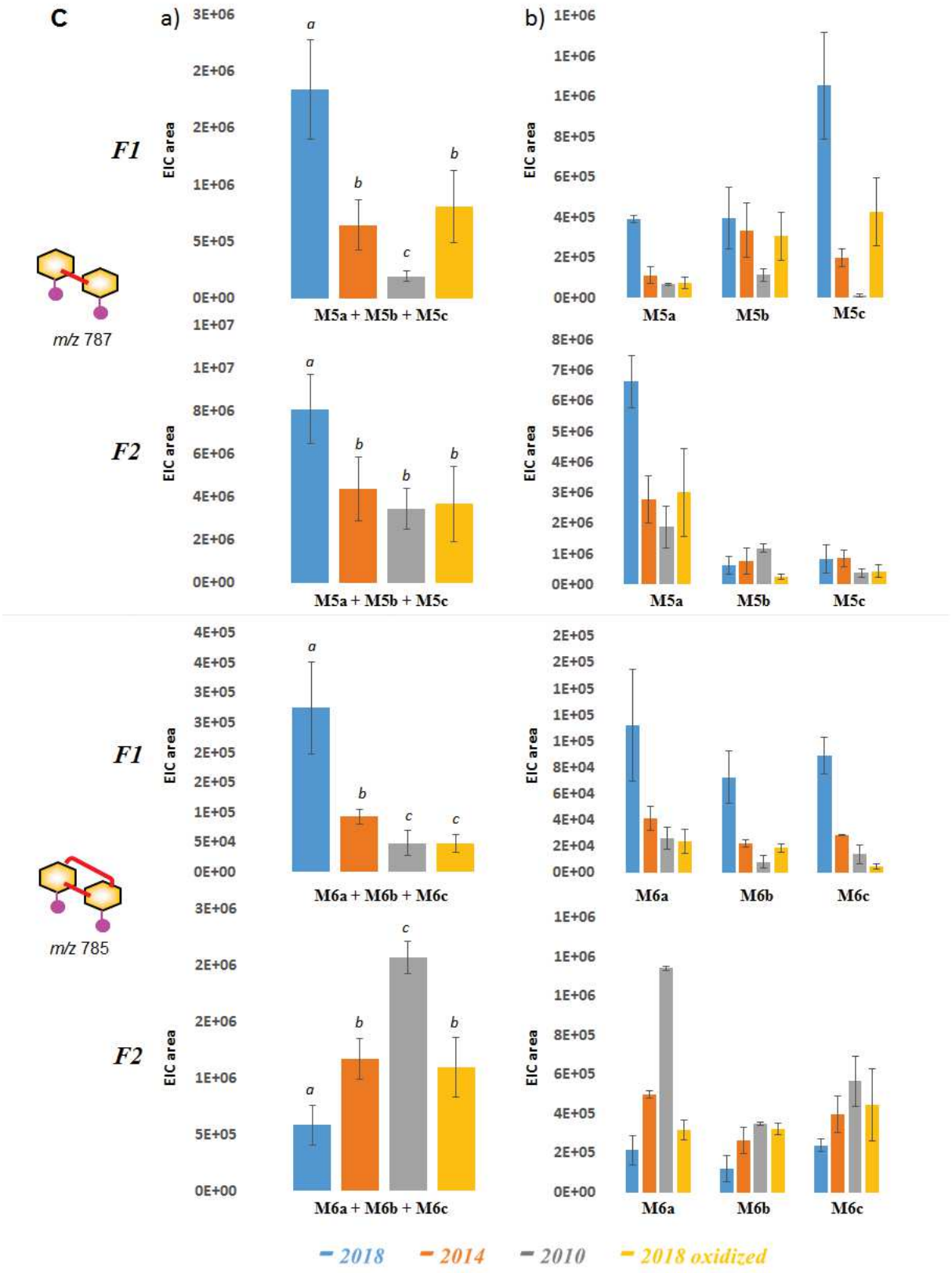

Figure 3: Comparative evolution of each oxidation markers (A) terminal units, (B) terminal/extension units and (C) extension units: (a) global evolution markers in fractions F1

and F2; (b) evolution of each marker isomer in fractions F1 and F2. Different letters indicate the significant differences between samples according to Tukey's test, $p<0.05$.

For the F1 fraction of the 2018 oxidized wine the concentration of markers:

- of the first oxidation level is comparable to that obtained for the wine of the 2014 vintage;
- of the second oxidation level evolved depending on the marker type: *m/z* 577 is absent (terminal marker), *m/z* 681 close to 2014 wine (terminal/extension marker) and *m/z* 785 similar to 2010 wine (extension marker).

For the second level oxidation markers of the F2 fraction, there is a clear increase in the terminal M2 (*m/z* 577) and extension markers M6 (*m/z* 785) over aging for the 2018, 2014 and 2010 wines while for the terminal/extension markers M4 (*m/z* 681) the concentrations are similar in the 2014 and 2010 wines and lower in the 2018 wine. The 2018 oxidized wine has similar levels to the 2014 wine for the global evolution of terminal/extension markers while it is higher for the terminal/extension markers. This difference is mainly due to the M4c marker in the F2 fraction of the 2018 oxidized wine whose content is close to two times higher than the 2018, 2014 and 2010 wines (as observed in the whole tannin fraction, see part 2.b.). For this fraction, the M4a marker follows the trend of the other marker types in the second oxidation level (**Figure 3B.b.**).

According to the monitoring of these six marker types, the oxidation level of the tannins in the F1 and F2 fractions seems to differ for the three marker types of the second oxidation level (M2, M4 and M6). They increase over time for the majority of them (except M4a) in the F2 fraction while they tend to decrease in the F1 fraction. The trend of the evolution of the F2 markers follows the global trend of the whole tannin fraction of the wines. The relative intensity of the markers obtained for F1 and F2 also were higher in F2 than in F1 (on average 10 times lower) with a total amount of tannins 1.5 to 2 times higher in F2 (1.5 times for 2018 and 2 times for 2014, 2010 and 2018 oxidized) which reflects a structural difference of the tannins between the F1 and F2 fractions. Thus, upon fractionation the tannins eluted first (F1) seem to have less evolved structures and lower degree of polymerization (**Table 1**, apparent mDP 2.1 to 2.6 for F1 and apparent mDP 5.8 to 8.7 for F2).

4. Conclusion

This study showed for the first time that it was possible to follow the oxidative evolution of wine tannins by monitoring some relevant dimeric tannin oxidation markers generated after chemical depolymerization. At four-year intervals, significant differences were observed for the wines studied. The accelerated oxidation of the 2018 wine resulted in a greater evolution of tannins than those obtained during the natural aging of the wine but the markers of the first level of oxidation were similar to those of the 2014 vintage. Thus for the studied wines, the accelerated oxidation allows predicting the natural evolution of tannins at four years by the monitoring of oxidation markers of the first level. While the monitoring of the oxidation markers of the second level gives a more realistic reflection of the global oxidation state of the tannic fraction of the wines.

In order to estimate the relative quantities from the area of the EIC, it is essential to determine the ionization coefficient of the constituent units of the tannins released after chemical depolymerization. So far, this work performed on unmodified tannin units has shown that the extension units ionize 2 to 3 times more than the terminal units under our experimental conditions. Thus, knowledge of this corrective factor is essential if the content of the various oxidation markers in a sample is to be estimated. This study should therefore be continued and extended to the oxidation markers to determine the ionization factor of each of them. For that, the chemical synthesis of these various markers will be carried out in order to obtain a sufficient quantity of each of these markers with a sufficient purity to enable us to use them as a standard product. Calibration curves can then be established after UHPLC-MS analysis of the standard range of each marker. These curves will allow us to determine the ionization coefficient specific to each marker on the one hand and to make a relative quantification of these markers from the EIC in the samples on the other hand.

Funding

This work was supported in part by a PhD grant (Stacy Deshaies) from the University of Montpellier (Bourse école doctorale GAIA).

Abbreviations

mDP: mean degree of polymerization; BFF: benzofuran forming; CAT: catechin; EC: epicatechin; ECG: epicatechin gallate; EGC: epigallocatechin gallate; EIC: extracted ion chromatogram; ESI: electrospray ionization; HRF: heterocyclic ring fission; MS/MS: tandem

mass spectrometry; Nu: nucleophilic reagent; UHPLC: ultra-high performance liquid chromatography; RDA: Retro-Diels-Alder.

References

Akoh, C. C. (2017). *Food Lipids—Chemistry, Nutrition and Biotechnology*. https://www.taylorfrancis.com/books/mono/10.1201/9781315151854/food-lipids-casimir-akoh

Alcade-Eon, C., Escribano-Bailón, M. T., Santos-Buelga, C., & Rivas-Gonzalo, J. C. (2006). Changes in the detailed pigment composition of red wine during maturity and ageing : A comprehensive study. *Analytica Chimica Acta*, *563*(1-2), 238-254.

Allgrove, J., & Davison, G. (2014). Chapter 19—Dark Chocolate/Cocoa Polyphenols and Oxidative Stress. In R. R. Watson, V. R. Preedy, & S. Zibadi (Éds.), *Polyphenols in Human Health and Disease* (p. 241-251). Academic Press. https://doi.org/10.1016/B978-0-12-398456-2.00019-0

Antoniolli, A., Fontana, A. R., Piccoli, P., & Bottini, R. (2015). Characterization of polyphenols and evaluation of antioxidant capacity in grape pomace of the cv. Malbec. *Food Chemistry*, *178*, 172-178. https://doi.org/10.1016/j.foodchem.2015.01.082

Arapitsas, P., Speri, G., Angeli, A., Perenzoni, D., & Mattivi, F. (2014). The influence of storage on the “chemical age” of red wines. *Metabolomics*, *10*, 816-832.

Atanasova, V., Fulcrand, H., Cheynier, V., & Moutounet, M. (2002a). Effect of oxygenation on polyphenol changes occurring in the course of wine-making. *Analytica Chimica Acta*, *458*(1), 15-27. https://doi.org/10.1016/S0003-2670(01)01617-8

Atanasova, V., Fulcrand, H., Cheynier, V., & Moutounet, M. (2002b). Effect of oxygenation on polyphenol changes occurring in the course of wine-making. *Analytica Chimica Acta*, *458*(1), 15-27. https://doi.org/10.1016/S0003-2670(01)01617-8

Avizcuri, J.-M., Sáenz-Navajas, M.-P., Echávarri, J.-F., Ferreira, V., & Fernández-Zurbano, P. (2016). Evaluation of the impact of initial red wine composition on changes in color and anthocyanin content during bottle storage. *Food Chemistry*, *213*, 123-134. https://doi.org/10.1016/j.foodchem.2016.06.050

Bakker, J., & Timberlake, C. F. (1997). Isolation, identification, and characterization of new color-stable anthocyanins occuring in some red wines. *Journal of Agricultural and Food Chemistry*, *45*(1), 35-43.

Barril, C., Clark, A. C., Prenzler, P. D., Karuso, P., & Scollary, G. R. (2009). Formation of Pigment Precursor (+)-1″-Methylene-6″-hydroxy-2H-furan-5″-one-catechin Isomers from (+)-Catechin and a Degradation Product of Ascorbic Acid in a Model Wine System. *Journal of Agricultural and Food Chemistry*, *57*(20), 9539-9546.

Barril, C., Clark, A. C., & Scollary, G. R. (2012). Chemistry of ascorbic acid and sulfur dioxide as an antioxidant system relevant to white wine. *Analytica Chimica Acta*, *732*, 186-193. https://doi.org/10.1016/j.aca.2011.11.011

Bartosz, G., Grzesik-Pietrasiewicz, M., & Sadowska-Bartosz, I. (2020). Fluorescent Products of Anthocyanidin and Anthocyanin Oxidation. *Journal of Agricultural and Food Chemistry*, *68*(43), 12019-12027. https://doi.org/10.1021/acs.jafc.0c04755

Benbouguerra, N., Richard, T., Saucier, C., & Garcia, F. (2020). Voltammetric Behavior, Flavanol and Anthocyanin Contents, and Antioxidant Capacity of Grape Skins and Seeds during Ripening (Vitis vinifera var. Merlot, Tannat, and Syrah). *Antioxidants*, *9*(9), 800. https://doi.org/10.3390/antiox9090800

Berké, B., Chèze, C., Vercauteren, J., & Deffieux, G. (1998). Bisulfite addition to anthocyanins : Revisited structures of colourless adducts. *Tetrahedron Letters*, *39*(32), 5771-5774. https://doi.org/10.1016/S0040-4039(98)01205-2

Berrueta, L. A., Rasines-Perea, Z., Prieto, N., Asensio-Regalado, C., Alonso-Salces, R. M., Sanchez-Ilarduya, M. B., & Gallo, B. (2020). Formation and evolution profiles of anthocyanin derivatives and tannins during fermentations and aging of red wines. *European Food Research and Technology*, *246*, 149-165.

Bradshaw, M. P., Barril, C., Clark, A. C., Prenzler, P. D., & Scollary, G. R. (2011). Ascorbic Acid : A Review of its Chemistry and Reactivity in Relation to a Wine Environment. *Critical Reviews in Food Science and Nutrition*, *51*(6), 479-498. https://doi.org/10.1080/10408391003690559

Brossaud, F., Cheynier, V., & Noble, A. C. (2008, mars 12). Bitterness and astringency of grape and wine polyphenols. *Australian Journal of Grape and Wine Research*.

Brouillard, R., & Dangles, O. (1994). Anthocyanin molecular interactions : The first step in the formation of new pigments during wine aging? *Food Chemistry*, *51*(4), 365-371. https://doi.org/10.1016/0308-8146(94)90187-2

Cacho, J., Castells, J., Esteban, A., Laguna, B., & Sagrista, N. (1995). Iron, Copper, and Manganese Influence on Wine Oxidation. *American Journal of Enology and Viticulture*, *46*(3), 380-384.

Canals, R., Llaudy, M. C., Valls, J., & Canals, J. M. (2005). Influence of Ethanol Concentration on the Extraction of Color and Phenolic Compounds from the Skin and Seeds of Tempranillo Grapes at Different Stages of Ripening | Journal of Agricultural and Food Chemistry. *Journal of Agricultural and Food Chemistry*, *53*(10), 4019-4025.

Carrascon, V., Fernandez-Zurbano, P., Bueno, M., & Ferreira, V. (2015). Oxygen Consumption by Red Wines. Part II: Differential Effects on Color and Chemical Composition Caused by Oxygen Taken in Different Sulfur Dioxide-Related Oxidation Contexts. *Journal of Agricultural and Food Chemistry*, *63*(51), 10938-10947.

Carrascón, V., Vallverdú-Queralt, A., Meudec, E., Sommerer, N., Fernandez-Zurbano, P., & Ferreira, V. (2018). The kinetics of oxygen and SO2 consumption by red wines. What do they tell about oxidation mechanisms and about changes in wine composition? *Food Chemistry*, *241*, 206-214. https://doi.org/10.1016/j.foodchem.2017.08.090

Castañeda-Ovando, A., Pacheco-Hernández, Ma. de L., Páez-Hernández, Ma. E., Rodríguez, J. A., & Galán-Vidal, C. A. (2009). Chemical studies of anthocyanins : A review. *Food Chemistry*, *113*(4), 859-871. https://doi.org/10.1016/j.foodchem.2008.09.001

Castro, C. C., Martins, R. C., Teixeira, J. A., & Silva Ferreira, A. C. (2014a). Application of a high-throughput process analytical technology metabolomics pipeline to Port wine forced ageing process. *Food Chemistry*, *143*, 384-391. https://doi.org/10.1016/j.foodchem.2013.07.138

Castro, C. C., Martins, R. C., Teixeira, J. A., & Silva Ferreira, A. C. (2014b). Application of a high-throughput process analytical technology metabolomics pipeline to Port wine forced ageing process. *Food Chemistry*, *143*, 384-391. https://doi.org/10.1016/j.foodchem.2013.07.138

Chevion, S., Roberts, M. A., & Chevion, M. (2000). The use of cyclic voltammetry for the evaluation of antioxidant capacity. *Free Radical Biology and Medicine*, *28*(6), 860-870. https://doi.org/10.1016/S0891-5849(00)00178-7

Cheynier, V., Basire, N., & Rigaud, J. (1989a). Mechanism of trans-caffeoyltartaric acid and catechin oxidation in model solutions containing grape polyphenoloxidase. *Journal of Agricultural and Food Chemistry*, *37*(4), 1069-1071. https://doi.org/10.1021/jf00088a055

Cheynier, V., Basire, N., & Rigaud, J. (1989b). Mechanism of trans-caffeoyltartaric acid and catechin oxidation in model solutions containing grape polyphenoloxidase. *Journal of Agricultural and Food Chemistry*, *37*(4), 1069-1071. https://doi.org/10.1021/jf00088a055

Cheynier, V., Dueñas, M., Salas, E., Maury, C., Souquet, J. M., Sarni-Manchado, & Fulcrand, H. (2006). Structure and Properties of Wine Pigments and Tannins. *American Journal of Enology and Viticulture*, *57*, 298-305.

Cheynier, V., Dueñas-Paton, M., Salas, E., Maury, C., Souquet, J.-M., Sarni-Manchado, P., & Fulcrand, H. (2006). Structure and Properties of Wine Pigments and Tannins. *American Journal of Enology and Viticulture*, *57*(3), 298-305.

Cheynier, V. F., Trousdale, E. K., Singleton, V. L., Salgues, M. J., & Wylde, R. (1986). Characterization of 2-S-glutathionyl caftaric acid and its hydrolysis in relation to grape wines. *Journal of Agricultural and Food Chemistry*, *34*(2), 217-221. https://doi.org/10.1021/jf00068a016

Cheynier, V., Hidalgo Arellano, Souquet, J. M., & Moutounet, M. (1997). Estimation of the Oxidative Changes in Phenolic Compounds of Carignane During Winemaking. *American Journal of Enology and Viticulture*, *48*, 225-228.

Cheynier, V., Owe, C., & Rigaud, J. (1988). Oxidation of Grape Juice Phenolic Compounds in Model Solutions. *Journal of Food Science*, *53*(6), 1729-1732.

Cheynier, V., Prieur, C., Guyot, S., Rigaud, J., & Moutounet, M. (1997). The Structures of Tannins in Grapes and Wines and Their Interactions with Proteins. In *Wine* (Vol. 661, p. 81-93). American Chemical Society. https://doi.org/10.1021/bk-1997-0661.ch008

Cheynier, V., & Ricardo da Silva, J. M. (1991). Oxidation of grape procyanidins in model solutions containing trans-caffeoyltartaric acid and polyphenol oxidase. *Journal of Agricultural and Food Chemistry*, *39*(6), 1047-1049. https://doi.org/10.1021/jf00006a008

Cheynier, V., Souquet, J. M., Kontek, A., & Moutounet, M. (1994). Anthocyanin degradation in oxidising grape musts. *Journal of the Science of Food and Agriculture*, *66*(3), 283-288.

Cheynier, V., Souquet, J. M., & Moutounet, M. (1989). Glutathione Content and Glutathione to Hydroxycinnamic Acid Ratio in Vitis vinifera Grapes and Musts. *American Journal of Enology and Viticulture*, *40*(4), 320-324.

Cheynier, Veronique., & Moutounet, Michel. (1992). Oxidative reactions of caffeic acid in model systems containing polyphenol oxidase. *Journal of Agricultural and Food Chemistry*, *40*(11), 2038-2044. https://doi.org/10.1021/jf00023a002

Chira, K., Suh, J.-H., Saucier, C., & Teissèdre, P.-L. (2008). Les polyphénols du raisin. *Phytothérapie*, *6*(2), 75-82. https://doi.org/10.1007/s10298-008-0293-3

Choe, E., & Min, D. B. (2009). Mechanisms of Antioxidants in the Oxidation of Foods. *Comprehensive Reviews in Food Science and Food Safety*, *8*(4), 345-358. https://doi.org/10.1111/j.1541-4337.2009.00085.x

Cillard, J., & Cillard, P. (2006). Mécanismes de la peroxydation lipidique et des anti-oxydations. *Oilseeds & fats Crops and Lipids*, *13*(1), 24-29.

Claus, H. (2003). Laccases and their occurrence in prokaryotes. *Archives of Microbiology*, *179*(3), 145-150. https://doi.org/10.1007/s00203-002-0510-7

Coppola, F., Picariello, L., Forino, M., Moio, L., & Gambuti, A. (2021). Comparison of Three Accelerated Oxidation Tests Applied to Red Wines with Different Chemical Composition. *Molecules*, *26*(4), 815. https://doi.org/10.3390/molecules26040815

Dallas, C., Ricardo da Silva, J. M., & Laureano, O. (1996). Products Formed in Model Wine Solutions Involving Anthocyanins, Procyanidin B2, and Acetaldehyde | Journal of Agricultural and Food Chemistry. *Journal of Agricultural and Food Chemistry*, *44*(8), 2402-2407.

Danilewicz, J. C. (2003a). *Review of Reaction Mechanisms of Oxygen and Proposed Intermediate Reduction Products in Wine : Central Role of Iron and Copper*. 13.

Danilewicz, J. C. (2003b). Review of Reaction Mechanisms of Oxygen and Proposed Intermediate Reduction Products in Wine : Central Role of Iron and Copper. *American Journal of Enology and Viticulture*, *54*(2), 73-85.

Danilewicz, J. C. (2007). Interaction of Sulfur Dioxide, Polyphenols, and Oxygen in a Wine-Model System : Central Role of Iron and Copper. *American Journal of Enology and Viticulture*, *58*(1), 53-60.

Danilewicz, J. C. (2011). Mechanism of Autoxidation of Polyphenols and Participation of Sulfite in Wine : Key Role of Iron. *American Journal of Enology and Viticulture*, *62*(3), 319-328. https://doi.org/10.5344/ajev.2011.10105

Danilewicz, J. C., Seccombe, J. T., & Whelan, J. (2008). Mechanism of Interaction of Polyphenols, Oxygen, and Sulfur Dioxide in Model Wine and Wine. *American Journal of Enology and Viticulture*, *59*(2), 128-136.

de Beer, D., Joubert, E., Marais, J., du Toit, W., Fouché, B., & Manley, M. (2016). Characterisation of Pinotage Wine During Maturation on Different Oak Products. *South African Journal of Enology and Viticulture*, *29*(1). https://doi.org/10.21548/29-1-1450

Deshaies, S., Cazals, G., Enjalbal, C., Constantin, T., Garcia, F., Mouls, L., & Saucier, C. (2020). Red Wine Oxidation : Accelerated Ageing Tests, Possible Reaction

Mechanisms and Application to Syrah Red Wines. *Antioxidants*, *9*(8), 663. https://doi.org/10.3390/antiox9080663

Drava, G., & Minganti, V. (2019). Mineral composition of organic and conventional white wines from Italy. *Heliyon*, *5*(9), e02464. https://doi.org/10.1016/j.heliyon.2019.e02464

Duval, A., & Avérous, L. (2016). Characterization and Physicochemical Properties of Condensed Tannins from Acacia catechu. *Journal of Agricultural and Food Chemistry*, *64*(8), 1751-1760.

Echave, J., Barral, M., Fraga-Corral, M., Prieto, M. A., & Simal-Gandara, J. (2021). Bottle Aging and Storage of Wines : A Review. *Molecules*, *26*(3), 713. https://doi.org/10.3390/molecules26030713

Elias, R. J., & Waterhouse, A. L. (2010). Controlling the Fenton Reaction in Wine. *Journal of Agricultural and Food Chemistry*, *58*(3), 1699-1707. https://doi.org/10.1021/jf903127r

Escribano-Bailón, M. T., Guerra, M. T., Rivas-Gonzalo, J. C., & Santos-Buelga, C. (1995). Proanthocyanidins in skins from different grape varieties. *Zeitschrift Für Lebensmittel-Untersuchung Und Forschung*, *200*(3), 221-224. https://doi.org/10.1007/BF01190499

Es-Safi, N.-E., Le Guernevé, C., Cheynier, V., & Moutounet, M. (2000). New Phenolic Compounds Formed by Evolution of (+)-Catechin and Glyoxylic Acid in Hydroalcoholic Solution and Their Implication in Color Changes of Grape-Derived Foods | Journal of Agricultural and Food Chemistry. *Journal of Agricultural and Food Chemistry*, *48*(9), 4233-4240.

Fayeulle, N., Vallverdu-Queralt, A., Meudec, E., Hue, C., Boulanger, R., Cheynier, V., & Sommerer, N. (2018). Characterization of new flavan-3-ol derivatives in fermented cocoa beans. *Food Chemistry*, *259*, 207-212. https://doi.org/10.1016/j.foodchem.2018.03.133

Ferreira, C., Sáenz-Navajas, M.-P., Carrascón, V., Næs, T., Fernández-Zurbano, P., & Ferreira, V. (2021). An assessment of voltammetry on disposable screen printed electrodes to predict wine chemical composition and oxygen consumption rates. *Food Chemistry*, *365*, 130405. https://doi.org/10.1016/j.foodchem.2021.130405

Ferreira, V., Carrascon, V., Bueno, M., Ugliano, M., & Fernandez-Zurbano, P. (2015). Oxygen Consumption by Red Wines. Part I : Consumption Rates, Relationship with Chemical Composition, and Role of SO_2. *Journal of Agricultural and Food Chemistry*, *63*(51), 10928-10937. https://doi.org/10.1021/acs.jafc.5b02988

Forino, M., Picariello, L., Lopatriello, A., Moio, L., & Gambuti, A. (2020). New insights into the chemical bases of wine color evolution and stability : The key role of acetaldehyde. *European Food Research and Technology*, *246*, 733-743.

Francia-Aricha, E., Guerra, M. T., Rivas-Gonzalo, J. C., & Santos-Buelga, C. (s. d.). New Anthocyanin Pigments Formed after Condensation with Flavanols | Journal of Agricultural and Food Chemistry. *Journal of Agricultural and Food Chemistry*, *45*(6), 2262-2266.

Freitas, V. D., & Mateus, N. (2011). Formation of pyranoanthocyanins in red wines : A new and diverse class of anthocyanin derivatives. *Analytical and Bioanalytical Chemistry*, *401*, 1463-1473.

Fulcrand, H., Dueñas, M., Salas, E., & Cheynier, V. (2006). Phenolic Reactions during Winemaking and Aging. *American Journal of Enology and Viticulture*, *57*(3), 289-297.

Gambuti, A., Han, G., Peterson, A. L., & Waterhouse, A. L. (s. d.). Sulfur Dioxide and Glutathione Alter the Outcome of Microoxygenation. *American Journal of Enology and Viticulture*, *66*(4), 411-423.

Gambuti, A., Picariello, L., Rinaldi, A., & Moio, L. (2018). Evolution of Sangiovese Wines With Varied Tannin and Anthocyanin Ratios During Oxidative Aging. *Frontiers in Chemistry*, *0*. https://doi.org/10.3389/fchem.2018.00063

Gambuti, A., Rinaldi, A., Ugliano, M., & Moio, L. (2013). Evolution of phenolic compounds and astringency during aging of red wine : Effect of oxygen exposure before and after bottling. *Journal of Agricultural and Food Chemistry*, *61*(8), 1618-1627. https://doi.org/10.1021/jf302822b

Gambuti, A., Siani, T., Picariello, L., Rinaldi, A., Lisanti, M. T., Ugliano, M., Dieval, J. B., & Moio, L. (2017a). Oxygen exposure of tannins-rich red wines during bottle aging.

Influence on phenolics and color, astringency markers and sensory attributes. *European Food Research and Technology*, *243*(4), 669-680. https://doi.org/10.1007/s00217-016-2780-3

Gambuti, A., Siani, T., Picariello, L., Rinaldi, A., Lisanti, M. T., Ugliano, M., Dieval, J. B., & Moio, L. (2017b). Oxygen exposure of tannins-rich red wines during bottle aging. Influence on phenolics and color, astringency markers and sensory attributes. *European Food Research and Technology*, *243*(4), 669-680. https://doi.org/10.1007/s00217-016-2780-3

Gaulejac, N. V. de, Vivas, N., Nonier, M.-F., Absalon, C., & Bourgeois, G. (2001). Study and quantification of monomeric flavan-3-ol and dimeric procyanidin quinonic forms by HPLC/ESI-MS. Application to red wine oxidation. *Journal of the Science of Food and Agriculture*, *81*(12), 1172-1179. https://doi.org/10.1002/jsfa.926

Geană, E.-I., Ciucure, C. T., Artem, V., & Apetrei, C. (2020). Wine varietal discrimination and classification using a voltammetric sensor array based on modified screen-printed electrodes in conjunction with chemometric analysis. *Microchemical Journal*, *159*, 105451. https://doi.org/10.1016/j.microc.2020.105451

Giribaldi, J., Besson, M., Suc, L., Fulcrand, H., & Mouls, L. (2020). The use of extracted-ion chromatograms to quantify the composition of condensed tannin subunits. *Rapid Communications in Mass Spectrometry*, *34*(7), e8619. https://doi.org/10.1002/rcm.8619

Gonzalez, A., Vidal, S., & Ugliano, M. (2018). Untargeted voltammetric approaches for characterization of oxidation patterns in white wines. *Food Chemistry*, *269*, 1-8. https://doi.org/10.1016/j.foodchem.2018.06.104

Goto, T., & Kondo, T. (1991). Structure and Molecular Stacking of Anthocyanins. *Angewandte Chemie International Edition*, 17-33.

Guyot, S., Vercauteren, J., & Cheynier, V. (1996). Structural determination of colourless and yellow dimers resulting from (+)-catechin coupling catalysed by grape

polyphenoloxidase. *Phytochemistry*, *42*(5), 1279-1288. https://doi.org/10.1016/0031-9422(96)00127-6

Hagerman, A. E., & Butler, L. G. (1978). Protein precipitation method for the quantitative determination of tannins. *Journal of Agricultural and Food Chemistry*, *26*(4), 809-812. https://doi.org/10.1021/jf60218a027

Hayasaka, Y., & Asenstorfer, R. E. (2002). Screening for Potential Pigments Derived from Anthocyanins in Red Wine Using Nanoelectrospray Tandem Mass Spectrometry. *Journal of Agricultural and Food Chemistry*, *50*(4), 756-761. https://doi.org/10.1021/jf010943v

He, F., Liang, N.-N., Mu, L., Pan, Q.-H., Wang, J., Reeves, M. J., & Duan, C.-Q. (2012). Anthocyanins and Their Variation in Red Wines I. Monomeric Anthocyanins and Their Color Expression. *Molecules*, *17*(2), 1571-1601. https://doi.org/10.3390/molecules17021571

He, F., Pan, Q.-H., Shi, Y., & Duan, C.-Q. (2008). Chemical Synthesis of Proanthocyanidins in Vitro and Their Reactions in Aging Wines. *Molecules*, *13*(12), 3007-3032. https://doi.org/10.3390/molecules13123007

Hopfer, H., Ebeler, S. B., & Heymann, H. (10754). The Combined Effects of Storage Temperature and Packaging Type on the Sensory and Chemical Properties of Chardonnay. *Journal of Agricultural and Food Chemistry*, *60*(43), 10743.

Hoyos-Arbeláez, J., Vázquez, M., & Contreras-Calderón, J. (2017). Electrochemical methods as a tool for determining the antioxidant capacity of food and beverages : A review. *Food Chemistry*, *221*, 1371-1381. https://doi.org/10.1016/j.foodchem.2016.11.017

Hui, Y. H., Nip, W.-K., Nollet, L. M. L., Paliyath, G., & Simpson, B. K. (2008). *Food Biochemistry and Food Processing*. John Wiley & Sons.

Jackson, R. S. (2008, avril 30). Wine Science : Principles and Applications. *Wine Science, Third Edition*.

Jackson : Wine science : Principles and applications—Google Scholar. (s. d.).

Jiang, H., Shii, T., Matsuo, Y., Tanaka, T., Jiang, Z.-H., & Kouno, I. (2011). A new catechin oxidation product and polymeric polyphenols of post-fermented tea. *Food Chemistry*, *129*(3), 830-836. https://doi.org/10.1016/j.foodchem.2011.05.031

Jiménez-Atiénzar, M., Cabanes, J., Gandía-Herrero, F., & García-Carmona, F. (2004). Kinetic analysis of catechin oxidation by polyphenol oxidase at neutral pH. *Biochemical and Biophysical Research Communications*, *319*(3), 902-910. https://doi.org/10.1016/j.bbrc.2004.05.077

Jurd, L. (1969). Review of Polyphenol Condensation Reactions and their Possible Occurrence in the Aging of Wines | American Journal of Enology and Viticulture. *American Journal of Enology and Viticulture*, 191-195.

Kamiya, H., Yanase, E., & Nakatsuka, S. (2014). Novel oxidation products of cyanidin 3-O-glucoside with 2,2′-azobis-(2,4-dimethyl)valeronitrile and evaluation of anthocyanin content and its oxidation in black rice. *Food Chemistry*, *155*, 221-226. https://doi.org/10.1016/j.foodchem.2014.01.077

Karbowiak, T., Gougeon, R. D., Alinc, J.-B., Brachais, L., Debeaufort, F., Voilley, A., & Chassagne, D. (2009). Wine Oxidation and the Role of Cork. *Food science and Nutrition*, *50*(1), 20-52.

Kennedy, J. A., Ferrier, J., Harbertson, J. F., & Gachons, C. P. des. (2006). Analysis of Tannins in Red Wine Using Multiple Methods : Correlation with Perceived Astringency. *American Journal of Enology and Viticulture*, *57*(4), 481-485.

Kennedy, J. A., & Jones, G. P. (2001). Analysis of Proanthocyanidin Cleavage Products Following Acid-Catalysis in the Presence of Excess Phloroglucinol. *Journal of Agricultural and Food Chemistry*, *49*(4), 1740-1746.

Khan, N., & Mukhtar, H. (2007). Tea polyphenols for health promotion. *Life Sciences*, *81*(7), 519-533. https://doi.org/10.1016/j.lfs.2007.06.011

Kilmartin, P. A. (2016). Electrochemistry applied to the analysis of wine : A mini-review. *Electrochemistry Communications*, *67*, 39-42. https://doi.org/10.1016/j.elecom.2016.03.011

Kilmartin, P. A., Zou, H., & Waterhouse, A. L. (2001). A Cyclic Voltammetry Method Suitable for Characterizing Antioxidant Properties of Wine and Wine Phenolics. *Journal of Agricultural and Food Chemistry*, *49*(4), 1957-1965.

Kilmartin, P. A., Zou, H., & Waterhouse, A. L. (2002). Correlation of Wine Phenolic Composition versus Cyclic Voltammetry Response. *American Journal of Enology and Viticulture*, *53*(4), 294-302.

Lambropoulos, I., & Roussis, I. G. (2007). Inhibition of the decrease of volatile esters and terpenes during storage of a white wine and a model wine medium by caffeic acid and gallic acid. *Food Research International*, *40*(1), 176-181. https://doi.org/10.1016/j.foodres.2006.09.003

Lavigne, V., Pons, A., & Dubourdieu, D. (2007). Assay of glutathione in must and wines using capillary electrophoresis and laser-induced fluorescence detection : Changes in concentration in dry white wines during alcoholic fermentation and aging. *Journal of Chromatography A*, *1139*(1), 130-135. https://doi.org/10.1016/j.chroma.2006.10.083

Leontieş, A.-R., Răducan, A., Gîfu, I. C., & Anghel, D. F. (2017). Catechin oxidation products : Mechanistic aspects and kinetics. *Studia Universitatis Babeș-Bolyai Chemia*, *62*(4), 11-19. https://doi.org/10.24193/subbchem.2017.4.01

Leopoldini, M., Russo, N., & Toscano, M. (2011). The molecular basis of working mechanism of natural polyphenolic antioxidants. *Food Chemistry*, *125*(2), 288-306. https://doi.org/10.1016/j.foodchem.2010.08.012

Li, H., Guo, A., & Wang, H. (2008). Mechanisms of oxidative browning of wine. *Food Chemistry*, *108*(1), 1-13. https://doi.org/10.1016/j.foodchem.2007.10.065

Lopes, P., Richard, T., Saucier, C., Teissedre, P.-L., Monti, J.-P., & Glories, Y. (2007). Anthocyanone A : A Quinone Methide Derivative Resulting from Malvidin 3-O-Glucoside Degradation. *Journal of Agricultural and Food Chemistry*, *55*(7), 2698-2704. https://doi.org/10.1021/jf062875o

Lorrain, B., Ky, I., Pechamat, L., & Teissedre, P.-L. (2013). Molecules | Free Full-Text | Evolution of Analysis of Polyhenols from Grapes, Wines, and Extracts. *Molecules*, *18*(1), 1076-1100.

Ma, W., Guo, A., Zhang, Y., Wang, H., Liu, Y., & Li, H. (2014). A review on astringency and bitterness perception of tannins in wine. *Trends in Food Science & Technology*, *40*(1), 6-19. https://doi.org/10.1016/j.tifs.2014.08.001

Macías, V. M. P., Pina, I. C., & Rodríguez, L. P. (2001). *Factors Influencing the Oxidation Phenomena of Sherry Wine*. 5.

Makhotkina, O., & Kilmartin, P. A. (2009). Uncovering the influence of antioxidants on polyphenol oxidation in wines using an electrochemical method : Cyclic voltammetry. *Journal of Electroanalytical Chemistry*, *633*(1), 165-174. https://doi.org/10.1016/j.jelechem.2009.05.007

Makhotkina, O., & Kilmartin, P. A. (2010). The use of cyclic voltammetry for wine analysis : Determination of polyphenols and free sulfur dioxide. *Analytica Chimica Acta*, *668*(2), 155-165.

Makkar, H. P. S., Blümmel, M., Borowy, N. K., & Becker, K. (1993). Gravimetric determination of tannins and their correlations with chemical and protein precipitation methods. *Journal of the Science of Food and Agriculture*, *61*(2), 161-165.

Mateus, N., Silva, A. M. S., Vercauteren, J., & de Freitas, V. (2001a). Occurrence of Anthocyanin-Derived Pigments in Red Wines. *Journal of Agricultural and Food Chemistry*, *49*(10), 4836-4840. https://doi.org/10.1021/jf001505b

Mateus, N., Silva, A. M. S., Vercauteren, J., & de Freitas, V. (2001b). Occurrence of Anthocyanin-Derived Pigments in Red Wines. *Journal of Agricultural and Food Chemistry*, *49*(10), 4836-4840. https://doi.org/10.1021/jf001505b

McRae, J. M., & Kennedy, J. A. (2011). Wine and Grape Tannin Interactions with Salivary Proteins and Their Impact on Astringency : A Review of Current Research. *Molecules*, *16*(3), 2348-2364. https://doi.org/10.3390/molecules16032348

Mercurio, M., & Smith, P. A. (2008). *Tannin Quantification in Red Grapes and Wine : Comparison of Polysaccharide- and Protein-Based Tannin Precipitation Techniques and Their Ability to Model Wine Astringency | Journal of Agricultural and Food Chemistry*. *56*(14), 5528-5537.

Merrell, C., & Hansen, M. (2018). Improving Red Wine Color and Mouthfeel Over Time. *Wines Vines Analytics*, *Wines&Vines*. https://winesvinesanalytics.com/features/203972

Miller, D. M., Buettner, G. R., & Aust, S. D. (1990). Transition metals as catalysts of "autoxidation" reactions. *Free Radical Biology and Medicine*, *8*(1), 95-108. https://doi.org/10.1016/0891-5849(90)90148-C

Millet, M., Poupard, P., Guilois-Dubois, S., Zanchi, D., & Guyot, S. (2019). Self-aggregation of oxidized procyanidins contributes to the formation of heat-reversible haze in apple-based liqueur wine. *Food Chemistry*, *276*, 797-805. https://doi.org/10.1016/j.foodchem.2018.09.171

Monagas, M., & Bartolomé, B. (2009). Anthocyanins and Anthocyanin-Derived Compounds. In M. V. Moreno-Arribas & M. C. Polo (Éds.), *Wine Chemistry and Biochemistry* (p. 439-462). Springer New York. https://doi.org/10.1007/978-0-387-74118-5_21

Monagas, M., Bartolomé, B., & Gomez-Cordoves, C. (2005). Evolution of polyphenols in red wines from Vitis vinifera L. during aging in the bottle. *European Food Research and Technology*, *220*, 331-340.

Monagas, M., Bartolomé, B., & Gómez-Cordovés, C. (2005). Evolution of polyphenols in red wines from Vitis vinifera L. during aging in the bottle. *European Food Research and Technology*, *220*(3), 331-340. https://doi.org/10.1007/s00217-004-1109-9

Motta, S., Guaita, M., Cassino, C., & Bosso, A. (2020). Relationship between polyphenolic content, antioxidant properties and oxygen consumption rate of different tannins in a model wine solution ScienceDirect. *Food Chemistry*, *313*. https://www.sciencedirect.com/science/article/pii/S0308814619321910?casa_token=

F5Za7fqUobkAAAAA:hwgLXeXveMPoNL9XDEjcAvkCPWJ0kBx_10jXTzvEW-2LNhfSXibf9VJfJpPLV8S88MxeXgIthwrWcA

Mouls, L., & Fulcrand, H. (2012). UPLC-ESI-MS study of the oxidation markers released from tannin depolymerization : Toward a better characterization of the tannin evolution over food and beverage processing. *Journal of Mass Spectrometry*, *47*(11), 1450-1457. https://doi.org/10.1002/jms.3098

Mouls, L., & Fulcrand, H. (2015a). Identification of new oxidation markers of grape-condensed tannins by UPLC–MS analysis after chemical depolymerization. *Tetrahedron*, *71*(20), 3012-3019. https://doi.org/10.1016/j.tet.2015.01.038

Mouls, L., & Fulcrand, H. (2015b). Identification of new oxidation markers of grape-condensed tannins by UPLC–MS analysis after chemical depolymerization. *Tetrahedron*, *71*(20), 3012-3019. https://doi.org/10.1016/j.tet.2015.01.038

Mouls, L., Mazauric, J.-P., Sommerer, N., Fulcrand, H., & Mazerolles, G. (2011a). Comprehensive study of condensed tannins by ESI mass spectrometry : Average degree of polymerisation and polymer distribution determination from mass spectra. *Analytical and Bioanalytical Chemistry*, *400*(2), 613-623. https://doi.org/10.1007/s00216-011-4751-7

Mouls, L., Mazauric, J.-P., Sommerer, N., Fulcrand, H., & Mazerolles, G. (2011b). Comprehensive study of condensed tannins by ESI mass spectrometry : Average degree of polymerisation and polymer distribution determination from mass spectra. *Analytical and Bioanalytical Chemistry*, *400*(2), 613-623. https://doi.org/10.1007/s00216-011-4751-7

Nave, F., Teixeira, N., Mateus, N., & de Freitas, V. (2010). The fate of flavanol–anthocyanin adducts in wines : Study of their putative reaction patterns in the presence of acetaldehyde. *Food Chemistry*, *121*(4), 1129-1138. https://doi.org/10.1016/j.foodchem.2010.01.060

Noble, A. C. (1994). Bitterness in wine. *Physiology & Behavior*, *56*(6), 1251-1255. https://doi.org/10.1016/0031-9384(94)90373-5

Oliveira, C. M., Barros, A. S., Ferreira, A. C. S., & Silva, A. M. S. (2016). Study of quinones reactions with wine nucleophiles by cyclic voltammetry. *Food Chemistry*, *211*, 1-7. https://doi.org/10.1016/j.foodchem.2016.05.020

Oliveira, C. M., Barros, A. S., Silva Ferreira, A. C., & Silva, A. M. S. (2015). Influence of the temperature and oxygen exposure in red Port wine : A kinetic approach. *Food Research International*, *75*, 337-347. https://doi.org/10.1016/j.foodres.2015.06.024

Oliveira, C. M., Ferreira, A. C. S., De Freitas, V., & Silva, A. M. S. (2011). Oxidation mechanisms occurring in wines. *Food Research International*, *44*(5), 1115-1126. https://doi.org/10.1016/j.foodres.2011.03.050

Oszmianski, J., Cheynier, V., & Moutounet, M. (1996). Iron-Catalyzed Oxidation of (+)-Catechin in Model Systems. *Journal of Agricultural and Food Chemistry*, *44*(7), 1712-1715. https://doi.org/10.1021/jf9507710

Oszmianski, J., Sapis, J.-C., & Macheix, J.-J. (1985). Changes in Grape Seed Phenols as Affected By Enzymic and Chemical Oxidation in vitro. *Journal of Food Science*, *50*(5), 1505-1506. https://doi.org/10.1111/j.1365-2621.1985.tb10515.x

Özkan, M. (2002). Degradation of anthocyanins in sour cherry and pomegranate juices by hydrogen peroxide in the presence of added ascorbic acid. *Food Chemistry*, *78*(4), 499-504. https://doi.org/10.1016/S0308-8146(02)00165-6

Peterson, A. L., & Waterhouse, A. L. (2016). 1H NMR: A Novel Approach To Determining the Thermodynamic Properties of Acetaldehyde Condensation Reactions with Glycerol, (+)-Catechin, and Glutathione in Model Wine. *Journal of Agricultural and Food Chemistry*, *64*(36), 6869-6878.

Petrozziello, M., Torchio, F., Piano, F., Giacosa, S., Ugliano, M., Bosso, A., & Rolle, L. (2018). Impact of Increasing Levels of Oxygen Consumption on the Evolution of Color, Phenolic, and Volatile Compounds of Nebbiolo Wines. *Frontiers in Chemistry*, *6*. https://doi.org/10.3389/fchem.2018.00137

Picariello, L., Gambuti, A., Picariello, B., & Moio, L. (2017). Evolution of pigments, tannins and acetaldehyde during forced oxidation of red wine : Effect of tannins addition. *LWT*, *77*, 370-375. https://doi.org/10.1016/j.lwt.2016.11.064

Ployon, S., Attina, A., Vialaret, J., Walker, A. S., Hirtz, C., & Saucier, C. (2020). Laccases 2 & 3 as biomarkers of Botrytis cinerea infection in sweet white wines. *Food Chemistry*, *315*, 126233. https://doi.org/10.1016/j.foodchem.2020.126233

P. McManus, J., G. Davis, K., E. Beart, J., H. Gaffney, S., H. Lilley, T., & Haslam, E. (1985). Polyphenol interactions. Part 1. Introduction; some observations on the reversible complexation of polyphenols with proteins and polysaccharides. *Journal of the Chemical Society, Perkin Transactions 2*, *0*(9), 1429-1438. https://doi.org/10.1039/P29850001429

Poncet-Legrand, C., Cabane, B., Bautista-Ortín, A.-B., Carrillo, S., Fulcrand, H., Pérez, J., & Vernhet, A. (2010). Tannin Oxidation : Intra- versus Intermolecular Reactions. *Biomacromolecules*, *11*(9), 2376-2386. https://doi.org/10.1021/bm100515e

Pourova, J., Kottova, M., Voprsalova, M., & Pour, M. (2010). Reactive oxygen and nitrogen species in normal physiological processes. *Acta Physiologica*, *198*(1), 15-35.

Prieur, C., Rigaud, J., Cheynier, V., & Moutounet, M. (1994). Oligomeric and polymeric procyanidins from grape seeds. *Phytochemistry*, *36*(3), 781-784. https://doi.org/10.1016/S0031-9422(00)89817-9

Quideau, S., Jourdes, M., Lefeuvre, D., Montaudon, D., Saucier, C., Glories, Y., Pardon, P., & Pourquier, P. (2005). The Chemistry of Wine Polyphenolic C-Glycosidic Ellagitannins Targeting Human Topoisomerase II. *Chemistry – A European Journal*, *11*(22), 6503-6513. https://doi.org/10.1002/chem.200500428

Rentzsch, M., Schwarz, M., & Winterhalter, P. (2007). Pyranoanthocyanins–an overview on structures, occurrence, and pathways of formation. *Trends in Food Science & Technology*, *18*(10), 526-534.

Ribéreau-Gayon, P., Glories, Y., Maujean, A., & Dubourdieu, D. (2006). *Handbook of Enology, Volume 2 : The Chemistry of Wine - Stabilization and Treatments*. John Wiley & Sons.

Ricci, A., Teslic, N., Petropolus, V.-I., Parpinello, G. P., & Versari, A. (2019). Fast Analysis of Total Polyphenol Content and Antioxidant Activity in Wines and Oenological Tannins Using a Flow Injection System with Tandem Diode Array and Electrochemical Detections. *Food Analytical Methods*, *12*(2), 347-354. https://doi.org/10.1007/s12161-018-1366-z

Rigaud, J., Cheynier, V., Souquet, J.-M., & Moutounet, M. (1991). Influence of must composition on phenolic oxidation kinetics. *Journal of the Science of Food and Agriculture*, *57*(1), 55-63. https://doi.org/10.1002/jsfa.2740570107

Rigaud, J., Perez-Ilzarbe, J., Da Silva, J. M. R., & Cheynier, V. (1991a). Micro method for the identification of proanthocyanidin using thiolysis monitored by high-performance liquid chromatography. *Journal of Chromatography A*, *540*, 401-405. https://doi.org/10.1016/S0021-9673(01)88830-0

Rigaud, J., Perez-Ilzarbe, J., Da Silva, J. M. R., & Cheynier, V. (1991b). Micro method for the identification of proanthocyanidin using thiolysis monitored by high-performance liquid chromatography. *Journal of Chromatography A*, *540*, 401-405. https://doi.org/10.1016/S0021-9673(01)88830-0

Rimbach, G., Melchin, M., Moehring, J., & Wagner, A. E. (2009). Polyphenols from Cocoa and Vascular Health—A Critical Review. *International Journal of Molecular Sciences*, *10*(10), 4290-4309. https://doi.org/10.3390/ijms10104290

Robards, K., Prenzler, P. D., Tucker, G., Swatsitang, P., & Glover, W. (1999). Phenolic compounds and their role in oxidative processes in fruits. *Food Chemistry*, *66*(4), 401-436. https://doi.org/10.1016/S0308-8146(99)00093-X

Robichaud, J. L., & Noble, A. C. (1990). Astringency and bitterness of selected phenolics in wine. *Journal of the Science of Food and Agriculture*, *53*(3), 343-353. https://doi.org/10.1002/jsfa.2740530307

Roles of o-quinones and their polymers in the enzymic browning of apples. (1990). *Phytochemistry*, *29*(2), 435-440.

Roussis, I. G., Lambropoulos, I., & Tzimas, P. (2007). Protection of Volatiles in a Wine with Low Sulfur Dioxide by Caffeic Acid or Glutathione. *American Journal of Enology and Viticulture*, *58*(2), 274-278.

Roussis, I. G., & Sergianitis, S. (2008). Protection of some aroma volatiles in a model wine medium by sulphur dioxide and mixtures of glutathione with caffeic acid or gallic acid—Roussis. *Flavour and Fragrance Journal*, *23*(1), 35-39.

Sadilova, E., Carle, R., & Stintzing, F. C. (2007). Thermal degradation of anthocyanins and its impact on color and in vitro antioxidant capacity. *Molecular Nurition Food Research*, *51*(12), 1461-1471.

Salas, E., Atanasova, V., Poncet-Legrand, C., Meudec, E., Mazauric, J. P., & Cheynier, V. (2004). Demonstration of the occurrence of flavanol–anthocyanin adducts in wine and in model solutions. *Analytica Chimica Acta*, *513*(1), 325-332. https://doi.org/10.1016/j.aca.2003.11.084

Sanoner, P., Guyot, S., Bernillon, S., Fulcrand, H., Drilleau, J.-F., & Renard, C. (2002, septembre 9). *Procyanidin B2 oxidation products, multi linked dimers ?* 21. International Conference on Polyphenols. https://hal.inrae.fr/hal-02763559

Sarneckis, C. J., Dambergs, R. G., Jones, P., Mercurio, M., Herderich, M. J., & Smith, P. A. (2006). Quantification of condensed tannins by precipitation with methyl cellulose : Development and validation of an optimised tool for grape and wine analysis. *Australian Journal of Grape and Wine Research*, *12*(1), 39-49. https://doi.org/10.1111/j.1755-0238.2006.tb00042.x

Sarni, P., Fulcrand, H., Souillol, V., Souquet, J. M., & Cheynier, V. (1995). Mechanisms of anthocyanin degradation in grape must-like model solutions. *Journal of the Science of Food and Agriculture*, *69*(3), 385-391.

Sarni-Manchado, P., & Cheynier, V. (s. d.). *Les polyphénols en agroalimentaire*.

Sarni-Manchado, P., Cheynier, V., & Moutounet, M. (1997). Reactions of polyphenoloxidase generated caftaric acid o-quinone with malvidin 3-O-glucoside. *Phytochemistry*, *45*(7), 1365-1369. https://doi.org/10.1016/S0031-9422(97)00190-8

Satake, R., & Yanase, E. (2018). Mechanistic studies of hydrogen-peroxide-mediated anthocyanin oxidation. *Tetrahedron*, *74*(42), 6187-6191. https://doi.org/10.1016/j.tet.2018.09.012

Saucier, C. (2010). How do wine polyphenols evolve during wine ageing? *Cerevisia*, *35*(1), 11-15. https://doi.org/10.1016/j.cervis.2010.05.002

Schwarz, M., Wabnitz, T. C., & Winterhalter, P. (2003). Pathway Leading to the Formation of Anthocyanin−Vinylphenol Adducts and Related Pigments in Red Wines. *Journal of Agricultural and Food Chemistry*, 3682-3687.

Scrimgeour, N., Nordestgaard, S., Lloyd, N. D. R., & Wikes, E. N. (2015). Exploring the effect of elevated storage temperature on wine composition. *Australian Journal of Grape and Wine Research*, *21*(S1), 713-722.

Shchepinov, M. S. (2007). Reactive Oxygen Species, Isotope Effect, Essential Nutrients, and Enhanced Longevity. *Rejuvenation Research*, *10*(1), 47-60.

Sheridan, M. K., & Elias, R. J. (2015). Exogenous acetaldehyde as a tool for modulating wine color and astringency during fermentation. *Food Chemistry*, *177*, 17-22. https://doi.org/10.1016/j.foodchem.2014.12.077

Singleton, V. L. (1987a). *Oxygen with Phenols and Related Reactions in Musts, Wines, and Model Systems : Observations and Practical Implications*. *38*(1), 9.

Singleton, V. L. (1987b). *Oxygen with Phenols and Related Reactions in Musts, Wines, and Model Systems : Observations and Practical Implications*. *38*(1), 9.

Singleton, V. L. (2001). A survey of wine aging reactions, especially with oxygen. *Proceedings of the ASEV 50th Anniversary Annual Meeting, Seattle, Washington, June 19-23, 2000, 2001, ISBN 0-9630711-4-9, Págs. 323-336*, 323-336. https://dialnet.unirioja.es/servlet/articulo?codigo=590527

Singleton, V. L., Salgues, M., Zaya, J., & Trousdale, E. (1985). Caftaric Acid Disappearance and Conversion to Products of Enzymic Oxidation in Grape Must and Wine. *American Journal of Enology and Viticulture*, *36*(1), 50-56.

Soares, S., Brandão, E., Mateus, N., & De Freitas, V. (2017). Sensorial properties of red wine polyphenols : Astringency and bitterness. *Food science and Nutrition*, *57*(5), 937-948.

Somers, T. C., & Wescombe, L. G. (1987). Evolution of red wines part II. An assessment of the role of acetaldehyde. *VITIS - Journal of Grapevine Research*, *26*(1), 27-27.

Souquet, J.-M., Cheynier, V., Brossaud, F., & Moutounet, M. (1996). Polymeric proanthocyanidins from grape skins. *Phytochemistry*, *43*(2), 509-512. https://doi.org/10.1016/0031-9422(96)00301-9

Sousa, C., Mateus, N., Silva, A. M. S., González-Paramás, A. M., Santos-Buelga, C., & Freitas, V. de. (2007). Structural and chromatic characterization of a new Malvidin 3-glucoside–vanillyl–catechin pigment. *Food Chemistry*, *102*(4), 1344-1351. https://doi.org/10.1016/j.foodchem.2006.04.050

Suc, L., Rigou, P., & Mouls, L. (2021). Detection and Identification of Oxidation Markers of the Reaction of Grape Tannins with Volatile Thiols Commonly Found in Wine. *Journal of Agricultural and Food Chemistry*, *69*(10), 3199-3208.

Tanaka, T., & Kouno, I. (2003). Oxidation of Tea Catechins : Chemical Structures and Reaction Mechanism. *food science and technology research*, *9*(2), 128-133.

Teng, B., Hayasaka, Y., Smith, P. A., & Bindon, K. A. (2019). *Effect of Grape Seed and Skin Tannin Molecular Mass and Composition on the Rate of Reaction with Anthocyanin and Subsequent Formation of Polymeric Pigments in the Presence of Acetaldehyde* | *Journal of Agricultural and Food Chemistry*. *67*(32), 8938-8949.

Timberlake, C. F., & Bridle, P. (1976). Interactions Between Anthocyanins, Phenolic Compounds, and Acetaldehyde and Their Significance in Red Wines. *American Journal of Enology and Viticulture*, *27*(3), 97-105.

Tindal, R. A., Jeffery, D. W., & Muhlack, R. A. (2021). Mathematical modelling to enhance winemaking efficiency : A review of red wine colour and polyphenol extraction and evolution. *Australian Journal of Grape and Wine Research*, *27*(2), 219-233.

Toit, W. J. du, Marais, J., Pretorius, I. S., & Toit, M. du. (2006). Oxygen in Must and Wine : A review. *South African Journal of Enology and Viticulture*, *27*(1), 76-94. https://doi.org/10.21548/27-1-1610

Ugliano, M. (2013). Oxygen Contribution to Wine Aroma Evolution during Bottle Aging. *Journal of Agricultural and Food Chemistry*, *61*(26), 6125-6136. https://doi.org/10.1021/jf400810v

Ugliano, M. (2016). Rapid fingerprinting of white wine oxidizable fraction and classification of white wines using disposable screen printed sensors and derivative voltammetry. *Food Chemistry*, *212*, 837-843. https://doi.org/10.1016/j.foodchem.2016.05.156

Ugliano, M., Wirth, J., Bégrand, S., Dieval, J.-B., & Vidal, S. (2015). Oxidation Signature of Grape Must and Wine by Linear Sweep Voltammetry Using Disposable Carbon Electrodes. In S. B. Ebeler, G. Sacks, S. Vidal, & P. Winterhalter (Éds.), *Advances in Wine Research* (Vol. 1203, p. 325-334). American Chemical Society. https://doi.org/10.1021/bk-2015-1203.ch020

Vernhet, A., carillo, S., & Poncet-Legrand, C. (2014). Condensed Tannin Changes Induced by Autoxidation : Effect of the Initial Degree of Polymerization and Concentration. *Journal of Agricultural and Food Chemistry*, *62*(31), 7833-7842.

Vivar-Quintana, A. M., Santos-Buelga, C., Francia-Aricha, E., & Rivas-Gonzalo, J. C. (1999). Formation of anthocyanin-derived pigments in experimental red wines / Formación de pigmentos derivados de antocianos en vinos tintos experimentales. *Food Science and Technology International*, *5*(4), 347-352. https://doi.org/10.1177/108201329900500407

Vivas, N. (1997). Composition et propriétés des préparations commerciales de tanins à usage oenologique. *Revue des oenologues et des techniques vitivinicoles et oenologiques: magazine trimestriel d'information professionnelle*, *24*(84), 15-21.

Vivas, N. (2000). Propriétés et intérêts des tanins œnologiques extraits du raisin. *Revue française d'oenologie*, *183*, 15-18.

Vivas, N., & Glories, Y. (1996). Role of Oak Wood Ellagitannins in the Oxidation Process of Red Wines During Aging. *American Journal of Enology and Viticulture*, *47*(1), 103-107.

von Baer, D., Rentzsch, M., Hitschfeld, M. A., Mardones, C., Vergara, C., & Winterhalter, P. (2008). Relevance of chromatographic efficiency in varietal authenticity verification of red wines based on their anthocyanin profiles : Interference of pyranoanthocyanins formed during wine ageing. *Analytica Chimica Acta*, *621*(1), 52-56.

Waterhouse, A. L., & Laurie, V. F. (2006a). Oxidation of Wine Phenolics : A Critical Evaluation and Hypotheses. *American Journal of Enology and Viticulture*, *57*(3), 306-313.

Waterhouse, A. L., & Laurie, V. F. (2006b). Oxidation of Wine Phenolics : A Critical Evaluation and Hypotheses. *American Journal of Enology and Viticulture*, *57*(3), 306-313.

Whitaker, J. R., & Lee, C. Y. (1995). Recent Advances in Chemistry of Enzymatic Browning. In *Enzymatic Browning and Its Prevention* (Vol. 600, p. 2-7). American Chemical Society. https://doi.org/10.1021/bk-1995-0600.ch001

Wrolstad, R. E., Durst, R. W., & Lee, J. (2005). Tracking color and pigment changes in anthocyanin products. *Trends in Food Science & Technology*, *16*(9), 423-428. https://doi.org/10.1016/j.tifs.2005.03.019

Zanchi, D., Poulain, C., Konarev, P., Tribet, C., & Svergun, D. (2008). Colloidal stability of tannins : Astringency, wine tasting and beyond. *journal of physics: condensed matter*.

Zhang, Z., Li, J., Fan, L., & Duan, Z. (2020). Effect of organic acid on cyanidin-3-O-glucoside oxidation mediated by iron in model Chinese bayberry wine. *Food Chemistry*, *310*, 125980. https://doi.org/10.1016/j.foodchem.2019.125980

Conclusion générale et perspectives

Au terme de ce manuscrit, une conclusion générale sur les résultats et observations obtenus sur « l'étude de l'oxydation des polyphénols des vins rouges » s'impose. Dans un premier temps, une étude bibliographique préliminaire a permis de mettre en lumière les enjeux des recherches sur l'oxydation des vins rouges, et en particulier l'oxydation des polyphénols. Majoritairement présents dans le vin rouge, ces derniers sont des cibles privilégiées pour les phénomènes d'oxydation et impactent grandement les propriétés organoleptiques du produit.

Trois tests d'oxydation accélérée des vins rouges ont été mis au point :

- Un test à 60°C ;
- Un test chimique au peroxyde d'hydrogène ;
- Un test enzymatique utilisant une solution de Laccases de *Trametes versicolor*.

Ces tests ont été appliqués à un vin de Syrah de 2018 et les différents résultats ont été comparés à l'évolution naturelle de ce même vin de Syrah (millésimes 2014 et 2010). Chaque test a permis de mettre en évidence, par analyse des ions moléculaires, des cibles d'oxydation spécifiques et de potentiels marqueurs d'oxydation, parmi lesquels les anthocyanes et les polyphénols contenant un groupement catéchol ou galloyl. Les spectres MS de l'évolution naturelle du vin ont également montré une diminution, avec les temps, de l'intensité des ions correspondant aux anthocyanes libres et une augmentation de ceux correspondant aux flavanols monomériques. Des résultats similaires ont été obtenus pour le test de vieillissement accéléré au peroxyde d'hydrogène. Ce dernier test semble être plus proche de l'évolution naturelle par rapport aux deux autres tests.

Le comportement oxydatif de ces mêmes vins (Syrah 2018, 2014 et 2010) a ensuite été étudié par voltammétrie cyclique. L'échantillonnage a été complété par six autres vins de Syrah et d'autres cépages, chacun des vins ayant subi les trois tests de vieillissement accélérées décrits précédemment. Les résultats obtenus ont confirmé que chacun des tests engendrent des résultats différents en fonction des cibles chimiques impliqués. Un classement en trois groupes a alors été possible entre les différents vins rouges selon leurs cépages et leurs millésimes, en considérant leur comportement électrochimique, leur composition chimique et leurs réponses aux tests de vieillissement.

L'analyse des paramètres électrochimiques des vins non oxydés corrélés aux tests de vieillissement impliquant la laccases et la température a également permis de mettre en

évidence le potentiel de la voltammétrie cyclique dans la prédiction de l'évolution des vins rouges.

Dans des travaux futurs, il pourrait être envisagé d'appliquer ces méthodes (tests accélérés et tests électrochimiques) à un plus grand nombre d'échantillons de vins rouges afin de valider ces méthodes et de confirmer les résultats obtenus jusqu'à présent. De plus, le vieillissement naturel est actuellement basé sur trois millésimes différents, un vieillissement naturel directement en bouteille au fil des années pourrait être envisagé.

Lors d'une étude ciblée sur l'oxydation de la catéchine, les produits de réaction issus de l'oxydation enzymatique par différentes oxydoréductases ont été étudiés (laccases de *Botrytis cinerea*, laccases de *Trametes versicolor* et polyphénoloxidase extraites de pépins). Les profils LC_MS des produits de réaction se sont avérés similaires même si des différences mineures peuvent suggérer de potentielles différences de réactivité entre les enzymes.

La structure de six marqueurs d'oxydation issus de l'oxydation enzymatique des laccases de *Trametes versicolor* sur la catéchine a été obtenue de manière non ambiguë pour la première fois en RMN, grâce à l'ajout de nitrate de cadmium suivi d'une étape de resolubilisation et d'évaporation des échantillons avant analyse, permettant une amélioration de la résolution des OH phénoliques. Parmi ces composés ont été retrouvés deux marqueurs dimériques possédants une liaison bi-aryl (C-C) entre deux unités catéchine, trois marqueurs (dont deux énantiomères) dimériques possédants une liaison bi-aryl ether (C-O-C) et un marqueur correspondant à un niveau d'oxydation évolué que les précédents (déhydrodicatéchine).

Ces marqueurs ont ensuite été détectés pour la première fois dans des échantillons de vins rouges (Syrah 2018, 2014, 2010) ainsi que dans des extraits de pépins de raisins de différents cépages (Merlot, Tannat, Syrah) grâce à l'utilisation de la spectrométrie de masse haute résolution. D'autres marqueurs non élucidés par RMN ont également été étudiés. Des fragmentations spécifiques à chaque type de dimère ont été observées, permettant de les différencier des dimères de type B possédant la même masse moléculaire :

- Un fragment *m/z* = 393 Th (même masse mais structures différentes) pour les marqueurs dimériques contenant une liaison bi-aryl ou bi-aryl ether. Ce fragment est absent pour les dimères de type B.
- Un fragment *m/z* = 291 Th exclusivement présent pour les marqueurs contenant une liaison bi-aryl ether.

Trois des marqueurs ont été détectés dans les extraits de pépins avec une tendance croissante de leur concentration avec l'évolution de la maturation de la baie (stade vert - veraison - maturité).

Trois marqueurs ont également été détectés dans les échantillons de vins avec, cette fois, une tendance décroissante de leur concentration avec l'évolution du vin.

Les perspectives de cette partie de nos travaux pourraient impliquer des substrats différents de la catéchine (flavonoïdes ou non-flavonoïdes) afin d'obtenir davantage de marqueurs d'oxydation. Les analyses RMN utilisant le cadmium et l'étape supplémentaire d'évaporation pourraient également être approfondies afin d'améliorer la compréhension du mode d'action du cadmium dans la résolution des signaux des OH phénoliques en RMN. La caractérisation enzymatique complète des trois enzymes utilisées pourrait également être envisagée après purification afin de valider leur mode d'action et leurs paramètres cinétiques.

La recherche des marqueurs au sein d'échantillons complexes tels que le vin ou les extraits de pépins pourrait être complétée par une étude quantitative ainsi que par une étude utilisant la spectrométrie de masse en tandem quadripôle-temps de vol à mobilité ionique (IM-QTof-MS) permettant de détecter et d'identifier des molécules d'intérêt par mesure de leur masse monoisotopique et leur mobilité ionique, notamment les marqueurs possédant les mêmes masses étudiés dans ce manuscrit. Cela permettrait de séparer les différents isomères non séparables par UHPLC dans la mobilité ionique et d'avoir le spectre MS/MS propre à chacun marqueur au lieu d'avoir un spectre MS/MS mélangé (mélange des ions fragments des deux isomères)

Finalement, l'évolution oxydative des tannins après dépolymérisation chimique a été réalisée sur les mêmes vins de Syrah (2018, 2014 et 2010) ainsi que sur la Syrah 2018 oxydée chimiquement (peroxyde d'hydrogène). Trois types de marqueurs à deux niveaux d'oxydation (soit 6 types au total) ont été détectés, identifiés et comparés :

- Marqueurs des unités terminales des tannins ;
- Marqueurs des unités terminales et d'extension des tannins ;
- Marqueurs des unités d'extension des tannins.

Chaque type de marqueurs présentant 3 isomères, 18 marqueurs au total ont été suivis. A quatre années d'intervalle, des différences significatives ont été observées pour les vins étudiés.

L'oxydation accélérée du vin 2018 a entrainé une évolution de tannins à priori plus importante que celles obtenues lors du vieillissement du vin même si les marqueurs du premier niveau d'oxydation suivis ont des teneurs comparables à celles du millésime 2014.

Afin de pouvoir estimer les quantités relatives à partir de l'aire des EIC, il est indispensable de déterminer le coefficient d'ionisation des unités constitutives des tannins libérés après dépolymérisation chimique. Des travaux antérieurs, réalisés au laboratoire, ont montré que les unités d'extension non modifiées s'ionisaient 2 à 3 fois plus que les unités terminales non modifiées dans nos conditions expérimentales. Ainsi, la connaissance de ce facteur correctif à appliquer aux marqueurs d'oxydation est incontournable si l'on veut estimer leur teneur dans un échantillon. Cette étude devra donc être poursuivie et étendue aux marqueurs d'oxydation pour déterminer le facteur d'ionisation de chacun d'entre eux. Pour cela, la synthèse chimique de ces différents marqueurs devra être réalisée afin d'obtenir une quantité suffisante de chacun de ces marqueurs qui seront utilisés comme étalon externe. Des courbes de calibration pourront alors être établies après analyse UHPLC-MS de la gamme étalon de chacun des marqueurs. Ces courbes permettront de déterminer le coefficient d'ionisation propre à chaque marqueur d'une part et de faire une quantification relative de ces marqueurs à partir de l'EIC dans les échantillons d'autre part.

Liste des figures et schémas

Chapitre I : Etude bibliographique

Chapitre II : Approche polyphénomique globale semi-ciblée

Chapitre III : Propriétés redox des vins rouges

Figure 1 - Cyclic voltammograms of different standards with SWCNT: catechin (A); caffeic acid (B); gallic acid (C); oenin chloride (D) and quercetin (E) at a concentration of 0.1mM (blank subtracted); SWCNT-SPCE: Single Walled Carbon Nanotubes modified Screen Printed Carbon Electrodes

Figure 2 - Cyclic voltammogram of *R2* wine non-oxidized (ref) and oxidized with three different protocols: temperature (60°C), chemical (H2O2) and enzymatic (laccases) with SWCNT.

Figure 3 - Representation of the loadings (variables) and the scores (wines) in the plane defined by respectively the first (F1) and second (F2) factor (explained variance: 69.87%)

Figure 4 - Representation of the loadings (variables – electrochemical parameters (except Q_{240mV} / Q_{800mV} ratio) for the reference wines with blank subtracted) and the scores (wines) in the plane defined by respectively the first (F1) and second (F2) factor (explained 97.74%)

Chapitre IV : Approche ciblée : identification et obtention de marqueurs d'oxydation

PARTIE I

Figure 1 - 1D ^{1}H spectra of the fractions N2, N3, N4, N6 and N8 at 25°C solubilized in acetone-d_6 (A), at 25°C in acetone-d_6 in the presence of cadmium (B), at 15°C in acetone-d_6 in the presence of Cd (with additional step of dryness evaporation of fractions N2, N3 and N4) (C), expansion of the phenolic (D) and the aliphatic (E) OH regions in same physicochemical conditions as (C)

Figure 2 - 1D ^{1}H spectra of fraction N6 in acetone-d_6 in the presence of Cd at 25°C and 15°C. The expansions show the effect of temperature upon the aromatic and aliphatic OH signal chemical shifts

Figure 3 - 2D ^{1}H DOSY of a sample containing both fractions N4 and N2

Figure 4 - Scheme of catechin dimers (N2, N3 and N8) showing OH protons implied either in $^{1}H/^{13}C$ long range or $^{1}H/^{1}H$ ROEs correlations allowing linkage position determination.

Figure 5 - Structures of five dimeric oxidation products formally identified by NMR analysis

PARTIE II

Figure 1 - five identified oxidation markers with different oxidation states : N2, N3, N4 and N6 ion at m/z 579 Da and N8 (dehydrodicatechin A) corresponding to a superior oxidation state at m/z 577 Da

Figure 2 - TIC MS (total ion chomatogram) of qualitative dimeric mixture containing four B-type dimeric procyanidins (B1 to B4) and eight oxidation dimeric markers (N1 to N8).

Figure 3 - Positive ion tandem mass spectra of the procyanidin B1 (a) , the oxidation dimer N2 (b) and oxidation dimer N8 (c) with Stepped Normalized Collision Energy (SNCE), 30% midpoint, 15% range and three steps

Figure 4 - EIC chromatogram of ion at m/z 577.13405 (+/-1ppm) of three 10g/L grape extracts of Merlot variety at different stage of ripening : green stage (a) ; veraison (b) ; maturity (c) and tandem mass spectra of compound at 22.03min (d) (for maturity) corresponding to N7 and at 26.7 min (e) (for 03/09/2018) corresponding to N8

Chapitre V : Recherche de marqueurs d'oxydation issus des tannins

Figure 0 - Abstract

Figure 1 – Tannins concentration evolution ($g.L^{-1}$) in 4 red wine samples: 2018, 2014, 2010 and 2018 oxidized with hydrogen peroxide: (a) total tannin fraction, (b) F1 and (c) F2.**Scheme 1**: Structure hypotheses for some oxidation markers, resulting from their MS/MS spectra.

Figure 2: Comparative evolution of each oxidation markers (a) in different Syrah wines: 2018, 2014, 2010 and 2018 oxidized (b) and global evolution marker. Different letters indicate the significant differences between samples according to Tukey's test, $p<0.05$.

Figure 3: Comparative evolution of each oxidation markers (A) terminal units, (B) terminal/extension units and (C) extension units: (a) global evolution markers in fractions F1 and F2; (b) evolution of each marker isomer in fractions F1 and F2. Different letters indicate the significant differences between samples according to Tukey's test, $p<0.05$.

Liste des tableaux

Chapitre I : Etude bibliographique

Chapitre II : Approche polyphénomique globale semi-ciblée

Chapitre III : Propriétés redox des vins rouges

Chapitre IV : Approche ciblée : identification et obtention de marqueurs d'oxydation

PARTIE I

Table 1 - (a) Analytical reversed-phase UHPLC retention times, absorbance maxima, corresponding m/z (Da) and yields (%) of the eight major oxidation collected products. (b) Qualitative comparison of analytical reversed-phase UHPLC retention times of eight major oxidation products with the three different oxidative enzymes: laccases from *Trametes versicolor*, laccases from *Botrytis cinerea* and polyphenoloxidase extracted from grapes.

PARTIE II

Table 1 - EIC (extracted ion chromatogram) evolution trend of oxidation markers in three different grape varieties (Merlot, Tannat, Syrah) at different stages of ripening: green stage, veraison and maturity.

Table 2 - identification of oxidation markers in three Syrah wines at different vintages (2018, 2014 and 2010)

Chapitre V : Recherche de marqueurs d'oxydation issus des tannins

Table 1 - Dry weight, percentage of unmodified and modified units, apparent mDP (estimated by UV and EIC) of both F1 and F2 fractions for 4 different Syrah wine samples

Table 2: Studied oxidation markers: retention time (UHPLC) and principal fragments ions observed on the MS/MS spectrum.

Annexes

Chapitre II : Approche polyphénomique globale semi-ciblée

Article 1 - *Red Wine Oxidation: Accelerated Ageing Tests, Possible Reaction Mechanisms and Application to Syrah Red Wines*

- ***Table S1 -*** *analytical characterization of 2018 Syrah wine*

	Result	***Unit***	***Quantification limit***	***Detection limit***	***Uncertainty (95%)***
Alcoholic strength	14.25	% vol.	/	/	0.150
Glucode + Fructose	≤ 1.0	g/L	1.0	0.33	N/V
Total acidity	3.41	g/L eq. H_2SO_4	2.0	/	0.180
Volatil acidity	0.52	g/L eq. H_2SO_4	/	/	0.050
Total SO_2	19	mg/L	10.0	3.3	15.0
Free SO_2	14	mg/L	5.0	1.667	6.0
pH	3.94	/	/	/	0.080
Malic acid	ND	g/L	0.2	0.1	N/V
Lactic acid	2	g/L	0.2	0.1	0.30
Total polyphenol content	65	/	5.0	/	6.0
CO_2	260	mg/L	100.0	/	130
Active SO_2	0.17	mg/L	/	/	0.000
Copper	0.3	mg/L	0.2	/	0.20
Iron	2.7	mg/L	0.5	/	0.50

- ***Table S2 -*** *analytical characterization of 2014 Syrah wine*

	Result	***Unit***	***Quantification limit***	***Detection limit***	***Uncertainty (95%)***
Alcoholic strength	14.24	% vol.	/	/	0.150
Glucode + Fructose	nd	g/L	1.0	0.33	N/V
Total acidity	3.27	g/L eq. H_2SO_4	2.0	/	0.180
Volatil acidity	0.5	g/L eq. H_2SO_4	/	/	0.050
Total SO_2	≤ 10.0	mg/L	10.0	3.3	N/A
Free SO_2	≤ 5.0	mg/L	5.0	1.667	N/A
pH	3.73	/	/	/	0.080
Malic acid	nd	g/L	0.2	0.1	N/V
Lactic acid	1.5	g/L	0.2	0.1	0.30
Total polyphenol content	58	/	5.0	/	6.0
CO_2	510	mg/L	100.0	/	130
Active SO_2	0.1	mg/L	/	/	0.000
Copper	0.3	mg/L	0.2	/	0.20
Iron	2.7	mg/L	0.5	/	0.50

- ***Table S3 -*** *analytical characterization of 2010 Syrah wine*

	Result	***Unit***	***Quantification limit***	***Detection limit***	***Uncertainty (95%)***
Alcoholic strength	14.13	% vol.	/	/	0.150
Glucode + Fructose	nd	g/L	1.0	0.33	N/V
Total acidity	3.03	g/L eq. H_2SO_4	2.0	/	0.180
Volatil acidity	0.43	g/L eq. H_2SO_4	/	/	0.050
Total SO_2	nd	mg/L	10.0	3.3	N/V
Free SO_2	≤ 5.0	mg/L	5.0	1.667	N/V
pH	3.83				0.080
Malic acid	nd	g/L	0.2	0.1	N/V
Lactic acid	1.2	g/L	0.2	0.1	0.30
Total polyphenol content	72		5.0		6.0
CO_2	440	mg/L	100.0		130
Active SO_2	0.06	mg/L			0.000
Copper	0.3	mg/L	0.2		0.20
Iron	2.7	mg/L	0.5		0.50

Chapitre III : Propriétés redox des vins rouges

***Article 2** – Red wine oxidation characterization by accelerated ageing tests and cyclic voltammetry*

- ***Table S1** – Enological analytic characterization of the red wines*

Wine sample	Alcoholic strength (%)	Total acidity (g/L eq. H_2SO_4)	Volatil acidity (g/L eq. H_2SO_4)	pH	Cu (mg/L)	Fe(mg/L)	Total SO2	Free SO2 after oxygen saturation (mg/L) *GC-MS analysis*
R1	14.41 ± 0.01	2.98 ± 0.02	0.55 ± 0.01	3.86 ± 0.01	0.3 ± 0.01	2.55 ± 0.05	22 ± 1.00	14.13 ± 0.22
R2	14.31 ± 0.02	3.00 ± 0.04	0.53 ± 0.01	3.68 ± 0.01	nd	2.1 ± 0.01	≤ 10	2.42 ± 0.03
R3	14.21 ± 0.04	2.78 ± 0.01	0.45 ± 0.01	3.77 ± 0.01	nd	1.2 ± 0.01	nd	0
R4	14.38 ± 0.10	3.00 ± 0.01	0.51 ± 0.01	3.45 ± 0.01	nd	2.85 ± 0.05	nd	0
R5	14.16 ± 0.04	2.67 ± 0.01	0.55 ± 0.01	3.71 ± 0.01	≤ 0.2	2.95 ± 0.05	≤ 10	1.42 ± 0.03
R6	13.55 ± 0.01	2.86 ± 0.01	0.66 ± 0.01	3.71 ± 0.01	nd	0.75 ± 0.05	29	5.5 ± 1.2
R7	13.75 ± 0.01	3.05 ± 0.01	0.34 ± 0.01	3.49 ± 0.01	≤ 0.2	2.3 ± 0.01	12.0	0
R8	15.42 ± 0	3.40 ± 0.01	0.55 ± 0.01	3.42 ± 0.01	0.5 ± 0.01	6.4 ± 0.01	21.5 ± 0.5	0
R9	16.26 ± 0.01	3.13 ± 0.01	0.64 ± 0.01	3.66 ± 0.01	0.3 ± 0.01	1.1 ± 0.01	70.5 ± 0.5	27.1 ± 0.15

- ***Table S2** – Free SO_2 measurements of enzymatic oxidized wine samples*

Wine sample	Free SO_2 (mg/L)
R1 - laccases oxidation	*0*
R2 - laccases oxidation	*0*
R3 - laccases oxidation	*0*
R4 - laccases oxidation	*0*
R5 - laccases oxidation	*0*
R6 - laccases oxidation	*5.5* ± 1.2
R7- laccases oxidation	*0*
R8 - laccases oxidation	*0*
R9 - laccases oxidation	*26.7* ± 0.15

Free SO2 was equal to 0 for both chemical and temperature oxidations

- ***Figure S1*** - *Representation of the scores (wines) (variables - electrochemical parameters for the reference wines (Q) and oxidized wines by the three protocols minus reference wines (ΔQ)) in the plane defined by respectively the first (F1) and second (F2) factor (explained variance: 79.55%)*

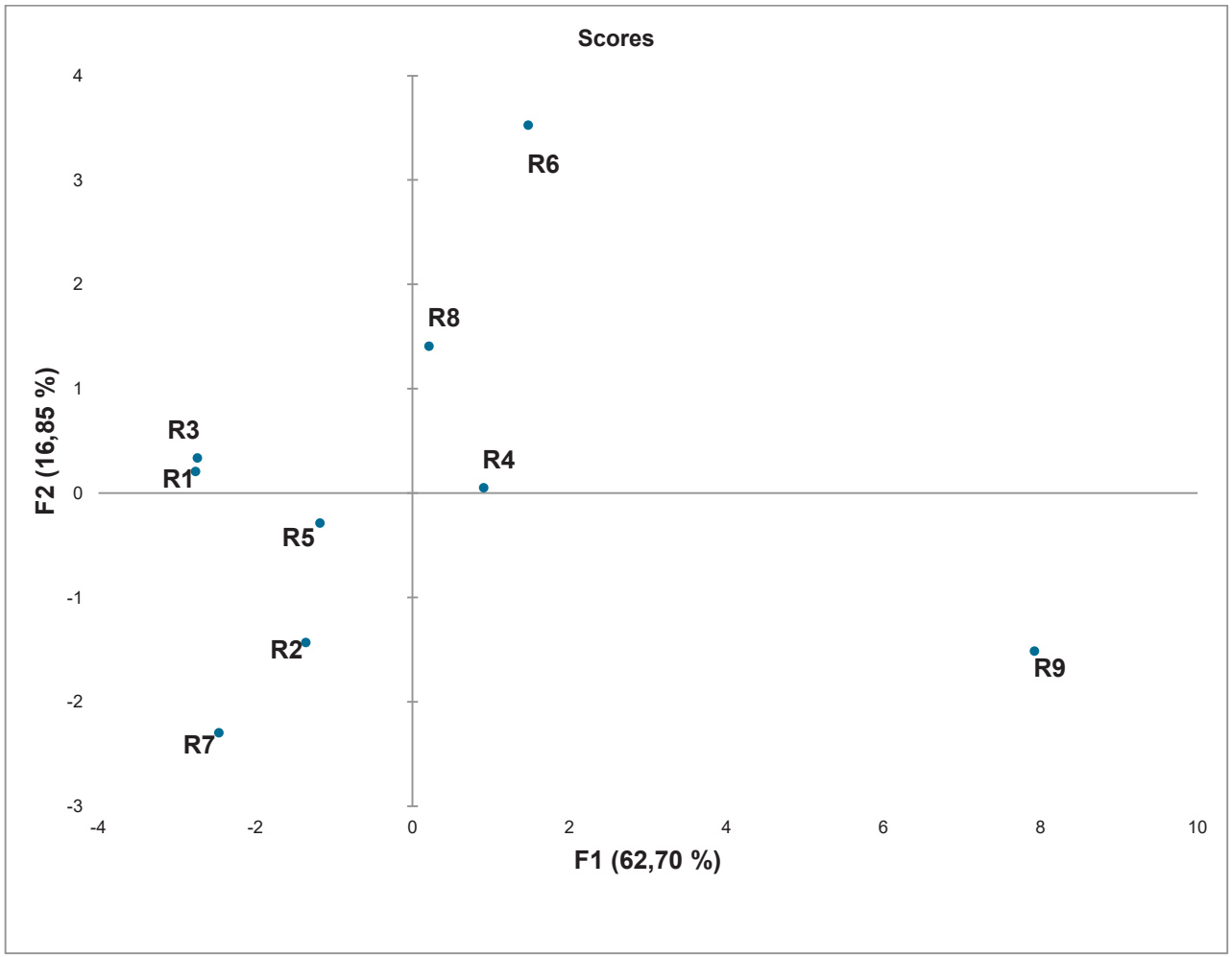

Chapitre IV : Approche ciblée : identification et obtention de marqueurs d'oxydation

Article 3 - *Unambiguous NMR structural determination of (+)-Catechin-Laccases dimeric reaction products as potential markers of grape and wine oxidation.*

- ***Figure S1 -*** *Classification of enzymes responsible for enzymatic browning*

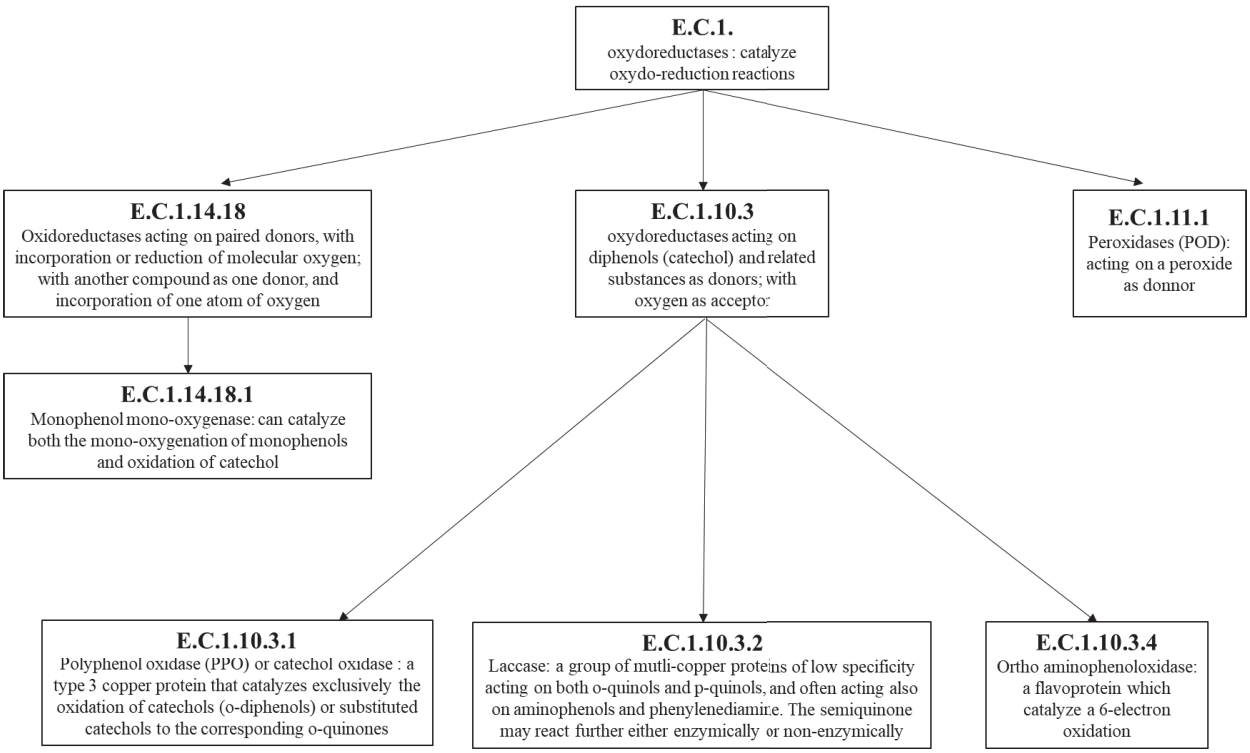

- ***Table S1*** *- ^{1}H and ^{13}C NMR assignments of compounds N2, N3, N4, N6 and N8. The analyses were carried out in the solvent acetone-d_6*

Compound	ring	H/C position	Chemical shift/ppm (δH)	Multiplicity pattern	J-coupling/Hz	Chemical shift/ppm (δC)
N2	**A-u**	4a	-	-	-	100.08
		5 (OH)	8.17	s	-	156.76
		6	5.96	d	2.29 (^{4}J)	95.53
		7 (OH)	8.02	s	-	157.24
		8	5.79	d	2.29 (^{4}J)	95.13
		8a	-	-	-	157.03
	C-u	2	4.54	d	2.17 (^{3}J)	67.92

		3	4.03	m	-	67.95
		3 (OH)	4.33	s		
		4α	2.89	dd	15.08 (^{2}J) / 5.41 (^{3}J)	28.93
		4β	2.38	dd	15.85 (^{2}J) / 8.79 (^{3}J)	
	B-u	1'	-	-	-	130.94
		2'	-	-	-	122.17
		3' (OH)	7.04	s	-	143.53
		4' (OH)	7.79	s	-	144.96
		5'	6.76	d	8.34 (^{3}J)	115.00
		6'	6.81	d	8.36 (^{3}J)	118.63
	A-l	4a	-	-	-	100.93
		5 (OH)	8.35	s	-	156.49
		6	6.13	s	-	96.71
		7 (OH)	7.47	s	-	155.05
		8	-	-	-	101.96
		8a	-	-	-	153.78
	C-l	2	4.52	d	1.89 (^{3}J)	67.96
		3	3.92	m	-	67.91
		3 (OH)	4.08	s	-	
		4α	2.93	dd	15.08 (^{2}J) / 5.22 (^{3}J)	28.37
		4β	2.54	dd	16.53 (^{2}J) / 8.77 (^{3}J)	
	B-l	1'	-	-	-	131.97
		2'	6.89	d	1.78 (^{4}J)	114.57
		3' (OH)	7.86	s	-	145.07
		4' (OH)	7.74	s	-	145.07
		5'	6.70	d	8.09 (^{3}J)	115.09
		6'	6.73	dd	8.79 (^{3}J) / 1.79 (^{4}J)	119.79
N3	**A-u**	4a	-	-	-	100.67
		5 (OH)	8.32	s	-	157.18
		6	6.01	d	2.26 (^{4}J)	96.22
		7 (OH)	8.08	s	-	157.79
		8	5.82	d	2.22 (^{4}J)	96.42
		8a	-	-	-	196.92
	C-u	2	4.53	d	8.38 (^{3}J)	82.80
		3	3.99	m	-	68.47
		3 (OH)	4.33	s	-	
		4α	2.98	dd	16.24 (^{2}J) / 5.89 (^{3}J)	29.42
		4β	2.52	dd	15.81 (^{2}J) / 9.36 (^{3}J)	
	B-u	1'	-	-	-	131.57
		2'	7.00	d	1.92 (^{4}J)	116.45
		3'	-	-	-	147.32

		4' (OH)	7.90	s	-	147.34
		5'	6.805	d	8.14 (^{3}J)	116.45
		6'	6.94	dd	8.06 (^{3}J) / 1.9 (^{4}J)	122.43
	A-l	4a	-	-	-	101.69
		5 (OH)	8.32	s	-	153.27
		6	6.15	s	-	96.18
		7 (OH)	8.2	s	-	149.62
		8	-	-	-	124.97
		8a	-	-	-	149.00
	C-l	2	4.62	d	7.57 (^{3}J)	82.71
		3	3.96	m	-	68.20
		3 (OH)	4.08	s	-	
		4α	2.90	dd	16.42 (^{2}J) / 5.18 (^{3}J)	28.6
		4β	2.58	dd	16.38 (^{2}J) / 8.23 (^{3}J)	
	B-l	1'	-	-	-	131.63
		2'	6.75	d	1.85 (^{4}J)	114.81
		3' (OH)	7.95	s	-	145.44
		4' (OH)	7.74	s	-	145.78
		5'	6.67	d	8.12 (^{3}J)	115.58
		6'	6.63	dd	8.15 (^{3}J) / 1.85 (^{4}J)	120.23
N4-A	**A-u**	4a	-	-	-	100.71
		5 (OH)	8.30	s	-	157.26
		6	6.02	d	2.33 (^{4}J)	96.16
		7 (OH)	8.08	s	-	157.76
		8	5.9	d	2.29 (^{4}J)	95.5
		8a	-	-	-	154.05
	C-u	2	4.57	d	6.13 (^{3}J)	83.15
		3	4.09	m	-	
		3 (OH)	4.34 or under H3C	s	-	68.83
		4α	2.96	dd	16.39 (^{2}J) / 7.12 (^{3}J)	28.91
		4β	2.55	dd	15.53 (^{2}J) / 8.95 (^{3}J)	
	B-u	1'	-	-	-	123.79
		2'	6.80	d	2.21 (^{4}J)	114.25
		3' (OH)	7.65	s	-	146.36
		4' (OH)	7.30	s	-	143.94
		5'	-	-	-	121.33
		6'	6.85	d	2.24 (^{4}J)	157.08
	A-l	4a	-	-	-	100.89
		5 (OH)	8.41	s	-	156.79
		6	6.15	s	-	96.55

		7 (OH)	7.43	s	-	155.05
		8	-	-	-	104.99
		8a	-	-	-	153.84
	C-l	2	4.73	d	6.21 (^{3}J)	81.93
		3	4.06	m	-	
		3 (OH)	4.34 or under H3C	s	-	67.66
		4α	2.84	dd	16.63 (^{2}J) / 5.1 (^{3}J)	28.02
		4β	2.62	dd	10.47 (^{2}J) / 6.94 (^{3}J)	
	B-l	1'	-	-	-	131.84
		2'	6.84	d	1.83 (^{4}J)	114.82
		3' (OH)	8.08	s	-	145.45
		4' (OH)	7.70	s	-	145.59
		5'	6.72	d	8.48 (^{3}J)	115.67
		6'	6.69	dd	8.04 (^{3}J) / 1.92 (^{4}J)	119.31
N4-B	**A-u**	4a	-	-	-	100.78
		5 (OH)	8.26	s	-	157.17
		6	6.00	d	2.37 (^{4}J)	96.13
		7 (OH)	8.08	s	-	157.71
		8	5.82	d	2.34 (^{4}J)	95.51
		8a	-	-	-	157.71
	C-u	2	4.42	d	8.26 (^{3}J)	83.07
		3	3.82	m	-	
		3 (OH)	4.34 or under H3C	s	-	68.86
		4α	2.96	dd	16.52 (^{2}J) / 8.63(^{3}J)	28.98
		4β	2.46	dd	16.29 (^{2}J) / 9.1 (^{3}J)	
	B-u	1'	-	-	-	124.51
		2'	6.82	d	2.08 (^{4}J)	113.30
		3' (OH)	7.83	s	-	146.65
		4' (OH)	7.29	s	-	144.45
		5'	-	-	-	122.01
		6'	6.71	d	2.58 (^{4}J)	157.02
	A-l	4a	-	-	-	101.03
		5 (OH)	8.42	s	-	156.69
		6	6.15	s	-	96.31
		7 (OH)	7.23	s	-	155.06
		8	-	-	-	104.55
		8a	-	-	-	153.84
	C-l	2	4.55	d	5.71 (^{3}J)	82.93
		3	3.99	m	-	68.25

		3 (OH)	4.34 or under H3C	s	-	
		4α	2.93	dd	15.77 (^{2}J) / 6.55(^{3}J)	28.91
		4β	2.59	dd	9.48 (^{2}J) / 6.32 (^{3}J)	
	B-l	1'	-	-	-	132.10
		2'	6.94	d	2.00 (^{4}J)	115.08
		3' (OH)	8.00	s	-	145.38
		4' (OH)	7.79	s	-	145.61
		5'	6.69	d	8.23 (^{3}J)	115.60
		6'	6.77	dd	8.16 (^{3}J) / 2.04 (^{4}J)	120.05
N6	**A-u**	4a	-	-	-	100.66
		5 (OH)	8.23	s	-	157.23
		6	6.03	d	2.04 (^{4}J)	96.25
		7 (OH)	8.03	s	-	157.80
		8	5.89	d	2.04 (^{4}J)	95.49
		8a	-	-	-	156.86
	C-u	2	4.60	d	8.05 (^{3}J)	82.63
		3	4.01	m	-	68.36
		3 (OH)	4.14	s	-	
		4α	2.96	dd	9.57 (^{2}J) / 5.62(^{3}J)	29.16
		4β	2.55	dd	15.85 (^{2}J) / 8.64 (^{3}J)	
	B-u	1'	-	-	-	134.69
		2'	6.92	d	1.71 (^{4}J)	115.72
		3' (OH)	7.80	s	-	147.25
		4'	-	-	-	147.45
		5'	6.22	d	8.38 (^{3}J)	115.96
		6'	6.78	dd	8.38 (^{3}J) / 1.8 (^{4}J)	119.72
	A-l	4a	-	-	-	101.79
		5 (OH)	8.27	s	-	153.33
		6	6.19	s	-	96.17
		7 (OH)	8.17	s	-	149.67
		8	-	-	-	125.03
		8a	-	-	-	149.05
	C-l	2	4.66	d	7.32 (^{3}J)	82.68
		3	3.98	m	-	67.97
		3 (OH)	4.05	s	-	
		4α	2.93	dd	10.17 (^{2}J) / 5.02 (^{3}J)	28.60
		4β	2.62	dd	16.34 (^{2}J) / 7.86 (^{3}J)	
	B-l	1'	-	-	-	131.63
		2'	6.71	d	1.71 (^{4}J)	114.88
		3' (OH)	7.83	s	-	146.72

		4'	-	-	-	145.90
		5'	6.73	d	8.11 (^{3}J)	115.69
		6'	6.64	dd	7.93 (^{3}J) / 1.59 (^{4}J)	119.92
N8	**A-u**	4a	-	-	-	100.24
		5 (OH)	8.36	s	-	157.41
		6	6.01	d	2.1 (^{4}J)	95.90
		7 (OH)	7.88	s	-	157.92
		8	5.61	d	2.34 (^{4}J)	96.98
		8a	-	-	-	155.97
	C-u	2	4.06	d	9.58 (^{3}J)	79.04
		3	4.01	m	-	66.22
		4α	2.95	dd	10.12 (^{2}J) / 5.40 (^{3}J)	27.95
		4β	2.53	dd	14.29 (^{2}J) / 11.08 (^{3}J)	
	B-u	1'	-	-	-	89.61
		2'α	2.71	d	12.03 (^{2}J)	45.20
		2'β	2.49	d	12.03 (^{2}J)	
		3' (OH)	5.78	s	-	94.80
		4'	-	-	-	192.69
		5'	6.38	s	-	112.91
		6'	-	-	-	162.57
	A-l	4a	-	-	-	103.96
		5 (OH)	9.72	s	-	164.46
		6	6.22	s	-	90.84
		7	-	-	-	167.13
		8	-	-	-	105.43
		8a	-	-	-	154.73
	C-l	2	4.86	d	7.84 (^{3}J)	83.46
		3	4.12	m	-	67.70
		3 (OH)	4.23	s	-	
		4α	2.98	dd	11.16 (^{2}J) / 5.40 (^{3}J)	28.55
		4β	2.95	dd	16.18 (^{2}J) / 8.41 (^{3}J)	
	B-l	1'	-	-	-	131.16
		2'	6.94	d	1.51 (^{4}J)	115.04
		3' (OH)	7.97	s	-	145.88
		4' (OH)	7.92	s	-	146.06
		5'	6.83	d	7.97 (^{3}J)	116.02
		6'	6.80	dd	7.97 (^{3}J) / 1.69 (^{4}J)	119.98

Figure S2 - *2D ^{1}H/^{13}C HMBC, top 1D ^{1}H, side 1D ^{13}C spectrum (a) N2; (b) N3; (c) N4; (d) N6 and (e) N8*

(a)- N2

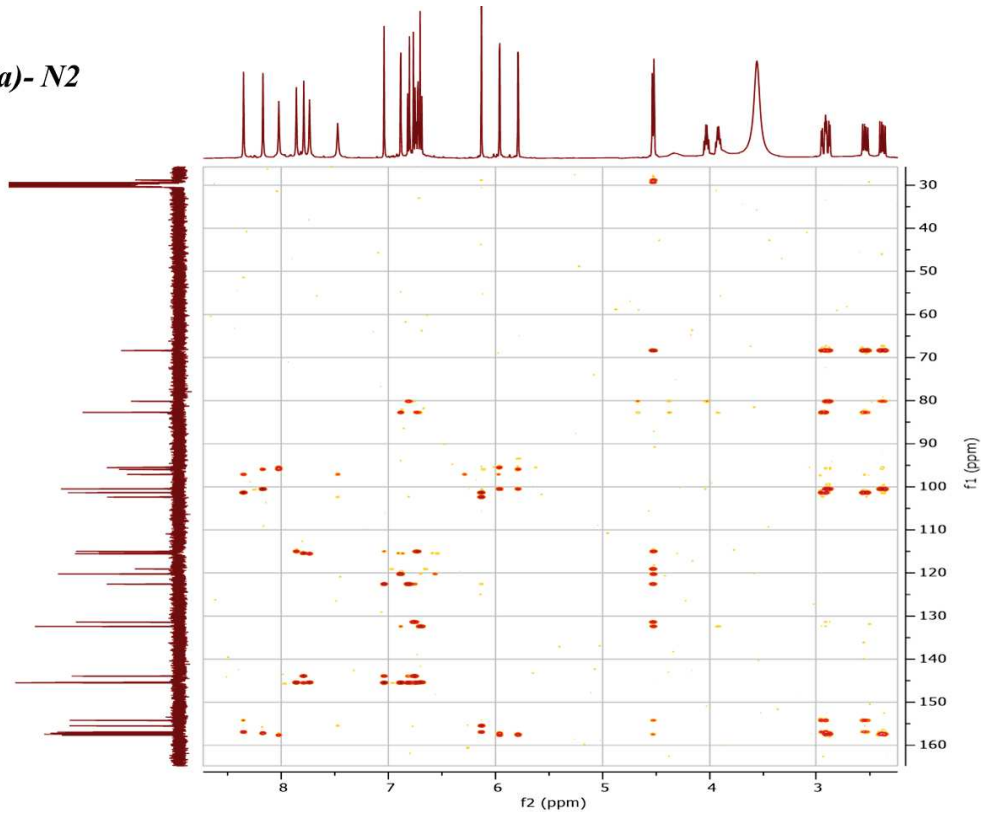

(b) – N3

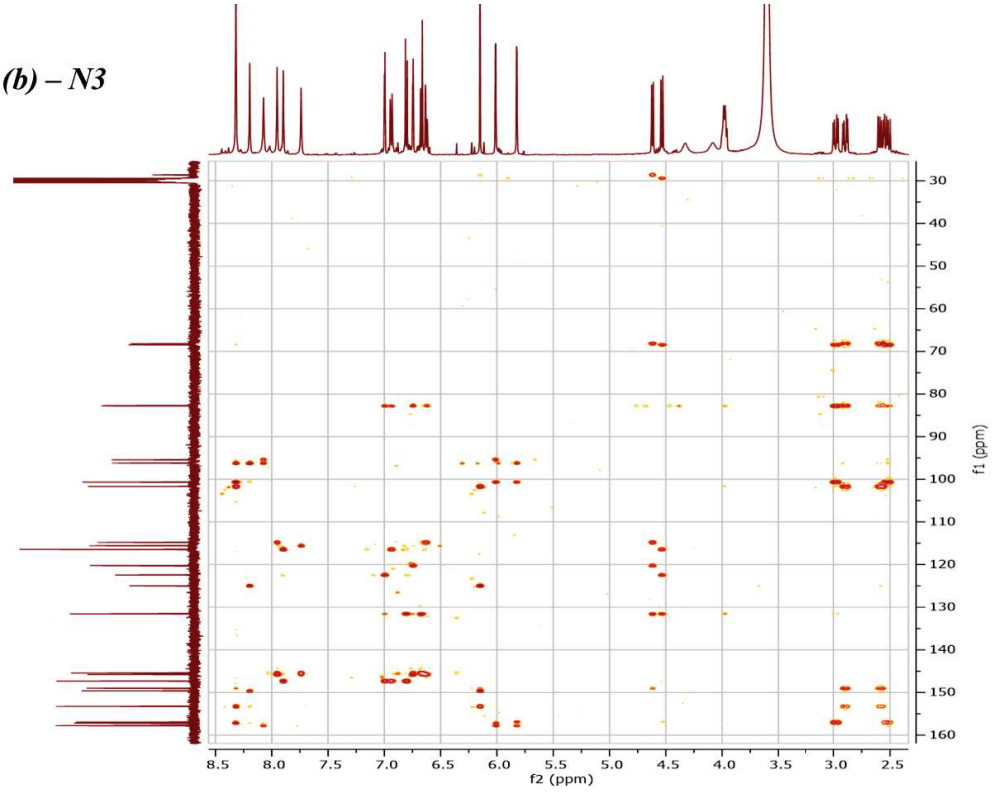

(c) – N4

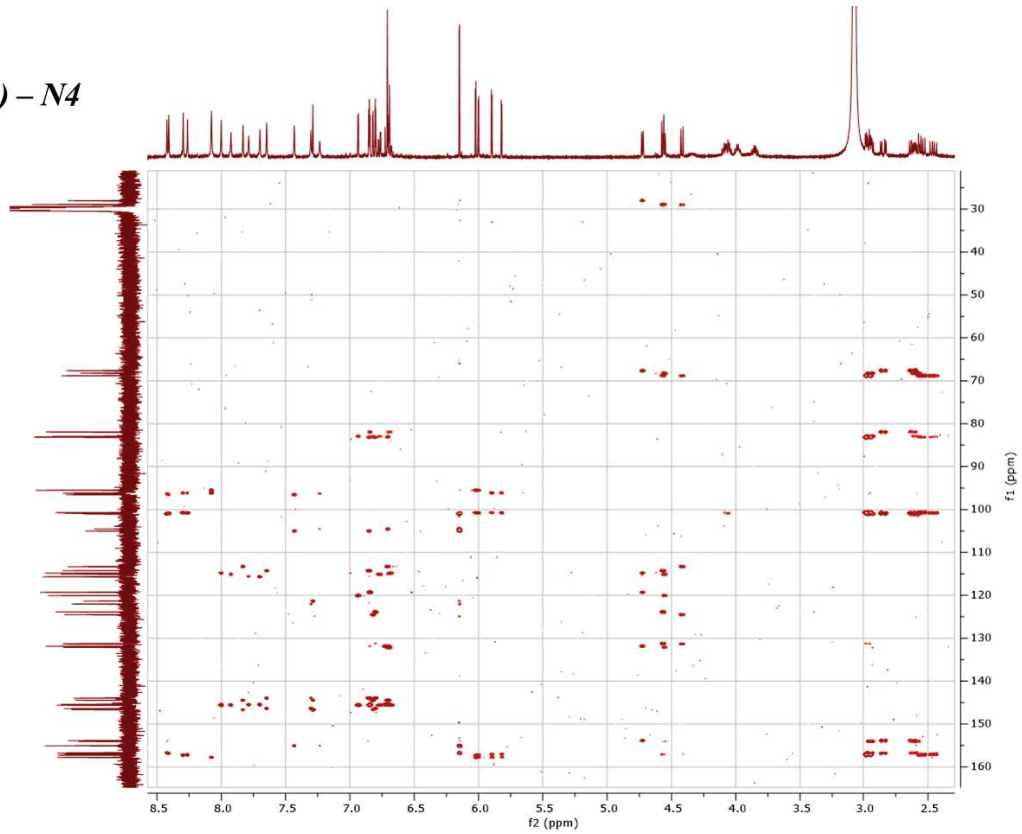

(d) – N6

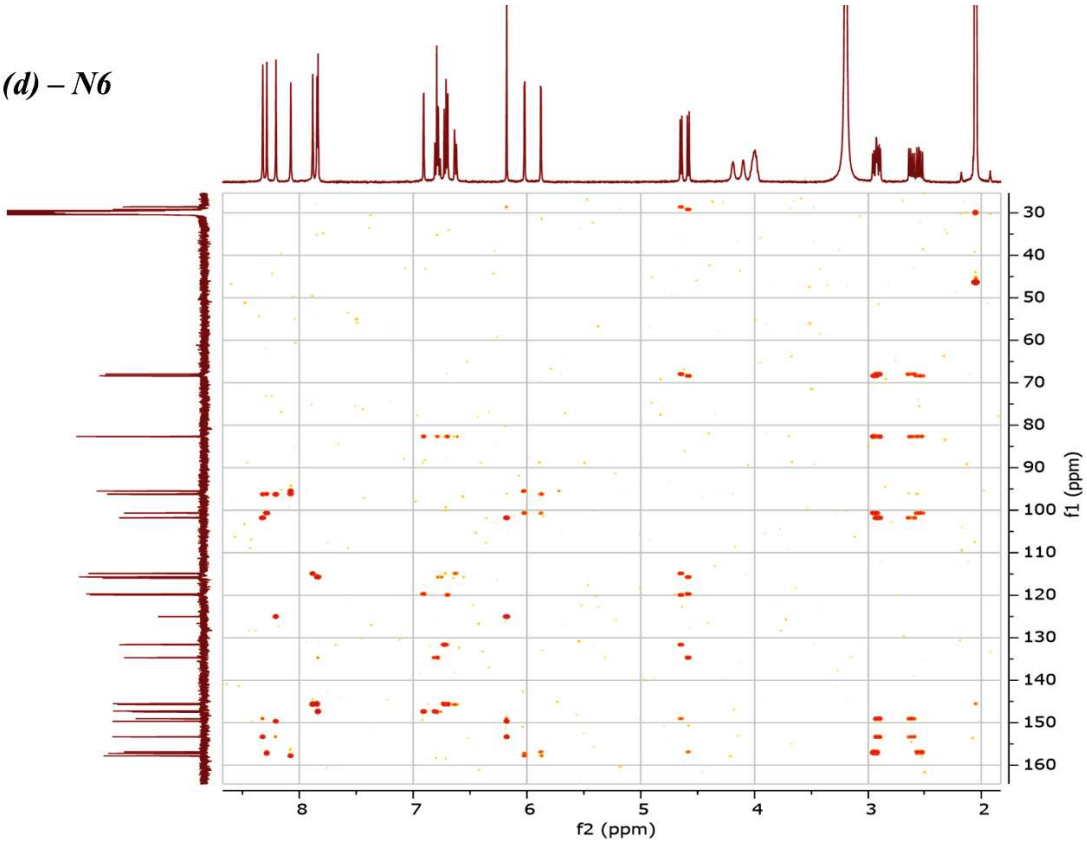

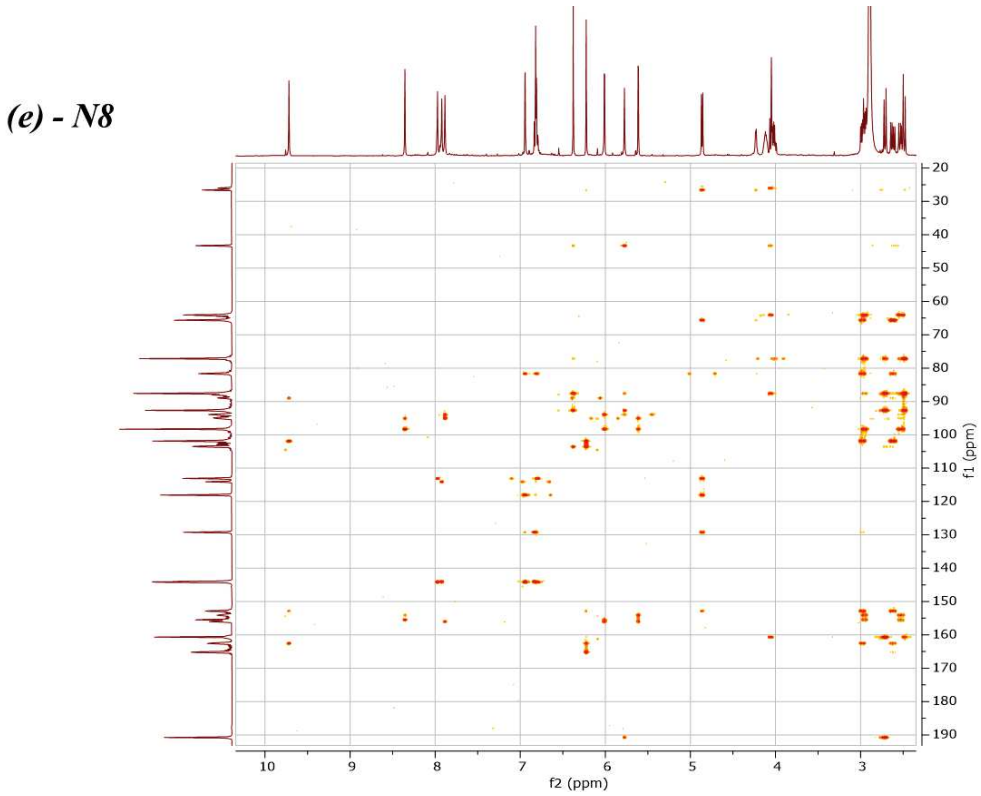

Figure S3 - *^{1}H 2D ROESY spectrum showing correlations (in blue) between phenolic and aromatic protons, ROE correlations between phenolic protons due to chemical exchange appear in red (a) N2; (b) N3; (c) N4; (d) N6 and (e) N8*

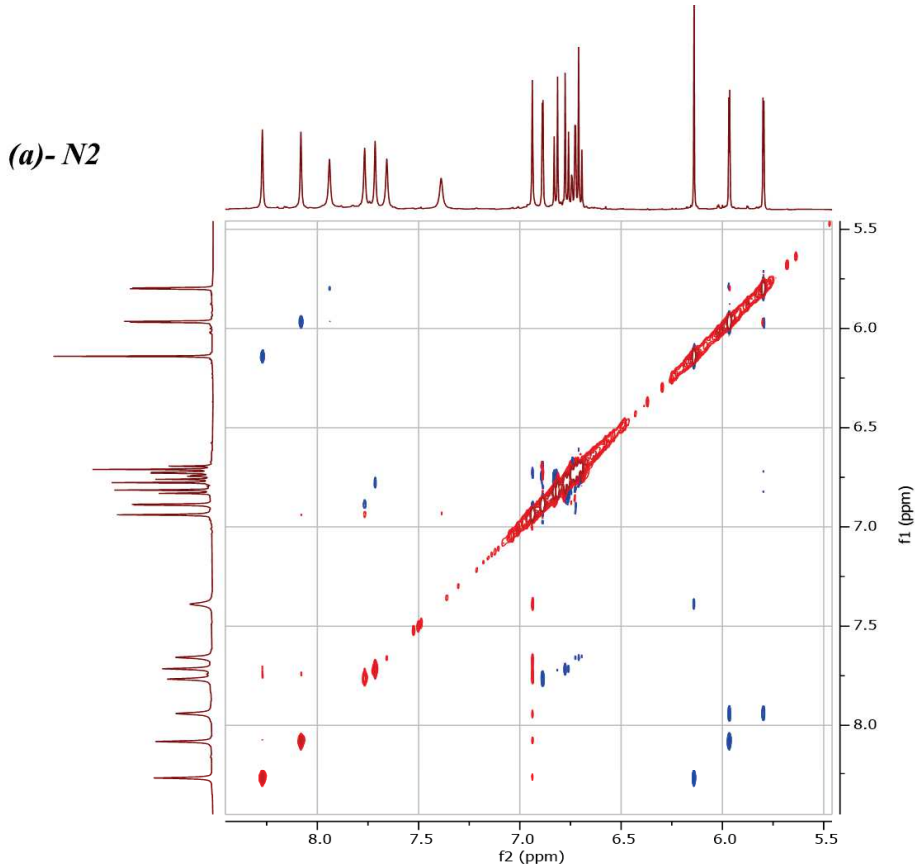

(b) – N3

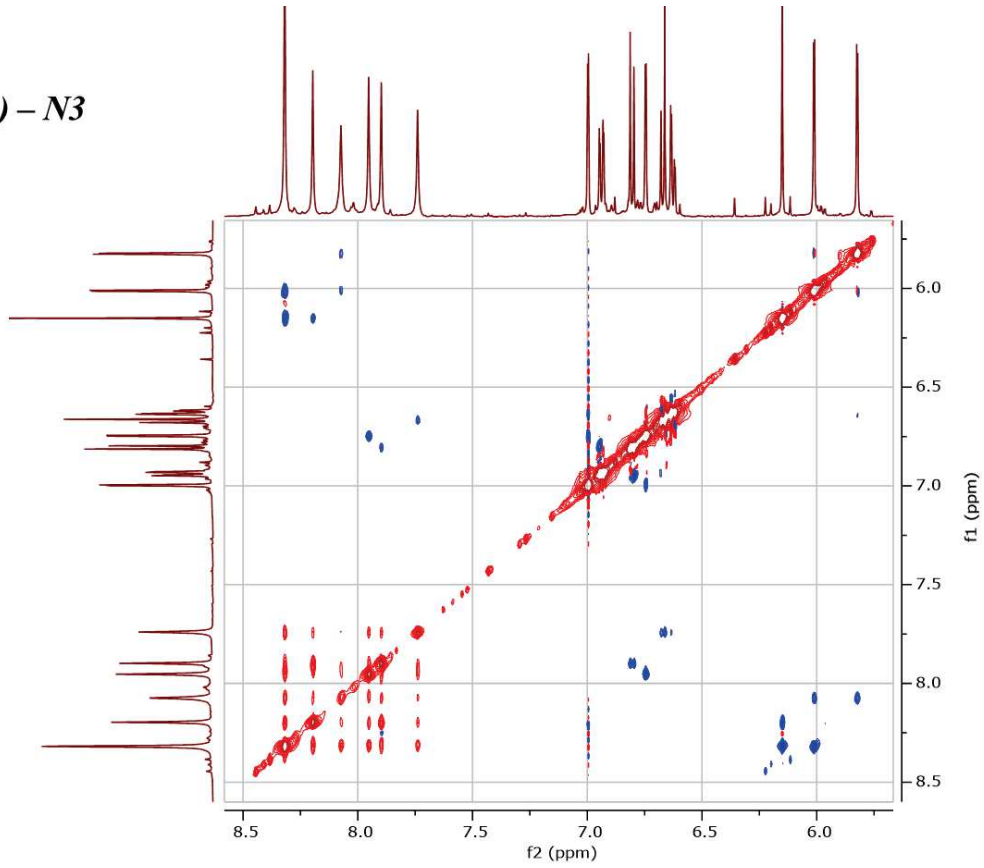

(c) – N4

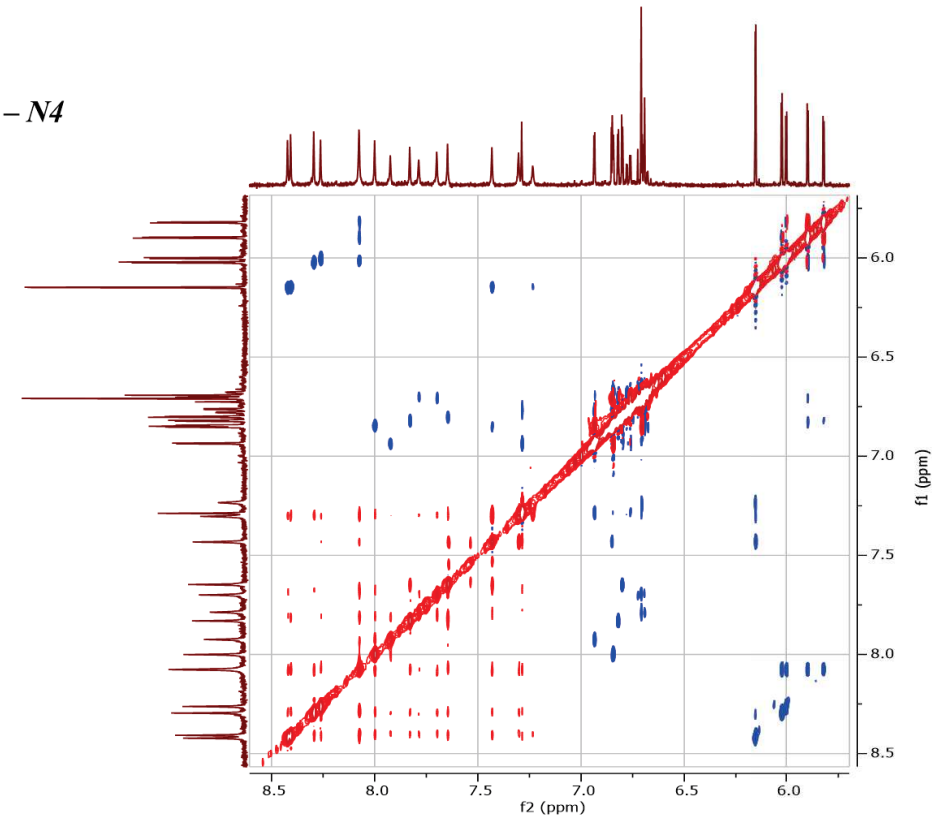

(d) – N6

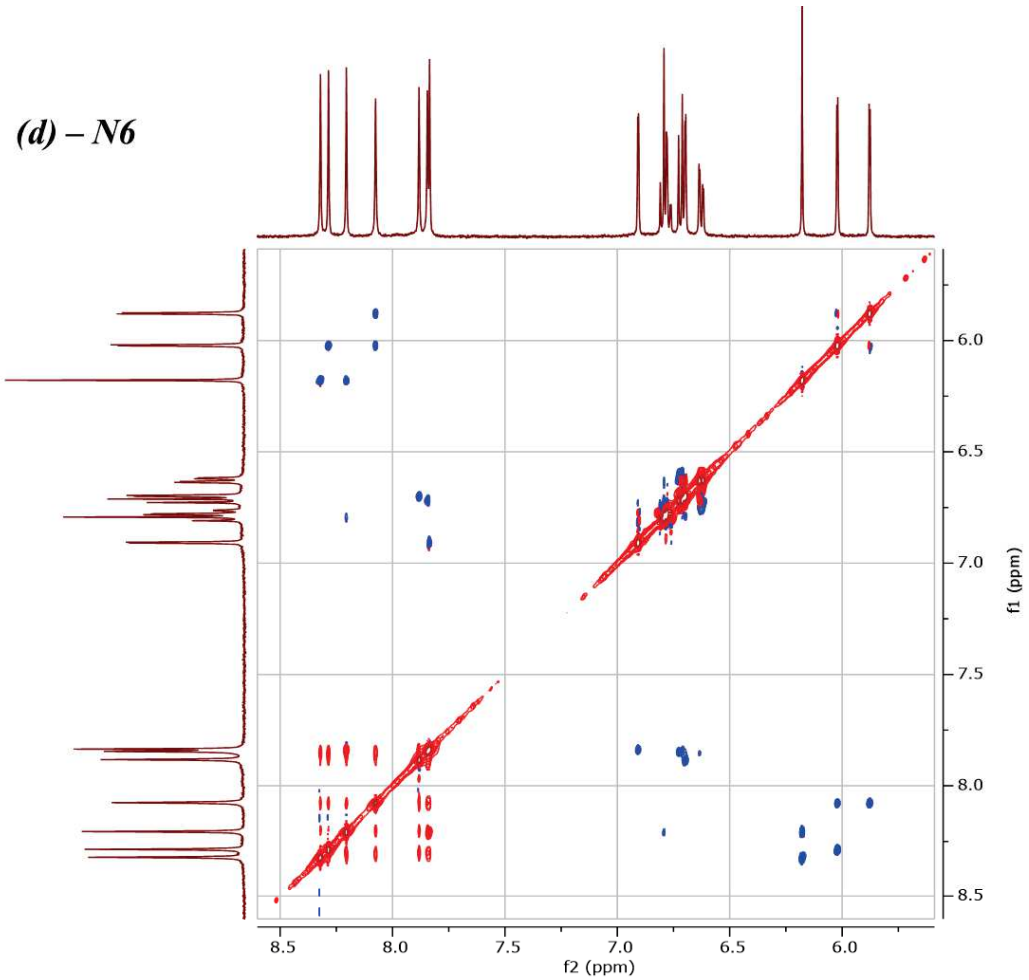

Partie 3 – *principaux spectres RMN ayant conduit à la détermination structurale des composés N2, N3, N4, N6 et N8*

N2 - Acd6+Cd – 15°C– Spectre 2D HMBC 1H/ 13C – Région des corrélations impliquant les protons H et OH des cycles A

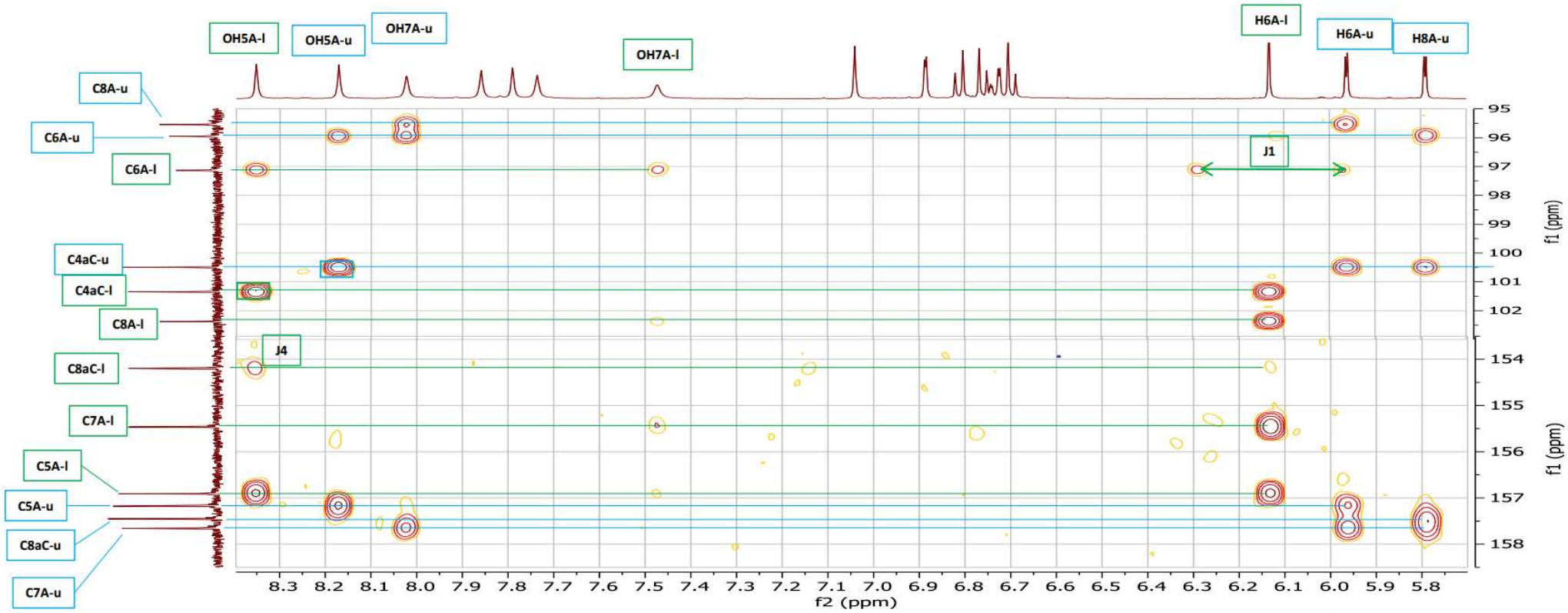

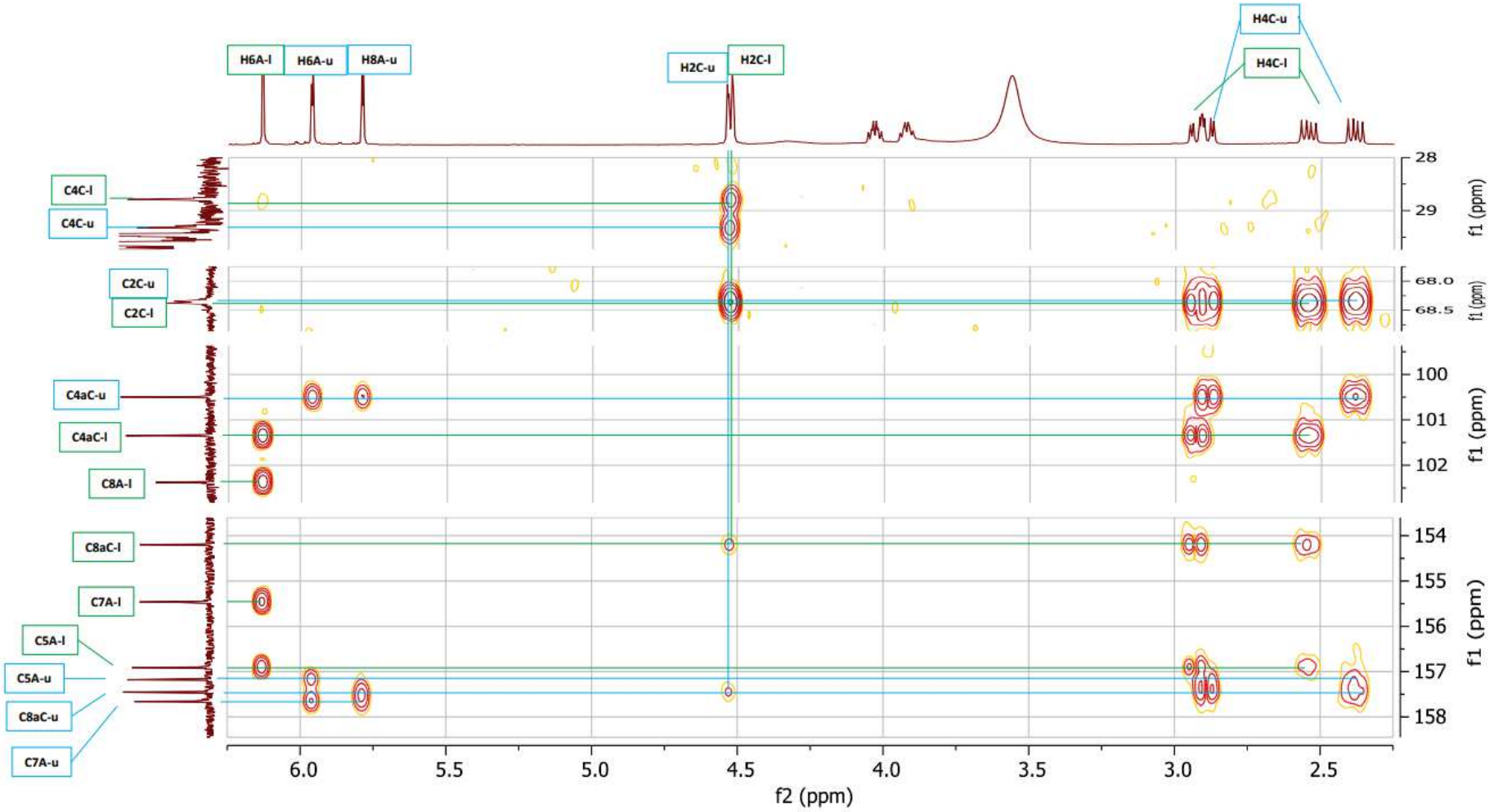
H6A-l
H6A-u
H8A-u
H2C-u
H2C-l
H4C-u
H4C-l
C4C-l
C4C-u
C2C-u
C2C-l
C4aC-u
C4aC-l
C8A-l
C8aC-l
C7A-l
C5A-l
C5A-u
C8aC-u
C7A-u
6.0
5.5
5.0
4.5
4.0
3.5
3.0
2.5
f2 (ppm)
28
29
68.0
68.5
100
101
102
154
155
156
157
158
f1 (ppm)

N2 - Acd6+Cd – 15°C – Spectre 2D HSQC 1H/ 13C – Région montrant les corrélations impliquant les protons HB et spectre 1D 1H 1H RMN

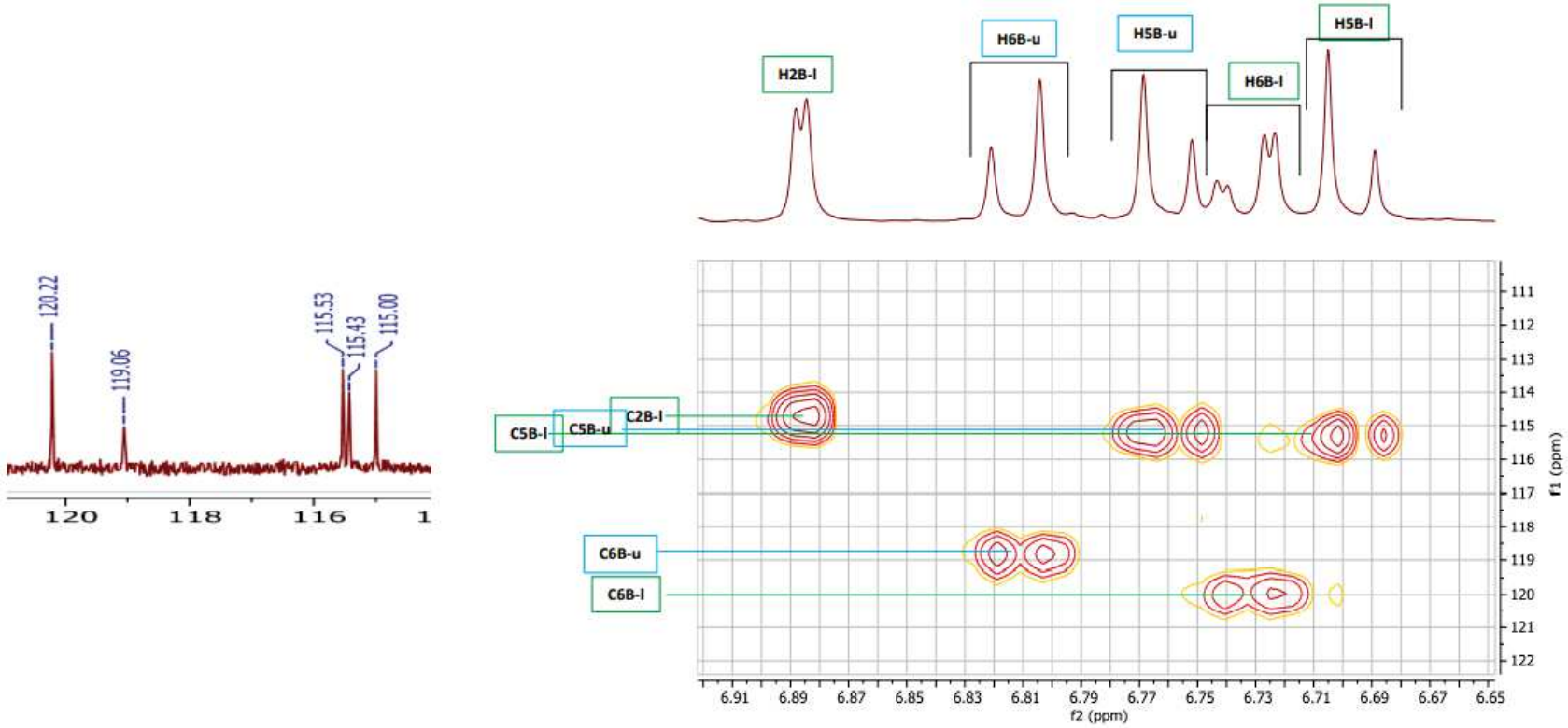

N2 - Acd6+Cd – 15°C– Spectre 2D HMBC 1H/ 13C – Région montrant les corrélations impliquant les protons H et OH des cycles B

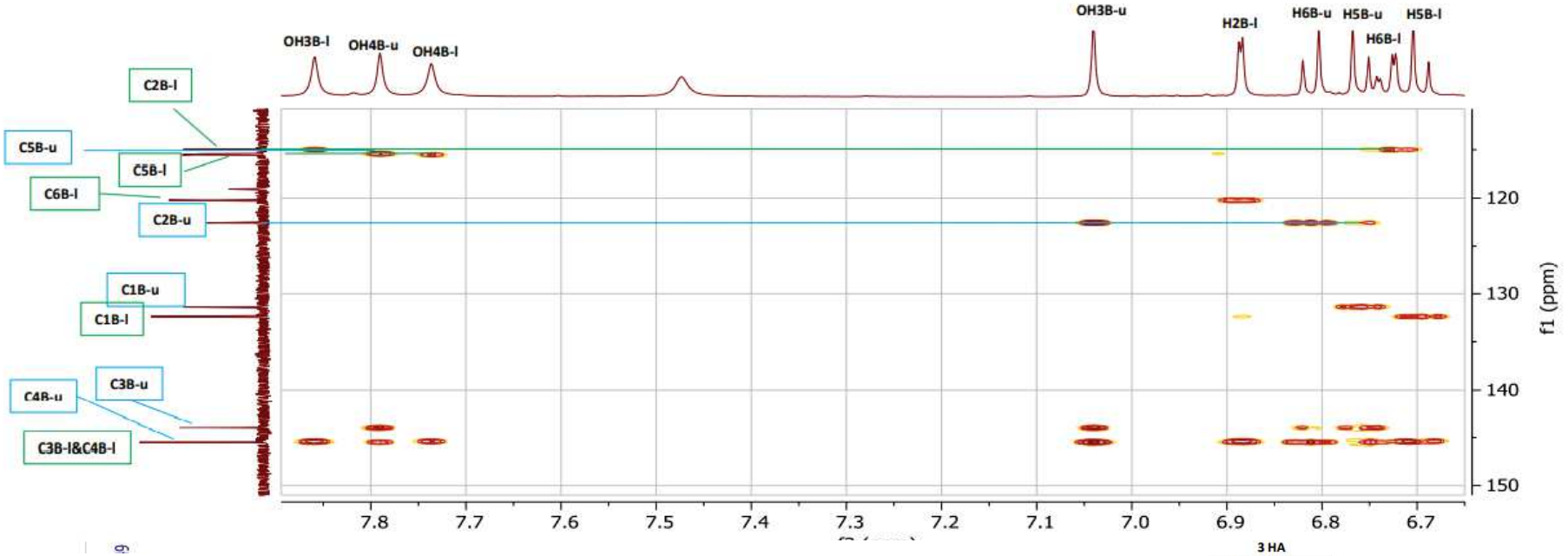

N2 - Acd6+Cd – 15°C– Spectre 2D 1H ROESY

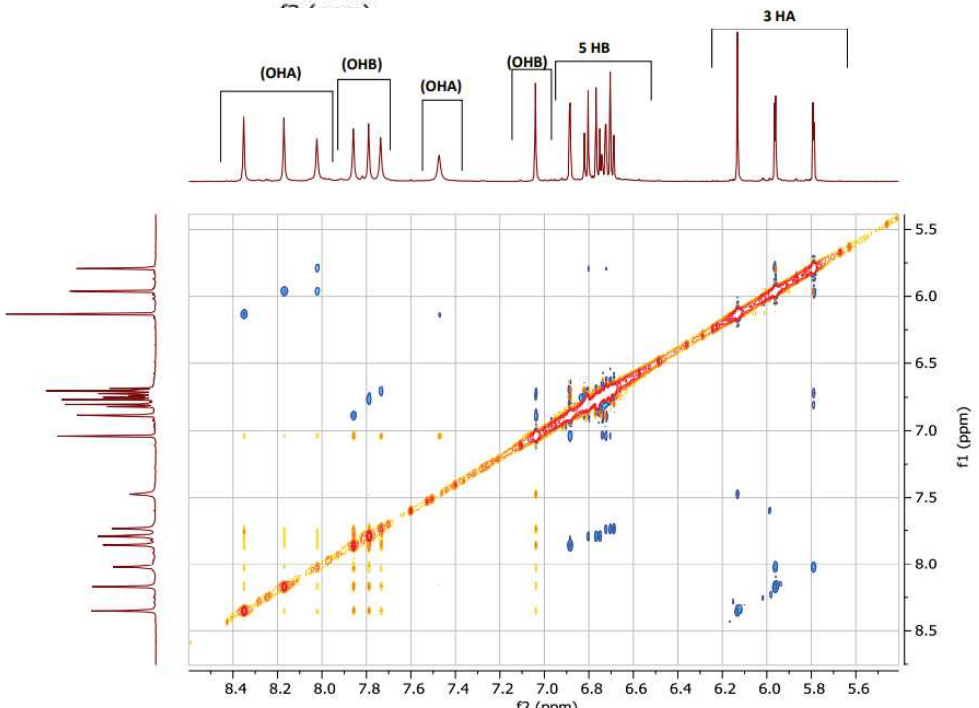

N3 - Acd6+Cd – 15°C – Spectre TOCSY - Régions montrant les systèmes de spins des cycles B et C

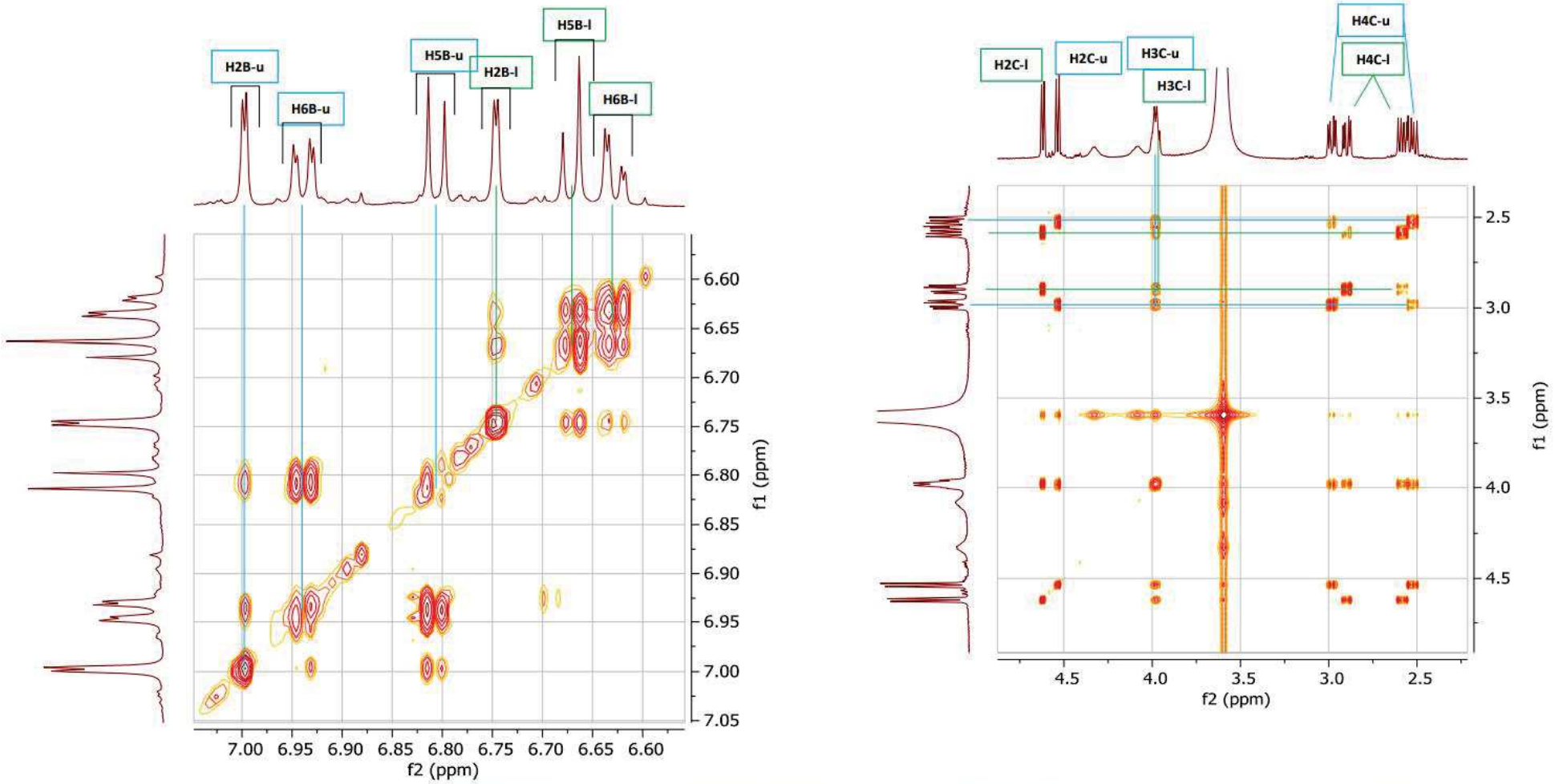

N3 Acd6+Cd – 15°C – Spectre HMBC – Attribution des protons et carbones protonés des cycles C

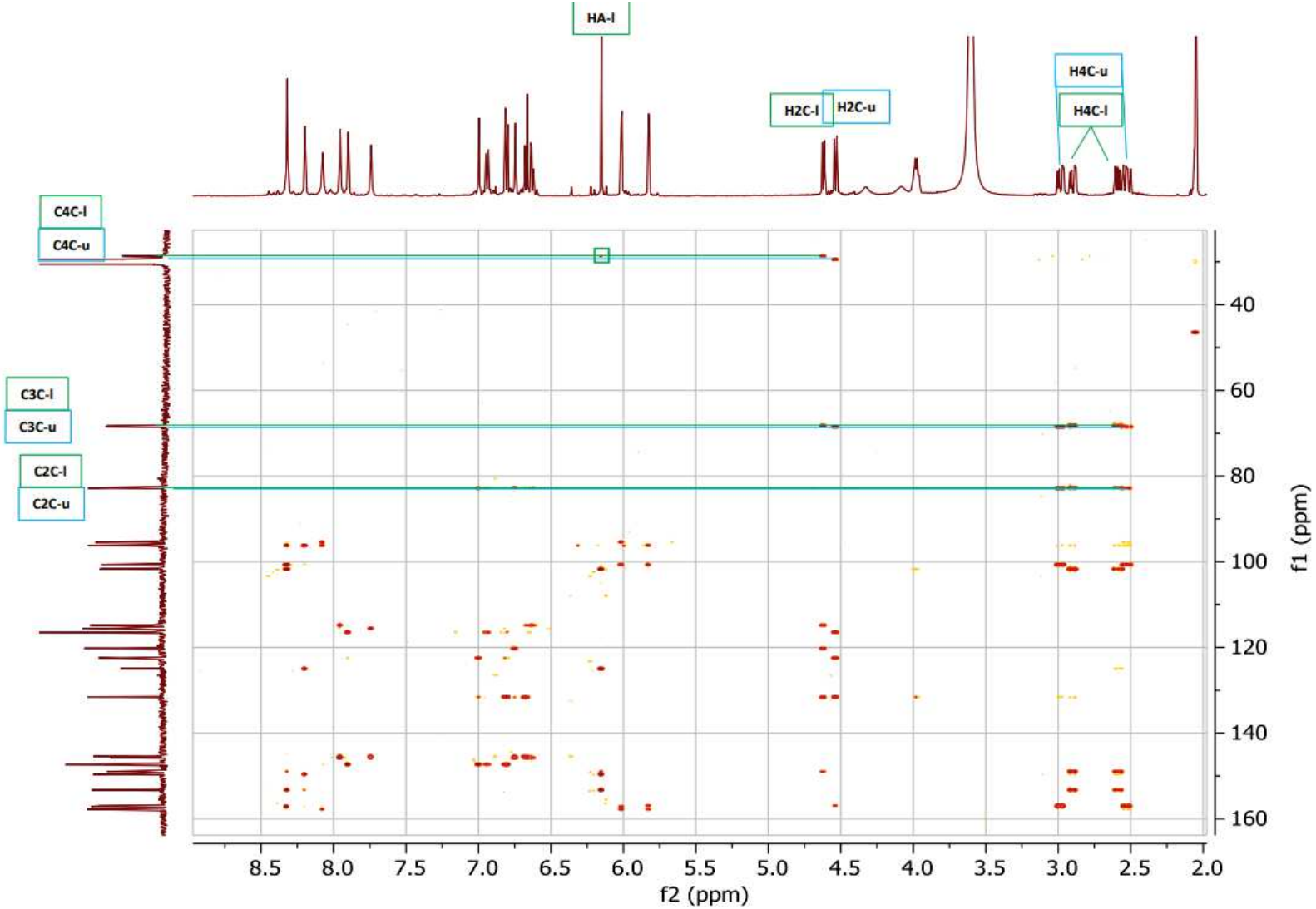

N3 Acd6+Cd – 15°C – Spectre HMBC- Région montrant les corrélations impliquant les protons H et OH des cycles B (Cf expansions ci-dessous pour les attributions)

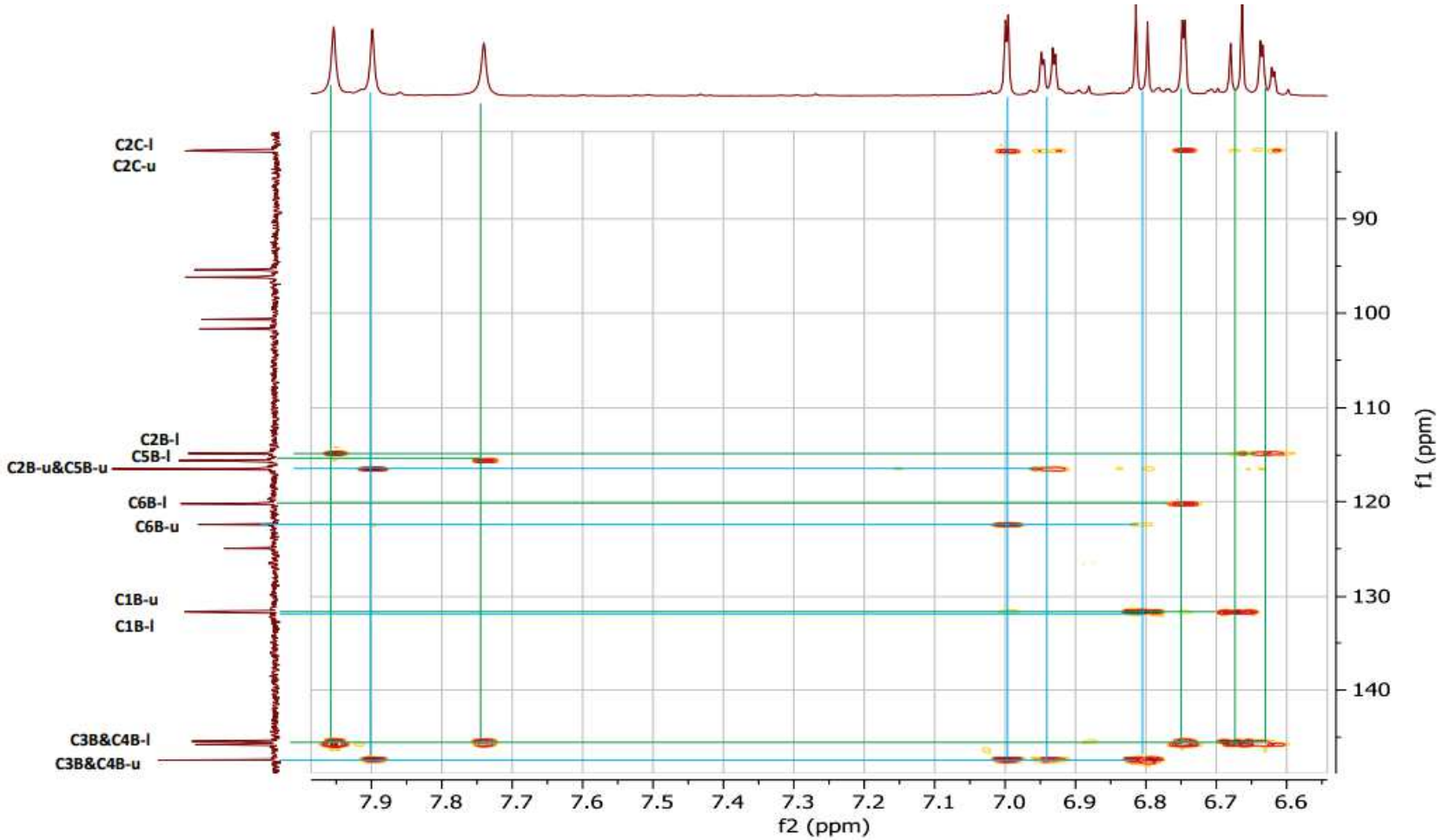

N3 - Acd6+Cd – 15°C – Spectre HMBC- Expansions du spectre montrant les corrélations impliquant les protons H et OH des cycles B

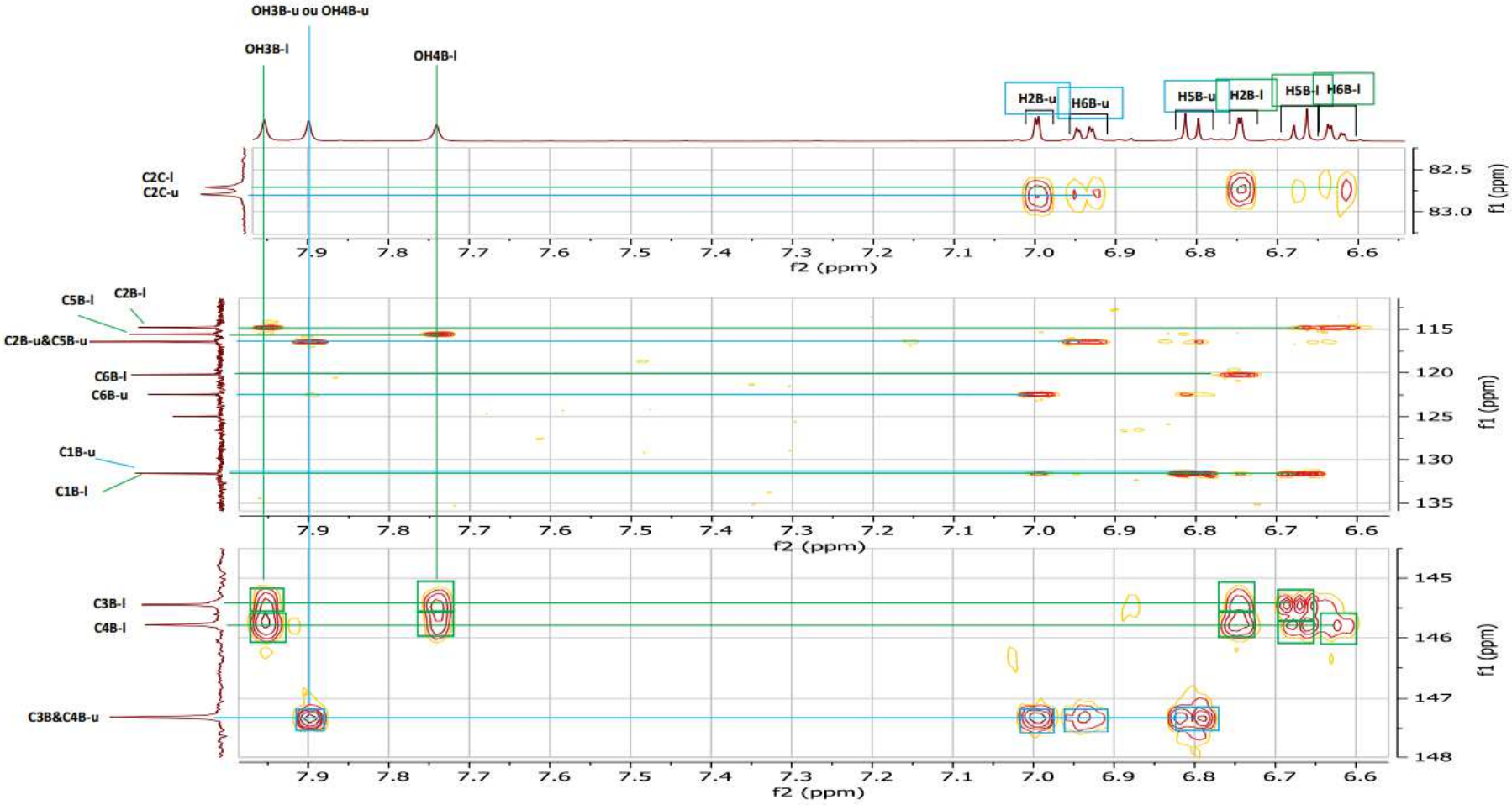

N3- Acd6+Cd – 15°C – Spectre ROESY- Expansion du spectre montrant les corrélations impliquant les protons H et OH des cycles B

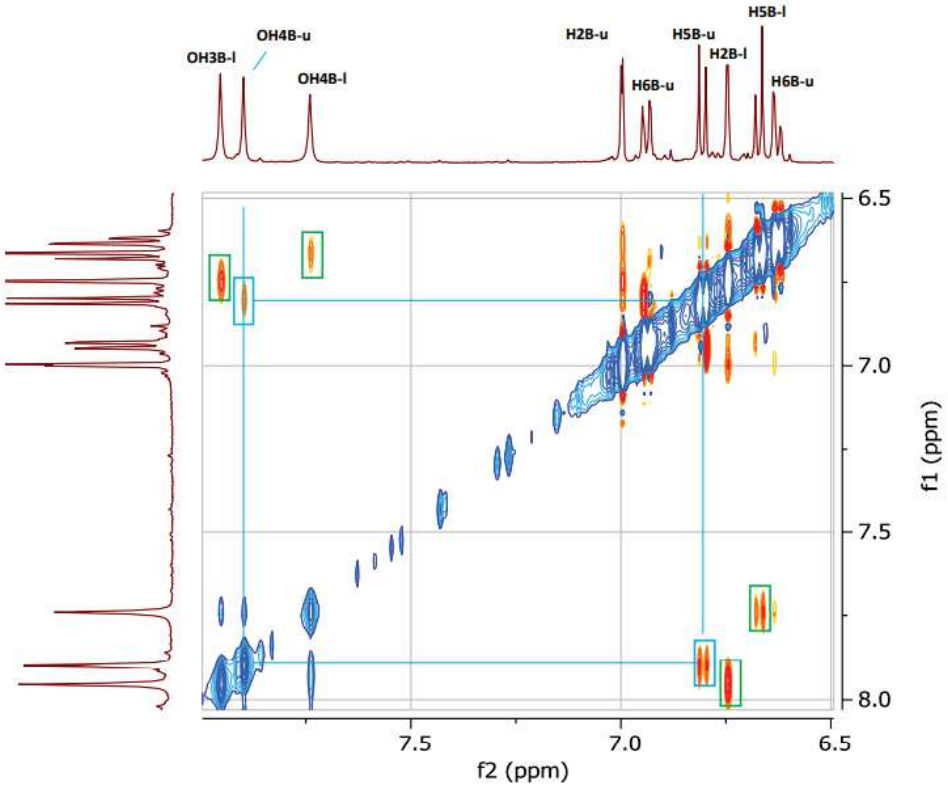

N3 Acd6+Cd – 15°C – Spectre HMBC- Attribution des H2C et confirmation des attributions ci-dessus

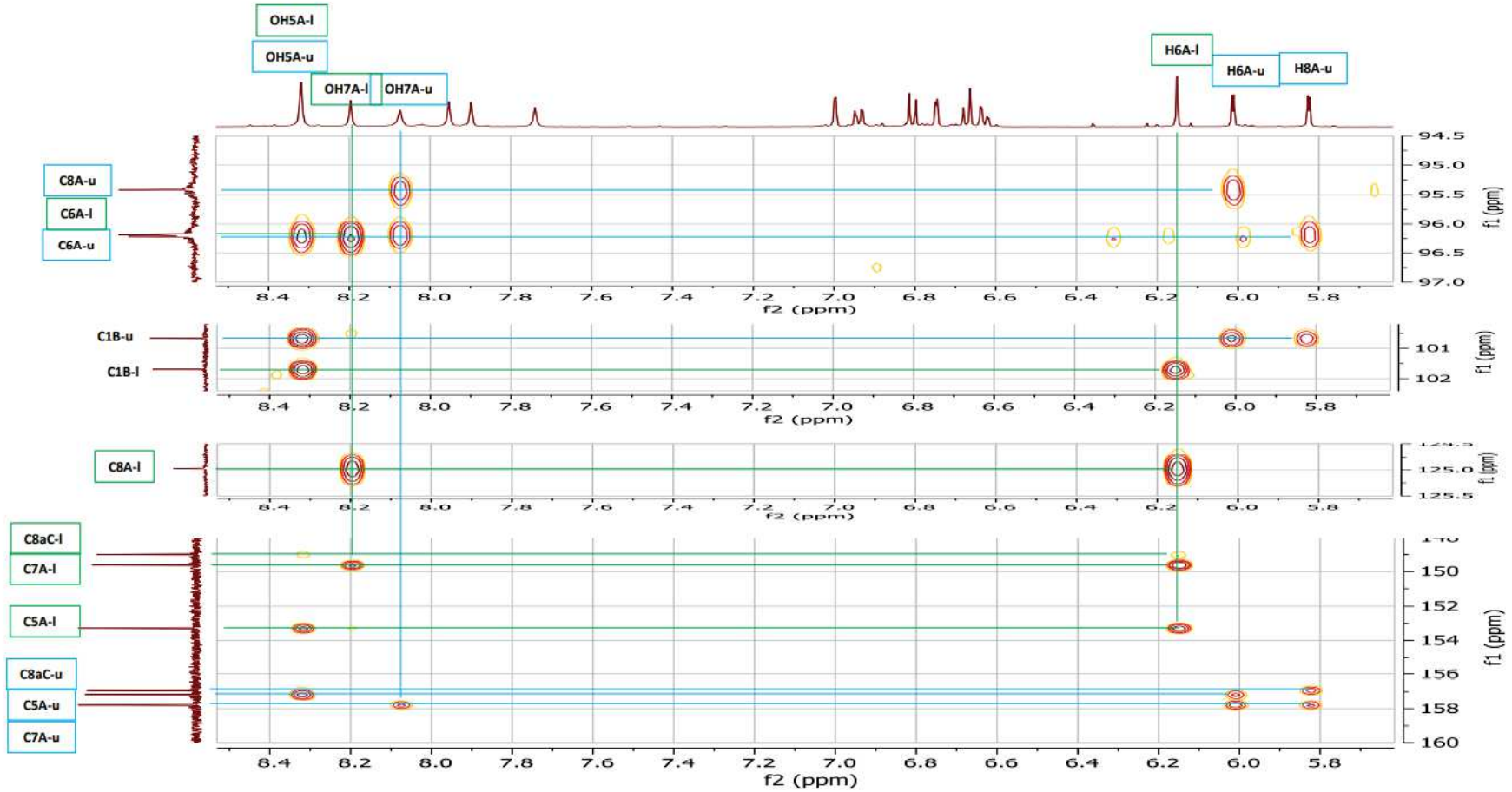

N3- Acd6+Cd – 15°C – Spectre HMBC- Attribution des H4C

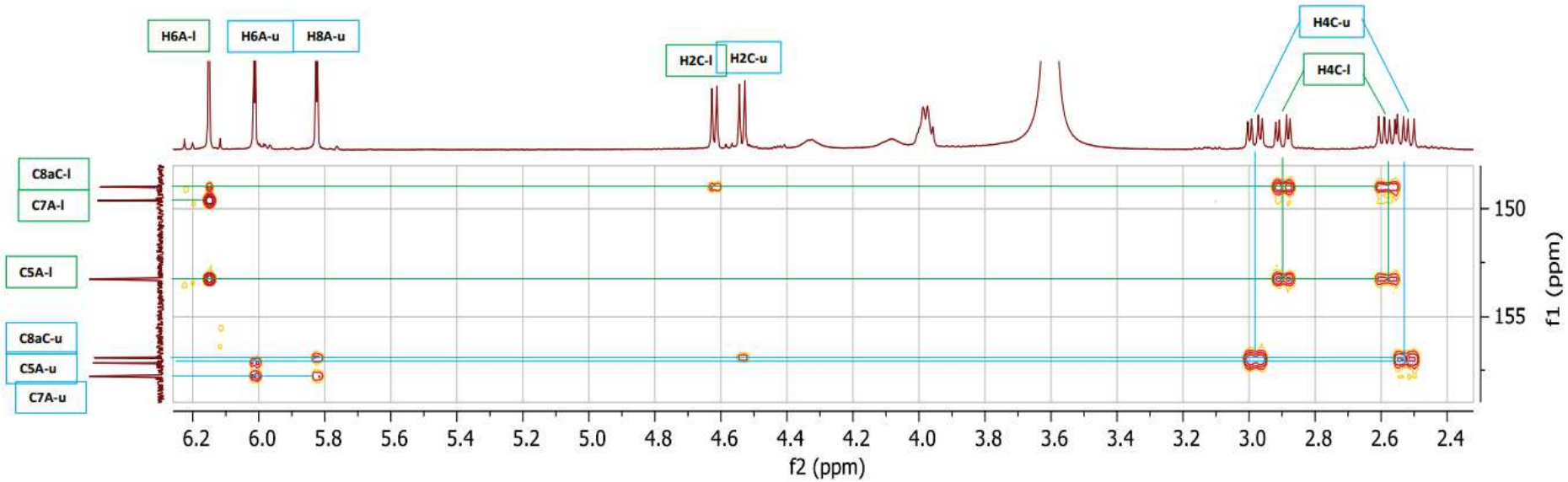

N4 - Acd6+Cd – 15°C – spectres TOCSY et HSQC

Spectre TOCSY : Région montrant les systèmes de spins des cycles B

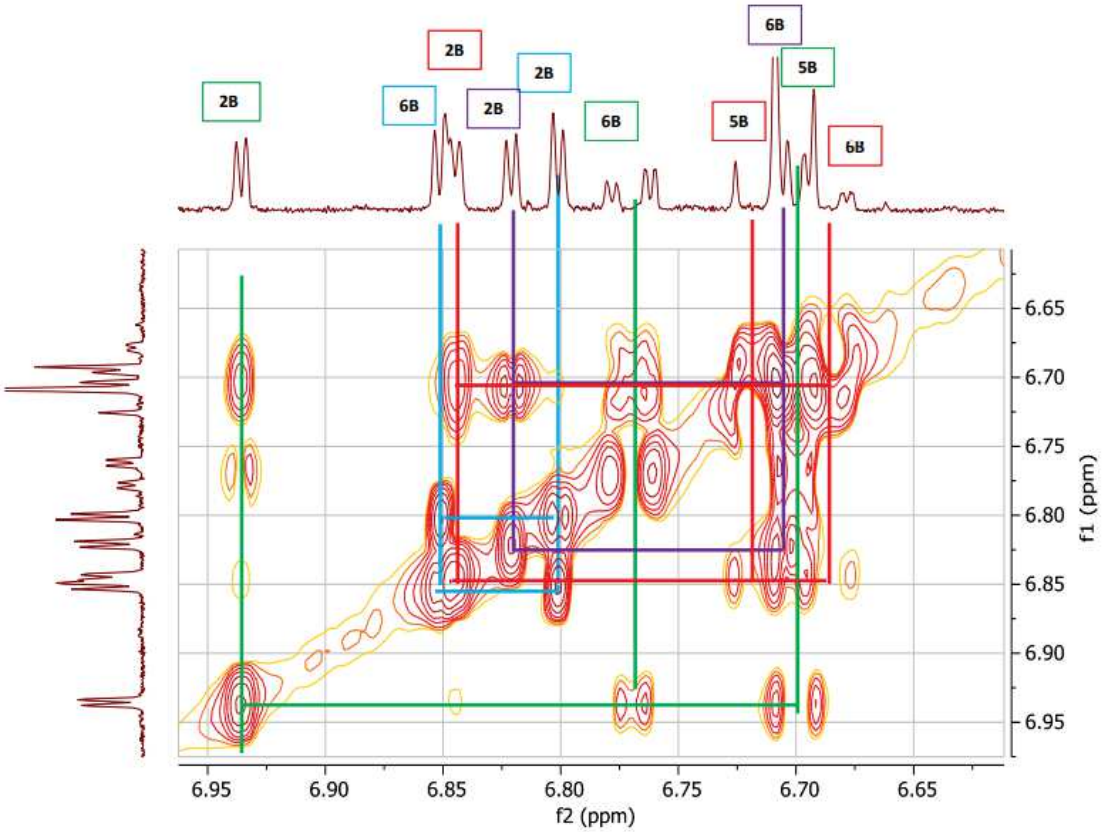

Spectre HSQC : Région des corrélations 1H-C13 des cycles B

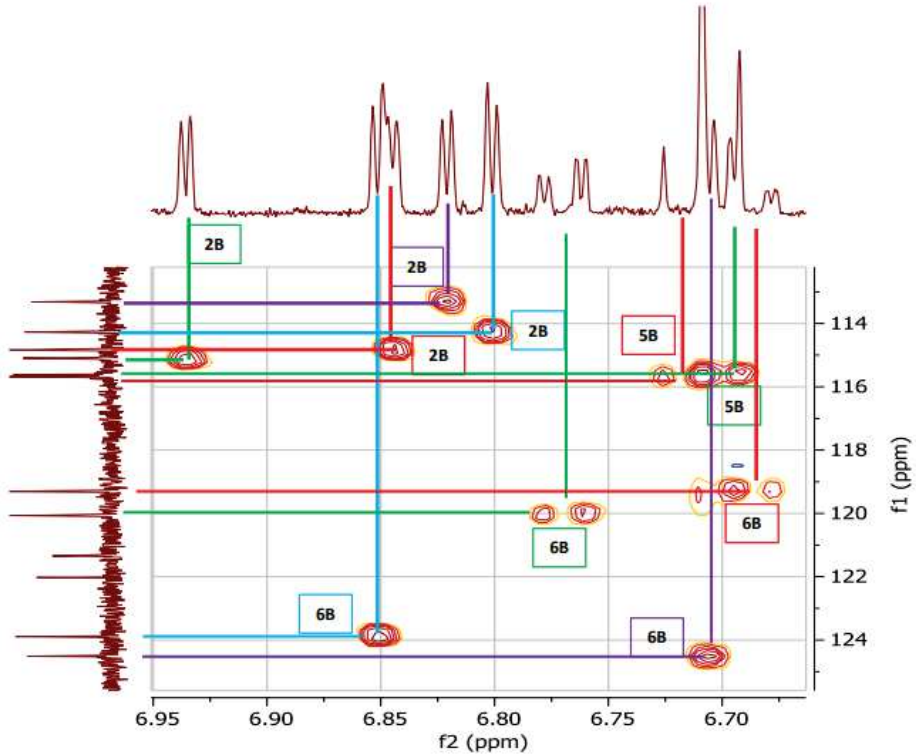

N4 - Acd6+Cd – 15°C– HMBC : Régions des corrélations impliquant les protons des cycles B (les attributions en bleu et vert correspondent à l'énantiomère 1, les attributions en rouge et violet à l'énantiomère 2)

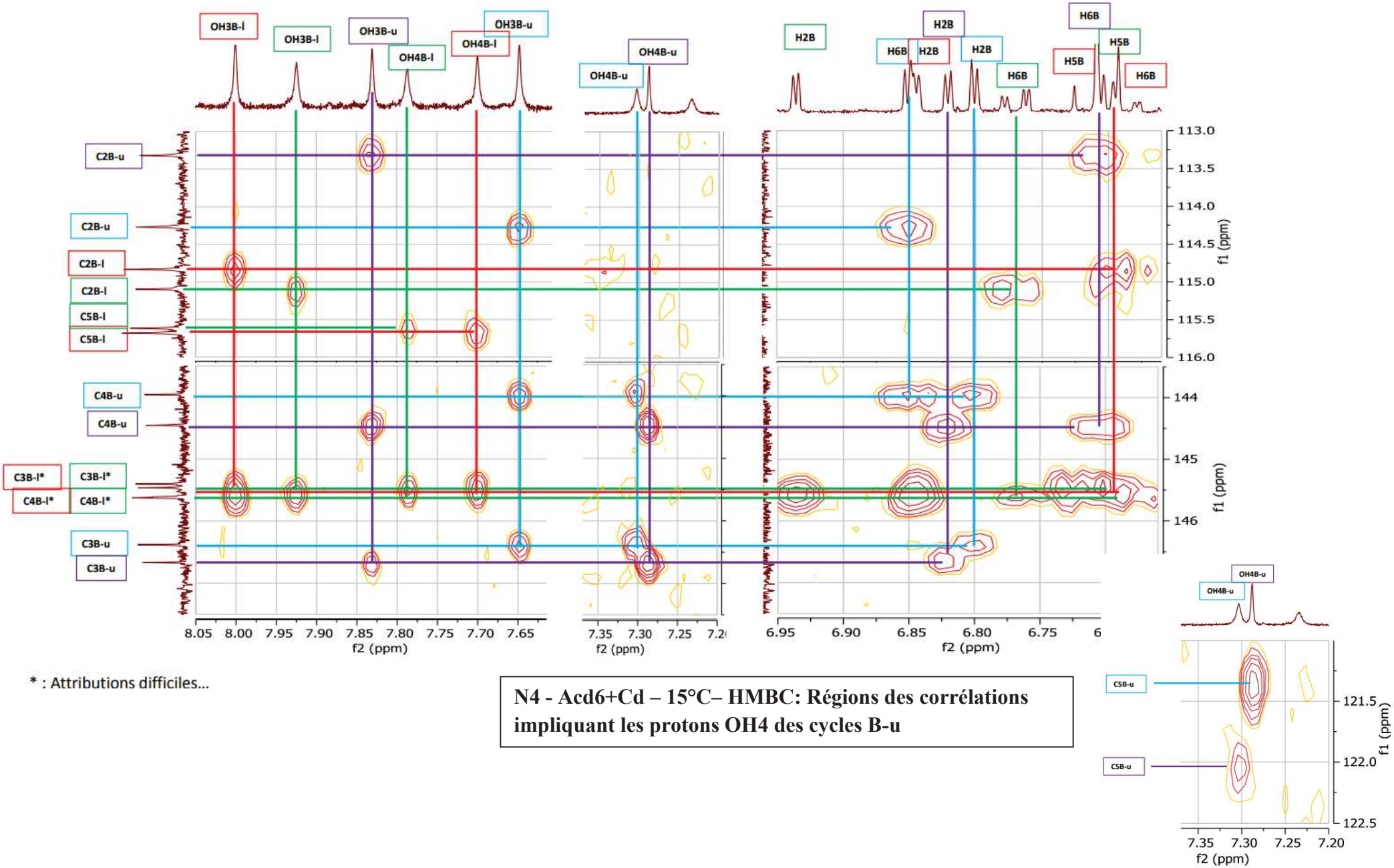

* : Attributions difficiles...

N4 - Acd6+Cd – 15°C– HMBC: Régions des corrélations impliquant les protons OH4 des cycles B-u

N4 - Acd6+Cd – 15°C– Attribution des C2C et H2C

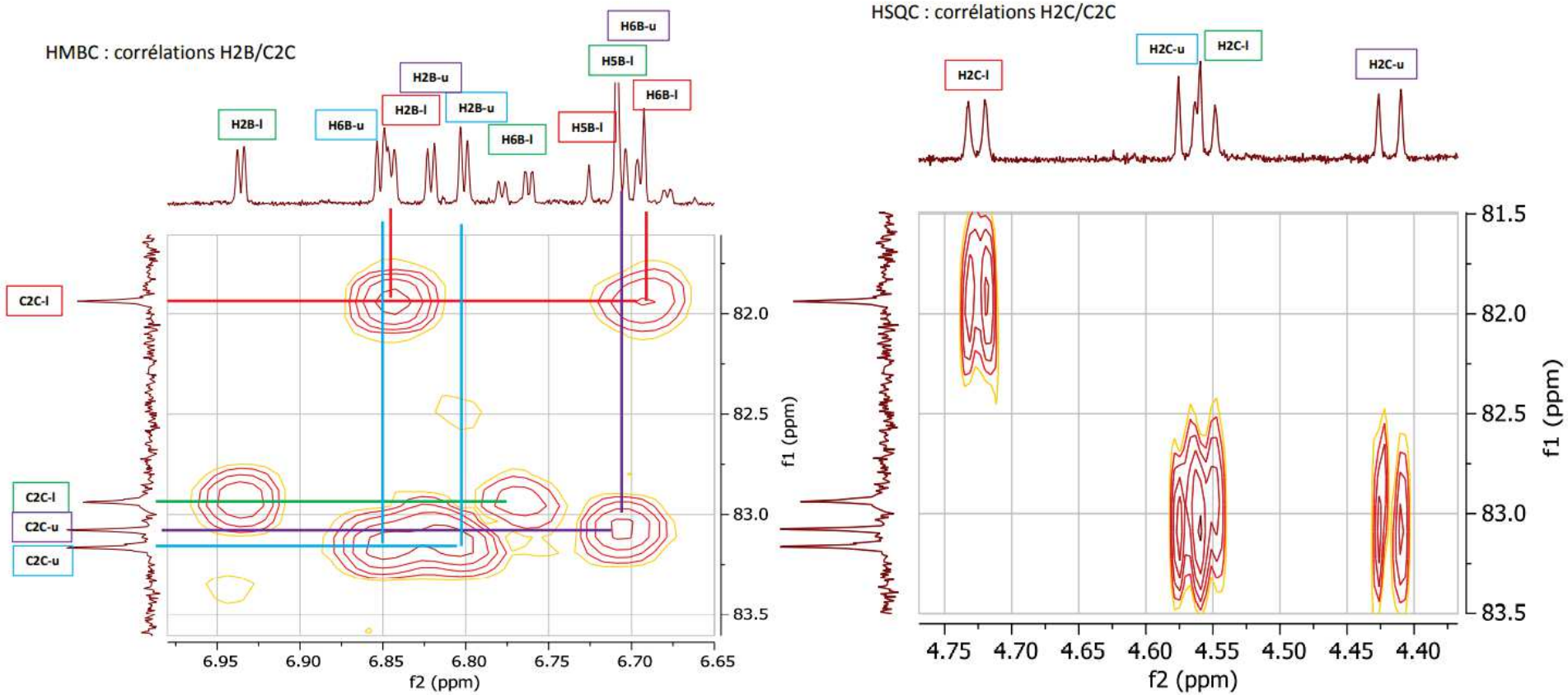

N4 - Acd6+Cd – 15°C– HMBC - Attribution des C4C et C3C

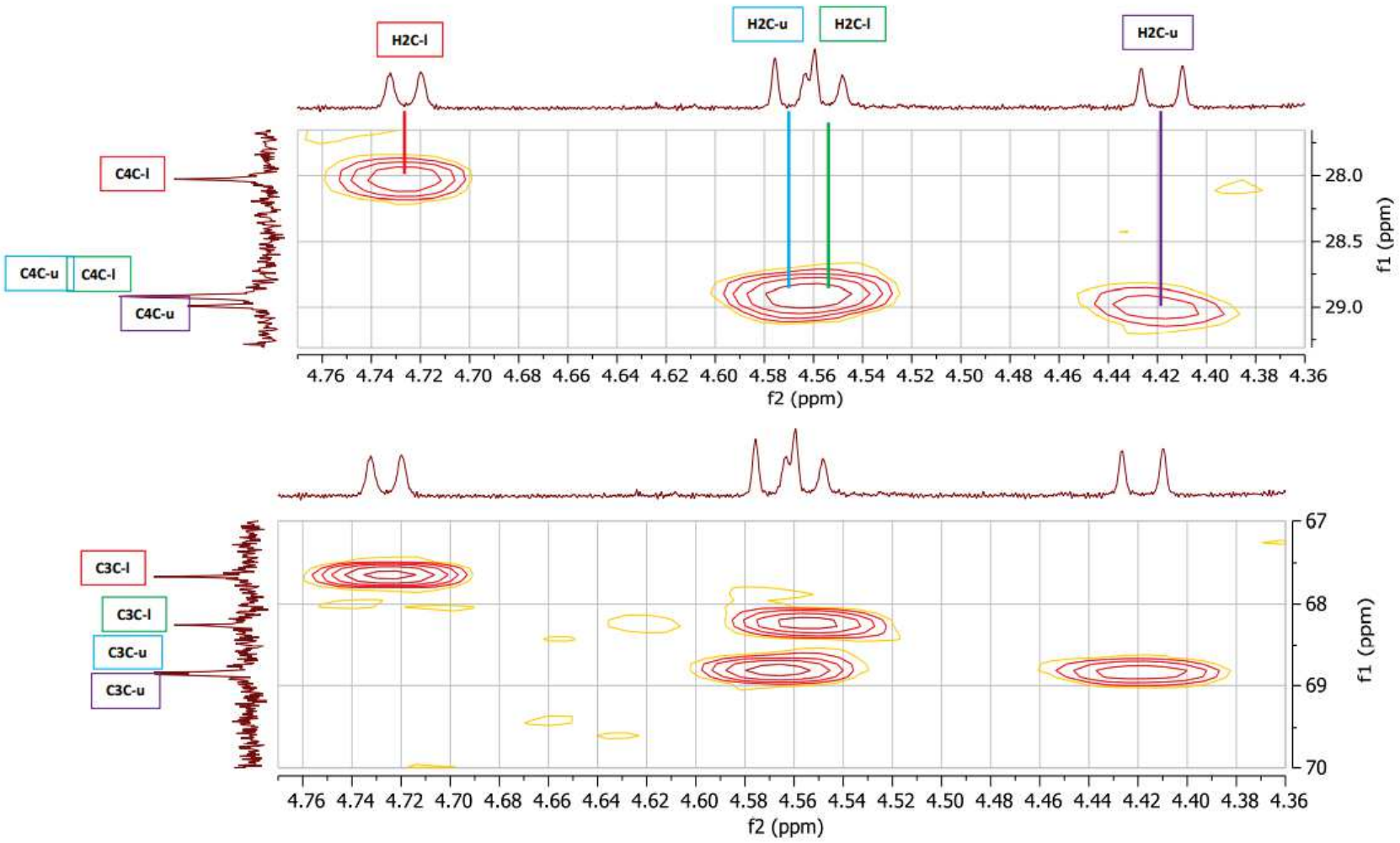

N4 Acd6+Cd – 15°C– TOCSY 2D 1H - Attribution des H3C et H4C

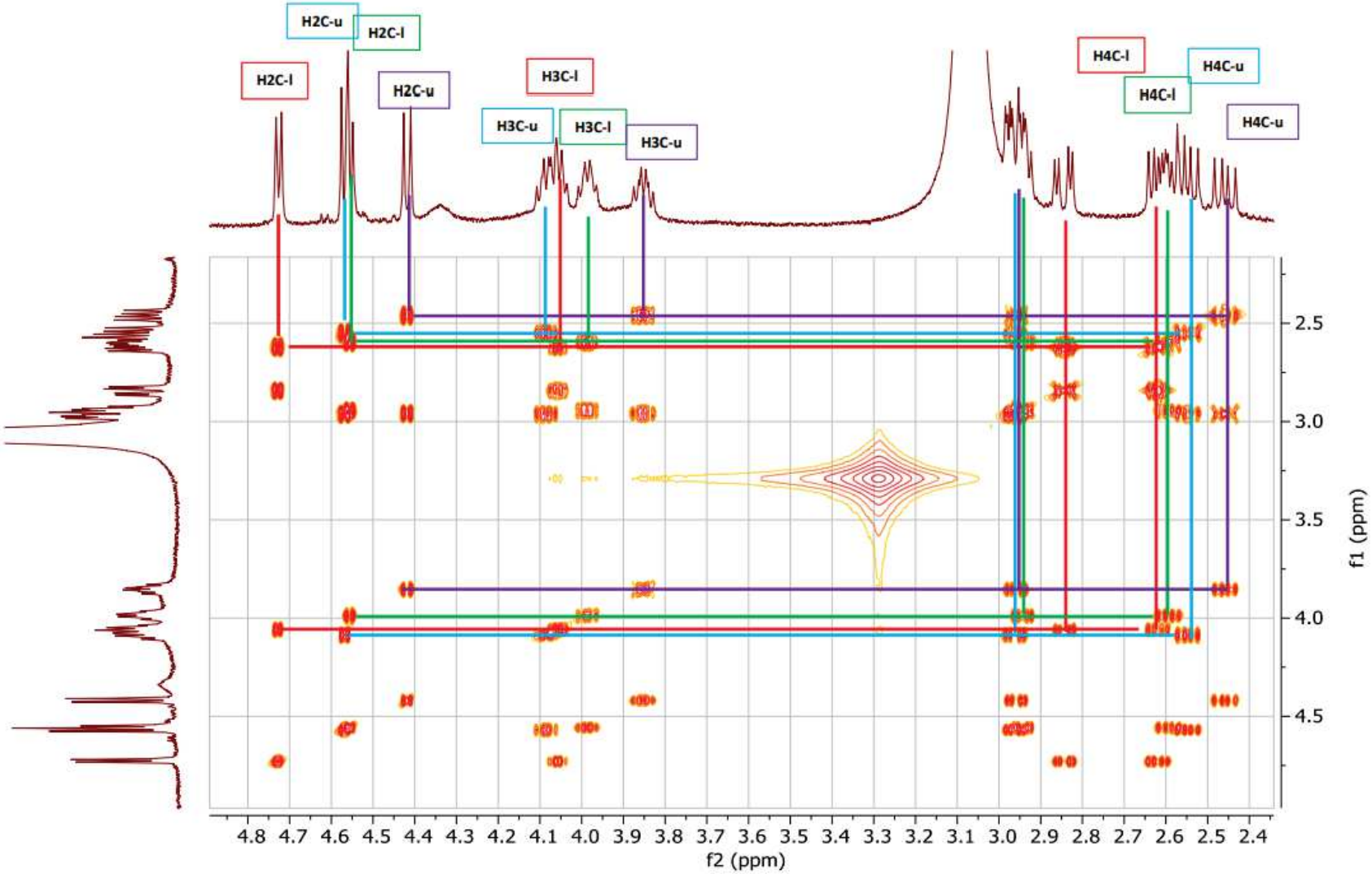

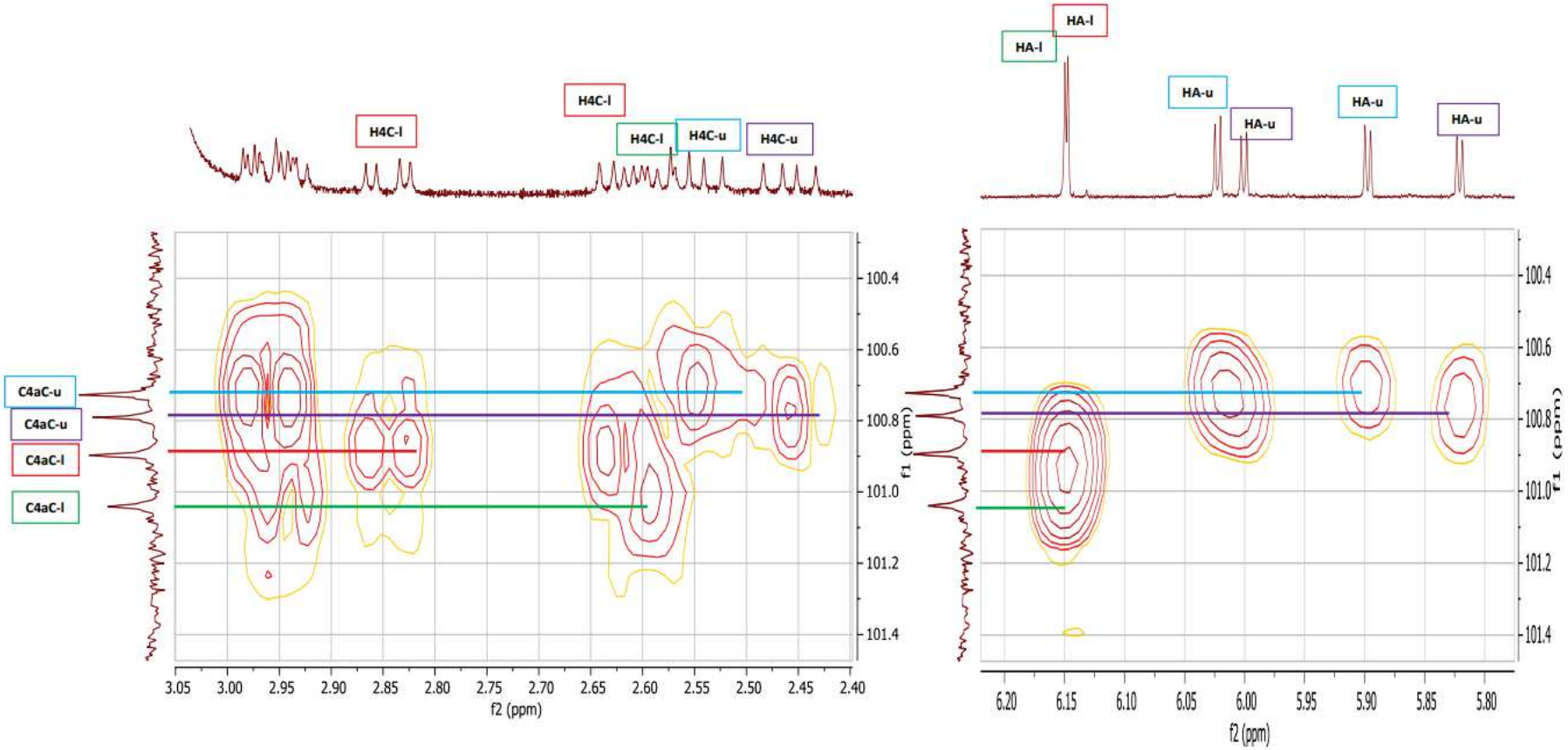
H4C-l
H4C-l
H4C-l
H4C-u
H4C-u
HA-l
HA-l
HA-u
HA-u
HA-u
HA-u
C4aC-u
C4aC-u
C4aC-l
C4aC-l
f1 (ppm)
f2 (ppm)
3.05 3.00 2.95 2.90 2.85 2.80 2.75 2.70 2.65 2.60 2.55 2.50 2.45 2.40
100.4 100.6 100.8 101.0 101.2 101.4
6.20 6.15 6.10 6.05 6.00 5.95 5.90 5.85 5.80

N4 Acd6+Cd – 15°C – TOCSY et ROESY

Spectre 1H TOCSY
Région montrant les systèmes de spins des cycles A

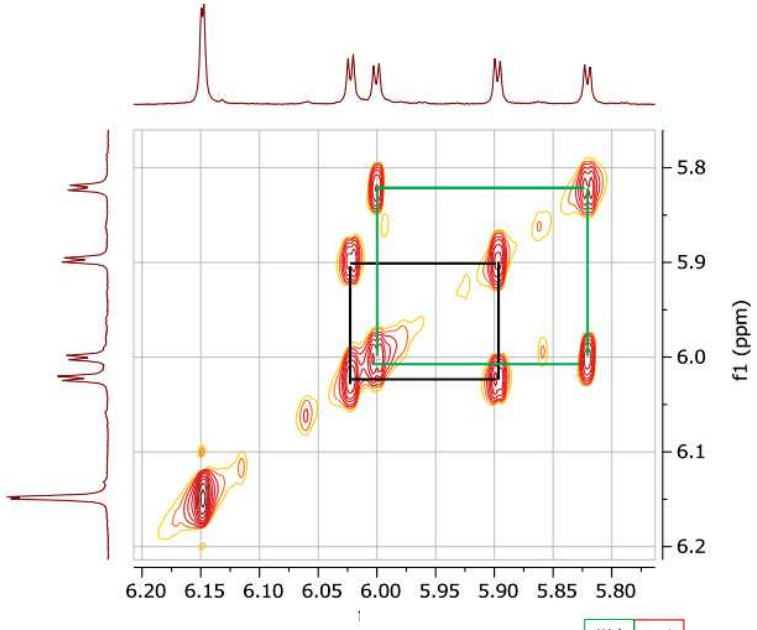

Spectre ROESY
Des corrélations ROEs négatives sont observées entre les protons des cycles A, signe d'un échange chimique, donc présence de conformères

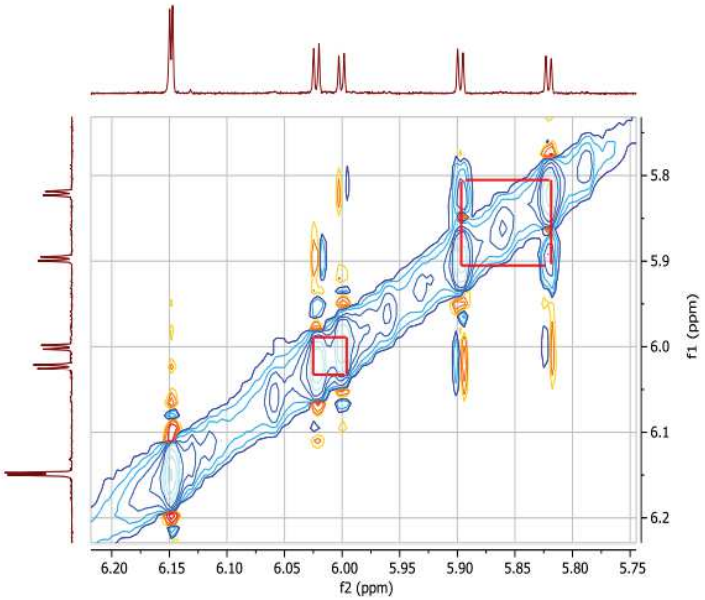

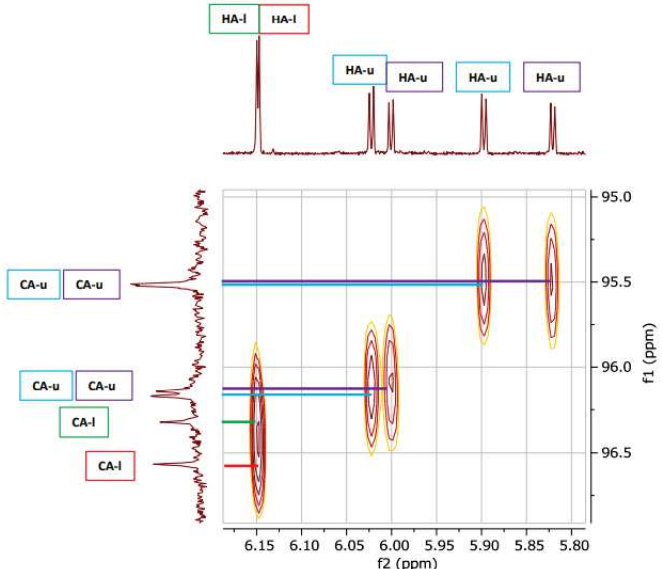

N4- Acd6+Cd – 15°C. Spectre HSQC : Région des corrélations 1H-13C des cycles A

N4 Acd6+Cd – 15°C– HMBC - Attribution protons (H et OH) et carbones des cycles A.

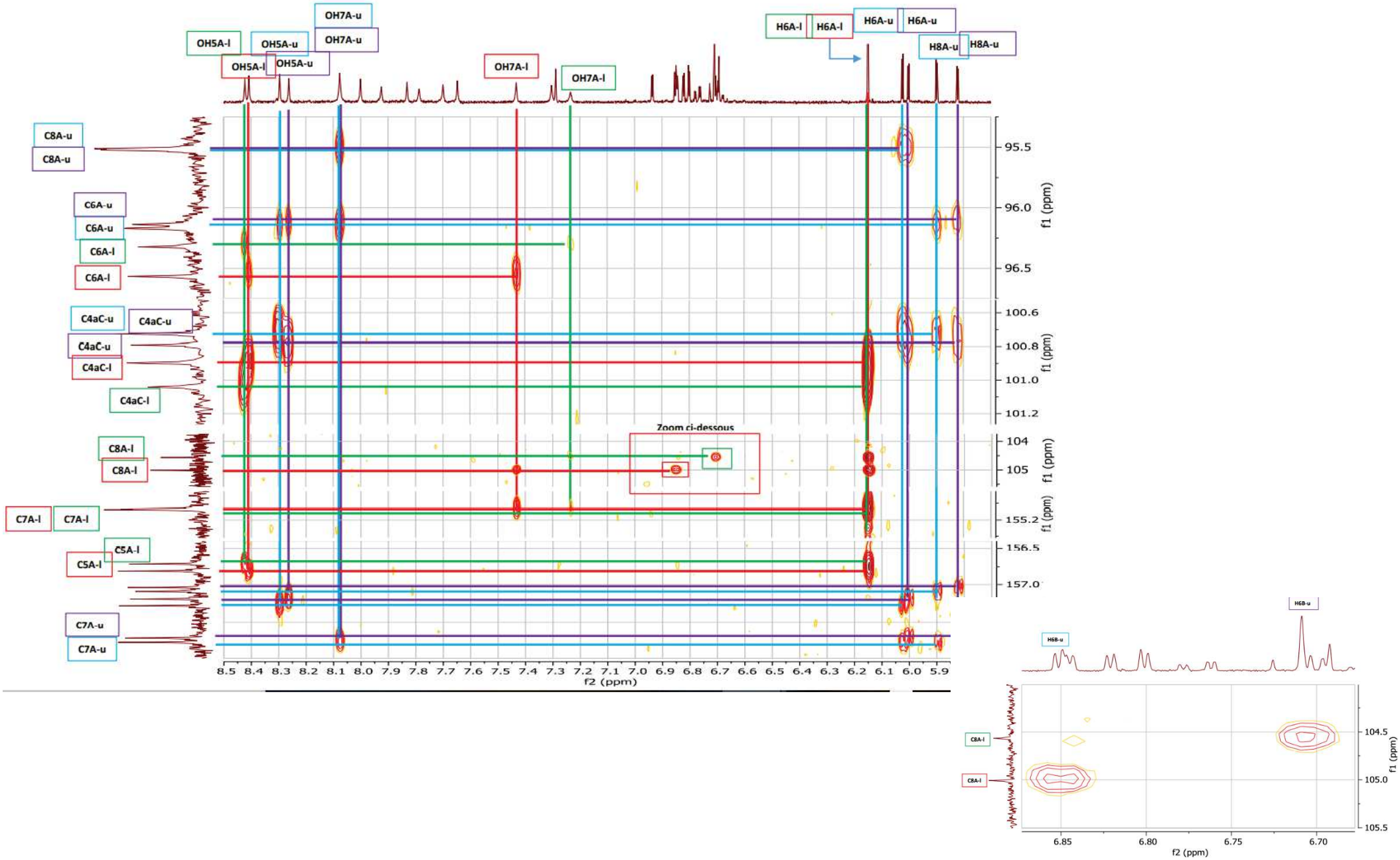

N4 Acd6+Cd – 15°C – Le spectre 1H TOCSY montre les corrélations entre les protons H2 et H3 des cycles C (C1,C2, C3,C4). Sur le spectre ROESY, des corrélations ROEs négatives sont observées entre les protons de ces cycles, signe d'un échange chimique, donc de la présence de conformères

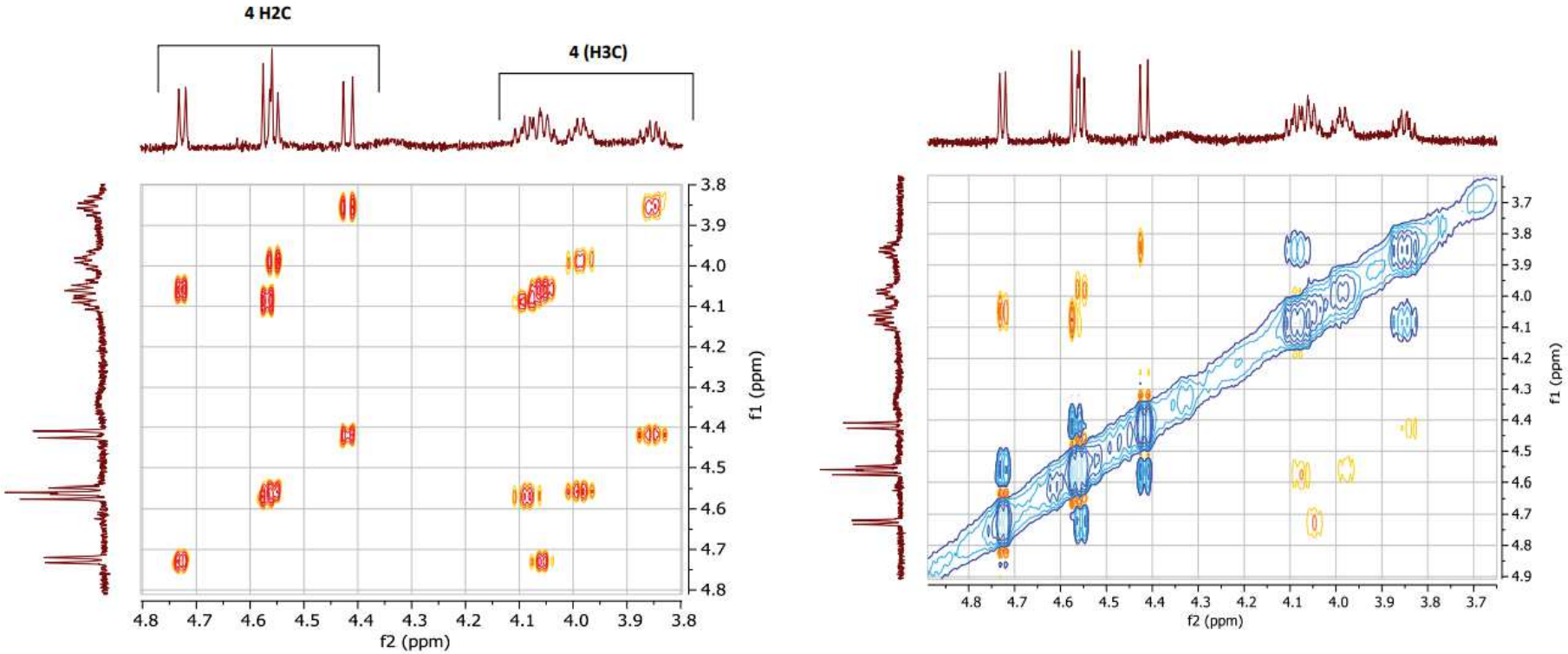

N6 – Acd6 + Cd – 25°C – HMBC 1H/13C

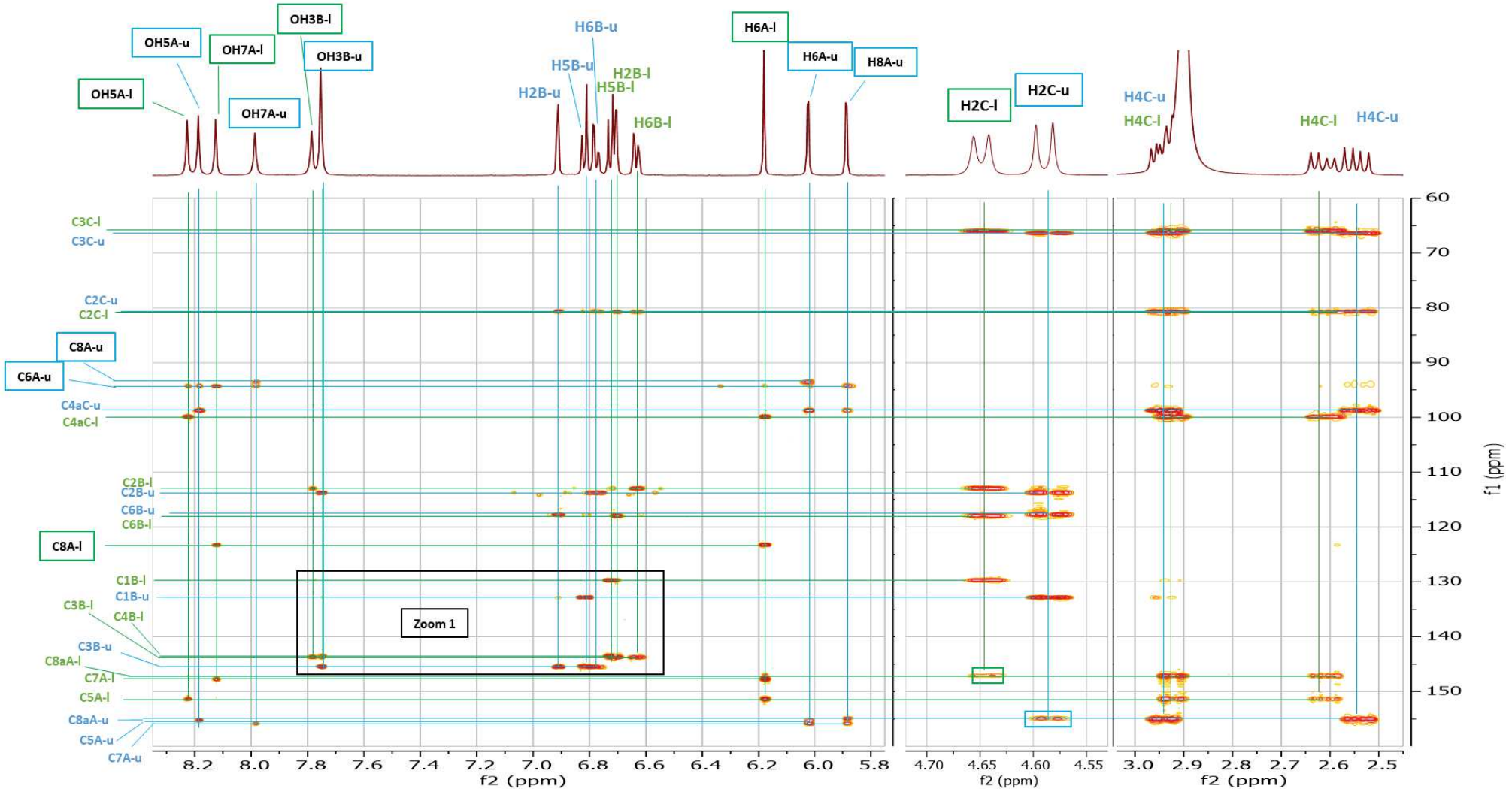
OH5A-u
OH7A-l
OH3B-l
OH3B-u
OH5A-l
OH7A-u
H6B-u
H5B-u
H2B-l
H5B-l
H2B-u
H6B-l
H6A-l
H6A-u
H8A-u
H2C-l
H2C-u
H4C-u
H4C-l
H4C-l
H4C-u
C3C-l
C3C-u
C2C-u
C2C-l
C8A-u
C6A-u
C4aC-u
C4aC-l
C2B-l
C2B-u
C6B-u
C6B-l
C8A-l
C1B-l
C1B-u
C3B-l
C4B-l
C3B-u
C8aA-l
C7A-l
C5A-l
C8aA-u
C5A-u
C7A-u
Zoom 1
8.2 8.0 7.8 7.6 7.4 7.2 7.0 6.8 6.6 6.4 6.2 6.0 5.8
f2 (ppm)
4.70 4.65 4.60 4.55
f2 (ppm)
3.0 2.9 2.8 2.7 2.6 2.5
f2 (ppm)
60 70 80 90 100 110 120 130 140 150
f1 (ppm)

N6- Acd6-Cd5ul-25°C - HMBC 1H/13C – zoom 1

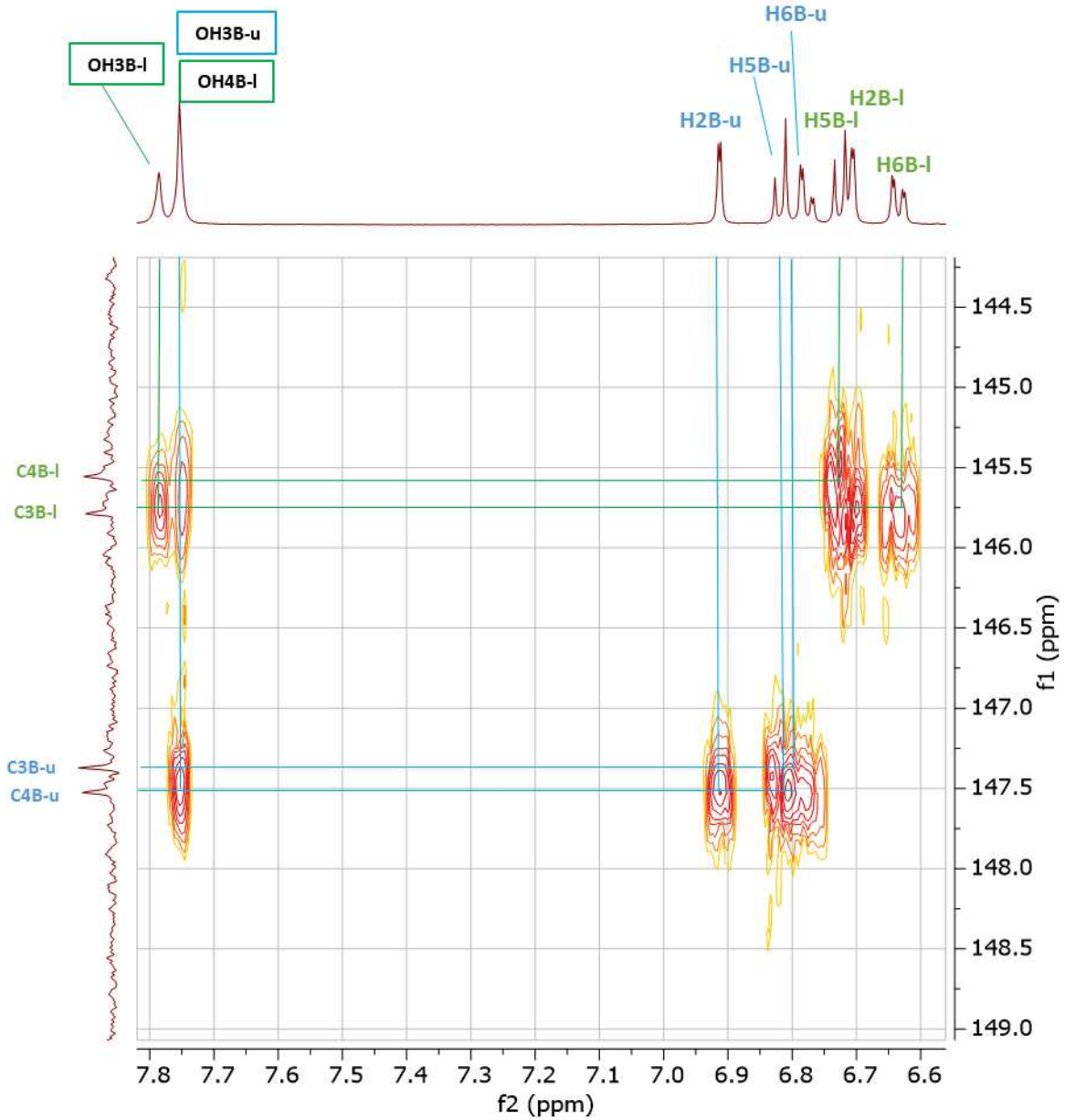

N6 15°C - Acd6+ Cd-5ul – Région du spectres ROESY montrant une corrélation inter-unité

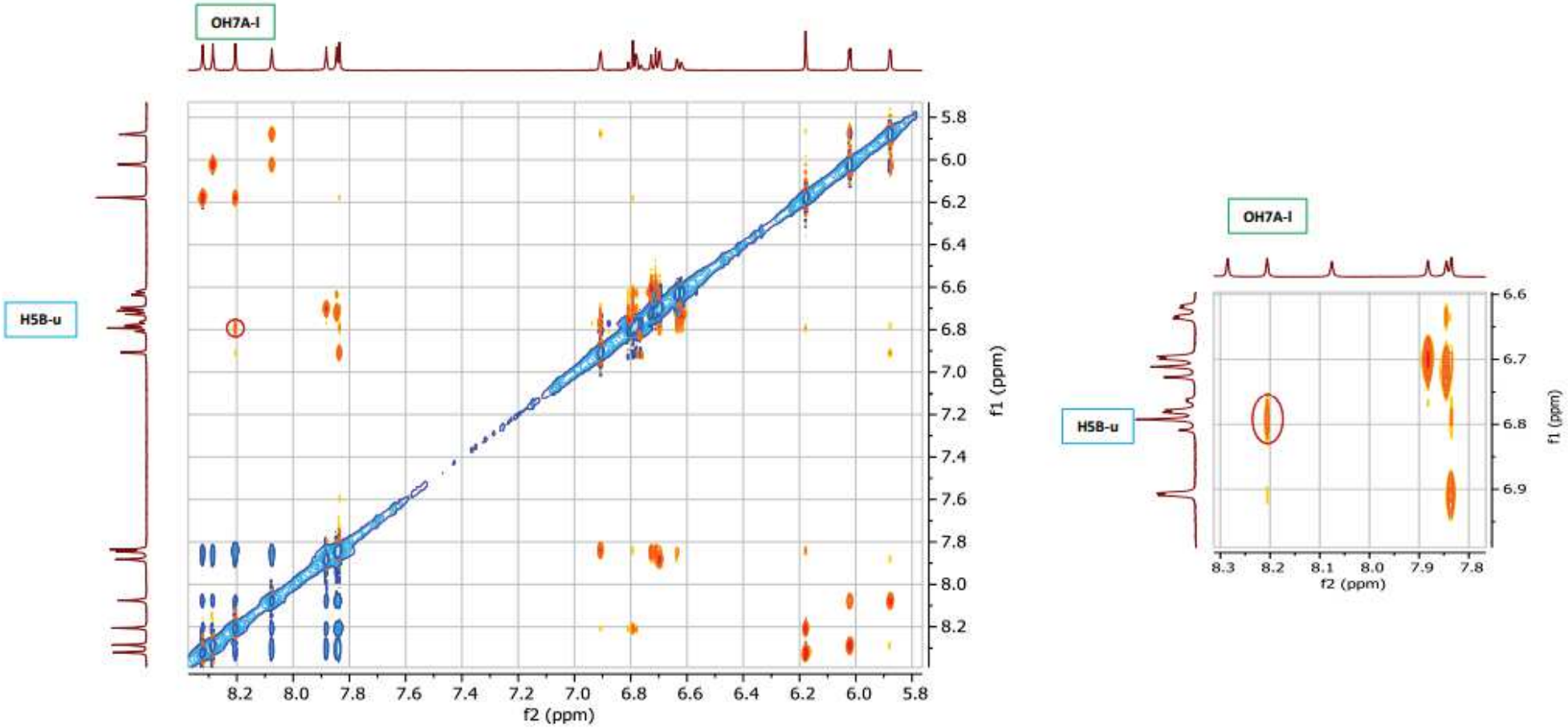

N6 Acd6 – 25°C - HMBC – Région 13C ~20-110ppm

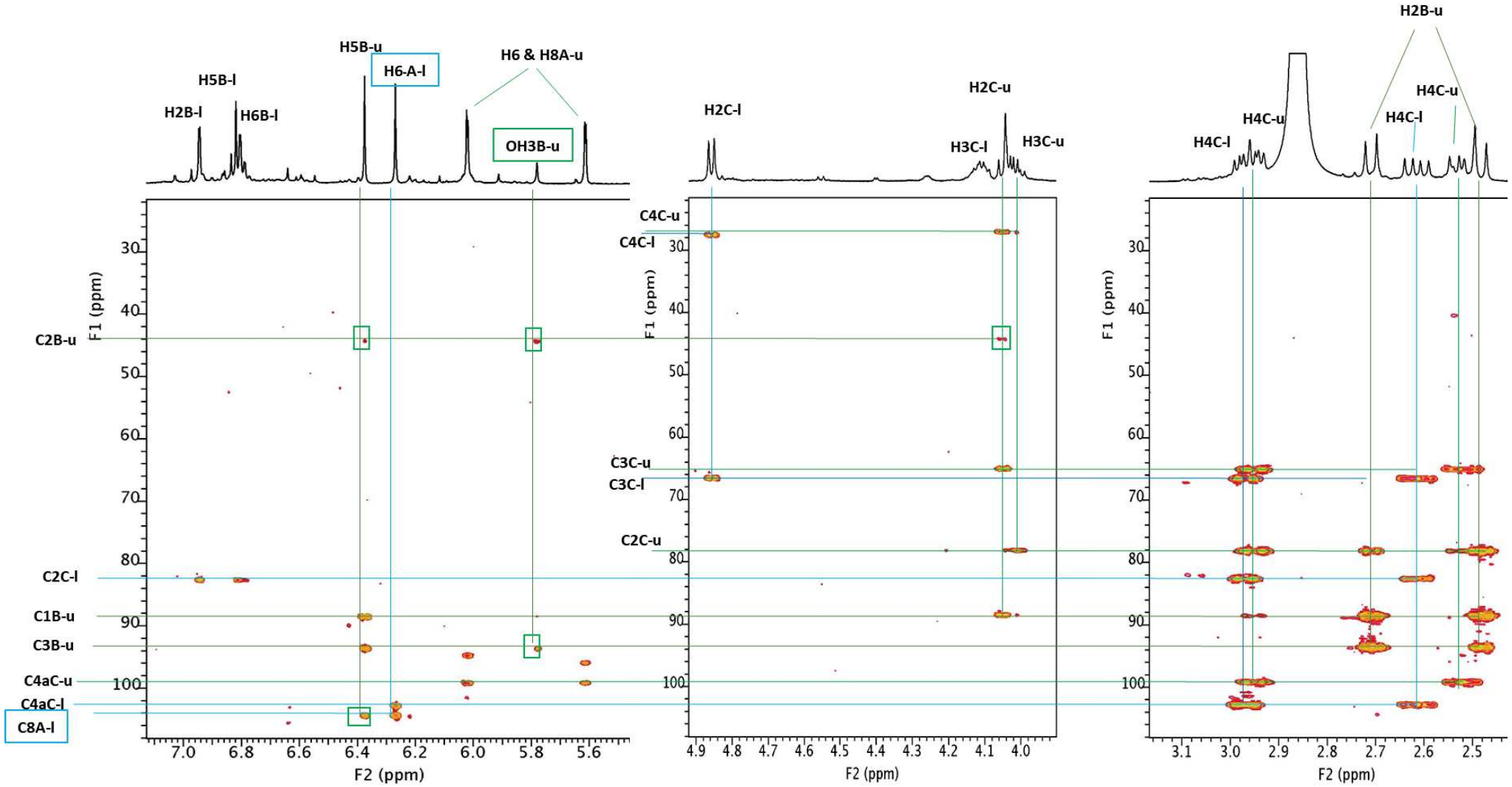

N8 Acd6 – 25°C - HMBC – Région 13C ~ 110-193ppm

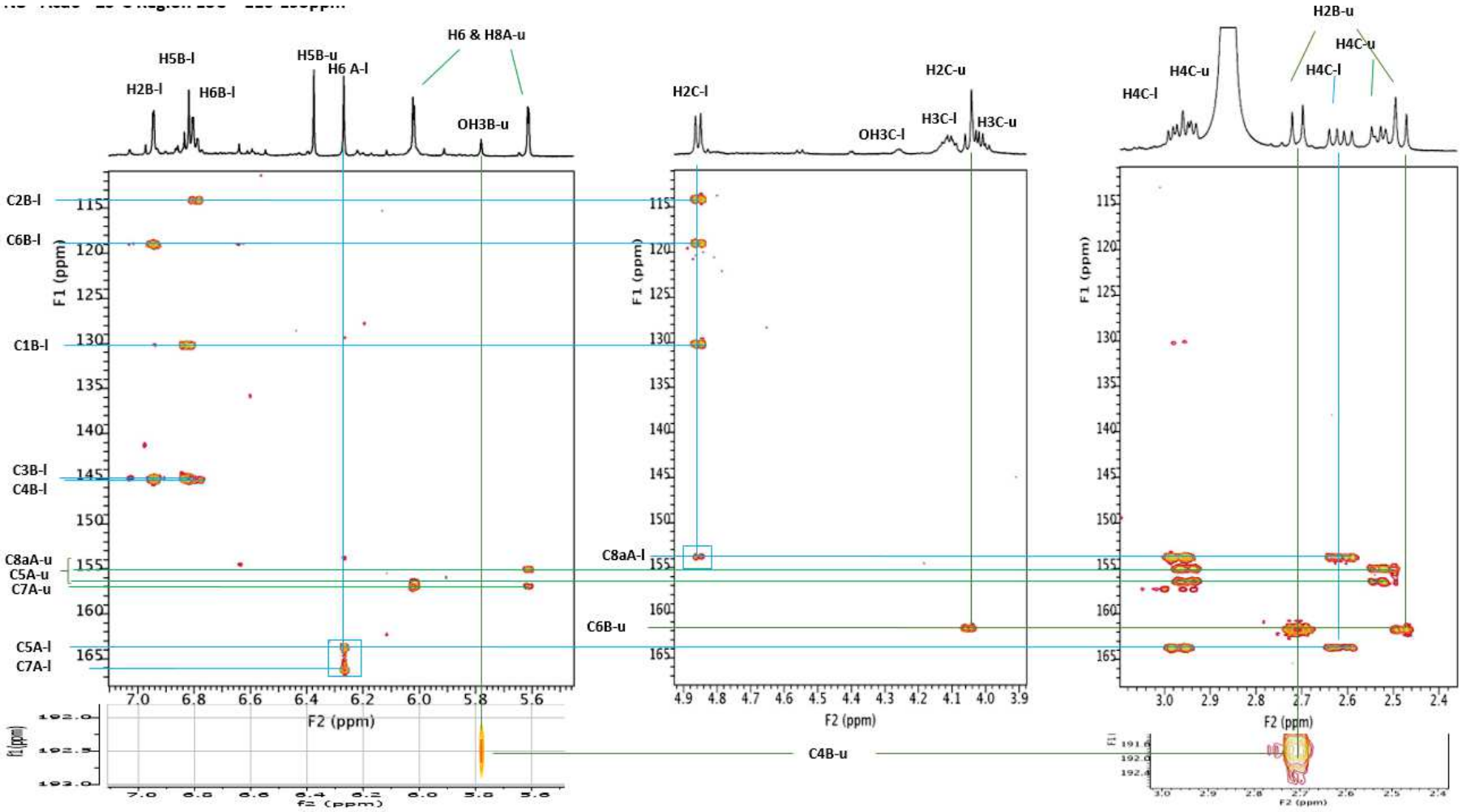

N8 Acd6 – 25°C - HMBC – Région 13C ~ 110-193ppm

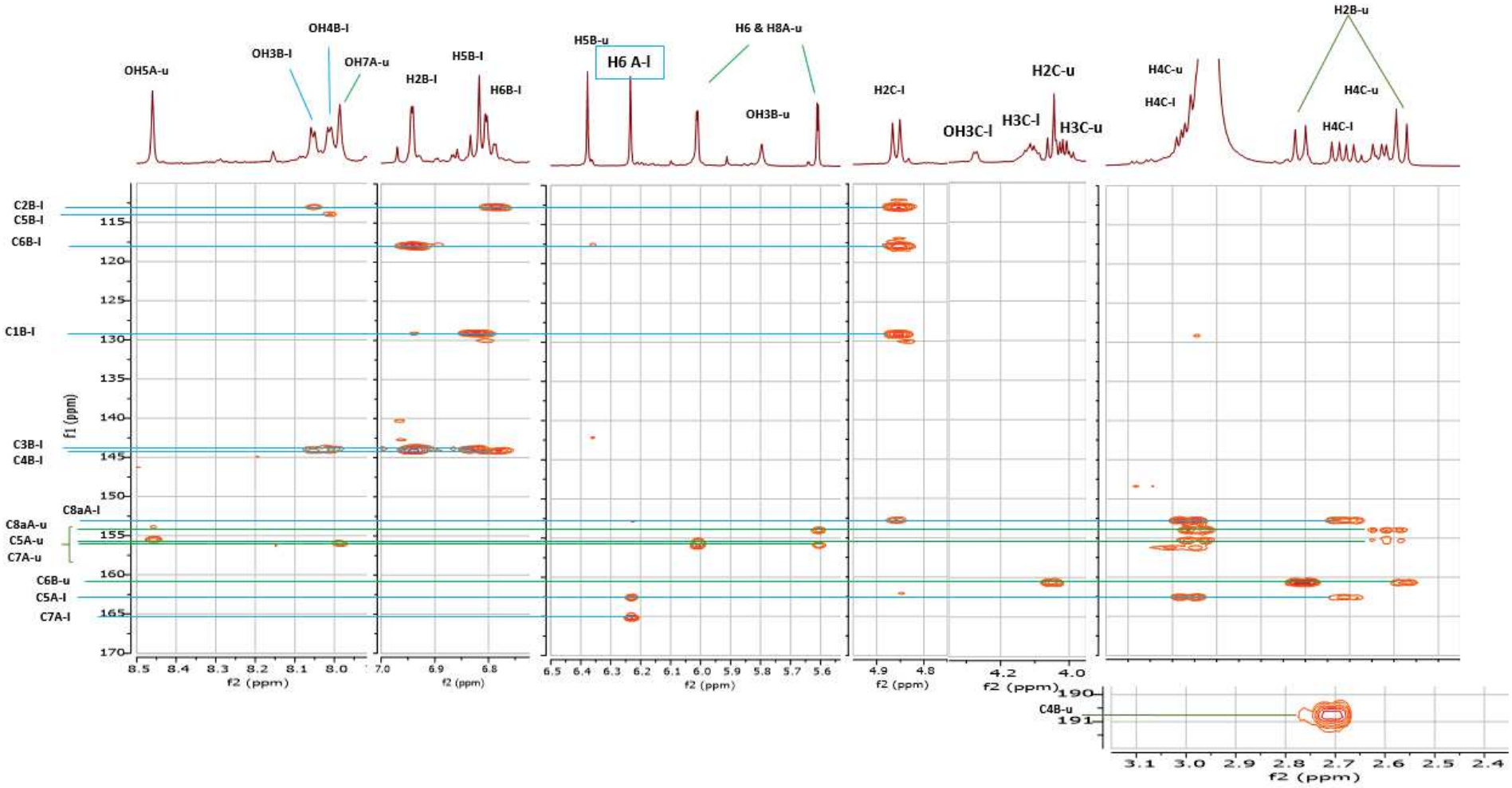

N8 Acd6 – Cd - 15°C - ROESY – Région 13C ~ 110-193ppm

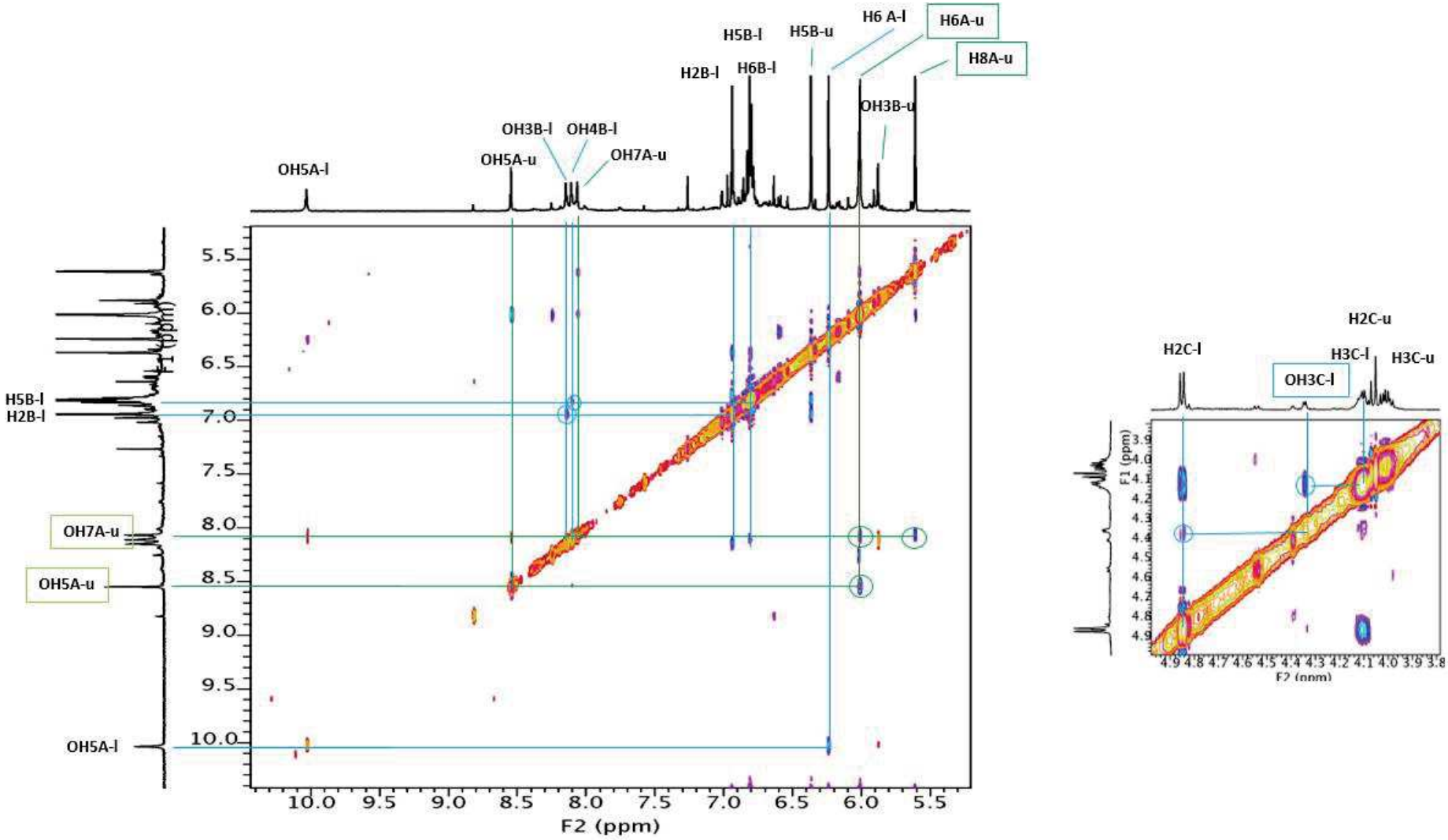

N8 Acd6 – Cd - 25°C - ROESY

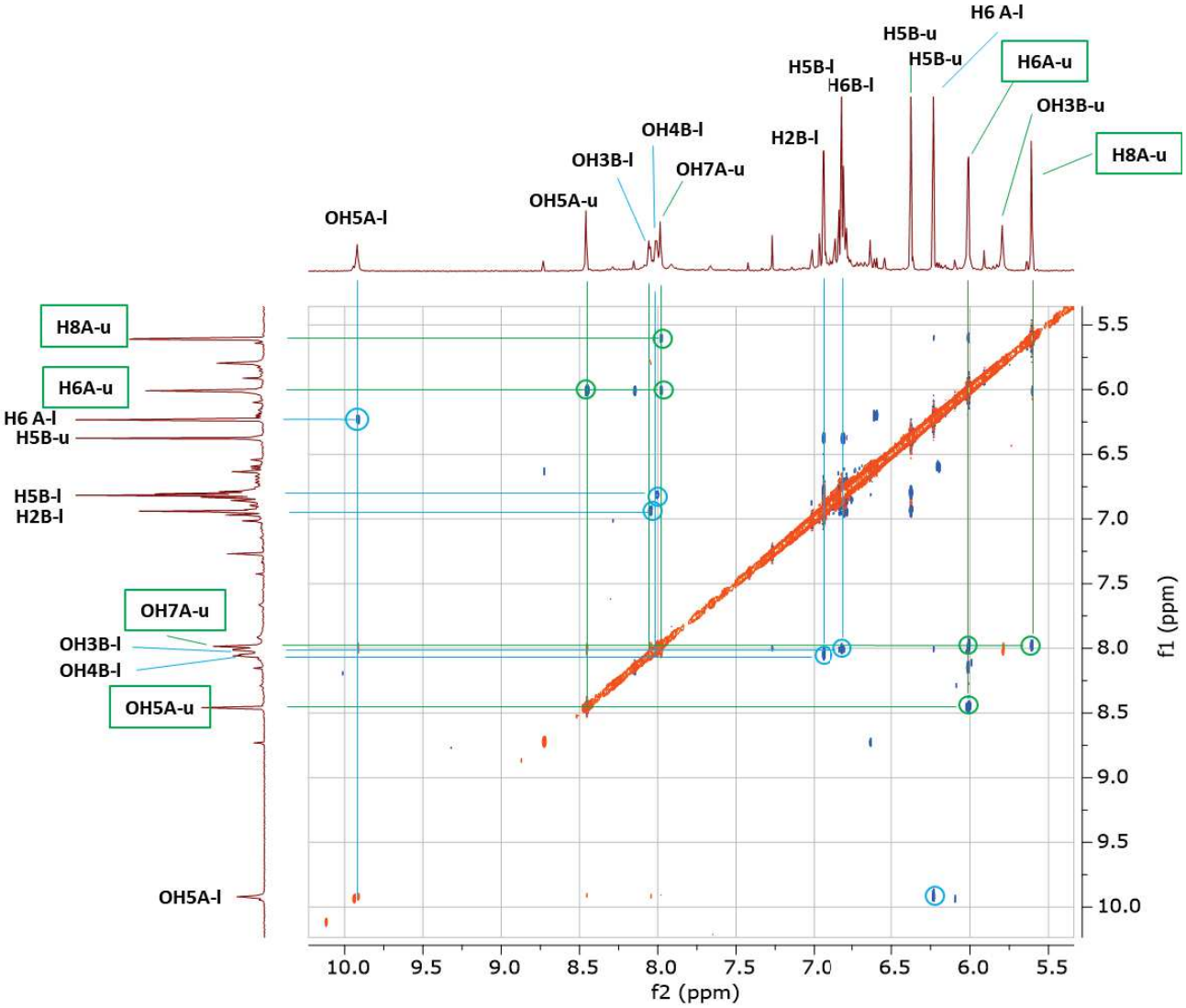
H6 A-l
H5B-u
H5B-u
H6A-u
H5B-l
H6B-l
OH3B-u
OH4B-l
H2B-l
H8A-u
OH3B-l
OH7A-u
OH5A-u
OH5A-l
H8A-u
H6A-u
H6 A-l
H5B-u
H5B-l
H2B-l
OH7A-u
OH3B-l
OH4B-l
OH5A-u
OH5A-l
10.0
9.5
9.0
8.5
8.0
7.5
7.0
6.5
6.0
5.5
f2 (ppm)
f1 (ppm)

Article 4 *- UHPLC-Q-Orbitrap /MS² identification of (+)-Catechin oxidation reaction dimeric products in red wines and grape seed extracts: Effect of grape maturation and wine age*

- ***Figure S1 -*** *Natural dimers structures. (a) procyanidin B1 with (-)-epicatechin and (+)-catechin units; (b) procyanidin B2 with two (-)-epicatechin units ; (c) procyanidin B3 with two (+)-catechin units ; (d) procyanidin B4 with (+)-catechin and (-)-epicatechin units.*

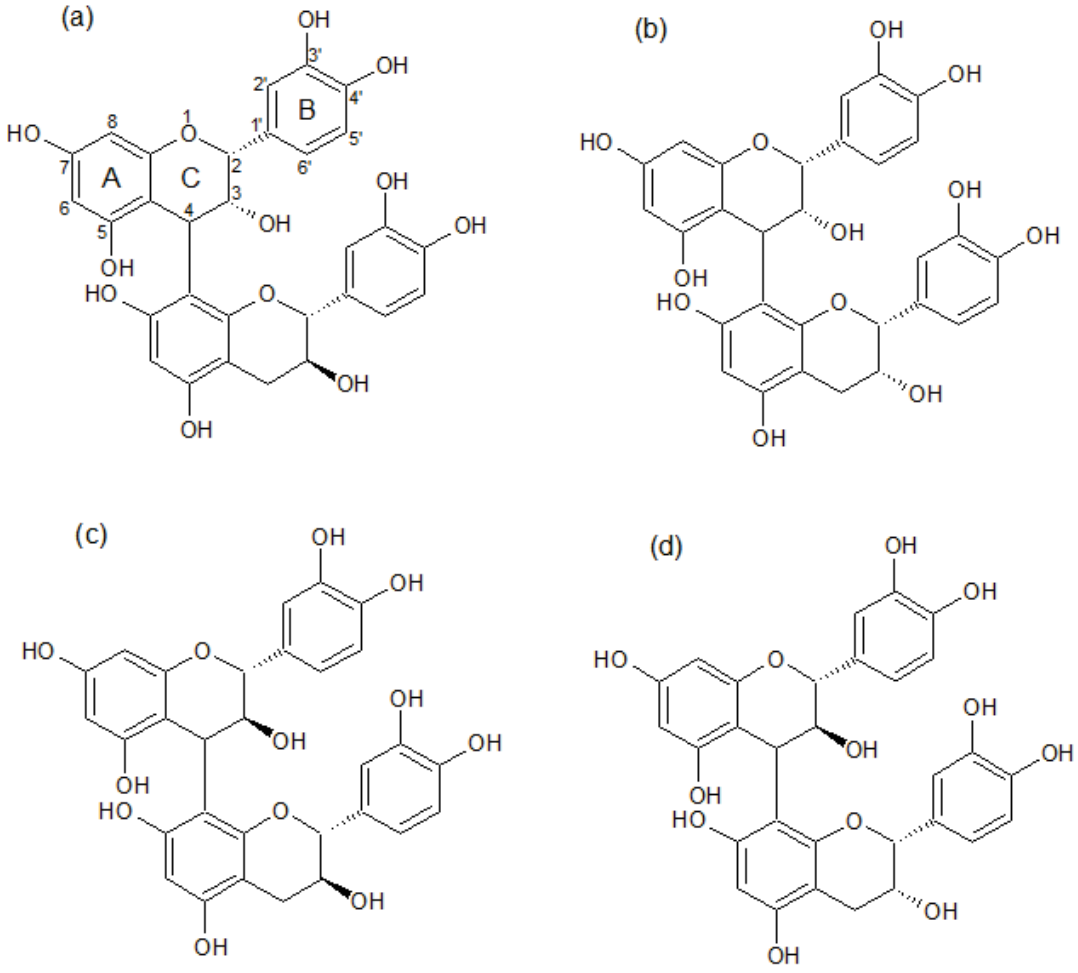

- ***Figure S2*** *- Representative tandem mass spectra in positive ion mode of natural procyanidins B2 (a); B3 (b) and B4 (c).*

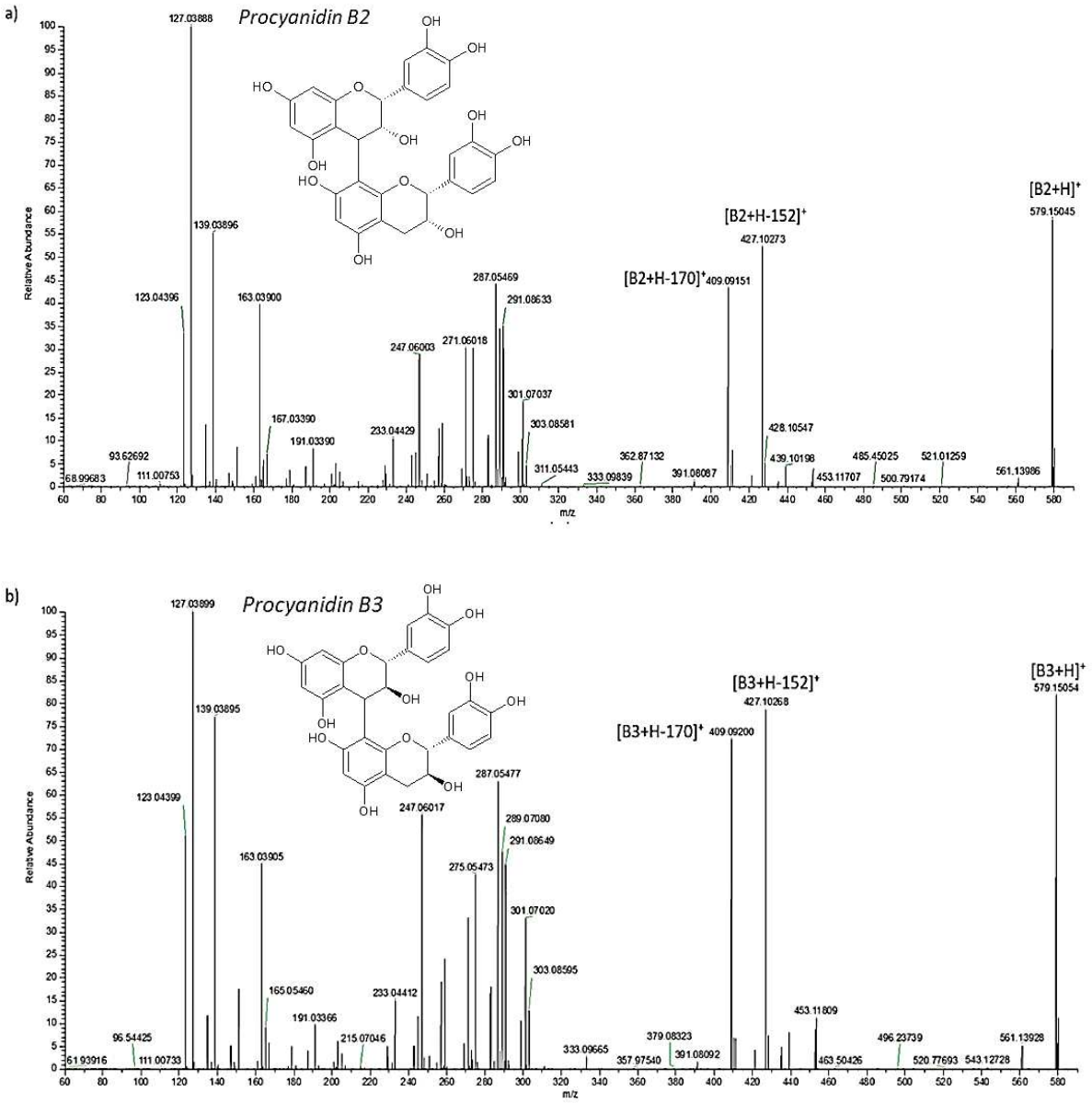

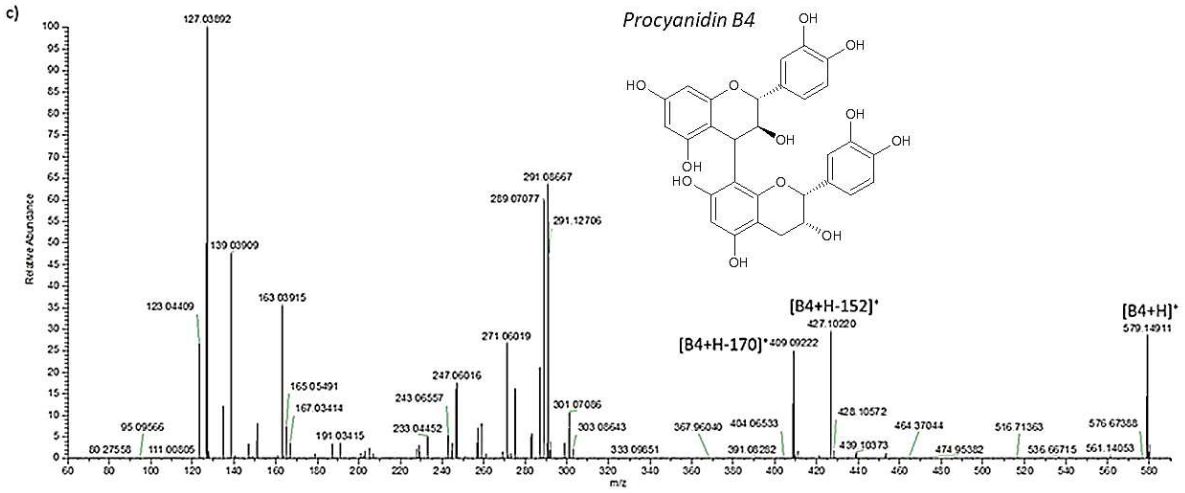

- ***Figure S3*** *- Representative tandem mass spectra in positive ion mode of oxidation dimers N1a (a); N1b (b) ; N3 (c) ; N4 (d) ; N5 (e) ; N6 (f) and N7 (g) with SNCE, 30% midpoint, 15% range and three steps*

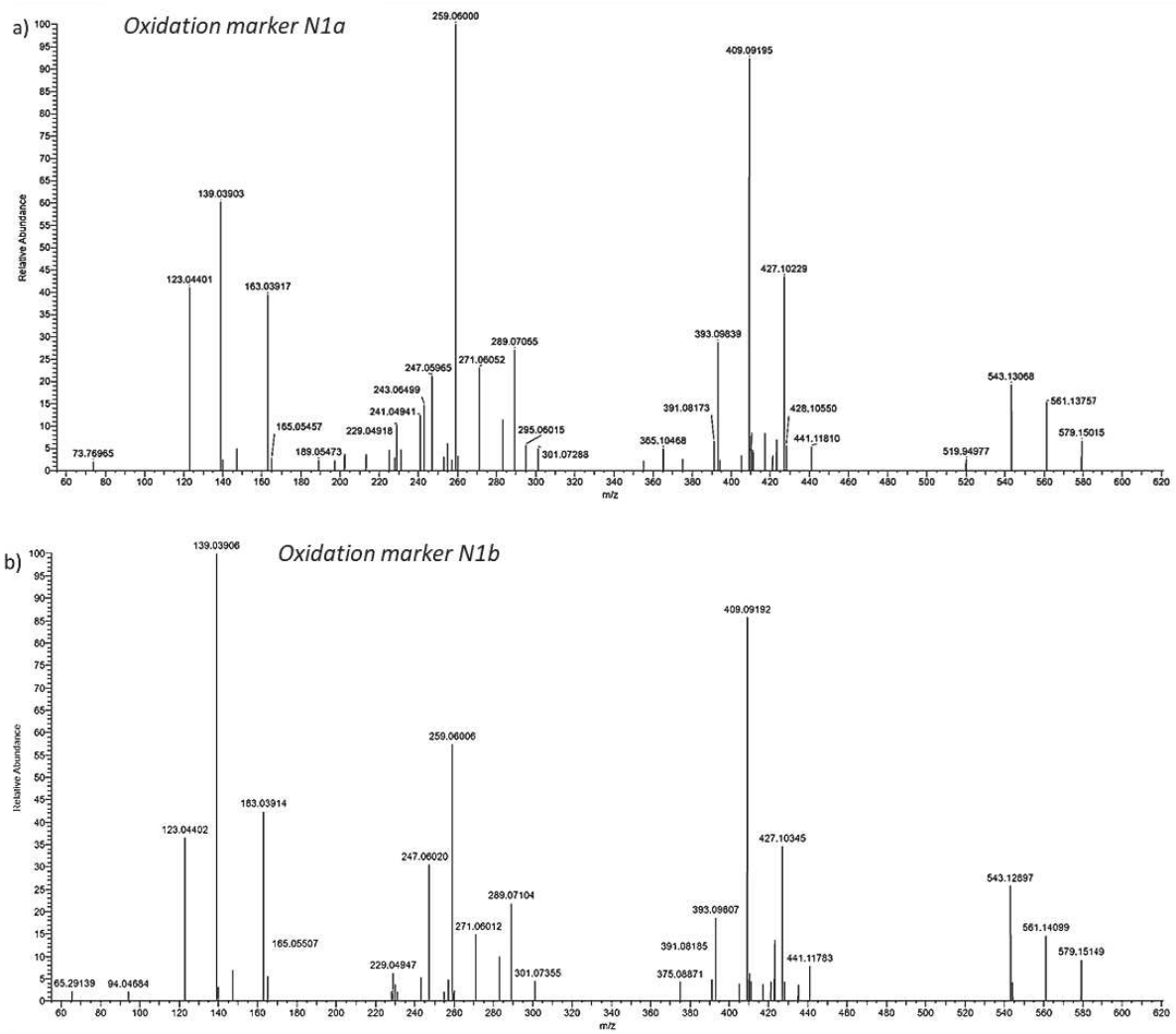

c)

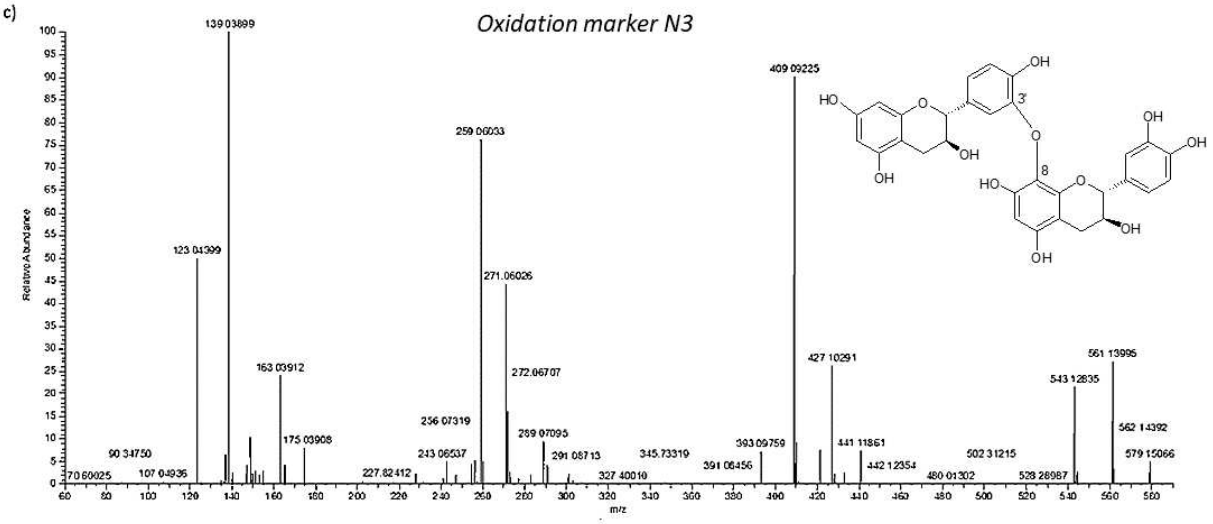
Oxidation marker N3
Relative Abundance
m/z
139.03899
409.09225
259.06033
123.04399
271.06026
163.03912
272.06707
427.10291
561.13995
543.12835
256.07319
175.03908
562.14392
579.15066
393.09759
441.11861
90.34750
243.06537
289.07095
291.08713
345.73319
502.31215
107.04936
227.82412
327.40019
391.06456
442.12354
480.01302
528.28987
70.60025
OH
HO
3'
8

d)

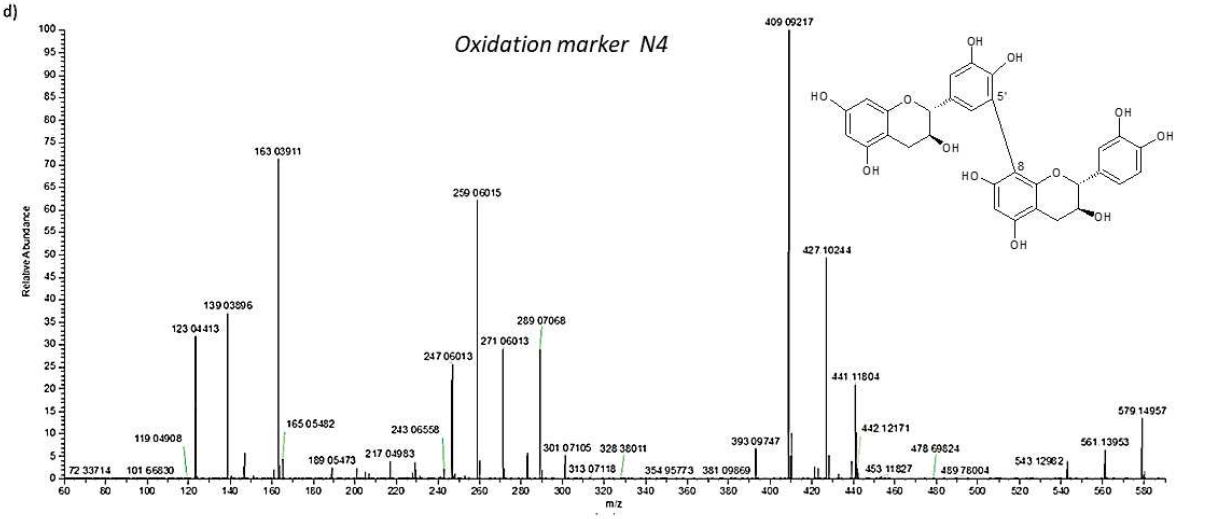
Oxidation marker N4
Relative Abundance
m/z
409.09217
163.03911
259.06015
427.10244
139.03896
123.04413
289.07068
271.06013
247.06013
441.11804
579.14957
165.05482
119.04908
243.06558
442.12171
393.09747
561.13953
301.07105
328.38011
478.69824
543.12982
72.33714
101.66830
189.05473
217.04983
313.07118
354.95773
381.09869
453.11827
489.78004
5'
8
OH
HO

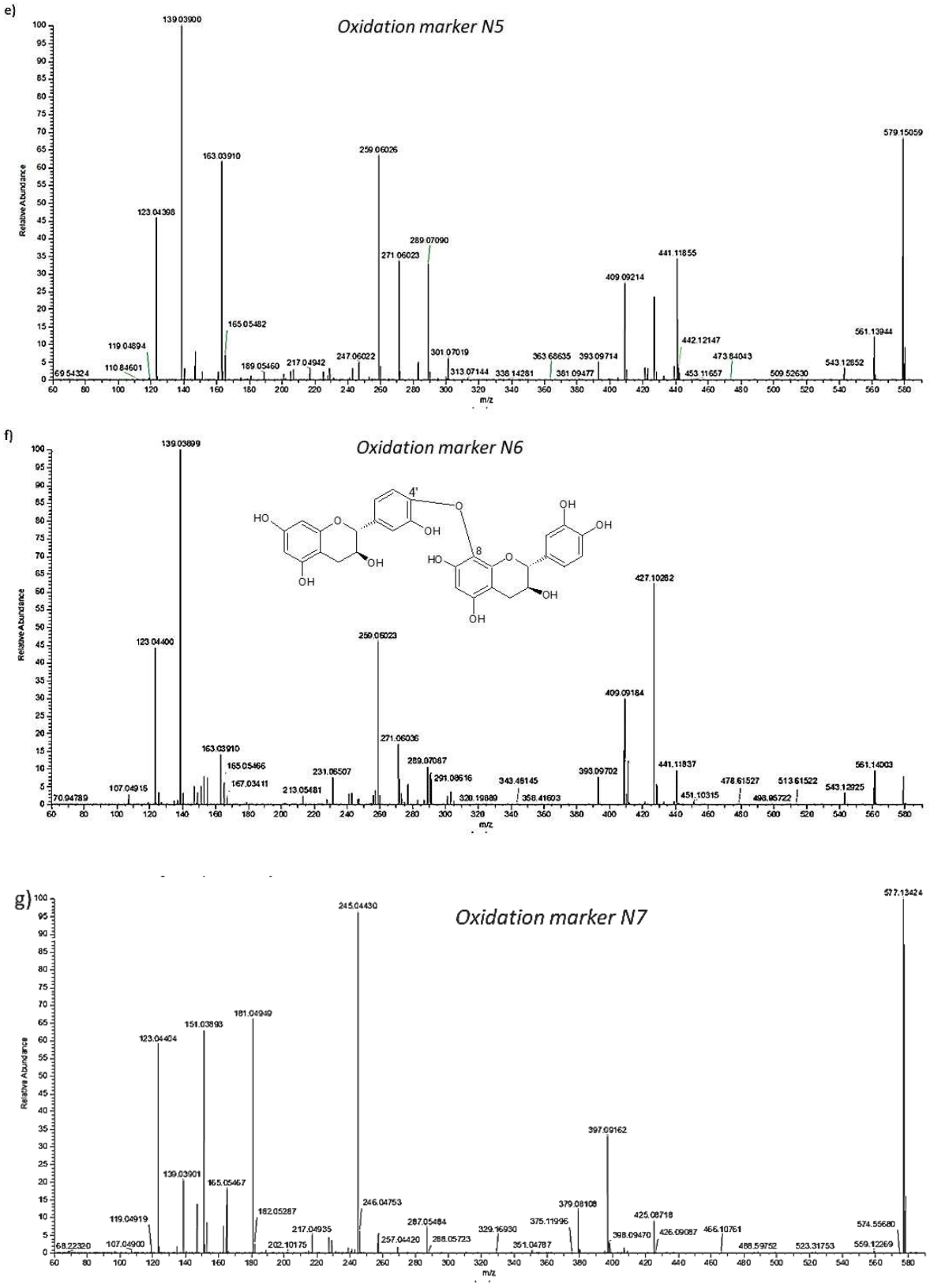

- ***Figure S4 -*** *Representative tandem mass spectra in positive ion mode of oxidation dimers N7 (a) and N8 dehydrodicatechin A (b) with SNCE, 40% midpoint, 20% range and three steps*

a)

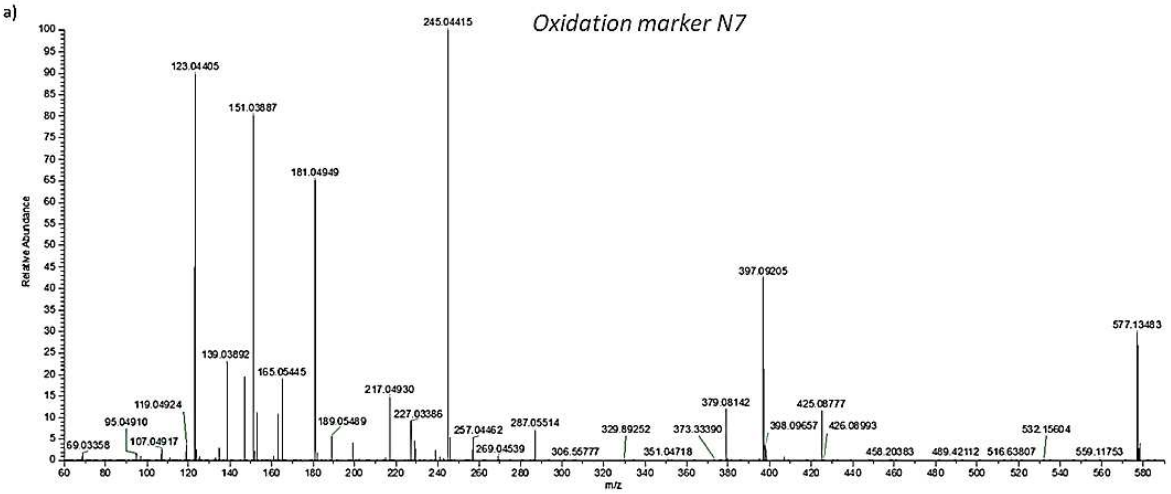
Oxidation marker N7
245.04415
123.04405
151.03887
181.04949
397.09205
577.13483
139.03892
165.05445
217.04930
119.04924
227.03386
379.08142
425.08777
95.04910
189.05489
257.04462
287.05514
329.89252
373.33390
398.09657
426.08993
532.15604
107.04917
269.04539
306.55777
351.04718
69.03358
Relative Abundance
m/z

b)

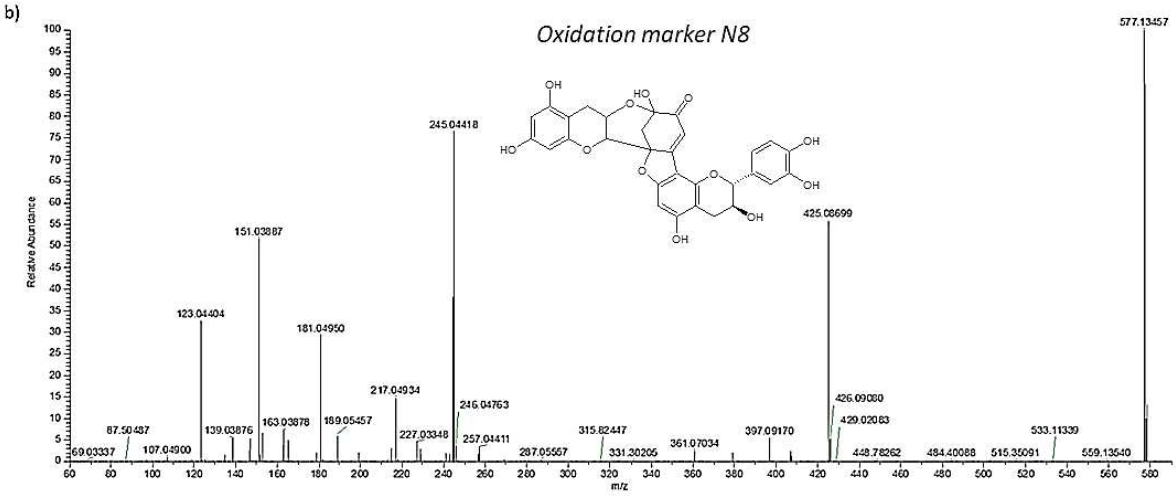
Oxidation marker N8
577.13457
245.04418
151.03887
425.08699
123.04404
181.04950
217.04934
246.04763
426.09080
429.02063
87.50487
139.03876
163.03878
189.05457
227.03348
257.04411
315.82447
397.09170
533.11339
69.03337
107.04900
287.05567
331.30205
361.07034
559.13540
Relative Abundance
m/z

- ***Figure S5*** *- Part of the fragment ions of a protonated oxidation dimer with a bi-aryl linkage*

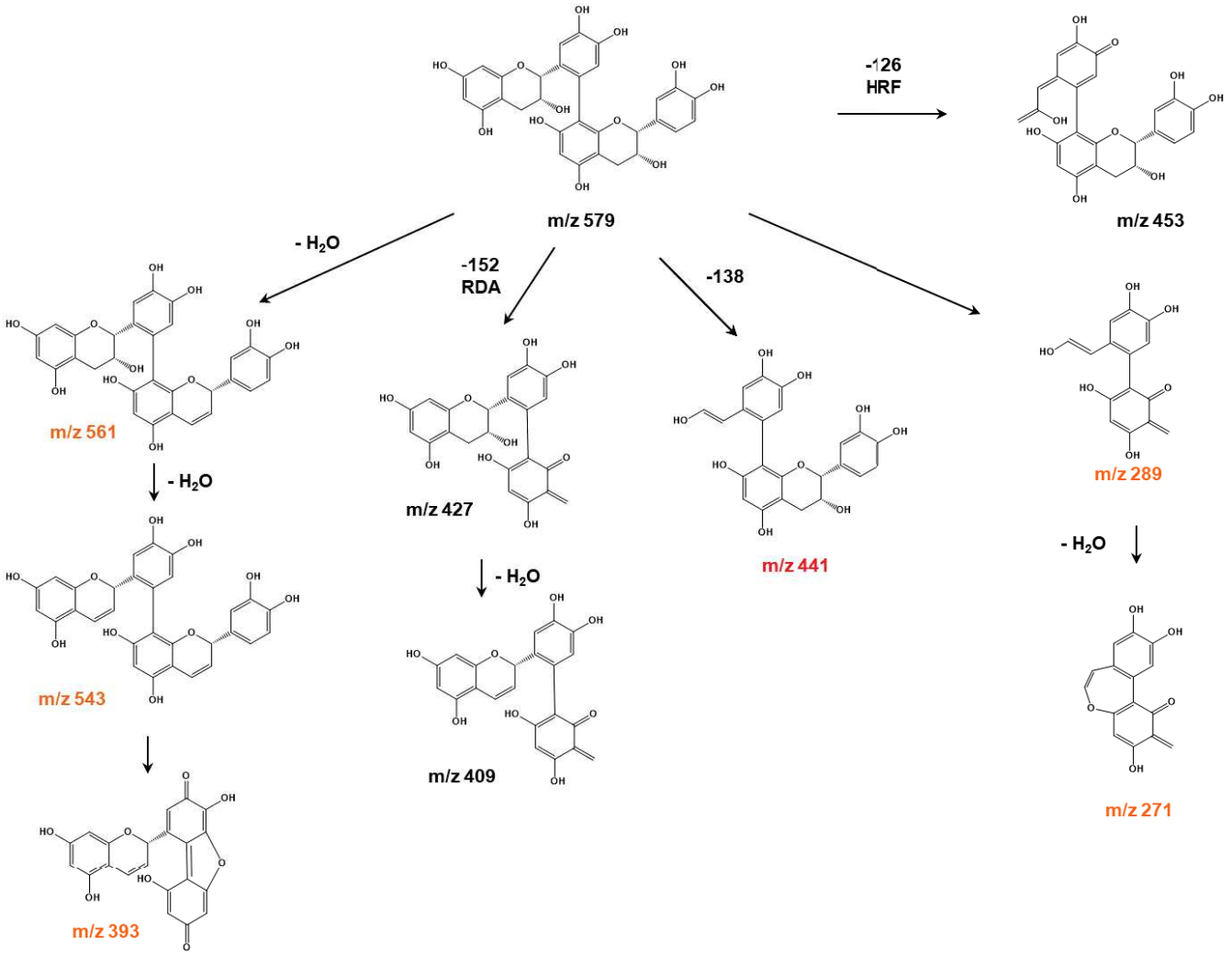

- ***Figure S6*** *- Part of the fragment ions of a protonated oxidation dimer with a bi-aryl ether linkage*

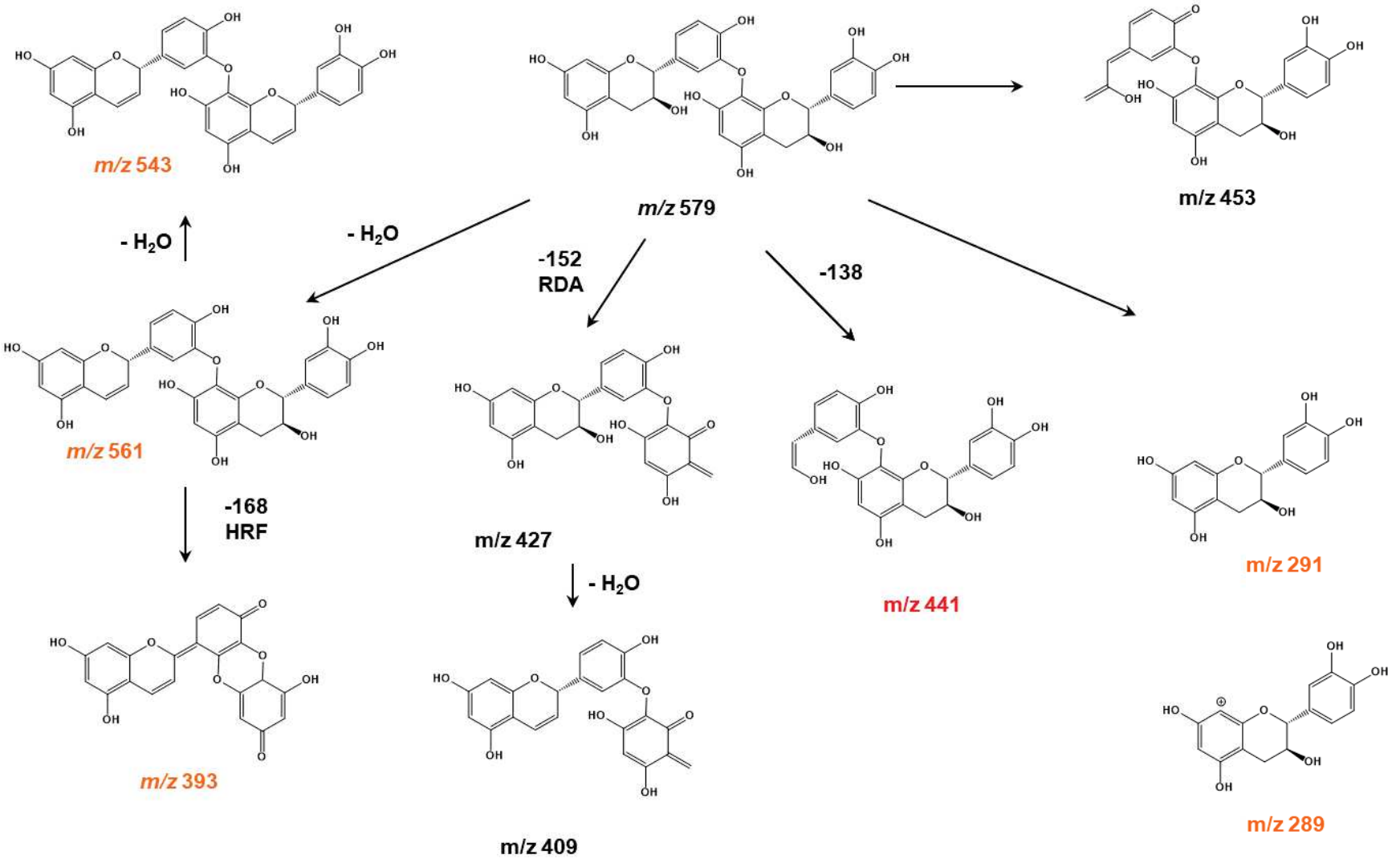
m/z 543
m/z 579
m/z 453
- H2O
- H2O
-152
RDA
-138
m/z 561
-168
HRF
m/z 427
- H2O
m/z 441
m/z 291
m/z 393
m/z 409
m/z 289

- ***Figure S7*** *- Part of the fragment ions of a protonated oxidation dimer N8 (dehydrodicatechin A)*

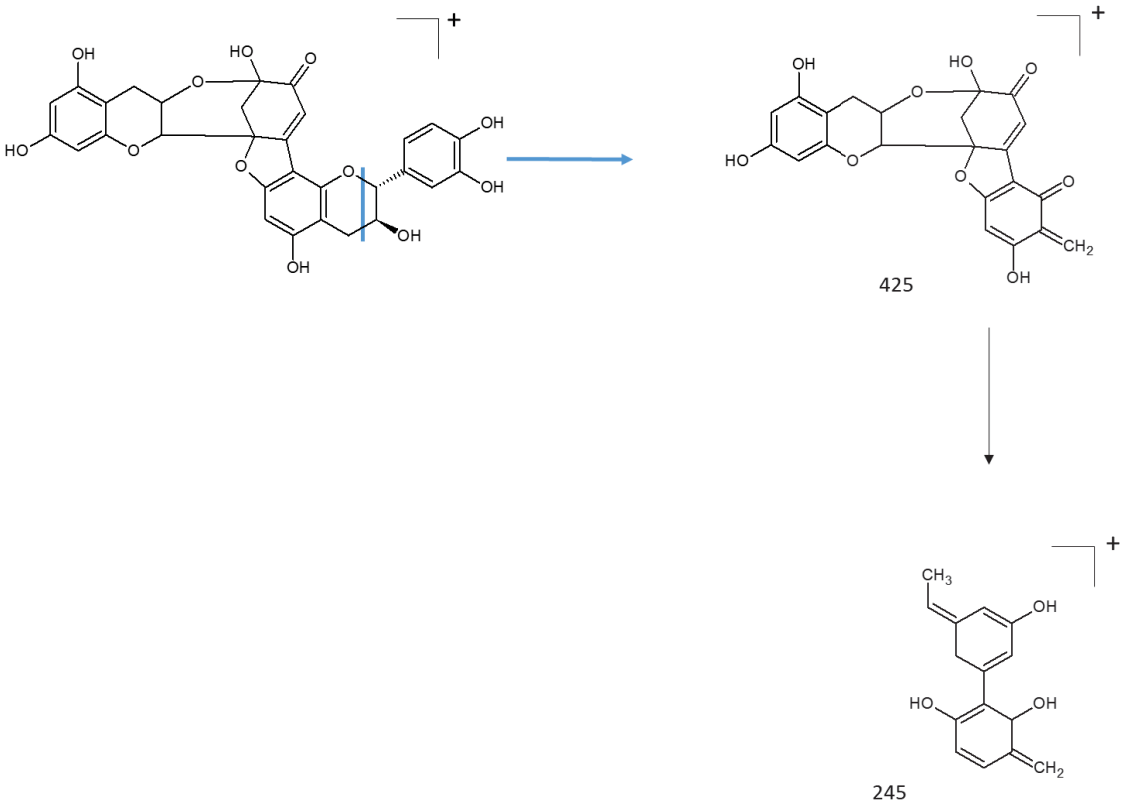

- ***Figure S8*** *- EIC chromatogram (Tr 19,4 – 22min) of three 10g/L grape extracts of Merlot variety at different stage of ripening: green stage (a); veraison (b) ; maturity (c) and tandem mass spectra of compound at 20.4min (d) (for maturity) corresponding to N6 - SNCE 30% midpoint, 15% range and three steps.*

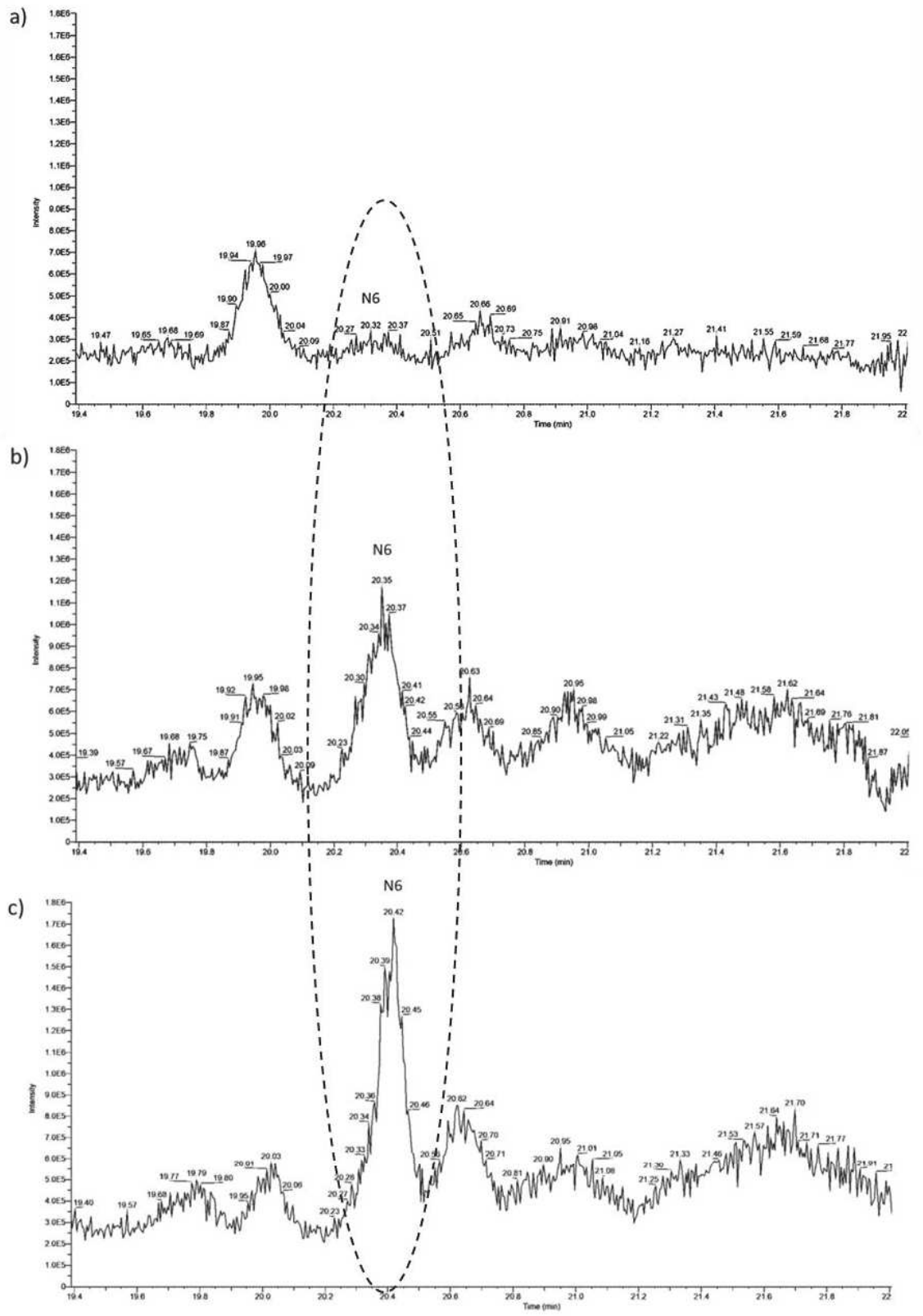

d)

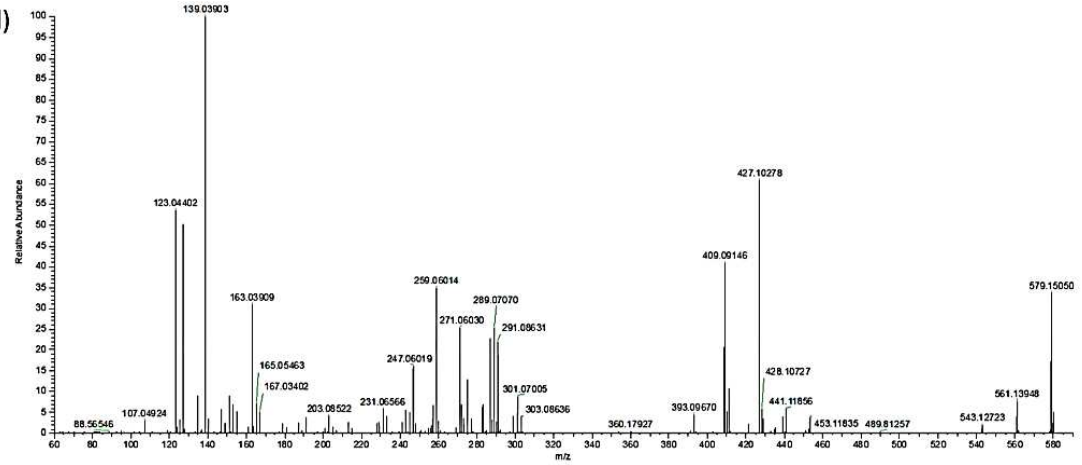
Relative Abundance
m/z
139.03903
123.04402
427.10278
409.09146
579.15050
259.06014
289.07070
271.06030
291.08631
163.03909
247.06019
165.05463
167.03402
428.10727
301.07005
441.11856
561.13948
231.06566
303.08636
203.08522
107.04924
88.56546
393.09670
360.17927
453.11835
489.81257
543.12723

- ***Figure S9 -*** *EIC chromatogram (Tr 19,4 – 22min) of three 10g/L grape extracts of Syrah variety at different stage of ripening: green stage (a); veraison (b); maturity (c) and tandem mass spectra of compound at 20.4min (d) (for maturity) corresponding to N6 - SNCE 30% midpoint, 15% range and three steps.*

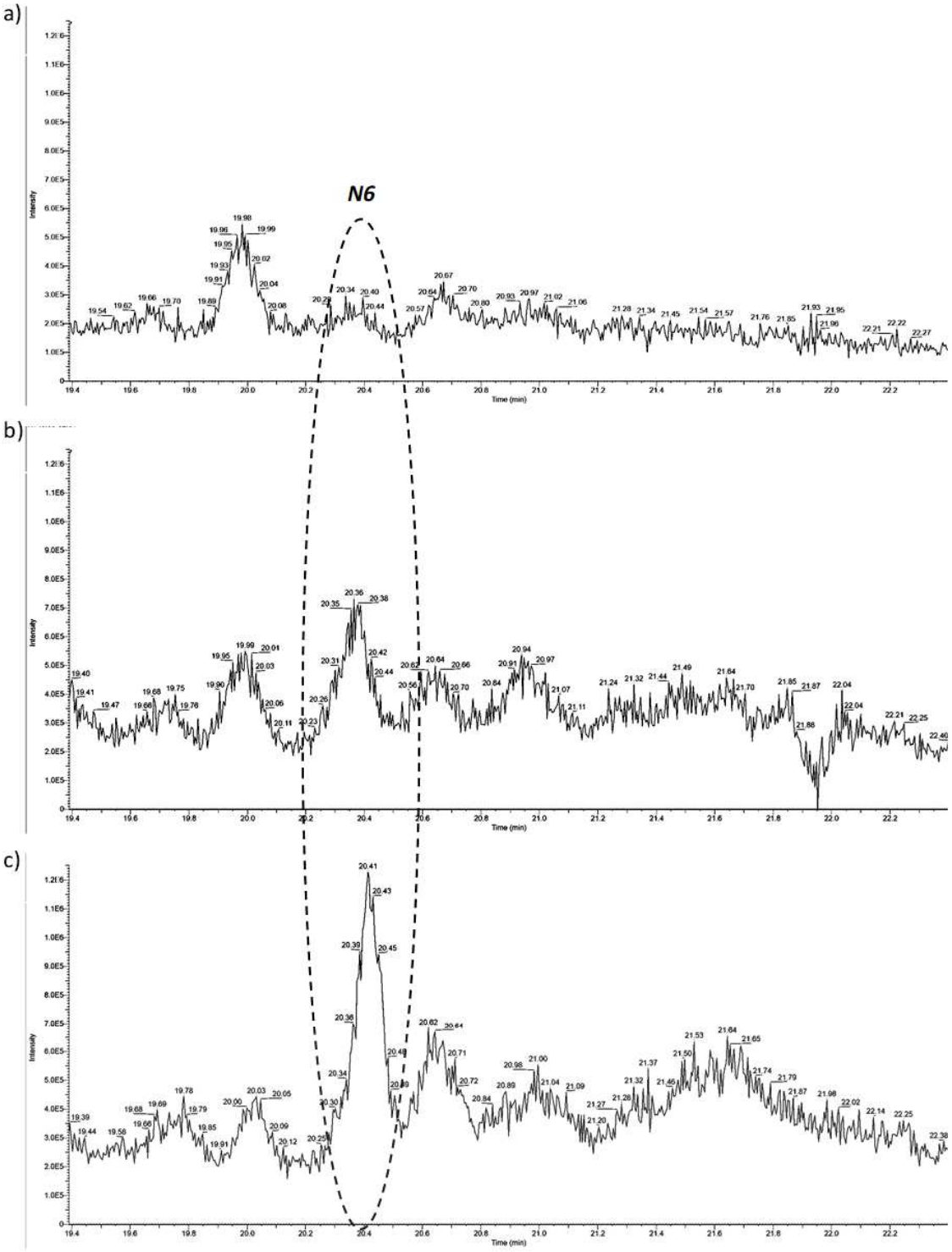

d)

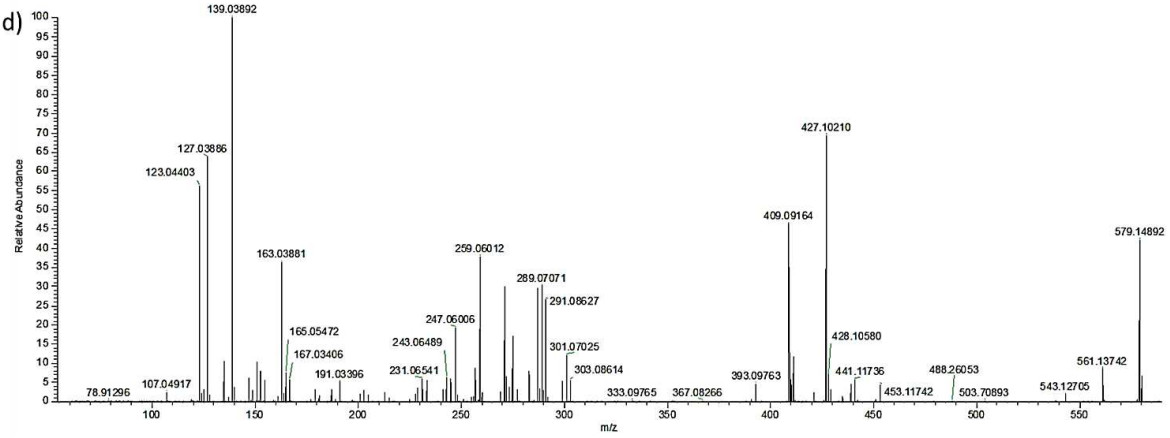
Relative Abundance
m/z
139.03892
127.03886
123.04403
163.03881
165.05472
167.03406
191.03396
78.91296
107.04917
259.06012
247.06006
243.06489
231.06541
289.07071
291.08627
301.07025
303.08614
333.09765
367.08266
427.10210
409.09164
428.10580
393.09763
441.11736
453.11742
488.26053
503.70893
543.12705
579.14892
561.13742

- ***Figure S10*** *- EIC chromatogram (Tr 19,4 – 22min) of three 10g/L grape extracts of Tannat variety at different stage of ripening: green stage (a) ; veraison (b) ; maturity (c) and tandem mass spectra of compound at 20.4min (d) (for maturity) corresponding to N6 - SNCE 30% midpoint, 15% range and three steps.*

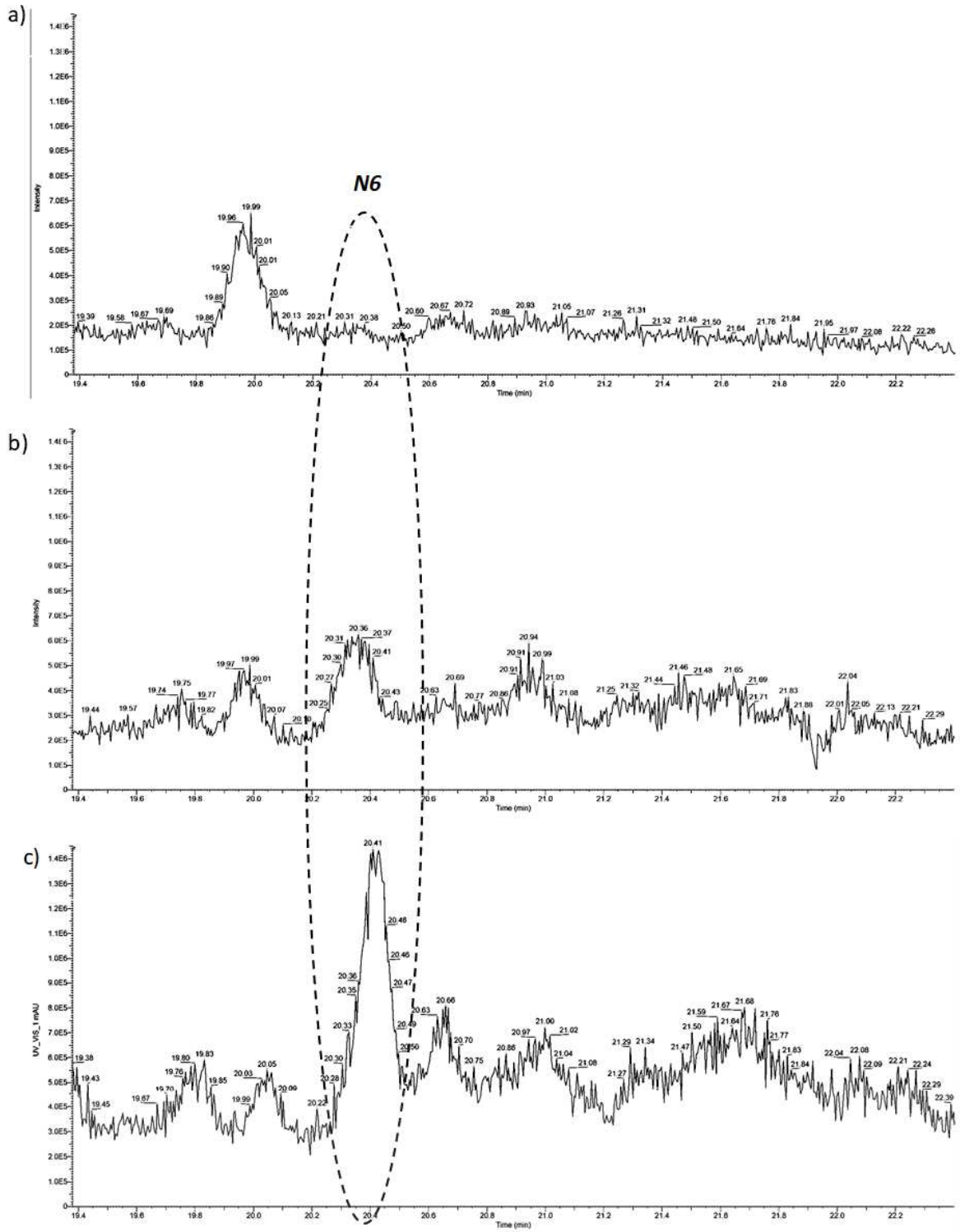

d)

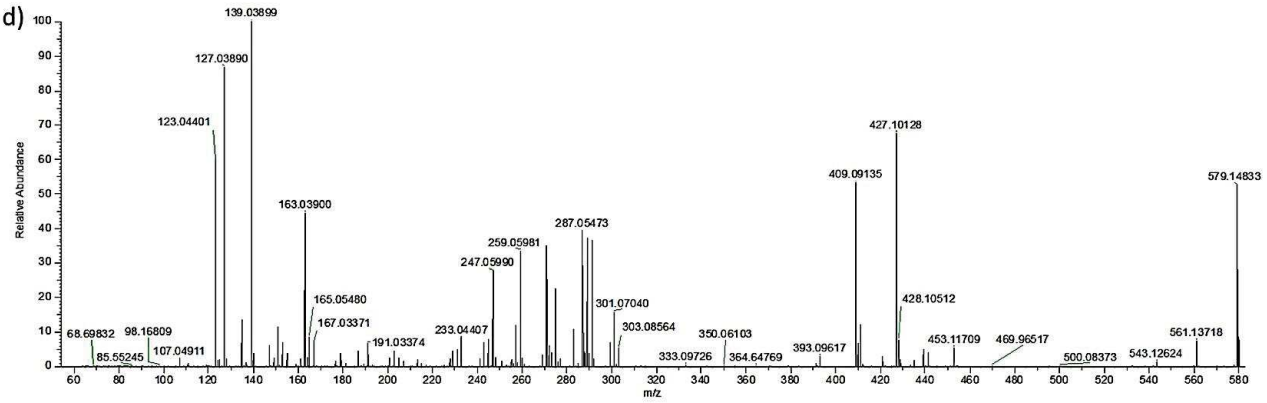
Relative Abundance
m/z
139.03899
127.03890
123.04401
163.03900
427.10128
409.09135
579.14833
287.05473
259.05981
247.05990
165.05480
167.03371
301.07040
428.10512
303.08564
68.69832
98.16809
107.04911
85.55245
191.03374
233.04407
350.06103
393.09617
453.11709
469.96517
561.13718
543.12624
500.08373
333.09726
364.64769

***Figure S11**: EIC chromatogram (Tr 20 – 27min) of three 10g/L grape extracts of Syrah variety at different stage of ripening: green stage (a) ; veraison (b) ; maturity (c) and tandem mass spectra of compound at 22.03min (d) (for maturity) corresponding to N7 and at 26.7 min (e) (for maturity) corresponding to N8 – SNCE 30% midpoint, 15% range and three steps.*

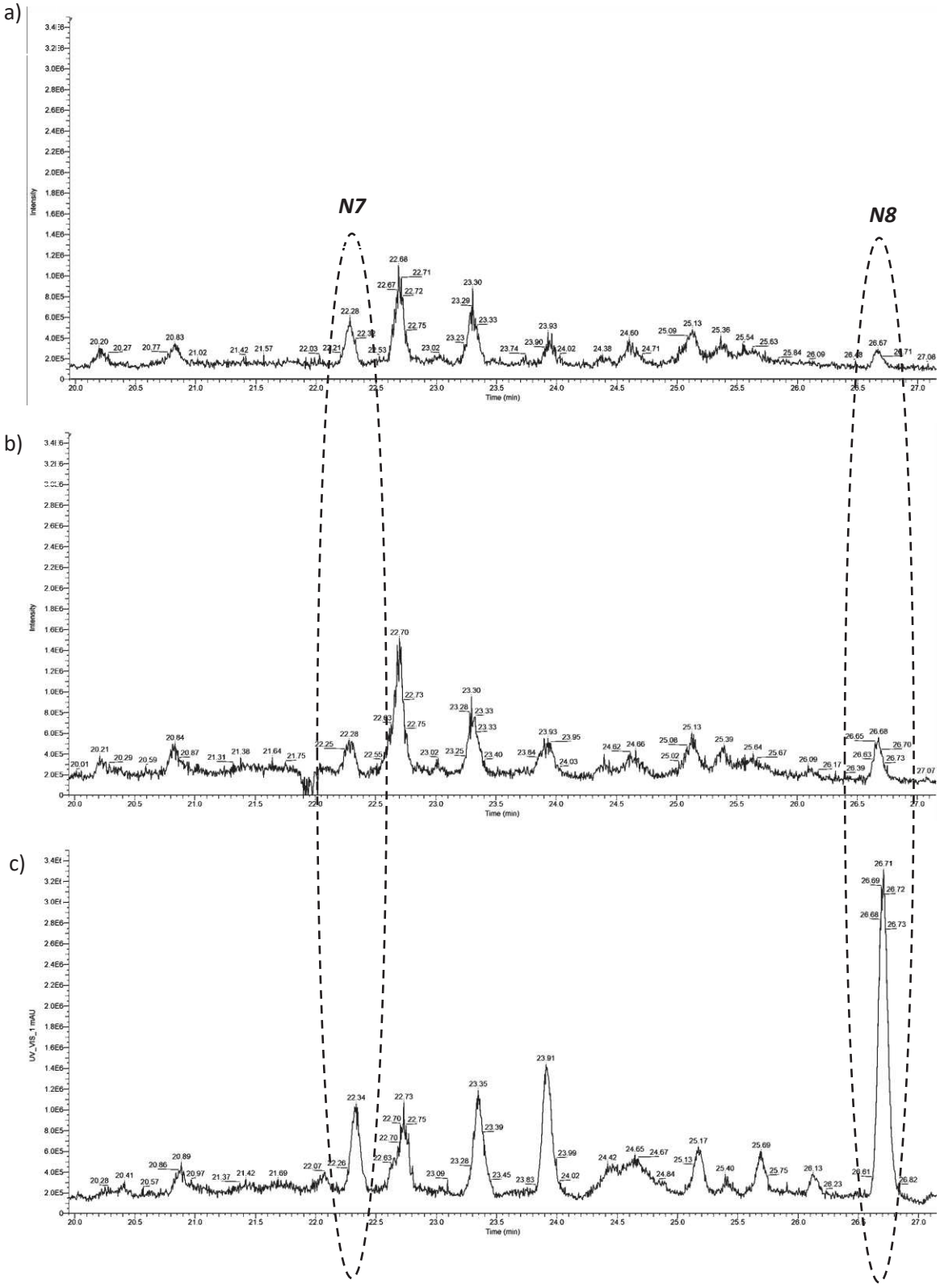

d)

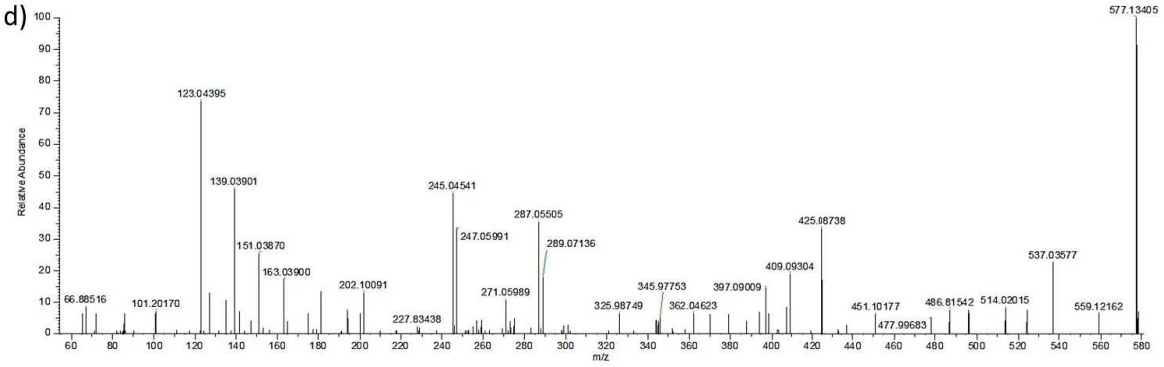
Relative Abundance
m/z
577.13405
123.04395
139.03901
245.04541
287.05505
247.05991
289.07136
425.08738
151.03870
163.03900
409.09304
537.03577
202.10091
271.05989
345.97753
397.09009
66.88516
101.20170
325.98749
362.04623
451.10177
486.81542
514.02015
559.12162
227.83438
477.99683

e)

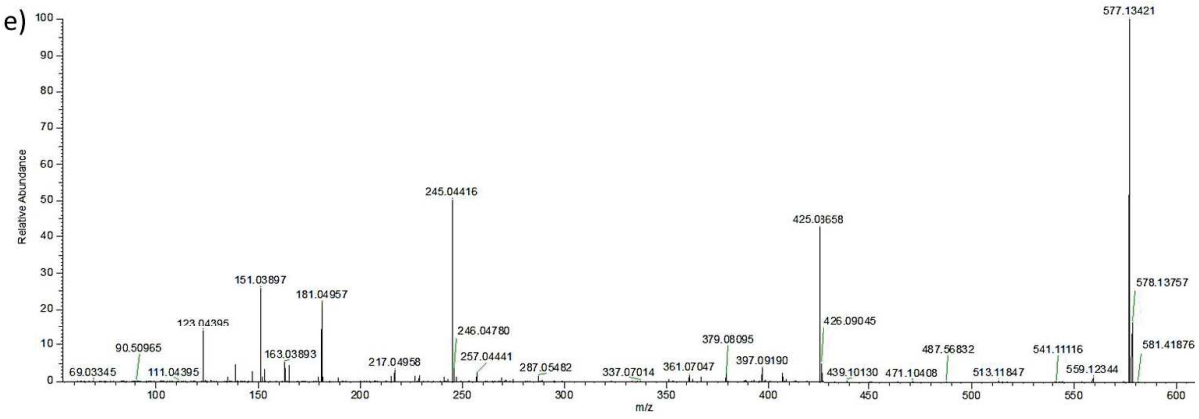
Relative Abundance
m/z
577.13421
245.04416
425.08658
151.03897
181.04957
578.13757
426.09045
246.04780
379.08095
257.04441
397.09190
581.41876
90.50965
163.03893
487.56832
541.11116
69.03345
111.04395
217.04958
287.05482
337.07014
361.07047
439.10130
471.10408
513.11847
559.12344

- ***Figure S12*** *- EIC chromatogram (Tr 20 – 27min) of three 10g/L grape extracts of Tannat variety at different stage of ripening: green stage (a) ; veraison (b) ; maturity (c) and tandem mass spectra of compound at 26.7 min (d) (for maturity) corresponding to N8 – SNCE 30% midpoint, 15% range and three steps.*

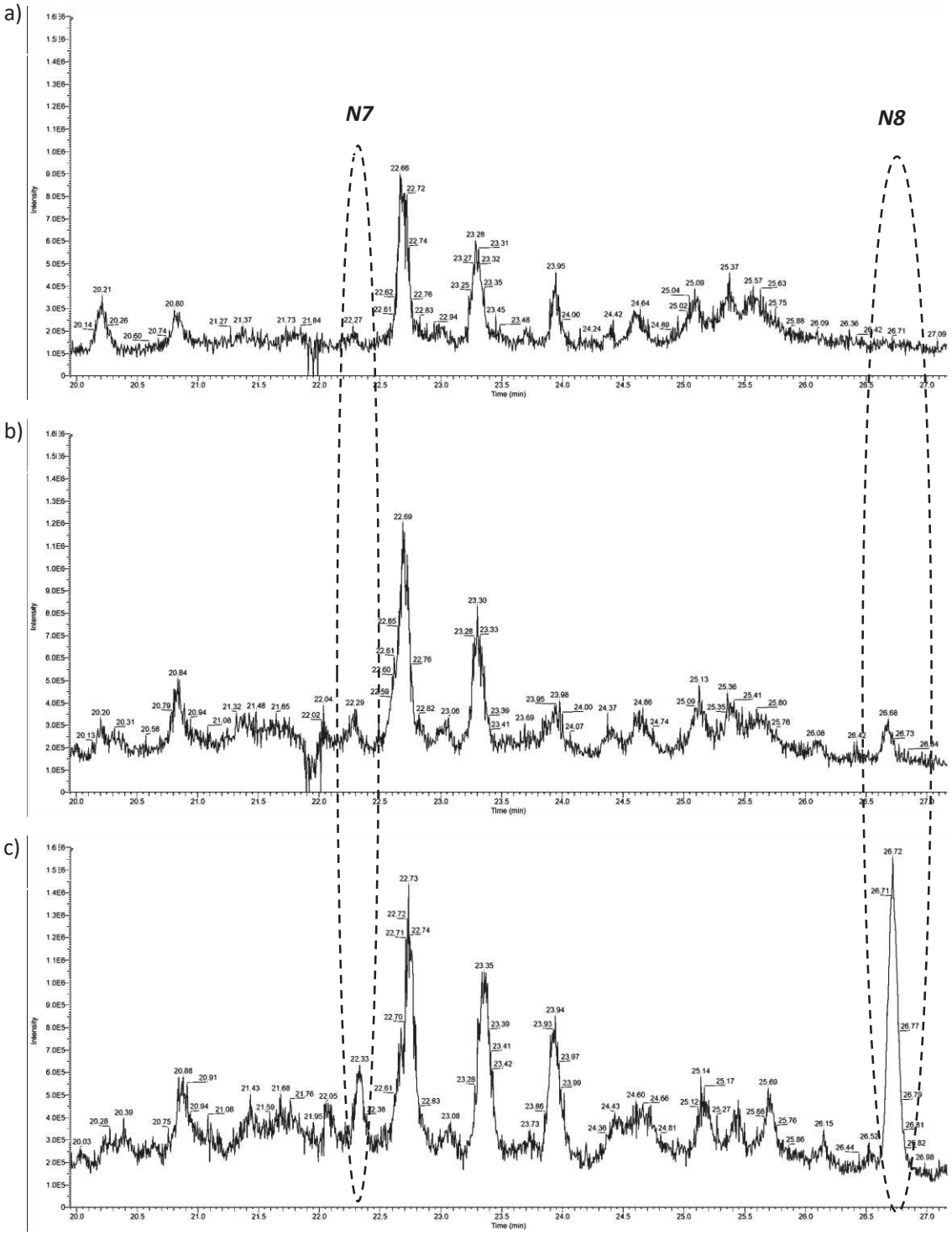

d)

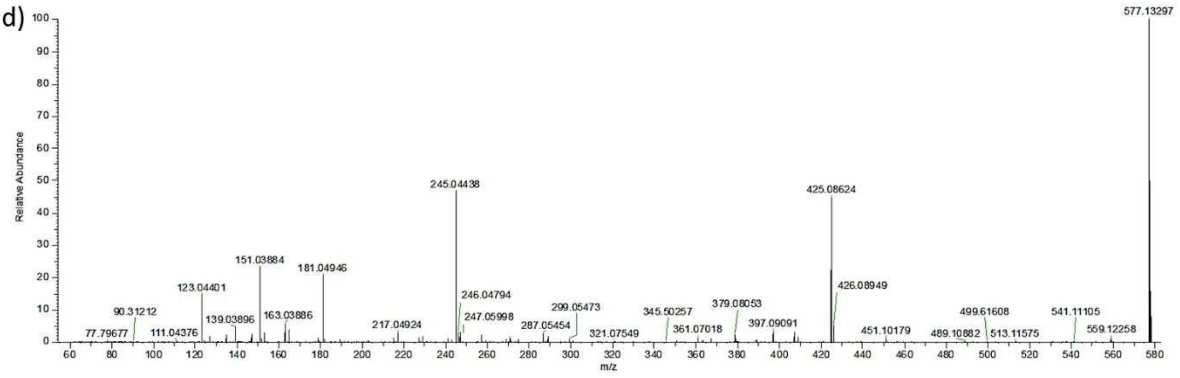
Relative Abundance
m/z
577.13297
245.04438
425.08624
151.03884
181.04946
123.04401
246.04794
426.08949
90.31212
247.05998
299.05473
345.50257
379.08053
499.61608
541.11105
139.03896
163.03886
217.04924
287.05454
321.07549
361.07018
397.09091
451.10179
489.10882
513.11575
559.12258
77.79677
111.04376

Chapitre V : Recherche de marqueurs d'oxydation issus des tannins

Article 5 – *Study of the oxidative evolution of tannins during Syrah red wines aging by tandem mass spectrometry*

- ***Table S1*** *Retention time (min) of (+)-catechin-laccases and (-)-epicatechin-laccases dimeric reaction products.*

	Total catechin units			***Total epicatechin units***				
Sample (fraction)	Rt (min)	EIC area	UV area	Rt (min)	EIC area	UV area	EC/CAT (EIC)	EC/CAT UV
2018 (F2)	3.7	21418442	109	4.1	325658492	480	15.2	4.4
2014 (F2)	3 .7	23212462	90	4.1	274183034	383	11.8	4.3
2010 (F2)	3.7	17651247	94	4.1	337232590	406	19.1	4.3
Oxidized 2018 (F2)	3.7	21092882	156	4.1	317910453	475	15.1	3.0

- ***Figure S1****: UV chromatograms (280 nm) of fractions F1(A) and F2(B) before depolymerization obtained for 2018, 2014, 2010 and 2018 oxidized Syrah winesamples.*

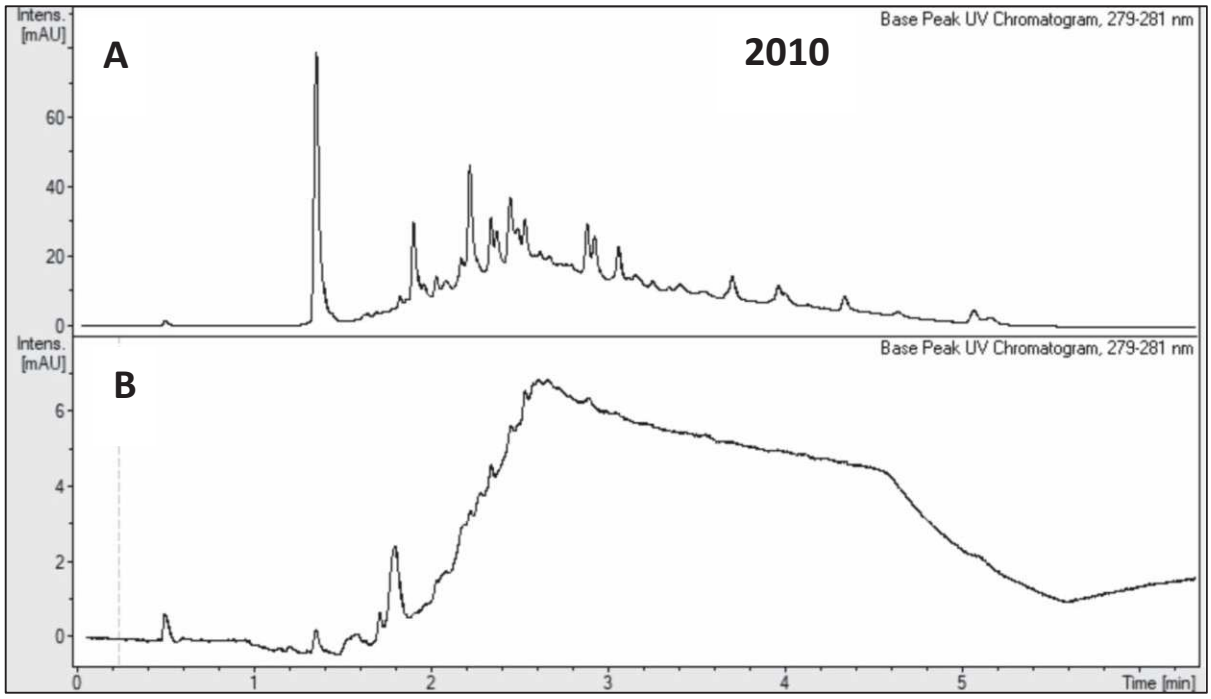
Intens. [mAU]
A
2010
Base Peak UV Chromatogram, 279-281 nm
60
40
20
0
Intens. [mAU]
B
Base Peak UV Chromatogram, 279-281 nm
6
4
2
0
0
1
2
3
4
5
Time [min]

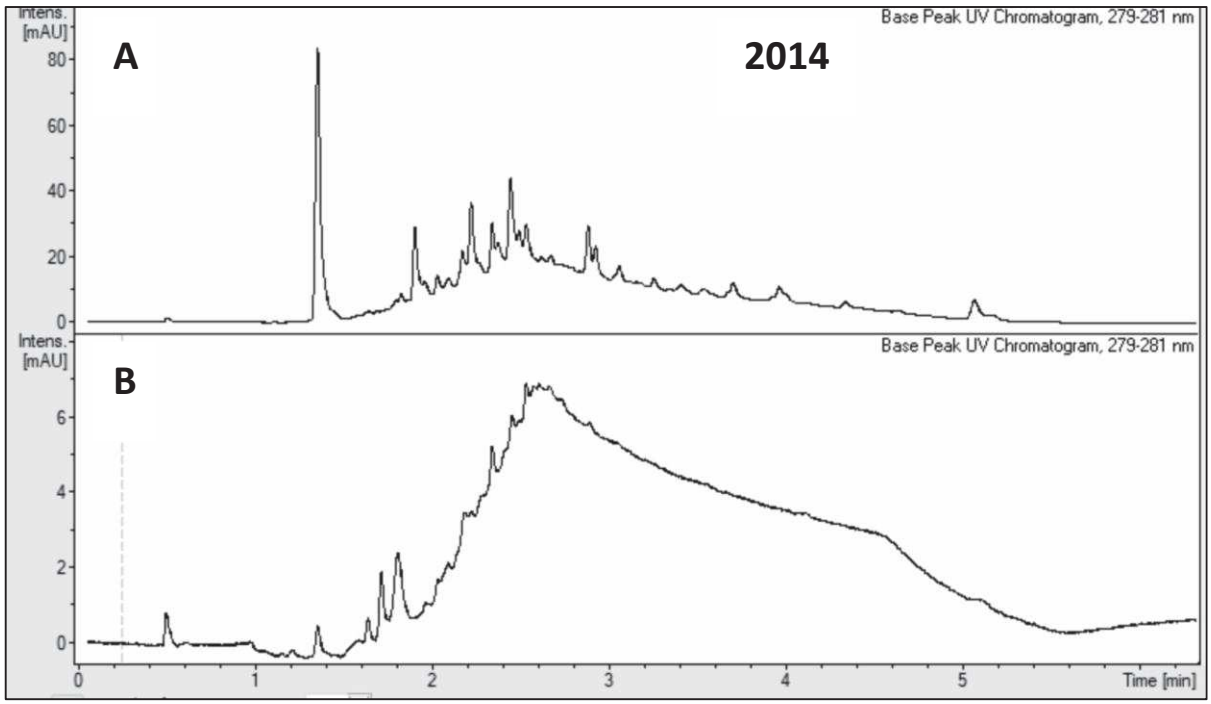
Intens. [mAU]
A
2014
Base Peak UV Chromatogram, 279-281 nm
80
60
40
20
0
Intens. [mAU]
B
Base Peak UV Chromatogram, 279-281 nm
6
4
2
0
0
1
2
3
4
5
Time [min]

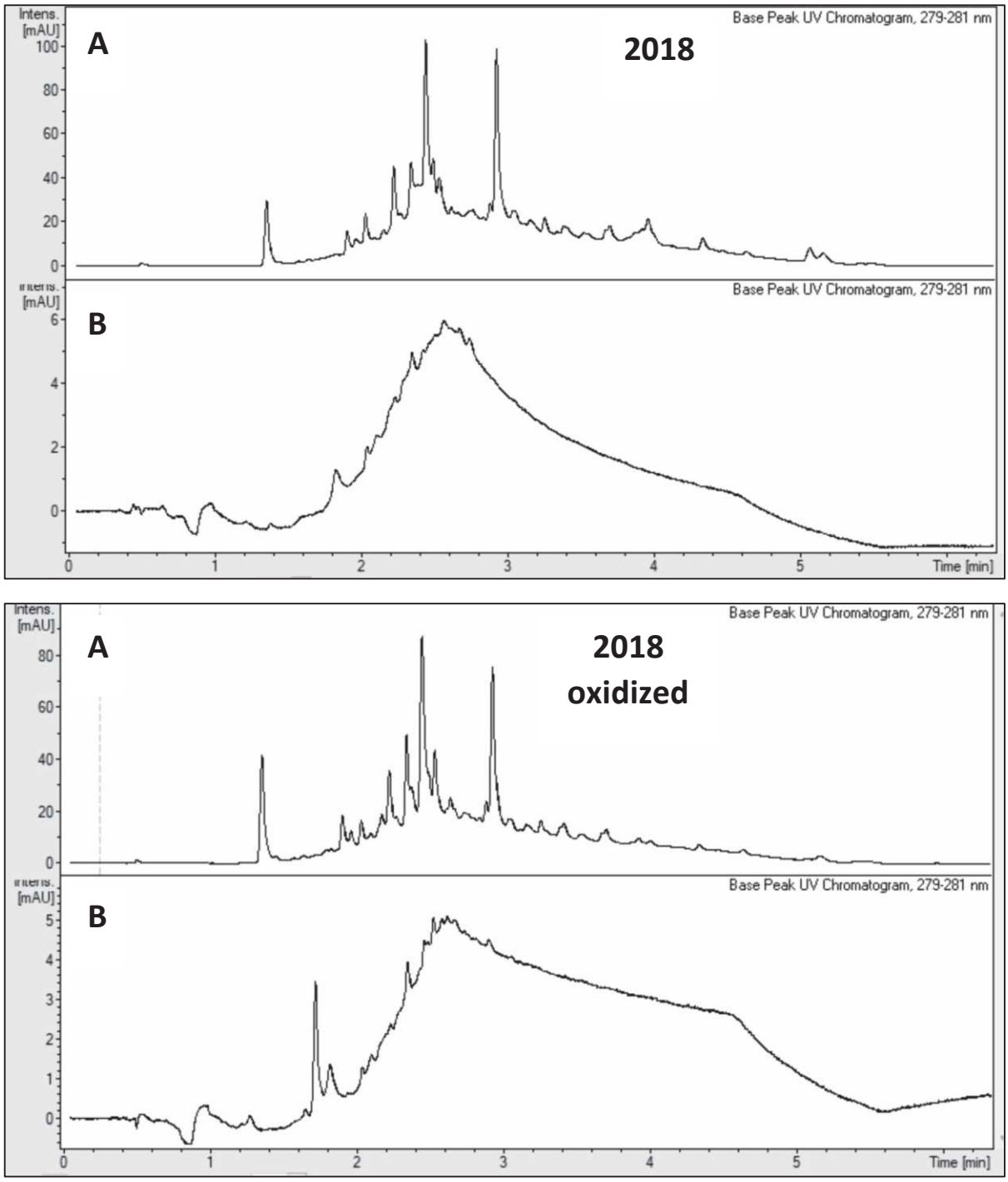

- ***Scheme S1****: Chemical depolymerization of condensed tannins.*

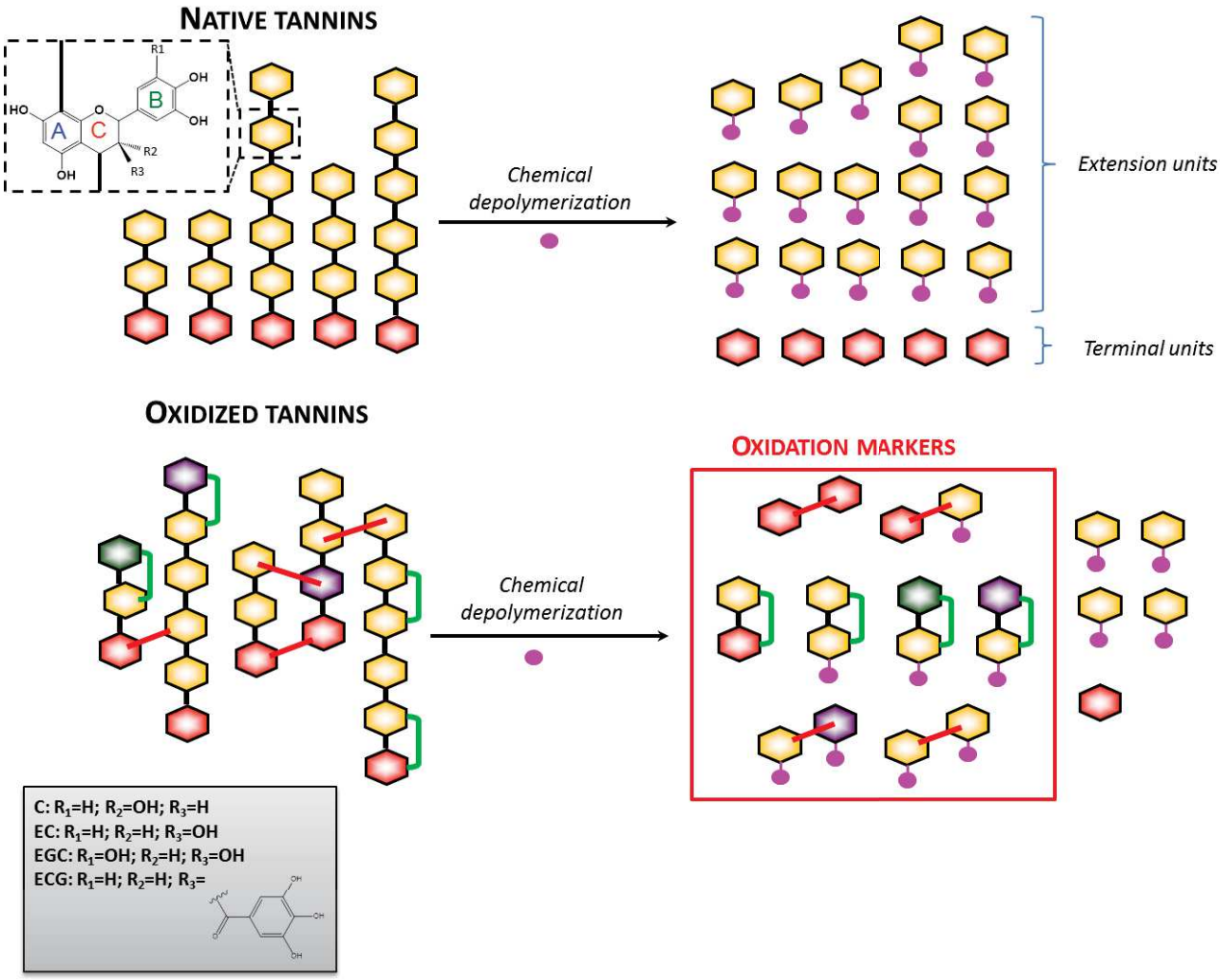

- ***Scheme S2****: A typical UHPLC chromatogram of depolymerization products (Δ) from Syrah 2018 wine tannins (Ω) the hump stained in yellow corresponds to the unresolved oxidation products from the tannins.*

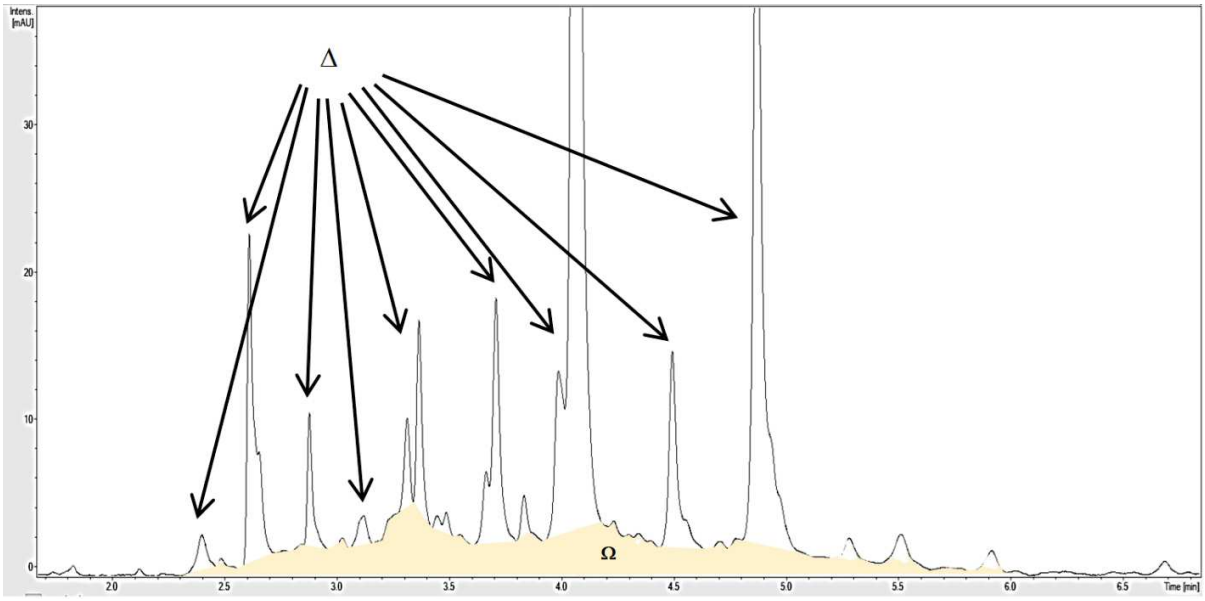

- ***Scheme S3****: Chemical depolymerization of condensed tannins using thioglycolic acid.*

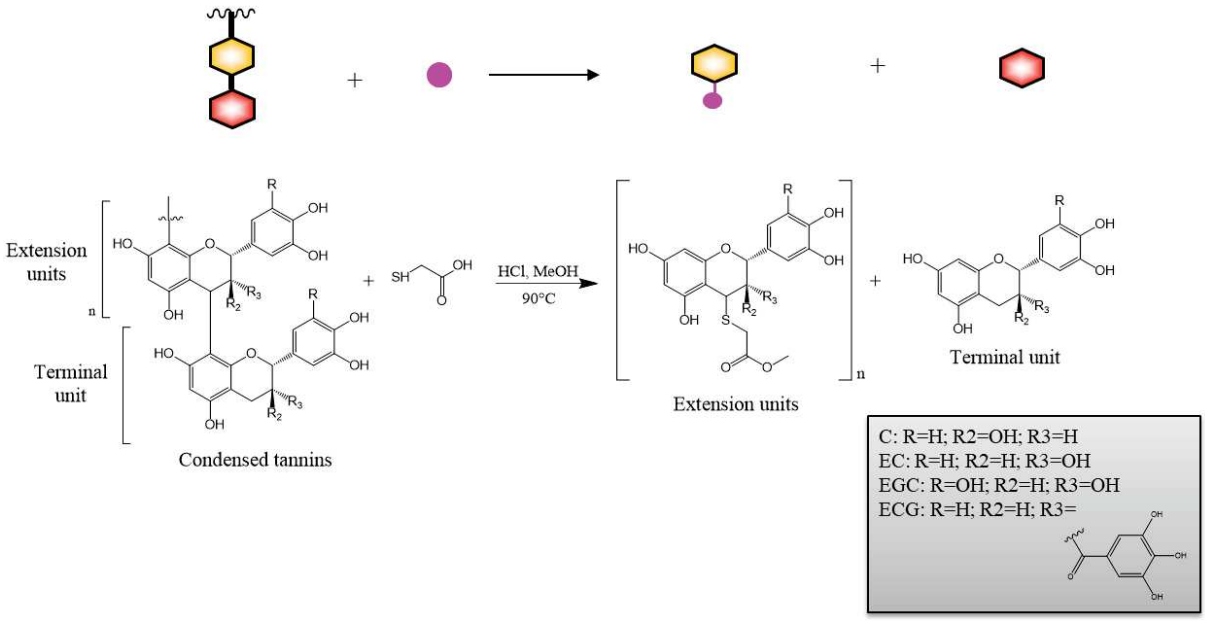

- ***Scheme S4****: Dissociation mass spectrometry of epicatechin/catechin monomer.*

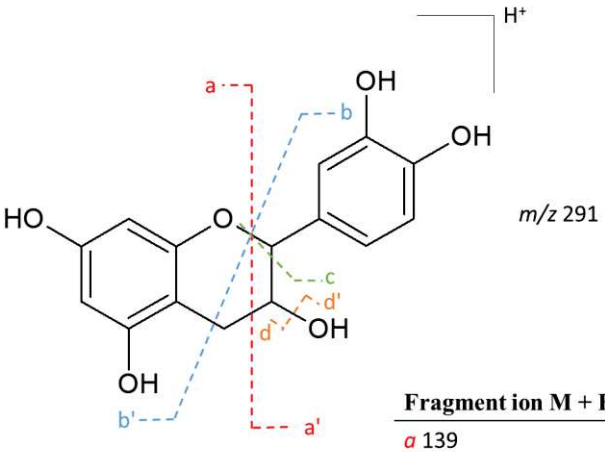

Fragment ion M + H +	Neutral loss M	Mechanism
a 139	*a'* 152	Retro-Diels-Alder (RDA)
b 165	*b'* 126	Heterocyclic Ring Fission (HRF)
d 273	*d'* 18	Loss of water molecule
a' 151		Rearrangements
c 123		Rearrangements

Fragment ions observed on the MS/MS spectra from oxidation markers M3, M4, M5 and M6:

- M3 (*m/z* 683):

→ 577 Th (-106 Da, -Nu) → 425 Th (-152 Da, RDA, - B-ring) → 299 Th (-126 Da, - A-ring): M3a, M3b and M3c.

→ 577 Th (-106 Da, -Nu) → 451 Th (-126 Da, - A-ring): M3a

→ 531 Th (-152 Da, RDA, - B-ring) → 425 Th (-106 Da, -Nu) → 299 Th (-126 Da, - A-ring): M3c

✓ M4 (*m/z* 681):

→ 575 Th (-106 Da, -Nu) → 425 Th (-152 Da, RDA, - B-ring): M4a → 299 Th (-126 Da, - B-ring +2): M4b

→ 575 Th (-106 Da, -Nu) → 449 Th (-126 Da, - A-ring): M4a

→ 529 Th (-152 Da, RDA, - B-ring): M4a and M4b.

✓ M5 (*m/z* 787):

→ 681 Th (-106 Da, -Nu) → 529 Th (-152 Da, RDA, - B-ring): M5a and M5c

→ 681 Th (-106 Da, -Nu) → 575 Th (-106 Da, -Nu) → 449 Th (-126 Da, - A-ring): M5a and M5c

✓ M6 (*m/z* 785):

→ 679 Th (-106 Da, -Nu) → 573 Th (-106 Da, -Nu) → 529 Th (-152 Da, RDA, - B-ring +2): M6a

- ***Figure S1*** *Dissociation mass spectrometry of epicatechin/catechin monomer (Mouls & Fulcrand, 2012)*

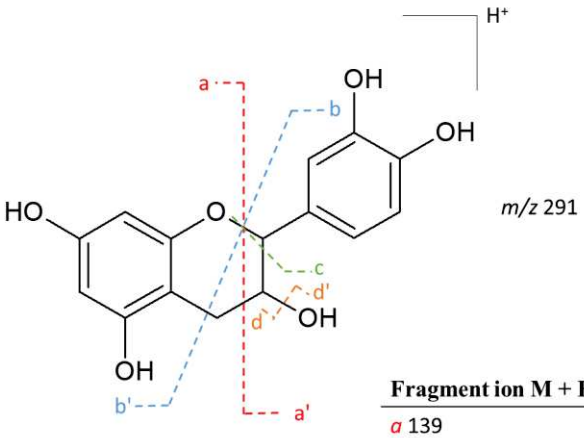

Fragment ion M + H +	Neutral loss M	Mechanism
a 139	*a'* 152	Retro-Diels-Alder (RDA)
b 165	*b'* 126	Heterocyclic Ring Fission (HRF)
d 273	*d'* 18	Loss of water molecule
a' 151		Rearrangements
c 123		Rearrangements

Références

Akoh, C. C. (2017). *Food Lipids—Chemistry, Nutrition and Biotechnology*. https://www.taylorfrancis.com/books/mono/10.1201/9781315151854/food-lipids-casimir-akoh

Alcade-Eon, C., Escribano-Bailón, M. T., Santos-Buelga, C., & Rivas-Gonzalo, J. C. (2006). Changes in the detailed pigment composition of red wine during maturity and ageing : A comprehensive study. *Analytica Chimica Acta*, *563*(1-2), 238-254.

Allgrove, J., & Davison, G. (2014). Chapter 19—Dark Chocolate/Cocoa Polyphenols and Oxidative Stress. In R. R. Watson, V. R. Preedy, & S. Zibadi (Éds.), *Polyphenols in Human Health and Disease* (p. 241-251). Academic Press. https://doi.org/10.1016/B978-0-12-398456-2.00019-0

Antoniolli, A., Fontana, A. R., Piccoli, P., & Bottini, R. (2015). Characterization of polyphenols and evaluation of antioxidant capacity in grape pomace of the cv. Malbec. *Food Chemistry*, *178*, 172-178. https://doi.org/10.1016/j.foodchem.2015.01.082

Arapitsas, P., Speri, G., Angeli, A., Perenzoni, D., & Mattivi, F. (2014). The influence of storage on the “chemical age” of red wines. *Metabolomics*, *10*, 816-832.

Atanasova, V., Fulcrand, H., Cheynier, V., & Moutounet, M. (2002a). Effect of oxygenation on polyphenol changes occurring in the course of wine-making. *Analytica Chimica Acta*, *458*(1), 15-27. https://doi.org/10.1016/S0003-2670(01)01617-8

Atanasova, V., Fulcrand, H., Cheynier, V., & Moutounet, M. (2002b). Effect of oxygenation on polyphenol changes occurring in the course of wine-making. *Analytica Chimica Acta*, *458*(1), 15-27. https://doi.org/10.1016/S0003-2670(01)01617-8

Avizcuri, J.-M., Sáenz-Navajas, M.-P., Echávarri, J.-F., Ferreira, V., & Fernández-Zurbano, P. (2016). Evaluation of the impact of initial red wine composition on changes in color and anthocyanin content during bottle storage. *Food Chemistry*, *213*, 123-134. https://doi.org/10.1016/j.foodchem.2016.06.050

Bakker, J., & Timberlake, C. F. (1997). Isolation, identification, and characterization of new color-stable anthocyanins occuring in some red wines. *Journal of Agricultural and Food Chemistry*, *45*(1), 35-43.

Barril, C., Clark, A. C., Prenzler, P. D., Karuso, P., & Scollary, G. R. (2009). Formation of Pigment Precursor (+)-1″-Methylene-6″-hydroxy-2H-furan-5″-one-catechin Isomers from (+)-Catechin and a Degradation Product of Ascorbic Acid in a Model Wine System. *Journal of Agricultural and Food Chemistry*, *57*(20), 9539-9546.

Barril, C., Clark, A. C., & Scollary, G. R. (2012). Chemistry of ascorbic acid and sulfur dioxide as an antioxidant system relevant to white wine. *Analytica Chimica Acta*, *732*, 186-193. https://doi.org/10.1016/j.aca.2011.11.011

Bartosz, G., Grzesik-Pietrasiewicz, M., & Sadowska-Bartosz, I. (2020). Fluorescent Products of Anthocyanidin and Anthocyanin Oxidation. *Journal of Agricultural and Food Chemistry*, *68*(43), 12019-12027. https://doi.org/10.1021/acs.jafc.0c04755

Benbouguerra, N., Richard, T., Saucier, C., & Garcia, F. (2020). Voltammetric Behavior, Flavanol and Anthocyanin Contents, and Antioxidant Capacity of Grape Skins and Seeds during Ripening (Vitis vinifera var. Merlot, Tannat, and Syrah). *Antioxidants*, *9*(9), 800. https://doi.org/10.3390/antiox9090800

Berké, B., Chèze, C., Vercauteren, J., & Deffieux, G. (1998). Bisulfite addition to anthocyanins : Revisited structures of colourless adducts. *Tetrahedron Letters*, *39*(32), 5771-5774. https://doi.org/10.1016/S0040-4039(98)01205-2

Berrueta, L. A., Rasines-Perea, Z., Prieto, N., Asensio-Regalado, C., Alonso-Salces, R. M., Sanchez-Ilarduya, M. B., & Gallo, B. (2020). Formation and evolution profiles of anthocyanin derivatives and tannins during fermentations and aging of red wines. *European Food Research and Technology*, *246*, 149-165.

Bradshaw, M. P., Barril, C., Clark, A. C., Prenzler, P. D., & Scollary, G. R. (2011). Ascorbic Acid : A Review of its Chemistry and Reactivity in Relation to a Wine Environment. *Critical Reviews in Food Science and Nutrition*, *51*(6), 479-498. https://doi.org/10.1080/10408391003690559

Brossaud, F., Cheynier, V., & Noble, A. C. (2008, mars 12). Bitterness and astringency of grape and wine polyphenols. *Australian Journal of Grape and Wine Research*.

Brouillard, R., & Dangles, O. (1994). Anthocyanin molecular interactions : The first step in the formation of new pigments during wine aging? *Food Chemistry*, *51*(4), 365-371. https://doi.org/10.1016/0308-8146(94)90187-2

Cacho, J., Castells, J., Esteban, A., Laguna, B., & Sagrista, N. (1995). Iron, Copper, and Manganese Influence on Wine Oxidation. *American Journal of Enology and Viticulture*, *46*(3), 380-384.

Canals, R., Llaudy, M. C., Valls, J., & Canals, J. M. (2005). Influence of Ethanol Concentration on the Extraction of Color and Phenolic Compounds from the Skin and Seeds of Tempranillo Grapes at Different Stages of Ripening | Journal of Agricultural and Food Chemistry. *Journal of Agricultural and Food Chemistry*, *53*(10), 4019-4025.

Carrascon, V., Fernandez-Zurbano, P., Bueno, M., & Ferreira, V. (2015). Oxygen Consumption by Red Wines. Part II: Differential Effects on Color and Chemical Composition Caused by Oxygen Taken in Different Sulfur Dioxide-Related Oxidation Contexts. *Journal of Agricultural and Food Chemistry*, *63*(51), 10938-10947.

Carrascón, V., Vallverdú-Queralt, A., Meudec, E., Sommerer, N., Fernandez-Zurbano, P., & Ferreira, V. (2018). The kinetics of oxygen and SO2 consumption by red wines. What do they tell about oxidation mechanisms and about changes in wine composition? *Food Chemistry*, *241*, 206-214. https://doi.org/10.1016/j.foodchem.2017.08.090

Castañeda-Ovando, A., Pacheco-Hernández, Ma. de L., Páez-Hernández, Ma. E., Rodríguez, J. A., & Galán-Vidal, C. A. (2009). Chemical studies of anthocyanins : A review. *Food Chemistry*, *113*(4), 859-871. https://doi.org/10.1016/j.foodchem.2008.09.001

Castro, C. C., Martins, R. C., Teixeira, J. A., & Silva Ferreira, A. C. (2014a). Application of a high-throughput process analytical technology metabolomics pipeline to Port wine forced ageing process. *Food Chemistry*, *143*, 384-391. https://doi.org/10.1016/j.foodchem.2013.07.138

Castro, C. C., Martins, R. C., Teixeira, J. A., & Silva Ferreira, A. C. (2014b). Application of a high-throughput process analytical technology metabolomics pipeline to Port wine forced ageing process. *Food Chemistry*, *143*, 384-391. https://doi.org/10.1016/j.foodchem.2013.07.138

Chevion, S., Roberts, M. A., & Chevion, M. (2000). The use of cyclic voltammetry for the evaluation of antioxidant capacity. *Free Radical Biology and Medicine*, *28*(6), 860-870. https://doi.org/10.1016/S0891-5849(00)00178-7

Cheynier, V., Basire, N., & Rigaud, J. (1989a). Mechanism of trans-caffeoyltartaric acid and catechin oxidation in model solutions containing grape polyphenoloxidase. *Journal of Agricultural and Food Chemistry*, *37*(4), 1069-1071. https://doi.org/10.1021/jf00088a055

Cheynier, V., Basire, N., & Rigaud, J. (1989b). Mechanism of trans-caffeoyltartaric acid and catechin oxidation in model solutions containing grape polyphenoloxidase. *Journal of Agricultural and Food Chemistry*, *37*(4), 1069-1071. https://doi.org/10.1021/jf00088a055

Cheynier, V., Dueñas, M., Salas, E., Maury, C., Souquet, J. M., Sarni-Manchado, & Fulcrand, H. (2006). Structure and Properties of Wine Pigments and Tannins. *American Journal of Enology and Viticulture*, *57*, 298-305.

Cheynier, V., Dueñas-Paton, M., Salas, E., Maury, C., Souquet, J.-M., Sarni-Manchado, P., & Fulcrand, H. (2006). Structure and Properties of Wine Pigments and Tannins. *American Journal of Enology and Viticulture*, *57*(3), 298-305.

Cheynier, V. F., Trousdale, E. K., Singleton, V. L., Salgues, M. J., & Wylde, R. (1986). Characterization of 2-S-glutathionyl caftaric acid and its hydrolysis in relation to grape wines. *Journal of Agricultural and Food Chemistry*, *34*(2), 217-221. https://doi.org/10.1021/jf00068a016

Cheynier, V., Hidalgo Arellano, Souquet, J. M., & Moutounet, M. (1997). Estimation of the Oxidative Changes in Phenolic Compounds of Carignane During Winemaking. *American Journal of Enology and Viticulture*, *48*, 225-228.

Cheynier, V., Owe, C., & Rigaud, J. (1988). Oxidation of Grape Juice Phenolic Compounds in Model Solutions. *Journal of Food Science*, *53*(6), 1729-1732.

Cheynier, V., Prieur, C., Guyot, S., Rigaud, J., & Moutounet, M. (1997). The Structures of Tannins in Grapes and Wines and Their Interactions with Proteins. In *Wine* (Vol. 661, p. 81-93). American Chemical Society. https://doi.org/10.1021/bk-1997-0661.ch008

Cheynier, V., & Ricardo da Silva, J. M. (1991). Oxidation of grape procyanidins in model solutions containing trans-caffeoyltartaric acid and polyphenol oxidase. *Journal of Agricultural and Food Chemistry*, *39*(6), 1047-1049. https://doi.org/10.1021/jf00006a008

Cheynier, V., Souquet, J. M., Kontek, A., & Moutounet, M. (1994). Anthocyanin degradation in oxidising grape musts. *Journal of the Science of Food and Agriculture*, *66*(3), 283-288.

Cheynier, V., Souquet, J. M., & Moutounet, M. (1989). Glutathione Content and Glutathione to Hydroxycinnamic Acid Ratio in Vitis vinifera Grapes and Musts. *American Journal of Enology and Viticulture*, *40*(4), 320-324.

Cheynier, Veronique., & Moutounet, Michel. (1992). Oxidative reactions of caffeic acid in model systems containing polyphenol oxidase. *Journal of Agricultural and Food Chemistry*, *40*(11), 2038-2044. https://doi.org/10.1021/jf00023a002

Chira, K., Suh, J.-H., Saucier, C., & Teissèdre, P.-L. (2008). Les polyphénols du raisin. *Phytothérapie*, *6*(2), 75-82. https://doi.org/10.1007/s10298-008-0293-3

Choe, E., & Min, D. B. (2009). Mechanisms of Antioxidants in the Oxidation of Foods. *Comprehensive Reviews in Food Science and Food Safety*, *8*(4), 345-358. https://doi.org/10.1111/j.1541-4337.2009.00085.x

Cillard, J., & Cillard, P. (2006). Mécanismes de la peroxydation lipidique et des anti-oxydations. *Oilseeds & fats Crops and Lipids*, *13*(1), 24-29.

Claus, H. (2003). Laccases and their occurrence in prokaryotes. *Archives of Microbiology*, *179*(3), 145-150. https://doi.org/10.1007/s00203-002-0510-7

Coppola, F., Picariello, L., Forino, M., Moio, L., & Gambuti, A. (2021). Comparison of Three Accelerated Oxidation Tests Applied to Red Wines with Different Chemical Composition. *Molecules*, *26*(4), 815. https://doi.org/10.3390/molecules26040815

Dallas, C., Ricardo da Silva, J. M., & Laureano, O. (1996). Products Formed in Model Wine Solutions Involving Anthocyanins, Procyanidin B2, and Acetaldehyde | Journal of Agricultural and Food Chemistry. *Journal of Agricultural and Food Chemistry*, *44*(8), 2402-2407.

Danilewicz, J. C. (2003a). *Review of Reaction Mechanisms of Oxygen and Proposed Intermediate Reduction Products in Wine : Central Role of Iron and Copper*. 13.

Danilewicz, J. C. (2003b). Review of Reaction Mechanisms of Oxygen and Proposed Intermediate Reduction Products in Wine : Central Role of Iron and Copper. *American Journal of Enology and Viticulture*, *54*(2), 73-85.

Danilewicz, J. C. (2007). Interaction of Sulfur Dioxide, Polyphenols, and Oxygen in a Wine-Model System : Central Role of Iron and Copper. *American Journal of Enology and Viticulture*, *58*(1), 53-60.

Danilewicz, J. C. (2011). Mechanism of Autoxidation of Polyphenols and Participation of Sulfite in Wine : Key Role of Iron. *American Journal of Enology and Viticulture*, *62*(3), 319-328. https://doi.org/10.5344/ajev.2011.10105

Danilewicz, J. C., Seccombe, J. T., & Whelan, J. (2008). Mechanism of Interaction of Polyphenols, Oxygen, and Sulfur Dioxide in Model Wine and Wine. *American Journal of Enology and Viticulture*, *59*(2), 128-136.

de Beer, D., Joubert, E., Marais, J., du Toit, W., Fouché, B., & Manley, M. (2016). Characterisation of Pinotage Wine During Maturation on Different Oak Products. *South African Journal of Enology and Viticulture*, *29*(1). https://doi.org/10.21548/29-1-1450

Deshaies, S., Cazals, G., Enjalbal, C., Constantin, T., Garcia, F., Mouls, L., & Saucier, C. (2020). Red Wine Oxidation : Accelerated Ageing Tests, Possible Reaction Mechanisms and Application to Syrah Red Wines. *Antioxidants*, *9*(8), 663. https://doi.org/10.3390/antiox9080663

Drava, G., & Minganti, V. (2019). Mineral composition of organic and conventional white wines from Italy. *Heliyon*, *5*(9), e02464. https://doi.org/10.1016/j.heliyon.2019.e02464

Duval, A., & Avérous, L. (2016). Characterization and Physicochemical Properties of Condensed Tannins from Acacia catechu. *Journal of Agricultural and Food Chemistry*, *64*(8), 1751-1760.

Echave, J., Barral, M., Fraga-Corral, M., Prieto, M. A., & Simal-Gandara, J. (2021). Bottle Aging and Storage of Wines : A Review. *Molecules*, *26*(3), 713. https://doi.org/10.3390/molecules26030713

Elias, R. J., & Waterhouse, A. L. (2010). Controlling the Fenton Reaction in Wine. *Journal of Agricultural and Food Chemistry*, *58*(3), 1699-1707. https://doi.org/10.1021/jf903127r

Escribano-Bailón, M. T., Guerra, M. T., Rivas-Gonzalo, J. C., & Santos-Buelga, C. (1995). Proanthocyanidins in skins from different grape varieties. *Zeitschrift Für Lebensmittel-Untersuchung Und Forschung*, *200*(3), 221-224. https://doi.org/10.1007/BF01190499

Es-Safi, N.-E., Le Guernevé, C., Cheynier, V., & Moutounet, M. (2000). New Phenolic Compounds Formed by Evolution of (+)-Catechin and Glyoxylic Acid in Hydroalcoholic Solution and Their Implication in Color Changes of Grape-Derived Foods | Journal of Agricultural and Food Chemistry. *Journal of Agricultural and Food Chemistry*, *48*(9), 4233-4240.

Fayeulle, N., Vallverdu-Queralt, A., Meudec, E., Hue, C., Boulanger, R., Cheynier, V., & Sommerer, N. (2018). Characterization of new flavan-3-ol derivatives in fermented cocoa beans. *Food Chemistry*, *259*, 207-212. https://doi.org/10.1016/j.foodchem.2018.03.133

Ferreira, C., Sáenz-Navajas, M.-P., Carrascón, V., Næs, T., Fernández-Zurbano, P., & Ferreira, V. (2021). An assessment of voltammetry on disposable screen printed electrodes to predict wine chemical composition and oxygen consumption rates. *Food Chemistry*, *365*, 130405. https://doi.org/10.1016/j.foodchem.2021.130405

Ferreira, V., Carrascon, V., Bueno, M., Ugliano, M., & Fernandez-Zurbano, P. (2015). Oxygen Consumption by Red Wines. Part I : Consumption Rates, Relationship with

Chemical Composition, and Role of SO_2. *Journal of Agricultural and Food Chemistry*, *63*(51), 10928-10937. https://doi.org/10.1021/acs.jafc.5b02988

Forino, M., Picariello, L., Lopatriello, A., Moio, L., & Gambuti, A. (2020). New insights into the chemical bases of wine color evolution and stability : The key role of acetaldehyde. *European Food Research and Technology*, *246*, 733-743.

Francia-Aricha, E., Guerra, M. T., Rivas-Gonzalo, J. C., & Santos-Buelga, C. (s. d.). New Anthocyanin Pigments Formed after Condensation with Flavanols | Journal of Agricultural and Food Chemistry. *Journal of Agricultural and Food Chemistry*, *45*(6), 2262-2266.

Freitas, V. D., & Mateus, N. (2011). Formation of pyranoanthocyanins in red wines : A new and diverse class of anthocyanin derivatives. *Analytical and Bioanalytical Chemistry*, *401*, 1463-1473.

Fulcrand, H., Dueñas, M., Salas, E., & Cheynier, V. (2006). Phenolic Reactions during Winemaking and Aging. *American Journal of Enology and Viticulture*, *57*(3), 289-297.

Gambuti, A., Han, G., Peterson, A. L., & Waterhouse, A. L. (s. d.). Sulfur Dioxide and Glutathione Alter the Outcome of Microoxygenation. *American Journal of Enology and Viticulture*, *66*(4), 411-423.

Gambuti, A., Picariello, L., Rinaldi, A., & Moio, L. (2018). Evolution of Sangiovese Wines With Varied Tannin and Anthocyanin Ratios During Oxidative Aging. *Frontiers in Chemistry*, *0*. https://doi.org/10.3389/fchem.2018.00063

Gambuti, A., Rinaldi, A., Ugliano, M., & Moio, L. (2013). Evolution of phenolic compounds and astringency during aging of red wine : Effect of oxygen exposure before and after bottling. *Journal of Agricultural and Food Chemistry*, *61*(8), 1618-1627. https://doi.org/10.1021/jf302822b

Gambuti, A., Siani, T., Picariello, L., Rinaldi, A., Lisanti, M. T., Ugliano, M., Dieval, J. B., & Moio, L. (2017a). Oxygen exposure of tannins-rich red wines during bottle aging. Influence on phenolics and color, astringency markers and sensory attributes. *European Food Research and Technology*, *243*(4), 669-680. https://doi.org/10.1007/s00217-016-2780-3

Gambuti, A., Siani, T., Picariello, L., Rinaldi, A., Lisanti, M. T., Ugliano, M., Dieval, J. B., & Moio, L. (2017b). Oxygen exposure of tannins-rich red wines during bottle aging. Influence on phenolics and color, astringency markers and sensory attributes. *European Food Research and Technology*, *243*(4), 669-680. https://doi.org/10.1007/s00217-016-2780-3

Gaulejac, N. V. de, Vivas, N., Nonier, M.-F., Absalon, C., & Bourgeois, G. (2001). Study and quantification of monomeric flavan-3-ol and dimeric procyanidin quinonic forms by HPLC/ESI-MS. Application to red wine oxidation. *Journal of the Science of Food and Agriculture*, *81*(12), 1172-1179. https://doi.org/10.1002/jsfa.926

Geană, E.-I., Ciucure, C. T., Artem, V., & Apetrei, C. (2020). Wine varietal discrimination and classification using a voltammetric sensor array based on modified screen-printed electrodes in conjunction with chemometric analysis. *Microchemical Journal*, *159*, 105451. https://doi.org/10.1016/j.microc.2020.105451

Giribaldi, J., Besson, M., Suc, L., Fulcrand, H., & Mouls, L. (2020). The use of extracted-ion chromatograms to quantify the composition of condensed tannin subunits. *Rapid Communications in Mass Spectrometry*, *34*(7), e8619. https://doi.org/10.1002/rcm.8619

Gonzalez, A., Vidal, S., & Ugliano, M. (2018). Untargeted voltammetric approaches for characterization of oxidation patterns in white wines. *Food Chemistry*, *269*, 1-8. https://doi.org/10.1016/j.foodchem.2018.06.104

Goto, T., & Kondo, T. (1991). Structure and Molecular Stacking of Anthocyanins. *Angewandte Chemie International Edition*, 17-33.

Guyot, S., Vercauteren, J., & Cheynier, V. (1996). Structural determination of colourless and yellow dimers resulting from (+)-catechin coupling catalysed by grape polyphenoloxidase. *Phytochemistry*, *42*(5), 1279-1288. https://doi.org/10.1016/0031-9422(96)00127-6

Hagerman, A. E., & Butler, L. G. (1978). Protein precipitation method for the quantitative determination of tannins. *Journal of Agricultural and Food Chemistry*, *26*(4), 809-812. https://doi.org/10.1021/jf60218a027

Hayasaka, Y., & Asenstorfer, R. E. (2002). Screening for Potential Pigments Derived from Anthocyanins in Red Wine Using Nanoelectrospray Tandem Mass Spectrometry. *Journal of Agricultural and Food Chemistry*, *50*(4), 756-761. https://doi.org/10.1021/jf010943v

He, F., Liang, N.-N., Mu, L., Pan, Q.-H., Wang, J., Reeves, M. J., & Duan, C.-Q. (2012). Anthocyanins and Their Variation in Red Wines I. Monomeric Anthocyanins and Their Color Expression. *Molecules*, *17*(2), 1571-1601. https://doi.org/10.3390/molecules17021571

He, F., Pan, Q.-H., Shi, Y., & Duan, C.-Q. (2008). Chemical Synthesis of Proanthocyanidins in Vitro and Their Reactions in Aging Wines. *Molecules*, *13*(12), 3007-3032. https://doi.org/10.3390/molecules13123007

Hopfer, H., Ebeler, S. B., & Heymann, H. (10754). The Combined Effects of Storage Temperature and Packaging Type on the Sensory and Chemical Properties of Chardonnay. *Journal of Agricultural and Food Chemistry*, *60*(43), 10743.

Hoyos-Arbeláez, J., Vázquez, M., & Contreras-Calderón, J. (2017). Electrochemical methods as a tool for determining the antioxidant capacity of food and beverages : A review. *Food Chemistry*, *221*, 1371-1381. https://doi.org/10.1016/j.foodchem.2016.11.017

Hui, Y. H., Nip, W.-K., Nollet, L. M. L., Paliyath, G., & Simpson, B. K. (2008). *Food Biochemistry and Food Processing*. John Wiley & Sons.

Jackson, R. S. (2008, avril 30). Wine Science : Principles and Applications. *Wine Science, Third Edition*.

Jackson : Wine science : Principles and applications—Google Scholar. (s. d.).

Jiang, H., Shii, T., Matsuo, Y., Tanaka, T., Jiang, Z.-H., & Kouno, I. (2011). A new catechin oxidation product and polymeric polyphenols of post-fermented tea. *Food Chemistry*, *129*(3), 830-836. https://doi.org/10.1016/j.foodchem.2011.05.031

Jiménez-Atiénzar, M., Cabanes, J., Gandía-Herrero, F., & García-Carmona, F. (2004). Kinetic analysis of catechin oxidation by polyphenol oxidase at neutral pH. *Biochemical and Biophysical Research Communications*, *319*(3), 902-910. https://doi.org/10.1016/j.bbrc.2004.05.077

Jurd, L. (1969). Review of Polyphenol Condensation Reactions and their Possible Occurrence in the Aging of Wines | American Journal of Enology and Viticulture. *American Journal of Enology and Viticulture*, 191-195.

Kamiya, H., Yanase, E., & Nakatsuka, S. (2014). Novel oxidation products of cyanidin 3-O-glucoside with 2,2′-azobis-(2,4-dimethyl)valeronitrile and evaluation of anthocyanin content and its oxidation in black rice. *Food Chemistry*, *155*, 221-226. https://doi.org/10.1016/j.foodchem.2014.01.077

Karbowiak, T., Gougeon, R. D., Alinc, J.-B., Brachais, L., Debeaufort, F., Voilley, A., & Chassagne, D. (2009). Wine Oxidation and the Role of Cork. *Food science and Nutrition*, *50*(1), 20-52.

Kennedy, J. A., Ferrier, J., Harbertson, J. F., & Gachons, C. P. des. (2006). Analysis of Tannins in Red Wine Using Multiple Methods : Correlation with Perceived Astringency. *American Journal of Enology and Viticulture*, *57*(4), 481-485.

Kennedy, J. A., & Jones, G. P. (2001). Analysis of Proanthocyanidin Cleavage Products Following Acid-Catalysis in the Presence of Excess Phloroglucinol. *Journal of Agricultural and Food Chemistry*, *49*(4), 1740-1746.

Khan, N., & Mukhtar, H. (2007). Tea polyphenols for health promotion. *Life Sciences*, *81*(7), 519-533. https://doi.org/10.1016/j.lfs.2007.06.011

Kilmartin, P. A. (2016). Electrochemistry applied to the analysis of wine : A mini-review. *Electrochemistry Communications*, *67*, 39-42. https://doi.org/10.1016/j.elecom.2016.03.011

Kilmartin, P. A., Zou, H., & Waterhouse, A. L. (2001). A Cyclic Voltammetry Method Suitable for Characterizing Antioxidant Properties of Wine and Wine Phenolics. *Journal of Agricultural and Food Chemistry*, *49*(4), 1957-1965.

Kilmartin, P. A., Zou, H., & Waterhouse, A. L. (2002). Correlation of Wine Phenolic Composition versus Cyclic Voltammetry Response. *American Journal of Enology and Viticulture*, *53*(4), 294-302.

Lambropoulos, I., & Roussis, I. G. (2007). Inhibition of the decrease of volatile esters and terpenes during storage of a white wine and a model wine medium by caffeic acid

and gallic acid. *Food Research International*, *40*(1), 176-181. https://doi.org/10.1016/j.foodres.2006.09.003

Lavigne, V., Pons, A., & Dubourdieu, D. (2007). Assay of glutathione in must and wines using capillary electrophoresis and laser-induced fluorescence detection : Changes in concentration in dry white wines during alcoholic fermentation and aging. *Journal of Chromatography A*, *1139*(1), 130-135. https://doi.org/10.1016/j.chroma.2006.10.083

Leontieş, A.-R., Răducan, A., Gîfu, I. C., & Anghel, D. F. (2017). Catechin oxidation products : Mechanistic aspects and kinetics. *Studia Universitatis Babeş-Bolyai Chemia*, *62*(4), 11-19. https://doi.org/10.24193/subbchem.2017.4.01

Leopoldini, M., Russo, N., & Toscano, M. (2011). The molecular basis of working mechanism of natural polyphenolic antioxidants. *Food Chemistry*, *125*(2), 288-306. https://doi.org/10.1016/j.foodchem.2010.08.012

Li, H., Guo, A., & Wang, H. (2008). Mechanisms of oxidative browning of wine. *Food Chemistry*, *108*(1), 1-13. https://doi.org/10.1016/j.foodchem.2007.10.065

Lopes, P., Richard, T., Saucier, C., Teissedre, P.-L., Monti, J.-P., & Glories, Y. (2007). Anthocyanone A : A Quinone Methide Derivative Resulting from Malvidin 3-O-Glucoside Degradation. *Journal of Agricultural and Food Chemistry*, *55*(7), 2698-2704. https://doi.org/10.1021/jf062875o

Lorrain, B., Ky, I., Pechamat, L., & Teissedre, P.-L. (2013). Molecules | Free Full-Text | Evolution of Analysis of Polyhenols from Grapes, Wines, and Extracts. *Molecules*, *18*(1), 1076-1100.

Ma, W., Guo, A., Zhang, Y., Wang, H., Liu, Y., & Li, H. (2014). A review on astringency and bitterness perception of tannins in wine. *Trends in Food Science & Technology*, *40*(1), 6-19. https://doi.org/10.1016/j.tifs.2014.08.001

Macías, V. M. P., Pina, I. C., & Rodríguez, L. P. (2001). *Factors Influencing the Oxidation Phenomena of Sherry Wine*. 5.

Makhotkina, O., & Kilmartin, P. A. (2009). Uncovering the influence of antioxidants on polyphenol oxidation in wines using an electrochemical method : Cyclic voltammetry.

Journal of Electroanalytical Chemistry, *633*(1), 165-174. https://doi.org/10.1016/j.jelechem.2009.05.007

Makhotkina, O., & Kilmartin, P. A. (2010). The use of cyclic voltammetry for wine analysis : Determination of polyphenols and free sulfur dioxide. *Analytica Chimica Acta*, *668*(2), 155-165.

Makkar, H. P. S., Blümmel, M., Borowy, N. K., & Becker, K. (1993). Gravimetric determination of tannins and their correlations with chemical and protein precipitation methods. *Journal of the Science of Food and Agriculture*, *61*(2), 161-165.

Mateus, N., Silva, A. M. S., Vercauteren, J., & de Freitas, V. (2001a). Occurrence of Anthocyanin-Derived Pigments in Red Wines. *Journal of Agricultural and Food Chemistry*, *49*(10), 4836-4840. https://doi.org/10.1021/jf001505b

Mateus, N., Silva, A. M. S., Vercauteren, J., & de Freitas, V. (2001b). Occurrence of Anthocyanin-Derived Pigments in Red Wines. *Journal of Agricultural and Food Chemistry*, *49*(10), 4836-4840. https://doi.org/10.1021/jf001505b

McRae, J. M., & Kennedy, J. A. (2011). Wine and Grape Tannin Interactions with Salivary Proteins and Their Impact on Astringency : A Review of Current Research. *Molecules*, *16*(3), 2348-2364. https://doi.org/10.3390/molecules16032348

Mercurio, M., & Smith, P. A. (2008). *Tannin Quantification in Red Grapes and Wine : Comparison of Polysaccharide- and Protein-Based Tannin Precipitation Techniques and Their Ability to Model Wine Astringency | Journal of Agricultural and Food Chemistry*. *56*(14), 5528-5537.

Merrell, C., & Hansen, M. (2018). Improving Red Wine Color and Mouthfeel Over Time. *Wines Vines Analytics*, *Wines&Vines*. https://winesvinesanalytics.com/features/203972

Miller, D. M., Buettner, G. R., & Aust, S. D. (1990). Transition metals as catalysts of “autoxidation” reactions. *Free Radical Biology and Medicine*, *8*(1), 95-108. https://doi.org/10.1016/0891-5849(90)90148-C

Millet, M., Poupard, P., Guilois-Dubois, S., Zanchi, D., & Guyot, S. (2019). Self-aggregation of oxidized procyanidins contributes to the formation of heat-reversible haze in apple-

based liqueur wine. *Food Chemistry*, *276*, 797-805. https://doi.org/10.1016/j.foodchem.2018.09.171

Monagas, M., & Bartolomé, B. (2009). Anthocyanins and Anthocyanin-Derived Compounds. In M. V. Moreno-Arribas & M. C. Polo (Éds.), *Wine Chemistry and Biochemistry* (p. 439-462). Springer New York. https://doi.org/10.1007/978-0-387-74118-5_21

Monagas, M., Bartolomé, B., & Gomez-Cordoves, C. (2005). Evolution of polyphenols in red wines from Vitis vinifera L. during aging in the bottle. *European Food Research and Technology*, *220*, 331-340.

Monagas, M., Bartolomé, B., & Gómez-Cordovés, C. (2005). Evolution of polyphenols in red wines from Vitis vinifera L. during aging in the bottle. *European Food Research and Technology*, *220*(3), 331-340. https://doi.org/10.1007/s00217-004-1109-9

Motta, S., Guaita, M., Cassino, C., & Bosso, A. (2020). Relationship between polyphenolic content, antioxidant properties and oxygen consumption rate of different tannins in a model wine solution ScienceDirect. *Food Chemistry*, *313*. https://www.sciencedirect.com/science/article/pii/S0308814619321910?casa_token=F5Za7fqUobkAAAAA:hwgLXeXveMPoNL9XDEjcAvkCPWJ0kBx_10jXTzvEW-2LNhfSXibf9VJfJpPLV8S88MxeXgIthwrWcA

Mouls, L., & Fulcrand, H. (2012). UPLC-ESI-MS study of the oxidation markers released from tannin depolymerization : Toward a better characterization of the tannin evolution over food and beverage processing. *Journal of Mass Spectrometry*, *47*(11), 1450-1457. https://doi.org/10.1002/jms.3098

Mouls, L., & Fulcrand, H. (2015a). Identification of new oxidation markers of grape-condensed tannins by UPLC–MS analysis after chemical depolymerization. *Tetrahedron*, *71*(20), 3012-3019. https://doi.org/10.1016/j.tet.2015.01.038

Mouls, L., & Fulcrand, H. (2015b). Identification of new oxidation markers of grape-condensed tannins by UPLC–MS analysis after chemical depolymerization. *Tetrahedron*, *71*(20), 3012-3019. https://doi.org/10.1016/j.tet.2015.01.038

Mouls, L., Mazauric, J.-P., Sommerer, N., Fulcrand, H., & Mazerolles, G. (2011a). Comprehensive study of condensed tannins by ESI mass spectrometry : Average

degree of polymerisation and polymer distribution determination from mass spectra. *Analytical and Bioanalytical Chemistry*, *400*(2), 613-623. https://doi.org/10.1007/s00216-011-4751-7

Mouls, L., Mazauric, J.-P., Sommerer, N., Fulcrand, H., & Mazerolles, G. (2011b). Comprehensive study of condensed tannins by ESI mass spectrometry : Average degree of polymerisation and polymer distribution determination from mass spectra. *Analytical and Bioanalytical Chemistry*, *400*(2), 613-623. https://doi.org/10.1007/s00216-011-4751-7

Nave, F., Teixeira, N., Mateus, N., & de Freitas, V. (2010). The fate of flavanol–anthocyanin adducts in wines : Study of their putative reaction patterns in the presence of acetaldehyde. *Food Chemistry*, *121*(4), 1129-1138. https://doi.org/10.1016/j.foodchem.2010.01.060

Noble, A. C. (1994). Bitterness in wine. *Physiology & Behavior*, *56*(6), 1251-1255. https://doi.org/10.1016/0031-9384(94)90373-5

Oliveira, C. M., Barros, A. S., Ferreira, A. C. S., & Silva, A. M. S. (2016). Study of quinones reactions with wine nucleophiles by cyclic voltammetry. *Food Chemistry*, *211*, 1-7. https://doi.org/10.1016/j.foodchem.2016.05.020

Oliveira, C. M., Barros, A. S., Silva Ferreira, A. C., & Silva, A. M. S. (2015). Influence of the temperature and oxygen exposure in red Port wine : A kinetic approach. *Food Research International*, *75*, 337-347. https://doi.org/10.1016/j.foodres.2015.06.024

Oliveira, C. M., Ferreira, A. C. S., De Freitas, V., & Silva, A. M. S. (2011). Oxidation mechanisms occurring in wines. *Food Research International*, *44*(5), 1115-1126. https://doi.org/10.1016/j.foodres.2011.03.050

Oszmianski, J., Cheynier, V., & Moutounet, M. (1996). Iron-Catalyzed Oxidation of (+)-Catechin in Model Systems. *Journal of Agricultural and Food Chemistry*, *44*(7), 1712-1715. https://doi.org/10.1021/jf9507710

Oszmianski, J., Sapis, J.-C., & Macheix, J.-J. (1985). Changes in Grape Seed Phenols as Affected By Enzymic and Chemical Oxidation in vitro. *Journal of Food Science*, *50*(5), 1505-1506. https://doi.org/10.1111/j.1365-2621.1985.tb10515.x

Özkan, M. (2002). Degradation of anthocyanins in sour cherry and pomegranate juices by hydrogen peroxide in the presence of added ascorbic acid. *Food Chemistry*, *78*(4), 499-504. https://doi.org/10.1016/S0308-8146(02)00165-6

Peterson, A. L., & Waterhouse, A. L. (2016). 1H NMR: A Novel Approach To Determining the Thermodynamic Properties of Acetaldehyde Condensation Reactions with Glycerol, (+)-Catechin, and Glutathione in Model Wine. *Journal of Agricultural and Food Chemistry*, *64*(36), 6869-6878.

Petrozziello, M., Torchio, F., Piano, F., Giacosa, S., Ugliano, M., Bosso, A., & Rolle, L. (2018). Impact of Increasing Levels of Oxygen Consumption on the Evolution of Color, Phenolic, and Volatile Compounds of Nebbiolo Wines. *Frontiers in Chemistry*, *6*. https://doi.org/10.3389/fchem.2018.00137

Picariello, L., Gambuti, A., Picariello, B., & Moio, L. (2017). Evolution of pigments, tannins and acetaldehyde during forced oxidation of red wine : Effect of tannins addition. *LWT*, *77*, 370-375. https://doi.org/10.1016/j.lwt.2016.11.064

Ployon, S., Attina, A., Vialaret, J., Walker, A. S., Hirtz, C., & Saucier, C. (2020). Laccases 2 & 3 as biomarkers of Botrytis cinerea infection in sweet white wines. *Food Chemistry*, *315*, 126233. https://doi.org/10.1016/j.foodchem.2020.126233

P. McManus, J., G. Davis, K., E. Beart, J., H. Gaffney, S., H. Lilley, T., & Haslam, E. (1985). Polyphenol interactions. Part 1. Introduction; some observations on the reversible complexation of polyphenols with proteins and polysaccharides. *Journal of the Chemical Society, Perkin Transactions 2*, *0*(9), 1429-1438. https://doi.org/10.1039/P29850001429

Poncet-Legrand, C., Cabane, B., Bautista-Ortín, A.-B., Carrillo, S., Fulcrand, H., Pérez, J., & Vernhet, A. (2010). Tannin Oxidation : Intra- versus Intermolecular Reactions. *Biomacromolecules*, *11*(9), 2376-2386. https://doi.org/10.1021/bm100515e

Pourova, J., Kottova, M., Voprsalova, M., & Pour, M. (2010). Reactive oxygen and nitrogen species in normal physiological processes. *Acta Physiologica*, *198*(1), 15-35.

Prieur, C., Rigaud, J., Cheynier, V., & Moutounet, M. (1994). Oligomeric and polymeric procyanidins from grape seeds. *Phytochemistry*, *36*(3), 781-784. https://doi.org/10.1016/S0031-9422(00)89817-9

Quideau, S., Jourdes, M., Lefeuvre, D., Montaudon, D., Saucier, C., Glories, Y., Pardon, P., & Pourquier, P. (2005). The Chemistry of Wine Polyphenolic C-Glycosidic Ellagitannins Targeting Human Topoisomerase II. *Chemistry – A European Journal*, *11*(22), 6503-6513. https://doi.org/10.1002/chem.200500428

Rentzsch, M., Schwarz, M., & Winterhalter, P. (2007). Pyranoanthocyanins–an overview on structures, occurrence, and pathways of formation. *Trends in Food Science & Technology*, *18*(10), 526-534.

Ribéreau-Gayon, P., Glories, Y., Maujean, A., & Dubourdieu, D. (2006). *Handbook of Enology, Volume 2 : The Chemistry of Wine - Stabilization and Treatments*. John Wiley & Sons.

Ricci, A., Teslic, N., Petropolus, V.-I., Parpinello, G. P., & Versari, A. (2019). Fast Analysis of Total Polyphenol Content and Antioxidant Activity in Wines and Oenological Tannins Using a Flow Injection System with Tandem Diode Array and Electrochemical Detections. *Food Analytical Methods*, *12*(2), 347-354. https://doi.org/10.1007/s12161-018-1366-z

Rigaud, J., Cheynier, V., Souquet, J.-M., & Moutounet, M. (1991). Influence of must composition on phenolic oxidation kinetics. *Journal of the Science of Food and Agriculture*, *57*(1), 55-63. https://doi.org/10.1002/jsfa.2740570107

Rigaud, J., Perez-Ilzarbe, J., Da Silva, J. M. R., & Cheynier, V. (1991a). Micro method for the identification of proanthocyanidin using thiolysis monitored by high-performance liquid chromatography. *Journal of Chromatography A*, *540*, 401-405. https://doi.org/10.1016/S0021-9673(01)88830-0

Rigaud, J., Perez-Ilzarbe, J., Da Silva, J. M. R., & Cheynier, V. (1991b). Micro method for the identification of proanthocyanidin using thiolysis monitored by high-performance liquid chromatography. *Journal of Chromatography A*, *540*, 401-405. https://doi.org/10.1016/S0021-9673(01)88830-0

Rimbach, G., Melchin, M., Moehring, J., & Wagner, A. E. (2009). Polyphenols from Cocoa and Vascular Health—A Critical Review. *International Journal of Molecular Sciences*, *10*(10), 4290-4309. https://doi.org/10.3390/ijms10104290

Robards, K., Prenzler, P. D., Tucker, G., Swatsitang, P., & Glover, W. (1999). Phenolic compounds and their role in oxidative processes in fruits. *Food Chemistry*, *66*(4), 401-436. https://doi.org/10.1016/S0308-8146(99)00093-X

Robichaud, J. L., & Noble, A. C. (1990). Astringency and bitterness of selected phenolics in wine. *Journal of the Science of Food and Agriculture*, *53*(3), 343-353. https://doi.org/10.1002/jsfa.2740530307

Roles of o-quinones and their polymers in the enzymic browning of apples. (1990). *Phytochemistry*, *29*(2), 435-440.

Roussis, I. G., Lambropoulos, I., & Tzimas, P. (2007). Protection of Volatiles in a Wine with Low Sulfur Dioxide by Caffeic Acid or Glutathione. *American Journal of Enology and Viticulture*, *58*(2), 274-278.

Roussis, I. G., & Sergianitis, S. (2008). Protection of some aroma volatiles in a model wine medium by sulphur dioxide and mixtures of glutathione with caffeic acid or gallic acid—Roussis. *Flavour and Fragrance Journal*, *23*(1), 35-39.

Sadilova, E., Carle, R., & Stintzing, F. C. (2007). Thermal degradation of anthocyanins and its impact on color and in vitro antioxidant capacity. *Molecular Nurition Food Research*, *51*(12), 1461-1471.

Salas, E., Atanasova, V., Poncet-Legrand, C., Meudec, E., Mazauric, J. P., & Cheynier, V. (2004). Demonstration of the occurrence of flavanol–anthocyanin adducts in wine and in model solutions. *Analytica Chimica Acta*, *513*(1), 325-332. https://doi.org/10.1016/j.aca.2003.11.084

Sanoner, P., Guyot, S., Bernillon, S., Fulcrand, H., Drilleau, J.-F., & Renard, C. (2002, septembre 9). *Procyanidin B2 oxidation products, multi linked dimers ?* 21. International Conference on Polyphenols. https://hal.inrae.fr/hal-02763559

Sarneckis, C. J., Dambergs, R. G., Jones, P., Mercurio, M., Herderich, M. J., & Smith, P. A. (2006). Quantification of condensed tannins by precipitation with methyl cellulose :

Development and validation of an optimised tool for grape and wine analysis. *Australian Journal of Grape and Wine Research*, *12*(1), 39-49. https://doi.org/10.1111/j.1755-0238.2006.tb00042.x

Sarni, P., Fulcrand, H., Souillol, V., Souquet, J. M., & Cheynier, V. (1995). Mechanisms of anthocyanin degradation in grape must-like model solutions. *Journal of the Science of Food and Agriculture*, *69*(3), 385-391.

Sarni-Manchado, P., & Cheynier, V. (s. d.). *Les polyphénols en agroalimentaire*.

Sarni-Manchado, P., Cheynier, V., & Moutounet, M. (1997). Reactions of polyphenoloxidase generated caftaric acid o-quinone with malvidin 3-O-glucoside. *Phytochemistry*, *45*(7), 1365-1369. https://doi.org/10.1016/S0031-9422(97)00190-8

Satake, R., & Yanase, E. (2018). Mechanistic studies of hydrogen-peroxide-mediated anthocyanin oxidation. *Tetrahedron*, *74*(42), 6187-6191. https://doi.org/10.1016/j.tet.2018.09.012

Saucier, C. (2010). How do wine polyphenols evolve during wine ageing? *Cerevisia*, *35*(1), 11-15. https://doi.org/10.1016/j.cervis.2010.05.002

Schwarz, M., Wabnitz, T. C., & Winterhalter, P. (2003). Pathway Leading to the Formation of Anthocyanin−Vinylphenol Adducts and Related Pigments in Red Wines. *Journal of Agricultural and Food Chemistry*, 3682-3687.

Scrimgeour, N., Nordestgaard, S., Lloyd, N. D. R., & Wikes, E. N. (2015). Exploring the effect of elevated storage temperature on wine composition. *Australian Journal of Grape and Wine Research*, *21*(S1), 713-722.

Shchepinov, M. S. (2007). Reactive Oxygen Species, Isotope Effect, Essential Nutrients, and Enhanced Longevity. *Rejuvenation Research*, *10*(1), 47-60.

Sheridan, M. K., & Elias, R. J. (2015). Exogenous acetaldehyde as a tool for modulating wine color and astringency during fermentation. *Food Chemistry*, *177*, 17-22. https://doi.org/10.1016/j.foodchem.2014.12.077

Singleton, V. L. (1987a). *Oxygen with Phenols and Related Reactions in Musts, Wines, and Model Systems : Observations and Practical Implications*. *38*(1), 9.

Singleton, V. L. (1987b). *Oxygen with Phenols and Related Reactions in Musts, Wines, and Model Systems : Observations and Practical Implications*. *38*(1), 9.

Singleton, V. L. (2001). A survey of wine aging reactions, especially with oxygen. *Proceedings of the ASEV 50th Anniversary Annual Meeting, Seattle, Washington, June 19-23, 2000, 2001, ISBN 0-9630711-4-9, Págs. 323-336*, 323-336. https://dialnet.unirioja.es/servlet/articulo?codigo=590527

Singleton, V. L., Salgues, M., Zaya, J., & Trousdale, E. (1985). Caftaric Acid Disappearance and Conversion to Products of Enzymic Oxidation in Grape Must and Wine. *American Journal of Enology and Viticulture*, *36*(1), 50-56.

Soares, S., Brandão, E., Mateus, N., & De Freitas, V. (2017). Sensorial properties of red wine polyphenols : Astringency and bitterness. *Food science and Nutrition*, *57*(5), 937-948.

Somers, T. C., & Wescombe, L. G. (1987). Evolution of red wines part II. An assessment of the role of acetaldehyde. *VITIS - Journal of Grapevine Research*, *26*(1), 27-27.

Souquet, J.-M., Cheynier, V., Brossaud, F., & Moutounet, M. (1996). Polymeric proanthocyanidins from grape skins. *Phytochemistry*, *43*(2), 509-512. https://doi.org/10.1016/0031-9422(96)00301-9

Sousa, C., Mateus, N., Silva, A. M. S., González-Paramás, A. M., Santos-Buelga, C., & Freitas, V. de. (2007). Structural and chromatic characterization of a new Malvidin 3-glucoside–vanillyl–catechin pigment. *Food Chemistry*, *102*(4), 1344-1351. https://doi.org/10.1016/j.foodchem.2006.04.050

Suc, L., Rigou, P., & Mouls, L. (2021). Detection and Identification of Oxidation Markers of the Reaction of Grape Tannins with Volatile Thiols Commonly Found in Wine. *Journal of Agricultural and Food Chemistry*, *69*(10), 3199-3208.

Tanaka, T., & Kouno, I. (2003). Oxidation of Tea Catechins : Chemical Structures and Reaction Mechanism. *food science and technology research*, *9*(2), 128-133.

Teng, B., Hayasaka, Y., Smith, P. A., & Bindon, K. A. (2019). *Effect of Grape Seed and Skin Tannin Molecular Mass and Composition on the Rate of Reaction with Anthocyanin*

and Subsequent Formation of Polymeric Pigments in the Presence of Acetaldehyde | *Journal of Agricultural and Food Chemistry*. *67*(32), 8938-8949.

Timberlake, C. F., & Bridle, P. (1976). Interactions Between Anthocyanins, Phenolic Compounds, and Acetaldehyde and Their Significance in Red Wines. *American Journal of Enology and Viticulture*, *27*(3), 97-105.

Tindal, R. A., Jeffery, D. W., & Muhlack, R. A. (2021). Mathematical modelling to enhance winemaking efficiency : A review of red wine colour and polyphenol extraction and evolution. *Australian Journal of Grape and Wine Research*, *27*(2), 219-233.

Toit, W. J. du, Marais, J., Pretorius, I. S., & Toit, M. du. (2006). Oxygen in Must and Wine : A review. *South African Journal of Enology and Viticulture*, *27*(1), 76-94. https://doi.org/10.21548/27-1-1610

Ugliano, M. (2013). Oxygen Contribution to Wine Aroma Evolution during Bottle Aging. *Journal of Agricultural and Food Chemistry*, *61*(26), 6125-6136. https://doi.org/10.1021/jf400810v

Ugliano, M. (2016). Rapid fingerprinting of white wine oxidizable fraction and classification of white wines using disposable screen printed sensors and derivative voltammetry. *Food Chemistry*, *212*, 837-843. https://doi.org/10.1016/j.foodchem.2016.05.156

Ugliano, M., Wirth, J., Bégrand, S., Dieval, J.-B., & Vidal, S. (2015). Oxidation Signature of Grape Must and Wine by Linear Sweep Voltammetry Using Disposable Carbon Electrodes. In S. B. Ebeler, G. Sacks, S. Vidal, & P. Winterhalter (Éds.), *Advances in Wine Research* (Vol. 1203, p. 325-334). American Chemical Society. https://doi.org/10.1021/bk-2015-1203.ch020

Vernhet, A., carillo, S., & Poncet-Legrand, C. (2014). Condensed Tannin Changes Induced by Autoxidation : Effect of the Initial Degree of Polymerization and Concentration. *Journal of Agricultural and Food Chemistry*, *62*(31), 7833-7842.

Vivar-Quintana, A. M., Santos-Buelga, C., Francia-Aricha, E., & Rivas-Gonzalo, J. C. (1999). Formation of anthocyanin-derived pigments in experimental red wines / Formación de pigmentos derivados de antocianos en vinos tintos experimentales. *Food Science*

and Technology International, *5*(4), 347-352. https://doi.org/10.1177/108201329900500407

Vivas, N. (1997). Composition et propriétés des préparations commerciales de tanins à usage oenologique. *Revue des oenologues et des techniques vitivinicoles et oenologiques: magazine trimestriel d'information professionnelle*, *24*(84), 15-21.

Vivas, N. (2000). Propriétés et intérêts des tanins œnologiques extraits du raisin. *Revue française d'oenologie*, *183*, 15-18.

Vivas, N., & Glories, Y. (1996). Role of Oak Wood Ellagitannins in the Oxidation Process of Red Wines During Aging. *American Journal of Enology and Viticulture*, *47*(1), 103-107.

von Baer, D., Rentzsch, M., Hitschfeld, M. A., Mardones, C., Vergara, C., & Winterhalter, P. (2008). Relevance of chromatographic efficiency in varietal authenticity verification of red wines based on their anthocyanin profiles : Interference of pyranoanthocyanins formed during wine ageing. *Analytica Chimica Acta*, *621*(1), 52-56.

Waterhouse, A. L., & Laurie, V. F. (2006a). Oxidation of Wine Phenolics : A Critical Evaluation and Hypotheses. *American Journal of Enology and Viticulture*, *57*(3), 306-313.

Waterhouse, A. L., & Laurie, V. F. (2006b). Oxidation of Wine Phenolics : A Critical Evaluation and Hypotheses. *American Journal of Enology and Viticulture*, *57*(3), 306-313.

Whitaker, J. R., & Lee, C. Y. (1995). Recent Advances in Chemistry of Enzymatic Browning. In *Enzymatic Browning and Its Prevention* (Vol. 600, p. 2-7). American Chemical Society. https://doi.org/10.1021/bk-1995-0600.ch001

Wrolstad, R. E., Durst, R. W., & Lee, J. (2005). Tracking color and pigment changes in anthocyanin products. *Trends in Food Science & Technology*, *16*(9), 423-428. https://doi.org/10.1016/j.tifs.2005.03.019

Zanchi, D., Poulain, C., Konarev, P., Tribet, C., & Svergun, D. (2008). Colloidal stability of tannins : Astringency, wine tasting and beyond. *journal of physics: condensed matter*.

Zhang, Z., Li, J., Fan, L., & Duan, Z. (2020). Effect of organic acid on cyanidin-3-O-glucoside oxidation mediated by iron in model Chinese bayberry wine. *Food Chemistry*, *310*, 125980. https://doi.org/10.1016/j.foodchem.2019.125980

RESUME

L'oxydation des polyphénols des vins rouges lors de leurs vieillissements implique des réactions très complexes mais constitue un véritable enjeu de recherche car elle va modifier leurs propriétés organoleptiques. Certaines voies de formation des produits d'oxydation des polyphénols ont été décrites dans la littérature. Cependant, de nombreuses études restent à faire, notamment sur la formation et l'identification de nouveaux composés d'oxydation de vins rouges. Au cours de ce travail de thèse, des protocoles de vieillissement et d'oxydation accélérés ont été mis au point sur vins rouges de Syrah (oxydation chimique, enzymatique et par chauffage). Une approche globale et semi-ciblée utilisant la spectrométrie de masse haute résolution a permis de comparer les évolutions naturelles et accélérées de vins de Syrah (3 millésimes différents 2018, 2014 et 2010). Cet axe a été complété par une approche électrochimique utilisant la voltammétrie cyclique et permettant, pour la première fois, de prédire la sensibilité d'un vin rouge face aux phénomènes de certaines dégradations oxydatives.

L'hémisynthèse de marqueurs d'oxydation dimériques de catéchine obtenus par voie enzymatique a été réalisée et les structures de six d'entre eux ont été élucidées par RMN pour la première fois. Certains de ces marqueurs ont ensuite été identifiés dans des extraits plus complexes de pépins (Merlot, Tannat, Syrah) et de vins de Syrah précédemment utilisés. Un effet de la maturation des baies et des millésimes des vins a été observé.

Finalement les produits d'oxydation des tannins et leurs cinétiques de formation ont été étudiés au sein de ces mêmes vins de Syrah (2018, 2014 et 2010) et comparé au vin de Syrah 2018 oxydé chimiquement. Cette étude a été menée en utilisant la dépolymérisation chimique suivie d'une séparation chromatographique liquide couplée à un spectromètre de masse (UHPLC-ESI-MS / MS) et a permis de mieux appréhender l'évolution des tannins au sein des vins.

ABSTRACT

The oxidation of polyphenols in red wines during their aging involves very complex reactions but constitutes a real research challenge because it will modify their organoleptic properties. Certain routes of formation of the polyphenols oxidation products have been described in the literature. However, many studies remain to be done, particularly on the formation and identification of new oxidation compounds in red wines. During this thesis, accelerated aging and oxidation protocols were developed on Syrah red wines (chemical, enzymatic and heating oxidation). A global and semi-targeted approach using high resolution mass spectrometry made it possible to compare the natural and accelerated evolutions of Syrah wines (3 different vintages 2018, 2014 and 2010). This axis was supplemented by an electrochemical approach using cyclic voltammetry and making it possible, for the first time, to predict the sensibility of a red wine towards certain oxidative degradations.

The hemisynthesis of enzymatically obtained dimeric catechin oxidation markers was performed and the structures of six of them were elucidated by NMR for the first time. Some of these markers were then identified in more complex extracts of seeds (Merlot, Tannat, Syrah) and in Syrah wines previously used. An effect of the berries ripening and the vintage of the wines was observed.

Finally, the tannin oxidation products and their formation kinetics were studied in these same Syrah wines (2018, 2014 and 2010) and compared to the chemically oxidized 2018 Syrah wine. This study was carried out using chemical depolymerization followed by liquid chromatographic separation coupled with a mass spectrometer (UHPLC-ESI-MS / MS) and made it possible to better understand the evolution of tannins in wines.